Pertanika Journal of

TROPICAL AGRICULTURAL SCIENCE

JTAS

VOL. 46 (1) FEB. 2023

PERTANIKA JOURNALS

A scientific journal published by Universiti Putra Malaysia Press

Pertanika Journal of Tropical Agricultural Science
Pertanika Journal of Tropical Agricultural Science

PERTANIKA JOURNAL OF TROPICAL AGRICULTURAL SCIENCE

About the Journal

Overview

Pertanika Journal of Tropical Agricultural Science is an official journal of Universiti Putra Malaysia. It is an open-access online scientific journal. It publishes the scientific outputs. It neither accepts nor commissions third party content.

Recognised internationally as the leading peer-reviewed interdisciplinary journal devoted to the publication of original papers, it serves as a forum for practical approaches to improving quality in issues pertaining to tropical agriculture and its related fields.

Pertanika Journal of Tropical Agricultural Science is a **quarterly** (*February*, *May*, *August*, and *November*) periodical that considers for publication original articles as per its scope. The journal publishes in **English** and it is open for submission by authors from all over the world.

The journal is available world-wide.

Aims and scope

Pertanika Journal of Tropical Agricultural Science aims to provide a forum for high quality research related to tropical agricultural research. Areas relevant to the scope of the journal include agricultural biotechnology, biochemistry, biology, ecology, fisheries, forestry, food sciences, genetics, microbiology, pathology and management, physiology, plant and animal sciences, production of plants and animals of economic importance, and veterinary medicine.

History

Pertanika was founded in 1978. A decision was made in 1992 to streamline *Pertanika* into 3 journals as Pertanika Journal of Tropical Agricultural Science, Pertanika Journal of Science & Technology, and Pertanika Journal of Social Sciences & Humanities to meet the need for specialised journals in areas of study aligned with the interdisciplinary strengths of the university.

Currently, as an interdisciplinary journal of agriculture, the revamped journal, a leading agricultural journal in Malaysia now focuses on tropical agricultural research and its related fields.

Vision

To publish journals of international repute.

Mission

Our goal is to bring the highest quality research to the widest possible audience.

Quality

We aim for excellence, sustained by a responsible and professional approach to journal publishing. Submissions are guaranteed to receive a decision within 90 days. The elapsed time from submission to publication for the articles averages 180 days. We are working towards decreasing the processing time with the help of our editors and the reviewers.

Abstracting and indexing of Pertanika

Pertanika is now over 42 years old; this accumulated knowledge has resulted in Pertanika Journal of Tropical Agricultural Science being abstracted and indexed in SCOPUS (Elsevier), Clarivate Web of Science (ESCI), EBSCO, DOAJ, Agricola, ASEAN CITATION INDEX, ISC, Microsoft Academic, Google Scholar, National Agricultural Science (NAL), and MyCite.

Citing journal articles

The abbreviation for Pertanika Journal of Tropical Agricultural Science is *Pertanika J. Trop. Agric. Sci*.

Pertanika Journal of Tropical Agricultural Science
Pertanika Journal of Tropical Agricultural Science

Publication policy

Pertanika policy prohibits an author from submitting the same manuscript for concurrent consideration by two or more publications. It prohibits as well publication of any manuscript that has already been published either in whole or substantial part elsewhere. It also does not permit publication of manuscript that has been published in full in proceedings.

Code of Ethics

The *Pertanika* journals and Universiti Putra Malaysia take seriously the responsibility of all its journal publications to reflect the highest publication ethics. Thus, all journals and journal editors are expected to abide by the journal's codes of ethics. Refer to *Pertanika*'s **Code of Ethics** for full details, or visit the journal's web link at http://www.pertanika.upm.edu.my/code_of_ethics.php

Originality

The author must ensure that when a manuscript is submitted to *Pertanika*, the manuscript must be an original work. The author should check the manuscript for any possible plagiarism using any program such as Turn-It-In or any other software before submitting the manuscripts to the *Pertanika* Editorial Office, Journal Division.

All submitted manuscripts must be in the journal's acceptable **similarity index range**:
≤ 20% – *PASS*; **> 20%** – *REJECT*.

International Standard Serial Number (ISSN)

An ISSN is an 8-digit code used to identify periodicals such as journals of all kinds and on all media–print and electronic. All *Pertanika* journals have an e-ISSN.

Pertanika Journal of Tropical Agricultural Science: e-ISSN 2231-8542 (Online).

Lag time

A decision on acceptance or rejection of a manuscript is expected within 90 days (average). The elapsed time from submission to publication for the articles averages 180 days.

Authorship

Authors are not permitted to add or remove any names from the authorship provided at the time of initial submission without the consent of the journal's Chief Executive Editor.

Manuscript preparation

Most scientific papers are prepared according to a format called IMRAD. The term represents the first letters of the words ***I****ntroduction*, ***M****aterials and Methods*, ***R****esults*, ***A****nd* ***D****iscussion*. IMRAD is simply a more 'defined' version of the "IBC" (*Introduction*, *Body*, *Conclusion*) format used for all academic writing. IMRAD indicates a pattern or format rather than a complete list of headings or components of research papers; the missing parts of a paper are: *Title*, *Authors*, *Keywords*, *Abstract*, *Conclusions*, *References*, and *Acknowledgement*. Additionally, some papers include *Appendices*.

The *Introduction* explains the scope and objective of the study in the light of current knowledge on the subject; the *Materials and Methods* describes how the study was conducted; the *Results* section reports what was found in the study; and the *Discussion* section explains meaning and significance of the results and provides suggestions for future directions of research. The manuscript must be prepared according to the journal's **Instruction to Authors** (http://www.pertanika.upm.edu.my/Resources/regular_issues/Regular_Issues_Instructions_to_ Authors.pdf).

Editorial process

Authors who complete any submission are notified with an acknowledgement containing a manuscript ID on receipt of a manuscript, and upon the editorial decision regarding publication.

Pertanika follows a double-**blind peer review** process. Manuscripts deemed suitable for publication are sent to reviewers. Authors are encouraged to suggest names of at least 3 potential reviewers at the time of submission of their manuscripts to *Pertanika*. The editors are not, however, bound by these suggestions.

Notification of the editorial decision is usually provided within 90 days from the receipt of manuscript. Publication of solicited manuscripts is not guaranteed. In most cases, manuscripts are accepted conditionally, pending an author's revision of the material.

As articles are double-blind reviewed, material that may identify authorship of the paper should be placed only on page 2 as described in the first-4-page format in *Pertanika*'s **Instruction to Authors** (http://www.pertanika.upm.edu.my/Resources/regular_issues/Regular_Issues_Instructions_to_Authors.pdf).

The journal's peer review

In the peer review process, 2 or 3 referees independently evaluate the scientific quality of the submitted manuscripts. At least 2 referee reports are required to help make a decision.

Peer reviewers are experts chosen by journal editors to provide written assessment of the **strengths** and **weaknesses** of written research, with the aim of improving the reporting of research and identifying the most appropriate and highest quality material for the journal.

Operating and review process

What happens to a manuscript once it is submitted to *Pertanika*? Typically, there are 7 steps to the editorial review process:

1. The journal's Chief Executive Editor and the Editor-in-Chief examine the paper to determine whether it is relevance to journal needs in terms of novelty, impact, design, procedure, language as well as presentation and allow it to proceed to the reviewing process. If not appropriate, the manuscript is rejected outright and the author is informed.

2. The Chief Executive Editor sends the article-identifying information having been removed, to 2 or 3 reviewers. They are specialists in the subject matter of the article. The Chief Executive Editor requests that they complete the review within 3 weeks.

   Comments to authors are about the appropriateness and adequacy of the theoretical or conceptual framework, literature review, method, results and discussion, and conclusions. Reviewers often include suggestions for strengthening of the manuscript. Comments to the editor are in the nature of the significance of the work and its potential contribution to the research field.

3. The Editor-in-Chief examines the review reports and decides whether to accept or reject the manuscript, invite the authors to revise and resubmit the manuscript, or seek additional review reports. In rare instances, the manuscript is accepted with almost no revision. Almost without exception, reviewers' comments (to the authors) are forwarded to the authors. If a revision is indicated, the editor provides guidelines to the authors for attending to the reviewers' suggestions and perhaps additional advice about revising the manuscript.

4. The authors decide whether and how to address the reviewers' comments and criticisms and the editor's concerns. The authors return a revised version of the paper to the Chief Executive Editor along with specific information describing how they have answered' the concerns of the reviewers and the editor, usually in a tabular form. The authors may also submit a rebuttal if there is a need especially when the authors disagree with certain comments provided by reviewers.

5. The Chief Executive Editor sends the revised manuscript out for re-review. Typically, at least 1 of the original reviewers will be asked to examine the article.

6. When the reviewers have completed their work, the Editor-in-Chief examines their comments and decides whether the manuscript is ready to be published, needs another round of revisions, or should be rejected. If the decision is to accept, the Chief Executive Editor is notified.

7. The Chief Executive Editor reserves the final right to accept or reject any material for publication, if the processing of a particular manuscript is deemed not to be in compliance with the S.O.P. of *Pertanika.* An acceptance notification is sent to all the authors.

   The editorial office ensures that the manuscript adheres to the correct style (in-text citations, the reference list, and tables are typical areas of concern, clarity, and grammar). The authors are asked to respond to any minor queries by the editorial office. Following these corrections, page proofs are mailed to the corresponding authors for their final approval. At this point, **only essential changes are accepted**. Finally, the manuscript appears in the pages of the journal and is posted on-line.

Pertanika Journal of

TROPICAL AGRICULTURAL SCIENCE

Vol. 46 (1) Feb. 2023

A scientific journal published by Universiti Putra Malaysia Press

PJTAS

***Pertanika* Journal of Tropical Agricultural Science**

AN INTERNATIONAL PEER-REVIEWED JOURNAL

EDITORIAL OFFICE

JOURNAL DIVISION
Putra Science Park
1st Floor, IDEA Tower II
UPM-MTDC Technology Centre
Universiti Putra Malaysia
43400 Serdang, Selangor Malaysia.

Gen Enquiry
Tel. No: +603 9769 1622 | 1616
E-mail:
executive_editor.pertanika@upm.edu.my
URL: www.journals-jd.upm.edu.my

PUBLISHER

UPM PRESS
Universiti Putra Malaysia
43400 UPM, Serdang, Selangor, Malaysia.
Tel: +603 9769 8851
E-mail: penerbit@putra.upm.edu.my
URL: http://penerbit.upm.edu.my

ABSTRACTING AND INDEXING OF PERTANIKA JOURNALS

The journal is indexed in SCOPUS (Elsevier), Clarivate-Emerging Sources Citation Index (ESCI), BIOSIS, National Agricultural Science (NAL), Google Scholar, MyCite, ISC. In addition, Pertanika JSSH is recipient of "CREAM" Award conferred by Ministry of Higher Education (MoHE), Malaysia.

Pertanika Journal of Tropical Agricultural Science
Vol. 46 (1) Feb. 2023

Contents

Foreword

Welcome to the first issue of 2023 for the Pertanika Journal of Tropical Agricultural Science (PJTAS)!

PJTAS is an open-access journal for studies in Tropical Agricultural Science published by Universiti Putra Malaysia Press. It is independently owned and managed by the university for the benefit of the world-wide science community.

This issue contains 20 articles; three review articles, one short communication, and the rest are regular articles. The authors of these articles come from different countries namely Germany, Indonesia, Jamaica, Kingdom of Saudi Arabia, Malaysia, Nigeria, Sudan, Thailand, United Kingdom, and United State of America.

A selected article, by Nurdianah Harif Fadzilah and Wan Adnan Wan Omar from Universiti Sains Malaysia, evaluated the therapeutic effect of ethanolic bee pollen extract (BPE) from Malaysian stingless bee in cultured breast adenocarcinoma human cell lines (MCF-7) and mammary epithelial human cell lines (MCF-10A). Three stingless bee species were used to prepare bee pollen ethanolic extracts: *Geniotrigona thoracica*, *Heterotrigona itama*, and *Tetrigona apicalis*. The trypan blue exclusion assay was applied for cell proliferation activity in MCF-7 and MCF-10A. Besides that, the therapeutic index (TI) was analyzed to assess the relative antiproliferative activity of BPE on cancer versus normal cells. The results showed that the therapeutic index of *G. thoracica* BPE was the highest, which is potentially developing as a chemotherapeutic agent. The detailed information of this article is available on page 37.

Another article entitled "The Effect of Cadmium, Copper, and Lead on *Brassica juncea* in Hydroponic Growth Medium" investigated the accumulation of heavy metals, including copper, cadmium, and lead, in the different parts of *Brassica juncea* planted by the hydroponic method. The research results show that the accumulation of these heavy metals in the different parts of *B. juncea* varied over time. Full information of this study is presented on page 253.

A regular article entitled "Phylogeny Study of 20 Selected Species of Zingiberaceae from *Ex situ* Collections in Peninsular Malaysia" provided additional biological information to the 20 selected Zingiberaceae species, which were collected from the Agricultural Conservatory Park, Institute of Bioscience, Universiti Putra Malaysia. The combined random amplified polymorphic DNA (RAPD) and inter simple sequence repeat unweighted pair group method with arithmetic mean (ISSR UPGMA) phylogenetic tree classed them according to their three tribes (Alpinieae, Zingiberaceae, and Globbeae). The further details of this study are found on page 329.

We anticipate that you will find the evidence presented in this issue to be intriguing, thought-provoking and useful in reaching new milestones in your own research. Please recommend the journal to your colleagues and students to make this endeavour meaningful.

A special thanks to the Editor-in-Chief, Prof. Dr. Amin Ismail for serving Pertanika Journal of Tropical Agricultural Science for the past two years, in ensuring Pertanika plays a vital role in shaping the minds of researchers, enriching their lives, and encouraging them to continue their quest for new knowledge. We welcome the new Editor-in-Chief, Assoc. Prof. Dr. Phebe Ding on board. We hope that her involvement and contributions towards Pertanika would not only improve its quality but also support the development efforts in making it an international journal of good standing.

We would also like to express our gratitude to all the contributors, namely the authors, reviewers, and Editorial Board Members of PJTAS, who have made this issue possible.

All the papers published in this edition underwent Pertanika's stringent peer-review process involving a minimum of two reviewers comprising internal as well as external referees. This was to ensure that the quality of the papers justified the high ranking of the journal, which is renowned as a heavily-cited journal not only by authors and researchers in Malaysia but by those in other countries around the world as well.

PJTAS is currently accepting manuscripts for upcoming issues based on original qualitative or quantitative research that opens new areas of inquiry and investigation.

Chief Executive Editor
Mohd Sapuan Salit
executive_editor.pertanika@upm.edu.my

Pertanika J. Trop. Agric. Sci. 46 (1): 1 - 15 (2023)

PERTANIKA JOURNALS

TROPICAL AGRICULTURAL SCIENCE

Journal homepage: http://www.pertanika.upm.edu.my/

Profiling Primary Metabolites of Governor's Plum *Flacourtia indica* (Burm.f.) Merr. at Two Different Ripe Stages

Omnia Momen Ahmed Khalifa Attallah[1], Rupika Delgoda[2] and Noureddine Benkeblia[3,4]*

[1]Department of Pharmacology, Faculty of Medical Sciences, The University of the West Indies, Mona Campus, Kingston 7, Jamaica
[2]Natural Products Institute, Faculty of Science and Technology, The University of the West Indies, Mona Campus, Kingston 7, Jamaica
[3]Department of Life Sciences, Faculty of Science and Technology, The University of the West Indies, Mona Campus, Kingston 7, Jamaica
[4]The Biotechnology Centre, Faculty of Science and Technology, The University of the West Indies, Mona Campus, Kingston 7, Jamaica

ABSTRACT

To date, no study has investigated the variation of the primary metabolite profile of the fruit of *Flacourtia indica* (Burm.f.) Merr. (commonly known as governor's plum), an underutilised fruit in Jamaica. To fill this gap, the current study aimed to bring novel data on this fruit at two different ripe stages (light = deep wine-red colour and dark = fully darkened brown colour) and explore the variation of their metabolome profiles. The gas chromatography-mass spectrometry (GC-MS) profiling identified 10 saccharides, 4 sugar alcohols, 11 organic acids, 24 fatty acids, and 8 amino acids in the light and dark colour fruits. However, some metabolites were not shared by both fruit ripening stages. The principal component analysis (PCA) of the different classes of the primary metabolites showed that the significant difference between the light and dark colour governor's plum fruit is mainly determined by the content of sugars and organic acids, with the fully ripe (dark) stage expressing significant high levels of both. The hierarchical cluster analysis (HCA) showed that the profiled sugars, sugar alcohols, and fatty acids were grouped into two main clusters. In contrast, organic acids and amino acids were grouped into one cluster. However, some metabolites were related to the clusters observed. With these profiles, it was concluded that the

ARTICLE INFO

Article history:
Received: 08 July 2022
Accepted: 05 September 2022
Published: 25 November 2022

DOI: https://doi.org/10.47836/pjtas.46.1.01

E-mail addresses:
omniaattallah178@gmail.com (Omnia Momen Ahmed Khalifa Attallah)
thejani.delgoda@uwimona.edu.jm (Rupika Delgoda)
noureddine.benkeblia@uwimona.edu.jm (Noureddine Benkeblia)
* Corresponding author

ISSN: 1511-3701
e-ISSN: 2231-8542

dark colour governor's plum is in the true ripe stage, although the light colour fruit is commercially considered ripe.

Keywords: *Flacourtia indica*, primary metabolites, profiling, ripening

INTRODUCTION

Fruit science is being deeply transformed because of unprecedented and incommensurate developments and advances in analytical chemistry. As sugars and other primary metabolites play a central role in maturation and ripening processes, the use of metabolomics in quantifying these primary metabolites is undoubtedly being established as a key analytical tool. This promising approach attempts to elucidate the variations of the primary metabolite profiles through the maturation process. In fact, following the changes in primary and secondary metabolites help establish the fact that they are not merely the end product of the expression of their respective genes but that they form a part of the regulatory system of maturation and ripening in an integrated manner (Goodacre et al., 2004).

In the tropics, fruits present large biodiversity varying in structure, characteristics, and physiology (Wongs-Aree & Noichinda, 2018). Bananas, pineapples, papaya, and avocado fall within the category of major tropical fruits, while others, such as lychee, durian, rambutan, guava, passionfruit, mangosteen, and tamarind, are considered minor tropical fruits (Paull & Duarte, 2011a, 2011b). As in many parts of the world, numerous not-so-well-known, unknown, and underutilized fruits grow island-wide, as exemplified by governor's plum (*Flacourtia inidca*), rose apple (*Syzygium malaccense*), jimbilin (*Phyllanthus acidus*), and mammee apple (*Mammea americana*). These indigenous introduced and native fruits are consumed by the rural communities and people living in the island's countryside and constitute an important source of vitamin and mineral requirements in their diet.

Governor's plum (*Flacourtia indica*), also known as 'Indian plum' or 'boichi, belongs to the family of Flacourtiaceae and grows widely in dry tropical forests. It is native to India, Bangladesh, Sri Lanka, Ethiopia, and South Africa, and was introduced to Jamaica (Chatterjee et al., 2015; Eramma, 2016). The edible fruit is round, cherry-sized, fleshy with a sour or sweet taste, and astringent (Lim, 2013). The unripe fruit is green, the ripe is deep wine red, and the very ripe fruit is dark brown (Chatterjee et al., 2015).

Ripening is defined as the total changes in fruit tissue metabolism and is characterized by softening fruit tissue. It is accompanied by an increase in a unique combination of numerous volatile compounds derived from primary metabolites, which confer a delicate aroma and an attractive and appealing fruit (Adams-Phillips et al., 2004; Giovannoni, 2001; Pott et al., 2019).

The variations of the primary metabolites, i.e., sugar and sugar alcohols, organic acids, fatty acids, and amino acids, depend on the fruit type and the environmental conditions of the parent plant

(Haruenkit, 2004). Overall, there is a general decrease in organic acids and an increase in sugar content as the fruit develops and ripens due to the decarboxylation of organic acids and the breakdown of stored carbohydrates to produce sugars (Batista-Silva et al., 2018). Studies using omics technologies have shown evidence of a shift from the accumulation of organic acids to sugar synthesis in the final stage of fruit development in several fruit species (Etienne et al., 2013). The respiratory pathways commonly involved in the reduction of fruit sugars are glycolysis, the oxidative pentose phosphate (OPP) pathway, and the tricarboxylic acid (TCA) pathway (Tucker, 2012), triggering fruit ripening and leading to the formation of hundreds and even thousands of different metabolites (Pech et al., 2013). Although extensive literature is readily available on the metabolic changes during certain fruits' maturation, ripening and senescence, work is scarce on many tropical fruits (Fabi et al., 2010). There has been no study on the variation of the primary metabolites in the governor's plum.

Therefore, to bring novel data on the governor's plum fruit and explore the variation of the metabolites profile, this study aimed to perform profiling of the primary metabolites of the fruit harvested at two ripe (light colour and dark colour) stages. The importance of the study is to screen the change in the metabolites of ripe governor's plum and determine the most appropriate commercial ripening stage, which is associated with the quality of fruits. Hence, using metabolomics will provide a comprehensive and unbiased analysis of the primary metabolites of the governor's plum at two different ripe stages. In addition, comprehensive metabolite profiling of sugars, organic acids, and amino acids is lacking in the governor's plum. Therefore, the findings of this study may provide the basis for further investigation of the physiological and biochemical changes in ripe fruit.

MATERIALS AND METHODS

Fruit Samples

The fruit of *Flacourtia indica* (governor's plum) was collected freshly from trees growing in Shortwood, St. Andrew, Jamaica. Fruits were collected at two commercial and ripe stages practised by farmers and the local market retailers: light colour fruit and dark colour fruit. Immediately after harvesting, fruits were transported to the laboratory and leaves, branches, and fruit were identified by the herbarium curator (Mr Patrick Lewis, botanist) of the Department of Life Sciences, UWI Mona campus, and deposited under voucher No: UWI-Mona 35 250. Afterwards, samples were sorted, and any sample with visible defect, contamination, or injury was discarded. The fruits were separated visually into two ripening stages based on the skin colour: light = deep wine-red colour and dark = fully darkened brown colour (Figure 1). The fruits were quickly washed with distilled water, left to drain for one hour at room temperature, and then freeze-dried for 72 hours using a Labconco freeze drier (Labconco Corp., USA) and stored under a vacuum at -20 °C until use.

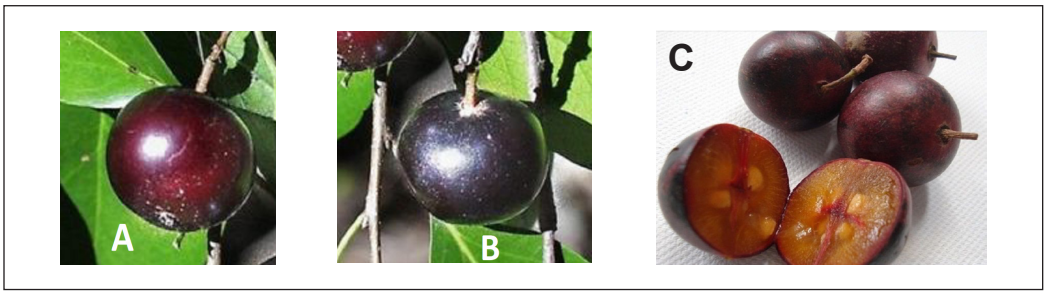

Figure 1. Governor's plum *Flacourtia indica* at the two ripe commercial stages. (A) Deep wine red (light) fruit; (B) Fully darkened brown (dark) very ripe fruit; and (C) Whole and sliced fruit

Metabolomics Profiling of *Flacourtia indica* Fruit

Sample Preparation. The metabolites of the extracts were profiled using gas chromatography-mass spectrometry (GC-MS) according to the method described by Broeckling et al. (2005) and Roessner-Tunali et al. (2003). Freeze-dried samples (300 mg) were extracted with 1 mL pure methanol (Sigma-Aldrich, USA) at 60 °C for 1 hour. Subsequently, 100 µL of ribitol (Sigma-Aldrich, USA) (0.2 mg/mL in distilled water) was added to the mixture as an internal standard. For separating polar and non-polar compounds, 1 mL of chloroform (Sigma-Aldrich, USA) was added to the mixture and then centrifuged at 1,400 × *g* for 10 min. Then the supernatant layer was separated and reduced to dryness. After dryness, the residues were redissolved in pyridine (Sigma-Aldrich, USA) (150 µL) for non-polar fractions. For polar fractions, the residues were redissolved in 150 µL of 20 mg/mL methoxyamine hydrochloride (Sigma-Aldrich, USA) in pyridine and incubated at 50 °C until the residue was completely dissolved. Subsequently, all the extracts were derivatized by the addition of 150 µL MSTFA (N-methyl-N-(trimethylsilyl) trifluoroacetamide) (Sigma-Aldrich, USA) + 1% TMCS (Trimethylchlorosilane) (Sigma-Aldrich, USA) and incubated at 50 °C for 1 hour. Afterwards, 200 µL of the extracts were transferred to a glass insert for GC-MS analysis.

GC-MS Analysis. GC-MS analysis was conducted using an Agilent Technologies gas chromatograph (model 6890N, USA) coupled to a mass spectrometric detector (model MSD 5973N). The operating conditions are as follows: electron impact mode, 70 eV; splitless mode (injection purge off = 0.75 min); injector temperature 250 °C; transfer line temperature 280 °C; column, DB-1701, 30 m, 0.25 mm i.d., 0.25 µm film thickness. A ramped temperature program was employed, starting at 80 °C, holding for 2 min, and increasing the temperature by 20 °C per min for 10 min and holding for 10 min. The solvent delay was 3 min, and the carrier gas helium was at a flow rate of 1.2 mL/min. All the operations were conducted in scan mode. The deconvolution of the metabolites was

done using AMDIS (Automated Mass Spectral Deconvolution and Identification System), and the metabolites were identified as TMS (trimethylsilyl) derivatives using the NIST (National Institute of Standards and Technology) database (NIST Mass Spectral Database, PC-Version 5.0, 2005, National Institute of Standardisation and Technology, USA). Other plant-specific databases, such as the Golm Metabolome Database (http://www.csbdb.mpimp-Golm.mpg.de/csbdb/gmd/home/gmd_sm.html) and RIKEN database (http://prime.psc.riken.jp/compms/msdial/main.html#MSP), based on matching mass and the highest match (probability).

Statistical Analysis. Data were treated by *t*-test to compare the means of the metabolites in the light and dark ripe fruits. Differences among means were determined by the least significant difference (LSD) test, with significance defined at $P < 0.05$. For multivariate analysis, data were transformed, and principal component (PCA) and hierarchical cluster (HCA) analyses were computed using the SPSS software package (version 25.0, IBM Corp., USA). Pearson's correlation coefficients and the furthest neighbour as the clustering method were selected to ensure that groups share a good correlation for the HCA analysis.

RESULTS

Sugars and Sugar Alcohols

The profiling of the primary sugars and sugar alcohols led to the identification of 10 saccharides and 4 sugar alcohols (Table 1). Ten (10) saccharides, were identified, including 3 pentoses, 4 hexoses, and 2 disaccharides in light colour fruit extracts, but fructose and melibiose were not detected. In dark colour fruit extracts, 11 saccharides, including 3 pentoses, 5 hexoses, and 2 disaccharides, were also identified, but sucrose was not detected. Similarly, only mannitol and galactitol were identified in light colour fruit extracts, while mannitol, arabinitol, and myo-inositol were detected in dark colour fruit extracts. In light colour fruit extracts, significantly

Table 1
Sugars and sugar alcohols profiled and identified in governor's plum Flacourtia indica *fruit at two different ripe stages*

Sugars and sugar alcohols	Light colour fruit (mg/g D.W.)	Dark colour fruit (mg/g D.W.)
Ribose	0.351[a]	76.11[b]
Galactose	2.1[a]	178.9[b]
Mannose	4.3[a]	25.4[b]
Xylose	1.3[a]	44.3[b]
Arabinose	1.1[a]	126.4[b]
Glucose	4.5[a]	32.8[b]
Fructose	(< 0.001)*[a]	0.5[b]
Sucrose	0.2[a]	(< 0.001)*[b]
Sorbose	0.2[a]	6.0[b]
Melibiose	(< 0.001)*[a]	1.0[b]
Maltose	(< 0.001)*[a]	0.2[b]
Myo-Inositol	(< 0.001)*[a]	11.8[b]
Xylitol	0.1[a]	(< 0.001)*[b]
Mannitol	(< 0.001)*[a]	(< 0.001)*[a]
Arabinitol	(< 0.001)*[a]	(< 0.001)*[b]
Galactitol	0.005[a]	(< 0.001)*[a]

Note. (< 0.001)* indicates concentrations that were not detected and below the limit of detection of the GC-MS. Values of the same row with different superscript letters are significantly different

high concentrations (> 1 mg/g D.W.) of sugars were noted, yielding 2.12, 4.31, 1.29, 1.12, and 4.48 mg/g for galactose, mannose, xylose, arabinose, and glucose, respectively totalizing 95% of the identified saccharides. In dark colour fruit extracts, significantly high concentrations (> 1 mg/g D.W.) of sugars were noted, yielding 76.10, 178.86, 25.39, 44.27, 126.36, 32.84, 6.01, and 1.02 mg/g for ribose, galactose, mannose, xylose, arabinose, glucose, sorbose, and melibiose, respectively totalizing 99% of the identified saccharides. On the other hand, sugar alcohols were found at significantly low concentrations (< 1 mg/g D.W.), except myo-inositol, which yielded 11.75 mg/g D.W. in dark colour fruit extract. These significantly low concentrations of sugar alcohols are likely due to their physiological role as they function as phloem-translocated carbohydrates, even though a few of them, such as sorbitol and mannitol, also serve as storage carbon but at low concentrations. Comparatively, the total concentration of sugars and sugar alcohols in light colour fruit extracts was significantly lower (14.06 mg/g D.W.) compared to dark colour fruit extracts (491.50 mg/g D.W.).

Organic Acids (OA)

The profiled samples led to the identification of a total of 11 different OAs, which were found in the dark colour fruit extracts. In contrast, 8 organic acids were found in the light colour extracts at a concentration higher than 1 mg/g D.W. (Table 2). Surprisingly, most OAs were found at significantly low concentrations except arabinonic and mannonic acids, which yielded 92% and 93% of the total organic acids in light and dark fruit extracts, respectively. Indeed, in ripe fruits, the amount of organic acids decreases since they are metabolized by oxidation, amino acid synthesis, or serve as precursors for synthesising secondary metabolites. It was also noted that in light colour fruit extracts, total OAs concentration was significantly lower (1.1775 mg/g D.W.) compared to dark colour fruit extracts (20.6646 mg/g D.W.).

Fatty Acids (FAs)

In the fruit samples, analysis of the fruit extracts led to identifying 24 different FAs (Table 3). However, 3 FAs, ethanimidic, pelargonic, and linoleic acids were not

Table 2
Organic acids profiled and identified in governor's plum Flacourtia indica *fruit at two different ripe stages*

Organic acids	Light colour fruit (mg/g D.W.)	Dark colour fruit (mg/g)
Malonic acid	0.001[a]	0.003[a]
Citric acid	(< 0.001)*[a]	0.495[b]
Malic acid	0.002[a]	0.005[a]
Phenylacetic acid	0.005[a]	0.363[b]
Mannonic acid	0.002[a]	19.206[b]
Gluconic acid	0.001[a]	0.099[b]
Hexahydro-benzoic acid	(< 0.001)*[a]	0.005[a]
Azelaic acid	(< 0.001)*[a]	0.010[a]
Tartaric acid	0.001[a]	0.001[a]
Arabinonic acid	1.090[a]	0.470[b]
Succinic acid	0.077[a]	0.009[b]

Note. (< 0.001)* indicates concentrations that were not detected and below the limit of detection of the GC-MS. Values of the same row with different superscript letters are significantly different

Table 3
Fatty acids profiled and identified in governor's plum Flacourtia indica *fruit at two different ripe stages*

Fatty acids	Number of carbons	Light colour fruit (mg/g D.W.)	Dark colour fruit (mg/g D.W.)
Propanoic acid	C3	0.254[a]	0.165[a]
Butanoic acid	C4	0.909[a]	4.527b
Ethanimidic acid	C4	(< 0.001)*[a]	(< 0.001)*[a]
Valeric acid	C5	0.508[a]	0.010[b]
Caproic acid	6	0.016[a]	0.099[a]
Enanthic acid	C7	0.010[a]	0.010[a]
Caprylic acid	C8	0.021[a]	0.099[b]
Pelargonic acid	C9	(< 0.001)*[a]	(< 0.001)*[a]
Capric acid	C10	(< 0.001)*[a]	0.067[b]
Sebacic acid	C10	0.010[a]	0.080[b]
Undecanoic acid	C11	(< 0.001)*[a]	(< 0.001)*[a]
Lauric acid	C12:0	0.333[a]	0.010[b]
Myristic acid	C14:0	(< 0.001)*[a]	0.007[a]
Pentadecanoic acid	C15:0	0.010[a]	0.010[a]
Palmitic acid	C16:0	0.203[a]	0.116[a]
Margaric acid	C17:0	0.010[a]	0.005[a]
Stearic acid	C18:0	0.096[a]	4.189[b]
Oleic acid	C18:1	0.057[a]	0.569[b]
Linoleic acid	C18:2	(< 0.001)*[a]	(< 0.001)*[a]
Linolenic acid	C18:3	0.032[a]	(< 0.001)*[b]
Nonadecanoic acid	C19:0	0.010[a]	0.066[a]
Arachidic acid	C20:0	0.010[a]	0.002[a]
Behenic acid	C22:0	0.002[a]	(< 0.001)*[a]
Lignoceric acid	C24:0	(< 0.001)*[a]	0.033[b]

Note. (< 0.001)* indicates concentrations that were not detected and below the limit of detection of the GC-MS. Values of the same row with different superscript letters are significantly different

detected (< 1 mg/g D.W.) in both light and dark fruit extracts. In light colour fruit extracts, 17 FAs were identified with two yielding more than 0.5 mg/g D.W., butanoic acid (0.909 mg/g D.W.), and valeric acid (0.508 mg/g D.W.). In dark colour fruit extracts, 18 FAs were identified with 3 yielding more than 0.5 mg/g D.W., butanoic acid (4.527 mg/g D.W.), stearic acid (4.189 mg/g D.W.), and oleic acid (0.569 mg/g D.W.). From the structural point of view, 7 FAs are of an odd number of carbons yielding 21.9% and 1.06% of the total FAs in light and dark colour fruit extracts, respectively. The other FAs, 13 FAs, are saturated, yielding 74% and 98.3% in light and dark fruit extract, respectively. Interestingly, 1 monosaturated (MOFA: oleic acid). Furthermore, 2 polyunsaturated (PUFA: linoleic and linolenic acids) FAs

were identified; however, only oleic, linoleic acids, and linolenic acids were significantly higher (> 1 mg/g D.W.) in light and dark colour fruit extracts, respectively. Furthermore, MOFA and PUFA yielded 2.3% and 1.3%, and 0.56% and 0.02% of the total FAs in light and dark colour fruit extracts, respectively.

Amino Acids (AAs)

Although eight different AAs were identified in the fruit extracts, only two, glycine and proline; and four, glycine, proline, leucine, and glutamine, showed concentrations significantly high than 1 mg/g D.W. in the light colour and dark colour fruit extracts, respectively (Table 4). These predominant AAs yielded 97% and 96% of the total AAs in light and dark colour fruit extracts, respectively.

Table 4
Amino acids profiled and identified in governor's plum Flacourtia indica *fruit at two different ripe stages*

Amino acids	Light colour fruit (mg/g)	Dark colour fruit (mg/g)
Methionine	(< 0.001)*[a]	(< 0.001)*[a]
Glycine	0.0172[a]	0.660[b]
Proline	0.009[a]	0.149[b]
Tryptophan	(< 0.001)*[a]	(< 0.001)*[a]
Arginine	(< 0.001)*[a]	(< 0.001)*[a]
Aspartic acid	(< 0.001)*[a]	(< 0.001)*[a]
Leucine	(< 0.001)*[a]	0.002[a]
Glutamine	(< 0.001)*[a]	0.033[b]

Note. (< 0.001)* indicates concentrations that were not detected and below the limit of detection of the GC-MS. Values of the same row with different superscript letters are significantly different

DISCUSSION

Based on the literature available, extensive research was carried out on profiling primary metabolites of numerous temperate fruits such as tomato, apple, pear, strawberry, persimmon, and other citrus species. In addition, extensive literature reported the metabolic changes during the maturation and ripening of fresh crops, such as peach (Lombardo et al., 2011), strawberry (Zhang et al., 2011), pear (Oikawa et al., 2015), and pitaya (Wu et al., 2019), while very scarce work was reported on some tropical fruits (Fabi et al., 2010).

Unfortunately, out of the seven *Flacourtia* accepted species, most of the work was conducted on the biological and therapeutic activities of some secondary metabolites, phenolic compounds mainly, while no referenced work reported on the profile of the primary metabolites of any *Flacourtia* species, including governor's plum *F. indica*. In general, fruits' organoleptic and commercial quality attributes are determined by their ripening stage (Kader, 1999). Colour and sugars content is commonly used as an index to determine the ripe stage, and the colour of the skin is one of the most important criteria for ripening in many fruits like stony fruits (Crisosto, 1994; Usenik et al., 2008), mango (Lalel et al., 2003; Malevski et al., 1977), guava (Mercado-Silva et al., 1998), and pomegranate (Manera et al., 2013). Nevertheless, many tropical fruits remain unknown, and neither appropriate harvesting time nor ripening index has been reported. Our results showed that

total sugars and OAs were significantly higher in dark colour fruit compared to light colour fruit, showing that this stage (light colour) is not the appropriate ripe stage for harvesting the governor's plum. However, the taste of the fruit is almost similar, i.e., very astringent due to the high content of phenolics and tannins (personal data).

The untargeted profiling of primary metabolites of fruits is a good approach to provide better insight into their metabolome changes. Metabolomics studies on temperate fruits revealed similar dynamic variations in the levels of sugars and organic acids, as well as other primary metabolites during ripening (Oikawa et al., 2015). Our results showing patterns of variation in sugars and sugar alcohols, organic acids, fatty acids, and amino acid levels in two ripe governor's plums provided fundamental metabolomic data that is useful for understanding this unknown fruit. The significant trend of sugars is due to photosynthates import or starch degradation, while organic acids accumulated in young fruits significantly decrease by being converted to other metabolites, including volatiles (Beauvoit et al., 2018; Carrari et al., 2006). Moreover, the relative levels of sugars and organic acids in fruits are of great importance for harvesting time and are one of the determinants of the organoleptic quality attributes of fruits, particularly sweetness (Itai & Tanahashi, 2008). Although barely comparable, Pandit et al. (2010) used transcriptomics markers to understand the maturation and ripening programmes in mango (*Mangifera indica* L.) fruit. Among eighteen genes related to fruit physiology and biochemistry, genes related to primary metabolism showed a significantly high expression in comparison to that of the genes related to flavour production, and this agrees with our results showing a significant increase in sugars and sugar alcohols in the dark colour fruit compared to the light colour fruit.

Ripe fruit is defined as the total changes in tissue metabolism leading to increased attractiveness and organoleptic quality attributes (Adams-Phillips et al., 2004). The ripe stage is characterised by tissue softness and increased volatile compounds and pigments, such as carotenoids and flavonoids, resulting in a more appealing fruit (Giovannoni, 2001). The concentration of sugars and organic acids in fruits varies in ripe fruits. Overall, a decrease in organic acids and an increase in sugar content as fruit ripen are due to the decarboxylation of organic acids and the breakdown of stored carbohydrates to produce sugars (Batista-Silva et al., 2018). Several studies have shown evidence of a shift from the accumulation of organic acids to sugar synthesis in the ripe fruit of several species using metabolomics and other advanced omics technologies. Indeed, this shift results from the respiratory pathways commonly involved in the reduction of sugars by the glycolysis pathway, oxidative pentose phosphate (OPP) pathway, and the tricarboxylic acid (TCA) pathway (Etienne et al., 2013; Tucker, 2012). These pathways dramatically alter the complex network of primary metabolites, as well as other secondary metabolites and proteins, and

our findings showed how the profile of the primary metabolites was significantly altered, highlighting the difference between the two ripe stages of the governor's plum.

Factoring and Clustering of the Profiled Metabolites

The principal component analysis of the data sets revealed that the distribution of the metabolites seems to be governed by the ripening stage of the fruits (Figure 2). In the present analysis, the PCA of sugars and sugar alcohols showed a loading plot scoring 16% and 98% in PC1 and PC2 for both light colour and dark colour governor's plum fruit. On the contrary, the PCA of organic acids showed a different loading plot scoring less than 1% and more than 99% in PC1 and PC2 for both light colour and dark colour governor's plum fruit. The PCA of fatty acids showed that light and dark colour fruit scores were closer, with a score of 32% and 94% for both light colour and dark colour governor's plum fruit. Interestingly, The PCA of amino acids showed that light and dark colour fruit scores were very close, with a score of 60% and 80% for both light colour and dark colour governor's plum fruit. Overall, hierarchically separated sugars and sugar alcohols, as well as organic acids in the light colour and dark colour governor's plum fruit, and the 2D PCA graphs depicted this result. Thus, the loading plots of the different classes of the primary metabolites revealed that the difference observed between the light colour and dark colour governor's plum fruit is mainly due to the content of sugars and organic acids,

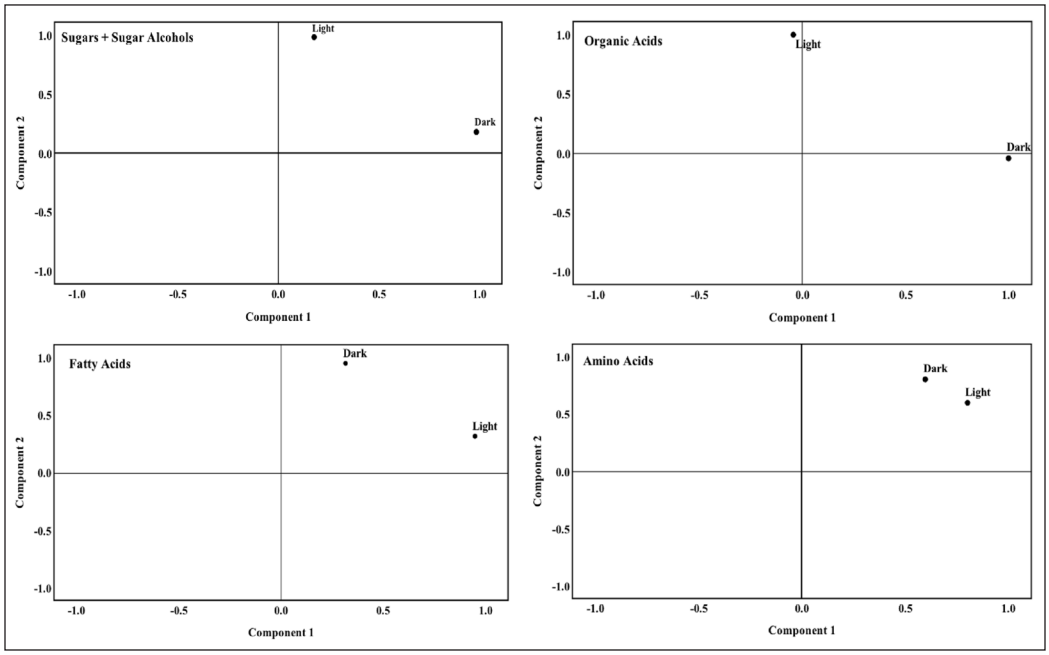

Figure 2. Score plots of the principal component analysis (PCA) of the profiled primary metabolites: sugars, organic acids, fatty acids, and amino acids of governor's plum (*Flacourtia indica*) fruit of two different ripe stages (light colour and dark colour skin)

to less extent to fatty acids. In contrast, amino acids cannot be considered markers to differentiate the governor's plum fruit's light and dark colour.

Hierarchical cluster analysis (HCA) was applied to a data set of the profiled and detected metabolites of light and dark colour governor's plum fruit (Figure 3). The dendrogram shows that the profiled sugars and sugar alcohols are distributed into different groups (clusters). Two clusters are observed at the first clustering level, while xylose, ribose, arabinose, and galactose are separated from the two main clusters. Similarly to sugars and sugar alcohols, fatty acids are grouped into two main clusters. However, the one formed by two FAs (behenic acid and stearic acid) is less related to the first cluster formed by the 22 other FAs. Interestingly, the organic acids dendrogram shows one cluster grouping all the organic acids except mannonic acid, which is separated from the unique cluster. Similarly to organic acids, the amino acids dendrogram shows one cluster grouping all AAs except proline and glycine, which

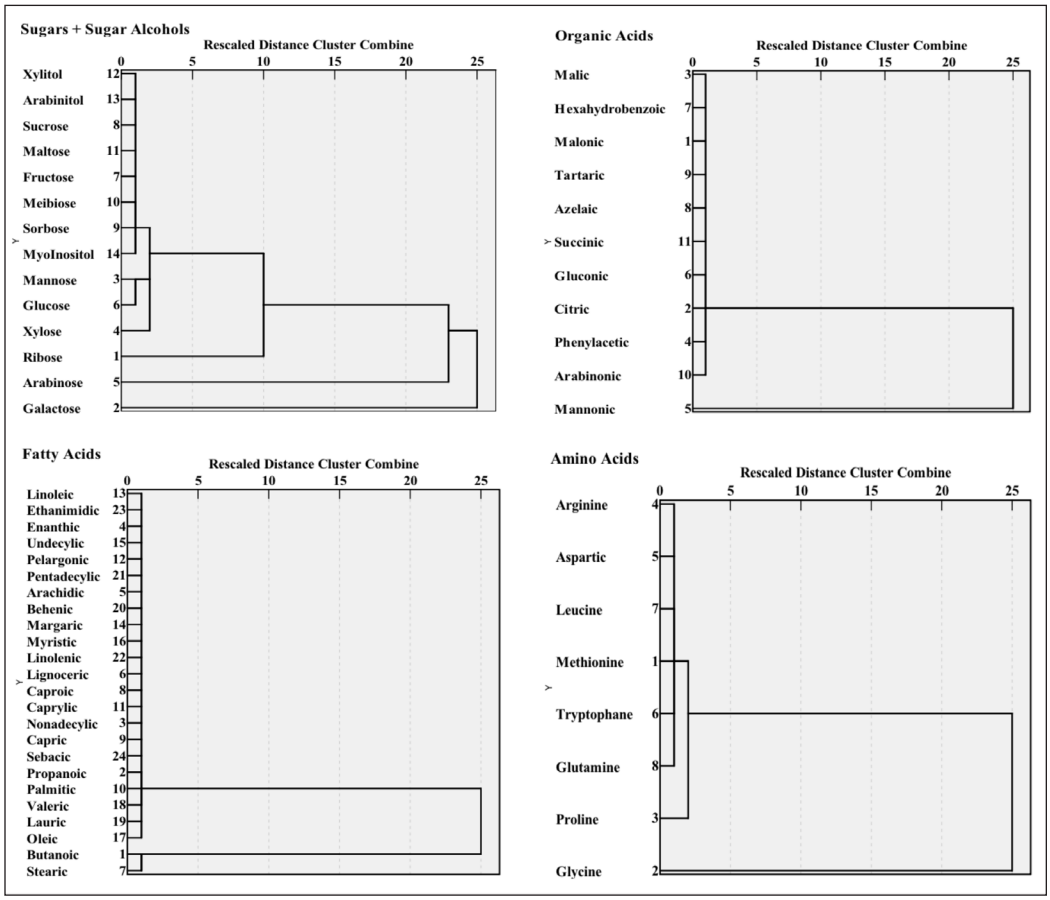

Figure 3. Dendrogram showing the hierarchical cluster analysis (HCA) of the profiled primary metabolites: sugars, organic acids, fatty acids, and amino acids of governor's plum (*Flacourtia indica*) fruit of two different ripe stages (light colour and dark colour skin)

seems unrelated to the unique cluster formed by the other AAs. Furthermore, as shown by the heatmap (Figure 4), sugars and sugar alcohols concentrate at the highest levels (higher colour intensity scale), followed by fatty acids, organic acids, and lastly, amino acids (lowest colour intensity.

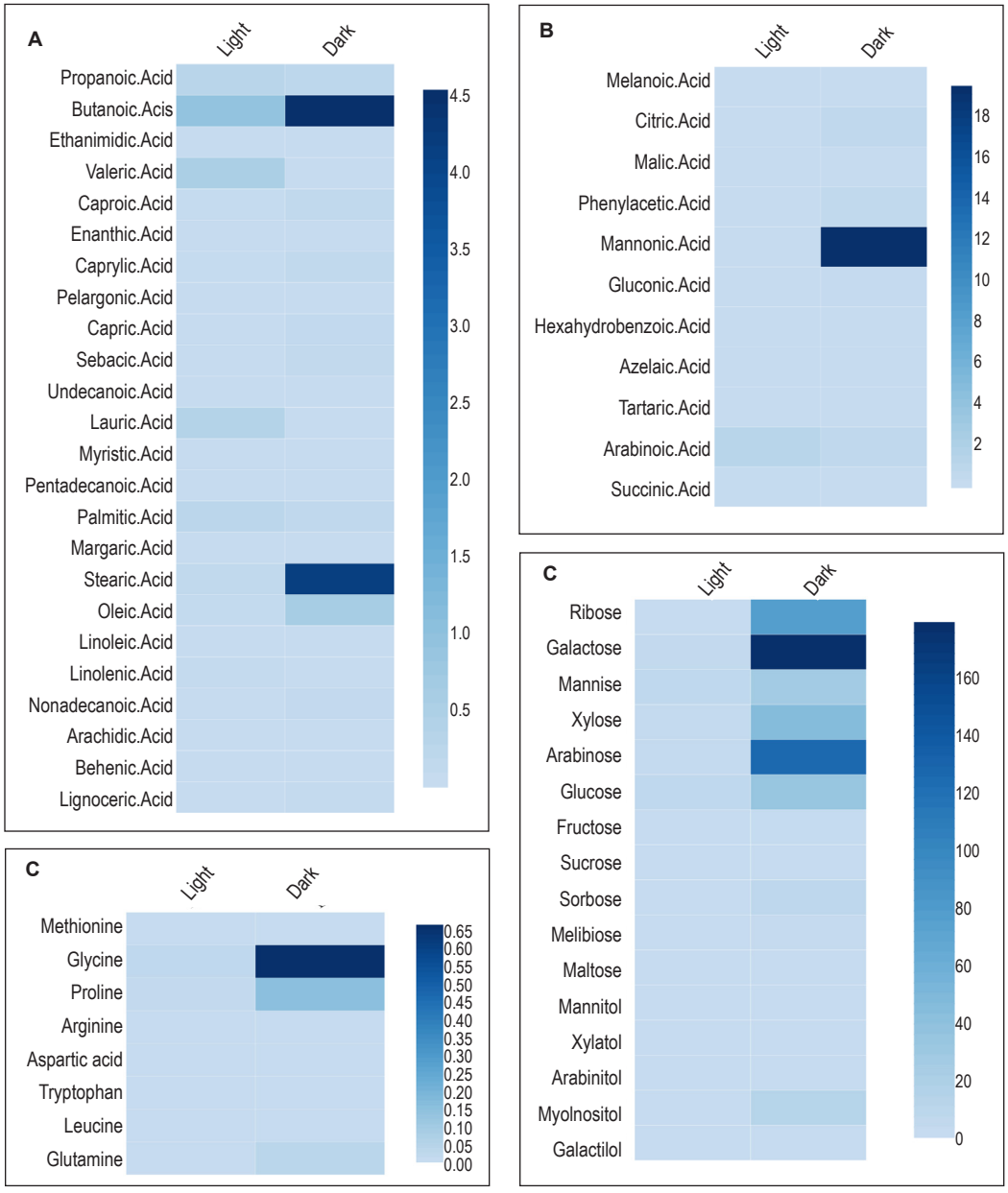

Figure 4. Heatmap of the primary metabolites: (A) sugars + sugar alcohols, (B) organic acids, (C) amino acids and (D) of governor's plum (*Flacourtia indica*) fruit of two different ripe stages (light colour and dark colour skin)

CONCLUSION

The data presented here have indicated that the profiled sugars and sugars alcohols, and organic acids varied significantly between the light and dark colours of the governor's plum fruit. However, fatty acids and amino acids did not govern the ripening stage. Multivariate analysis showed that fatty acids and amino acids of the two ripe stages fruit were much closer compared to sugars, sugar alcohols, and organic acids. Comparatively, dark colour fruit showed a significantly high content of sugars and sugar alcohols, while amino acids showed the lowest level with a significant statistical difference between the light and the dark colour fruit. The different groups of profiled primary metabolites suggest that sugars and sugar alcohols can be considered the "marker metabolites" of the ripe stage of dark colour governor's plum. In contrast, light colour fruit cannot be considered a ripe stage even though it is commercially harvested at this stage.

This study represents the first report on the profiling of the primary metabolites of governor's plum *Flacourtia indica*, and the observed variations therein are suggestive of the need to profile the secondary metabolites (mainly phenolics and volatiles) also, for a full understanding of the difference in the two ripe stages characterized by the fully darkened and red colour fruit.

ACKNOWLEDGEMENTS

This work was supported partly by the Department of Pharmacology, Faculty of Medical Sciences, UWI Mona, and partly by a grant from the Office of the Graduate Studies and Research, UWI, Mona.

REFERENCES

Adams-Phillips, L., Barry, B., & Giovannoni, J. (2004). Signal transduction systems regulating fruit ripening. *Trends in Plant Science*, *9*(7), 331–338. https://doi.org/10.1016/j.tplants.2004.05.004

Batista-Silva, W., Nascimento, V. L., Medeiros, D. B., Nunes-Nesi, A., Ribeiro, D. M., Zsögön, A., & Araújo, R. W. L. (2018). Modifications in organic acid profiles during fruit development and ripening: Correlation or causation? *Frontiers in Plant Science*, *9*, 1689. https://doi.org/10.3389/fpls.2018.01689

Beauvoit, B., Beelouah, I., Bertin, N., Cakpo, C. B., Colombié, S., Dai, Z., Gautier, H., Génard, M., Moing, A., Roch, L., Vercambre, G., & Gibon, Y. (2018). Putting primary metabolism into perspective to obtain better fruits. *Annals of Botany*, *122*(1), 1–21. https://doi.org/10.1093/aob/mcy057

Broeckling, C. D., Huhman, D. V., Farag, M. A., Smith, J. T., May, G. D., Mendes, P, Dixon, R. A., & Sumner, L. W. (2005). Metabolic profiling of *Medicago truncatula* cell cultures reveals the effects of biotic and abiotic elicitors on metabolism. *Journal of Experimental Botany*, *56*(410), 323–336. https://doi.org/10.1093/jxb/eri058

Carrari, F., Baxter, C., Usadel, B., Urbanczyk-Wochniak, E., Zanor, M. I., Nunes-Nesi, A., Nikiforova, V., Centero, D., Ratzka,A., Pauly, M., Sweetlove, L. J., & Fernie A. R. (2006). Integrated analysis of metabolite and transcript levels reveals the metabolic shifts that underlie tomato fruit development and highlight regulatory aspects of metabolic network behavior. *Plant Physiology*, *142*(4), 1380–1396. https://doi.org/10.1104/pp.106.088534

Chatterjee, M., Chandra, I., & Chatterjee, S. (2015). *Flacourtia indica* (Burm.f.) Merr. –An ethnopharmacologicaly valuable plant. *International Journal of Herbo Medica*, *2*(1), 26–27.

Crisosto, C. H. (1994). Stone fruit maturity indices: A descriptive review. *Postharvest News and Information*, *5*, 65N–68N.

Eramma, N. K. (2016). A comprehensive review on pharmacology of *Flacourtia indica* (Burm.f.) Merr. (governor's plum). *International Journal of Pharmaceutical and Chemical Sciences*, *5*(3), 176–184.

Etienne, A., Génard, M., Lobit, P., Mbeguié-A-Mbéguié, D., & Bugaud, C. (2013). What controls fleshy fruit acidity? A review of malate and citrate accumulation in fruit cells. *Journal of Experimental Botany*, *64*(6), 1451–1469. https://doi.org/10.1093/jxb/ert035

Fabi, J. P., Peroni, F. H. G., & Araújo Gomez, M. L. P. (2010). Papaya, mango and guava fruit metabolism during ripening: Postharvest changes affecting tropical fruit nutritional content and quality. *Fresh Produce*, *4*(1), 56–64.

Giovannoni, J. (2001). Molecular biology of fruit maturation and ripening. *Annual Review of Plant Biology*, *52*(1), 725–749. https://doi.org/10.1146/annurev.arplant.52.1.725

Goodacre, R., Vaidyanathan, S., Dunn, W. B., Harrigan, G. G., & Kell, D. B. (2004). Metabolomics by numbers: acquiring and understanding global metabolite data. *Trends in Biotechnology*, *22*(5), 245–252. https://doi.org/10.1016/j.tibtech.2004.03.007

Haruenkit, R. (2004). Analysis of sugars and organic acids in pineapple, papaya and star fruit by HPLC using an Aminex HPx-87 H column. *Warasan Kaset Phrachomklao*, *22*, 11–18.

Itai, A., & Tanahashi, T. (2008). Inhibition of sucrose loss during cold storage in Japanese pear (*Pyrus pyrifolia* Nakai) by 1-MCP. *Postharvest Biology and Technology*, *48*(3), 355-363. https://doi.org/10.1016/j.postharvbio.2007.10.015

Kader, A. A. (1999). Fruit maturity, ripening and quality relationships. *Acta Horticulturae*, *485*, 203–208. https://doi.org/10.17660/ActaHortic.1999.485.27

Lalel, H. J. D., Singh, Z., Tan, S. C., & Agusti, M. (2003). Maturity stage at harvest affects fruit ripening, quality and biosynthesis of aroma volatile compounds in 'Kensington Pride' mango. *Journal of Horticultural Science and Biotechnology*, *78*(2), 225–233. https://doi.org/10.1080/14620316.2003.11511610

Lim, T. K. (2013). *Flacourtia rukam*. In T. K. Lim (Ed.), *Edible medicinal and non-medicinal plants* (pp. 776-779). Springer. https://doi.org/10.1007/978-94-007-5653-3_41

Lombardo, V. A., Odorio, S., Borsani, J., Lauxmann, M. A., Bustamante, C. A., Budde, C. O., Andreo, C. S., Lara, M. V., Fernie, A. R., & Drincovich, M. F. (2011). Metabolic profiling during peach fruit development and ripening reveals the metabolic networks that underpin each developmental stage. *Plant Physiology*, *157*(4), 1696–1710. https://doi.org/10.1104/pp.111.186064

Malevski, Y., Brito, L. G. Z., Peleg, M., & Silberg, M. (1977). External color as maturity index of mango. *Journal of Food Science*, *42*(5), 1316–1318. https://doi.org/10.1111/j.1365-2621.1977.tb14486.x

Manera, F. J., Legua, P., Melgarejo, P., Brotons. J. M., Hernández, F., & Martínez, J. J. (2013). Determination of a colour index for fruit of pomegranate varietal group "Mollar de Elche". *Scientia Horticulturae*, *150*, 360–364. https://doi.org/10.1016/j.scienta.2012.11.036

Mercado-Silva, E., Benito-Bautista, P., & de los Angeles García-Velasco, M. (1998). Fruit

development, harvest index and ripening changes of guavas produced in central Mexico. *Postharvest Biology and Technology*, *13*(2), 143–150. https://doi.org/10.1016/S0925-5214(98)00003-9

Oikawa, A., Otsuka, T., Nakabayashi, R., Jikumaru, Y., Isuzugawa, K., Murayama, H., Saito, K., & Shiratake, K. (2015). Metabolic profiling of developing pear fruits reveals dynamic variation in primary and secondary metabolites, including plant hormones. *PLOS One*, *10*(7), e0131408. https://doi.org/10.1371/journal.pone.0131408

Pandit, S. S., Kulkarni, U, R. S., Giri, A. P., Köllner, T. G., Degenhardt, J., Gershenzon, J., & Gupta, V. S. (2010). Expression profiling of various genes during the fruit development and ripening of mango. *Plant Physiology and Biochemistry*, *48*(6), 426–433. https://doi.org/10.1016/j.plaphy.2010.02.012

Paull, R. E., & Duarte, O. (2011a). *Tropical fruits* (Vol. 1.). C. A. B. International.

Paull, R. E., & Duarte, O. (2011b). *Tropical fruits* (Vol. 2). C. A. B. International.

Pech, J. C., Purgatto, E., Girardi, C. L., Rombaldi, C. V., & Latche, A. (2013). Current challenges in postharvest biology of fruit ripening. *Current Agricultural Science and Technology*, *19*, 1–18.

Pott, D. M., Osorio, S., & Vallarino, J. G. (2019). From central to specialized metabolism: An overview of some secondary compounds derived from the primary metabolism for their role in conferring nutritional and organoleptic characteristics to fruit. *Frontiers in Plant Science*, *10*, 835. https://doi.org/10.3389/fpls.2019.00835

Roessner-Tunali, U., Hegemann, B., Lytovchenko, A., Carrari, F., Bruedigam, C., Granot, D., & Fernie, A. R. (2003). Metabolic profiling of transgenic tomato plants overexpressing hexokinase reveals that the influence of hexose phosphorylation diminishes during fruit development. *Plant Physiology*, *133*(1), 84–99. https://doi.org/10.1104/pp.103.023572

Tucker, G. A. (2012). Introduction. In G. B. Seymour, J. E. Taylor, & G. A. Tucker (Eds.), *Biochemistry of fruit ripening* (pp. 1–51). Springer. https://doi.org/10.1007/978-94-011-1584-1_1

Usenik, V., Kastelec, D., Veberic, R., & Štampar, F. (2008). Quality changes during ripening of plums (*Prunus domestica* L.). *Food Chemistry*, *111*(4), 830–836. https://doi.org/10.1016/j.foodchem.2008.04.057

Wongs-Aree, C., & Noichinda, S. (2018). Glycolysis fermentative by-products and secondary metabolites involved in plant adaptation under hypoxia during pre- and postharvest. In K. Das & M. S. Biradar (Eds.), *Hypoxia and anoxia*. IntechOpen. https://doi.org/10.5772/intechopen.80226

Wu, Y., Xu J., He, Y., Shi, M., Han, X., Li, W., Zhang, X., & Wen, X. (2019). Metabolic profiling of pitaya (*Hylocereus polyrhizus*) during fruit development and maturation. *Molecules*, *24*(6), 1114. https://doi.org/10.3390/molecules24061114

Zhang, J., Wang, X., Yu, O., Tang, J., Gu, X., Wan X., & Fang, C. (2011). Metabolic profiling of strawberry (*Fragaria* × *ananassa* Duch.) during fruit development and maturation. *Journal of Experimental Botany*, *62*(3), 1103–1118. https://doi.org/10.1093/jxb/erq343

Pertanika J. Trop. Agric. Sci. 46 (1): 17 - 35 (2023)

PERTANIKA JOURNALS

TROPICAL AGRICULTURAL SCIENCE

Journal homepage: http://www.pertanika.upm.edu.my/

Short Communication

The Occurrence of *Pteroptyx tener* Olivier Firefly (Coleoptera: Lampyridae) in Malaysia

Nurhafizul Abu Seri[1], Azimah Abd Rahman[1]*, Nur Faeza Abu Kassim[2] and Noor Fazeera Ahmad Fuzi[1]

[1]Geoinformatic Unit, Geography Section, School of Humanities, Universiti Sains Malaysia, 11800 USM, Pulau Pinang, Malaysia
[2]School of Biological Sciences, Universiti Sains Malaysia, 11800 USM, Pulau Pinang, Malaysia

ABSTRACT

A field survey of synchronized fireflies (*Pteroptyx tener* Olivier) was conducted in Kuala Sepetang, Perak. It involved sampling efforts for six months, from November 2021 to April 2022. A total of 10 sampling stations were selected along 5.63 km from the upstream to the downstream of the river. A sweep net was used for sampling at each station, and the net was swept for two minutes. Such sampling was replicated twice at each station. At the same time, collecting vegetation samples was done by taking the leaves, flowers, fruits, tree trunks, and roots. For species identification, collected specimens were taken to the Laboratory of the School of Biological Sciences, Universiti Sains Malaysia (USM). From this survey, a total of 111,622 individuals were recorded. This species has been observed on *Rhizophora mucronata*, *Rhizophora apiculata*, and *Sonneratia caseolaris*. The distribution and abundance of fireflies in the sampling area were undocumented prior to this study. This study is being conducted to understand *Pteroptys tener*'s distribution in Malaysia better and to add knowledge about the undocumented area of Kuala Sepetang. By adding an undocumented location for this species, this study can contribute to and expand the knowledge of the distribution and occurrence of fireflies in Malaysia, particularly in Perak.

Keywords: Distribution, fireflies, *Hibiscus tilliaceus* L. Engl., *Nypa fruticans*, *Pteroptyx tener* Olivier, *Rhizophora apiculata*, *Sonneratia caseolaris* Engl.

ARTICLE INFO

Article history:
Received: 14 July 2022
Accepted: 06 September 2022
Published: 25 November 2022

DOI: https://doi.org/10.47836/pjtas.46.1.02

E-mail addresses:
nurhafizul.abuseri97@gmail.com (Nurhafizul Abu Seri)
azimahrahman@usm.my (Azimah Abd Rahman)
nurfaeza@usm.my (Nur Faeza Abu Kassim)
fazeeraa@gmail.com (Noor Fazeera Ahmad Fuzi)
* Corresponding author

ISSN: 1511-3701
e-ISSN: 2231-8542

INTRODUCTION

Fireflies are insects belonging to the Coleoptera order and Lampyridae family capable of emitting flashing bioluminescent light (Lewis et al., 2020; Shahara et al., 2017). They are also known as glow worms or lightning bugs, and their taxonomic diversity encompasses more than 2,000 species in around 100 genera and 8 subfamilies across the globe (Shahara et al., 2017). González-Oreja (2008) and Wilson (2003) report that approximately 3,000 species per year perish, or 8 per day, out of a total of 3-100 million species in the globe. In the previous 600 years, around 70 species have gone extinct (Dunn, 2005). In Malaysia, a study by Asri et al. (2021) and Jusoh et al. (2012) revealed a significant decrease in mangrove fireflies in Sungai Rembau-Linggi.

Southeast Asia, encompassing Singapore, the Philippines, Thailand, Cambodia, Indonesia, Sulawesi, Papua New Guinea, Thailand, and Malaysia, is home to the *Pteroptyx* species of bent-winged fireflies (Ballantyne, 2001; Ballantyne & Lambkin, 2001; Ballantyne & McLean, 1970; Jusoh et al., 2018; Sartsanga et al., 2018). Malaysia is home to 13 species of the *Pteroptyx*, all of which may be found congregating on the mangrove vegetation of *Sonneratia caseolaris* (Shahara et al., 2017; Sulaiman et al., 2016, 2017). Compared to other species, *Pteroptyx tener* Olivier was the most common species in Malaysia (Jusoh et al., 2011, 2018). The *Pteroptyx tener* Olivier population on Peninsular's west coast differs from those on the east coast and in Borneo, even though there are no physical differences (Jusoh et al., 2020).

The locations of adult *Pteroptyx tener* Olivier fireflies recorded through the field surveys in Kuala Sepetang, Perak (Peninsular Malaysia), have existed for decades, but they are undocumented. Although this location is one of the most popular destinations for ecotourism, it is also one of the few places to watch fireflies where individuals can synchronize their flashing lights at night. The researchers, who studied the distribution and the occurrence of fireflies in the state of Perak, have concentrated solely on fireflies discovered in Kampung Dew, Perak. *Pteroptyx* fireflies, according to Mahadimenakbar et al. (2009), have the potential as ecotourism goods and contribute to wildlife tourism called entomotourism (Lemelin et al., 2019). Figure 1 shows the current study area for this field survey in Kuala Sepetang, Perak, compared to the previous study area in Kampung Dew, Perak. The map in Figure 1 also shows the documented and undocumented areas in Kuala Sepetang for *Pteroptyx tener* Olivier. Indirectly, this study adds information on the undocumented area for this firefly species.

The synchronized flashing light emitted by *Pteroptyx tener* Olivier makes them a valuable resource to promote ecotourism and significantly increases the local community income by creating jobs and procuring goods and services for some areas in Peninsular Malaysia (K. Nallakumar, 2003). For example, in Kuala Selangor (Khoo et al., 2012), Kuala Sepetang and Rembau-Linggi (Jusoh et al., 2010a,

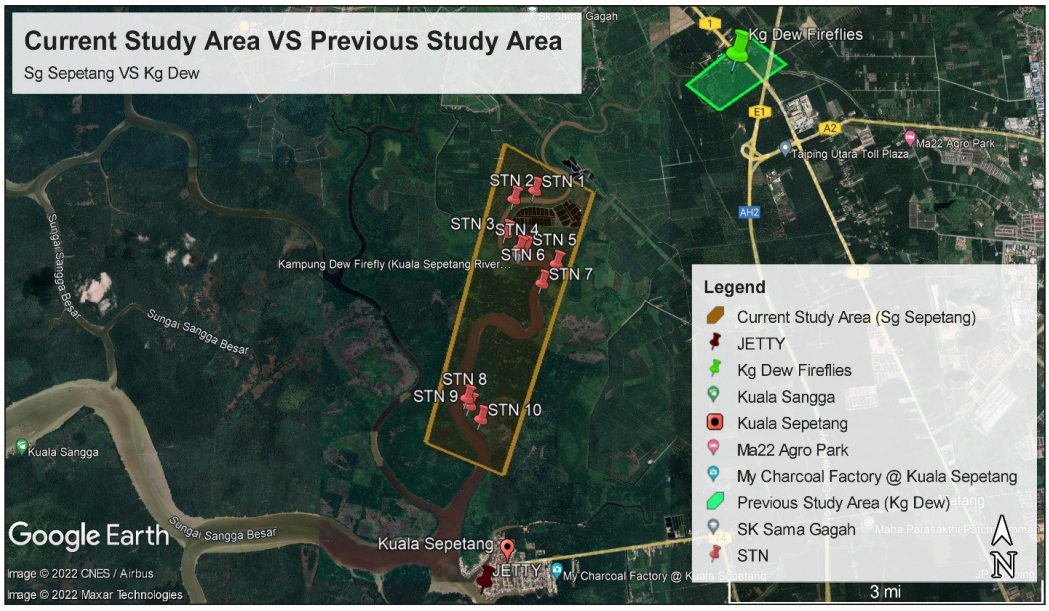

Figure 1. The current study area is in Kuala Sepetang, Perak, and the previous study area was in Kampung Dew, Perak
Note. Map was generated using Geographical Information System (GIS) software

2010b), Sungai Garama (Mahadimenakbar et al., 2007), Kg. Kuantan (Ballantyne & Menayah, 2000), Paitan River (Chey, 2006), Bernam River (Shahara et al., 2017), and Cherating River (Mohd et al., 2019). However, due to this human interference, the fireflies lost their natural habitat in mangrove forests, resulting in extinction in some places (Ballantyne et al., 2011). Hence, preserving and conserving firefly habitats is crucial (Foo & Mahadimenakbar, 2015). Furthermore, other human activities, such as speedboats operation, generate waves that erode the riverbanks, disrupting the habitat of adult fireflies by destroying the trees on which they rely. Thus, the population of fireflies is endangered (Lewis, 2016).

Therefore, this study collates records of adult *Pteroptyx tener* Olivier fireflies reported in the Malaysian peninsular, including Sabah and Sarawak. The records used in this study are from a compilation of field surveys conducted by authors (i.e., in Kuala Sepetang, Perak, situated in Peninsular Malaysia) and from published journal articles to construct lists of the distribution of this species. Moreover, the purpose of this study is to comprehend *Pteroptys tener*'s distribution in Malaysia. The authors discovered that it is crucial to record every location where fireflies are present to conserve them in the future. It would be challenging for the Forestry Department and other related organizations to precisely determine the number of firefly populations, the distribution, and the diversity of firefly species, particularly species that have never been discovered, if many places are undocumented. Thus, this

study attempts to bridge the knowledge gap while adding information about the undocumented area where fireflies were found.

METHODS

Study Site

This study was conducted along the Sepetang River in Kuala Sepetang, Perak. Kuala Sepetang is surrounded by mangrove swamps and is a focus for fireflies-watching activities at night; and one of the Congregating Firefly Zones (CFZs) in Malaysia, aiming to protect the river's firefly colonies, especially *Pteroptyx tener* Olivier. The main vegetation species that dominate the area are mangroves, such as *Sonneratia caseolaris*, *Rhizophora mucronata*, and *Rhizophora apiculata*. Malaysia's mangrove forests are the sixth largest in the world. In Malaysia, mangrove forests are categorized as permanent forest reserves (PFR), which include protected forest reserves, domestic forest reserves, mangrove forest reserves (MFR), virgin forest reserves (VJR), and wildlife reserves (Tangah et al., 2022). In Kuala Sepetang, the largest mangrove forest reserve in Malaysia, with an area of about 40,000 ha, is Matang Mangrove Forest Reserve (MMFR) (Romañach et al., 2018). Figure 3 shows the distribution of mangroves in Matang, Perak, Malaysia, including Kuala Sepetang, Kuala Trong, and Kerang River.

During the initial sampling, a display tree with a large congregation of fireflies and well-synchronized *Pteroptyx tener* Olivier fireflies was used to identify ten sampling locations, as shown in Figure 2. Those ten sampling points from the upstream river to the downstream river with each sampling

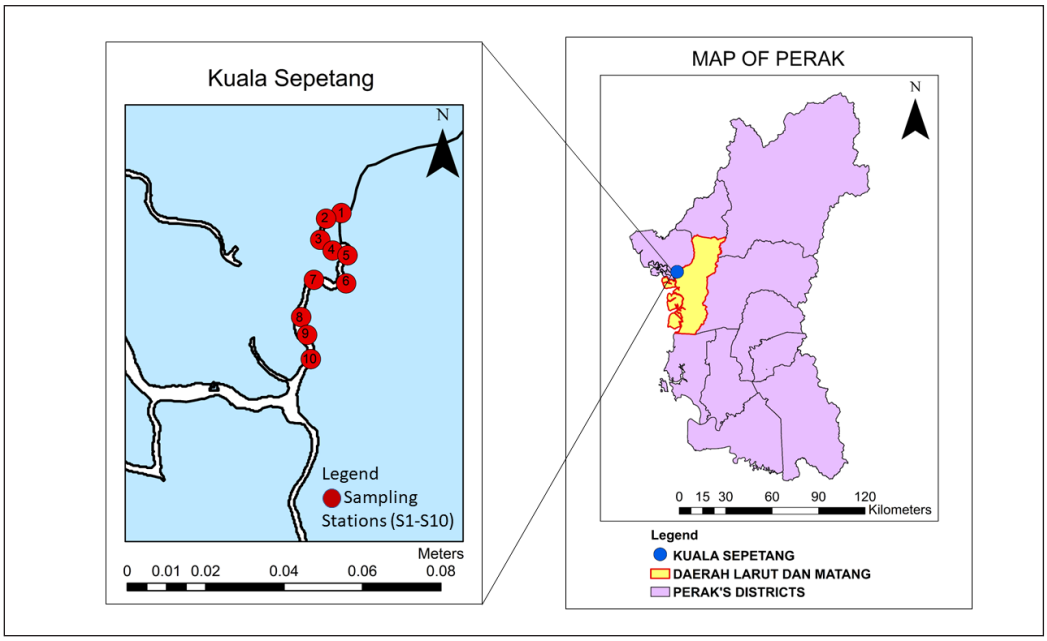

Figure 2. Sampling points located at Kuala Sepetang, Perak

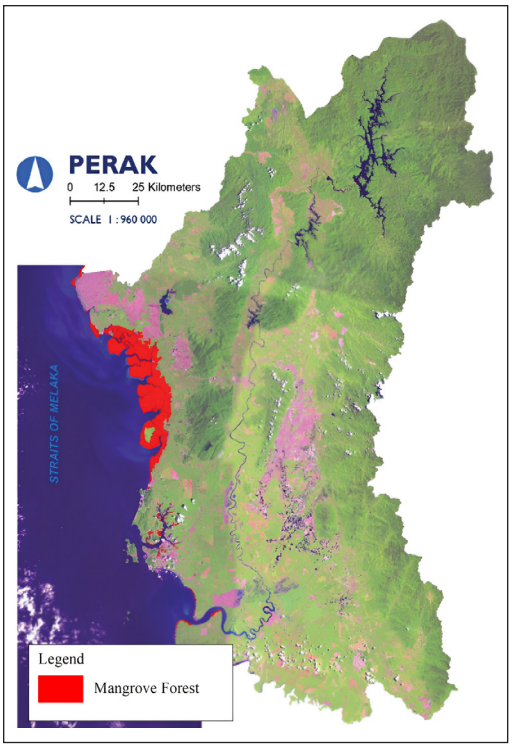

Figure 3. Distribution of mangroves in Perak (Omar et al., 2020)

point were recorded at night using a Global Positioning System (GPS) receiver (version 4.7.3) (Handheld Altimeter GPS+ via iPhone X, USA). Then, the data were analyzed using the Geographic Information System (GIS) application technique using ArcGis software (version 10.3). The coordinates for each sampling point in this study range from Station 1 to Station 10, as shown in Table 1. There had been no scientific documentation of *Pteroptyx tener* in this sampling point location before this study.

It is very relevant for this study to be conducted because the sampling point area in this study is a developing area. While conducting this study, it was found that human activities, such as ecotourism and aquaculture (shrimp and fishponds), are increasingly carried out. It is feared that many nearby human activities would damage the mangrove firefly habitat. The fireflies' existence will be at risk if the mangroves are disrupted (please refer to the Results and Discussion section for more information). There is no documentation for fireflies in this area. Although tourism activities have been very active almost every day, especially on weekends, many boats bring local and foreign tourists to the area. The lack of documentation on the firefly population makes it challenging to know further about these fireflies from time to time. The documentation in this study is crucial to preserve and understanding the fireflies' status.

Sampling and Identification Process

The samplings were conducted for six consecutive months, from November 2021 until April 2022, from 5.30 p.m. to 9:00 p.m. Firstly, collecting vegetation samples

Table 1
Sampling points (Station 1 - Station 10) coordinates

Sampling point	Coordinate
Station 1	4° 53' 17.02" N, 100° 38' 03.73" E
Station 2	4° 53' 13.09" N, 100° 37' 53.02" E
Station 3	4° 52' 55.72" N, 100° 37' 48.92" E
Station 4	4° 52' 47.90" N, 100° 37' 55.77" E
Station 5	4° 52' 47.70" N, 100° 37' 58.92" E
Station 6	4° 52' 40.18" N, 100° 38' 14.73" E
Station 7	4° 52' 30.50" N, 100° 38' 07.31" E
Station 8	4° 51' 33.69" N, 100° 37' 29.31" E
Station 9	4° 51' 30.22" N, 100° 37' 30.60" E
Station 10	4° 51' 31.40" N, 100° 37' 37.75" E

(display trees) were collected by taking the leaves, flowers, fruits, tree trunks, and roots. Further identification of the vegetation from the field survey done at the Laboratory of the School of Biological Sciences, Universiti Sains Malaysia (USM), where the description follows a book by Lee et al. (2015), which is entitled "Mangrove Guidebook for Malaysia".

Next, the adult firefly samples were collected using the sweep method (using a sweep net). The sampling was replicated twice at each station, and the net was swept for two minutes. Then the samples were stored in bottles containing 95% ethanol and labeled according to their respective collection dates and sampling station. Finally, all the samples were taken to the Entomology Laboratory of the School of Biological Sciences, Universiti Sains Malaysia (USM), for further identification. The identification of firefly species concerning the taxonomic description was published by Ballantyne and Lambkin (2013), and the sex of fireflies followed the taxonomic description established by Jusoh et al. (2018).

RESULTS AND DISCUSSION

The Locality of *Pteroptyx tener* Olivier was Recorded

Table 2 to Table 7 list the *Pteroptyx tener* Olivier Firefly specimens examined in six states in Peninsular Malaysia, including Selangor, Johor, Negeri Sembilan, Pahang, Perak, and Terengganu. Tables 8 and 9 list the *Pteroptyx tener* Olivier Firefly samples found in East Malaysia (Sarawak and Sabah). In addition, two digital information maps, such as in Figure 4, which show the map of the occurrence of *Pteroptyx tener* Olivier in Peninsular Malaysia, were developed using GIS software. Figure 5, meanwhile, depicts the occurrence map of *Pteroptyx tener* Olivier in East Malaysia (Sabah and Sarawak). *Pteroptyx tener* Olivier only occurs in six Peninsular Malaysia states: Terengganu, Perak, Pahang, Negeri Sembilan, Selangor, and Johor, including East Malaysia (Sabah and Sarawak). As stated by Wong and Yeap (2012), the distribution of this assemblage of firefly habitats in riverine mangroves is still primarily undocumented and unrecorded. Therefore, there is a possibility that no samples were taken or no previously published information about the distribution of this species in other states in Malaysia (Perlis, Kedah, Penang, Kelantan, Kuala Lumpur, Putrajaya, and Melaka). Another piece of evidence is the absence of records indicating the presence of fireflies in Penang, despite the presence of unknown species of fireflies in the Nibong Tebal region of the state. Therefore, future research should concentrate on documenting more firefly locations in Malaysia, particularly this species, which has the potential to boost the local economy.

Pteroptyx tener Olivier's Dependence on Their Habitat

Pteroptyx tener Olivier fireflies are frequently seen in Malaysia along the mangrove estuary's banks, and they are similar at the sampling points (S1–S10) in Kuala

Table 2
The samples were found in Peninsular Malaysia, Selangor

Coordinate	Location	Data acquisition			Habitat	Study period	Sources of information
		♂	♀	Other specimens			
Data not available	Kampung Kuantan	88	92	245 newly hatched larvae	Data not available	March 2000 to June 2000	Ballantyne and Menayah (2000)
3° 14' 24.00" N, 101° 07' 12.01" E	Kuala Selangor	Data not available	Data not available	Data not available	Data not available	25 April 1975, found by J. E. Lloyd	Jusoh et al. (2013)
Data not available	Selangor River, Kampung Kuantan	40	40	Data not available	Data not available	January to May 2014	Salleh et al. (2019)
Data not available	Selangor River	Data not available	Data not available	Data not available	*Sonneratia caseolaris* Engl.	May 2006 to April 2009	Khoo et al. (2012)

Table 3
The samples were found in Peninsular Malaysia, Johor

Coordinate	Location	Data acquisition			Habitat	Study period	Sources of information
		♂	♀	Other specimens			
Data not available	Benut	Data not available	Data not available	Data not available	Data not available	October 1965, found by J. M. Bassot	Jusoh et al. (2013)
01° 22' 48.00" N, 103° 09' 00.00" E	Benut	Data not available	Data not available	Data not available	Data not available	June 1967, found by I. Polunin	Jusoh et al. (2013)
1° 44' 36.10" N, 103° 54' 54.71" E; 1° 41' 31.25" N, 103° 55' 44.26" E	Johor River, Kota Tinggi	1,104	612	Data not available	*Sonneratia caseolaris* Engl.	December 2007 until January 2008	Sulaiman et al. (2016)
1° 25' 12.00" N, 103° 21' 00.00" E	Kota Tinggi, Kupia Labong, Endau River	Data not available	Data not available	Data not available	Data not available	12 December 1970, found by I. Polunin	Jusoh et al. (2013)
1° 31' 12.00" N, 103° 34' 12.00" E	Mawai	Data not available	Data not available	Data Not Available	Data not available	19 December 1970, found by I. Polunin	Jusoh et al. (2013)

Table 4
The samples were found in Peninsular Malaysia, Negeri Sembilan

Coordinate	Location	Data acquisition			Habitat	Study period	Sources of information
		♂	♀	Other specimens			
Data not available	Linggi River	Data not available	Data not available	Two adults (*Pteroptyx* sp.). No specific species was mentioned	*Sonneratia caseolaris*	November 2008 until April 2009	Jusoh et al. (2010a)
2° 25' 08.76" N, 102° 03' 55.44" E; 2° 26' 54.24" N, 102° 03' 55.44" E	Rembau River	835	313	Data not available	*Sonneratia caseolaris* Engl., and *Nypa fruticans*	November 2017 to October 2018	Asri et al. (2021)
Data not available	Rembau River	Data not available	Data not available	658,104 adults	*Sonneratia caseolaris, Rhizophora apiculata*, *Hibiscus tiliaceus*, and *Ficus* sp.	November 2008 to April 2009	Jusoh et al. (2010a)
2° 25' 08.76" - 2° 26' 54.24" N, 102° 03' 55.44" E	Rembau River	Data not available	Data not available	525 adults	Found next to the jetty, human settlement area, horticulture activity, jetty, mangrove, aquaculture activity, and oil palm plantation (specific tree species were not mentioned by the author). Data not available	January 2018 to November 2018	Abdullah et al. (2021)
Data not available	Ramuan China Besar River	Data not available	Data not available	103 adults	*Sonneratia caseolaris* and *Rhizophora apiculata*	November 2008 until April 2009	Jusoh et al. (2010a)
Data not available	Ramuan China Kechil River	Data not available	Data not available	182 adults	*Sonneratia caseolaris* and *Rhizophora apiculata*	November 2008 until April 2009	Jusoh et al. (2010a)

Table 5
The samples were found in Peninsular Malaysia, Pahang

Coordinate	Location	Data acquisition			Habitat	Study period	Sources of information
		♂	♀	Other specimens			
Data not available	Cherating River	Data not available	Data not available	243 adults	Data not available	March 2019	Faudzi et al. (2021)

Table 6
The samples were found in Peninsular Malaysia, Perak

Coordinate	Location	Data acquisition			Habitat	Study period	Sources of information
		♂	♀	Other specimens			
Data not available	Sepetang River, Kampung Dew	Data not available	Data not available	3,044 adults	*Sonneratia caseolaris* Engl.	March 2014 to June 2014	Hazmi and Sagaff (2017)
4° 50' 27.3012" N, 100° 38' 04.92" E	Sepetang estuary	Data not available	Data not available	Data not available	*Sonneratia caseolaris*, *Nypa fruticans,* and *Rhizophora apiculata*	December 2006 until February 2007	Jusoh et al. (2010b)
4° 52' 13.26" N, 100° 38' 01.20" E	Sepetang estuary	Data not available	Data not available	14 adults	Data not available	Found by W. F. A. Jusoh (Forest Research Institute Malaysia – B. Nada, C.-K. Phon)	Jusoh et al. (2018)
4° 53' 17.02" N, 100° 38' 03.73" E; 4° 51' 31.40" N, 100° 37' 37.75" E	Sepetang River	Data not available	Data not available	111,622 adults	*Sonneratia caseolaris, Rhizophora* mucronata, and *Rhizophora apiculata*	November 2021 to April 2022, found by N. A. Seri, A. A. Rahman, N. F. A. Kassi, and N. F. A. Fuzi	Field survey

Table 7
The samples were found in Peninsular Malaysia, Terengganu

Coordinate	Location	Data acquisition			Habitat	Study period	Sources of information
		♂	♀	Other specimens			
Data not available	Chukai River, Kemaman	Data not available	Data not available	503 adults	*Sonneratia caseolaris*, *Hibiscus tilliaceus* L. Engl., *Nypa fruticans* Wurmb., *Barringtonia* sp., and *Guilandina bonduc* L.	November 2017 to April 2018	Mahmod et al. (2018)
5° 33' 00" N, 102° 44' 08" E	Kampung Mangkuk, Setiu	5	1	Data not available	*Avicennia alba* and *Sonneratia alba*	July 2005 until January 2006	Azmi et al. (2015)
Data not available	Kerteh River	Data not available	Data not available	Data not available	*Gluta velutina* Blume, *Hibiscus tiliaceus* L., *Xylocarpus granatum* J. König, *Avicennia alba* Blume, *Rhizophora apiculata* Blume, *Excoecaria agallocha* L., *Barringtonia racemosa* (L.) Spreng., *Ficus microcarpa* L.f., *Bruguiera gymnorrhiza* (L.) Lam., and *Nypa fruticans* Wurmb	18 to 20 July 2009	Jusoh et al. (2011)

Table 8
The samples were found in East Malaysia, Sarawak

Coordinate	Location	Data acquisition			Habitat	Study period	Sources of information
		♂	♀	Other specimens			
2° 55' 44.82" N, 112° 32' 41.28" E	Balingian River	Data not available	Data not available	Data not available	Data not available	Found by M. Musbah	Jusoh et al. (2018)
1° 19' 12.00" N, 110° 12' 00.00" E	Kuching	Data not available	Data not available	Data not available	Data not available	26 September 1965, found by J. Buck	Jusoh et al. (2013)
4° 29' 24.00" N, 115° 06' 00.00" E	Limbang	Data not available	Data not available	Data not available	Data not available	4 October 1970, found by I. Polunin	Jusoh et al. (2013)
2° 53' 48.59" N, 112° 07' 54.30" E	Mukah River	Data not available	Data not available	Data not available	Data not available	Found by T. Musa	Jusoh et al. (2018)
Data not available	Miri River	23	11	Data not available	Data not available	Found by M. Musbah	Jusoh et al. (2018)
Data not available	Kuching	Data not available	Data not available	Data not available	Data not available	5 February 1909, found by J. E. A. Lewis	Jusoh et al. (2013)
2° 15' 36.00" N, 111° 09' 36.00" E	Paya Paloh	Data not available	Data not available	Data not available	Data not available	27 September 1965, found by J. Buck	Jusoh et al. (2013)
Data not available	Pending	Data not available	Data not available	Data not available	Data not available	26 September 1965, found by J. Buck	Jusoh et al. (2013)
1° 26' 24.00" N, 111° 12' 00.00" E	Saratok	Data not available	Data not available	Data not available	Data not available	23 September 1970, found by I. Polunin	Jusoh et al. (2013)
3° 31' 08.40" N, 113° 19' 43.20" E	Similajau River	Data not available	Data not available	Data not available	Data not available	Data not available	Jusoh et al. (2018)

Table 9
The samples were found in East Malaysia, Sabah

Coordinate	Location	Data acquisition			Habitat	Study period	Sources of information
		♂	♀	Other specimens			
5° 24' 00.00" N, 118° 15' 00.00" E	Abai	Data not available	Data not available	Data not available	Data not available	21 October 1970, found by I. Polunin	Jusoh et al. (2013)
5º 31' 27" N 115º42' 03.2" E	Binsulok River	Data not available	Data not available	5 adults	Data not available	9 September 2017	Mahadimenakbar et al. (2018)
5° 10' 00.00" N, 115° 19' 60.00" E; 5° 30' 00.00" N, 115° 40' 00.00" E	Garama River	261	158	316 adults	*Rhizophora apiculata*, *Excoecaria indica*, and *Nypa fruticans*	April 2004 to June	Mahadimenakbar et al. (2007)
(5° 24' 37.32" N, 115° 31' 54.54" E	Garama River	308	263	Data not available	*Excoecaria agallocha* L., *Rhizophora apiculata*, and *Sonneratia alba*	January 2015 to August 2015	Foo and Mahadimenakbar (2017)
Data not available	Garama River	Data not available	Data not available	Data not available	*Ficus microcarpa*, *Clerodendrum inerme*	September 2009	Chey (2010)
Data not available	Klias River	Data not available	Data not available	Data not available	*Glochidion littorale*, *Rhizophora apiculata*	September 2009	Chey (2010)
Data not available	Klias River	Data not available	Data not available	Data not available	*Sonneratia caseolaris*, *Heritiera littoralis* Dryand. ex Aiton), *Rhizophora apiculata* Bl., *Excoecaria indica* (Willd.) Muell. Arg.	April 2004	Chey (2004)
Data not available	Kudat, Kanibongan	Data not available	Data not available	Data not available	Data not available	24 September 1965, found by K. H. Kong	Jusoh et al. (2013)
Data not available	Kulamba XPDC (expedition) Sungai Terusan	2	23 unassigned females		Presumed to be a species of *Sonneratia* locally known as 'Pedada')	In 2006 found by Nordin and Zaidi	Jusoh et al. (2018)

Table 9 *(continue)*

Coordinate	Location	Data acquisition			Habitat	Study period	Sources of information
		♂	♀	Other specimens			
Data not available	Sandakan Bay, Sapagaya Lumber Camp	Data not available	Data not available	Data not available	Data not available	7 November 1957, J. L. found by Gressit	Jusoh et al. (2013)
05° 39' 43.56" N 118° 24' 07.56" E	Kinabatangan River	Data not available	Data not available	Data not available	*Sonneratia caseolaris*, *Excoecaria indica*	2002	Mahadimenakbar et al. (2002)
5° 04' 12.00" N, 115° 19' 48.00" E	Sipitang River	Data not available	Data not available	Data not available	Data not available	22 October 1970, found by I. Polunin	Jusoh et al. (2013)
Data not available	Tawau Residency	Data not available	Data not available	Data not available	Data not available	19 November 1958, found by L. W. Quate	Jusoh et al. (2013)
5° 19' 38.9" N; 115° 31' 06.7" E	Teratak River	656	104	Data not available	*Excoecaria agallocha* L., *Rhizophora apiculata*, and *Sonneratia alba*	January 2015 to August 2015	Foo and Mahadimenakbar (2017)
5° 11' 37.82" N, 115° 34' 38.54" E	Weston River	Data not available	Data not available	Data not available	*Excoecaria agallocha* L., *Rhizophora apiculata*, and *Sonneratia alba*	January 2015 to August 2015	Foo and Mahadimenakbar (2017)
05° 19' 38.9" N, 115° 31' 06.7" E	Teratak River	Data not available	Data not available	2 adults	*Avicennia alba* (Avicenniaceae)	March 2014 to April 2014	Foo and Mahadimenakbar (2015)

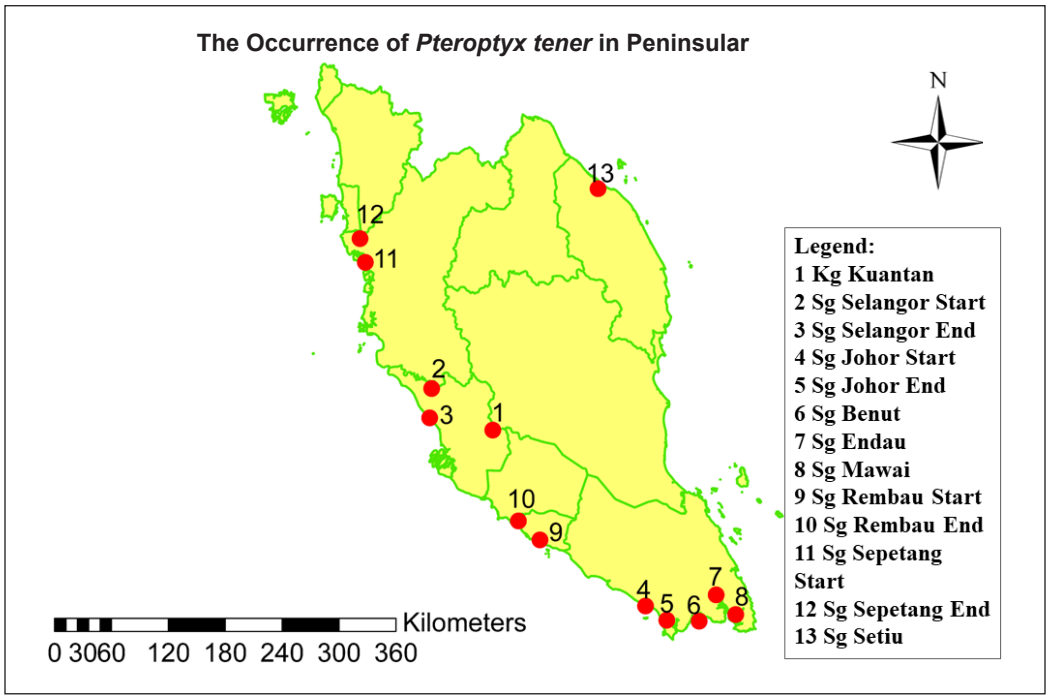

Figure 4. The occurrence of *Pteroptyx tener* Olivier in Peninsular Malaysia

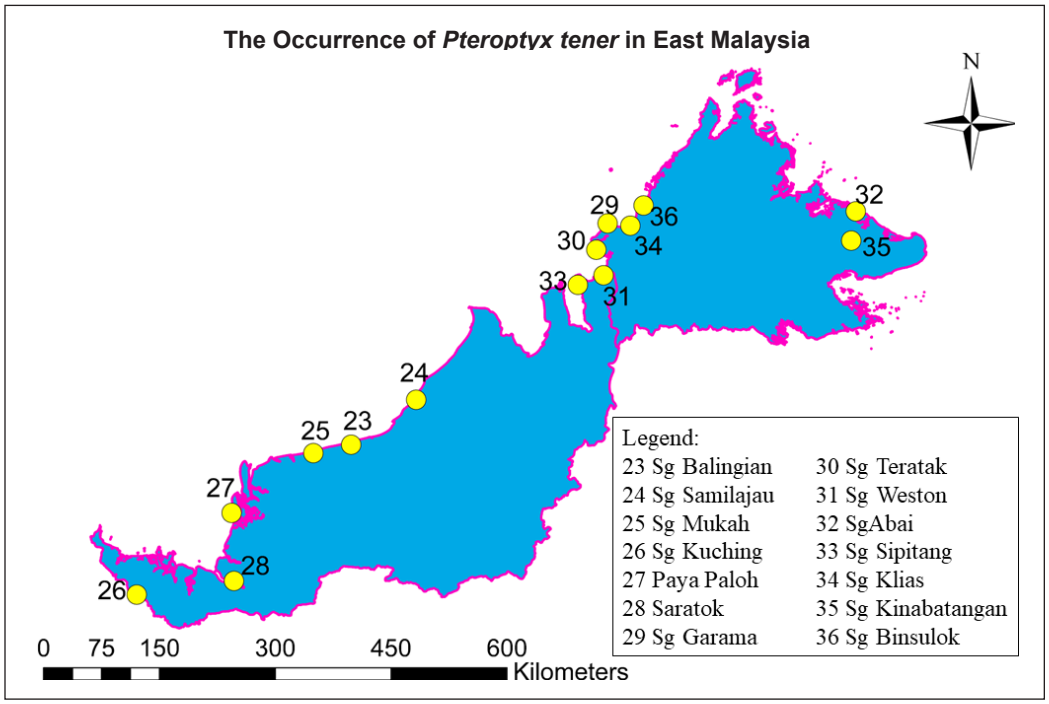

Figure 5. The occurrence of *Pteroptyx tener* Olivier in East Malaysia (Sabah and Sarawak)

Sepetang, Perak. There are no other firefly species found in the area. This study found that mangrove trees, including *Sonneratia caseolaris* Engl., *Rhizophora mucronata*, and *Rhizophora apiculata*, are found along the entire river of the sampling locations. *Pteroptyx tener* uses these trees as display trees, covering them with varying densities of small, medium, and big firefly colonies on a single tree. Other than these three mangrove trees, *Hibiscus tiliaceus*, *Sapium indicum*, *Metroxylon sagu*, *Gigantochloa ligulata*, *Ficus microcarpa*, *Ficus retusa*, *Urena lobata*, *Tetracera indica*, *Avicennia* sp., *Durio* sp., and *Garcinia* sp. trees are among the mangrove trees species that has firefly species inhabiting there or nearby (Ohba & Wong, 2004).

The observations of this study also revealed that *Pteroptyx tener* favors young and low mangrove trees (*Sonneratia caseolaris* Engl.) over older trees, possibly because of the smaller, waxier leaves of this tree. More research is required to determine whether this species' adult fireflies will likely be displayed on old *Sonneratia caseolaris* Engl. The authors' observations confirm those of A. Nallakumar (2002), who discovered that some Kuala Selangor, Malaysia's *Pteroptyx* fireflies, only use young *Sonneratia caseolaris* trees as their display trees. Jusoh et al. (2010b) found that *Sonneratia caseolaris* and *Nypa fruticans* trees are the most preferred display trees. This preference may be owing to the availability of sugar in the sap of *Sonneratia caseolaris*, a food source for fireflies (A. Nallakumar, 2002; Ohba & Sim, 1994).

According to Jusoh et al. (2010b), five more criteria in tree selection by fireflies are being examined. The first is that trees must be located near the water's edge to allow firefly communication. The second criterion is that the leaf arrangement of each tree on display must be conducive to mating. Thirdly, the display tree must contain nectar or sap if the adult fireflies consume food. Next, the display tree must be close to the food plant for the larval prey. Then, the tree must be in good health. The tree's health is important because healthy mangrove trees have a higher leaf density, which increases the amount of surface area for insects to perch on and gives more protection from direct sunlight during the day (Foo & Mahadimenakbar, 2015).

In addition, the association between firefly abundance and vegetation assemblages may be related to the fact that fireflies do not mate while flying; instead, they use trees as mating locations (Buck & Buck, 1966). Adult female fireflies fly to the muddy bank behind the tree and lay their eggs near the intertidal zone of rivers (Barrows et al., 2008; Lewis et al., 2020).

The life cycle and habitat of Lampyridae (fireflies) are incredibly complex. It is because, throughout their life cycle, the surroundings and environmental circumstances play a crucial role (Salvador-Caabay, 2022). For instance, adult fireflies mainly inhabit the canopies of mangroves and other trees and will only lay their eggs in wetlands farther from their mating sites. The eggs are put on the ground or moss. When the larvae hatch, they become mobile

on the ground and feed on their prey. The pupa may remain on the ground or logs or other plants for protection until the adult firefly emerges (Salvador-Caabay, 2022). Eggs of fireflies require moist soil and shady areas, such as *Rhizophora* spp., so they are not easily harmed by heat and dryness (Jusoh et al., 2010b). In Sungai Selangor, for example, firefly larvae were found in greater abundance at the base of sago trees near the riverbank. On the other hand, areas with a high density of human activity are less suitable for larvae and snail prey. It could be owing to the soil's condition in the location, which has low humidity, high temperatures, and the prevalence of light invasion (Kirton et al., 2006).

Moreover, riverside palm trees like *Nypa fruticans* and *Metroxylon sago* provide an essential food source for snail prey that firefly larvae consume (Nada & Kirton, 2004). As a result, fireflies will make these trees their display tree. Another preferred assumption that fireflies consider when selecting a display tree as a favorable display tree is that fireflies feed exudates (sugary substances secreted by *Sonneratia caseolaris*) from leaf stipules (K. Nallakumar, 2003). This relationship between mangrove assemblage and firefly abundance (Jusoh et al., 2010) demonstrates how crucial it is to protect firefly species, as their display trees and habitat are threatened (Jusoh & Hashim, 2012). Consequently, any mangrove alterations will lead to a declining firefly population (Nallakumar, 2002; Yuma, 2007), and the loss of mangrove forests has resulted in their extinction in some localities (Ballantyne et al., 2011). Therefore, it is crucial to take fireflies and their habitat in mangrove forests seriously as a research topic to protect these fireflies from extinction.

CONCLUSION

This study adds an undocumented location for *Pteroptyx tener* Olivier's and could contribute to the knowledge of the distribution and occurrence of fireflies in Malaysia. On the other hand, this study collected a record of the distribution and occurrence of *Pteroptyx tener* Olivier, which was then mapped using GIS software, which researchers rarely utilize to present their data visually to make it more comprehensible. However, because the records from previous researchers are limited, the mapping results indicate that there are still some locations of *Pteroptyx tener* Olivier that have been discovered that cannot be mapped; because the researcher did not record the coordinates where the species was discovered. Therefore, many locations of fireflies were found unavailable. From this study also, the literature review found that the most preferred tree for this species was *Sonneratia caseolaris* Engl. A few identified associated trees: *Rhizophora mucronata*, *Rhizophora apiculata*, *Hibiscus tilliaceus* L. Engl., and *Nypa fruticans*. In addition, the authors recommend protecting the mangrove forests along Kuala Sepetang to ensure the firefly's long-term survival. Fireflies are a keystone species in mangrove forests because maintaining the mangrove habitat will benefit both fireflies and humans.

ACKNOWLEDGEMENTS

The Ministry of Higher Education Malaysia finances this research under the Fundamental Research Grant Scheme with project code: FRGS/1/2020/SS0/USM/02/6.

REFERENCES

Abdullah, N. A., Asri, L. N., Husin, S. M., Shukor, A. M., Darbis, N. D. A., Ismail, K., & Hazmi, I. R. (2021). Influence of physico-chemical characteristics of Rembau River, peninsular Malaysia, on congregating *Pteroptyx* fireflies. *Environmental Monitoring and Assessment*, *193*, 634. https://doi.org/10.1007/s10661-021-09426-y

Asri, L. N., Abdullah, N. A., Sulaiman, A., Asri, M. H. M., Sulaiman, N., Satiman, E. M. F. E. N., Husin, S. M., Shukor, A. M., & Darbis, N. D. A. (2021). Abundance and species composition of synchronous flashing firefly at Sungai Rembau, Negeri Sembilan, Malaysia. *International Journal of Tropical Insect Science*, *41*, 1095-1106. https://doi.org/10.1007/s42690-020-00295-5

Azmi, W. A., Zainudin, A., & Salam, M. R. (2015). Notes on *Pteroptyx tener* (Coleoptera: Lampyridae) in Mangrove Forest of Setiu, Terengganu. In F. Mohamad, J. M. Salim, J. M. J., & R. Shahrudin (Eds.), *Setiu Wetlands: Species, ecosystems and livelihoods* (pp. 67-72). Penerbit Universiti Malaysia Terengganu.

Ballantyne, L. A. (2001). The bent winged fireflies of Cambodia, Indonesia, Malaysia, Philippines and Thailand (Coleoptera: Lampyridae: Luciolinae: Luciolini). *Serangga*, *6*(1), 51-95.

Ballantyne, L. A., & Lambkin, C. (2001). A new firefly, *Luciola* (Pygoluciola) *kinabalua*, new species (Coleoptera: Lampyridae), from Malaysia, with observations on a possible copulation clamp. *The Raffles Bulletin of Zoology*, *49*(2), 363-378.

Ballantyne, L. A., & Lambkin, C. L. (2013). Systematics and phylogenetics of Indo-Pacific Luciolinae fireflies (Coleoptera: Lampyridae) and the description of new genera. *Zootaxa*, *3653*(1), 1-162. https://doi.org/10.11646/zootaxa.3653.1.1

Ballantyne, L. A., & McLean, M. R. (1970). Revisional studies on the firefly genus *Pteroptyx* Olivier (Coleoptera: Lampyridae: Luciolinae: Luciolini). *Transactions of the American Entomological Society (1890-)*, *96*(2), 223–305.

Ballantyne, L. A., & Menayah, R. (2000). Redescription of the synchronous firefly, *Pteroptyx tener* Olivier (Coleoptera: Lampyridae), of Kampung Kuantan, Selangor. *Malayan Nature Journal*, *54*(4), 323-328.

Ballantyne, L., Xin, H. F., Shih, C. H., Cheng, C. Y., & Yiu, V. (2011). *Pteroptyx maipo* Ballantyne, a new species of bent-winged firefly (Coleoptera: Lampyridae) from Hong Kong, and its relevance to firefly biology and conservation. *Zootaxa*, *2931*(1), 8-34. https://doi.org/10.11646/zootaxa.2931.1.2

Barrows, E. M., Arsenault, S. B., & Grenier, N. P. (2008). Firefly (Coleoptera: Lampyridae) flight periods, sex ratios, and habitat frequencies in a United States Mid-Atlantic freshwater tidal marsh, low forest, and their ecotone. *Banisteria*, *31*, 47-52.

Buck, J., & Buck, E. (1966). Biology of synchronous flashing of fireflies. *Nature*, *211*, 562-564. https://doi.org/10.1038/211562a0

Chey, V. K. (2004). Fireflies of Sungai Klias and their display trees. *Sepilok Bulletin*, *1*, 67–69.

Chey, V. K. (2006). Fireflies of Sungai Paitan. *Sepilok Bulletin*, *5*(1), 1-6.

Chey, V. K. (2010). Fireflies of Beaufort with special reference to Sungai Garama and Sungai Klias. *Sepilok Bulletin*, *12*(1), 13–19.

Dunn, R. R. (2005). Modern insect extinctions, the neglected majority. *Conservation Biology*, *19*(4), 1030-1036. https://doi.org/10.1111/j.1523-1739.2005.00078.x

Faudzi, R., Abas, A., Othman, N. W., & Mazlan, S. M. (2021). Effect of water quality on the abundance of firefly populations at Cherating River, Pahang, Malaysia. *Environment Asia*, *14*(1), 69-79. https://doi.org/10.14456/ea.2021.8

Foo, K., & Mahadimenakbar, M. D. (2015). Diversity of fireflies (Coleoptera: Lampyridae) of Sungai Teratak, Sabah, Malaysia. *Journal of Tropical Biology and Conservation*, *12*, 1-11.

Foo, K., & Mahadimenakbar, M. D. (2017). Diversity of *Pteroptyx* fireflies (Coleoptera: Lampyridae) and their display trees at Klias Peninsula, Sabah, Malaysia. *Journal of Tropical Biology and Conservation*, *14*, 95–103.

González-Oreja, J. A. (2008). The encyclopedia of life vs. the brochure of life: Exploring the relationships between the extinction of species and the inventory of life on Earth. *Zootaxa*, *1965*(1), 61-68. https://doi.org/10.11646/zootaxa.1965.1.3

Hazmi, I. R., & Sagaff, S. A. S. (2017). Fireflies population and the aquaculture industry (Coleoptera: Lampyridae) of the Sungai Sepetang, Kampung Dew, Perak, Malaysia. *Serangga*, *22*(2), 217-237.

Jusoh, W. F. A. W., & Hashim, N. R. (2012). The effect of habitat modification on firefly populations at the Rembau-Linggi estuary, Peninsular Malaysia. *Lampyrid*, *2*, 149-155.

Jusoh, W. F. A. W., Hashim, N. R., & Ibrahim, Z. Z. (2010a). Distribution and abundance of *Pteroptyx* fireflies in Rembau-Linggi estuary, Peninsular Malaysia. *EnvironmentAsia*, *3*(special issue), 56-60. https://doi.org/10.14456/EA.2010.40

Jusoh, W. F. A. W., Hashim, N. R., & Ibrahim, Z. Z. (2010b). Firefly distribution and abundance on mangrove vegetation assemblages in Sepetang estuary, Peninsular Malaysia. *Wetlands Ecology and Management*, *18*, 367-373. https://doi/org/10.1007/s11273-009-9172-4

Jusoh, W. F. A. W., Wong, C. H., & Hashim, N. R. (2011). Zonation of firefly species and their display trees along Kerteh River, Terengganu. *Serangga*, *16*(2), 57-64.

Jusoh, W. F. A., Ballantyne, L., & Chan, K. O. (2020). DNA-based species delimitation reveals cryptic and incipient species in synchronous flashing fireflies (Coleoptera: Lampyridae) of Southeast Asia. *Biological Journal of the Linnean Society*, *130*(3), 520-532. https://doi.org/10.1093/biolinnean/blaa072

Jusoh, W. F. A., Ballantyne, L., Lambkin, C. L., Hashim, N. R., & Wahlberg, N. (2018). The firefly genus *Pteroptyx* Olivier revisited (Coleoptera: Lampyridae: Luciolinae). *Zootaxa*, *4456*(1), 1-71. https://doi.org/10.11646/zootaxa.4456.1.1

Jusoh, W. F. A., Hashim, N. R., & Adam, N. A. (2013). Distribution of the synchronous flashing beetle *Pteroptyx tener* Olivier (Coleoptera: Lampyridae) in Malaysia. *The Coleopterists Bulletin*, *67*(4), 604-605. https://doi.org/10.1649/0010-065X-67.4.604

Khoo, V., Nada, B., Kirton, L. G., & Phon, C. K. (2012). Monitoring the population of the firefly *Pteroptyx tener* along the Selangor River, Malaysia for conservation and sustainable ecotourism. *Lampyrid*, *2*, 162-173.

Kirton, L. G., Nada, B., Tan, S. A., Ang, L. H., Tang, L. K., Hui, T. F., & Ho, W. M. (2006). *The Kampung Kuantan firefly project: A preliminary assessment of the habitat requirements of* Pteroptyx tener *(Coleoptera: Lampyridae)*. https://www.researchgate.net/publication/237235622_The_Kampung_Kuantan_Firefly_Project_A_Preliminary_Assessment_of_the_Habitat_Requirements_of_Pteroptyx_tener_Coleoptera_Lampyridae

Lee, S. S., Muhamad, A., & Tong, J. (Eds.) (2015). *Mangrove guidebook for Malaysia*. Wetlands International Malaysia.

Lemelin, R. H., Boileau, E. Y., & Russell, C. (2019). Entomotourism: The allure of the arthropod. *Society and Animals*, *27*(7), 733-750.

Lewis, S. (2016). *Silent sparks: The wondrous world of fireflies*. Princeton University Press. https://doi.org/10.1515/9781400880317

Lewis, S. M., Wong, C. H., Owens, A., Fallon, C., Jepsen, S., Thancharoen, A., Wu, C., De Cock, R., Novák, M., López-Palafox, T., & Khoo, V., Reed, J. M. (2020). A global perspective on firefly extinction threats. *BioScience*, *70*(2), 157-167. https://doi.org/10.1093/biosci/biz157

Mahadimenakbar, M. D., Fiffy, H. S., & Godoong, E. (2009). *Studies on the potential of fireflies watching tourism for firefly (Coleoptera: Lampyridae;* Pteroptyx *spp.) conservation*. https://www.researchgate.net/publication/268523025_Studies_on_the_Potential_of_Fireflies_Watching_Tourism_for_Firefly_Coleoptera_Lampyridae_Pteroptyx_spp_Conservation

Mahadimenakbar, M. D., Jeperi, S. R., Fiffy Hanidah, S., & Bagul, A. H. B. P. (2018). Notes on congregating fireflies (Coleoptera, Lampyridae) of Binsulok River, Sabah. *Journal of Tropical Biology and Conservation*, *15*, 155-162.

Mahadimenakbar, M. D., Mahsol, H. H., & Ghani, M. A., (2007). The distribution and phenology of *Pteroptyx* fireflies (Coleoptera; Lampyridae) along Garama River, Sabah, Malaysia. *Journal of Tropical Biology and Conservation*, *3*, 1-9.

Mahadimenakbar, M. D., Menno, S., & Zulhazman, H. (2002). *Preliminary survey of fireflies (Coleoptera: Lampyridae) in Lower Kinabatangan, Sabah*. https://www.academia.edu/27971071/Mahadimenakbar_M_Dawood_Menno_Schilthuizen_and_Zulhazman_Hamzah_2003_Preliminary_Survey_of_Fireflies_Coleoptera_Lampyridae_in_Lower_Kinabatangan_Sabah_Lower_Kinabatangan_Scientific_Expedition_2002_Universiti_Malaysia_Sabah_Pp27_36

Mahmod, A. M., Sulaiman, A., Asri, L. N., Abdullah, N. A., Husin, S. M., Shukor, A., Darbis, N. D. A, Satiman, Faris, E. M., & Sulaiman, N. (2018). *Kelimpahan kelip kelip bersinkroni di Sungai Chukai, Kemaman, Terengganu* [Abundance of synchronize firefly at Chukai River, Kemaman, Terengganu]. *Undergraduate Research Journal for Integrative Biology*, *2*, 117-123.

Mohd, F. A., Maulud, K. N. A., Karim, O. A., Begum, R. A., Awang, N. A., Ahmad, A., Azhary, W. A. H. W. M., Kamarudin, M. K. A., Jaafar, M., & Mohtar, W. H. M. W. (2019). Comprehensive coastal vulnerability assessment and adaptation for Cherating-Pekan coast, Pahang, Malaysia. *Ocean and Coastal Management*, *182*, 104948. https://doi.org/10.1016/j.ocecoaman.2019.104948

Nada, B., & Kirton, L. G. (2004). The secret life of fireflies. *IRBM Updates*, *3*(December 2004), 2-4.

Nallakumar, A. (2002). *The management and conservation of fireflies in Peninsular Malaya* [Unpublished Doctoral dissertation]. Imperial College London.

Nallakumar, K. (2003). The synchronously flashing aggregative fireflies of Peninsular Malaysia. *Biodiversity*, *4*(2), 11-16. https://doi.org/10.1080/14888386.2003.9712684

Ohba, N., & Sim, S. H. (1994). The morphology, behaviour and life cycle of *Pteroptyx valida* (Coleoptera: Lampyridae) in Singapore. *Science Report of the Yokosuka City Museum*, *42*, 1-11.

Ohba, N., & Wong, C. H. (2004). External morphology and ecological study of the firefly, *Pteroptyx tener* at Kampong Kuantan, Selangor, Malaysia. *Science Report of Yokosuka City Museum*, *51*, 1-33.

Omar, H., Misman, M. A., Parlan, I. (Eds.) (2020). *Status of mangroves in Malaysia*. Forest Research Institute Malaysia.

Romañach, S. S., DeAngelis, D. L., Koh, H. L., Li, Y., Teh, S. Y., Barizan, R. S. R., & Zhai, L. (2018). Conservation and restoration of mangroves: Global status, perspectives, and prognosis. *Ocean and Coastal Management*, *154*, 72-82. https://doi.org/10.1016/j.ocecoaman.2018.01.009

Salleh, N. K., Othman, N. W., Sulaiman, N., & Sahid, I. (2019). Ultrastructure on the light organ of tropical synchronize firefly, *Pteroptyx tener*. *Sains Malaysiana*, *48*(4), 727-733. https://doi.org/10.17576/jsm-2019-4804-04

Salvador-Caabay, J. M. (2022). Ecology and diversity of Lampyridae (firefly): Checklist, state of knowledge, and priorities for future research and conservation in the Philippines. *Biodiversity Journal*, *13*(2), 409–416. https://doi.org/10.31396/Biodiv.Jour.2022.13.2.409.416

Sartsanga, C., Swatdipong, A., & Sriboonlert, A. (2018). Distribution of the firefly genus *Pteroptyx* Olivier and a new record of *Pteroptyx asymmetria* Ballantyne (Coleoptera: Lampyridae: Luciolinae) in Thailand. *The Coleopterists Bulletin*, *72*(1), 171-183. https://doi.org/10.1649/0010-065X-72.1.171

Shahara, A., Nura, A. M. R., Maimon, A., & Norela, S. (2017). Assessment of firefly abundance at a new ecotourism site of Sungai Bernam, Selangor, Malaysia. *Malayan Nature Journal*, *69*(2), 67-74.

Sulaiman, N., Loo, M. C., & Abdullah, M. (2017). Association between the firefly population and some biotic and abiotic factors along the Sungai Sepetang river banks at Kampung Dew, Taiping, Perak, Malaysia. *Malayan Nature Journal*, *69*(3), 159-167.

Sulaiman, N., Shahril, M. H., Noh, A. N. M., Maimon, A., & Nur Khairunnisa, S. (2016). Abundance of Lampyridae in relation to the vegetation and abiotic conditions along the Sungai Johor, Johor, Malaysia. *Malayan Nature Journal*, *67*(4), 395-402.

Tangah, J., Ashton, E. C., Chan, H. T., Baba, S. (2022). Mangroves of Malaysia. In S. C. Das, Pullaiah, & E. C. Ashton (Eds.), *Mangroves: Biodiversity, livelihoods and conservation* (pp. 373–395). Springer. https://doi.org/10.1007/978-981-19-0519-3_15

Wilson, E. O. (2003). On global biodiversity estimates. *Paleobiology*, *29*(1), 14. https://doi.org/10.1666/0094-8373(2003)029<0014:OGBE>2.0.CO;2

Wong, C. H., & Yeap, C. A. (2012). Conservation of congregating firefly zones (CFZs) in Peninsular Malaysia. *Lampyrid*, *2*, 174-187.

Yuma, M. (2007). Effect of rainfall on the long-term population dynamics of the aquatic firefly *Luciola cruciata*. *Entomological Science*, *10*(3), 237-244. https://doi.org/10.1111/j.1479-8298.2007.00219.x

Pertanika J. Trop. Agric. Sci. 46 (1): 37 - 48 (2023)

PERTANIKA JOURNALS

TROPICAL AGRICULTURAL SCIENCE

Journal homepage: http://www.pertanika.upm.edu.my/

Therapeutic Evaluation of Ethanolic Bee Pollen Extract from Malaysian Stingless Bee in MCF-7 and MCF-10A Cell Lines

Nurdianah Harif Fadzilah and Wan Adnan Wan Omar*

Advanced Medical and Dental Institute, Universiti Sains Malaysia, Bertam, 13200 Kepala Batas, Penang, Malaysia

ABSTRACT

Bee pollen is a complete food containing comprehensive nutrients and therapeutic properties that could eliminate free radicals. Three stingless bee species native to Malaysia were used to prepare bee pollen ethanolic extracts (BPE): *Geniotrigona thoracica*, *Heterotrigona itama*, and *Tetrigona apicalis*. The methodology used in this study was a trypan blue exclusion assay for cell proliferation activity in cultured breast adenocarcinoma human cell lines (MCF-7) and mammary epithelial human cell lines (MCF-10A). In addition, the therapeutic index (TI) was analyzed to assess the relative antiproliferative activity of BPE on cancer versus normal cells. *Geniotrigona thoracica* BPE exhibited the highest therapeutic index (TI = 3.12) compared to *H. itama* (TI = 1.16) and *T. apicalis* (TI = 0.90) BPE. Each species represents different bioactive compounds due to different pollen foraging activities. Therefore, the highest TI species (*G. thoracica*) could be a potential candidate to be developed as a potential chemotherapeutic agent.

Keywords: MCF-7, MCF-10A, stingless bee pollen, therapeutic index

INTRODUCTION

Environment, nutrition, and lifestyle factors play a significant role in influencing cancer development. Cancer could be considered a leading cause of mortality globally, including breast cancer. It is the most common cancer to cause mortality in women (Azamjah et al., 2019; Seely & Alhassan, 2018). Therefore, there is a lot of research on cancer chemoprevention and therapy using nutritional supplementation and

ARTICLE INFO

Article history:
Received: 29 June 2022
Accepted: 22 September 2022
Published: 22 December 2022

DOI: https://doi.org/10.47836/pjtas.46.1.03

E-mail addresses:
nurdianaharif@usm.my (Nurdianah Harif Fadzilah)
wanadnan@usm.my (Wan Adnan Wan Omar)
* Corresponding author

ISSN: 1511-3701
e-ISSN: 2231-8542

traditional medicines to treat cancer using various natural compounds (Cha et al., 2005; Choudhari et al., 2013).

Compounds in natural products, such as herbal and bee products, offer many research opportunities in developing anticancer agents that have nutraceutical properties, are non-toxic, and safe for human health (Kuppusamy et al., 2014; Premratanachai & Chanchao, 2014; Wang et al., 2012). Natural compounds in bee products, including honey, propolis, and bee pollen, were found to significantly inhibit cell growth and reduce tumor cells proliferation (Ahmad et al., 2019; Choudhari et al., 2013; Franchi et al., 2012; Kustiawan et al., 2014; T-Johari et al., 2019). In Malaysia, 45 stingless bee species from 14 genera were documented (Norowi et al., 2010; Samsudin et al., 2018), including *Geniotrigona thoracica*, *Heterotrigona itama*, and *Tetrigona apicalis*, which are commonly domesticated for honey production.

Other than honey, stingless bee produces bee pollen that serves as a source of nutrients for both adult bees and larvae. It is known as a complete food since the food energy produced is relatively high, ranging from 396.4 to 411.1 kcal/100 g of pollen (Kocot et al., 2018). Bee pollen is also a popular health supplement for maintaining health and longevity. Studies have demonstrated that 70% of bee pollen compositions are biologically active and exhibit numerous benefits, including cardioprotection, hepatoprotection, antioxidation, anticarcinogen, antibacterial, antiosteoporosis, antiprostatitis, anti-anemia, anti-aging, anti-inflammatory, and immunostimulant (Campos et al., 2010; Rzepecka-Stojko et al., 2015; Yang et al., 2013).

In vitro antiproliferative activity of bee pollen extract can be determined based on the minimum effective concentrations (EC_{50}) in cancer cells and the minimum inhibitory concentrations (IC_{50}) in normal cells. EC_{50} and IC_{50}, however, are often used interchangeably. The terms determine the tested compounds or drugs with the desired properties and qualities (Sebaugh, 2011). EC_{50} is expressed as the effective concentration of a molecule where 50% of the bioactivity is observed and is commonly used to describe the stimulation of responses (MarÉchal, 2011). IC_{50}, on the other hand, is defined as the inhibitor concentration that decreases the response to 50% of its maximum. That maximum response (or binding) is inhibited due to an inhibitor's action that binds to a receptor (MarÉchal, 2011).

In drug development, the therapeutic index (TI) is expressed as the ratio of dosage with the maximum exposure that is not toxic (with fewer adverse effects) to the dosage that indicates the preferred pharmacological outcome (Muller & Milton, 2012). TI is a quantitative relationship between the drug's safety (toxicology) and efficacy (pharmacology). *In vitro* safety assays, such as cytotoxicity tests, determine the IC50 (minimum toxic concentrations), and *in vitro* efficacy assays, such as growth inhibition of tumor cells, determine the EC_{50} (minimum effective concentrations) (Muller

& Milton, 2012). IC_{50}/EC_{50} is typically used to measure the effectiveness of a compound in biochemical or biological studies in cells.

TI provides a semiquantitative evaluation of the concentrations used to attain the expected response with a tolerable level of adverse effects. It is expressed as the ratio of the IC_{50} of normal/non-tumor cells to the EC_{50} of tumor cells (Deepa et al., 2012). TI with a high value indicates more safety and specificity in targeting cancer cells (Abughazaleh & Tracy, 2014; Muller & Milton, 2012). The United States Food and Drug Administration (FDA) describes drugs with a low TI as less than a 2-fold difference in the IC_{50} and EC_{50} (Abughazaleh & Tracy, 2014). However, there is no clear FDA guidance on the use of TI for clinical trials, believing that each drug is unique.

In antiproliferative or cytotoxicity assay, *in vitro* cell cultures are frequently identified as alive or dead based on membrane integrity. Different assays can detect dead cells accumulation, including the measurement of cytoplasm's component leakage into the culture medium (by enzyme or fluorescent marker) or non-permeable dye penetration into cells with damaged membranes (trypan blue or fluorogenic DNA binding dyes) (Riss et al., 2019).

By using the trypan blue exclusion method, the toxicity of compounds and inhibition of tumor cells can be evaluated. This method observes cell membrane integrity and detects nonviable cells in non-dividing cell populations (Aslantürk, 2018). The number of viable cells can be determined based on the fundamental that intact membranes of living cells exclude trypan blue dye, exhibiting a perfect cytoplasm. Meanwhile, a nonviable cell exhibits blue ruptured cytoplasm.

Antiproliferative and cytotoxicity are terms that are being used interchangeably. The term cytotoxic refers to chemicals that cause cell toxicity, such as anticancer agents or chemotherapy treatments that aim to kill cancer cells and stop their growth (Kandaswami, 2014). On the other hand, the antiproliferative assay determines cell viability and cell proliferation, a measure of mammalian cell growth and survival (Kandaswami, 2014). Thus, the trypan blue exclusion method is better known as an antiproliferative viability assay that can estimate the rate of proliferation and the percentage of viable/nonviable cells (Strober, 2015).

This study evaluated the antiproliferative effect of three stingless bee pollen extracts, *G. thoracica*, *H. itama*, and *T. apicalis*, on two cell lines (MCF-7 and MCF-10A). In addition, the therapeutic index was analyzed to assess the relative antiproliferative activity of BPE on cancer versus normal cells.

MATERIALS AND METHODS

Preparation of Bee Pollen Extract (BPE)

Malaysian stingless bee species were collected from Syamille Agrofarm, Kuala Kangsar, Perak, Malaysia, i.e., *Geniotrigona thoracica* (*G. thoracica*), *Heterotrigona itama* (*H. itama*), and *Tetrigona apicalis*

(*T. apicalis*). The pollen samples were collected from two different colonies for each species. They were extracted in ethanol (10% w/v), sonicated in an ultrasound bath at 41°C (90 min), centrifuged at 2,800 × *g* (5 min), filtered, and dried in a rotary evaporator (EYELA OSB-2100, Japan). The BPE was then freeze-dried for four days (Martin Christ Alpha freeze dryer, Germany) and kept at 4°C to be used later in the experiment.

Cell Lines

Mammary epithelial human cell lines (MCF-10A) were maintained in a 75 cm^3 cell culture flask containing Dulbecco's Modified Eagle Medium/Nutrient Mixture F-12 (DMEM/F-12) medium supplemented with serum from the horse (5% v/v), recombinant insulin from human (10 µg/mL), recombinant epidermal growth factor from human (hEGF, 20 ng/mL), hydrocortisone (0.5 µg/mL) and penicillin-streptomycin (1% v/v).

Breast adenocarcinoma human cell lines (MCF-7) were grown in a 75 cm^3 cell culture flask containing RPMI 1640 medium supplemented with serum from fetal bovine (10% v/v) and penicillin-streptomycin (1% v/v). All media and supplements were purchased from Sigma (USA) and Gibco (USA).

Cell lines were preserved in humidified air with 5% CO_2 at 37°C and subcultured every two to three days. Trypsin was used to detach cells with 80% viability for trypan blue exclusion assay. MCF-10A and MCF-7 ATCC cell lines were obtained from Advanced Medical and Dental Institute, Universiti Sains Malaysia (USM).

Trypan Blue Exclusion Assay

Antiproliferative activity was evaluated using the trypan blue dye exclusion assay. MCF-10A and MCF-7 cells were seeded at 5.0×10^4 cells/well in 24-well plates and allowed to adhere for 36 h to 48 h. After reaching 70% to 80% confluency, cells were treated for 24 h with different BPE concentrations ranging from 0.3 to 5.0 mg/mL dissolved in the growth medium, while in control cells, no BPE treatment was applied.

After 24 h treatment with BPE, phosphate-buffered saline (PBS) was used to wash the cells, followed by centrifuging the cells at 112 × *g* (5 min) and discarding the supernatant. PBS was used again to resuspend the cell pellet and mixed with trypan blue (0.4%, 10:10 µL) in a microplate well. Ten µL of the trypan blue/cell mixture was taken into a hemocytometer, and cells were observed under a microscope. The unstained (viable) and stained (nonviable) cells attached to the hemocytometer were calculated. The viable cells' total number was multiplied by the trypan blue dilution factor (×2) to obtain viable cells per mL. The percentage of viable cells was estimated as (viable cells number per mL/total number of cells per mL) × 100 (Strober, 2019).

A dose-response curve of sample concentration versus cell viability was consequently plotted. Finally, the 50% inhibitory concentration in MCF-10A cells (IC_{50}) and 50% effective concentration in

MCF-7 were calculated by interpolating the plotted graph using Microsoft Excel (version 16.37). All three experiments were done as independent experiments, each performed in duplicate.

Therapeutic Index

The therapeutic index (TI) was estimated as follows: TI = (IC_{50} non-neoplastic cell) / (EC_{50} neoplastic cell) (Deepa et al., 2012). MCF-10A was non-neoplastic (normal) cells and MCF-7 was neoplastic (cancer) cells. A compound with a high therapeutic index is potent compared with a low therapeutic index compound.

Statistical Analysis

All experiments were duplicated and presented as mean ± standard deviation (SD). The significant differences between experimental groups were assessed by Student's *t*-test using IBM SPSS Statistics version 24.0. (IBM Corp., USA). Statistically significant data was presented with *P* values ≤ 0.05.

RESULTS

Antiproliferative Activity of *T. apicalis* BPE in MCF-7 and MCF-10A Cells

Different concentrations of *T. apicalis* BPE on the viability of MCF-7 and MCF-10A cells treated at 24 h were demonstrated in Figure 1. The effect of BPE from *T. apicalis* showed a dose-dependent increase in MCF-7 cell inhibition. Both colonies of *T. apicalis* BPE inhibited MCF-7 cells at EC_{50} of 1.60 + 0.10 mg/mL (Figure 1a). Meanwhile, the IC_{50} of *T. apicalis* in MCF-10A cells was 1.46 + 0.51 mg/mL (Figure 1b).

When the EC_{50} and IC_{50} values were evaluated using Student's *t*-test, no significant difference was seen with *p*-values of 0.161 and 0.567 for both colonies of *T. apicalis* (i) and (ii), respectively. In addition, the result showed no difference in EC_{50} value in MCF-7 cells compared with the IC_{50} value in MCF-10A cells.

Antiproliferative Activity of *H. itama* BPE in MCF-7 and MCF-10A Cells

Extrapolation from Figure 2a showed that the EC_{50} for MCF-7 cells was 1.72 + 0.28 mg/mL for *H. itama*. In MCF-10A cells, the IC_{50} was 1.91 + 0.72 mg/mL for *H. itama* as depicted in Figure 2b. Comparing IC_{50} of MCF-10A and EC_{50} of MCF-7 in two colonies of *H. itama* did not show any statistically significant difference [$p = 0.212$ in *H. itama* (i) and $p = 0.172$ in *H. itama* (ii)].

Antiproliferative Activity of *G. thoracica* BPE in MCF-7 and MCF-10A Cells

Geniotrigona thoracica BPE showed the MCF-7 EC_{50} mean value of 1.61 + 0.30 mg/mL (Figure 3a). While in MCF-10A, the IC_{50} was 4.93 + 0.81 mg/mL for colony i and the IC_{40} was 4.93 + 0.51 mg/mL for colony ii (Figure 3b).

The IC_{40} value was used in the second colony of *G. thoracica* because the IC_{50} value was outside the data range (Figure 3b). All variables were standardized in each experiment, where the maximum

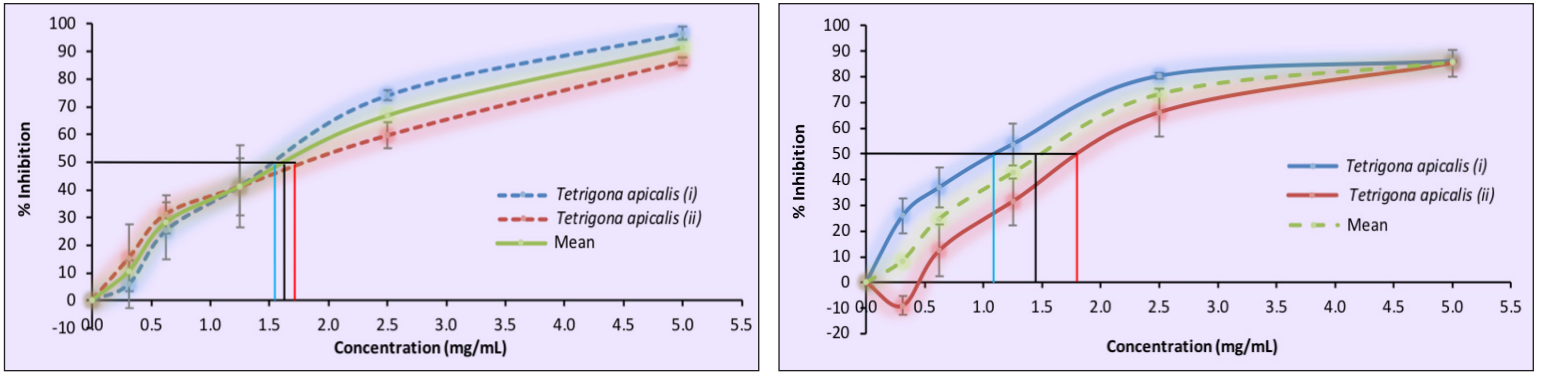

Figure 1. Antiproliferation of *T. apicalis* BPE against MCF-7 and MCF-10A cells

Note. (a) Antiproliferation of *T. apicalis* BPE against MCF-7 cells at 24 h treatment, mean = 1.60 mg/mL; (b) Antiproliferation of *T. apicalis* BPE against MCF-10A cells at 24 h treatment, mean =1.46 mg/mL. Each point indicates three independent experiments' mean values ± SD

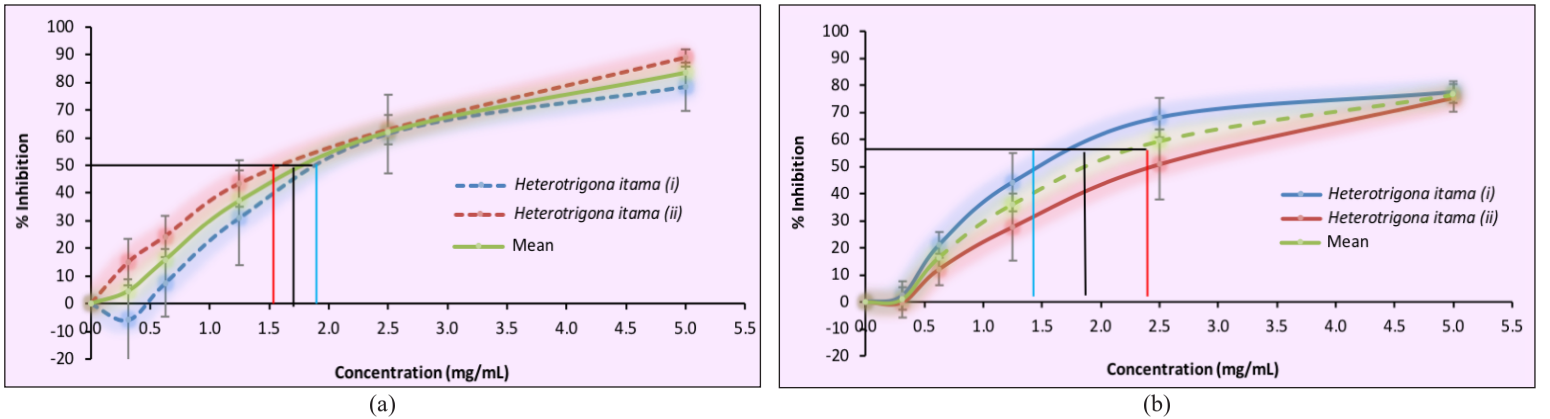

Figure 2. Antiproliferation of *H. itama* BPE against MCF-7 and MCF-10A cells

Note. (a) Antiproliferation of *H. itama* BPE in MCF-7 cells, mean =1.72 ± 0.28 mg/mL; (b) Antiproliferation of *H. itama* BPE in MCF-10A cells at 24 h treatment, mean = 1.91 ± 0.72 mg/mL. The results presented are means of three separate experiments ± SD

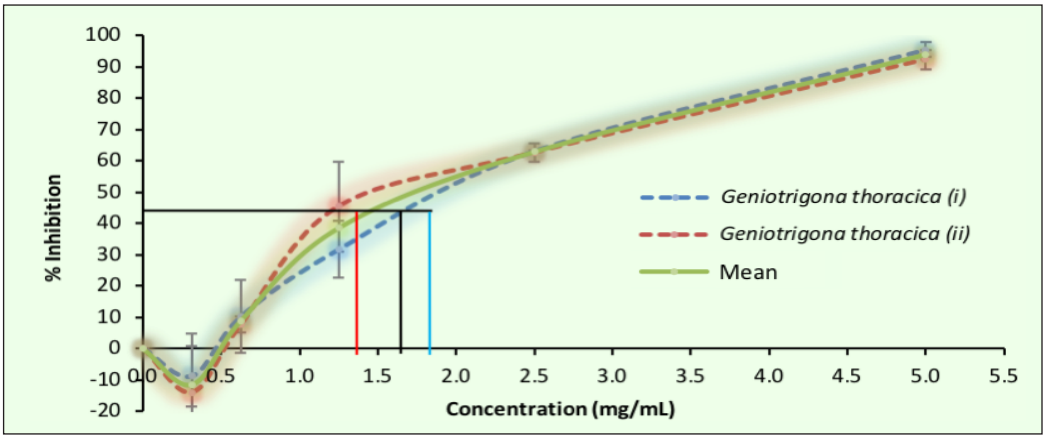

(a)

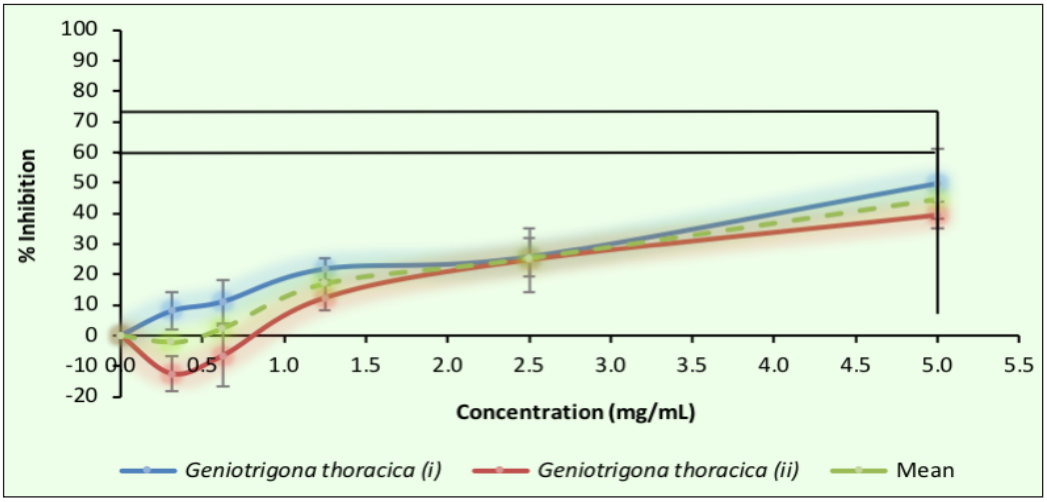

(b)

Figure 3. Antiproliferation of *G. thoracica* BPE against MCF-7 and MCF-10A cells
Note. (a) Antiproliferation of *G. thoracica* BPE in MCF-7 cells, mean = 1.61 ± 0.30 mg/mL; (b) Antiproliferation of *G. thoracica* BPE in MCF-10A cells at 24 h treatment, mean = 4.93 ± 0.51 mg/mL. The results presented are means of three separate experiments ± SD

concentration was 5.0 mg/mL. Both IC_{50} and IC_{40} values were applicable and consistent with treatment doses of less than 50% inhibition used in the clinical setting (Stordal et al., 2006).

A significant difference was found in EC_{50} values in MCF-7 cells compared with the IC_{50}/IC_{40} values in MCF-10A cells for both colonies of *G. thoracica* species. In colony i, the *p*-value was 0.018, while in colony ii, the *p*-value was 0.001. Only *G. thoracica* species indicated a significant result compared to the other two species.

Therapeutic Index (TI)

The therapeutic index is a ratio of concentration that inhibits 50% proliferation of normal cells (IC_{50}) to the concentration

that inhibits 50% proliferation of tumor cells (EC_{50}). The TI values of each colony of BPE species differed from each other. The order of TI values is as follows: *G. thoracica* > *H. itama* > *T. apicalis*.

The average of two colonies of each species was calculated, where *G. thoracica* showed the highest TI value of 3.12, followed by *H. itama* (1.16), and *T. apicalis* (0.90) (Figure 4).

DISCUSSION

Antiproliferative Assay

In this study, a trypan blue exclusion assay has been used to assess the antiproliferative activity of *T. apicalis*, *H. itama*, and *G. thoracica* BPE in MCF-7 and MCF-10A cell lines. The minimum effective concentrations (EC_{50}) in MCF-7 cells and the minimum inhibitory concentrations (IC_{50}) in MCF-10A cells were determined from the graph based on extrapolation from the antiproliferative curve after 24 h treatment.

MCF-7, the breast adenocarcinoma human cell line, was developed in 1970, and since then, more than 25,000 publications have been reported (Lee et al., 2015). In addition, MCF-7 is a frequently studied cell line that serves as a valuable model system in hormone-receptor-positive breast cancer research (Lee et al., 2015).

Among the commonly used normal breast cells as an *in vitro* model is MCF-10A, the mammary epithelial human cell line that was isolated in 1984 (American Type Culture Collection [ATCC], n.d.). These cells originated from benign immortalized breast tissue proliferation, no estrogen receptors expression, and exhibited some features of normal breast epithelium (Qu et al., 2015).

Antiproliferative Activity of BPE

In the present study, the antiproliferative activity revealed that three BPE species demonstrated the capacity to decrease

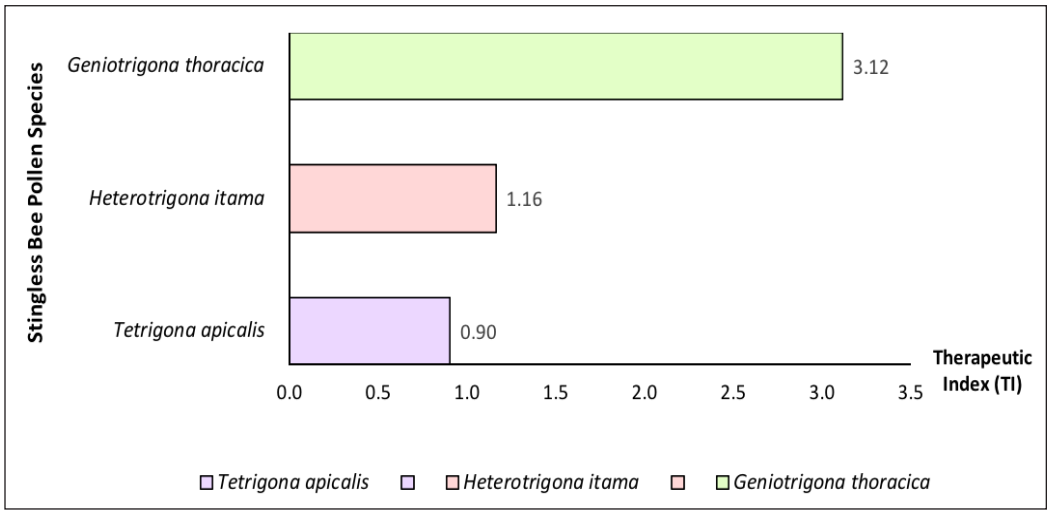

Figure 4. Comparison of therapeutic index (TI) in different BPE species with respect to MCF-10A cells
Note. Bars illustrate the TI values of three BPE species

the MCF-7 and MCF-10A cell viability in a dose-dependent manner. However, *T. apicalis* (EC_{50} = 1.60 mg/mL, IC_{50} = 1.46 mg/mL, TI = 0.90) and *H. itama* (EC_{50} = 1.72 mg/mL, IC_{50} = 1.91 mg/mL, TI = 1.16) showed a lower antiproliferative effect compared to *G. thoracica* (EC_{50} = 1.61 mg/mL, IC_{50} = 4.93 mg/mL, TI = 3.12).

The antiproliferative effect of *G. thoracica* (colonies i and ii) strongly increased by reaching a maximum of 92-95% inhibition in MCF-7 and only 39-49% inhibition in MCF-10A cell lines. Among the three species, *G. thoracica* showed a significant result ($p < 0.05$) with the highest antiproliferative effect on MCF-7 and the least antiproliferative activity seen in MCF-10A [$p = 0.018$ in *G. thoracica* (i), $p = 0.001$ in *G. thoracica* (ii)]. According to FDA, the TI value of more than a 2-fold difference in the IC_{50} and EC_{50} gives the distinction that *G. thoracica* is better than *T. apicalis* and *H. itama*; thus, *G. thoracica* could act as a potent antiproliferative agent (Tamargo et al., 2015).

Kustiawan et al. (2014) showed that the proliferation of five cancer cell lines was inhibited by four different species of stingless bee products, i.e., honey, bee pollen, and propolis (Kustiawan et al., 2014). The result showed BPE from n-hexane and ethyl acetate (EtOAc) extract from two species gave <50% relative viable cell number after 48 h treatment on two cancer cell lines. In their study, *T. apicalis* was the least cytotoxic species with a lower antiproliferative effect on cancer cells than other species. Our data showed a similar finding (EC_{50} of *T. apicalis* = 1.60 mg/mL, TI = 0.90).

BPE's ability to inhibit the growth of cancer cells depends on the bee species and cell line in *in vitro* study, representing different bioactive compounds due to different pollen foraging activities displayed by each species. In addition, it was previously shown that BPE contained different antioxidant activity and phenolic/flavonoid content (Harif Fadzilah et al., 2017), which could contribute to its bioactivity and antiproliferative effects on cell lines tested in this study.

CONCLUSION

Geniotrigona thoracica BPE showed a strong antiproliferative effect on MCF-7 cells, and less antiproliferative activity was seen on MCF-10A cells. The calculated therapeutic index in this study showed that the specificity of *G. thoracica* BPE was more effective in killing MCF-7 cells with less toxicity to MCF-10A cells compared with *T. apicalis* and *H. itama*. The therapeutic index of *G. thoracica* BPE was the highest, potentially developing as a chemotherapeutic agent.

ACKNOWLEDGEMENTS

The authors gratefully acknowledge the financial support from Universiti Sains Malaysia (Research University Grant: 1001/CIPPT/8012317).

REFERENCES

Abughazaleh, R. D., & Tracy, T. S. (2014). *Therapeutic index*. Wiley StatsRef: Statistics Reference Online. https://doi.org/10.1002/9781118445112.stat07121

Ahmad, F., Seerangan, P., Mustafa, M. Z., Osman, Z. F., Abdullah, J. M., & Idris, Z. (2019). Anti-cancer properties of *Heterotrigona itama* sp. honey via induction of apoptosis in malignant glioma cells. *Malaysian Journal of Medical Sciences*, *26*(2), 30–39. https://doi.org/10.21315/mjms2019.26.2.4

American Type Culture Collection. (n.d.). *MCF 10A (CRL-10317™)*. ATCC. https://www.atcc.org/products/all/CRL-10317.aspx#history

Aslantürk, Ö. S. (2018). *In vitro* cytotoxicity and cell viability assays: Principles, advantages, and disadvantages. In M. L. Larramendy & S. Soloneski (Eds.), *Genotoxicity - A predictable risk to our actual world*. IntechOpen. https://doi.org/10.5772/intechopen.71923

Azamjah, N., Soltan-Zadeh, Y., & Zayeri, F. (2019). Global trend of breast cancer mortality rate: A 25-year study. *Asian Pacific Journal of Cancer Prevention*, *20*(7), 2015–2020. https://doi.org/10.31557/APJCP.2019.20.7.2015

Campos, M. G. R., Frigerio, C., Lopes, J., & Bogdanov, S. (2010). What is the future of Bee-Pollen?. *Journal of ApiProduct and ApiMedical Science*, *2*(4), 131–144. https://doi.org/10.3896/ibra.4.02.4.01

Cha, M. C., Lin, A., & Meckling, K. A. (2005). Low dose docosahexaenoic acid protects normal colonic epithelial cells from araC toxicity. *BMC Pharmacology*, *5*, 7. https://doi.org/10.1186/1471-2210-5-7

Choudhari, M. K., Haghniaz, R., Rajwade, J. M., & Paknikar, K. M. (2013). Anticancer activity of Indian stingless bee propolis: An *in vitro* study. *Evidence-Based Complementary and Alternative Medicine*, *2013*, 928280. https://doi.org/10.1155/2013/928280

Deepa, P. R., Vandhana, S., Jayanthi, U., & Krishnakumar, S. (2012). Therapeutic and toxicologic evaluation of anti-lipogenic agents in cancer cells compared with non-neoplastic cells. *Basic and Clinical Pharmacology and Toxicology*, *110*(6), 494–503. https://doi.org/10.1111/j.1742-7843.2011.00844.x

Franchi, G. C., Moraes, C. S., Toreti, V. C., Daugsch, A., Nowill, A. E., & Park, Y. K. (2012). Comparison of effects of the ethanolic extracts of brazilian propolis on human leukemic cells as assessed with the MTT assay. *Evidence-Based Complementary and Alternative Medicine*, *2012*, 918956. https://doi.org/10.1155/2012/918956

Harif Fadzilah, N., Jaapar, M. F., Jajuli, R., & Wan Omar, W. A. (2017). Total phenolic content, total flavonoid and antioxidant activity of ethanolic bee pollen extracts from three species of Malaysian stingless bee. *Journal of Apicultural Research*, *56*(2), 130–135. https://doi.org/10.1080/00218839.2017.1287996

Kandaswami, C. C. (2014). *Re: What is the difference between an antiproliferative assay and a cytotoxicity assay?*. ResearchGate. https://www.researchgate.net/post/What-is-the-difference-between-an-antiproliferative-assay-and-a-cytotoxicity-assay/53a079e2d4c1188e0a8b4626/citation/download

Kocot, J., Kiełczykowska, M., Luchowska-Kocot, D., Kurzepa, J., & Musik, I. (2018). Antioxidant potential of propolis, bee pollen, and royal jelly: Possible medical application. *Oxidative Medicine and Cellular Longevity*, *2018*, 7074209. https://doi.org/10.1155/2018/7074209

Kuppusamy, P., Yusoff, M. M., Maniam, G. P., Ichwan, S. J. A., Soundharrajan, I., & Govindan, N. (2014). Nutraceuticals as potential therapeutic

agents for colon cancer: A review. *Acta Pharmaceutica Sinica B*, *4*(3), 173–181. https://doi.org/10.1016/j.apsb.2014.04.002

Kustiawan, P. M., Puthong, S., Arung, E. T., & Chanchao, C. (2014). *In vitro* cytotoxicity of Indonesian stingless bee products against human cancer cell lines. *Asian Pacific Journal of Tropical Biomedicine*, *4*(7), 549–556. https://doi.org/10.12980/APJTB.4.2014APJTB-2013-0039

Lee, A. V., Oesterreich, S., & Davidson, N. E. (2015). MCF-7 cells - Changing the course of breast cancer research and care for 45 years. *Journal of the National Cancer Institute*, *107*(7), djv073. https://doi.org/10.1093/jnci/djv073

MarÉchal, E. (2011). Measuring bioactivity: KI, IC50 and EC50. In E. Marechal, S. Roy, L. Lafanechère (Eds.), *Chemogenomics and chemical genetics* (pp. 55–65). Springer. https://doi.org/10.1007/978-3-642-19615-7_5

Muller, P. Y., & Milton, M. N. (2012). The determination and interpretation of the therapeutic index in drug development. *Nature Reviews Drug Discovery*, *11*(10), 751–761. https://doi.org/10.1038/nrd3801

Norowi, M. H., Mohd, F., Sajap, A. S., Rosliza, J., & Suri, R. (2010). *Conservation and sustainable utilization of stingless bees for pollination services in agricultural ecosystems in Malaysia*. ResearchGate. https://www.researchgate.net/publication/318338675

Premratanachai, P., & Chanchao, C. (2014). Review of the anticancer activities of bee products. *Asian Pacific Journal of Tropical Biomedicine*, *4*(5), 337–344. https://doi.org/10.12980/APJTB.4.2014C1262

Qu, Y., Han, B., Yu, Y., Yao, W., Bose, S., Karlan, B. Y., Giuliano, A. E. & Cui, X. (2015). Evaluation of MCF10A as a reliable model for normal human mammary epithelial cells. *PLOS One*, *10*(7), e0131285. https://doi.org/10.1371/journal.pone.0131285

Riss, T., Niles, A., Moravec, R., Karassina, N., Vidugiriene, J., Markossian, S., Grossman, A., Brimacombe, K., Arkin, M., Auld, D., Austin, C., Baell, J., Chung, T. D. Y., Coussens, N. P., Dahlin, J. L., Devamarayan, V., Foley, T. L., Glicksman, M., Hass, J. V., … Xu, X. (Eds.). Cytotoxicity assays: *In vitro* methods to measure dead cells. In *Assay guidance manual*. Eli Lilly & Company and the National Center for Advancing Translational Sciences. https://pubmed.ncbi.nlm.nih.gov/31070879/

Rzepecka-Stojko, A., Stojko, J., Kurek-Górecka, A., Górecki, M., Kabała-Dzik, A., Kubina, R., Moździerz, A., & Buszman, E. (2015). Polyphenols from bee pollen: Structure, absorption, metabolism and biological activity. *Molecules*, *20*(12), 21732–21749. https://doi.org/10.3390/molecules201219800

Samsudin, S. F., Mamat, M. R., & Hazmi, I. R. (2018). Taxonomic study on selected species of stingless bee (Hymenoptera: Apidae: Meliponini) in Peninsular Malaysia. *Serangga*, *23*(2), 203–258.

Sebaugh, J. L. (2011). Guidelines for accurate EC50/IC50 estimation. *Pharmaceutical Statistics*, *10*(2), 128–134. https://doi.org/10.1002/pst.426

Seely, J. M., & Alhassan, T. (2018). Screening for breast cancer in 2018 — What should we be doing today?. *Current Oncology*, *25*(s1), 115–124. https://doi.org/10.3747/co.25.3770

Stordal, B. K., Davey, M. W., & Davey, R. A. (2006). Oxaliplatin induces drug resistance more rapidly than cisplatin in H69 small cell lung cancer cells. *Cancer Chemotherapy and Pharmacology*, *58*(2), 256–265. https://doi.org/10.1007/s00280-005-0148-7

Strober, W. (2015). Trypan blue exclusion test of cell viability. *Current Protocols in Immunology*, *111*, A3.B1-A3.B3. https://doi.org/10.1002%2F0471142735.ima03bs111

Tamargo, J., Le Heuzey, J. Y., & Mabo, P. (2015). Narrow therapeutic index drugs: A clinical

pharmacological consideration to flecainide. *European Journal of Clinical Pharmacology*, *71*(5), 549–567. https://doi.org/10.1007/s00228-015-1832-0

T-Johari, S. A. T., Hashim, F., Ismail, W. I. W., & Ali, A. M. (2019). Combinatorial cytotoxic effects of gelam honey and 5-fluorouracil against human adenocarcinoma colon cancer HT-29 cells *in vitro*. *International Journal of Cell Biology*, *2019*, 9050626. https://doi.org/10.1155/2019/9050626

Wang, H., Khor, T. O., Shu, L., Su, Z., Fuentes, F., Lee, J.-H., & Kong, A.-N. T. (2012). Plants against cancer: A review on natural phytochemicals in preventing and treating cancers and their druggability. *Anti-cancer Agents in Medical Chemistry*, *12*(10), 1281–1305. https://doi.org/10.2174%2F187152012803833026

Yang, K., Wu, D., Ye, X., Liu, D., Chen, J., & Sun, P. (2013). Characterization of chemical composition of bee pollen in China. *Journal of Agricultural and Food Chemistry*, *61*(3), 708–718. https://doi.org/10.1021/jf304056b

Pertanika J. Trop. Agric. Sci. 46 (1): 49 - 65 (2023)

PERTANIKA JOURNALS

TROPICAL AGRICULTURAL SCIENCE

Journal homepage: http://www.pertanika.upm.edu.my/

Fermentation of White and Brown Rice Water Increases Plant Nutrients and Beneficial Microbes

Abba Nabayi[1, 2], Christopher Boon Sung Teh[1]*, Ali Kee Zuan Tan[1] and Ngai Paing Tan[1]

[1]*Department of Land Management, Faculty of Agriculture, Universiti Putra Malaysia, 43400 Serdang, Selangor, Malaysia*

[2]*Department of Soil Science, Faculty of Agriculture, Federal University Dutse, Nigeria, PMB 7156, Ibrahim Aliyu Bye-pass Jigawa State, Nigeria*

ABSTRACT

The wastewater after washing rice grains is known as washed rice water (WRW). WRW is often recommended for reuse as plant fertilizer, but little is known about the difference in the nutrient and microbial contents of WRW between white and brown rice. The study aims to answer this question and determine how much the nutrient contents in the WRW would change with fermentation and how fermentation would affect the phosphorus (P)- and potassium (K)-solubilization bacteria in the WRW. Medium-grained rice was washed at a volumetric rice-to-water ratio of 1:3 for 90 seconds at 0.357 × *g*. WRW was then fermented for 0 (fresh), 3, 6, and 9 days. The rice grains and WRW were analyzed for pH, electrical conductivity (EC), carbon (C), nitrogen (N), sulfur (S), ammonium (NH_4^+), nitrate (NO_3^-), phosphorus (P), potassium (K), calcium (Ca), magnesium (Mg), copper (Cu), zinc (Zn), and boron (B), as well as for total microbial population and P- and K-solubilizing bacteria. Brown rice grains had 26 to 324% higher P, K, Mg, and Zn than white rice. Nutrient contents in the WRW increased with increasing fermentation, except for C, which decreased with fermentation. At 9 days of fermentation, P, Ca, Mg, Cu, and B in the white rice water increased by 4 to 207%, which were also higher than in the brown rice water. The microbial population increased with fermentation for 3 days, then decreased after that, following the same C trend in the WRW from both rice types. P-and K-solubilization by bacteria in the WRW from both rice types increased with fermentation. The P solubilization was 25% higher in brown rice water, while the

ARTICLE INFO

Article history:
Received: 24 June 2022
Accepted: 12 October 2022
Published: 22 December 2022

DOI: https://doi.org/10.47836/pjtas.46.1.04

E-mail addresses:
abba.nabayi@fud.edu.ng (Abba Nabayi)
chris@upm.edu.my (Christopher Boon Sung Teh)
tkz@upm.edu.my (Ali Kee Zuan Tan)
ngaipaing@upm.edu.my (Ngai Paing Tan)
* Corresponding author

ISSN: 1511-3701
e-ISSN: 2231-8542

K solubilization was 67% higher in white rice water. Fermented rice water from white and brown rice was revealed to potentially improve plant growth and increase overall soil health due to their plant nutrient and microbial contents.

Keywords: Elements, fermentation, ratio, rice, rice water, wastewater

INTRODUCTION

Washed rice water (WRW) is obtained when milled rice grains are washed to remove the bran, dust, and dirt from the rice before the rice is cooked (Juliano, 1993). However, significant proportions of water-soluble nutrients are removed because of rice washing. Several studies have indicated that rice washing leads to the leaching of different proportions of nutrients from the rice grains into the WRW (Juliano, 1985; Nabayi, Sung, Zuan, Paing, & Akhir, 2021). For example, Nabayi, Sung, Zuan, Paing, and Akhir (2021) reviewed that WRW contains between 40 to 150 mg L^{-1} N, 43 to 16306 mg L^{-1} P, 51 to 200 mg L^{-1} K, 8 to 3574 mg L^{-1} Ca, 36 to 1425 mg L^{-1} Mg, and 27 to 212 mg L^{-1} S. It indicates that these leached nutrients have enriched the WRW, which potentially could be utilized as a liquid plant fertilizer, rather than WRW being discarded (Nabayi, Sung, Paing, & Zuan, 2021b). Other studies have reported that WRW can be used as a plant nutrient source (Bahar, 2016; Suryana et al., 2017; Wardiah & Rahmatan, 2014) due to the presence of carbohydrates, proteins, vitamins, and other minerals at various concentrations (Juliano, 1985; Purnami et al., 2014).

Recently, WRW was reused as part of communal programs, whereby WRW from different households is collected, pooled centrally, then used for fertilizing crops. For instance, in Lambangkuning Village, Indonesia, a WRW reuse program was established. This program comprised about 30 households, each producing about 5 L of WRW daily, totaling 150 L per day. The collected WRW was then pooled for reuse later to irrigate the crops in the village homes (Supraptiningsih et al., 2019). Similarly, Polo Geulis, a village in Central Bogor, Indonesia, practiced a centralized water-saving system, where WRW was collected from the residents and used to irrigate and fertilize the village herbs and vegetables (The Jakarta Post, 2017). Kalsum et al. (2011) reported that fermented WRW contains numerous nutrients essential to plant growth and development. Hapsoh et al. (2019) found higher vegetative growth of pepper due to the bacterial content of fermented WRW. Similarly, several studies have reported using WRW to increase the growth of other crops (Bahar, 2016; Hariyadi, 2020; Karlina et al., 2013; Yulianingsih, 2017).

Sairi et al. (2018) found and biochemically identified the presence of beneficial microbes in WRW and suggested its use as a biofertilizer. Biofertilizer is recommended as part of sustainable agriculture, which aims to use fewer chemical fertilizers. The addition of beneficial microbes into the soil could

increase plant nutrient availability, thereby reducing the demand for chemical fertilizers (Çakmakçi et al., 2007). N_2-fixing and P and K solubilizing bacteria are of great importance for plant nutrition because they can increase plants' N, P, and K uptake (Çakmakçi et al., 2006; Ekin, 2010). In addition, the direct application of plant growth-promoting (PGP) microbes can improve plant growth (Kumar et al., 2014). PGP bacteria and rhizobia are vital in supplying nutrients to plants, particularly in less fertile soils (Tan et al., 2014). However, these WRW studies, mostly done on white rice, lacked scientific details, such as whether the WRW use was fresh or fermented, and if fermented, for how long and how rigorously the rice grains were washed, and what were the nutrient contents in the WRW.

Rice is a vital source of carbohydrates, protein, and other essential nutrients for billions of people worldwide, particularly in developing nations (Huang et al., 2016). It is usual to wash rice to remove dirt and dust before cooking. Considering the rate at which rice is consumed, the practice of reusing WRW has the potential to save significant amounts of water and fertilizers. In addition, it will lead to less reliance on energy, particularly during the current environment of detrimental climate change.

Rice parboiling ensures the retention of some nutrients contained in the rice bran (Roy et al., 2011). However, removing the outer bran layers while milling the white rice renders it low in nutrients and bioactive chemicals (Saleh, Wang, Wang, S. Yang, et al., 2019). Compared with white rice, whole brown rice grain has higher mineral contents because of the remaining presence of the outer bran layer (Babu et al., 2009; de Simone Carlos Iglesias Pascual et al., 2013; Saleh, Wang, Wang, L. Yang, et al., 2019). Nabayi, Sung, Paing, and Zuan (2021b), as well as Srinuttrakul and Busamongkol (2014), have reported that the elemental concentrations in white rice and brown rice grains ranged from (in mg kg^{-1}) 1298 to 3830 P, 1109 to 1928 K, 72 to 437 Ca, 240 to 1284 Mg, 0.31 to 0.37 B, 4.96 to 5.31 Cu, 5.10 to 9.75 Fe, 22 to 44 Mn, and 23 to 33 Zn. However, there is no comparative study of rice water from white and brown rice grains in terms of their nutrient and microbial contents and how the nutrient and microbial contents change when the rice water is fermented. Nabayi, Sung, Zuan, and Paing (2021a) reported the presence of beneficial bacteria in white rice water, but there has been no similar study on brown rice water. In addition, there are limited studies on assessing P- and K-solubilizing bacteria in rice water, which could play a significant role in the higher plant growth of many crops, as reported by Nabayi, Sung, Zuan, Paing, and Akhir (2021). Therefore, the objectives of this paper were to (1) analyze the nutrient contents in white and brown rice grains and their respective rice water at different fermentation periods and (2) assess the P and K solubilization in the white and brown rice water at different fermentation periods.

MATERIALS AND METHODS

Materials

"Rambutan" (Padiberas Nasional Berhad, Malaysia) and "Eco-brown" (Serba Wangi Sdn. Bhd., Malaysia) brands of white rice and brown rice grains, respectively, were used in this study. A mixing machine (Bossman Kaden matte BK-100S, Japan) was used for washing the rice grains at a volumetric rice-to-water ratio of 1:3 for 90 seconds at a speed of 0.357 × *g* to ensure consistency, repeatability, and uniformity in rice washing. WRW from the white rice and brown rice grains were then subjected to a series of fermentation periods of 0 (fresh), 3, 6, and 9 days. The choice of fermentation periods followed Akib et al. (2015), who fermented rice water for 0, 2, 4, and 6 days, and they reported an increase in microbial count over time. Therefore, this study selected 0, 3, 6, and 9 days to observe the nutrient and microbial population before the fourth and after the sixth days. The fermentation was carried out without adding additives by covering the WRW container for 0, 3, 6, and 9 days. The containers were opened daily for about 20 minutes for aeration.

Elemental Analyses

Dry ashing of rice samples was carried out following Enders and Lehmann (2012). About 1 g of the oven-dried (at 105 °C) ground rice grain samples were placed in a muffle furnace and heated sequentially from 200 to 550 °C for 6 hours to obtain complete ash for additional tests. The rice samples' total C, N, and S content were determined using the CNS analyzer (LECO Corp., MI, USA). In contrast, P, K, Ca, Mg, Cu, Zn, and B were determined using Inductively Coupled Plasma Optical Emission Spectrophotometry (ICP-OES) (Thermo Fisher Scientific, iCAP 6000, Germany). The rice water samples at different fermentation periods were filtered using Whatman 1 filter paper (11 µm size). The total C, N, and S of the rice water were determined by a CNS analyzer (LECO Corp., MI, USA). At the same time, the P, K, Ca, Mg, Cu, Zn, and B were analyzed using an atomic absorption spectrophotometer (AAS) (PerkinElmer, PinAAcle, 900T, USA). The Kjeldahl procedure (Nelson & Sommers, 1983) was employed for ammonium and nitrate determination. The 827 pH and EC lab meters were used to determine the pH and EC, respectively (Metrohm AG, Switzerland) (McLean, 1983).

Culture Media Preparation and Microbial Population Determination

Tryptic soy agar (TSA) and potato dextrose agar (PDA) were used to assess the bacteria and fungi population, respectively, in the different samples of the fermented rice water of the two rice grains, following Tan et al. (2014). The media were prepared by dissolving about 40 g each of TSA and PDA media and autoclaved at 121 psi for 20 minutes. The media were removed and poured into Petri dishes, then allowed to solidify under laminar flow. A serial dilution of up to 10^8 was performed on the different rice waters (from white and brown

rice) at different fermentation periods (0-, 3-, 6-, and 9-day). After that, the serially diluted rice water was introduced onto the plates containing the TSA and PDA-prepared media for bacteria and fungi determination, respectively. The inoculated plates were incubated for 24 hours at 33 °C, and subsequently, the bacterial and fungi populations were counted for each plate (in triplicates). Plates having between 30 to 300 colony-forming units were selected to calculate the microbial population per mL of sample (Thomas et al., 2015).

Phosphorus and Potassium Solubilization Ability of the WRW Culture

The National Botanical Research Institute's Phosphate (NBRIP) broth was used to measure the amount of soluble phosphate in the culture supernatants using the vanado-molybdo-phosphoric acid method (Ribeiro & Cardoso, 2012). A combination of a stock solution containing phosphoric acid (KH_2PO_4) and 5 mL of concentrated sulfuric acid (H_2SO_4) was made up to 1 L using distilled water to form a standard curve. Each NBRIP broth was inoculated with 10 µL of each WRW culture suspension. A flask containing 100 mL of NBRIP culture medium with no inoculum was used as the control. Tan et al. (2014) described that the flasks were incubated at room temperature between 25 to 29 °C for 12 days, with a steady agitation at 100 rpm. The P solubilization of the cultures was assessed at various fermentation periods at 12 days of incubation. At each assessment, 25 mL of each culture media was transferred to 50 mL tubes and centrifuged at 8,000 × *g* for 20 minutes. Next, the 2.5 mL of the supernatant was transferred to a 50 mL beaker, then 20 mL of distilled water was added. A 2.5 mL of Barton's reagent was promptly added for the mixing reaction (Barton, 1948), and color development was permitted for 10 minutes. A spectrophotometer (Agilent Technologies 8453 7 Cuvette UV Vis Spectrophotometer, USA) set to 430 nm was used to determine the absorbance.

The bacterial ability to release potassium from the Aleksandrov broth was used to calculate the potassium solubilization rate quantitatively. One mL of the WRW culture was inoculated into 100 mL of the broth overnight. The amount of K released in the broth was quantified from three flask replicates after 12 days of incubation (Nabayi, Sung, Zuan, Paing, & Akhir, 2021). The inoculated broth cultures were centrifuged at 6,700 × *g* for 10 minutes to separate the supernatant from the broth and bacterial cells. One mL of the supernatant was transferred to a 50 mL volumetric flask, which was then marked up with distilled water and carefully mixed. AAS was used to determine the amount of available K in the supernatant (PerkinElmer, PinAAcle, 900T, USA).

Statistical Analysis

All data were subjected to analysis of variance (ANOVA) using Minitab software package version 20 (Pennsylvania State University, USA). The data were analyzed based on a randomized design in factorial

arrangement with fermentation periods (0, 3, 6, and 9 days) and rice water types (white and brown rice water) as factors, and the Tukey's test procedure ($p < 0.05$) was used for the mean separations.

RESULTS AND DISCUSSION

Elemental Amount of Rice Grains

The highest element in white and brown rice grains was C which comprised about 40% of the total elements in the grains (Table 1). The inner endosperm of rice kernels is densely packed with starch, mainly carbohydrates (Saleh, Wang, Wang, L. Yang, et al., 2019; Zhou et al., 2002). The results showed that the nutrient contents are in the order: C > N > P > K > S > Mg > Ca > Zn > Cu > B for both rice types (Table 1). The elemental content of both rice grains was similar to the results obtained by Srinuttrakul and Busamongkol (2014), who also found that the nutrient contents of brown rice grains to be in the same order and ranged between (in mg kg^{-1}) 3024 to 3830 P, 140 to 1927 K, 980 to 1284 Mg, 72 to 128 Ca, and 23 to 33 Zn.

Nitrogen was the second highest element in both the rice grains, which agreed with Saleh, Wang, Wang, L. Yang, et al. (2019), who reported that protein, a source of N, is the second highest element in rice grains after C. Furthermore, Saleh, Wang, Wang, S. Yang, et al. (2019) reported that brown rice grains have greater N content than white rice grains because of their outer bran layer, which is the main source of N in the rice, which corroborated the results obtained in this study as brown rice grains had 2.4% higher N content than in white rice grains. The nutrient contents of the white and brown rice grains were generally similar to each

Table 1
Mean (± SE) nutrient content of the white and brown rice grains

Parameters	White rice grains	Brown rice grains
Ash content (%)	0.95 ± 0.04	1.76 ± 0.05
Moisture content (%)	14.39 ± 0.21	17.42 ± 0.18
Organic carbon (%)	30.30 ± 0.02	30.68 ± 0.06
C (%)	40.30 ± 0.01	40.80 ± 0.01
N (%)	1.25 ± 0.01	1.28 ± 0.01
C: N ratio	32.24 ± 0.01	31.87 ± 0.01
S (%)	0.10 ± 0.004	0.12 ± 0.03
NH_4^+ (mg kg^{-1})	215.45 ± 4.41	174.08 ± 4.13
NO_3^- (mg kg^{-1})	100.82 ± 8.53	131.76 ± 9.10
P (mg kg^{-1})	1320.83 ± 34.04	3284.62 ± 43.67
K (mg kg^{-1})	1130.83 ± 22.64	2081.17 ± 25.40
Ca (mg kg^{-1})	427.08 ± 5.72	163.32 ± 3.92
Mg (mg kg^{-1})	244.93 ± 10.26	759.50 ± 21.52
B (mg kg^{-1})	0.33 ± 0.09	1.40 ± 0.02
Cu (mg kg^{-1})	5.25 ± 0.12	5.15 ± 0.10
Zn (mg kg^{-1})	5.01 ± 0.09	6.30 ± 0.06

other for C, N, S, and Cu, but not for P, K, Ca, Mg, Zn, and B. Brown rice grains had 26 to 324% higher in P, K, Mg, and Zn, but lower in Ca by 162% than the white rice grains. The greater amount of Ca in the white rice grains could be due to rice varietal differences. Nutrient content in rice can vary between genotypes and environmental conditions (Huang et al., 2016). However, the higher P, K, Mg, Zn, and B in the brown rice grains were because of the intact bran layer in the brown rice, as compared with its absence in white rice grains. When the outer bran layers are removed during polishing or milling, the polished grain has fewer nutrients and bioactive chemicals because these elements are concentrated in the rice grain's outer bran layers (Saleh, Wang, Wang, S. Yang, et al., 2019; Sharif et al., 2014). The study also revealed a higher ash percentage (85%) in brown rice than in the white rice grains, indicating higher amounts of inorganic elements in brown rice (Table 1). Overall, the chemical analyses of the rice grains agreed with several studies that also reported greater nutrient content in brown rice as compared to white rice (Babu et al., 2009; de Simone Carlos Iglesias Pascual et al., 2013; Saleh, Wang, Wang, L. Yang, et al., 2019).

Effect of Fermentation on the Nutrient Content of WRW from White Rice and Brown Rice Grains

Nutrient analyses of white and brown rice water showed increasing levels of EC, (NH_4^+), N, S, P, K, Ca, Mg, Cu, and B with increasing fermentation periods. In contrast, increasing fermentation decreased pH, C, NO_3^-, and Zn levels (Table 2). Brown rice water was found to have significantly ($p < 0.01$) higher NH_4^+, N, S, and K contents on day 9 of the fermentation period at 4, 5, 7, and 122%, respectively, than the white rice water at the same fermentation period. However, white rice water recorded significantly ($p < 0.01$) higher contents in P, Ca, Mg, Cu, and B by 47, 4, 49, 77, and 207%, respectively, on day 9 of the fermentation period than on the brown rice water. The higher Ca, and Cu content in the white rice water could be due to the higher content of Ca and Cu in the white rice grains (Table 1), as reported too by other studies (Nabayi, Sung, Paing, & Zuan, 2021b; Saleh, Wang, Wang, L. Yang, et al., 2019). However, the higher P, Mg, and B in white rice water could be because of the mineralization of WRW by the microbes, which would lead to an increase in these elements due to the utilization of the highly available C as an energy source by the microbes. These results agreed with several studies that reported that fermentation of cereals had increased the concentrations of P, Ca, Mg, and Zn, mainly due to the loss of dry matter, as microbes mineralized the carbohydrate and protein contents in the cereals, leading to the availability of these elements (Blandino et al., 2003; Pranoto et al., 2013). Similarly, Nabayi, Sung, Paing, and Zuan (2021b) reported an increase in the nutrient content of white rice water with an increase in the fermentation period due to the mineralization by the microbes present in the fermented WRW. The greater P in the

white rice water, despite its lower content in the rice grains, could be attributed to the P solubilization by the beneficial microbes in the white rice water. Earlier studies had isolated and identified the presence of *Bacillus velezensis* and *Enterobacter mori* species in fermented white rice water (Nabayi, Sung, Zuan, & Paing, 2021a; Sairi et al., 2018), which were reported as plant growth-promoting bacteria that could solubilize P and K (Bhattacharyya & Jha, 2012; Deepa et al., 2008). The presence of nutrients and microbes in the rice water and their increase with fermentation could be the reasons for the higher growth of various plants, as found by several studies (Bahar, 2016; Hariyadi, 2020; Karlina et al., 2013; Yulianingsih, 2017). Iskarlia (2018) opined that rice water could be used as an organic fertilizer for plant use, while Supraptiningsih et al. (2019) stated that rice water could enhance soil fertility.

Higher levels of N, S, and K were found in the brown rice water because of their relatively higher concentrations in the brown rice grains (Table 2). Most of these elements are higher in the outer layer of the brown rice grains and washing the rice would lead to the leaching of these elements into the water. Protein, for instance, is concentrated in the outer bran layer of rice grains; hence, brown rice has a higher protein concentration than milled rice (Saleh, Wang, Wang, L. Yang, et al., 2019). The NO_3^- content in WRW increased with fermentation for the white and brown rice for 3 days, then declined after that. However, significantly higher ($p < 0.01$) NO_3^- was recorded in brown rice water at 3 days of fermentation, which was 20% more than in white rice water during the same fermentation period. The decline in NO_3^- after 3 days of fermentation could be due to denitrification during fermentation. The higher concentration of NO_3^- at 3 days was attributed to the higher bacterial population, which could indicate the presence of beneficial bacteria, such as N-fixing bacteria. Nabayi, Sung, Zuan, and Paing (2021a) found higher N-fixation bacteria in white rice water fermented for 3 days compared to other fermentation periods. Similarly, the increase in N and NH_4^+ with the fermentation period indicating the presence of N-fixation bacteria.

C content decreased with increasing fermentation by 71% and 62% in white and brown rice water, respectively, throughout the fermentation period. The higher C in the white rice water at day 0 of the fermentation period was because of the lack of the outer layer, which exposed the endosperm of the white rice grains and led to the higher leaching of C during the rice washing (unlike in the brown rice grains that still had their outer layer). The inner endosperm of rice kernels is densely packed with starch (Zhou et al., 2002). The decrease in C with fermentation was because C is an energy source for microbes. Significantly higher ($p < 0.05$) C at the lower fermentation period could indicate the limited activity of microbes, which agreed with the microbial population results (Figure 1).

Generally, the increase in the concentrations of the elements with increasing fermentation could be explained

Table 2
Mean (± SE) of the interaction between fermentation period and WRW types on pH, EC, N, C, S, NH_4^+, NO_3^-, P, K, Ca, Mg, Cu, Zn, and B

Parameters	Fermentation period (days)							
	0	3	6	9	0	3	6	9
	White rice water				Brown rice water			
pH	6.5 ± 0.20a	5.2 ± 0.12b	4.3 ± 0.10c	3.7 ± 0.11d	6.7 ± 0.21a	5.8 ± 0.13b	4.7 ± 0.10c	4.1 ± 0.08d
EC (µS cm^{-1})	563.7 ± 21.42a	613.3 ± 19.54b	677.0 ± 23.64b	783.4 ± 27.12c	291.1 ± 13.32c	332.0 ± 12.5c	382.7 ± 13.76d	412.7 ± 16.04d
C (%)	0.34 ± 0.021b	0.22 ± 0.016c	0.19 ± 0.017d	0.10 ± 0.010fg	0.21 ± 0.018a	0.14 ± 0.010e	0.11 ± 0.010ef	0.08 ± 0.008g
N (%)	0.015 ± 0.001c	0.017 ± 0.001bc	0.021 ± 0.002a	0.021 ± 0.002a	0.017 ± 0.001bc	0.018 ± 0.001b	0.021 ± 0.002a	0.022 ± 0.002a
S (%)	0.012 ± 0.001abc	0.011 ± 0.001bc	0.012 ± 0.001abc	0.014 ± 0.002a	0.010 ± 0.001c	0.013 ± 0.001ab	0.014 ± 0.002ab	0.015 ± 0.002a
NH_4^+ (mg L^{-1})	10.5 ± 0.71c	11.8 ± 0.67bc	13.9 ± 0.84a	13.9 ± 0.82a	11.4 ± 0.69bc	12.3 ± 0.82b	14.0 ± 0.91a	14.4 ± 0.92a
NO_3^- (mg L^{-1})	4.33 ± 0.39b	6.86 ± 0.54d	5.56 ± 0.48c	5.06 ± 0.51cd	5.30 ± 0.47c	8.20 ± 0.83a	4.30 ± 0.45d	5.17 ± 0.42cd
P (mg L^{-1})	90.8 ± 8.60e	209.7 ± 14.20b	264.1 ± 13.26a	264.9 ± 12.87a	84.0 ± 8.10e	106.7 ± 9.69e	153.7 ± 14.30d	180.7 ± 16.02c
K (mg L^{-1})	118.1 ± 10.90e	135.7 ± 11.41de	162.4 ± 12.10d	164.3 ± 13.54d	264.0 ± 14.90c	283.2 ± 18.93c	321.6 ± 18.39b	364.5 ± 17.92a
Ca (mg L^{-1})	8.48 ± 0.94b	13.53 ± 0.98a	13.69 ± 1.01a	14.61 ± 1.03a	8.06 ± 0.85b	13.08 ± 0.99a	14.03 ± 1.02a	14.01 ± 1.06a
Mg (mg L^{-1})	27.9 ± 1.16e	66.8 ± 3.20b	81.9 ± 5.32a	87.0 ± 5.95a	20.8 ± 0.87e	45.1 ± 3.24d	54.7 ± 4.11c	58.4 ± 4.63c
Cu (mg L^{-1})	0.08 ± 0.006a	0.104 ± 0.011b	0.112 ± 0.010c	0.115 ± 0.011a	0.026 ± 0.001c	0.031 ± 0.002c	0.040 ± 0.003c	0.065 ± 0.004c
Zn (mg L^{-1})	0.201 ± 0.012e	0.124 ± 0.011d	0.099 ± 0.006cd	0.032 ± 0.002e	0.585 ± 0.042a	0.436 ± 0.031b	0.333 ± 0.021c	0.311 ± 0.021c
B (mg L^{-1})	0.100 ± 0.072c	0.191 ± 0.081c	0.201 ± 0.013b	0.319 ± 0.021a	0.075 ± 0.004c	0.095 ± 0.004c	0.171 ± 0.083b	0.104 ± 0.067c

Note. Means that different letter(s) within the same rows are statistically different ($p < 0.05$) according to Tukey's test

in two ways. First, the solubility of these elements in water could have played a role in their higher availability, as some elements have a higher solubility in water than others (Petrucci et al., 2011). Second, the presence of these elements in the water led to the colonization of the WRW by microbes. In the process, they break down the C content and fix and solubilize additional elements, such as N, P, and K. Therefore, the increase in the elements with fermentation was because of the beneficial microbes in the fermented rice water, which corroborated with other studies that reported the presence of beneficial microorganisms in fermented white rice water (Nabayi, Sung, Zuan, & Paing, 2021a, Nabayi, Sung, Paing, & Zuan, 2021b; Sairi et al., 2018).

Effect of Fermentation Period on the Microbial Population in WRW from White Rice and Brown Rice

Higher bacteria and fungi populations were found on day 3 of the fermentation in the white and brown rice water, while the least was recorded on day 0 (Figure 1). However, brown rice water had a greater bacterial population at all levels of fermentation than white rice water. For instance, on day 3 of the fermentation period, the brown rice water had an 89% increase in bacterial population than the white rice water. The higher bacterial population in brown rice water could be attributed to the brown rice grains' higher P, K, Mg, B, and Zn elements (Table 1). In addition, Brown rice grains have higher mineral elements because of the outer bran layer, which contains significant proportions of elements compared to white rice grains (Saleh, Wang, Wang, L. Yang, et al., 2019).

In contrast, the white rice water had a 71% higher fungi population than the brown rice water on day 3 of the fermentation period, which decreased with increasing fermentation regardless of the rice type. The decrease in microbial population (bacteria and fungi) with increasing fermentation was because of microbial competition, as the C was the only energy source for the microbes. Therefore, this indicated that the rice water could not sustain the proliferation of the microbes beyond 3 days. These results agreed with studies that reported a decrease in the microbial population in white rice water with increasing fermentation due to the decrease in the C content of the white rice water (Akib et al., 2015; Nabayi, Sung, Zuan, & Paing, 2021a, Nabayi, Sung, Paing, & Zuan, 2021b). For the different fermentation periods (except for day 0) and rice water types, the bacterial populations were within the range expected for microbial colonization (10^6 colony-forming units per mL), as stated by Thomas et al. (2015). The pH of the WRW decreased with increasing fermentation, irrespective of the rice type. The decrease in pH of the rice water agreed with Nabayi, Sung, Zuan, and Paing (2021a) as well as Rousk et al. (2009), who reported a lower pH (acidic) with fermentation due to the microbial activity that produced organic acids and thereby lowering the pH of the culture.

Effect of Fermentation Period on Phosphorus and Potassium Solubilization of WRW from White Rice and Brown Rice Grains

After each fermentation period, i.e., 0-, 3-, 6-, and 9-day, the WRW was incubated for 12 days and tested for P and K solubilization (Figure 2). The highest P solubilization was found at 6-and 9-day fermentation periods for brown rice and white rice water. On average, brown rice water had 22% higher P solubilization across all fermentation periods than white rice water. However, K solubilization was highest on 3-day fermentation and decreased with increasing fermentation for rice water. The white rice water had 67% higher K solubilization than the brown rice water, despite having a lower K grain content. This increase could be explained by P and K solubilizing microbes, as indicated by the microbial population results (Figure 1). The general decrease in the microbial population after 3 days of fermentation could indicate the decrease in the K solubilization bacteria in the rice water. This result agreed with other studies that reported a decrease in microbial population because of the decrease in the C content of white rice water (Akib et al., 2015; Nabayi, Sung, Zuan, & Paing, 2021a, Nabayi, Sung, Paing, & Zuan, 2021b). The P and K solubilization of rice water by microorganisms is sustained by the C content of the rice water, which the microbes use as energy. He et al. (2016) stated that WRW could be used as a source of C for microorganisms. In addition, Adugna (2016) stated that the effectiveness and availability of microorganisms depend on the availability of C.

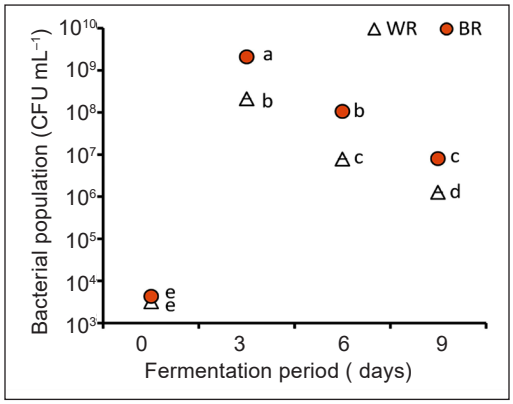

(a)

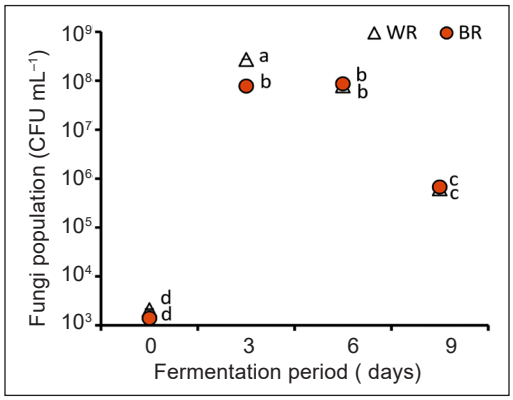

(b)

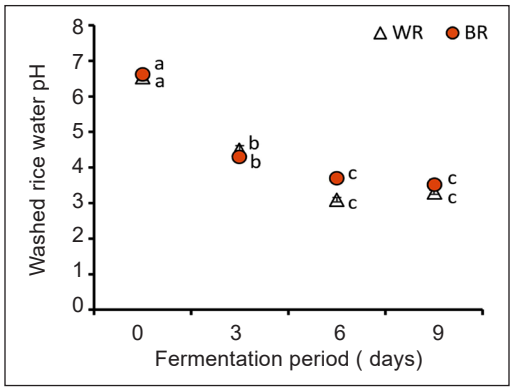

(c)

Figure 1. Mean (±SE) of (a) total bacteria population, (b) fungi population, and (c) pH in white rice water (WR) and brown rice water (BR) at different fermentation periods. For the same chart, means with different letters are significantly ($p < 0.05$) different from each other using Tukey's test

Note. BR = Brown rice water; WR = White rice water; CFU = Colony forming unit

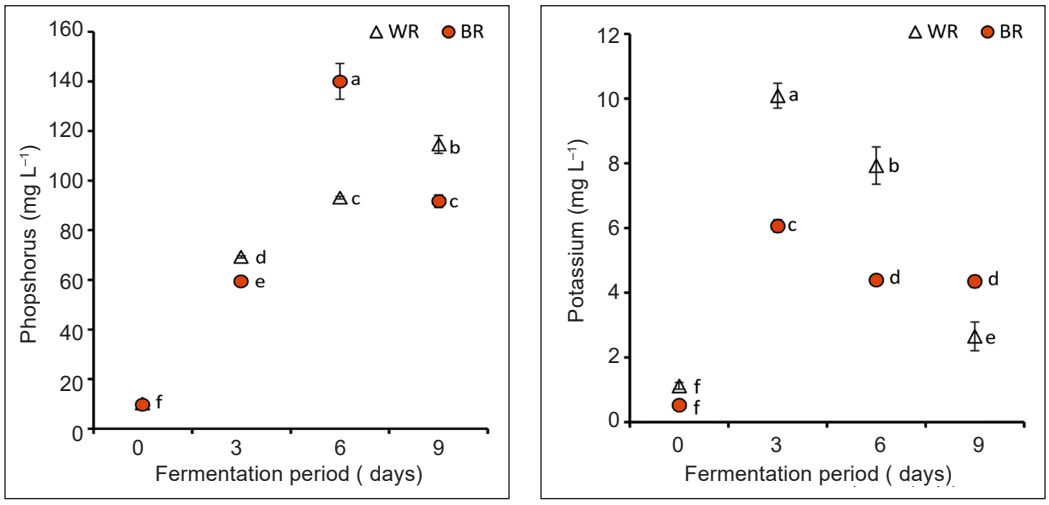

(a) (b)

Figure 2. Mean (±SE) of quantitative solubilization of (a) phosphorus and (b) potassium of white rice water (WR) and brown rice water (BR) fermented at different periods. For the same chart, means with different letters are significantly ($p < 0.05$) different from each other using Tukey's test
Note. WR = White rice water; BR = Brown rice water; CFU = Colony forming unit

Therefore, the increase in P and K in the rice water was because of the presence of P and K solubilizing bacteria that colonized the rice water due to fermentation. Nabayi, Sung, Zuan, and Paing (2021a) reported the presence of *Bacillus* spp. and *Enterobacter* spp. in white rice water, and studies have identified the *Bacillus* and *Enterobacter* species as plant growth-promoting bacteria that could solubilize P and K (Bhattacharyya & Jha, 2012; Deepa et al., 2008). The P solubilization rates of both rice water found in this study were higher than the bacterial strains used by Sugumaran and Janarthanum (2007) as well as Tan et al. (2014), which solubilized a maximum of 14.15 mg L^{-1} and 4.29 mg L^{-1}, respectively, after 5 and 4 days of incubation. The use of microbes as biofertilizer components to improve soil health and plant productivity is considered an alternative to chemical fertilizers (Suhaimee et al., 2021). Park and DuPonte (2008) reported that beneficial microbes provide their benefits to crops through root colonization to stimulate growth and development. Bacteria that can solubilize nutrients like P and K are essential because they can convert insoluble P and K in soils into soluble forms. P and K solubilization could significantly benefit the plants because phosphorus is relatively immobile, making soils and plants deficient in P since this nutrient is unavailable for plant uptake. The enhanced P and K release by bacteria is linked to the bacteria synthesizing acids, alkalis, or chelates (Tan et al., 2014). The use of fermented rice water could reduce the need for inorganic fertilizers through the beneficial roles of the microbes present, such as P and K solubilizing microbes found in this study and through catalase and indole acetic acid production and N-fixation ability

of the microbes as reported by other studies (Akib et al., 2015; Nabayi, Sung, Zuan, & Paing, 2021a; Sairi et al., 2018).

CONCLUSION

White rice water had 5 to 208% higher nutrients than brown rice water, despite the higher nutrient content of the brown rice grains. The elements in both rice water increased with increasing fermentation. The microbial population in rice water was the highest on day 3 and, after that, decreased. Both rice waters showed microbial P- and K-solubilizing activities throughout the fermentation period. Other essential microbial analyses of the rice water, such as N-fixation, catalase, and phytohormone production potentials due to the presence of the microbes in the WRW, need to be further carried out to prove the worth of using WRW as a source of plant nutrients. Therefore, the results of this study suggest that continuous application of WRW into the soil as a nutrient source would positively impact plant growth and soil fertility. The presence of beneficial microorganisms in the fermented WRW, common wastewater in households, makes it suitable for sustainable agriculture as these microbes would impact plant growth and soil fertility without endangering the environment, as is the case with chemical fertilizers.

FUNDING

This research was funded by the Universiti Putra Malaysia Grant 2022, Geran Inisiatif Putra Siswazah (GP IPS) (No. GP IPS/2022/9709600).

ACKNOWLEDGMENTS

The authors would like to acknowledge TETFund Nigeria for providing a Ph.D. scholarship to the first author. The authors also acknowledged colleagues and staff at Universiti Putra Malaysia Selangor Campus for their support and cooperation.

DECLARATION OF COMPETING INTEREST

The authors declare that they have no known competing financial interests or personal relationships that could have appeared to influence the work reported herein.

REFERENCES

Adugna, G. (2016). A review on impact of compost on soil properties, water use and crop productivity. *Academic Research Journal of Agricultural Science and Research*, *4*(3), 93-104. https://doi.org/ 10.14662/ARJASR2016.010

Akib, M. A., Setiawaty, H., Haniarti, H., & Sulfiah, S. (2015). Improving the quality of "Leri" rice washing waste by different period of fermentation and yeast concentration as an alternative liquid organic fertilizer. *International Journal of Agriculture System*, *2*(2), 153-162. https://doi.org/10.20956/ijas.v2i2.31

Babu, P. D., Subhasree, R. S., Bhakyaraj, R., & Vidhyalakshmi, R. (2009). Brown rice - Beyond the color reviving a lost health food – A review. *American-Eurasian Journal of Agronomy*, *2*(2), 67–72.

Bahar, A. E. (2016). Pengaruh pemberian limbah air cucian beras terhadap pertumbuhan tanaman kangkung darat (*Ipomoea reptans* Poir) [Effect of applying washed rice wastewater on the growth of land spinach (*Ipomoea reptans* Poir)]. *Jurnal Ilmiah Mahasiswa Fakultas Pertanian*, *3*(2).

Barton, C. J. (1948). Photometric analysis of phosphate rock. *Analytical Chemistry*, *20*(11), 1068–1073. https://doi.org/10.1021/ac60023a024

Bhattacharyya, P. N., & Jha, D. K. (2012). Plant growth-promoting rhizobacteria (PGPR): Emergence in agriculture. *World Journal of Microbiology and Biotechnology*, *28*(4), 1327–1350. https://doi.org/10.1007/s11274-011-0979-9

Blandino, A., Al-Aseeri, M. E., Pandiella, S. S., Cantero, D., & Webb, C. (2003). Cereal-based fermented foods and beverages. *Food Research International*, *36*(6), 527–543. https://doi.org/10.1016/S0963-9969(03)00009-7

Çakmakçi, R., Dönmez, F., Aydın, A., & Şahin, F. (2006). Growth promotion of plants by plant growth-promoting rhizobacteria under greenhouse and two different field soil conditions. *Soil Biology and Biochemistry*, *38*(6), 1482-1487. https://doi.org/10.1016/j.soilbio.2005.09.019

Çakmakçi, R., Dönmez, M. F., & Erdoğan, Ü. (2007). The effect of plant growth promoting rhizobacteria on barley seedling growth, nutrient uptake, some soil properties, and bacterial counts. *Turkish Journal of Agriculture and Forestry*, *31*(3), 189-199.

de Simone Carlos Iglesias Pascual, C., Massaretto, I. L., Kawassaki, F., Barros, R. M. C., Noldin, J. A., & Marquez, U. M. L. (2013). Effects of parboiling, storage and cooking on the levels of tocopherols, tocotrienols and γ-oryzanol in brown rice (*Oryza sativa* L.). *Food Research International*, *50*(2), 676–681. https://doi.org/10.1016/j.foodres.2011.07.013

Deepa, G., Singh, V., & Naidu, K. A. (2008). Nutrient composition and physicochemical properties of Indian medicinal rice – Njavara. *Food Chemistry*, *106*(1), 165-171. https://doi.org/10.1016/j.foodchem.2007.05.062

Ekin, Z. (2010). Performance of phosphate solubilizing bacteria for improving growth and yield of sunflower (*Helianthus annuus* L.) in the presence of phosphorus fertilizer. *African Journal of Biotechnology*, *9*(25), 3794-3800.

Enders, A., & Lehmann, J. (2012). Comparison of wet-digestion and dry-ashing methods for total elemental analysis of biochar. *Communication in Soil Science and Plant Analysis*, *43*(7), 1042–1052. https://doi.org/10.1080/00103624.2012.656167

Hapsoh., Dini, I. R., Salbiah, D., & Kusmiati. (2019). Growth and pepper yields (*Capsicum annuum* L.) by giving a formulation of biological fertilizer of cellulolytic bacteria based on organic liquid waste. In *Journal of Physics: Conference Series* (Vol. 1351, No. 1, p. 012097). IOP Publishing. https://doi.org/10.1088/1742-6596/1351/1/012097

Hariyadi, S. P. (2020). The effect of watering on rice washing water, MSG water, and AC (air conditioner) wastewater on yields components and tomato yields (*Lycopersicon esculentum* L.) in the deep peatland. *Universal Journal*, *2*(4).

He, Q., Feng, C., Hu, Q., Li, R., & Chen, N. (2016). Biological denitrification using rice washing drainage (RWD) as carbon source for removing nitrate from groundwater. *Desalination and Water Treatment*, *57*(46), 21990–21999. https://doi.org/10.1080/19443994.2015.1127780

Huang, Y., Tong, C., Xu, F., Chen, Y., Zhang, C., & Bao, J. (2016). Variation in mineral elements in grains of 20 brown rice accessions in two environments. *Food Chemistry*, *192*, 873–878. https://doi.org/10.1016/j.foodchem.2015.07.087

Iskarlia, G. R. (2018). Pertumbuhan sayur sawi hidroponik menggunakan nutrisi air cucian beras dan cangkang telur ayam [The growth of hydroponic mustard plant (*Brassica rapa* L.) using the nutrition of washed rice water and chicken egg shells]. *AgricSains*, *3*(2), 42-51.

Juliano, B. O. (Ed.) (1985). *Rice: Chemistry and technology* (2nd ed.). American Association of Cereal Chemists.

Juliano, B. O. (1993). *Rice in human nutrition*. Food and Agriculture Organization of the United Nations.

Kalsum, U. S., Fatimah, & Wasonowati, C. (2011). Efektivitas pemberian air leri terhadap pertumbuhan dan hasil jamur tiram putih (*Pleurotus ostreatus*) [Effectiveness of washed rice water provision on growth and yield of white oyster mushroom (*Pleurotus ostreatus*)]. *Journal of Agrovigor*, *4*(2), 86-92. https://doi.org/10.21107/agrovigor.v4i2.297

Karlina, A., Yursida, & Ruli, J. P. (2013). Tanggap pertumbuhan kangkung (*Ipomea reptans*) terhadap aplikasi poc urin sapi dan pupuk organik di lahan pasang surut tipe luapan C [Growth response of water spinach (*Ipomea reptans*) to the application of liquid organic fertilizer from cow urine and organic fertilizer in tidal land overflow type C]. *JurnalIlmiah AgrIBA*, *1*, 1158-2303.

Kumar, A., Maurya, B. R., & Raghuwanshi, R. (2014). Isolation and characterization of PGPR and their effect on growth, yield and nutrient content in wheat (*Triticum aestivum* L.). *Biocatalysis and Agricultural Biotechnology*, *3*(4), 121-128. https://doi.org/10.1016/j.bcab.2014.08.003

McLean, E. O. (1983). Soil pH and lime requirement. In A. L. Page (Ed.), *Methods of soil analysis: Part 2 Chemical and microbiological properties* (2nd ed., pp. 199–224). American Society of Agronomy, Crop Science Society of America, and Soil Science Society of America. https://doi.org/10.2134/agronmonogr9.2.2ed.c12

Nabayi, A., Sung, C. T. B., Zuan, A. T. K., & Paing, T. N. (2021a). Fermentation of washed rice water increases beneficial plant bacterial population and nutrient concentrations. *Sustainability*, *13*(23), 13437. https://doi.org/10.3390/su132313437

Nabayi, A., Sung, C. T. B., Zuan, A. T. K., Paing, T. N., & Akhir, N. I. M. (2021). Chemical and microbial characterization of washed rice water waste to assess its potential as plant fertilizer and for increasing soil health. *Agronomy*, *11*(12), 2391. https://doi.org/10.3390/agronomy11122391

Nabayi, A., Sung, C. T. B., Paing, T. N., & Zuan, A. T. K. (2021b). Wastewater from washed rice water as plant nutrient source: current understanding and knowledge gaps. *Pertanika Journal of Science and Technology*, *29*(3), 1347–1369. https://doi.org/10.47836/pjst.29.3.11

Nelson, D. W., & Sommers, L. (1983). Total carbon, organic carbon, and organic matter. In A. L. Page (Ed.), *Methods of soil analysis: Part 2 Chemical and microbiological properties* (2nd ed., pp. 539–579). American Society of Agronomy, Crop Science Society of America, and Soil Science Society of America. https://doi.org/10.2134/agronmonogr9.2.2ed.c29

Park, H., & DuPonte, M. W. (2008). *How to cultivate indigenous microorganisms*. https://www.ctahr.hawaii.edu/oc/freepubs/pdf/bio-9.pdf

Petrucci, R. H., Herring, F. G., Bissonnette, C., & Madura, J. D. (2011). *General chemistry: Principles and modern applications* (10th ed.). Prentice Hall.

Pranoto, Y., Anggrahini, S., & Efendi, Z. (2013). Effect of natural and *Lactobacillus plantarum* fermentation on *in-vitro* protein and starch digestibilities of sorghum flour. *Food Bioscience*, *2*, 46–52. https://doi.org/10.1016/j.fbio.2013.04.001

Purnami, W. G., Yuswanti, N. H., & Astiningsih, M. A. (2014). Effect of type and frequency of washed rice water on growth of orchid seeds (*Phalaenopsis* sp.) after acclimatization. *Jurnal of Agroekoteknologi Tropica*, *3*(1), 22-31.

Ribeiro, C. M., & Cardoso, E. J. B. N. (2012). Isolation, selection and characterization of root-associated growth promoting bacteria

in Brazil Pine (*Araucaria angustifolia*). *Microbiology Research*, *167*(2), 69–78. https://doi.org/10.1016/j.micres.2011.03.003

Rousk, J., Brookes, P. C., & Bååth, E. (2009). Contrasting soil pH effects on fungal and bacterial growth suggest functional redundancy in carbon mineralization. *Applied and Environmental Microbiology*, *75*(6), 1589–1596. https://doi.org/10.1128/AEM.02775-08

Roy, P., Orikasa, T., Okadome, H., Nakamura, N., & Shiina, T. (2011). Processing conditions, rice properties, health and environment. *International Journal of Environmental Research and Public Health*, *8*(6), 1957-1976. https://doi.org/10.3390/ijerph8061957

Sairi, F., Ismail, N., & Ibrahim, N. (2018). The effect of FRAW towards the growth of chilli seedlings and its associated microorganisms. *Malaysian Journal of Microbiology*, *14*(6), 606-610. https://doi.org/10.21161/mjm.1461822

Saleh, A. S. M., Wang, P., Wang, N., Yang, S., & Xiao, Z. (2019). Technologies for enhancement of bioactive components and potential health benefits of cereal and cereal-based foods: Research advances and application challenges. *Critical Reviews in Food Science and Nutrition*, *59*(2), 207-227. https://doi.org/10.1080/10408398.2017.1363711

Saleh, A. S. M., Wang, P., Wang, N., Yang, L., & Xiao, Z. (2019). Brown rice versus white rice: Nutritional quality, potential health benefits, development of food products, and preservation technologies. *Comprehensive Reviews in Food Science and Food Safety*, *18*(4), 1070-1096. https://doi.org/10.1111/1541-4337.12449

Sharif, M. K., Butt, M. S., Anjum, F. M., & Khan, S. H. (2014). Rice bran: A novel functional ingredient. *Critical Reviews in Food Science and Nutrition*, *54*(6), 807–816. https://doi.org/10.1080/10408398.2011.608586

Srinuttrakul, W., & Busamongkol, A. (2014). Elemental analysis of brown rice by inductively coupled plasma atomic emission spectrometry and instrumental neutron activation analysis. *Energy Procedia*, *56*, 85–91. https://doi.org/10.1016/j.egypro.2014.07.135

Sugumaran, P., & Janarthanam, B. (2007). Solubilization of potassium containing minerals by bacteria and their effect on plant growth. *World Journal of Agricultural Sciences*, *3*(3), 350-355.

Suhaimee, S., Ibrahim, I. Z., & Abdul Wahab, M. A. M. (2021). *Organic agriculture in Malaysia*. Food and Fertilizer Technology Center for the Asian and Pacific Region – Agricultural Policy Platform. https://ap.fftc.org.tw/article/1010

Supraptiningsih, L. K., Nuriyanti, R., & Sutrisno, A. (2019). Processing household waste (washed rice water) into liquid organic fertilizer in Probolinggo Regency Empowering. *Journal Pengabdian Masyarakat Fakulti Psikologi*, *3*, 12-20.

Suryana, H., Titiaryanti, M., & Yuniasih, B. (2017). Pengaruh macam dan dosis limbah terhadap pertumbuhan bibit kelapa sawit (pre nursery) **[**Effect of types and doses of waste on the growth of oil palm seedlings (pre nursery)]. *Jurnal Agromast*, *2*(1).

Tan, K. Z., Radziah, O., Halimi, M. S., Khairuddin, A. R., Habib, S. H., & Shamsuddin, Z. H. (2014). Isolation and characterization of rhizobia and plant growth-promoting rhizobacteria and their effects on growth of rice seedlings. *American Journal of Agricultural and Biological Sciences*, *9*(3), 342–360. https://doi.org/10.3844/ajabssp.2014.342.360

The Jakarta Post. (2017). *Village in Bogor uses leftover rice water to grow plants*. The Jakarta Post. https://www.thejakartapost.com/news/2017/10/07/village-in-bogor-uses-leftover-rice-water-to-grow-plants.html

Thomas, P., Sekhar, A. C., Upreti, R., Mujawar, M. M., & Pasha, S. S. (2015). Optimization of single plate-serial dilution spotting (SP-SDS) with sample anchoring as an assured method for bacterial and yeast cfu enumeration and single colony isolation from diverse samples. *Biotechnology Reports*, *8*, 45–55. https://doi.org/10.1016/j.btre.2015.08.003

Wardiah, L., & Rahmatan, H. (2014). Potensi limbah air cucian beras sebagai pupuk organik cair pada pertumbuhan pakchoy (*Brassica rapa* L.) [The capacity of rice water as organic liquid fertilizer for the growth of pakchoy (*Brassica rapa* L.)]. *Jurnal Biologi Edukasi*, *6*(1), 34-38.

Yulianingsih, R. (2017). Pengaruh air cucian beras terhadap pertumbuhan dan hasil terung ungu (*Solanum melongena* L.) [Effect of rice washing water on growth and yield of superior eggplant (*Solanum melongea* L.)]. *Publikasi Informasi Pertanian*, *13*(24), 61-68.

Zhou, Z., Robards, K., Helliwell, S., & Blanchard, C. (2002). Composition and functional properties of rice. *International Journal of Food Science and Technology*, *37*(8), 849–868. https://doi.org/10.1046/j.1365-2621.2002.00625.x

Pertanika J. Trop. Agric. Sci. 46 (1): 67 - 90 (2023)

PERTANIKA JOURNALS

TROPICAL AGRICULTURAL SCIENCE

Journal homepage: http://www.pertanika.upm.edu.my/

In silico Analysis of *OsNRT2.3* Reveals *OsAMT1.3*, *OsZIFL9*, *OsbZIP27*, and *OsIRT1* as Potential Drought-Related Genes During Nitrogen Use Efficiency in *Oryza sativa* L.

Muhammad-Redha Abdullah-Zawawi[1], Karwatik Busiri[2], Syafiqah Johan[2], Mohammad Asad Ullah[2] and Zamri Zainal[2,3]*

[1]*UKM Medical Molecular Biology Institute (UMBI), UKM Medical Centre, Jalan Ya'acob Latiff, Bandar Tun Razak, 56000 Cheras, Kuala Lumpur, Malaysia*
[2]*Faculty of Science and Technology, Universiti Kebangsaan Malaysia, 43600, Bangi, Selangor, Malaysia*
[3]*Institute of Systems Biology, Universiti Kebangsaan Malaysia, 43600, Bangi, Selangor, Malaysia*

ABSTRACT

Nitrate transporter (NRT) is responsible for the molecular mechanism of the root nitrate (NO_3^-) uptake system for plant development. Although several *NRT* genes are identified and characterised in plants, knowledge of the *NRT2* gene family and its nitrogen use efficiency (NUE) function in drought stress has remained elusive in rice. This study conducted an *in silico* analysis on 20 NRT2 family genes of rice, wheat, soybean, barley, maize, and papaya. Phylogenetic and motifs analysis clustered genes encoding NRT2 proteins into four monophyletic groups, and the motifs of *NRT2* genes were significantly conserved for the specific domain of NO_3^- transmembrane transporter. Interestingly, co-expression analysis revealed that potential drought-related genes were expressed similarly to the functional NUE gene, *OsNRT2.3*. Furthermore, half of the co-expressed genes were enriched in nitrogen use efficiency (NUE)-related processes, such as transport, stress, macromolecule metabolic pathways, and transcription regulation. Expression pattern analysis of *OsNRT2.3* and its co-expressed genes in tissue-specific and nitrogen (N) response led to the discovery of *OsAMT1.3*, *OsZIFL9*, *OsbZIP27*, and *OsIRT1* as four strong candidates to participate in drought stress during NO_3^- uptake system. The co-expression of iron (Fe) uptake genes, *OsZIFL9* and *OsIRT1*, with *OsNRT2.3* also suggested a possible interaction of Fe and

ARTICLE INFO

Article history:
Received: 28 July 2022
Accepted: 05 October 2022
Published: 22 December 2022

DOI: https://doi.org/10.47836/pjtas.46.1.05

E-mail addresses:
mraz@ukm.edu.my (Muhammad-Redha Abdullah-Zawawi)
karwatik96@gmail.com (Karwatik Busiri)
syafiqahjohan96@gmail.com (Syafiqah Johan)
P95693@siswa.ukm.edu.my (Mohammad Asad Ullah)
zz@ukm.edu.my (Zamri Zainal)
* Corresponding author

ISSN: 1511-3701
e-ISSN: 2231-8542

nitrogen (N) during an increasing amount of Fe, which led to the acidification of rice apoplasts during water deficiency. Together, this study will provide a valuable resource for potential candidate genes that can further investigate their molecular response to drought during NUE.

Keywords: Drought stress, *in silico*, nitrogen use efficiency, *NRT2.3*, *Oryza sativa* L.

INTRODUCTION

Rice (*Oryza sativa* L.) is a major staple food consumed by the world's population, particularly in Asian countries. According to the Food and Agriculture Organization of the United Nations (FAO) (2017), the global population is expected to reach 9 billion by 2050, with food supplies increasing by 70% to 100%. Therefore, rice production must be significantly increased to meet the outburst of the world population. As one of the world's largest consumers, Malaysia has been importing 30% to 40% of its rice consumption annually for the last 30 years and will continue to be a net rice importer in the future (Khazanah Research Institute, 2019). To ensure the country's demand in the future, Malaysia must alleviate the production of high-quality rice by adhering to good agricultural practices. However, farmers face frequent diseases and pests, resulting in significant economic loss. Therefore, nutrient management has emerged as a critical, cost-effective strategy for increasing crop productivity in intensive agricultural practices worldwide, considering the abovementioned points.

Nitrogen (N) is an essential macro element for plant growth and development. N availability is a major limiting factor in rice crop growth and yield among the macroelements. Nitrogen is required in large quantities compared to other nutrients (Djaman et al., 2018). Thus, proper N fertiliser applications are crucial to enhance grain yield and grain quality in rice farming. Unfortunately, excessive use of N fertiliser in rice farming causes irreparable damage to soil structure, mineral cycles, soil microbial flora, and plants (K. Wu et al., 2021).

NUE, in general, consists of two key components: N uptake efficiency (NUpE), which is the efficiency of absorption of supplied N, and N utilisation efficiency (NUtE), which is the efficiency of assimilation and remobilisation of plant N in producing grain. NUE is inherently complex, owing to the interaction of multiple genes with environmental factors. N was primarily obtained by the plant in the form of nitrate (NO_3^-) or ammonium (NH_4^+) (Ranade-Malvi, 2011; Xu et al., 2012). The anionic form of NO_3^- is easily soluble in water and easily mobilised in soil (Jin et al., 2015). NO_3^- is absorbed through roots and transported to all parts of the plant via NO_3^- transporters or by producing amino acids through an assimilation process before being redistributed (Xu et al., 2012). Plants developed two nitrate transport systems to regulate nitrate: a high-affinity NO_3^- transport system (HATS) and a low-affinity NO_3^- transport system (LATS) (Huang et al., 2018).

Nitrate transporters are divided into four prominent protein families, including nitrate transporter 1 (NRT1) or peptide transporter (PTR), also known as NPF, nitrate transporter 2 (NRT2), chloride channel (CLC), and slow anion channel (SLAC1/SLAH) (Y. Y. Wang et al., 2012). Many studies on the molecular mechanism of the root nitrate uptake system have revealed that nitrate transporter gene families, *NRT1* and *NRT2*, were involved in the LATS and HATS systems, respectively (Fenchel et al., 2012; Forde, 2000; Orsel et al., 2002). In *Arabidopsis*, *AtNRT2.1* was reported as crucial in root architecture response due to low nitrate accumulation during lateral root initiation (Little et al., 2005; Remans et al., 2006). However, most of the NRT2 family members cannot transport NO_3^- independently as a pair protein called nitrate transporter-activating protein 2 (NAR2) is required to play a role in nitrate assimilation. In rice, three *OsNRT2* members, including *OsNRT2.1*, *OsNRT2.2*, and *OsNRT2.3a*, need the paired protein, *OsNAR2.1*, to absorb nitrate, whereas *OsNRT2.3b* and *OsNRT2.4* can function independently (Wei et al., 2018). Interestingly, few studies were conducted on *OsNRT2.3*, despite its importance in regulating NO_3^- transport in the root system as the root architecture changes in response to N-deficiency, thereby improving the NUE.

Drought and N deficiency induce adaptative responses such as root elongation, cell-damaging ROS production, and photosynthesis reduction. For example, reactive oxygen species (ROS) levels were reported to elevate in certain root areas during N deficiency due to reduced photosynthesis caused by drought stress (Safavi-Rizi et al., 2021). Previous studies have reported that drought stress affects the expression of key genes or QTLs associated with nitrogen management in rice. For instance, *ARE1* is associated with high yield under N-deficiency (Q. Wang et al., 2018), *qGYLN7* and *qGYPP-4b* increase grain yield under low N conditions (H. H. Tong et al., 2011; Rao et al., 2018), and *qRL6.1* enhances root elongation under deficient NH_4^+ condition (Obara et al., 2010).

In this study, *in silico* analyses were conducted to gain insights into an exhaustive knowledge of the function of the high-affinity nitrate transporter gene 2.3 (*NRT2.3*) in *O. sativa*. The members of the NRT family in rice and selected plants, such as soybean, maize, papaya, *Arabidopsis*, wheat, and barley, were analysed by executing bioinformatics approaches on the publicly available genome and protein sequences. In particular, a common and distinct organisation of functional motifs was identified among the phylogenetic tree of the NRT family, depicting evolutionary relationships among them. Subsequently, a *cis*-element regulatory analysis was also examined to determine the involvement of *OsNRT2.3* as a stress-responsive protein during NUE. Finally, co-expression analysis was performed to decipher the potential function of *OsNRT2.3* with correlated genes in NUE processes and later observed their expression profiles using publicly available microarray data. Protein-protein interaction analysis suggests that most correlated *OsNRT2.3* genes may interact

under the NUE functionally. The findings may contribute to a better understanding of its role in NUE for the genetic improvement of agronomic crops.

MATERIALS AND METHODS

Retrieval of NRT2 Family Gene Sequences from Databases

The complete coding sequence and protein sequence of the high-affinity nitrate transporter 2, NRT2 family genes from rice (*Oryza sativa*) and selected species, such as soybean (*Glycine max*), maize (*Zea mays*), papaya (*Carica papaya*), and *Arabidopsis* (*Arabidopsis thaliana*), were obtained from Plaza v3.0 (https://bioinformatics.psb.ugent.be/plaza/) (Proost et al., 2015). Meanwhile, *NRT2* sequences of wheat (*Triticum aestivum*) were obtained from the National Center for Biotechnology Information (NCBI) (https://www.ncbi.nlm.nih.gov) (Sayers et al., 2021) and barley (*Hordeum vulgare*) from GrainGenes (https://wheat.pw.usda.gov) (Matthews et al., 2003). The pI/Mw tool (https://web.expasy.org/compute_pi/) was employed to calculate the molecular weight (Mw) and isoelectric point (pI) of the NRT2 encoding protein by setting the resolution set to average (Gasteiger et al., 2005).

Phylogenetic Analysis

The multiple sequence alignment and phylogenetic analyses were conducted to evaluate the evolutionary relationships of the NRT2 family in their respective monophyletic groups or clades. First, the NRT2 protein sequences of rice, wheat, soybean, barley, maize, and papaya were aligned at default settings to determine their consensus and conserved regions using the MUltiple Sequence Comparison by Log-Expectation (MUSCLE) algorithm (https://www.ebi.ac.uk/Tools/msa/muscle/) (Edgar, 2004). Subsequently, the MUSCLE alignment file was used to conduct the phylogenetic analysis using Molecular Evolutionary Genetics Analysis (MEGA7) software (https://www.megasoftware.net/) (Kumar et al., 2016). Next, the Maximum Likelihood (ML) phylogenetic tree was generated using the bootstrap method of 1,000 replications and the substitution method of the Jones-Taylor-Thornton (JTT) model at uniform rates. The phylogenetic tree was then annotated using Interactive Tree Of Life (iTOL) (https://itol.embl.de) (Letunic & Bork, 2007).

Conserved Motif Analysis and Motif Function Prediction

The conserved motif searching for the protein sequence of *NRT2* was conducted using the Multiple Expectation Maximisation for Motif Elicitation (MEME 5.3.3) online tool (https://meme-suite.org/meme/tools/meme) (Bailey et al., 2009). The search parameters used to discover the motifs were as follows: number of motifs = 20; minimum width = 6; maximum width = 50; minimum sites = 2; and maximum sites = 600. The HyperText Markup Language (HTML) output file exported from MEME was used to manually illustrate the organisation of the motifs on the protein sequences using the Illustrator for Biological Sequences (IBS) online tool (http://ibs.biocuckoo.org)

(Liu et al., 2015). The 20 consensus motifs sequences in *NRT2* were then annotated for their putative function using the Conserved Domains Database (CDD) (https://www.ncbi.nlm.nih.gov/Structure/cdd/cdd.shtml) (Marchler-Bauer et al., 2015), Pfam (http://pfam.xfam.org) (Mistry et al., 2021), and PROSITE (https://prosite.expasy.org) (Hulo et al., 2006).

Promoter Analysis

In this study, the 2.0 kb upstream genomic region from the transcription site of *OsNRT2.3* was extracted from PLAZA 3.0 Monocots (https://bioinformatics.psb.ugent.be/plaza/) to perform promoter analysis (Proost et al., 2015). The 2.0 kb upstream region of the promoter sequence was searched against PlantCARE (http://bioinformatics.psb.ugent.be/webtools/plantcare/html/) to investigate the putative role of the *cis*-element (Lescot et al., 2002).

Analysis of Gene Co-Expression Network, GO Annotation, and Expression Patterns

The Gene Co-expression Network Analysis (GCNA) was conducted by retrieving publicly available co-expression data from the Rice Expression Database (RED) (http://expression.ic4r.org/) (Xia et al., 2017). The *OsNRT2.3* identity (LOC_Os01g50820/ Os01g0704100) was used as a query to identify and obtain the *NRT2.3* co-expression network, with Pearson's *r*-value set at 0.85. The network was later downloaded and visualised in the Cytoscape software (version 3.7.1) for further observation (Shannon et al., 2003). The Gene Ontology (GO) annotation of the co-expressed genes was then conducted to discover their function using the AgriGO database (http://bioinfo.cau.edu.cn/agriGO/index.php) (Tian et al., 2017). The Fisher statistical test method < 0.05 was selected for complete GO analysis. For expression profile analysis of genes of interest, the ePlant database (http://bar.utoronto.ca/eplant/) (Waese et al., 2017) was employed to examine co-expressed genes manifesting similar expression profiles to *OsNRT2.3* at a tissue-specific level. Rice whole-genome Affymetrix GeneChip array data for transcript analysis of N response was obtained from NCBI Gene Expression Omnibus (https://www.ncbi.nlm.nih.gov/geo/) (Cao et al., 2012) under accession number GSE61370 (Coneva et al., 2014).

Protein-Protein Interaction Network Analysis

After identifying co-expressed genes to *OsNRT2.3*, the protein-protein interactions (PPIs) data from STRING (https://string-db.org) (Mering et al., 2003) were retrieved using Cytoscape StringApp plugin to construct the PPI network of *NRT2.3* protein. The PPIs with a confidence score of > 0.400 were retained and visualised in the Cytoscape software (Shannon et al., 2003). However, in this study, only evidence of known interactions was selected, such as from a curated database, and experimentally determined to supply strong evidence of PPI via validated physical interactions between

the proteins. The PPI between *OsNRT2.3* and co-expressed gene encoding protein will strongly support their critical role in NUE at the functional level.

RESULTS

Identification of NRT2 Family Genes from Selected Organisms

The present study identified 20 selected NRT2 proteins and gene sequences, including four *NRT2* in rice named *OsNRT2.1* to *OsNRT2.4*, followed by seven *Arabidopsis NRT2* (*AtNRT2.1* to *AtNRT2.7*), four maize *NRT2* (*ZmNRT2.1* to *ZmNRT2.3*, and *ZmNRT2.5*), and two barley *NRT2* (*HvNRT2.5* and *HvNRT2.6*). Single *NRT2* was identified in soybean (*GmNRT2*), papaya (*CpNRT2*), and wheat (*TaNRT2.1*). The size of the proteins encoded by *NRT2* genes varies substantially. The length of NRT2 family proteins ranged from 485 to 542 amino acid residues. The shortest NRT2 protein is OsNRT2.4, 485 amino acids, and the most extended NRT2 protein is AtNRT2.6, 542 amino acids. The Expasy analysis demonstrated a large variation in isoelectric point (pI) values ranging from 5.40 to 9.21 and molecular weights ranging from 50.199 to 58.637 kDa. The information on the NRT2 proteins is reported in Table 1.

Table 1
The list of high-affinity nitrate transporter 2 (NRT 2) protein families

Protein ID	Gene name	Species	ORF length (bp)	Protein		
				Length (aa)	MW (kDa)	pI
OS02G02170	*OsNRT2.1*	*Oryza sativa*	1,602	533	57.230	8.43
OS02G02190	*OsNRT2.2*	*Oryza sativa*	1,602	533	57.230	8.43
OS01G50820	*OsNRT2.3*	*Oryza sativa*	1,551	516	55.407	8.99
OS01G36720	*OsNRT2.4*	*Oryza sativa*	1,452	485	50.199	8.37
ABG20828	*HvNRT2.5*	*Hordeum vulgare*	1,545	514	55.376	8.98
ABG20829	*HvNRT2.6*	*Hordeum vulgare*	1,524	507	54.673	8.39
AAG01172	*TaNRT2.1*	*Triticum aestivum*	1,796	507	54.708	8.39
ZM04G41480	*ZmNRT2.1*	*Zea mays*	1,755	524	56.675	8.20
ZM04G41500	*ZmNRT2.2*	*Zea mays*	1,855	524	56.644	8.20
ZM05G17230	*ZmNRT2.3*	*Zea mays*	2,001	522	56.099	8.35
ZM08G26310	*ZmNRT2.5*	*Zea mays*	2,094	520	55.775	8.94
AT1G08090	*AtNRT2.1*	*Arabidopsis thaliana*	2,111	530	57.709	8.85
AT1G08100	*AtNRT2.2*	*Arabidopsis thaliana*	1,709	522	56.615	8.72
AT5G60780	*AtNRT2.3*	*Arabidopsis thaliana*	1,922	539	58.230	8.96
AT5G60770	*AtNRT2.4*	*Arabidopsis thaliana*	1,716	527	57.768	9.04
AT1G12940	*AtNRT2.5*	*Arabidopsis thaliana*	1,852	502	54.261	8.97
AT3G45060	*AtNRT2.6*	*Arabidopsis thaliana*	1,912	542	58.637	8.84
AT5G14570	*AtNRT2.7*	*Arabidopsis thaliana*	1,917	493	52.677	5.40
GM08G39140	*GmNRT2*	*Glycine max*	2,099	508	55.259	9.21
CP00056G00130	*CpNRT2*	*Carica papaya*	1,638	534	57.986	9.12

Note. ORF = Open reading frame ; MW = Molecular weight ; pI = Isoelectric point

Phylogenetic Classification of NRT2 Family Genes

A phylogenetic tree using full-length protein sequences was constructed to decipher the evolutionary relationships of NRT2 family genes among monocot (rice, barley, wheat, and maize) and eudicot (*Arabidopsis*, soybean, and papaya). The phylogenetic tree demonstrated that NRT2 family genes were divided into four clades (I to IV), including one outgroup gene named *ZmNRT2.3* with > 38.4% bootstrap values (Figure 1). Clade II has the fewest *NRT2* gene members (2), while clade IV consists of the most members (7), followed by clade III (6) and clade II (4). The NRT2 family members indicated a high degree of similarities. They were clustered into their respective monophyletic groups, reflecting the highly conserved nature of *NRT2* genes within the plant, particularly for monocot species in clades I and II and eudicot species in clade III. Based on phylogenetic analysis, eight sister pairs were discovered among them: (i) paralogous pairs of *OsNRT2.1/OsNRT2.2*, *ZmNRT2.1/ZmNRT2.2*, *AtNRT2.3/AtNRT2.6*, and *AtNRT2.1/AtNRT2.2*; and (ii) orthologous pairs of *TaNRT2.1/HvNRT2.6*, *AtNRT2.7/OsNRT2.4*, *GmNRT2/AtNRT2.5*, and *OsNRT2.3/HvNRT2.5*. Most paralogous pairs had high bootstrap support with > 99.9% bootstrap values, while bootstrap values of orthologous pairs were between 45.1% and 100%.

Functional Motifs of NRT2 Family Genes

Aside from conserved 60 amino acid residues, the rest of the protein sequence contains other motifs potentially involved in unknown functions or structural roles. Hence, twenty distinctive motifs were determined by analysing conserved amino acids ranging from 6 to 50 amino acid

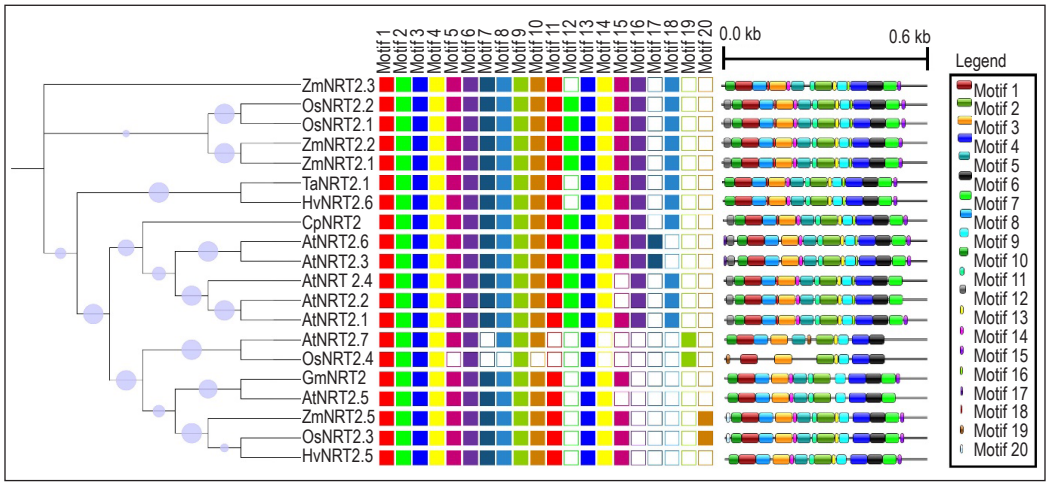

Figure 1. Illustrative diagram of motifs organisation for NRT2 family protein in the phylogenetic tree. The coloured box represents the presence and absence of distinctive motifs in NRT2 proteins. The arrangement of 6–50 amino acid motifs is shown in an orderly sequence of NRT2 proteins. The information on the motif is shown in Table 2

residues within the NRT2 protein sequences. The information is demonstrated in Figure 1 and Table 2. Generally, two or more motifs that have remained close to each other are considered domain regions. The function annotation of putative motifs was obtained from Pfam, PROSITE, and CDD searches. The conserved motif 1 to 11 comprises the nitrate transmembrane transporter domain, which is highly present in most NRT2 family proteins (Table 2). The orthologous pair of *AtNRT2.7/OsNRT2.4* had the least conserved motifs, with several motifs (motifs 7, 11, 12, 14 to 18, and 20)

Table 2
Twenty motifs of NRT family genes were identified using MEME Suite 5.3.3. Each motif consensus was annotated against CDD, Pfam, and PROSITE

Motif	Motif consensus	Motif length (aa)	Motif name
1	PHMRTFHLSWISFFTCFVSTFAAAPLVPIIRDNLNLTKADI GNAGVASVS	50	[1, 2, 4, 5]
2	YRTWIFVLLYGYSMGVELTTDNVIAEYFYDRFDLDLRTA GIIAASFGMAN	50	[1, 6]
3	RFLIGFSLATFVSCQYWMSTMFNSKIIGLVNGLAAGWG NMGGGATQLJMP	50	[1]
4	MVLFSFFAQAACGATFGVVPFVSRRSLGIISGMTGAGGN VGAGLTQLLFF	50	[1, 3, 6, 8]
5	TAWRIAFFVPGLLHVVMGILVLTLGQDLPDGNLRSLQK	38	[1, 6, 7]
6	TSSRYSTETGJEYMGIMIMACTLPVTLVHFPQWGSMFLP PSADA	44	[1]
7	TEEHYYASEWSEEEKSKGLHEASLKFAENSRSERGRRNVI	40	[1, 5, 6, 8, 9]
8	GSIFSRLAMGAVCDLLGPRYGCAFLIMLSAPTVFCMSFIDS	41	[1, 5, 6]
9	ARRFGMRGRLWNJWILQTAGGAFCIWLGR	29	[1]
10	EAADAKSKFDLPVDSEHKAKVFRLFSFAN	29	[1, 5]
11	AKDSFSKVLWYAVTN	15	[1]
12	EPGSSLHGVTGREQAFAFSVE	21	[5, 8]
13	VARPGGGLLSD	11	[6]
14	VYEAIRKCGAT	11	[10]
15	ATPPNNTPEHV	11	[10]
16	ASTLPTSV	8	[10]
17	MAHNHSNE	8	[4]
18	AGYIAV	6	[10]
19	EEEEKLVEEED	11	[10]
20	EFKPVAMZVE	10	[10]

Note.
[1]Nitrate transmembrane transporter; Provisional (cl30556)
[2]Leucine rich repeat (PF13516)
[3]Ubiquitinol-cytochrome C reductase Fe-S subunit TAT signal (PF10399)
[4]N-glycosylation site (PS00001)
[5]Casein kinase II phosphorylation site (PS00006)
[6]N-myristoylation site (PS00008)
[7]Major facilitator superfamily (MFS) (PS50850)
[8]Protein kinase C phosphorylation site (PS00005)
[9]Amidation site (PS00009)
[10]Unknown

found to be absent in both genes. Motifs 1 and 4 were putatively annotated as leucine-rich repeat, ubiquinol-cytochrome C reductase, Fe-S subunit, and twin-arginine translocation (TAT) signal, respectively. Meanwhile, motif five was identified as a short sequence region for a major facilitator superfamily that transports substrates across cell membranes. Several sites were annotated among the motifs, including the *N*-glycosylation site (motifs 1 and 17), casein kinase II phosphorylation site (motifs 1, 7, 8, 10, and 12), *N*-myristoylation site (motifs 2, 4, 5, 7, 8, and 13), protein kinase C phosphorylation site (motifs 4, 7, and 12) and amidation site (motif 7), which could play an essential role of protein structure. With motifs 1 to 11, it became clear that the most closely related clade members had similar motif distribution, suggesting functional similarities among NRT2 proteins within constructed phylogenetic trees.

Promoter Analysis of Putative Stress Responsive *OsNRT2.3*

The presence of *cis*-regulatory elements (CREs) in the promoter is critical for controlling gene transcription under particular conditions. As the functional motifs of *OsNRT2.3* are highly conserved among the orthologous and paralogous genes, responsive elements of *OsNRT2.3* was found to be implicated in vital biological processes. Therefore, the 2.0 kb promoter region of *OsNRT2.3* was analysed using PlantCare, resulting in four functional elements: hormone-, tissue-, stress-, and light-responsive elements. The promoter analysis revealed that stress-responsive elements were predominantly present in *OsNRT2.3*, with a total number of 19, followed by light-responsive elements (13), hormone-responsive elements (11), and tissue-specific elements (3). The information on these CREs and their locations are reported in Table 3 and Figure 2, respectively.

The identified CREs were discovered to be involved in numerous stress responses, for instance, Myb-binding site (MBS) (CAACTG), v-Myb myeloblastosis viral oncogene homolog (MYB) (CAACCA), and myelocytomatosis oncogenes (MYC) (GTTTAC) induced by drought; AU rich element (ARE) (AAACCA) responsive to anaerobic induction; GC-motif (GCCCCC) involved in oxygen deficiency; long terminal repeats (LTR) (CCGAAA) induced by low temperature; and wnt-responsive element 3 (WRE3) (CCACCTAC) responsive to wound. Interestingly, several hormone-responsive elements that are involved in various stresses were also discovered, including ABA-responsive element (ABRE) (CGGTGCG), ABA-responsive element 3a (ABRE3a) (TACGTG), and ABA-responsive element 4 (ABRE4) (ATGCAC) induced by abscisic acid and drought stress; CGTCA-motif (ACTGC) and TGACG-motif (TGACG) involved in methyl jasmonate responsiveness and biotic stress; ethylene-responsive element (ERE) (ATTTTAAA) responsive to ethylene; and gibberellic acid responsive element (GARE) (TCTGTTG) responsive to gibberellin. In addition, most of the light-responsible elements like Box-4

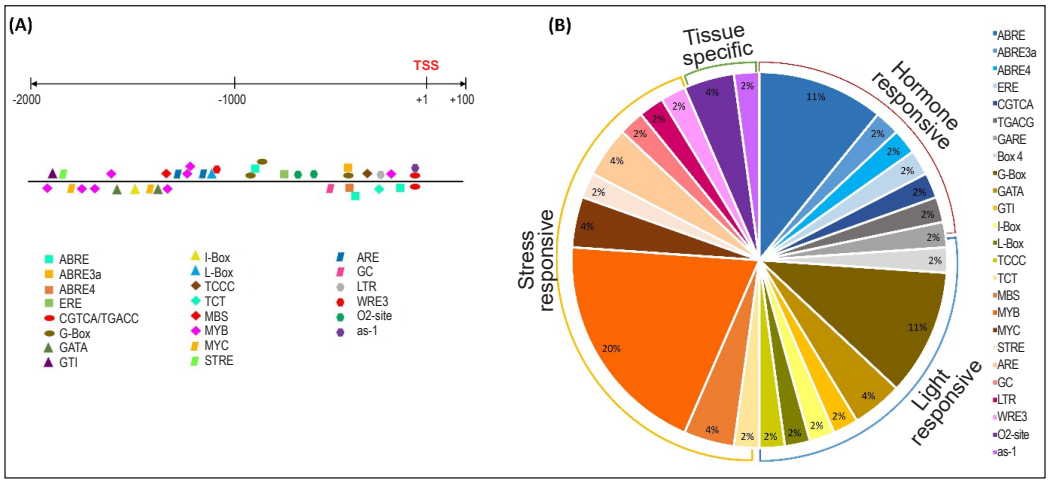

Figure 2. The information of plant stress-, hormone-, light- and tissue-specific-responsive elements (CREs) in the promoter regions of *OsNRT2.3*. (A) Predicted CREs in the promoter regions of *OsNRT2.3* gene; (B) Pie distribution of identified motifs in *O. sativa NRT2.3* gene from PlantCARE, based on their biological functions

Table 3
Description of putative cis*-acting regulatory elements in* OsNRT2.3 *promoter region from the PlantCARE database*

Type	Element	Sequence (5'-3')	Function	Abundance of element
Hormone-responsive element	ABRE	CGGTGCG	*Cis*-acting regulatory element involved in the ABA responsiveness	5
	ABRE3a	TACGTG	*Cis*-acting regulatory element involved in the ABA responsiveness	1
	ABRE4	ATGCAC	*Cis*-acting regulatory element involved in the ABA responsiveness	1
	ERE	ATTTTAAA	ethylene-responsive element	1
	CGTCA-motif	ACTGC	*Cis*-acting regulatory element involved in the MeJA-responsiveness	1
	TGACG-motif	TGACG	*Cis*-acting regulatory element involved in the MeJA-responsiveness	1
	GARE	TCTGTTG	Gibberellin responsive element	1
Light-responsive element	Box-4	ATTAAT	Part of a conserved DNA module involved in light responsiveness	1
	G-box	TAAACGTG	*Cis*-acting regulatory element involved in light responsiveness	5
	GATA-motif	GGAAGAGGAA	Part of a light-responsive element	2
	GTI-motif	GGTTAA	Light responsive element	1
	I-box	TCGGAGTAGAA	Part of a light-responsive element	1
	L-box	ATCCCACCT	Part of a light-responsive element	1
	TCCC-motif	TCTCCCT	Part of a light-responsive element	1
	TCT-motif	CATTCT	Part of a light-responsive element	1

Table 3 *(continue)*

Type	Element	Sequence (5'-3')	Function	Abundance of element
Stress-responsive element	MBS	CAACTG	MYB binding site involved in drought-inducibility	2
	MYB	CAACCA	MYB recognition site involved in drought responsiveness	9
	MYC	GTTTAC	MYB recognition site involved in drought responsiveness	2
	STRE	AGGGG	Stress-responsive element	1
	ARE	AAACCA	*Cis*-acting regulatory element essential for the anaerobic induction	2
	GC-motif	GCCCCC	Enhancer-like element involved in anoxic specific inducibility	1
	LTR	CCGAAA	*Cis*-acting element involved in low-temperature responsiveness	1
	WRE3	CCACCTAC	Wound responsive element	1
Tissue-specific element	O2-site	GATGATGTGG	*Cis*-acting regulatory element involved in zein metabolism regulation	2
	As-1	TGACG	*Cis*-acting regulatory element involved in the root-specific expression	1

(ATTAAT), G-box (TAAACGTG), GATA-motif (GGAAGAGGAA), GT1-motif (GGTTAA), I-box (TCGGAGTAGAA), L-box (ATCCCACCT), TCCC-motif (TCTCCCT), and TCT-motif (CATTCT) are responsible for responding to a broad spectrum and specific wavelength of light. In the case of tissue-specific elements, opaque 2 (O_2-site) (GATGATGTGG) and as-1 (TGACG) are essential in zein metabolism regulation and root-specific expression, respectively.

Identification of *OsNRT2.3* Co-Expressed Genes and GO Annotation Analysis

Co-expression analysis is widely used to perceive transcription regulators in rice. It was used as a query gene to retrieve the information of the co-expressed genes from Rice Expression Database (RED), with the selected Pearson's *r* value greater than 0.85 to exploit the transcription regulation of the *OsNRT2.3* gene. As a result, 18 genes were identified to be significantly co-expressed with *OsNRT2.3* (Table 4). Nine co-expressed genes were assigned to numerous GO annotations focusing on lipid transport and localisation, cellular macromolecule metabolic processes, stress response, and transcription regulation. Most of the genes encode proteins in the nucleus and membrane. The molecular functions discovered are transcriptional regulation, binding, protein kinase activity, transporter, protein dimerisation, oxidoreductase, and hydrolysis. These findings imply that annotated co-expressed genes may be associated with transport and localisation.

Table 4
Co-expressed genes of OsNRT2.3 *(*LOC_Os01g50820/Os01g0704100*) obtained from Rice Expression Database (http://expression.ic4r.org)*

MSU ID	Gene ID	Gene name	Protein name	Pearson's *r* value
LOC_Os01g22920	Os01g0332200	*GA2ox2*	Gibberellin 2-beta-dioxygenase 2	0.921323
LOC_Os01g42370	Os01g0609200	*PDR11*	Pleiotropic drug resistance 11	0.977791
LOC_Os02g26950	N/A	*Os02g0468900*	Hypothetical protein	0.873701
LOC_Os02g40710	Os02g0620500	*AMT1.3*	Ammonium transporter 1.3	0.899457
LOC_Os03g19375	Os03g0306700	*bZIP27*	bZIP transcription factor 27	0.918212
LOC_Os03g22390	N/A	*Os03g0344166*	Universal stress protein family protein	0.854134
LOC_Os03g46470	Os03g0667500	*IRT1*	Iron-regulated transporter 1	0.92206
LOC_Os03g58670	N/A	*Os03g0801200*	Plant lipid transfer/seed storage/ trypsin-alpha amylase inhibitor domain-containing protein	0.982927
LOC_Os05g28770	Os05g0355700 Os05g0355800	*GCRP9*	Glycine and cysteine-rich family protein	0.936195
LOC_Os05g29000	Os05g0358101	*Os05g0358101*	Expressed protein	0.861334
LOC_Os06g24460	N/A	*PDR2*	Pleiotropic drug resistance protein 2, putative	0.871721
LOC_Os06g30860	Os06g0504900	*WRKY31*	WRKY transcription factor 31	0.934795
LOC_Os07g24930	N/A	*N/A*	Retrotransposon protein, putative, Ty3-gypsy subclass	0.960406
LOC_Os07g24940	Os07g0431160	*Os07g0431160*	Transposon protein, putative, CACTA, En/Spm sub-class	0.870374
LOC_Os07g25300	N/A	*N/A*	Retrotransposon, putative, centromere-specific	0.972477
LOC_Os08g31890	Os08g0413200	*Os08g0413200*	Hypothetical protein	0.927934
LOC_Os08g44800	N/A	*N/A*	Hypothetical protein	0.874997
LOC_Os12g03830	Os12g0132500	*ZIFL9*	Zinc-induced facilitator-like 9	0.983711

From the co-expression network in Figure 3A, *OsNRT2.3* is co-expressed with several important genes in NUE; particularly genes that encode proteins involved in transport, such as zinc-induced facilitator-like 9 (*OsZIFL*) and ammonium transporter 1.3 (*OsAMT1.3*), plant lipid transfer/seed storage/trypsin-alpha amylase inhibitor domain-containing protein (*Os03g0801200*), in lipid transport and localisation, and universal stress protein (*Os03g0344166*) in stress response. *OsNRT2.3* is also co-expressed with fungus-inducible *OsbZIP27* and pathogen-inducible *OsWRKY31*, exhibiting these defense-related transcription factors (TFs) have a causal role in putatively controlling the transcriptional regulation of *OsNRT2.3* and its co-expressed genes under stresses. Based on bibliomic searching, the unannotated co-expressed genes, *gibberellin 2-beta-dioxygenase 2* (*OsGA2ox2*), enhanced

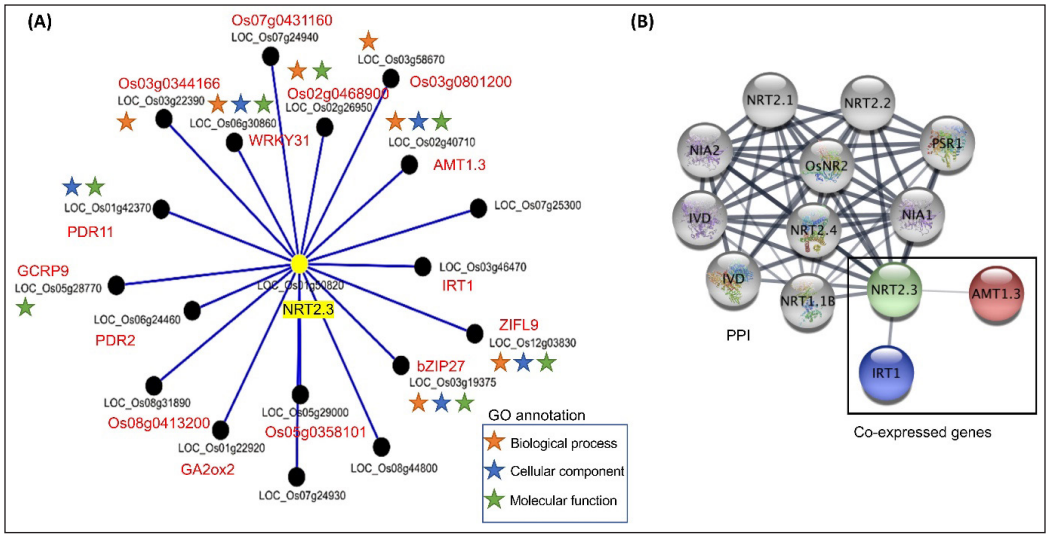

Figure 3. Interaction of (A) co-expressed genes with *OsNRT2.3* obtained from Rice Expression Database (http://expression.ic4r.org) and (B) gene network inference of *OsNRT2.3* and its co-expressed genes using PPI data from STRING database (https://string-db.org)

lodging resistance in rice. In contrast, *iron-regulated transporter 1* (*OsIRT1*) was critical in cadmium uptake and translocation during iron deficiency. Although knowledge of the reported co-expressed genes is still limited, these genes may play a possible role in directly or indirectly being involved in NUE in rice.

In silico Inference of Functional *OsNRT2.3* Co-Expressed Genes by PPI

To strongly support the co-expression analysis at the functional level, the PPI of *OsNRT2.3* and 18 co-expressed genes was conducted using StringApp, a Cytoscape plugin. Therefore, the *OsNRT2.3* PPI was discovered to consist of 13 genes with 50 interactions. This data was used to infer the function of *OsNRT2.3* co-expressed genes based on the interaction gene lists of a priori knowledge. From the STRING data, the *OsNRT2.3* interacts with *OsAMT1.3* and *OsIRT1*, which regulated the response of NH_4^+ and Fe uptake, exhibiting the interplay of the transporter proteins in rice under nutrient-deficient soil (Figure 3B). Despite the absence of the other co-expressed genes in PPI data, their association with several biological processes, including transport, response to stress, protein phosphorylation, and cellular macromolecule metabolic process, may suggest them as new candidate genes occurred in coordinating regulation of macromolecule metabolism and other critical physiological functions.

Nine proteins were also found functionally related to *OsNRT2.3* based on their gene ontology annotation information, whereas the other nine proteins' functions were classified as unknown (Figure 3A). The interacting annotated partners of *OsNRT2.3* comprised four nitrate transporters (*OsNRT2.1*, *OsNRT2.2*, *OsNRT2.3*, and *OsNRT1.1B*), three nitrate reductase (*OsNR2*,

OsNIA1, and *OsNIA2*), promoter of shoot regeneration (*OsPSR1*), and isovaleryl-CoA dehydrogenase (*OsIVD*). These proteins are associated with several NUE-related processes, including N utilisation, nitrate assimilation, and response to nitrate, ammonium, and chlorate, having similar biological processes to the *OsNRT2.3* protein.

Expression Patterns Analysis of *OsNRT2.3* Co-expressed Genes

To discover the transcript level of the *OsNRT2.3* gene and its co-expressed genes in the specific tissue, the similar expression profiles of selected genes were visualised in various tissues of rice using the ePlant, a data visualisation tool in the Bio-Analytic Resource for Plant Biology (BAR) database. Interestingly, the expression level of co-expressed genes, *OsAMT1.3*, *OsbZIP27*, *OsIRT1*, and *OsZIFL9*, were discovered to be relatively similar to *OsNRT2.3* in all 15 tissues. The transcript of all five genes demonstrated a higher expression level in the seedling root, with an average expression level from 850.99 to 12,511.73 (Figure 4). *OsIRT1* had the highest expression level in

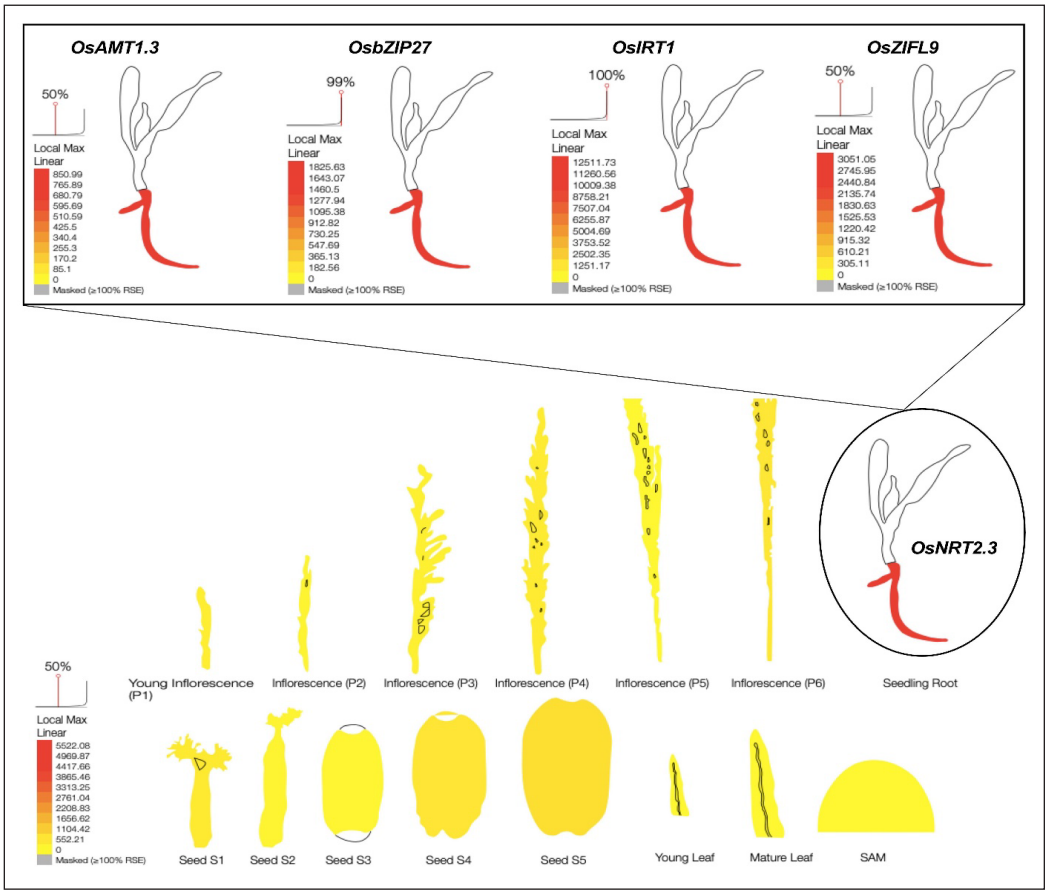

Figure 4. Expression levels of four co-expressed genes: *OsAMT1.3*, *OsbZIP27*, *OsIRT1*, and *OsZIFL9* with *OsNRT2.3* in 15 tissue-specific obtained from ePlant (http://bar.utoronto.ca/eplant/)

the seedling root, followed by *OsNRT2.3* (5522.08), *OsZIFL9* (3,051.05), *OsbZIP27* (1,825.63), and the lowest is *OsAMT1.3*. The particular genes may reflect their crucial role in the absorption and transportation of micronutrients available via root in rice.

The expression patterns of genes were observed to reveal more information on the potential involvement of co-expressed genes in N response using a rice whole-genome Affymetrix GeneChip array. Under different treatments of N response in leaf and root, *OsNRT2.3*, *OsAMT1.3*, and *OsIRT1* had similar expression patterns in the root and were highly expressed under low N and root-induced N (Figure 5). The decreased gene expression level under normal N conditions and root-reduced N may also suggest their importance in balancing the N uptake and utilisation due to nitrification in aerobic soils. Therefore, the involvement of the *OsAMT1.3* and *OsIRT1* were inferred to play a significant role in NUE and provided two putative candidates, *OsbZIP27* and *OsZIFL9*, to interact with *OsNRT2.3* during the control of N transportation in rice.

DISCUSSION

The nitrate transporter (NRT) is a vital gene family required for nitrate (NO_3^-) absorption and transport for plant growth. In addition, NRT is essential in motioning water and solutes across the cell membrane. A recent study about the importance of the NRT family was reported, such as the *NRT2* gene responsive to stresses in rapeseed (*Brassica napus* L.) (J. Tong et al., 2020) and the genetic effects of *NRT* genes in Chinese white poplar (*Populus tomentosa*) (Zhao et al., 2021). However, the roles of *OsNRT2.3* and its co-expressed genes in the association of drought and NUE in rice remain elusive, particularly in reporting the potential drought-related genes

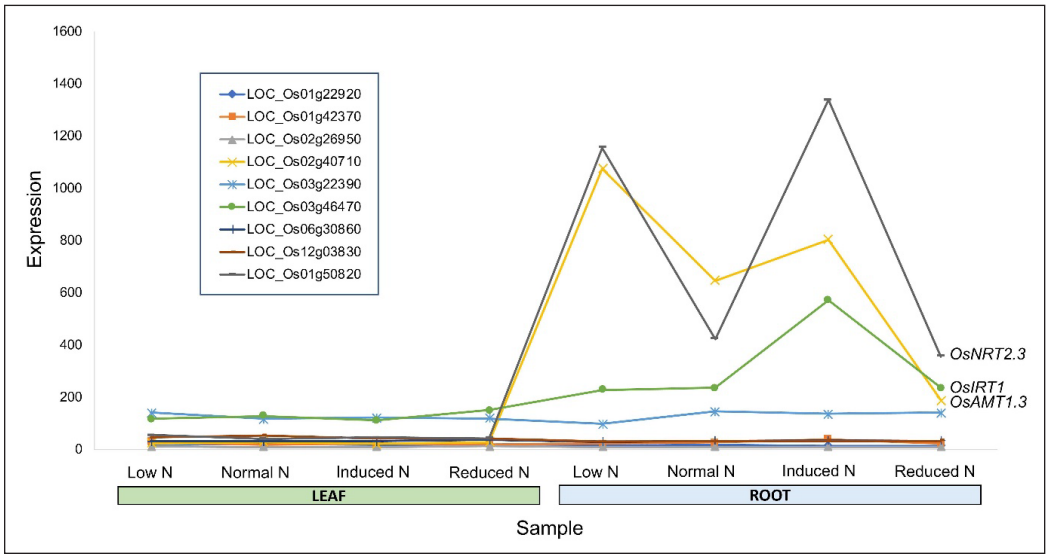

Figure 5. Expression patterns of *OsNRT2.3*, *OsAMT1.3*, and *OsIRT1* in the root and leaf under the different N conditions

during NUE. Thus, our study presents the *in silico* analysis of four *OsNRT2*, seven *AtNRT2*, four *ZmNRT2*, two *HvNRT2*, one *GmNRT2*, one *CpNRT2*, and one *TaNRT2* to comprehend the evolutionary relationship of *OsNRT2.3* with other *NRT2* genes of monocot and eudicot. Twenty *NRT2* genes are divided into four monophyletic groups in the phylogeny by introducing eight sister pairs of ortholog and paralog members. By analysing the distribution of the motif of *NRT2* genes, most of these genes were highly conserved by considering the motifs remaining close to each other in nitrate transmembrane transporter domain regions.

Nevertheless, some *NRT2* genes have distinct motif distributions, exhibiting that the protein domain likely evolved at different substitution rates to adapt to the environment (Schaeffer et al., 2016). The different lengths of the NRT2 protein sequences for the sister pairs may also suggest the possible insertion and/or deletion events throughout evolution that could further understand the functional diversity of genes encoding NRT2 proteins (Abdullah-Zawawi et al., 2021). Therefore, we found that *OsNRT2.3* is in a similar sub-clade phylogeny to *ZmNRT2.5* and *HvNRT2.5* and consists of similar motifs, which indicates that these genes may serve similar functions. From a previous study, H. Wang et al. (2017) discovered that *ZmNRT2.5* enhances the rapid accumulation of amino acids and increases N uptake in roots during a drought. The survival rate of transgenic lines of *OsNRT2.3* is not significantly different from *OsNRT2.1* transgenic lines under drought conditions and is considered relatively regulated in increasing drought tolerance in rice (Chen et al., 2019).

The CREs play a significant role in gene regulation by controlling a substantial gene network in biological function. The presence of prominent CREs in the promoter region of the *OsNRT2.3* gene highlights the potential involvement of the responsive gene in stress and hormone based on the predominant number of CREs that appeared in *OsNRT2.3,* such as MYB and ABRE. A study by M. Wang et al. (2020) reported that *NRT2.3* is induced by ABA signals in wheat roots through the transcript abundance of *TaNRT2.3* after being treated with nitrate. An abundant MYB element in the promoter region of drought-responsive genes also revealed its higher root expression in rice and other crops (Khan et al., 2017). Therefore, the co-expression interaction of the *OsNRT2.3* gene is observed to fully comprehend the regulation of the respective gene that controls other genes in NUE.

A combinatorial analysis of gene co-expression and gene expression pattern revealed that four co-expressed genes, including *OsAMT1.3*, *OsbZIP27*, *OsIRT1*, and *OsZIFL9*, are strongly co-regulated with *OsNRT2.3* in response to N availability based on Pearson correlation coefficient, PCC > 0.85 and expression pattern similarity. Furthermore, the expression levels of these five genes were found to be highly expressed in seedling roots. *OsAMT1.3* and *OsIRT1* showed similar expression patterns with *OsNRT2.3* under low and normal N conditions and root-induced and

root-reduced N conditions. *OsbZIP27* and *OsZIFL9*, on the other hand, only expressed similarly with *OsNRT2.3* under low and normal N conditions, suggesting that all these four genes may play an important role in the correlation between drought and NUE.

Plants develop various adaptation strategies, including tolerance mechanisms and N-use optimisation due to the drought response. Under drought stress, plant roots will absorb more water from the soil to seize an optimal amount of N for metabolism (Waraich et al., 2011), affecting the N assimilation process and resulting in the declination of NUE (Hoang et al., 2019). *OsAMT1.3* is a root-specific gene regulated by nitrogen supply and is also involved in enhancing rice growth and carbon-nitrogen metabolic status (Bao et al., 2015; Sonoda et al., 2003). There is no clear evidence of *OsIRT1* being involved in NUE; however, it was reported that *OsIRT1* is a preferential Fe (II) transporter whose function in NUE can be characterised using the reverse genetics approach (Z. Zhang et al., 2020). OsZIFL9, a Zn transporter, is known to have a crucial role in improving nutrient status in rice, although its status in N management is still understudied (Awasthi et al., 2021). Therefore, deciphering the correlations of potential drought-related genes' function with NUE is challenging but important. It is suggested that optimising N use could support drought tolerance in rice and require further validation of the genes in future studies.

Generally, in the flooded soil, N is usually distributed as NH_4^+, while in the upland, it is converted into NO_3^- due to nitrification by aerobic soils (Kabange et al., 2021; Qian et al., 2004). An NH_4^+ transporter, OsAMT1.3, acts as a signal sensor for regulating NUE under low NH_4^+ conditions (Ferreira et al., 2015). A recent study also suggested that *OsAMT1.3* co-expressed with the *NRT* gene after applying potassium chlorate ($KClO_3$) to simulate a drought (Kabange et al., 2021). *OsZIFL9* and *OsIRT1*, on the other hand, are reported to play a potential role in alleviating Fe deficiency by NH_4^+ in calcareous soils. In the case of *OsIRT1*, this transporter gene is induced by low Fe conditions, and ethylene (ET) will enhance the expression of the respective gene in the roots uptake system of Fe^{3+} and Fe^{2+} phytosiderophore (Ishimaru et al., 2006; J. Wu et al., 2011). Recently, García et al. (2021) discovered that ethylene (ET) plays a significant role in regulating crosstalk between the nutrient deficiency through activation of the ET transduction pathway for facilitating the plant response, particularly by enhancing the transporter activity. The assimilation of NH_4^+ and NO_3^- are different in apoplastic pH, influencing the uptake and utilisation of Fe in rice. First, NO_3^- reduces the xylem alkalinity by delivering Fe into the cell wall. Secondly, NH_4^+ enables the reduction of aerenchyma division, which ultimately adjusts the water uptake capacity of Fe from roots to different parts of the rice (X. Zhang et al., 2019). The above findings proposed that the presence of

OsNRT2.3, coupled with the *OsIRT1* activity in roots, would designate the prevalence of Fe uptake during NO_3^- and NH_4^+ transport.

A previous study showed that *OsbZIP27*, a bZIP-type transcription factor, was induced by dehydration stress under a mild water deficit of rice (Hossain et al., 2010). The bZIP proteins have a DNA-binding specificity for ACGT-containing DNA sequence motifs (Izawa et al., 1993). Despite the lack of a specific study of the *OsbZIP27* function in regulating *OsNRT2.3*, ACGT-binding specificity of G-box and ABRE3a elements were discovered in the *OsNRT2.3* promoter region. It reflects that OsbZIP27 proteins may activate transcription of ABA-induced *OsNRT2.3* by binding to the ABREa element for drought tolerance of rice. In addition, previous studies have also demonstrated that roots overexpressing *ZIFL* genes have significantly increased by Zn and Fe (Sharma et al., 2019). Under Fe-deficient conditions, FER-LIKE FE DEFICIENCY-INDUCED TRANSCRIPTION FACTOR (OsFIT) and its interacting partner, iron-related bHLH transcription factor 2 (*OsIRO2*), play a critical role in regulating Fe-acquisition genes for Fe homeostasis in the roots and leaves, including *OsZIFL9* that increased in expression level (Liang et al., 2020).

Interactions between essential nutrients, such as iron (Fe), nitrogen (N), sulfur (S), and phosphorus (P), were reported to influence transport, homeostasis, and assimilation processes for proper growth and development in plants (Kumar et al., 2021). For example, according to Singh et al. (2018), the concentration of Fe, Zn, and protein in wheat grains increased due to the interaction of Fe and Zn with N. Likewise, the concentration of micronutrients like Cu, Zn, Mn, and Na increased in the belowground tissue of *Bothriochloa ischaemum* when exposed to a high amount of N (Ai et al., 2017). Thus, our study demonstrates that the NUE system's potential drought-related genes, *OsAMT1.3*, *OsbZIP27*, *OsIRT1*, and *OsZIFL9,* are highly associated with *OsNRT2.3*, and *OsZIFL9* and *OsIRT1* might be key players in the interaction of macronutrient N and micronutrient Fe in rice.

CONCLUSION

Transporters involved in the uptake, transport, and re-translocation of nitrogen (N) are important targets in breeding programmes to combat environmental stress, particularly drought. Computational dissection of potential drought-related genes from *NRT2* will greatly advance our knowledge of the relationship between NUE and drought. This study has investigated 20 selected *NRT2* genes of various plants, and their motif compositions are mostly similar and conserved within the nitrate transmembrane transporter domain across the monophyletic group. In rice, *NRT2.3* genes interacted specifically with stress and phytohormone responsiveness elements. The correlation between genes has emerged as a growing research focus in crop improvement. The interaction of four potential genes, *OsAMT1.3*, *OsbZIP27*, *OsIRT1*, and *OsZIFL9*, with *OsNRT2.3*, provides an alternative explanation of the

relationship between NUE and drought response in rice. This knowledge will assist the future investigation, such as genome editing via the CRISPR-Cas9 system and reverse genetics, to understand better the function of potential genes in the N uptake system and drought stress. The present findings not only identified the genes that potentially govern drought and NUE but can also expedite the discovery and molecular validation of the biologically important gene in breeding strategies.

ACKNOWLEDGEMENTS

Dana Impak Perdana (DIP) funded this research under grant number DIP-2019-031, awarded to Zamri Zainal by Universiti Kebangsaan Malaysia (UKM).

REFERENCES

Abdullah-Zawawi, M. R., Afiqah-Aleng, N., Ikhwanuddin, M., Sung, Y. Y., Tola, S., Fazhan, H., & Waiho, K. (2021). Recent development in ecdysone receptor of crustaceans: Current knowledge and future applications in crustacean aquaculture. *Reviews in Aquaculture*, *13*(4), 1938-1957. https://doi.org/10.1111/raq.12552

Ai, Z., Wang, G., Liang, C., Liu, H., Zhang, J., Xue, S., & Liu, G. (2017). The effects of nitrogen addition on the uptake and allocation of macro- and micronutrients in *Bothriochloa ischaemum* on Loess Plateau in China. *Frontiers in Plant Science*, *8*, 1476. https://doi.org/10.3389/fpls.2017.01476

Awasthi, S., Chauhan, R., Indoliya, Y., Chauhan, A. S., Mishra, S. K., Agrawal, L., Dwivedi, S., Singh, S. N., Srivastava, S., Singh, P. C., Chauhan, P. S., Chakrabarty, D., Srivastava, S., & Tripathi, R. D. (2021). Microbial consortium mediated growth promotion and arsenic reduction in rice: An integrated transcriptome and proteome profiling. *Ecotoxicology and Environmental Safety*, *228*, 113004. https://doi.org/10.1016/j.ecoenv.2021.113004

Bailey, T. L., Boden, M., Buske, F. A., Frith, M., Grant, C. E., Clementi, L., Ren, J., Li, W. W., & Noble, W. S. (2009). MEME SUITE: Tools for motif discovery and searching. *Nucleic Acids Research*, *37*(suppl_2), W202–W208. https://doi.org/10.1093/nar/gkp335

Bao, A., Liang, Z., Zhao, Z., & Cai, H. (2015). Overexpressing of *OsAMT1-3*, a high affinity ammonium transporter gene, modifies rice growth and carbon-nitrogen metabolic status. *International Journal of Molecular Sciences*, *16*(5), 9037-9063. https://doi.org/10.3390/ijms16059037

Cao, P., Jung, K. H., Choi, D., Hwang, D., Zhu, J., & Ronald, P. C. (2012). The Rice Oligonucleotide Array Database: An atlas of rice gene expression. *Rice*, *5*, 17. https://doi.org/10.1186/1939-8433-5-17

Chen, J., Qi, T., Hu, Z., Fan, X., Zhu, L., Iqbal, M. F., Yin, X., Xu, G., & Fan, X. (2019). *OsNAR2.1* positively regulates drought tolerance and grain yield under drought stress conditions in rice. *Frontiers in Plant Science*, *10*, 197. https://doi.org/10.3389/fpls.2019.00197

Coneva, V., Simopoulos, C., Casaretto, J. A., El-Kereamy, A., Guevara, D. R., Cohn, J., Zhu, T., Guo, L., Alexander, D. C., Bi, Y. M., McNicholas, P. D., & Rothstein, S. J. (2014). Metabolic and co-expression network-based analyses associated with nitrate response in rice. *BMC Genomics*, *15*, 1056. https://doi.org/10.1186/1471-2164-15-1056

Djaman, K., Mel, V., Ametonou, F., El-Namaky, R., Diallo, M., & Koudahe, K. (2018). Effect of nitrogen fertilizer dose and application timing on yield and nitrogen use efficiency of irrigated

hybrid rice under semi-arid conditions. *Journal of Agricultural Science and Food Research*, *9*(2), 1000223.

Edgar, R. C. (2004). MUSCLE: Multiple sequence alignment with high accuracy and high throughput. *Nucleic Acids Research*, *32*(5), 1792-1797. https://doi.org/10.1093/nar/gkh340

Fenchel, T., King, G. M., & Blackburn, T. H. (2012). Transport mechanisms. *Bacterial Biogeochemistry*, *3*(10), 35–47. https://doi.org/10.1016/b978-0-12-415836-8.00002-5

Ferreira, L. M., de Souza, V. M., Tavares, O. C. H., Zonta, E., Santa-Catarina, C., de Souza, S. R., Fernandes, M. S., & Santos, L. A. (2015). *OsAMT1.3* expression alters rice ammonium uptake kinetics and root morphology. *Plant Biotechnology Reports*, *9*(4), 221–229. https://doi.org/10.1007/s11816-015-0359-2

Food and Agriculture Organization of the United Nations. (2017). *The future of food and agriculture – Trends and challenges*. FAO. https://www.fao.org/3/i6583e/i6583e.pdf

Forde, B. G. (2000). Nitrate transporters in plants: Structure, function and regulation. *Biochimica et Biophysica Acta-Biomembranes*, *1465*(1–2), 219–235. https://doi.org/10.1016/S0005-2736(00)00140-1

García, M. J., Angulo, M., García, C., Lucena, C., Alcántara, E., Pérez-Vicente, R., & Romera, F. J. (2021). Influence of ethylene signaling in the crosstalk between Fe, S, and P deficiency responses in *Arabidopsis thaliana*. *Frontiers in Plant Science*, *12*, 643585. https://doi.org/10.3389/fpls.2021.643585

Gasteiger, E., Hoogland, C., Gattiker, A., Duvaud, S., Wilkins, M. R., Appel, R. D., & Bairoch, A. (2005). Protein identification and analysis tools on the ExPASy server. In J. M. Walker (Eds.), *The proteomics protocols handbook* (pp. 571–607). Humana. https://doi.org/10.1385/1592598900

Hoang, D. T., Hiroo, T., & Yoshinobu, K. (2019). Nitrogen use efficiency and drought tolerant ability of various sugarcane varieties under drought stress at early growth stage. *Plant Production Science*, *22*(2), 250-261. https://doi.org/10.1080/1343943X.2018.1540277

Hossain, M. A., Lee, Y., Cho, J. I., Ahn, C. H., Lee, S. K., Jeon, J. S., Kang, H., Lee, C. H., An, G., & Park, P. B. (2010). The bZIP transcription factor OsABF1 is an ABA responsive element binding factor that enhances abiotic stress signaling in rice. *Plant Molecular Biology*, *72*(4), 557–566. https://doi.org/10.1007/s11103-009-9592-9

Huang, S., Zhao, C., Zhang, Y., & Wang, C. (2018). Nitrogen use efficiency in rice. In A. Amanullah & S. Fahad (Eds.), *Nitrogen in agriculture – Updates*. IntechOpen. https://doi.org/10.5772/intechopen.69052

Hulo, N., Bairoch, A., Bulliard, V., Cerutti, L., De Castro, E., Langendijk-Genevaux, P. S., Pagni, M., & Sigrist, C. J. A. (2006). The PROSITE database. *Nucleic Acids Research*, *34*(suppl_1), D227–D230. https://doi.org/10.1093/nar/gkj063

Ishimaru, Y., Suzuki, M., Tsukamoto, T., Suzuki, K., Nakazono, M., Kobayashi, T., Wada, Y., Watanabe, S., Matsuhashi, S., Takahashi, M., Nakanishi, H., Mori, S., & Nishizawa, N. K. (2006). Rice plants take up iron as an Fe_3^+-phytosiderophore and as Fe_2^+. *Plant Journal*, *45*(3), 335–346. https://doi.org/10.1111/j.1365-313X.2005.02624.x

Izawa, T., Foster, R., & Chua, N. H. (1993). Plant bZIP protein DNA binding specificity. *Journal of Molecular Biology*, *230*(4), 1131–1144. https://doi.org/10.1006/jmbi.1993.1230

Jin, Z., Zhu, Y., Li, X., Dong, Y., & An, Z. (2015). Soil N retention and nitrate leaching in three types of dunes in the Mu Us desert of China. *Scientific Reports*, *5*, 14222. https://doi.org/10.1038/srep14222

Kabange, N. R., Park, S. Y., Lee, J. Y., Shin, D., Lee, S. M., Kwon, Y., Cha, J. K., Cho, J. H., Duyen, D. Van, Ko, J. M., & Lee, J. H. (2021). New insights into the transcriptional regulation of genes involved in the nitrogen use efficiency under potassium chlorate in rice (*Oryza sativa* L.). *International Journal of Molecular Sciences*, *22*(4), 2192. https://doi.org/10.3390/ijms22042192

Khan, M. R., Khan, I., Ibrar, Z., Léon, J., & Naz, A. A. (2017). Drought-responsive genes expressed predominantly in root tissues are enriched with homotypic *cis*-regulatory clusters in promoters of major cereal crops. *Crop Journal*, *5*(3), 195–206. https://doi.org/10.1016/j.cj.2016.10.001

Khazanah Research Institute. (2019). *The status of the paddy and rice industry in Malaysia*. Khazanah Research Institute. http://www.krinstitute.org/assets/contentMS/img/template/editor/20190409_RiceReport_Full%20Report_Final.pdf

Kumar, S., Kumar, S., & Mohapatra, T. (2021). Interaction between macro- and micro-nutrients in plants. *Frontiers in Plant Science*, *12*, 665583. https://doi.org/10.3389/fpls.2021.665583

Kumar, S., Stecher, G., & Tamura, K. (2016). MEGA7: Molecular Evolutionary Genetics Analysis version 7.0 for bigger datasets. *Molecular Biology and Evolution*, *33*(7), 1870–1874. https://doi.org/10.1093/molbev/msw054

Lescot, M., Déhais, P., Thijs, G., Marchal, K., Moreau, Y., Van de Peer, Y., Rouzé, P., & Rombauts, S. (2002). PlantCARE, a database of plant *cis*-acting regulatory elements and a portal to tools for *in silico* analysis of promoter sequences. *Nucleic Acids Research*, *30*(1), 325–327. https://doi.org/10.1093/nar/30.1.325

Letunic, I., & Bork, P. (2007). Interactive Tree Of Life (iTOL): An online tool for phylogenetic tree display and annotation. *Bioinformatics*, *23*(1), 127–128. https://doi.org/10.1093/bioinformatics/btl529

Liang, G., Zhang, H., Li, Y., Pu, M., Yang, Y., Li, C., Lu, C., Xu, P., & Yu, D. (2020). *Oryza sativa* FER-LIKE FE DEFICIENCY-INDUCED TRANSCRIPTION FACTOR (OsFIT/OsbHLH156) interacts with OsIRO2 to regulate iron homeostasis. *Journal of Integrative Plant Biology*, *62*(5), 668–689. https://doi.org/10.1111/jipb.12933

Little, D. Y., Rao, H., Oliva, S., Daniel-Vedele, F., Krapp, A., & Malamy, J. E. (2005). The putative high-affinity nitrate transporter NRT2.1 represses lateral root initiation in response to nutritional cues. *Proceedings of the National Academy of Sciences of the United States of America*, *102*(38), 13693–13698. https://doi.org/10.1073/pnas.0504219102

Liu, W., Xie, Y., Ma, J., Luo, X., Nie, P., Zuo, Z., Lahrmann, U., Zhao, Q., Zheng, Y., Zhao, Y., Xue, Y., & Ren, J. (2015). IBS: An illustrator for the presentation and visualization of biological sequences. *Bioinformatics*, *31*(20), 3359–3361. https://doi.org/10.1093/bioinformatics/btv362

Marchler-Bauer, A., Derbyshire, M. K., Gonzales, N. R., Lu, S., Chitsaz, F., Geer, L. Y., Geer, R. C., He, J., Gwadz, M., Hurwitz, D. I., Lanczycki, C. J., Lu, F., Marchler, G. H., Song, J. S., Thanki, N., Wang, Z., Yamashita, R. A., Zhang, D., Zheng, C., & Bryant, S. H. (2015). CDD: NCBI's conserved domain database. *Nucleic Acids Research*, *43*(D1), D222–D226. https://doi.org/10.1093/nar/gku1221

Matthews, D. E., Carollo, V. L., Lazo, G. R., & Anderson, O. D. (2003). GrainGenes, the genome database for small-grain crops. *Nucleic Acids Research*, *31*(1), 183–186. https://doi.org/10.1093/nar/gkg058

Mering, C. Von, Huynen, M., Jaeggi, D., Schmidt, S., Bork, P., & Snel, B. (2003). STRING: A

database of predicted functional associations between proteins. *Nucleic Acids Research*, *31*(1), 258–261. https://doi.org/10.1093/nar/gkg034

Mistry, J., Chuguransky, S., Williams, L., Qureshi, M., Salazar, G. A., Sonnhammer, E. L. L., Tosatto, S. C. E., Paladin, L., Raj, S., Richardson, L. J., Finn, R. D., & Bateman, A. (2021). Pfam: The protein families database in 2021. *Nucleic Acids Research*, *49*(D1), D412–D419. https://doi.org/10.1093/nar/gkaa913

Obara, M., Tamura, W., Ebitani, T., Yano, M., Sato, T., & Yamaya, T. (2010). Fine-mapping of *qRL6.1*, a major QTL for root length of rice seedlings grown under a wide range of NH_4^+ concentrations in hydroponic conditions. *Theoretical and Applied Genetics*, *121*, 535-547. https://doi.org/10.1007/s00122-010-1328-3

Orsel, M., Krapp, A., & Daniel-Vedele, F. (2002). Analysis of the NRT2 nitrate transporter family in *Arabidopsis*. Structure and gene expression. *Plant Physiology*, *129*(2), 886–896. https://doi.org/10.1104/pp.005280

Proost, S., Van Bel, M., Vaneechoutte, D., Van de Peer, Y., Inzé, D., Mueller-Roeber, B., & Vandepoele, K. (2015). PLAZA 3.0: An access point for plant comparative genomics. *Nucleic Acids Research*, *43*(D1), D974–D981. https://doi.org/10.1093/nar/gku986

Qian, X., Shen, Q., Xu, G., Wang, J., & Zhou, M. (2004). Nitrogen form effects on yield and nitrogen uptake of rice crop grown in aerobic soil. *Journal of Plant Nutrition*, *27*(6), 1061–1076. https://doi.org/10.1081/PLN-120037536

Ranade-Malvi, U. (2011). Interaction of micronutrients with major nutrients with special reference to potassium. *Karnataka Journal of Agricultural Sciences*, *24*(1), 106–109.

Rao, I. S., Neeraja, C. N., Srikanth, B., Subrahmanyam, D., Swamy, K. N., Rajesh, K., Vijayalakshmi, P., Kiran, T. V., Sailaja, N., Revathi, P., Rao, P. R., Rao, L. V. S., Surekha, K., Babu, V. R., & Voleti, S. R. (2018). Identification of rice landraces with promising yield and the associated genomic regions under low nitrogen. *Scientific Reports*, *8*, 9200. https://doi.org/10.1038/s41598-018-27484-0

Remans, T., Nacry, P., Pervent, M., Girin, T., Tillard, P., Lepetit, M., & Gojon, A. (2006). A central role for the nitrate transporter NRT2.1 in the integrated morphological and physiological responses of the root system to nitrogen limitation in *Arabidopsis*. *Plant Physiology*, *140*(3), 909–921. https://doi.org/10.1104/pp.105.075721

Safavi-Rizi, V., Uellendahl, K., Öhrlein, B., Safavi-Rizi, H., & Stöhr, C. (2021). Cross-stress tolerance: Mild nitrogen (N) deficiency effects on drought stress response of tomato (*Solanum lycopersicum* L.). *Plant-Environment Interactions*, *2*(5), 217-228. https://doi.org/10.1002/pei3.10060

Sayers, E. W., Beck, J., Bolton, E. E., Bourexis, D., Brister, J. R., Canese, K., Comeau, D. C., Funk, K., Kim, S., Klimke, W., Marchler-Bauer, A., Landrum, M., Lathrop, S., Lu, Z., Madden, T. L., O'Leary, N., Phan, L., Rangwala, S. H., Schneider, V. A., … Sherry, S. T. (2021). Database resources of the National Center for Biotechnology Information. *Nucleic Acids Research*, *49*(D1), D10-D17. https://doi.org/10.1093/nar/gkaa892

Schaeffer, R. D., Kinch, L. N., Liao, Y., & Grishin, N. V. (2016). Classification of proteins with shared motifs and internal repeats in the ECOD database. *Protein Science*, *25*(7), 1188–1203. https://doi.org/10.1002/pro.2893

Shannon, P., Markiel, A., Ozier, O., Baliga, N. S., Wang, J. T., Ramage, D., Amin, N., Schwikowski, B., & Ideker, T. (2003). Cytoscape: A software environment for integrated models of biomolecular interaction networks. *Genome Research*, *13*(11), 2498-504. https://doi.org/10.1101/gr.1239303

Sharma, S., Kaur, G., Kumar, A., Meena, V., Kaur, J., & Pandey, A. K. (2019). Overlapping transcriptional expression response of wheat zinc-induced facilitator-like transporters emphasize important role during Fe and Zn stress. *BMC Molecular Biology*, *20*, 22. https://doi.org/10.1186/s12867-019-0139-6

Singh, B. R., Timsina, Y. N., Lind, O. C., Cagno, S., & Janssens, K. (2018). Zinc and iron concentration as affected by nitrogen fertilization and their localization in wheat grain. *Frontiers in Plant Science*, *9*, 307. https://doi.org/10.3389/fpls.2018.00307

Sonoda, Y., Ikeda, A., Saiki, S., Wirén, N. V., Yamaya, T., & Yamaguchi, J. (2003). Distinct expression and function of three ammonium transporter genes (*OsAMT1; 1–1; 3*) in rice. *Plant and Cell Physiology*, *44*(7), 726-734. https://doi.org/10.1093/pcp/pcg083

Tian, T., Liu, Y., Yan, H., You, Q., Yi, X., Du, Z., Xu, W., & Su, Z. (2017). AgriGO v2.0: A GO analysis toolkit for the agricultural community, 2017 update. *Nucleic Acids Research*, *45*(W1), W122–W129. https://doi.org/10.1093/nar/gkx382

Tong, J., Walk, T. C., Han, P., Chen, L., Shen, X., Li, Y., Gu, C., Xie, L., Hu, X., Liao, X., & Qin, L. (2020). Genome-wide identification and analysis of high-affinity nitrate transporter 2 (*NRT2*) family genes in rapeseed (*Brassica napus* L.) and their responses to various stresses. *BMC Plant Biology*, *20*, 464. https://doi.org/10.1186/s12870-020-02648-1

Tong, H. H., Chen, L., Li, W. P., Mei, H. W., Xing, Y. Z., Yu, X. Q., Xu, X. Y., Zhang, S. Q., & Luo, L. J. (2011). Identification and characterization of quantitative trait loci for grain yield and its components under different nitrogen fertilization levels in rice (*Oryza sativa* L.). *Molecular Breeding*, *28*, 495-509. https://doi.org/10.1007/s11032-010-9499-9

Waese, J., Fan, J., Pasha, A., Yu, H., Fucile, G., Shi, R., Cumming, M., Kelley, L. A., Sternberg, M. J., Krishnakumar, V., Ferlanti, E., Miller, J., Town, C., Stuerzlinger, W., & Provart, N. J. (2017). ePlant: Visualizing and exploring multiple levels of data for hypothesis generation in plant biology. *Plant Cell*, *29*(8), 1806–1821. https://doi.org/10.1105/tpc.17.00073

Wang, H., Yang, Z., Yu, Y., Chen, S., He, Z., Wang, Y., Jiang, L., Wang, G., Yang, C., Liu, B., & Zhang, Z. (2017). Drought enhances nitrogen uptake and assimilation in maize roots. *Agronomy Journal*, *109*(1), 39–46. https://doi.org/10.2134/agronj2016.01.0030

Wang, M., Zhang, P., Liu, Q., Li, G., Di, D., Xia, G., Kronzucker, H. J., Fang, S., Chu, J., & Shi, W. (2020). TaANR1-TaBG1 and TawAbi5-TaNRT2S/NARs link ABA metabolism and nitrate acquisition in wheat roots. *Plant Physiology*, *182*(3), 1440–1453. https://doi.org/10.1104/PP.19.01482

Wang, Y. Y., Hsu, P. K., & Tsay, Y. F. (2012). Uptake, allocation and signaling of nitrate. *Trends in Plant Science*, *17*(8), 458–467. https://doi.org/10.1016/j.tplants.2012.04.006

Wang, Q., Nian, J., Xie, X., Yu, H., Zhang, J., Bai, J., Dong, G., Hu, J., Bai, B., Chen, L., Xie, Q., Feng, J., Yang, X., Peng, J., Chen, F., Qian, Q., Li, J., & Zuo J. (2018). Genetic variations in *ARE1* mediate grain yield by modulating nitrogen utilization in rice. *Nature Communications*, *9*, 735. https://doi.org/10.1038/s41467-017-02781-w

Waraich, E. A., Ahmad, R., & Ashraf, M. Y. (2011). Role of mineral nutrition in alleviation of drought stress in plants. *Australian Journal of Crop Science*, *5*(6), 764-777

Wei, J., Zheng, Y., Feng, H., Qu, H., Fan, X., Yamaji, N., Ma, J. F., & Xu, G. (2018). *OsNRT2.4* encodes a dual-affinity nitrate transporter and

functions in nitrate-regulated root growth and nitrate distribution in rice. *Journal of Experimental Botany*, *69*(5), 1095–1107. https://doi.org/10.1093/jxb/erx486

Wu, J., Wang, C., Zheng, L., Wang, L., Chen, Y., Whelan, J., & Shou, H. (2011). Ethylene is involved in the regulation of iron homeostasis by regulating the expression of iron-acquisition-related genes in *Oryza sativa*. *Journal of Experimental Botany*, *62*(2), 667–674. https://doi.org/10.1093/jxb/erq301

Wu, K., Ali, I., Xie, H., Ullah, S., Iqbal, A., Wei, S., He, L., Huang, Q., Wu, X., Cheng, F., & Jiang, L. (2021). Impact of fertilization with reducing in nitrogen and phosphorous application on growth, yield and biomass accumulation of rice (*Oryza sativa* L.) under a dual cropping system. *PeerJ*, *9*, e11668. https://doi.org/10.7717/peerj.11668

Xia, L., Zou, D., Sang, J., Xu, X., Yin, H., Li, M., Wu, S., Hu, S., Hao, L., & Zhang, Z. (2017). Rice Expression Database (RED): An integrated RNA-Seq-derived gene expression database for rice. *Journal of Genetics and Genomics*, *44*(5), 235–241. https://doi.org/10.1016/j.jgg.2017.05.003

Xu, G., Fan, X., & Miller, A. J. (2012). Plant nitrogen assimilation and use efficiency. *Annual Review of Plant Biology*, *63*, 153–182. https://doi.org/10.1146/annurev-arplant-042811-105532

Zhang, X., Liu, H., Zhang, S., Wang, J., & Wei, C. (2019). NH_4^+-N alleviates iron deficiency in rice seedlings under calcareous conditions. *Scientific Reports*, *9*, 12712. https://doi.org/10.1038/s41598-019-49207-9

Zhang, Z., Gao, S., & Chu, C. (2020). Improvement of nutrient use efficiency in rice: Current toolbox and future perspectives. *Theoretical and Applied Genetics*, *133*, 1365-1384. https://doi.org/10.1007/s00122-019-03527-6

Zhao, L., Chen, P., Liu, P., Song, Y., & Zhang, D. (2021). Genetic effects and expression patterns of the nitrate transporter (NRT) gene family in *Populus tomentosa*. *Frontiers in Plant Science*, *12*, 661635. https://doi.org/10.3389/fpls.2021.661635

Pertanika J. Trop. Agri. Sci. 46 (1): 91 - 106 (2023)

PERTANIKA JOURNALS

TROPICAL AGRICULTURAL SCIENCE

Journal homepage: http://www.pertanika.upm.edu.my/

Growth Interaction of *Moina* sp. and *Chlorella* sp. for Sustainable Aquaculture

Afrina Batrisyia Aswazi[1,2,4], Ahmad Azfaralarriff[1], Douglas Law[3], Herryawan Ryadi Eziwar Dyari[2], Babul Airianah Othman[1], Muhammad Shahid[1], Mushrifah Idris[5], Nur Amelia Abas[5], Muhamad Syahmin Aiman Sahrir[5], Hanan Mohd Yusof[6] and Shazrul Fazry[1,5]*

[1]Department of Food Sciences, Faculty of Science and Technology, Universiti Kebangsaan Malaysia, 43600, Bangi, Selangor, Malaysia
[2]Department of Earth Sciences and Environment, Faculty of Science and Technology, Universiti Kebangsaan Malaysia, 43600, Bangi, Selangor, Malaysia
[3]Faculty of Health and Life Sciences, INTI International University, Persiaran Perdana BBN, 71800 Nilai, Negeri Sembilan, Malaysia
[4]Department of Biomedical Science, Faculty of Medicine and Health Sciences, Universiti Putra Malaysia, 43400, UPM Serdang, Selangor, Malaysia
[5]Tasik Chini Research Centre, Faculty of Science and Technology, Universiti Kebangsaan Malaysia, 43600, Bangi, Selangor, Malaysia
[6]Fisheries Research Institute, Glami Lemi, 71660 Titi Jelebu, Negeri Sembilan, Malaysia

ABSTRACT

Fish farmers' dependence on costly formulated fish feed has affected their income. The cost of formulated feed is also constantly rising. Efforts to mass-produce the locally available natural resource, namely water flea (*Moina* sp.), were initiated as an alternative to the commercially formulated fish feed. This study evaluates the most suitable growth medium for commercially culturing *Moina* sp. and *Chlorella* sp. and studies the effect of their growth activity on water quality. In this study, the growth behaviour of *Moina* sp. and *Chlorella* sp. was monitored individually before *Moina* sp. was cultured together with *Chlorella* sp. in a growth medium. *Chlorella* sp. was cultured in different mediums (BG-11, Bristol, and organic fertiliser). The first generation of *Moina* sp. took 96 h to mature and begin to reproduce, while the next generation took a

ARTICLE INFO

Article history:
Received: 10 August 2022
Accepted: 9 November 2022
Published: 22 December 2022

DOI: https://doi.org/10.47836/pjtas.46.1.06

E-mail addresses:
afrina.aswazi@gmail.com (Afrina Batrisyia Aswazi)
azfaralariff@ukm.edu.my (Ahmad Azfaralarriff)
douglas.law@gmail.com (Douglas Law)
herry@ukm.edu.my (Herryawan Ryadi Eziwar Dyari)
airianah@ukm.edu.my (Babul Airianah Othman)
mshahdaslam@gmail.com (Muhammad Shahid)
mushrifahidris@gmail.com (Mushrifah Idris)
amelia@ukm.edu.my (Nur Amelia Abas)
syahminaiman@ukm.edu.my (Muhamad Syahmin Aiman Sahrir)
hanan@dof.gov.my (Hanan Mohd Yusof)
shazrul@ukm.edu.my (Shazrul Fazry)
*Corresponding author

ISSN: 1511-3701
e-ISSN: 2231-8542

shorter time (from 24 h to 48 h). The brood size was between five and 15 neonates, while the maximum brood count recorded was eight. The *Chlorella* sp. culture had grown well on Day 5 (555.33 ug/L); thus, it was introduced with *Moina* sp. on Day 6. Although an organic fertiliser medium provided the optimum conditions for *Chlorella* sp. growth, it slightly inhibited the *Moina* sp. growth due to higher ammonia (NH_3) concentration. However, the organic fertiliser medium could sustain *Chlorella* sp. growth while being ingested by *Moina* sp. The growth activity of both species slightly affected the water quality. Meanwhile, the increase in ammonia (NH_3), carbon dioxide (CO_2), and calcium carbonate ($CaCO_3$) was recorded. In conclusion, organic fertiliser is the best medium for *Chlorella* sp. growth, which is the main food source for *Moina* sp. culture.

Keywords: *Chlorella* sp., live feed, *Moina* sp., organic fertiliser, sustainable aquaculture

INTRODUCTION

Live foods are living organisms that can move in water and are always available for fish or larvae, thus stimulating the larval feeding response (Das et al., 2012). Since commercial marine fish culture was developed in the late 1970s, the demand for *Artemia* sp. or brine shrimp cysts has gradually increased from a few tonnes to approximately 800 tonnes per annum (Rasdi & Qin, 2018). It represents approximately 40% of aquaculture feed demand during the early stages. Although applying *Artemia* sp. cysts as feed is simple, several factors are critical for hatching the large quantities needed in larval fish production. These include cyst disinfection or decapsulation before incubation and hatching under the following optimal conditions: constant temperature of 25–28°C, 15–35 parts per thousand (ppt) salinity, minimum pH value of 8.0, near-saturated oxygen levels, maximum cyst densities of 2 g/L, and strong illumination of 2,000 lux (Sorgeloos et al., 2001). The production cost of *Artemia* sp. cysts is relatively high, directly affecting fish production costs. Cheaper diets with the same nutritional values are needed to keep the price of fish competitive in the global market. The lack of suitable live feeds for feeding the fish at various production stages has hampered the industrial development of aquaculture (Das et al., 2012). Most formulated fish pellets are not suitable for feeding aquatic organism larvae. In addition, the high price and rapid consumption of fish pellets place a burden on small-scale fish farmers.

Moina sp., also known as the water flea, is a freshwater crustacean organism smaller than *Daphnia* sp., its closest relative. *Moina* sp. is capable of asexual and sexual reproduction. *Moina* sp. can produce up to 30 neonates asexually for each brood under optimal conditions. Usually, the population is made up entirely of females. The *Moina* sp. diet comprises bacterial, yeast, phytoplankton and decomposing organic matter (Rottmann et al., 2018). *Moina* sp. has a protein content equal to 50% of its dry weight (Rasdi & Qin, 2018). The fat content of adult *Moina* sp. is typically higher than its

juvenile (Conklin & Provasoli, 1977; Rasdi et al., 2020; Rottmann et al., 2018). *Moina* sp. can primarily be found in temporary ponds or ditches. It is smaller in size than its closest relative, *Daphnia* sp. *Moina* sp. has high protein content and is relatively easy to culture. Aside, it is a superior live food compared to *Artemia* sp., which is one of the commonly used live feeds. It is because of its high protein and nutrient content (Loh et al., 2012), thus making it a suitable substitute for *Artemia* in aquaculture hatcheries. The *Moina* sp. was widely utilised as live food in many hatcheries and the maintenance and cultivation of commercially significant ornamental fishes, finfish, crustaceans, teleost, and marine fish culture worldwide (Aguado et al., 2009; Das et al., 2012; He et al., 2001; Fermin, 1991; Fermin & Bolivar, 1994; Ingram, 2009; Poynton et al., 2013). In this study, *Moina* sp. was selected and utilised as a live food to produce sustainable fish feed, particularly for aquaculture production in Tasik Chini. *Moina* sp. cultivation is not as complex as *Artemia* sp. because these freshwater Cladoceras have higher reproduction rates, wide temperature tolerance, and the ability to thrive on phytoplankton and organic wastes; they can thrive in a relatively high content of un-ionised ammonia (Khoo et al., 2013).

Humans regularly use microalgae as a food source and in hatchery production for commercial fish and shellfish (Kay & Barton, 1991). These microscopic organisms are still consumed as food supplements, and their products are also used for different purposes like dyes, pharmaceuticals, animal feed, aquaculture, and cosmetics (Safi et al., 2014). Microalgae, such as *Chlorella* sp., *Dunaliella* sp., *Scenedesmus* sp., and *Spirulina* sp., are frequently utilised algae. *Chlorella* sp. is a collection of aquatic organisms that lack complex cell structures and are often found in plants (Slade & Bauen, 2013). *Chlorella* sp. can also be defined as prokaryotic or photosynthetic eukaryotic microorganisms with unicellular or compact multicellular structures capable of rapid reproduction and survival in harsh environments (Mata et al., 2010). In terms of nutrient content, *Chlorella* sp. has a protein content of appropriately 70% and a higher beta-carotene concentration than broccoli (Kay & Barton, 1991). *Chlorella* sp. has valuable components with potential in the food industry due to its high content of macro and micro components and low-calorie count. *Chlorella* sp. contains various vitamins and minerals, including calcium and magnesium, in addition to the basic nutrients.

As fish feed prices rise rapidly, identifying a reliable food source for livestock and a sustainable system that can produce affordable and sustainable food sources is critical. Given the correlation between *Chlorella* sp. and *Moina* sp., as well as their ability to reproduce in the laboratory, it is crucial to investigate the growing linkages between these two organisms and assess their potential. Therefore, this study aims to evaluate *Moina* sp. and *Chlorella* sp. growth. The suitable growth medium for both organisms was determined, and the effect of their growth activity on water quality was also evaluated. At the end of this

study, a suitable medium for *Moina* sp. and *Chlorella* sp. growth could be formulated.

MATERIALS AND METHODS

Organism and Culture Medium

The cultured *Chlorella* sp. was a gift from the Fisheries Research Institute Glami-Lemi. *Moina* sp. was obtained directly from a pet shop which sells wild *Moina* sp. Meanwhile, *Chlorella* sp. was cultured using two types of culture medium: BG-11, Bristol, and an organic fertiliser mix (Table 1). All chemicals were purchased from Chemiz (Malaysia).

Table 1
Composition for BG-11, Bristol, and organic fertiliser

Ingredient	Media		
	BG-11 (g/L)	Bristol (g/L)	Organic fertiliser (g/10 L)
Sodium nitrate ($NaNO_3$)	1	0.250	-
Magnesium sulphate ($MgSO_4$)	0.513	0.075	-
Dipotassium phosphate (K_2HPO_4)	0.250	0.075	-
Calcium chloride ($CaCl_2$)	0.058	0.250	-
Ammonium chloride (NH_4Cl)	0.050	-	-
Iron (III) chloride ($FeCl_3$)	0.003	-	-
Rice bran	-	-	0.60
Corn	-	-	1.20
Urea	-	-	0.10
Triple super phosphate	-	-	0.10
Agricultural lime	-	-	0.05

Culturing *Moina* sp. Biomass

Adult *Moina* sp. with neonate was placed in a separate container that contained water. New neonates were produced, and those less than 24 hours old were isolated and used as new adults. The new neonates were placed in test tubes that contained 20 ml of dechlorinated tap water to assess the first reproduction day, number of reproductions, and lifespan of *Moina* sp. The neonates were fed daily with 1 ml of *Chlorella* sp. cultivated in BG-11. When the neonates matured (adult *Moina* sp.) and started to reproduce, the average number of neonates produced (brood size) was determined, and they were isolated from the mother. This procedure was repeated to determine the brood number and female life expectancy (Martínez-Jerónimo & Gutierrez-Valdivia, 1991). This experiment was carried out in 10 replicates.

Culturing *Chlorella* sp. Under Laboratory Culture Condition

Chlorella sp. was cultured using a batch culture system (Laing, 1991). First, it was cultured in an initial culture volume of 10 mL and gradually transferred or subcultured in a larger culture volume (10 L). At Stage 1 of cultivation (small volume), *Chlorella* sp. was grown using BG-11 (1 ml). Then, it was to prepare as feed for *Moina* sp. and a subculture for a larger culture volume to be cultivated with *Moina* sp.

For Stage 2 of cultivation in the larger volume (10 L), *Chlorella* sp. was cultivated in three different mediums: BG-11, Bristol, and organic fertiliser. The cultures were exposed to continuous fluorescents illumination at 22°C to achieve the maximum growth rate and aerated by using an air pump (0.03 MPa, 50l/min, 220-240 V, 35W). It was to prevent sedimentation of the algae and ensure that all cells of the population were equally exposed to light and nutrients. Gas exchange between the culture medium and the air was simultaneously improved. *Chlorella* sp. culture was not bacteria-free; however, all culture mediums and liquids were autoclaved at a temperature of 120°C for 15 min. Algal biomass that was tested for its nutrient content was centrifuged and refrigerated.

Chlorophyll A Concentration

Chlorophyll A concentration of *Chlorella* sp. biomass cultured in the 10 L culture volume was recorded daily until it was ready to be fed to *Moina* sp. and continued until all *Chlorella* sp. was consumed by *Moina* sp. The following equation calculated the specific growth rate of the *Chlorella* sp.:

$$\text{Specific growth rate, } \mu = \text{Ln}\,(N_2 / N_1)/(t_2 - t_1)$$

where μ is the specific growth rate, and N_1 and N_2 are biomass at Time 1 (t_1) and Time 2 (t_2), respectively (Krishnan et al., 2015).

Chlorophyll A of *Chlorella* sp. biomass of more than 10 L was measured using YSI 600 OMS V2 Sonde (Xylem Analytics, USA) along with temperature and salinity. *Chlorella* sp. biomass (10 L) was moved to room temperature before *Moina* sp. was inoculated. Experiments were carried out in three replicates.

Moina sp. Weight

The initial wet weight of *Moina* sp. before being inoculated into 10 L of algae culture was determined. *Moina* sp. biomass was collected using a fine mesh sieve/strainer (<400 μm), which was also used to drain excess water simultaneously and weighted using a laboratory analytical scale. All measurements were carried out in triplicates.

Water Quality Tests on *Chlorella* sp. Culture

Several water parameter tests were carried out on the *Chlorella* sp. cultures to see if there were changes in water quality during *Chlorella* sp. growth and after *Moina* sp. inoculation. Water parameter test kits from (HACH, Malaysia) were used to check the water quality. The parameter test kits included acidity and alkalinity, carbon dioxide (CO_2), unionised ammonia, and

nitrite test kits. In addition, YSI-600-OMS V2 Sonde (Xylem Analytics, USA) was used to check the salinity, temperature, and dissolved oxygen (DO).

Statistical Analysis

All analysis was done in triplicate. Data were presented as mean ± standard deviation (SD).

RESULTS AND DISCUSSION

Growth and Reproduction of *Moina* sp.

The Cladocera species, especially *Moina* sp., were extensively studied worldwide concerning the effects of food abundance, growth, and reproduction parameters (Burak, 1997; He et al., 2001; Rasdi, Ikhwanuddin et al., 2021). In addition, other literature has addressed *Chlorella* sp. to be used as a primary food source for *Moina* sp. (Das et al., 2012; Shidik et al., 2021). Therefore, in this study, *Chlorella* sp. was used as feed for the *Moina* sp. growth. Figure 1 shows the *Moina* sp. count after a single neonate was fed daily with 1 ml of *Chlorella* sp. for six days.

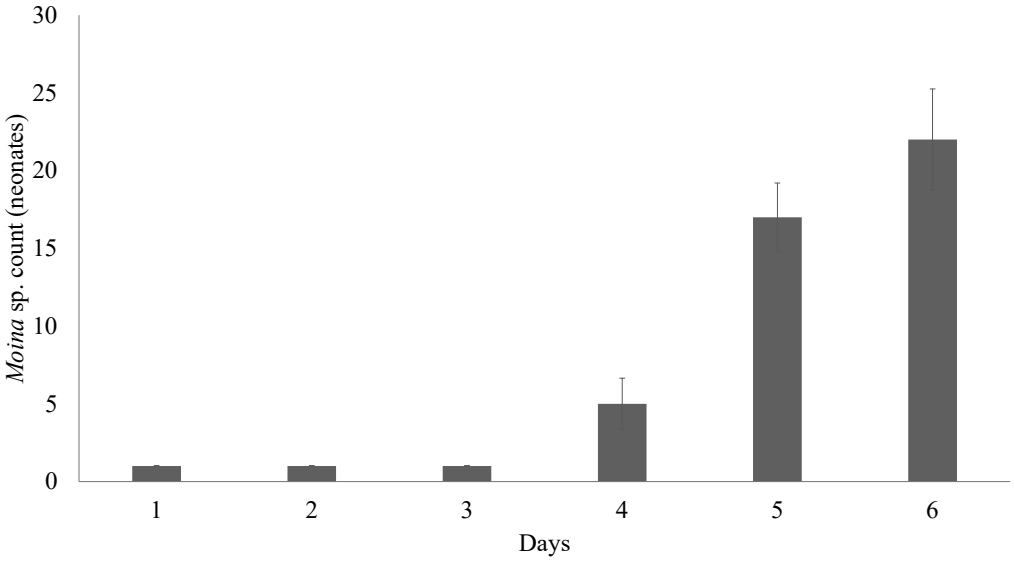

Figure 1. *Moina* sp. count. A neonate is fed 1 ml of *Chlorella* sp. and counted every day for six days to know the sex maturity and first reproduction time. Neonate-turned-adult and new neonates are counted together for the first and subsequent reproduction. The error bar represents the standard deviation of the results

Moina sp. feds *Chlorella* sp. took as early as four days to mature and began to produce brood. Subsequent broods are produced every 24 h after the first reproduction (First brood number). Figure 2 shows the brood size of each reproduction from a single

neonate after the first reproduction. The second reproduction shows the average highest brood size produced (15 neonates) and continues up to eight reproductions, with the brood size ranging from four to ten neonates on each reproduction. As reported previously, the *Moina* sp. reproduction activity ranges from 6 to 12 reproductions (Kamrunnahar et al., 2019; Martínez-Jerónimo & Gutierrez-Valdivia, 1991).

Effect of Medium on the *Chlorella* sp. Growth

Quality and quantity of food are the most important factors in determining biomass production by *Moina* sp. (Rasdi et al., 2020, Rasdi, Yuslan et al., 2021; Sipaúba-Tavares et al., 2014). To mass produce *Moina* sp., an adequate supplement of microalgal must be provided. For usage in aquaculture, a microalgal strain must meet various criteria, such as ease of culture, lack of toxicity, high nutritional value with correct cell size and shape, and a digestible cell wall to make nutrients available (Hemaiswarya et al., 2011; Rasdi, Yuslan, et al., 2021). Different kinds of literature have addressed *Chlorella* sp. as a primary food source for *Moina* sp. (Das et al., 2012; Shidik et al., 2021). Therefore, the growth of *Chlorella* sp. in different growth mediums was observed to identify the most suitable growth medium to be used and if there was any effect on *Chlorella* sp. growth. Figure 3 shows the chlorophyll A concentration in *Chlorella* sp. growth in different mediums.

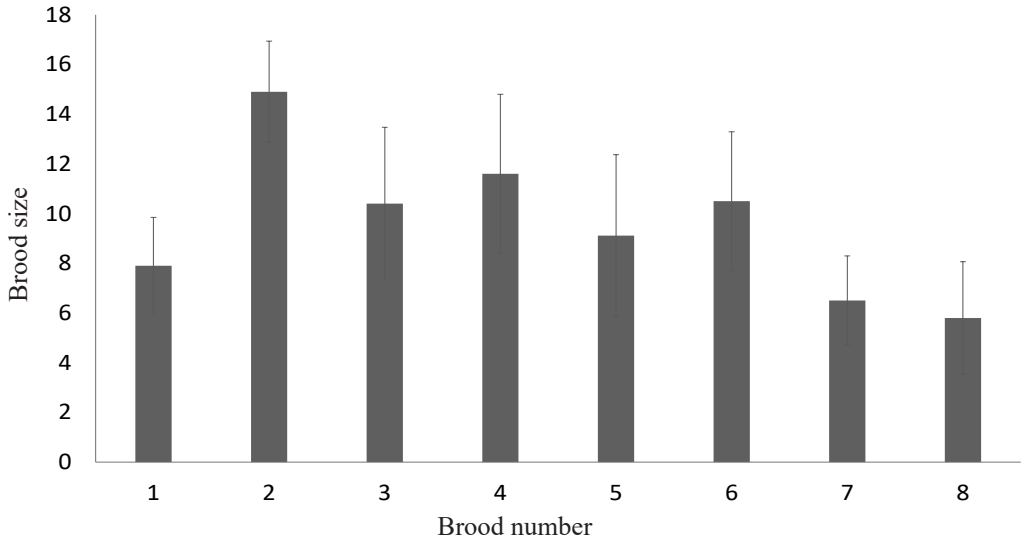

Figure 2. Average brood size and brood number (lifespan) of *Moina* sp. Each generation of juvenile *Moina* sp. produced from single adult *Moina* sp. is calculated and separated from the mother. Brooding *Moina* sp. is fed by 1 ml of *Chlorella* sp. The error bar represents the standard deviation of the results

After inoculation, *Chlorella* sp. grew well in the BG-11 medium, followed by Bristol medium and organic fertiliser. Chlorophyll A reached its maximum concentration of 552.5 ± 1.7 ug/L after 48 h in biomass cultured using BG-11 medium and 72 h in biomass cultured by Bristol medium and organic fertiliser. Although *Chlorella* sp. cultured in fertiliser showed a lag phase on Day 1, it has a significantly higher growth rate than the others. It indicated that the organic fertiliser not only had the basic nutrients required to culture *Chlorella* sp. but also had more macronutrients and micronutrients, such as potassium, zinc, iron, and copper, to help facilitate *Chlorella* sp. growth (Bhosale & Vijayalakshmi, 2015; Prasanthi et al., 2017). From Day 4 onwards, all cultures reached the maximum growth number. This phase occurred due to the depletion of nutrients in the medium (Krishnan et al., 2015). In this stationary phase, there was an equal rate of cell division and dying cells. Therefore, culture at this stage was suitable as a starter culture to produce a continuous supply of *Chlorella* sp. (Sánchez-Bayo et al., 2020).

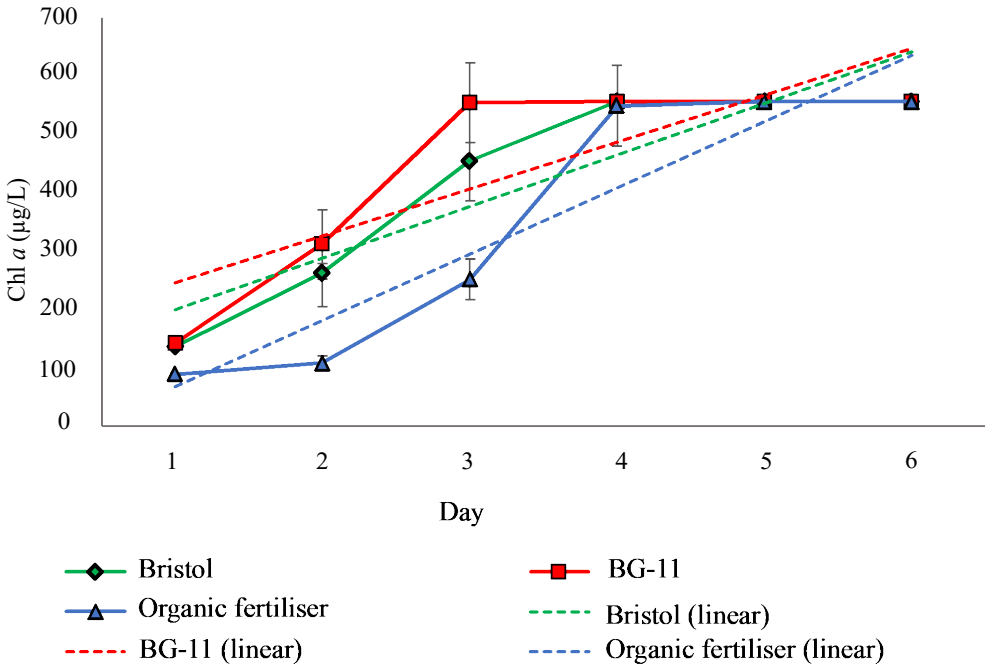

Figure 3. The concentration of chlorophyll A in *Chlorella* sp. culture cultured in different growth mediums at 22°C, 24 h of illuminated light and aeration for five days

The Growth of *Moina* sp. in Different Media

A single mature neonate (72 h old) was introduced into the six-day-old medium, which contained well growth chlorophyll A. Figure 4 shows the growth of *Chlorella* sp. from Day 1 until Day 6 and changes that occurred when *Moina* sp. was introduced on Day 6.

Results showed that the growth of *Chlorella* sp. in BG-11 and Bristol started to decrease, respectively, after 24 h and 48 h of *Moina* sp. introduction and depleted on Day 10. Meanwhile, the concentration of *Chlorella* sp. in the organic fertiliser medium was maintained until Day 15 and depleted on Day 17. The ability of *Chlorella* sp. to remain at the same concentration until Day 15 indicated that organic fertiliser could supply adequate nutrients (Ratomski & Hawrot-Paw, 2021) throughout the growth of *Chlorella* sp. for 15 days. Further tests from previous research findings on nutrient concentration effects (nitrogen and phosphorous) showed that low nitrogen concentrations could also stimulate algal growth (Blinova et al., 2015).

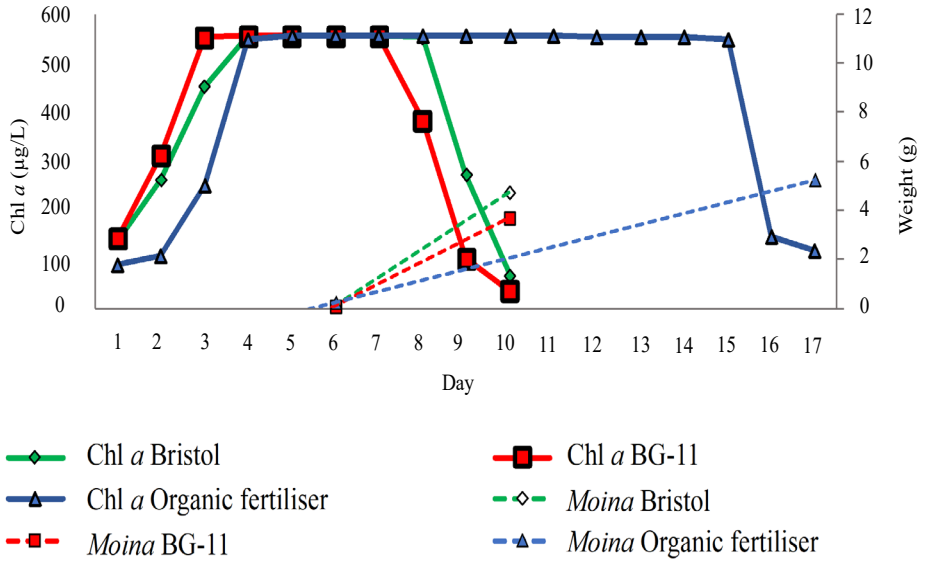

Figure 4. Changes in the concentration of chlorophyll A and wet weight (g) of *Moina* sp. straight line indicated the *Chlorella* sp. concentration changes while the dashed line represents the *Moina* sp. wet weight changes when inoculated on the sixth days of *Chlorella* sp. growth and final weight once *Chlorella* sp. biomass fully consumed

Of all *Moina* sp. growth in different mediums, *Moina* sp. growth in organic fertiliser showed the highest final weight (5.24 g), followed by *Moina* sp. growth in Bristol (4.73 g) and the lowest in BG-11 (3.69 g). Although *Moina* sp. in BG-11

started to feed on *Chlorella* sp. faster, it had the lowest final weight than the other two *Moina* sp. in different mediums. These differences probably happened due to differences in medium composition and thus influenced the growth, reproduction, and metabolism of *Moina* sp. and *Chlorella* sp. The presence of organic ingredients supported *Chlorella* sp. growth and *Moina* sp. as a nutrition source (Shidik et al., 2021). It was reported that the feed's protein and amino acid concentrations directly affected the fecundity and population growth of *M. macrocopa* (Mubarak et al., 2017). It was also reported that the high fertility and reproductive rate of Cladocera could be obtained when its food source had a high carbon/nitrogen ratio (Khoo et al., 2013). In addition, the higher growth rate of *Chlorella* sp. in an organic fertiliser medium (Figure 3) indicated that it could be a source of food supply for *Moina* sp. for a longer period. The highest final weight of *Moina* sp. was due to the adequacy of *Chlorella* sp. to ensure the growth and development of the brood generation produced.

Changes in Water Quality During *Moina* sp. Growth

Moina sp. is known to survive in poor water quality, especially in an oxygen-poor environment (Rottmann et al., 2018). However, there is not much to know about the chemical or physical requirements for *Moina* sp. Therefore, in this study, changes in water quality during *Moina* sp. growth were evaluated: Un-ionised ammonia (NH_3) level, salinity, dissolved oxygen (DO), average carbon dioxide (CO_2) content, and average calcium carbonate ($CaCO_3$) total alkalinity. The results are presented in Figure 5.

Organic fertiliser had a higher concentration of NH_3 (0.01098 mg/L) than the other two mediums used (Figure 5a), which were at 0 mg/L, respectively. Compared to the nutrient composition in BG-11 and Bristol medium that was in liquid form, organic fertiliser was composed of a solid substrate that would break down in the *Chlorella* sp. inoculated water, providing nutrients for *Chlorella* growth. Therefore, decomposition occurred in the *Chlorella* sp. biomass and inevitably released a much higher concentration of NH_3 (Shidik et al., 2021). The increase in NH_3 concentration in all mediums indicated that the growth activity of *Chlorella* sp. and *Moina* sp. unionised ammonia (NH_3) values in the *Chlorella* sp. cultured using organic fertiliser increased to 0.0015 mg/L on Day 3 and remained on the lag phase until Day 12. The high concentration of NH_3 might explain the higher growth rate of *Chlorella* sp. in organic fertiliser compared to the other mediums in the first four days (Figure 4).

Chlorella sp. could adapt to the high NH_3 concentration (Tam & Wong, 1996) on Day 4 after inoculation because there was no decrease in chlorophyll A concentration, albeit with a low reproduction on Day 1. The increased NH_3 level (Figure 5a) after the introduction of *Moina* sp. indicated that nitrogenous waste was produced during *Moina* sp. growth. The prolonged growth of *Moina* sp. in organic fertiliser for up to 12 days as compared to other mediums

(five days, respectively) was due to the prolonged growth and reproduction rate of *Chlorella* sp. It was also reported that when the NH_3 concentration was above 0.013 mg/L, the growth and reproduction activity of *Moina* sp. seemed to be affected as *Moina* sp. population could be seen in high yield on Day 4 of inoculation in *Chlorella* sp. biomass cultured by BG-11 and Bristol mediums. However, when the NH3 concentration reached 0.236 mg/L, it would kill the *Moina* sp. completely instead of affecting its reproduction and growth rate (He et al., 2001). *Chlorella* sp. and *Moina* sp. kept growing and number simultaneously up to Day 10 until the consumption rate of *Chorella* sp. by *Moina* sp. was higher than the *Chlorella* sp. reproduction (Figure 4). The last reproduction of *Moina* sp. was recorded on Day 12, probably due to the shortage of food supply as the *Moina* sp. could adapt to environmental stress.

In this study, *Chlorella* sp. was cultured in three different mediums with salinity values of 0.05 ppt to 0.015 ppt on the day of *Moina* sp. inoculation (Figure 5b). *Chlorella* sp. cultivated using organic fertiliser had a higher salinity value than BG-11 and Bristol mediums. This high salinity value corresponded to the high concentration of unionised ammonia NH_3, which slowed down the *Chlorella* sp. (Fakhri et al., 2017; Goto et al., 2018). However, all mediums had a salinity value below the limit of 0.5 ppt for proper Cladocera growth, although the optimal growth was suggested at 0 salinity (Yuslan et al., 2021) and limit at 2 ppt (Rasdi & Qin, 2018). Therefore, it was concluded that 0.015 ppt salinity value has no significant effect on *Moina* sp. growth.

Dissolved oxygen during *Moina* sp. inoculation in organic fertiliser medium was lower (7.09 mg/L) than BG-11 (11.71 mg/L) and Bristol (11.95 mg/L) mediums. Dissolved oxygen is an indicator of photosynthetic activity by microalgae. Low dissolved oxygen indicates problems with microalgal growth and possibly dissolved oxygen consumption by heterotrophic microorganisms (Morales et al., 2018). The decreased level of dissolved oxygen when *Moina* sp. was inoculated indicated the respiration activity of *Moina* sp. (Murakami et al., 2020). Meanwhile, dissolved oxygen levels in BG-11 and Bristol mediums decreased until all *Moina* sp. stopped reproducing (Day 5). Dissolved oxygen in the organic fertiliser medium started to increase on Day 5. Increased dissolved oxygen levels indicated that the *Chlorella* sp. growth rate was higher than *Moina* sp. consumption and respiration rate (Kazbar et al., 2019). These changes were caused by high NH_3 concentration, which inhibited *Moina* sp. growth and reproduction. However, on the Day 8 of *Moina* sp. growth, the dissolved oxygen concentration started to decrease. It indicated that *Moina* sp. could adapt to the environmental stress and started to reproduce, thus causing the increased consumption rate and respiration rate of *Moina* sp.

The increase in carbon dioxide rate was higher in the organic fertiliser medium than in other mediums after inoculation of *Moina* sp. This result was consistent with the changes in the dissolved oxygen concentration (Figure 5c). Although algae growth requires a source of carbon

dioxide (Slade & Bauen, 2013), the low photosynthesis rate of *Chlorella* sp. during the first four days caused a higher carbon dioxide concentration due to the *Moina* sp. respiration (Santoso et al., 2020). Therefore, it is viewed that high carbon dioxide does not necessarily increase the growth rate (Rashid et al., 2014). In addition, carbon dioxide was also reported to be produced partly from the decomposition of organic fertiliser and partly from the carbonate-bicarbonate system (Ventura & Enderez, 1980).

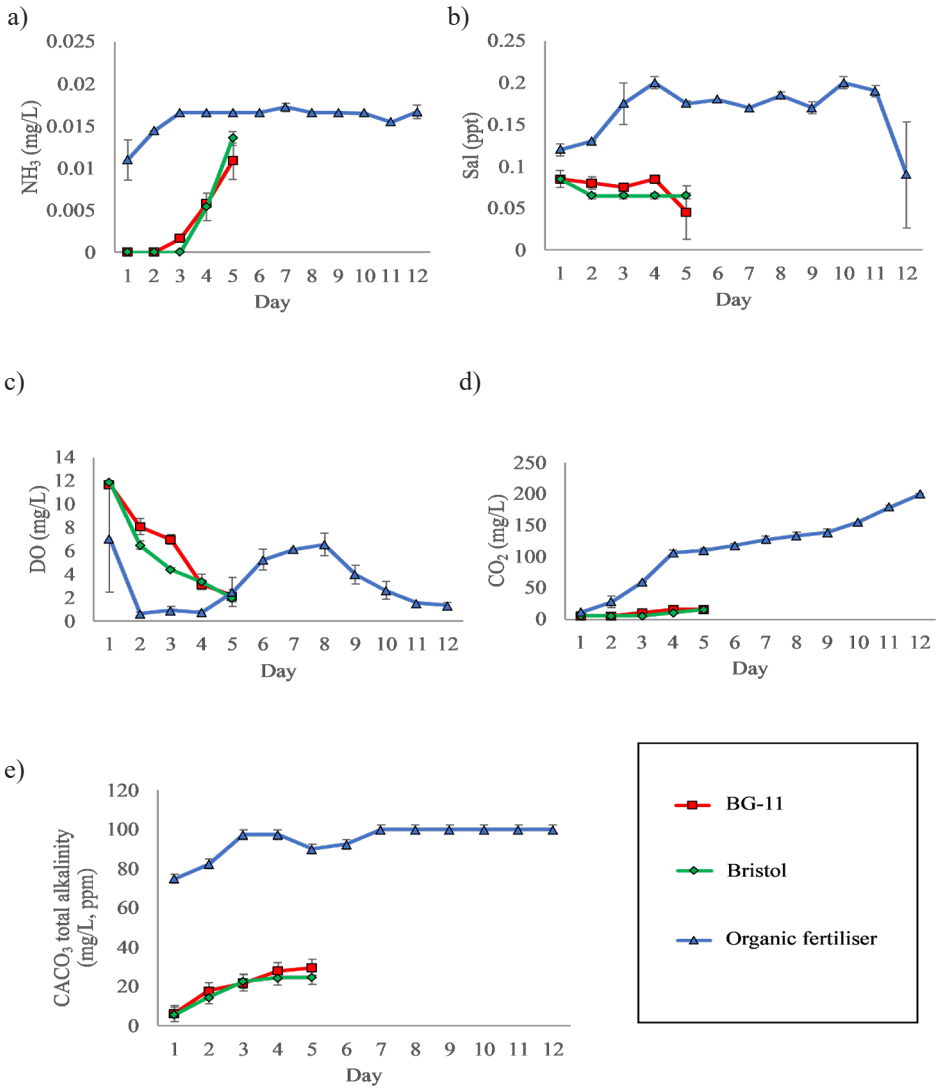

Figure 5. Water quality changes on three different mediums used to culture *Chlorella* sp. and *Moina* sp.: Day 1 indicated the first day of *Moina* sp. inoculation and the sixth day of *Chlorella* sp. cultivation. (a) Un-ionised ammonia level (NH_3); (b) Salinity of *Chlorella* sp. Culture (Sal); (c) Dissolved oxygen (DO); (d) Average carbon dioxide content (CO_2); and (e) Average $CaCO_3$ total alkalinity.

Organic fertiliser medium had higher $CaCO_3$ total alkalinity (19.6 ± 7.5 mg/L) than other mediums used, which only had a trace amount. It was due to agricultural lime ($CaCO_3$), an organic fertiliser ingredient, stabilising the pH value (Kar, 2016). However, when carbon dioxide was produced as a photosynthesis product, the dissolved carbon dioxide produced carbonic acid, which dissolved $CaCO_3$ (Qian et al., 2021). As a result, the concentration of carbon dioxide increased (Figure 5d), and the alkalinity also increased (Figure 5e). In addition, the high alkalinity (80 mg/L $CaCO_3$) might be the other factor which affected the *Chlorella* sp. growth on Day 1, as the limit for optimum *Chlorella* sp. growth was 63 mg/L $CaCO_3$ based on hardness (Kim & Kim, 2014).

CONCLUSION

This research showed that *Moina* sp. started to mature and reproduce after 72 h. The usage of different mediums affected the *Chlorella* sp. growth, whereby organic fertiliser medium showed the highest growth rate. *Moina* sp. reproduction in a *Chlorella* sp. biomass cultured using organic fertiliser showed a longer reproduction time, possibly due to growth inhibition by high NH_3 concentration and the rate of solid decomposition of the nutrient substrate in the culture. *Moina* sp. growth activity in all mediums used could slightly affect water quality but within the acceptable range. It was found that the most important factor determining the survival, longevity, and growth of *Moina* sp. was the medium used. *Moina* sp. could adapt to environmental stresses when the food supply was adequate. This study concludes that organic fertiliser with higher NH_3 content is more suitable for *Chlorella* sp. optimal growth and supports the growth of *Moina* sp.

ACKNOWLEDGEMENTS

The authors want to thank the Universiti Kebangsaan Malaysia (UKM) and Tasik Chini Research Centre, UKM, for supporting this project through DCP 2018-006/1 research grant and INTI International University through the INTI-FHLS-07-03-2021 research grant.

REFERENCES

Aguado, F. P., Nandini, S., & Sarma, S. S. S. (2009). Functional response of *Ameca splendens* (Family Goodeidae) fed cladocerans during the early larval stage. *Aquaculture Research*, *40*(14), 1594-1604. https://doi.org/10.1111/j.1365-2109.2009.02259.x

Bhosale, S., & Vijayalakshmi, D. (2015). Processing and nutritional composition of rice bran. *Current Research in Nutrition and Food Science*, *3*(1), 74–80. https://doi.org/10.12944/CRNFSJ.3.1.08

Blinova, L., Bartosova, A., & Gerulova, K. (2015). Cultivation of microalgae (*Chlorella vulgaris*) for biodiesel production. *Research Papers Faculty of Materials Science and Technology Slovak University of Technology*, *23*(36), 108–113. https://doi.org/10.1515/rput-2015-0010

Burak, E. S. (1997). Life tables of *Moina macrocopa* (Straus) in successive generations under food and temperature adaptation. *Hydrobiologia*, *360*, 101-107. https://doi.org/10.1023/A:1003161201737

Conklin, D. E., & Provasoli, L. (1977). Nutritional requirements of the water flea *Moina macrocopa*. *Biological Bulletin*, *152*(3), 337–350. https://doi.org/10.2307/1540422

Das, P., Mandal, S. C., Bhagabati, S. K., Akhtar, M. S., & Singh, S. K. (2012). Important live food organisms and their role in aquaculture. In *Frontiers in aquaculture* (pp. 69-86). Narendra Publishing House.

Fakhri, M., Arifin, N. B., Yuniarti, A., & Hariati, A. M. (2017). The influence of salinity on the growth and chlorophyll content of nannochloropsis sp. BJ17. *Nature Environment and Pollution Technology*, *16*(1), 209–212.

Fermin, A. C. (1991). Freshwater cladoceran *Moina macrocopa* (Strauss) as an alternative live food for rearing sea bass *Lates calcarifer* (Bloch) fry. *Journal of Applied Ichthyology*, *7*(1), 8-14. https://doi.org/10.1111/j.1439-0426.1991.tb00589.x

Fermin, A. C., & Bolivar, M. E. (1994). Feeding live or frozen *Moina macrocopa* (Strauss) to Asian sea bass, *Lates calcarifer* (Bloch), larvae. *Israeli Journal of Aquaculture*, *46*(3), 132-139.

Goto, M., Nagao, N., Yusoff, F. M., Kamarudin, M. S., Katayama, T., Kurosawa, N., Koyama, M., Nakasaki, K., & Toda, T. (2018). High ammonia tolerance on growth rate of marine microalga *Chlorella vulgaris*. *Journal of Environmental Biology*, *39*(5), 843–848. https://doi.org/10.22438/jeb/39/5(SI)/4

He, Z. H., Qin, J. G., Wang, Y., Jiang, H., & Wen, Z. (2001). Biology of *Moina mongolica* (Moinidae, Cladocera) and perspective as live food for marine fish larvae: Review. *Hydrobiologia*, *457*, 25–37. https://doi.org/10.1023/A:1012277328391

Hemaiswarya, S., Raja, R., Kumar, R. R., Ganesan, V., & Anbazhagan, C. (2011). Microalgae: A sustainable feed source for aquaculture. *World Journal of Microbiology and Biotechnology*, *27*(8), 1737–1746. https://doi.org/10.1007/s11274-010-0632-z

Ingram, B. A. (2009). Culture of juvenile Murray cod, trout cod and Macquarie perch (Percichthyidae) in fertilised earthen ponds. *Aquaculture*, *287*(1-2), 98-106. https://doi.org/10.1016/j.aquaculture.2008.10.016

Kamrunnahar, K., Md, A., Jeong, U. C., & Kang, S. J. (2019). Mass culture of *Moina macrocopa* using organic waste and its feeding effects on the performance of *Pagrus major* larvae. *The Egyptian Journal of Aquatic Research*, *45*(1), 75-80. https://doi.org/10.1016/j.ejar.2019.02.001

Kar, D. (2016). Control (Treatment) of epizootic ulcerative syndrome. In *Epizootic ulcerative fish disease syndrome* (pp. 233–245). Academic Press. https://doi.org/10.1016/b978-0-12-802504-8.00010-9

Kay, R. A., & Barton, L. L. (1991). Microalgae as food and supplement. *Critical Reviews in Food Science and Nutrition*, *30*(6), 555–573. https://doi.org/10.1080/10408399109527556

Kazbar, A., Cogne, G., Urbain, B., Marec, H., Le-Gouic, B., Tallec, J., Takache, H., Ismail, A., & Pruvost, J. (2019). Effect of dissolved oxygen concentration on microalgal culture in photobioreactors. *Algal Research*, *39*, 101432. https://doi.org/10.1016/j.algal.2019.101432

Khoo, G., Lock, M. M., Smith, T. J., Hii, Y. S., Ong, H. K. A., & Loh, J. Y. (2013). Impact of potential food sources on the life table of the cladoceran, *Moina macrocopa*. *Israeli Journal of Aquaculture - Bamidgeh*, *65*. https://doi.org/10.46989/001c.20668

Kim, S., & Kim, H. S. (2014). Effects of alkalinity and hardness on the chlorophyll-α concentration. *Journal of Korean Society on Water Environment*, *30*(1), 25–30. https://doi.org/10.15681/kswe.2014.30.1.025

Krishnan, V., Uemura, Y., Thanh, N. T., Khalid, N. A., Osman, N., & Mansor, N. (2015). Three types of marine microalgae and *Nannocholoropsis oculata* cultivation for potential source of biomass production. In *Journal of Physics: Conference Series* (Vol. 622, No. 1, p. 012034). IOP Publishing. https://doi.org/10.1088/1742-6596/622/1/012034

Laing, I. (1991). *Cultivation of marine: Unicellular algae*. Ministry of Agriculture, Fisheries and Food Directorate of Fisheries Research.

Loh, J. Y., Ong, H. K. A., Hii, Y. S., Smith, T. J., Lock, M. W., & Khoo, G. (2012). Highly unsaturated fatty acid (HUFA) retention in the freshwater cladoceran, *Moina macrocopa*, enriched with lipid emulsions. *Israeli Journal of Aquaculture*, *64*. https://doi.org/10.46989/001c.20648

Martínez-Jerónimo, F., & Gutierrez-Valdivia, A. (1991). Fecundity, reproduction, and growth of *Moina macrocopa* fed different algae. *Hydrobiologia*, *222*, 49–55. https://doi.org/10.1007/BF00017499

Mata, T. M., Martins, A. A., & Caetano, N. S. (2010). Microalgae for biodiesel production and other applications: A review. *Renewable and Sustainable Energy Reviews*, *14*(1), 217–232. https://doi.org/10.1016/j.rser.2009.07.020

Morales, M., Sánchez, L., & Revah, S. (2018). The impact of environmental factors on carbon dioxide fixation by microalgae. *FEMS Microbiology Letters*, *365*(3), fnx262. https://doi.org/10.1093/femsle/fnx262

Mubarak, A. S., Jusadi, D., Junior, M. Z., & Suprayudi, M. A. (2017). The population growth and the nutritional status of *Moina macrocopa* feed with rice bran and cassava bran suspensions. *Jurnal Akuakultur Indonesia*, *16*(2), 223-233. https://doi.org/10.19027/jai.16.2.223-233

Murakami, K., Kakazu, K., Ruike, K., & Shibata, K. I. (2020). Example assessments of the microcosm N-system. In Y. Inamori (Ed.), *Microcosm manual for environmental impact risk assessment* (pp. 69-158). Springer. https://doi.org/10.1007/978-981-13-6798-4_7

Poynton, S. L., Dachsel, P., Lehmann, M. J., & Steinberg, C. E. (2013). Culture of the cladoceran *Moina macrocopa*: Mortality associated with flagellate infection. *Aquaculture*, *416-417*, 374-379. https://doi.org/10.1016/j.aquaculture.2013.09.029

Prasanthi, P. S., Naveena, N., Vishnuvardhana Rao, M., & Bhaskarachary, K. (2017). Compositional variability of nutrients and phytochemicals in corn after processing. *Journal of Food Science and Technology*, *54*, 1080–1090. https://doi.org/10.1007/s13197-017-2547-2

Qian, C., Ren, X., Rui, Y., & Wang, K. (2021). Characteristics of bio-$CaCO_3$ from microbial bio-mineralization with different bacteria species. *Biochemical Engineering Journal*, *176*, 108180. https://doi.org/10.1016/j.bej.2021.108180

Rasdi, N. W., & Qin, J. G. (2018). Toleration of *Moina* sp. towards salinity and food types as the prominent factors in determining *Moin*a sp. abundance: A review. *Research and Reviews: Journal of Agriculture and Allied Sciences*, *7*, 35–40.

Rasdi, N. W., Arshad, A., Ikhwanuddin, M., Hagiwara, A., Yusoff, F. M., & Azani, N. (2020). A review on the improvement of cladocera (*Moina*) nutrition as live food for aquaculture: Using valuable plankton fisheries resources. *Journal of Environmental Biology*, *41*(5), 1239–1248. https://doi.org/10.22438/JEB/41/5(SI)/MS_16

Rasdi, N. W., Ikhwanuddin, M., Azman, S., Karim, M., Syukri, F., & Hagiwara, A. (2021). The effects of enriched *Moina* on the growth, survival, and proximate analysis of marine shrimp (*Penaeus monodon*). *Journal of Sustainability Science and Management*, *16*(3), 56-70. https://doi.org/10.46754/jssm.2021.04.005

Rasdi, N. W., Yuslan, A., Suhaimi, H., Qin, J. G., Naseer, N. M., Ikhwanuddin, M., Sung, Y. Y., Yusoff, F. M., & Hagiwara, A. (2021). The impact of feeding algae and canola oil on the growth, survival and reproduction of *Moina* sp. *Songklanakarin Journal of Science and Technology*, *43*(3), 864–870. https://doi.org/10.14456/sjst-psu.2021.114

Rashid, N., Rehman, M. S., Sadiq, M., Mahmood, T., & Han, J. I. (2014). Current status, issues and developments in microalgae derived biodiesel production. *Renewable and Sustainable Energy Reviews*, *40*, 760–778. https://doi.org/10.1016/j.rser.2014.07.104

Ratomski, P., & Hawrot-Paw, M. (2021). Influence of nutrient-stress conditions on *Chlorella vulgaris* biomass production and lipid content. *Catalysts*, *11*(5), 573. https://doi.org/10.3390/catal11050573

Rottmann, R. W., Graves, J. S., Watson, C., & Yanong, R. P. E. (2018, March 16). *Culture techniques of* Moina*: The ideal* Daphnia *for feeding freshwater fish fry*. University of Florida Institute of Food and Agricultural Sciences. https://edis.ifas.ufl.edu/publication/FA024

Safi, C., Zebib, B., Merah, O., Pontalier, P. Y., & Vaca-Garcia, C. (2014). Morphology, composition, production, processing and applications *of Chlorella vulgaris*: A review. *Renewable and Sustainable Energy Reviews*, *35*, 265–278. https://doi.org/10.1016/j.rser.2014.04.007

Sánchez-Bayo, A., Morales, V., Rodríguez, R., Vicente, G., & Bautista, L. F. (2020). Cultivation of microalgae and cyanobacteria: Effect of operating conditions on growth and biomass composition. *Molecules*, *25*(12), 2834. https://doi.org/10.3390/molecules25122834

Santoso, F., Krylov, V. V., Castillo, A. L., Saputra, F., Chen, H. M., Lai, H. T., & Hsiao, C. D. (2020). Cardiovascular performance measurement in water fleas by utilizing high-speed videography and ImageJ software and its application for pesticide toxicity assessment. *Animals*, *10*(9), 1587. https://doi.org/10.3390/ani10091587

Shidik, T. S. A. N., Ekasari, J., Jusadi, D., & Setiawati, M. (2021). Productivity and quality of *Moina* sp. cultivated with various culture medium. *Jurnal Akuakultur Indonesia*, *20*(2), 148–162. https://doi.org/10.19027/jai.20.2.148-162

Sipaúba-Tavares, L. H., Truzzi, B. S., & Berchielli-Morais, F. A. (2014). Growth and development time of subtropical Cladocera *Diaphanosoma birgei* Korinek, 1981 fed with different microalgal diets. *Brazilian Journal of Biology*, *74*(2), 464–471. https://doi.org/10.1590/1519-6984.12012

Slade, R., & Bauen, A. (2013). Micro-algae cultivation for biofuels: Cost, energy balance, environmental impacts and future prospects. *Biomass and Bioenergy*, *53*, 29–38. https://doi.org/10.1016/j.biombioe.2012.12.019

Sorgeloos, P., Dhert, P., & Candreva, P. (2001). Use of the brine shrimp, *Artemia* spp., in marine fish larviculture. *Aquaculture*, *200*(1-2), 147-159. https://doi.org/10.1016/S0044-8486(01)00698-6

Tam, N. F. Y., & Wong, Y. S. (1996). Effect of ammonia concentrations on growth of *Chlorella vulgaris* and nitrogen removal from media. *Bioresource Technology*, *57*(1), 45–50. https://doi.org/10.1016/0960-8524(96)00045-4

Ventura, R. F., & Enderez, E. M. (1980). Preliminary studies on *Moina* sp. production in freshwater tanks. *Aquaculture*, *21*(1), 93–96. https://doi.org/10.1016/0044-8486(80)90129-5

Yuslan, A., Najuwa, S., Hagiwara, A., Ghaffar, M. A., Suhaimi, H., & Rasdi, N. W. (2021). Production performance of *Moina macrocopa* (Straus 1820) (Crustacea, Cladocera) cultured in different salinities: The effect on growth, survival, reproduction, and fatty acid composition of the neonates. *Diversity*, *13*(3), 105. https://doi.org/10.3390/d13030105

Pertanika J. Trop. Agric. Sci. 46 (1): 107 - 128 (2023)

PERTANIKA JOURNALS

TROPICAL AGRICULTURAL SCIENCE

Journal homepage: http://www.pertanika.upm.edu.my/

Acclimatization of Tropical Palm Species Associated with Leaf Morpho-Physiological Traits to the Understorey Environment of *Hevea* Rubber Farms

Zar Ni Zaw, Piyanut Musigapong, Rawee Chiarawipa*, Surachart Pechkeo and Amonrat Chantanaorrapint

Agricultural Innovation and Management Division, Faculty of Natural Resources, Prince of Songkla University, Songkhla, 90112, Thailand

ABSTRACT

Hevea rubber farm is viable for agroforestry systems since its canopy lessens extreme weather conditions and contributes to the adaptation of shade-tolerant plants. However, some limitations in the availability of soil water and shades vary with the age of rubber trees and affect the understorey plants' acclimatization. Tropical palms are potentially associated plants for the rubber-based agroforestry systems because they are rainforest species adaptable to understorey environments. Two rubber farms, ages 12 and 25 years, intercropped with tropical palms were selected to investigate the acclimatization of the palms to the seasonal abiotic variations in the mature rubber farms. The studied palm species were *Chrysalidocarpus lutescens* and *Rhapis excelsa* in the 12-year-old rubber farm and *Livistona speciosa* and *Licuala spinosa* in the 25-year-old rubber farm, respectively. Leaf area, stomatal conductance, photosynthesis pigments, and leaf nitrogen content were identified as the palms' morpho-physiological traits. The 12-year-old rubber farm had a marked soil water deficit in all soil depths at the beginning of the rainy season, reaching around 200 kPa at the 80 cm soil depth, while the 25-year-old rubber farm received greater light transmissions, ranging between 37 and 46% in the late dry season. All palms adjusted leaf area to balance the photosynthetic capacity. The *Rhapis* palm had greater acclimatization with significant responses of stomatal conductance. Other than the *Licuala* palm, all palms exhibited the allocation of chlorophyll pigments and nitrogen content significantly in their leaves

ARTICLE INFO

Article history:
Received: 25 July 2022
Accepted: 11 October 2022
Published: 03 February 2023

DOI: https://doi.org/10.47836/pjtas.46.1.07

E-mail addresses:
6110630008@psu.ac.th (Zar Ni Zaw)
piyanut191161@gmail.com (Piyanut Musigapong)
rawee.c@psu.ac.th (Rawee Chiarawipa)
surachart.p@psu.ac.th (Surachart Pechkeo)
amonrat.b@psu.ac.th (Amonrat Chantanaorrapint)
* Corresponding author

ISSN: 1511-3701
e-ISSN: 2231-8542

in response to the different intensities of abiotic stresses in the understorey of the rubber farms.

Keywords: Agroforestry, Arecaceae, ecophysiological adaptation, *Hevea brasiliensis*, tropical palm species

INTRODUCTION

Natural rubber (*Hevea brasiliensis*) is a forest tree that naturally grows and thrives together with other forest species in its origin, the Amazon rainforest. However, it has been planted traditionally as a monocrop for many years in Southeast Asian countries where commercial plantings developed. Most commercial expansions have invaded tropical forests in the regions, resulting in environmental costs accumulated, such as loss of biodiversity, soil fertility, carbon stock, and forest ecosystem services (Ahrends et al., 2015; Fox & Castella, 2013; Sun et al., 2017). To recover these costs, agroforestry, a created forest ecosystem in which biodiversity could be restored with the interactions of tree and agricultural components ensuring ecological and economic sustainability (Leakey, 2017), is the most recommended option (Langenberger et al., 2017; Somboonsuke et al., 2011; Wu et al., 2016).

The understorey environment of rubber farms is viable for an agroforestry system since the overstorey lessens extreme weather conditions, such as high temperature and light intensity, and contributes to biodiversity enhancement complementing forestry ecosystem services in agricultural farms (Rappaport & Montagnini, 2014). Furthermore, with low irradiance and better light interception, greater light distribution under multi-layered canopy structures like the understorey environment of rubber-based agroforestry enhances the efficient light energy capture of the understorey plants, thus improving the photosynthetic rate in the system (Powles, 1984).

Typically, in smallholder rubber production, mature rubber farms aged between 10 and 20 deliver the highest yield, while the overaged rubber farms aged over 20 years start yield decreasing due to the high-frequency tapping system conventionally practiced by the farmers (Munasinghe & Rodrigo, 2017; Zaw et al., 2017). These different production potentials also implicate the above- and below-ground ecosystem components, such as seasonal variations of overstorey canopy and soil water conditions that tend to affect the ecophysiological adaptation of understorey plants. Unlike other crops, *Hevea* rubber is regularly exploited secondary metabolite, rubber latex, throughout the year (d'Auzac et al., 1997), which could lead to higher soil water consumption, particularly during high productive years (Tan et al., 2011). In addition, during the dry season, the rubber tree typically does not provide canopy shades to the understorey environment due to its deciduous nature (Premakumari & Saraswathyamma, 2000). Such changes in light intensity are interrelated to the above- and below-ground water availabilities of the understorey environment (Galhidy et al., 2005). These factors could be key considerations that affect the adaptability

performance of understorey plants in a rubber-based agroforestry system and vary with the age of the overstorey rubber trees (Pathiratna, 2006).

Therefore, acclimatization of the understorey plants to these factors is vital to facilitate interdependence among the component of the agroforestry system. Furthermore, since leaves play an important role in photosynthesis, closely influenced by environmental variations and stresses, tree acclimatization could be based on changes in leaves' morphological and physiological traits (Givnish et al., 1988; Valladares et al., 2016).

Although most plant species typically improve photosynthesis with higher vegetative growth under an optimal light intensity (Feng et al., 2019), shade-tolerant plants exhibit greater acclimatization to a light deficit condition with a higher resource allocation to leaves, thus increasing in total leaf area to achieve maximum exposure to irradiance for a greater light-harvesting capacity (Givnish, 1988; Poorter, 1999). However, typical adaptable plants reduce leaf surface area under a water deficit condition or extreme light intensity to improve water conservation in the plant (Chaves et al., 2003). As a vital mechanism to balance gas exchange between the plant and the adjacent atmosphere, stomatal traits such as its apertures and density are leaf anatomical responses closely associated with plant-water relationships (Aasamaa et al., 2001) and photosynthetic capacity (Farquhar & Sharkey, 1982). Photosynthetic pigments—chlorophyll *a* (Chl *a*), chlorophyll *b* (Chl *b*), and carotenoids (Car), and their ratios, notably Chl *a*/*b* and Chl/Car, reflect the physiological status of photosynthetic mechanism (Houborg et al., 2015) and adaptability to environmental stresses (Hendry & Price, 1993). The chlorophyll contents are positively associated with leaf nitrogen content that varies with the light availability (Evans, 1989). A plant with greater acclimatization allocates higher nitrogen concentration to leaves, thus higher chlorophyll pigments with larger leaf areas ensuring improved light harvesting under stress (Field & Mooney, 1986; Givnish, 1988).

Many studies confirmed that shade-tolerant plants like coffee, tea, cocoa, bamboo, and ginger could thrive with higher adaptability in the understorey environment of mature rubber farms and deliver sustainable benefits to the agroforestry ecosystem (Langenberger et al., 2017; Wu et al., 2016). Like these shade-tolerant plants, tropical palms belong to the Arecaceae (Palmae) family and are potentially associated plants for the rubber-based agroforestry system because most palms in rubber-growing regions are tropical rainforest species and are highly adaptable to understorey environments (Dransfield et al., 2004; Johnson, 2011). The distribution of tropical palm species is greatly concentrated in the equatorial regions of Southeast Asia, notably southern Thailand, the Malay Peninsula, and Indonesian islands (Dransfield et al., 2004; Saw et al., 2003), where the *Hevea* rubber has been planted extensively, and around 60% of the world's

total rubber growing area exists, producing over 50% of the world's total supply (Association of Natural Rubber Producing Countries [ANRPC], 2021). In addition, some palm species naturally grow and are cultivated traditionally as understorey plants in some smallholder rubber farms, supplying household subsistence for small rubber farmers (Jongrungrot et al., 2014; Supapvanich et al., 2014). For example, Jongrungrot et al. (2014) reported that tropical palm species like *Livistona* spp., *Licuala* spp., and *Chrysalidocarpus* spp. were commonly found in smallholder rubber farms in southern Thailand, providing not only household uses of non-timber forest products, such as food, decoration, and building materials but also greater on-farm economic performances. Thus, conserving these tropical palm species under smallholder rubber farming would deliver ecological and economic benefits and improve farmers' resilience. To ensure these benefits, the ecophysiological adaptation of tropical palm species to the rubber farm understorey environment is crucially important.

Scientific research studies on the combination of palms in rubber-based agroforestry systems are limited. Hence, an on-farm study was carried out to investigate the acclimatization of the common tropical palm species to the seasonal abiotic variations of the understorey environment in mature rubber farms. The study also identified the palm species ecologically compatible with the different ages of mature rubber farms.

MATERIALS AND METHODS

Experimental Location and Planting Materials

The study was conducted in the Namon district of Songkhla province, located at 6°59'30" N, 100°8'7" E in the east part of southern Thailand. The area is generally under the influence of Southwest Monsoon with a monthly rainfall of around 200 mm from June to September, and Northeast Monsoon with about 400 mm rainfall per month from October to December, resulting in a heavy rainy season, followed by a dry period with a mean temperature of around 28 °C from mid-January to mid-May (Thai Meteorological Department [TMD], 2019).

Two rubber farms, ages 12 and 25 years, intercropped with tropical palms, adjacently situated, were selected for the study. The studied palms were yellow butterfly palm (*Chrysalidocarpus lutescens* H. Wendl.) and lady palm (*Rhapis excelsa* (Thunb.) Henry) in the 12-year-old rubber farms and Livistona palm (*Livistona speciosa* Kurz.) and mangrove fan palm (*Licuala spinosa* Roxb.) in the 25-year-old rubber farm, respectively. All rubber trees were RRIM 600 and planted in a spacing of 3 m × 7 m, and the intercropped palms were spaced in 3 m × 7 m in the inter-rows of the rubber trees.

Abiotic Parameters

Rainfall, atmospheric temperature, and evapotranspiration data during the study period were obtained from a local agricultural meteorological station in the area. In addition, light intensities in the understorey

were measured from five different points in the farms compared with under full sun at the same time between 10:00 and 11:00 a.m. once a week using the Sun System – 748205 – photosynthesis active radiation meter (Sun System, Canada).

Soil moisture tensions at 20, 40, 60, and 80 cm depths were monitored monthly on the farms, using the WATERMARK sensor (IRROMETER Company, USA) installed horizontally from the ground between the rubber tree and the palms at 1.5 m far from them.

Changes in the farms' canopy areas were monitored by measuring the farms' leaf area index (LAI) using the hemispherical photography method (Chen et al., 1997). The canopy areas were captured using a Nikon Coolpix 8400 (Nikon, Japan) camera attached with a fish-eye lens upward positioned at 1.2 m from the ground. The photos were taken monthly from three points between the rubber trees and the palms at each farm. The photos were processed using the Gap Light Analyzer software version 2.0 (Simon Fraser University, Canada) to quantify the LAI of the farms.

Morphological Traits

Six palm leaves were sampled randomly from fully expanded fronds to quantify the understorey palm's leaf traits of leaf area (LA), leaf dry mass, and specific leaf area (SLA). An image analyzing software, the ImageJ program (National Institute of Health, USA) (Schneider et al., 2012), was used to process the leaf photos for the LA. The sample leaves were put in paper bags and oven-dried at 70 °C for 72 hours to calculate the leaf dry mass and the SLA (Awal et al., 2004).

Quantifying the palm leaves' stomatal and guard cells were carried out monthly by the impression method (Weyers & Meidner, 1990). First, 1 cm^2 of leaf specimens was prepared by sampling the middle portion of the leaves collected from each palm species between 09:00 and 10:00 a.m. Next, an impression solution, formalin acetic acid alcohol, was applied to the leaf specimens for replication. Once the solution hardened, the replica was detached from the specimen, located on a microscope slide, and investigated under a compound microscope (Zeiss CP-Achromat 40× Objective) (Carl Zeiss Microscopy, USA).

Physiological Traits

For the photosynthesis pigment determination, leaf samples in 1 cm^2 dimension were excised from five different points of each palm species. The pigments (chlorophylls and carotenoids) were extracted with 3 ml of *N*, *N*-dimethylformamide solvent by the direct immersion method and kept for 24 hours at 4 °C under a dark condition (Moran & Porath, 1980). The absorbances were measured at wavelengths of 647 nm, 664 nm, and 480 nm with a UV spectrophotometer— Ultrospec 3000 UV/VIS (Pharmacia Biotech, USA) for Chl *a*, Chl *b*, total Chl and Car, respectively (Wellburn, 1994). Calculations of the pigment contents followed the simultaneous equations devised by Inskeep and Bloom (1985).

The oven-dried sample leaves were ground and sieved through a 1 mm aperture mesh for the sample preparation of the total nitrogen content determination using the micro-Kjeldahl method (Sáez-Plaza et al., 2013). Leaf nitrogen contents in mass-based (N_m) and area-based (N_a) were then calculated based on the dry weight of the leaf and SLA.

Data Collection and Statistical Analysis

The data collection was carried out from July 2016 to June 2017 and split into four seasonal periods according to the typical weather patterns in the area, the southern peninsular of Thailand: Wet I (July–September 2016), Wet II (October–December 2016), Dry I (January–March 2017), and Dry II (April–June 2017), respectively.

The collected data were analyzed using the *F*-test in one-way analysis of variance (ANOVA) for the overall significance and then followed by Duncan's multiple range test at $P \leq 0.05$ to compare the significant data among the seasonal periods for each understorey palm species. R stat 3.6.2 software was performed for the data analysis.

RESULTS

Agroclimatic Situation of the Study Area

According to the weather data from the local meteorological station, the area received 2,560 mm of total rainfall, and it accumulated 286, 1177, 646, and 489 mm in the Wet I, Wet II, Dry I, and Dry II seasons, respectively (Figure 1). Monthly rainfall in the Wet I period was under 150 mm. It then increased

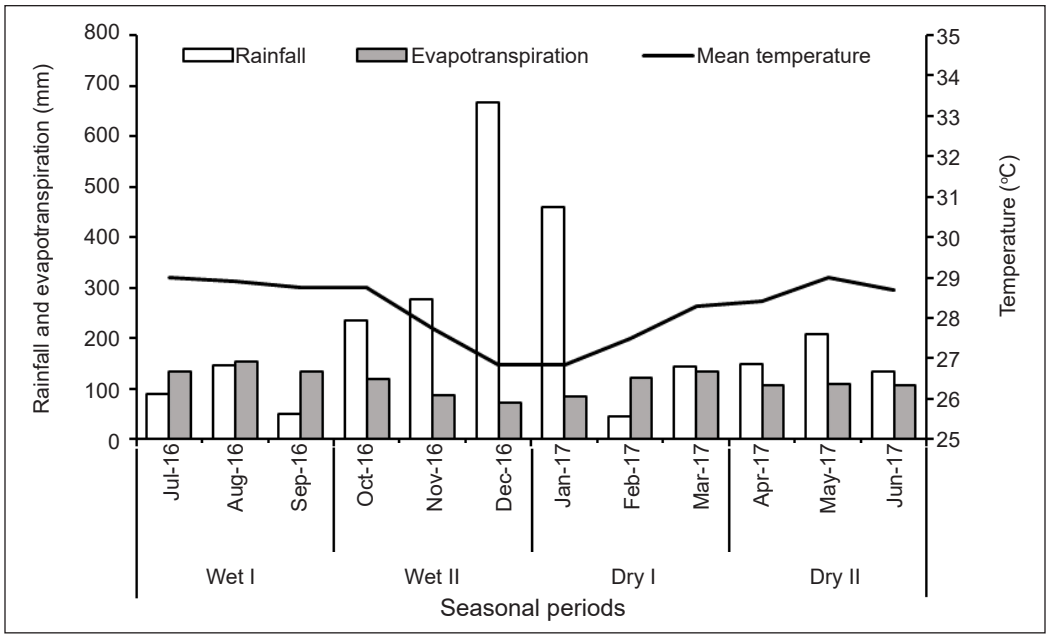

Figure 1. Monthly weather conditions: rainfall, evapotranspiration, and mean temperature of the study area (from July 2016 to June 2017)

in October from 235 to 666 mm in December during the Wet II season, a heavy rainy period. In January of the Dry I season, the rainfall decreased and reached its minimum of 44 mm in February. Then few light spots of rain started, with monthly rainfall ranging between 130 and 210 mm in the Dry II season.

It was observed that monthly evapotranspiration rates were at the highest between 130 and 155 mm during the Wet I season, followed by the Dry I and Dry II seasons. The minimum evapotranspiration rate of 72 mm per month was found in December in the Wet II season.

Soil Moisture Tensions at the Rubber Farms

Figure 2 shows the soil moisture tensions of the rubber farms during the study period. At the 12-year-old rubber farm (Figure 2A), during the Wet I season, higher soil moisture tensions were observed in all soil depths, reaching around 200 kPa at the 80 cm soil depth in September and October, and the tension reduced with the higher rainfall in the Wet II season. In the Dry II season, its soil moisture tension rose about 130 kPa at the 60 cm soil depth, while the other soil depths had relatively lower tension, less than 40 kPa.

On the other hand, the soil moisture tensions in the 25-year-old rubber farm (Figure 2B) were not as intense as those in the 12-year-old rubber farm. However, in September of the Wet I season, particularly at the 40 cm soil depth, significant tensions were observed at around 120 kPa.

LAI and Light Intensity in the Farms

Figures 3A and 3B exhibit the light transmission and the LAI of the 12-year-old and 25-year-old rubber farms, respectively, during the study period. Both farms showed the light transmissions in the farms were lower in the wet seasons and increased in the dry seasons, while conversely, higher LAI values in the wet seasons and lower values in the dry seasons. In comparing the two farms, the 25-year-old rubber farms showed lower LAI values than the 12-year-old rubber farms, particularly during the Dry II season. The LAIs of the farms reached their minimum values of less than one in February and April. Throughout the study period, the 25-year-old rubber farm received greater light transmissions than the 12-year-old rubber farm. It was observed that the light transmission in both farms increased during the Dry II season, but a marked increase in the 25-year-old rubber farm ranged between 46 and 37%.

Morpho-Physiological Traits of the Palms

***Chrysalidocarpus lutescens*.** Significant differences were investigated in seasonal comparisons of the LA and the guard cell length (Table 1). However, other morphological traits, notably SLA, stomatal density, and guard cell width, did not vary significantly. The LAs of the palm were exposed as the smallest at 15.71 m^2 in the Wet I season compared to other seasons.

The guard cell lengths in the Wet II and the Dry I exhibited significantly the longest at 24.27 and 23.89 μm, respectively.

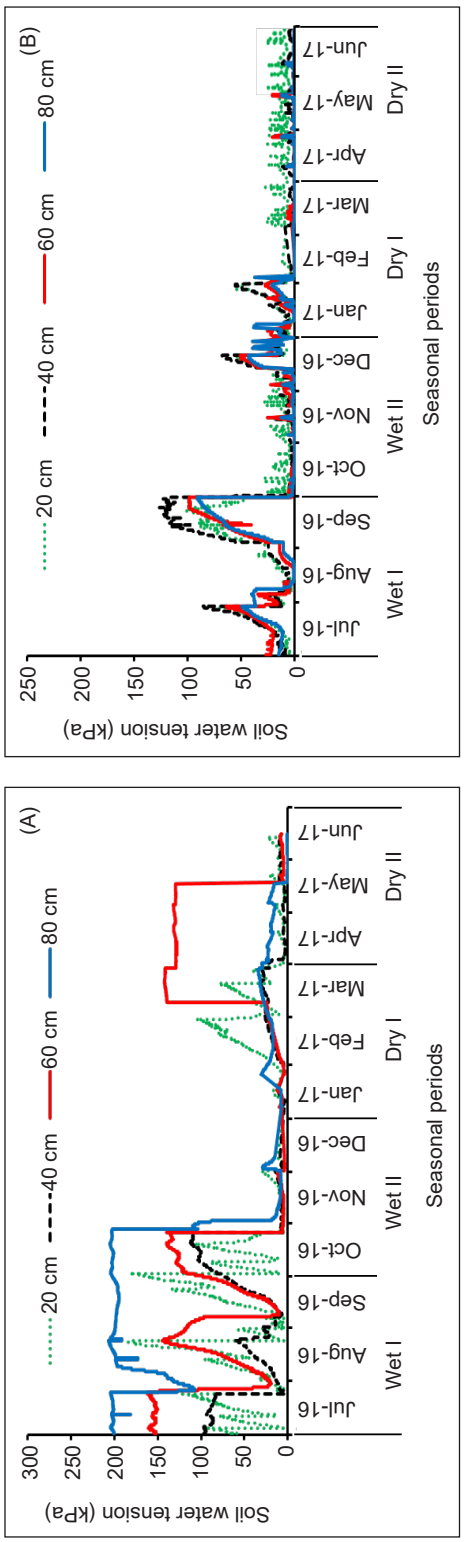

Figure 2. Monthly changes of soil water tension in (A) the 12-year-old rubber farm and (B) the 25-year-old rubber farm (from July 2016 to June 2017)

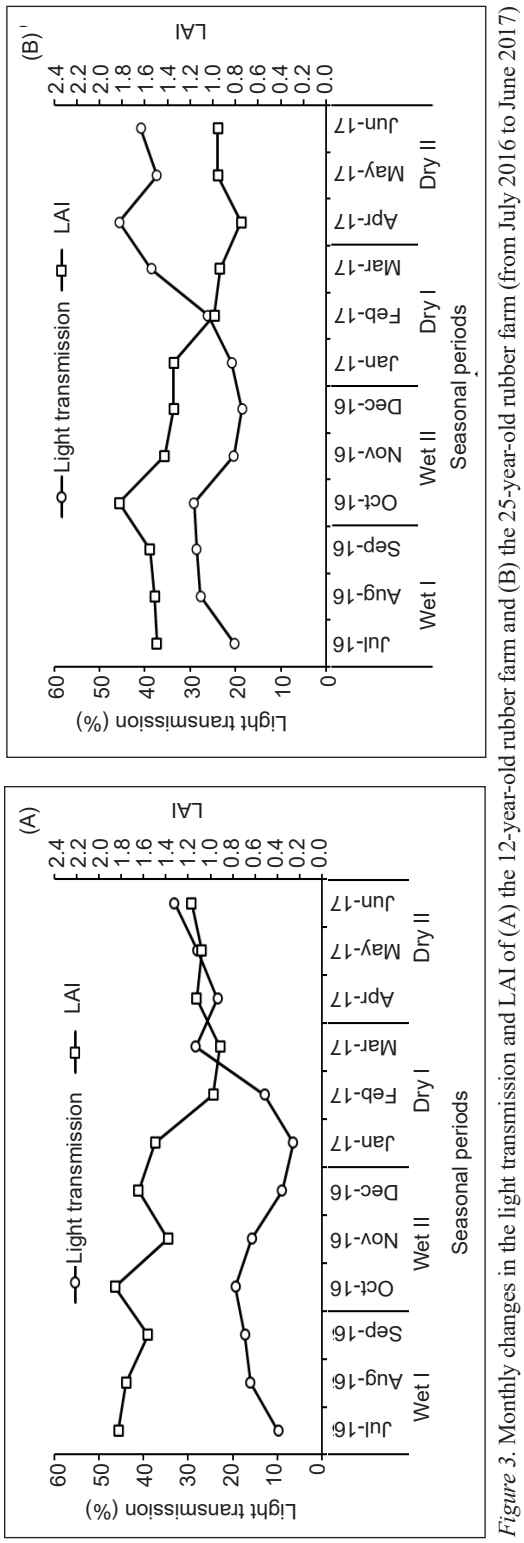

Figure 3. Monthly changes in the light transmission and LAI of (A) the 12-year-old rubber farm and (B) the 25-year-old rubber farm (from July 2016 to June 2017)

Table 1
Seasonal changes in morpho-physiological traits of the Chrysalidocarpus lutescens *H. Wendl. leaves under the 12-year-old rubber farm*

Parameters	Wet I	Wet II	Dry I	Dry II	*F*-test
Morphological traits					
LA (m^2)	15.71 b	23.73 a	20.21 ab	23.53 a	**
SLA ($cm^2\ g^{-1}$)	117.76	94.71	96.82	94.71	ns
Stomatal density (stomata mm^{-2})	44.32	45.81	44.04	44.36	ns
Guard cells width (µm)	16.43	19.26	18.87	17.59	ns
Guard cells length (µm)	22.03 ab	24.27 a	23.89 a	21.36 b	**
Physiological traits					
Chl *a* (mg cm^{-2})	14.19 a	14.15 a	11.24 b	10.72 b	**
Chl *b* (mg cm^{-2})	6.22 a	6.21 a	4.75 b	4.47 b	**
Total Chl (mg cm^{-2})	20.47 a	20.41 a	16.03 b	15.22 b	**
Car (mg cm^{-2})	2.70 a	2.70 a	2.12 b	1.98 b	**
Chl *a*/*b*	2.28 b	2.28 b	2.39 a	2.41 a	**
Chl/Car	7.58	7.76	7.58	7.69	ns
Total N (%)	1.81 a	1.71 ab	1.63 b	1.69 ab	*
N_m	0.24	0.33	0.40	0.35	ns
N_a	0.09	0.07	0.10	0.07	ns

Note. Wet I = from July to September 2016; Wet II = from October to December 2016; Dry I = from January to March 2017; Dry II = from April to June 2017. *, ** = Different letters in the same row indicate statistically significant differences by Duncan's multiple range test (DMRT) ($P \leq 0.05$, and $P \leq 0.01$), and ns = no significant difference

Likewise, the guard cell widths were broader in the Wet II and the Dry II than in the other seasons, but there were no statistical differences among their seasonal changes.

The major photosynthesis pigments, namely Chl *a*, Chl *b*, total Chl, and Car contents, were greater with a high significance in the wet seasons and less in the dry seasons. The higher ratios of Chl *a*/*b* resulted during the dry seasons, but their values in all seasons did not exceed 2.5. The highest content of total leaf nitrogen was investigated in the Wet I season.

***Rhapis excelsa*.** During the Wet II season, the LA of the *Rhapis* palm was the biggest at 7.26 m^2, while its SLAs were high values of over 79 $cm^2\ g^{-1}$ in the Wet II and the Dry II seasons, respectively (Table 2). The stomatal density found in the Wet II season was also the highest at 58.25 m m^{-2} among the seasons. The Wet II and the Dry I seasons resulted in the largest guard cell size, with over 21 and 25 µm in width and length, respectively.

Its seasonal changes in the Chl and Car contents were similar to those of the understorey *Chrysalidocarpus* palm growing together under the same farm. The Chl *a*, Chl *b*, total Chl, and Car contents were at the highest values in the Wet I season at 15.26, 5.67, 20.67, and 3.58 mg cm^2, respectively. Moreover, those contents

Table 2
Seasonal changes in morpho-physiological traits of the Rhapis excelsa *Thunb. leaves under the 12-year-old rubber farm*

Parameters	Wet I	Wet II	Dry I	Dry II	*F*-test
Morphological traits					
LA (m^2)	5.53 b	7.26 a	4.79 b	5.60 b	**
SLA ($cm^2\ g^{-1}$)	70.89 ab	79.00 a	64.41 b	79.50 a	*
Stomatal density (stomata mm^{-2})	44.93 b	58.25 a	48.64 b	50.12 ab	**
Guard cells width (µm)	14.56 b	21.21 a	22.27 a	16.55 b	**
Guard cells length (µm)	21.65 b	25.07 a	25.39 a	21.24 b	**
Physiological traits					
Chl *a* (mg cm^{-2})	15.26 a	14.53 ab	13.38 b	10.56 c	**
Chl *b* (mg cm^{-2})	5.67 a	5.25 ab	4.51 b	2.94 c	**
Total Chl (mg cm^{-2})	20.67 a	19.52 ab	17.62 b	13.23 c	**
Car (mg cm^{-2})	3.58 a	3.46 ab	3.28 b	2.82 c	**
Chl *a*/*b*	2.70 c	2.84 bc	3.00 b	3.60 a	**
Chl/Car	5.77 a	5.61 ab	5.36 b	4.68 c	**
Total N (%)	2.05 a	2.01 a	1.70 b	1.79 b	**
N_m	0.16 ab	0.19 a	0.10 b	0.12 ab	*
N_a	0.14 a	0.07 c	0.10 b	0.11 b	**

Note. Wet I = from July to September 2016; Wet II = from October to December 2016; Dry I = from January to March 2017; Dry II = from April to June 2017. *, ** = Different letters in the same row indicate statistically significant differences by Duncan's multiple range test (DMRT) ($P \leq 0.05$, and $P \leq 0.01$), and ns = no significant difference

gradually decreased to their smallest values in the Dry II season at 10.56, 2.94, 13.23, and 2.82 mg cm^2, respectively. The ratios of Chl *a* and Chl *b* were lower in the Wet seasons, with values less than three, whereas they were over three in the dry seasons. However, in contrast, the total Chl and Car ratio (Chl/Car) showed the highest value in the Wet I season at 5.77 and the lowest in the Dry II season at 4.68.

It was observed that the total nitrogen content was higher in the wet seasons than in the dry seasons. Nitrogen content per dry leaf mass (N_m) in the Wet II season was at 0.19, the highest among the seasons. On the other hand, leaf-area-based nitrogen (N_a) content was the highest in the Wet I season at 0.24, while that in the Wet II season resulted in the lowest value of 0.07.

***Livistona speciosa*.** During the Wet I season, the palm leaf area was the smallest, but later it expanded significantly in the Wet II and the dry seasons (Table 3). However, with respect to the SLA, the higher value was observed in the Wet I season, followed by a gradual decrease to the lowest value in the Dry II season.

The variations in the width and length of the guard cells were significant, and their respective lowest values were observed in the Dry II season.

All content of the major photosynthetic pigments was higher than those of other

Table 3
Seasonal changes in morpho-physiological traits of the Livistona speciosa *Kurz. leaves under the 25-year-old rubber farm*

Parameters	Wet I	Wet II	Dry I	Dry II	*F*-test
Morphological traits					
LA (m^2)	86.15 b	165.02 a	159.33 a	172.82 a	**
SLA ($cm^2\ g^{-1}$)	55.59 a	49.67 ab	45.75 bc	40.48 c	**
Stomatal density (stomata mm^{-2})	260.15	288.97	257.74	259.01	ns
Guard cells width (µm)	17.17 ab	18.83 a	16.62 ab	15.89 b	*
Guard cells length (µm)	21.28 a	21.53 a	21.65 a	18.42 b	**
Physiological traits					
Chl *a* (mg cm^{-2})	22.30 c	22.59 bc	24.85 a	23.73 ab	**
Chl *b* (mg cm^{-2})	10.95 c	11.15 bc	12.75 a	11.95 ab	**
Total Chl (mg cm^{-2})	30.67 c	31.14 bc	34.85 a	33.00 ab	**
Car (mg cm^{-2})	4.40 c	4.46 bc	4.93 a	4.70 ab	**
Chl *a*/*b*	2.04 a	2.03 ab	1.95 c	1.99 ab	**
Chl/Car	6.97 b	6.97 b	7.07 a	7.02 ab	**
Total N (%)	1.67 b	1.91 ab	1.95 a	1.70 ab	**
N_m	1.77 b	2.18 b	5.47 a	1.76 b	**
N_a	0.11 b	0.07 c	0.17 a	0.05 1c	**

Note. Wet I = from July to September 2016; Wet II = from October to December 2016; Dry I = from January to March 2017; Dry II = from April to June 2017. *, ** = Different letters in the same row indicate statistically significant differences by Duncan's multiple range test (DMRT) ($P \leq 0.05$, and $P \leq 0.01$), and ns = no significant difference

palms in the study. These pigments increased in the dry seasons and reduced in the wet seasons. The chlorophyll ratio (Chl *a*/*b*) was at the maximum of 2.04 during the Wet I season. The total Chl and Car ratio were lower in the Wet seasons and higher in the dry seasons. The total nitrogen content, N_m, and N_a were also highest, with a statistical significance at 1.95, 5.47, and 0.17, respectively, during the Dry I season.

***Licuala spinosa*.** The LA of the palm was the smallest in the Wet II season, followed by the largest in the Dry I season (Table 4). However, the SLA showed the highest in the Wet II season. The guard cells' width and length were minimal during the Dry II season. No significant changes were observed in the photosynthesis pigments and the total nitrogen content on the palm leaves among the seasons. Nevertheless, the N_m and N_a were at the minimum during the Wet I season and peaked at 0.62 and 0.64 in the Dry II season.

DISCUSSION

Seasonal Variations in the Agroecosystem of the Mature Rubber Farms

Agroclimatic Ecology. Based on the meteorological data, the study area received a relatively higher annual rainfall during the study period. However, some months of the Wet I season did not receive the

Table 4
Seasonal changes in morpho-physiological traits of the Licuala spinosa *Roxb. leaves under the 25-year-old rubber farm*

Parameters	Wet I	Wet II	Dry I	Dry II	*F*-test
Morphological traits					
LA (m^2)	18.70 ab	11.72 c	24.39 a	20.74 ab	**
SLA ($cm^2\ g^{-1}$)	73.76 ab	81.64 a	74.85 ab	65.67 b	*
Stomatal density (stomata mm^{-2})	195.56	197.00	189.71	180.62	ns
Guard cells width (µm)	19.41 ab	20.78 a	19.54 ab	16.92 b	*
Guard cells length (µm)	25.01 a	24.14 a	23.52 a	18.54 b	**
Physiological traits					
Chl *a* (mg cm^{-2})	14.48	14.42	16.03	14.13	ns
Chl *b* (mg cm^{-2})	5.91	5.81	6.76	5.72	ns
Total Chl (mg cm^{-2})	20.00	19.79	22.47	19.45	ns
Car (mg cm^{-2})	2.98	2.92	3.30	2.91	ns
Chl *a*/*b*	2.45	4.50	2.41	2.55	ns
Chl/Car	6.11	6.76	6.80	6.61	ns
Total N (%)	1.66	1.67	1.86	1.61	ns
N_m	0.18 b	0.27 b	0.44 ab	0.62 a	**
N_a	0.23 b	0.47 ab	0.44 ab	0.64 a	**

Note. Wet I = from July to September 2016; Wet II = from October to December 2016; Dry I = from January to March 2017; Dry II = from April to June 2017. *, ** = Different letters indicate statistically significant differences by DMRT ($P \leq 0.05$, and $P \leq 0.01$), and ns = no significant difference

normal rainfall of those months. In contrast, the peak rainfall in December was higher than the average monthly rainfall normally experienced during the Wet II season. These observations indicated that although the rainfall was above average in the study period, the rain distribution was intermittent, especially at the beginning of the rainy season. However, the high monthly evapotranspiration rate experienced during the Wet I season showed that the studied area could have a good water cycle of the agroecosystem during those months.

Seasonal Abiotic Stresses. It was noticed that overcanopy developments of both rubber farms reached their highest LAIs when the rainfall was less in the Wet I season, resulting in some extent of soil water tensions in both farms. Marked increased soil water tensions were observed in the 12-year-old rubber farm, particularly in the Wet I season, the beginning of the rainy season. However, the 25-year-old rubber farm had only slightly increased soil water tension in the Wet I season and considerably less in the dry season. Tan et al. (2011) found higher water consumption by mature rubber trees in the rainy season than in the dry season in tropical regions of China. Since the age of 25 years is normally considered the end of the economic lifespan of rubber farms (Saraswathyamma et al., 2000) because of the fewer number of productive

rubber trees that remain (Pathiratna, 2006), the soil water consumption in latex production considerably decreases with low productivity, thus less soil water deficit. Lin et al. (2011) reported that the soil water deficit decreased with the age of rubber farms because the water usage activity of overaged rubber trees gradually reduced with lesser transpiration and vegetative growth. Since the 25-year-old rubber farm had less vegetative development, the farm received a higher light transmission than the 12-year-old rubber farm throughout the year. Pathiratna (2006) reported that older rubber farms over 20 years tended to have a lesser canopy density and received a higher light transmission because of fewer trees remaining, the longer height of the trees, and the self-pruning of lower branches with age increased. Its prolonged low LAI value in the dry seasons was primarily due to the longer its deciduous period. In general, an overage rubber tree is less efficient in nutrient translocation leading to a greater duration to complete the deciduous process, which is internal nutrient storage activity for the next nutrient cycle of the deciduous tree (Jacob et al., 2018; Y. Li et al., 2016).

On the other hand, in the 12-year-old rubber farm, the soil water tension elevated slightly with the refoliation after the defoliation in the deciduous process during the Dry I season. These observations confirmed that the soil water tension markedly increased with the development of the leaf area, particularly when the water availability was limited.

Seasonal Variations of the Palm Leaf Morpho-physiological Traits under the Rubber Farms

LA and SLA. In the 12-year-old rubber farm, when the soil water tension reached the highest during the Wet I season, both understorey palms: the *Chrysalidocarpus* and the *Rhapis,* reduced their leaf areas. Plants minimize leaf area to inhibit transpiration, improving water use efficiency under certain water deficit conditions (Chaves et al., 2003; Xu & Zhou, 2005).

However, in the 25-year-old rubber farm, both understorey palms: the *Livistona* and the *Licuala*, increased the LA during the Dry I season when a greater light transmission was received because of the overstorey defoliation. In most species, optimal light intensity improves the photosynthesis process associated with biomass production with vegetative development unless considerable abiotic stress exists (Feng et al., 2019).

It was noticed that the SLA of the *Rhapis* palm was observed as the smallest in the Dry I season when the soil water tension was relatively lower than the other seasons, whereas that of the same understorey palm, the *Chrysalidocarpus*, did not vary significantly between the seasons. However, the SLAs of the understorey palms, the *Livistona* and the *Licuala*, in the 25-year-old rubber farm reduced to the smallest values in the Dry II season when there was no soil water tension but higher light transmission with dryer conditions leading to a slight water deficit in the air.

These different responses are consistent with the findings of previous studies that although a moderate drought increased the stomatal density, a severe water deficit decreased the stomatal density, which negatively correlated with the SLA (Liu et al., 2006; Meng et al., 1999; Xu & Zhou, 2005).

Stomatal Structure. The results of the stomatal density in the *Rhapis* palm also replicated the above finding of the association between the stomatal density and water stress intensity since the lowest stomatal density was found in the Wet I season when the soil water stress was significantly high. However, other palms did not significantly differ in stomatal density among the seasons.

Variation in stomatal density results from anatomical modification to balance the stomatal conductance with adaptation to prevailing environmental stresses (Casson & Hetherington, 2010) during new leaf development in which the stomatal pattern is adjusted (Hamanishi et al., 2012; Vaten & Bergmann, 2012). Stomatal pores respond instantly to weather fluctuations by regulating the aperture size by adjusting turgor pressure in adjacent guard cells (Farquhar & Sharkey, 1982; Franks & Beerling, 2009). When a plant experiences a moisture deficit, a reduction in turgor pressure decreases the guard cell size in width and length, resulting in a smaller stomatal aperture to minimize water loss (Schroeder et al., 2001). This adaptative stomatal dynamic was found significantly in the *Rhapis* palm under the 12-year-old rubber tree as the guard cell size in both width and length enlarged, thereby the stomatal aperture, in the Wet II and the Dry I seasons when the rainfall was the highest with less soil water tension. In contrast, the guard cells become smaller in the Wet I and Dry II seasons once the moisture deficit is markedly intense.

However, the *Chrysalidocarpus* palm under the same rubber farm did not significantly alter its stomatal density and guard cell width except for the guard cell length. Thus, it indicates that the palm could not actively perform the anatomical adjustment of its stomatal traits amidst the water stresses on the farm.

On the other hand, both palms under the 25-year-old rubber farm could adjust the stomatal aperture by significantly altering the guard cell in width and length by the seasons but the stomatal densities. The significant decreases in the width and length of the guard cells of both palms in the Dry II season contributed to the reduction in the stomatal pore size to lessen the leaf transpiration under the higher light transmission. Bertolino et al. (2019) reported that dynamic responses of the stomatal aperture were significant with light intensity variation rather than soil water deficit in most rainforest species.

Photosynthetic Pigments' Contents. Under the 12-year-old rubber farm, both understorey palms exhibited higher concentrations of the majority photosynthetic pigments (Chl *a*, Chl *b*, total Chl, and Car) per unit leaf

area in both wet seasons when the light transmission was poor with higher leaf area index. Typically, the photosynthesis process becomes less efficient with some decreases in the pigments under low light conditions (Feng et al., 2019). Shade-tolerant plants, however, adapt to the low-light environment with increases in the concentration of the pigments to maintain the photosynthetic capacity (Lei & Lechowicz, 1997; Niinemets & Tenhunen, 1997; T. Li et al., 2014). Furthermore, since these plants enhance light harvesting chlorophyll-protein complexes, present in Chl *b*, to improve the light-harvest function in response to low light conditions, the value of Chl *a*/*b* becomes lesser with a reduction in irradiance intensity of a shady environment (Mathur et al., 2018; Terashima & Hikosaka, 1995). Thus, with the lesser values of the Chl *a*/*b* during the Wet seasons, both palms could approve their adaptive acclimatization to the low light condition under the rubber farm.

It was previously reported that a marked increase in the value of Chl *a*/*b* indicated a greater intensity of stress mainly associated with light-harvesting function in the photosynthesis process but varied with different species, development stages, nutrient levels, and environmental conditions (Kitajima & Hogan, 2003; Feng et al., 2019). Furthermore, some studies have suggested that a value of Chl *a*/*b* more than three was considered stress that affects the photosynthetic capacity over the threshold level (Hartmut et al., 2007; Lichtenthaler et al., 1981). Thus, the values of the Chl *a*/*b* of the *Rhapis* palm higher than three during the dry seasons indicated that the palm experienced a stressful environment during that period.

In addition, the widest stomatal opening that continued in the Dry I season aggravated the stress more intensely in the Dry I and II seasons because of the higher transpiration rate. At the same time, the surrounding water availability was limited. However, its lesser values of the Chl/Car of 5.36 and 4.68 in the Dry I and II seasons, respectively, corresponded to the range observed in other acclimated plants under a stress condition (Hartmut et al., 2007; Sarijeva et al., 2007). The higher values of its Chl/Car ratio in the low light condition approved that the photosystem enhanced its light-harvesting complex through the significant increment of carotenoid content to balance with the light irradiance availability for the system (Hendry & Price, 1993).

On the other hand, the results of markedly higher contents of chlorophylls and carotenoid pigment in the *Livistona* palm compared to the other palms in the study agreed with the reports of Windsor-Collins et al. (2006) that palmate leaves of palms like *Livistona speciosa* were likely to change a darker color with higher concentrations of photosynthetic pigments under a low-light condition. In addition, the pigments of the palm were greater in the Dry seasons than in the Wet seasons. However, there were no significant variations of the pigments in the *Licuala* palm among the seasons.

Fan et al. (2018) and Feng et al. (2019) suggested that higher chlorophyll pigment content under a greater irradiance was related to leaf thickness associated with an increase of leaf nitrogen content per unit dry mass, which is a major source of chlorophyll pigments, contributed by optimal light intensity.

Higher values of the Chl *a*/*b* coupled with lower values of the Chl/Car in the Wet seasons and conversely, decreasing in the Chl *a/b* with increasing in the Chl/Car in the dry seasons reflected that the *Livistona* palm could have great adaptability to the seasonal irradiance variation in the understorey environment of the 25-year-old rubber farm. In addition, according to the findings by Hartmut et al. (2007), Lichtenthaler et al. (1981), and Sarijeva et al. (2007), the Chl *a*/*b* of less than three and the Chl/Car ratios of greater than six approved that there were no environmental stresses affected to the palm throughout the study period.

Leaf Nitrogen Concentration. Regarding the nitrogen contents of the leaves under the 12-year-old rubber farm, it was observed that they increased in both understorey palms, while the chlorophyll and carotenoid contents were at higher levels in the Wet seasons. Nitrogen-deficient leaves are normally found under stress conditions along with a marked reduction in chlorophyll pigments and leaf area together with photosynthetic capacity (Bojović & Marković, 2009). However, in contrast, a plant, which has greater acclimatization, allocates higher nitrogen concentration to leaves, thus higher chlorophyll pigments with larger leaf area to optimize the photosynthetic capacity under abiotic stress such as low irradiance and high-water deficit (Evans, 1989; Field & Mooney, 1986; Givnish, 1988).

However, a positive relationship between the leaf nitrogen content and the SLA was observed only in the palm leaf of the *Rhapis*. This correlated variation was also reported as the acclimation response of a shade-tolerant plant to a low-light environment (Bojović & Marković, 2009; Wang et al., 2012). The *Rhapis* palm also exhibited a closed positive correlation between the leaf nitrogen content per unit dry mass and the SLA. A higher allocation of nitrogen to the photosynthetic mechanism of a shade-resilient plant enlarges light-harvesting areas, which is a main limiting factor in the photosynthetic capacity (Evans, 1989; Niinemets & Tenhunen, 1997; Terashima & Hikosaka, 1995; Wang et al., 2012). Although a greater correlation between the SLA and the leaf nitrogen content per unit area was reported in some previous studies (Cornelissen et al., 1997; Dijkstra, 1990; Meziane & Shipley, 2001), the current study did not observe a consistent relationship between them.

Under the 25-year-old rubber farm, the leaf nitrogen concentration with both mass-based and area-based varied significantly with the seasons in the *Livistona* palm and expressed their highest levels in the Dry I season when the higher light intensity with the low LAI due to the natural leaf deciduous

process. Hollinger (1989) reported that greater mass-based leaf nitrogen content was investigated in the upper layer of an evergreen forest, reflecting a positive correlation between the leaf nitrogen content per unit of dry mass and light intensity. Vincent (2001) observed that leaf nitrogen content associated with photosynthetic capacity increased with canopy openness until a threshold level that varied in different species.

It was also noted that the mass-based leaf nitrogen contents of the *Livistona* palm were markedly higher than that of other palms. Conversely, its area-based leaf nitrogen contents were smaller than the others. They were associated with the distinctive morphological traits of the *Livistona* palm. Its average LA was significantly larger, and the SLA was smaller than the other palms. Thus, the leaf could be thinner and lighter than other leaves. With the normal nitrogen content of the leaf, the thin leaf led to the higher mass-based leaf nitrogen content, while the lighter leaf caused the area-based leaf nitrogen content to be smaller. Thus, the leaves were less likely to thicken during the Dry I season. The findings on these traits are consistent with a report by Loomis (1997) that a thin leaf had a higher mass-based leaf nitrogen content resulting in greater photosynthetic capacity.

CONCLUSION

The study highlighted those significant abiotic variations with the different ages of the rubber farms primarily influenced the morpho-physiological traits of the understorey palms. For example, the 12-year-old rubber farm had a marked soil water deficit at the beginning of the rainy season, while the 25-year-old rubber farm had a greater light transmission in the dry season.

Under these abiotic variations, all palms could adjust the leaf area in terms of the morphological traits to balance the photosynthetic capacity. However, the *Rhapis* palm had higher acclimatization with significant stomatal conductance responses than the other palms. Regarding the physiological traits, except the *Licuala* palm, all palms exhibited significant allocation of the chlorophyll pigments and nitrogen content in their leaves in response to the different intensities of the abiotic stresses in the understorey of the rubber farms.

Despite the study results showing the greater acclimatization with the adaptive morpho-physiological response of the palm leaves, it is suggested that the below-ground interactions of the system, linked with the current findings, should be further studied for a holistic understanding of their coexistence.

ACKNOWLEDGEMENTS

The National Research Council of Thailand financially supported the study through the project (NAT600122b) and Thailand's Education Hub for ASEAN Countries (THE-AC), Graduate School, Prince of Songkla University.

REFERENCES

Aasamaa, K., Sober, A., & Rahi, M. (2001). Leaf anatomical characteristics associated with shoot hydraulic conductance, stomatal conductance and stomatal sensitivity to changes of leaf water status in temperate deciduous trees. *Australian Journal of Plant Physiology*, *28*(8), 765-774. https://doi.org/10.1071/PP00157

Ahrends, A., Hollingsworth, P. M., Ziegler, A. D., Fox, J. M., Chen, H., Su, Y., & Xu, J. (2015). Current trends of rubber plantation expansion may threaten biodiversity and livelihoods. *Global Environmental Change*, *34*, 48-58. https://doi.org/10.1016/j.gloenvcha.2015.06.002

Association of Natural Rubber Producing Countries. (2021). *Natural rubber statistics March 2021*. ANRPC. http://www.anrpc.org/html/nrts.aspx?ID1=57&ID=58&PID=59

Awal, M. A., Wan Ishak, Endan, J., & Haniff, M. (2004). Determination of specific leaf area and leaf area-leaf mass relationship in oil palm plantation. *Asian Journal of Plant Sciences*, *3*(3), 264-268. https://doi.org/10.3923/AJPS.2004.264.268

Bertolino, L. T., Caine, R. S., & Gray, J. E. (2019). Impact of stomatal density and morphology on water-use efficiency in a changing world. *Frontiers in Plant Science*, *10*, 225.

Bojović, B., & Marković, A. (2009). Correlation between nitrogen and chlorophyll content in wheat (*Triticum aestivum* L.). *Kragujevac Journal of Sciences*, *31*, 69-74.

Casson S. A., & Hetherington, A. M. (2010). Environmental regulation of stomatal development. *Current Opinion Plant Biology*, *13*(1), 90-95. https://doi.org/10.1016/j.pbi.2009.08.005

Chaves, M. M., Morocco, J. P., & Pereira, J. S. (2003). Understanding plant responses to drought – From genes to the whole plant. *Functional Plant Biology*, *30*(3), 239-264. https://doi.org/10.1071/fp02076

Chen, J. M., Rich, P. M., Gower, S.T., Norman, J. M., & Plummer, S. (1997). Leaf area index of boreal forests: Theory, techniques, and measurements. *Journal of Geophysical Research: Atmospheres*, *102*(D24), 29429-29443. https://doi.org/10.1029/97JD01107

Cornelissen, J. H. C., Werger, M. J. A., Castro-Diez, P., van Rheenen, J. W. A., & Rowland, A. P. (1997). Foliar nutrients in relation to growth, allocation and leaf traits in seedlings of a wide range of woody plant species and types. *Oecologia*, *111*, 460-469. https://doi.org/10.1007/s004420050259

d'Auzac, J., Jacob, J. L., Prevot, J. C., Clement, A., Gallois, R., Cretin, H., Lecote, R., Pujade-Renaud, V., & Gohet, E. (1997). *The regulation of cis-polyisoprene production (natural rubber) from* Hevea brasiliensis. ResearchGate. https://www.researchgate.net/publication/235908218_The_regulation_of_cis-polyisoprene_production_natural_rubber_from_Hevea_brasiliensis

Dijkstra, P. (1990). Causes and effect of differences in specific leaf area. In H. Lambers, M. L. Cambridge, H. Konings, & T. L. Pons (Eds.), *Causes and consequences of variation in growth rate and productivity of higher plants* (pp. 125-140). SPB Academic Publishing.

Dransfield, J., Barfod, A. S., & Pongsattayapipat, R. (2004). A preliminary checklist to Thai palms. *Thai Forest Bulletin*, *32*, 32-72.

Evans, J. R., (1989). Photosynthesis and nitrogen relationships in leaves of C_3 plants. *Oecologia*, *78*, 9-19. https://doi.org/10.1007/bf00377192

Fan, Y., Chen, J., Cheng, Y., Raza, M. A., Mu, X., Wang, Z., Liu, Q., Wang, R., Wang, X., Yong, T., Liu, W., Liu, J., Du, J., Shu, K., Yang, W., & Feng, Y. (2018). Effect of shading and light recovery on the growth, leaf structure,

and photosynthetic performance of soybean in a maize-soybean relay-strip intercropping system. *PLOS One*, *13*(5), e0198159. https://doi.org/10.1371/journal.pone.0198159

Farquhar, G. D., & Sharkey, T. D. (1982). Stomatal conductance and photosynthesis. *Annual Review of Plant Physiology*, *33*, 317-345. https://doi.org/10.1146/annurev.pp.33.060182.001533

Feng, L., Raza, M. A., Li, Z., Chen, Y., Khalid, M. H. B., Du, J., Liu, W., Wu, X., Song, C., Yu, L., Zhang, Z., Yuan, S., Yang, W., & Yang, F. (2019). The influence of light intensity and leaf movement on photosynthesis characteristics and carbon balance of soybean. *Frontiers in Plant Science*, *9*, 1952. https://doi.org/10.3389/fpls.2018.01952

Field, C., & Mooney, H. A. (1986). The photosynthesis-nitrogen relationship in wild plants. In T. Givnish (Ed.), *On the economy of plant form and function* (pp. 25-55). Cambridge University Press.

Fox, J., & Castella, J. C. (2013). Expansion of rubber (*Hevea brasiliensis*) in mainland Southeast Asia: What are the prospects for smallholders?. *Journal of Peasant Studies*, *40*(1), 155-170. https://doi.org/10.1080/03066150.2012.750605

Franks, P. J., & Beerling, D. J. (2009). Maximum leaf conductance driven by CO_2 effects on stomatal size and density over geologic time. *Proceedings of National Academy of Sciences of the United States of America*, *106*(25), 10343-10347. https://doi.org/10.1073/pnas.0904209106

Galhidy, L., Mihok, B., Hagyo, A., Rajkai, K., & Standovar, T. (2005). Effects of gap size and associated changes in light and soil moisture on the understorey vegetation of a Hungarian beech forest. *Plant Ecology*, *183*, 133-145. https://doi.org/10.1007/s11258-005-9012-4

Givnish, T. J. (1988). Adaptation to sun and shade: A whole-plant perspective. *Australian Journal of Plant Physiology*, *15*(2), 63-92. https://doi.org/10.1071/PP9880063

Hamanishi, E. T., Thomas, B. R., & Campbell, M. M. (2012). Drought induces alterations in the stomatal development program in *Populus*. *Journal of Experimental Botany*, *63*(13), 4959-4971. http://doi.org/10.1093/jxb/ers177

Hartmut, K. L., Alexander, Ac., Michal, V. M., Jiri, K., & Urban, O. (2007). Differences in pigment composition, photosynthetic rates and chlorophyll fluorescence images of sun and shade leaves of four tree species. *Plant Physiology and Biochemistry*, *45*(8), 577-588. https://doi.org/10.1016/j.plaphy.2007.04.006

Hendry, G. A. F., & Price, A. H. (1993). Stress indicators: Chlorophylls and carotenoids. In G. A. F. Hendry & J. P. Grime (Eds.), *Methods in comparative plant ecology* (pp. 148-152). Springer. https://doi.org/10.1007/978-94-011-1494-3

Hollinger, D. Y. (1989). Canopy organization and foliage photosynthetic capacity in a broad-leaved evergreen montane forest. *Functional Ecology*, *3*(1), 53-62. https://doi.org/10.2307/2389675

Houborg, R., McCabe, M., Cescatti, A., Gao, F., Schull, M., & Gitelson, A. (2015). Joint leaf chlorophyll content and leaf area index retrieval from Landsat data using a regularized model inversion system (REGFLEC). *Remote Sensing of Environment*, *159*, 203-221. https://doi.org/10.1016/j.rse.2014.12.008

Inskeep, W. P., & Bloom, P. R. (1985). Extinction coefficients of chlorophyll *a* and *b* in *N*, *N*-dimethylformamide and 80% acetone. *Plant Physiology*, *77*(2), 483-485. https://doi.org/10.1104/pp.77.2.483

Jacob, J. L., Prévôt, J. C., Roussel, D., Lacote, R., Serres, E., d'Auzac, J., Eschback, J.-M., & Omont, H. (2018). Yield limiting factors, latex physiological parameters, latex diagnosis and clonal typology. In J. d'Auzac, J. L. Jacob, & H. Chrestin (Eds.), *Physiology of rubber tree latex: The laticiferous cell and latex – A model*

of cytoplasm (pp. 345-382). CRC Press. https://doi.org/10.1201/9781351075695-16

Johnson, D. V. (2011). *Tropical palms: 2010 revision*. Food and Agriculture Organization of the Unite Nations. https://www.fao.org/3/i1590e/i1590e00.htm

Jongrungrot, V., Thungwa, S., & Snoeck, D. (2014). Diversification des cultures pérennes dans les plantations d'hévéa pour augmenter les revenus des petits producteurs de caoutchouc du sud de la Thaïlande [Tree-crop diversification in rubber plantations to diversify sources of income for small-scale rubber farmers in Southern Thailand]. *Bios et Forets des Tropiques*, *321*, 21-32. http://doi.org/10.19182/bft2014.321.a31214

Kitajima, K., & Hogan, K. P. (2003). Increase of chlorophyll *a*/*b* ratios during acclimation of tropical woody seedlings to nitrogen limitation and high light. *Plant, Cell and Environment*, *26*(6), 857-865. https://doi.org/10.1046/j.1365-3040.2003.01017.x

Langenberger, G., Cadisch, G., Martin, K., Min, S., & Waibel, H. (2017). Rubber intercropping: A viable concept for the 21st century?. *Agroforestry System*, *91*, 577-596. https://doi.org/10.1007/s10457-016-9961-8

Leakey, R. R. B. (2017). Definition of agroforestry revisited. In *Multifunctional agriculture – Achieving sustainable development in Africa* (pp. 5-6). Academic Press. https://doi.org/10.1016/B978-0-12-805356-0.00001-5

Lei, T. T., & Lechowicz, M. J. (1997). The photosynthetic response of eight species of *Acer* to simulated light regimes from the centre and edges of gaps. *Functional Ecology*, *11*(1), 16-23.

Li, T., Liu, L., Jiang, C. D., Liu, Y. J., & Shi, L. (2014). Effects of mutual shading on the regulation of photosynthesis in field-grown sorghum. *Journal of Photochemistry and Photobiology B: Biology*, *137*, 31-38. https://doi.org/10.1016/j.jphotobiol.2014.04.022

Li, Y., Lan, G., & Xia, Y. (2016). Rubber trees demonstrate a clear retranslocation under seasonal drought and cold stresses. *Frontiers in Plant Science*, *7*, 1907. https://doi.org/10.3389/fpls.2016.01907

Lichtenthaler, H. K., Buschmann, C., Döll, M., Fietz, H. J., Bach, T., Koizel, U., Meir, D., & Rahmsdorf, U. (1981). Photosynthetic activity chloroplasts ultrastructure and leaf characteristics of high-light and low-light plants and of sun and shade leaves. *Photosynthesis Research*, *2*, 115-141. https://doi.org/10.1007/BF00028752

Lin, X. H., Chen, Q. B., Hua, Y. G., Yang, L. F., & Wang, Z. H. (2011). Soil moisture content and fine root biomass of rubber tree (*Hevea brasiliensis*) plantations at different ages. *Journal of Applied Ecology*, *22*(2), 331-336.

Liu, S., Liu, J., & Cao, J. (2006). Stomatal distribution and character analysis of leaf epidermis of jujube under drought stress. *Journal of Anhui Agricultural Science*, *34*, 1315-1318.

Loomis, R. S. (1997). On the utility of nitrogen in leaves. *Proceedings of National Academy Sciences of the United States of America*, *94*(25), 13378-13379. https://doi.org/10.1073/pnas.94.25.13378

Mathur, S., Jain, L., & Jajoo, A. (2018). Photosynthetic efficiency in sun and shade plants. *Photosynthetica*, *56*(1), 354-365. https://doi.org/10.1007/s11099-018-0767-y

Meng, L., Li, L., Chen, W., Xu, Z., & Liu, L. (1999). Effect of water stress on stomatal density, length, width and net photosynthetic rate I rice leaves. *Journal of Shenyang Agricultural University*, *30*(5), 477-480.

Meziane, D., & Shipley, B. (2001). Direct and indirect relationships between specific leaf area, leaf nitrogen and leaf gas exchange. Effects of irradiance and nutrient supply. *Annals of*

Botany, *88*(5), 915-927. https://doi.org/10.1006/anbo.2001.1536

Moran, R., & Porath, D. (1980). Chlorophyll determination in intact tissues using *N*, *N*-dimethylformamide. *Plant Physiology*, *65*(3), 478-479. https://doi.org/10.1104/pp.65.3.478

Munasinghe, E. S., & Rodrigo, V. H. L. (2017). Lifespan of rubber cultivation can be shortened for high returns: A financial assessment of stimulated conditions in Sri Lanka. *Experimental Agriculture*, *54*(3), 323-335. https://doi.org/10.1017/S0014479717000011

Niinemets, Ü., & Tenhunen, J. D. (1997). A model separating leaf structural and physiological effects on carbon gain along light gradients for the shade-tolerant species *Acer saccharum*. *Plant, Cell and Environment*, *20*(7), 845-866. https://doi.org/10.1046/j.1365-3040.1997.d01-133.x

Pathiratna, L. S. S. (2006). Management of intercrops under rubber: Implications of competition and possibilities for improvement. *Bulletin of Rubber Research Institution of Sri Lanka*, *47*, 8-16.

Poorter, H. (1999). Growth responses of 15 rain-forest tree species to a light gradient: The relative importance of morphological and physiological traits. *Functional Ecology*, *13*(3), 396-410. https://doi.org/10.1046/j.1365-2435.1999.00332.x

Powles, S. B. (1984). Photoinhibition of photosynthesis induced by visible light. *Annual Review of Plant Physiology*, *35*, 15-44. https://doi.org/10.1146/annurev.pp.35.060184.000311

Premakumari, D., & Saraswathyamma, C. K. (2000). The para rubber tree. In P. J. George & C. J. Kuruvilla (Eds.), *Natura rubber: Agromanagement and crop processing* (pp. 29-35). Rubber Research Institute of India.

Rappaport, D., & Montagnini, F. (2014). Tree species growth under a rubber (*Hevea brasiliensis*) plantation: Native restoration via enrichment planting in southern Bahia, Brazil. *New Forests*, *45*, 715-732. https://doi.org/10.1007/s11056-014-9433-9

Sáez-Plaza, P., Navas, M. J., Wybraniec, S., Michalowski, T., & Asuero, A. G. (2013). An overview of the Kjeldahl method of nitrogen determination. Part II. Sample preparation, working scale, instrumental finish and quality control. *Critical Reviews in Analytical Chemistry*, *43*(4), 224-272. https://doi.org/10.1080/10408347.2012.751787

Saraswathyamma, C. K., Licy, J., & Marattukalam, J. G. (2000). Planting materials. In P. J. Geroge & C. J. Kuruvilla (Eds.), *Natural rubber: Agromanagement and crop processing* (pp. 59-74). Rubber Research Institute of India.

Sarijeva, G., Knapp, M., & Lichtenthaler, H. K. (2007). Differences in photosynthetic activity, chlorophyll and carotenoid levels, and in chlorophyll fluorescence parameters in green sun and shade leaves of *Ginkgo* and *Fagus*. *Journal of Plant Physiology*, *164*(7), 950-955. https://doi.org/10.1016/j.jplph.2006.09.002

Saw, L. G., Dransfield, J., & Keith-Lucas, D. M. (2003). Morphological diversity of the genus *Licuala* (Palmae). *Telopea*, *10*(1), 187-206. https://doi.org/10.7751/telopea20035615

Schneider, C. A., Rasband, W. S., & Eliceiri, K. W. (2012). NIH Image to ImageJ: 25 years of image analysis. *Nature Methods*, *9*, 671-675. https://doi.org/10.1038/nmeth.2089

Schroeder, J. I., Allen, G. J., Hugouvierx, V., Kwak, J. M., & Waner, D. (2001). Guard cell signal transduction. *Annual Review of Plant Physiology and Plant Molecular Biology*, *52*, 627-658. https://doi.org/10.1146/annurev.arplant.52.1.627

Somboonsuke, B., Wetayaprasit, P., Chernchom, P., & Pacheerat, K. (2011). Diversification of smallholding rubber agroforestry system (SRAS)

Thailand. *Kasetsart Journal of Social Sciences*, *32*, 327-339.

Sun, Y., Ma, Y., Cao, K., Li, H., Shen, J., Liu, W., Di, L., & Mei, C. (2017). Temporal changes of ecosystem carbon stocks in rubber plantations in Xishuangbanna, Southwest China. *Pedosphere*, *27*(4), 737-746. https://doi.org/10.1016/S1002-0160(17)60327-8

Supapvanich, S., Megia, R., & Ding, P. (2014). Salak (*Salacca zalacca* (Gaertner) Voss). In E. M. Yahia (Ed.), *Postharvest biology and technology of tropical and subtropical fruits* (pp. 334-352). Woodhead Publishing. https://doi.org/10.1533/9780857092618.334

Tan, Z. H., Zhang, Y. P., Song, Q. H., Liu, W. J., Deng, X. B., Tang, J. W., Zhou, W. J., Yang, L. Y., Yu, G. R., Sun, M. X., & Liang, N. S. (2011). Rubber plantations act as water pumps in tropical China. *Geophysical Research Letters*, *38*(24), L24406. https://doi.org/10.1029/2011GL050006

Terashima, I., & Hikosaka, K. (1995). Comparative ecophysiology of leaf and canopy photosynthesis. *Plant, Cell and Environment*, *18*(10), 1111-1128. https://doi.org/10.1111/j.1365-3040.1995.tb00623.x

Thai Meteorological Department. (2019). *The climate of Thailand*. https://www4.tmd.go.th/en/archive/thailand_climate.pdf

Valladares, F., Laanisto, L., Niinemets, Ü., & Zavala, M. A. (2016). Shedding light on shade: Ecological perspectives of understory plant life. *Plant Ecology and Diversity*, *9*(3), 237-251. https://doi.org/10.1080/17550874.2016.1210262

Vaten, A., & Bergmann, D. C. (2012). Mechanisms of stomatal development: An evolutionary view. *EvoDevo*, *3*, 11. https://doi.org/10.1186/2041-9139-3-11

Vincent, G. (2001). Leaf photosynthetic capacity and nitrogen content adjustment to canopy openness in tropical forest tree seedlings. *Journal of Tropical Ecology*, *17*(4), 495-509. http://doi.org/10.1017/S0266467401001377

Wang, M., Shi, S., Lin, F., Hao, Z., Jiang, P., & Dai, G. (2012). Effects of soil water and nitrogen on growth and photosynthetic response of Manchurian ash (*Fraxinus mandshurica*) seedlings in Northeastern China. *PLOS One*, *7*, e30754. https://doi.org/10.1371/journal.pone.0030754

Wellburn, A. R. (1994). The spectral determination of chlorophylls *a* and *b*, as well as total carotenoids, using various solvents with spectrophotometers of different resolution. *Journal of Plant Physiology*, *144*(3), 307-313. https://doi.org/10.1016/S0176-1617(11)81192-2

Weyers, J. D. B., & Meidner, H. (1990). *Methods in stomatal research*. Longman.

Windsor-Collins, A., Cutler, D., & Atherton, M. (2006). The palm – A model for success?. *WIT Transactions on State-of-the-art in Science and Engineering*, *27,* 303-326. https://doi.org/10.2495/978-1-85312-853-0/10

Wu, J., Liu, W., & Chem, C. (2016). Can intercropping with the world's tree major beverage plants help improve the water use of rubber trees?. *Journal of Applied Ecology*, *53*(6), 1787-1799. https://doi.org/10.1111/1365-2664.12730

Xu, Z. Z., & Zhou, G. S. (2005). Effects of water stress and nocturnal temperature on carbon allocation in the perennial grass, *Leymus chinensis*. *Physiologia Plantarum*, *123*(3), 272-280. https://doi.org/10.1111/j.1399-3054.2005.00455.x

Zaw, Z. N., Sdoodee, S., & Lacote, R. (2017). Performances of low frequency tapping system with rainguard in high rainfall area in Myanmar. *Australian Journal of Crop Science*, *11*(11), 1451-1456. https://doi.org/10.21475/ajcs.17.11.11.pne593

Pertanika J. Trop. Agric. Sci. 46 (1): 129 - 151 (2023)

PERTANIKA JOURNALS

TROPICAL AGRICULTURAL SCIENCE

Journal homepage: http://www.pertanika.upm.edu.my/

Induced Biochemical Changes in *Ganoderma boninense* Infected *Elaeis guineensis* Seedlings in Response to Biocontrol Treatments

Tuan Muhammad Syafiq Tuan Hassan[1], Nusaibah Syd Ali[1]* and Mohd Rafii Yusop[2]

[1]*Department of Plant Protection, Faculty of Agriculture, Universiti Putra Malaysia, 43400 Serdang, Selangor, Malaysia*

[2]*Institute of Tropical Agriculture and Food Security, Universiti Putra Malaysia, 43400 Serdang, Selangor, Malaysia*

ABSTRACT

Despite massive economic contributions to Malaysia, the oil palm industry faces devastating threats from basal stem rot (BSR) disease. An array of treatments was designed to evaluate the potential of biological control agents (BCAs) as a single and combination of applications in a greenhouse study of six months. Oil palm enzymes, phenolic content, and metabolite induction in BSR-diseased seedlings were also assessed in response to the designed treatments. In the study, seedlings treated with *Trichoderma asperellum* (UPM16) demonstrated the highest disease reduction (DR) (57.2%). Peroxidase (PO), lignin, and total phenolic content (TPC) were evaluated. Treatments on *Ganoderma*-infected seedlings treated with *Bacillus cereus* (UPM15) exhibited the highest reading in all assays. Gas chromatography-mass spectrometry (GC-MS) analysis profiled phenol, 4-2-aminoethyl- as the most abundant metabolite detected in combination treatments with *B. cereus* and *T. asperellum* (BT). Both BCAs complimented and demonstrated huge potential in mitigating BSR diseases in oil palm. However, excessive chemical application to control BSRs negatively impacts biodiversity and the human population. In view of this, studies on biological control are crucial in selecting potential BCAs to counter BSR sustainably. Biological control would be an ideal alternative as a sustainable method for controlling oil palm BSR disease.

Keywords: Basal stem rot, biological control agents, lignin, metabolites, peroxidase, total phenolic content

ARTICLE INFO

Article history:
Received: 06 July 2022
Accepted: 11 October 2022
Published: 03 February 2023

DOI: https://doi.org/10.47836/pjtas.46.1.08

E-mail addresses:
capooxy04@gmail.com (Tuan Muhammad Syafiq Tuan Hassan)
nusaibah@upm.edu.my (Nusaibah Syd Ali)
mrafii@upm.edu.my (Mohd Rafii Yusop)
* Corresponding author

ISSN: 1511-3701
e-ISSN: 2231-8542

INTRODUCTION

A disease of oil palm, such as one caused by a genus of polypore fungi, *Ganoderma* spp., continues to cause significant yield reduction and losses through the collapse of standing palms. The most destructive and vital pathogen that causes basal stem rot (BSR) is *Ganoderma boninense*. This pathogen causes damage to up to 80% of palm stands when they are just about halfway through their economic lifespan (Bivi et al., 2010). Synthetic chemical control using hexaconazole is widely used when dealing with this soil-borne pathogen in the plantations. However, synthetic chemical control leads to groundwater pollution, evolving fungicidal resistance variants, and loss of non-target beneficial flora.

Against this background arising from excessive usage of chemicals, the oil palm industry must transform its current practices to more environment-friendly methods. Biological control agents (BCAs) could be the potential alternatives to chemical pesticides. Several potential BCAs, including *Trichoderma* spp. (Nusaibah et al., 2017; Sariah et al., 2005), and *Bacillus* spp. (Nusaibah et al., 2017) have shown their efficacy in inhibiting *G. boninense*'s growth and subsequently reducing infection. In justification, BCA generally occupies the rhizosphere of the soil profile and produces almost no toxic residues as opposed to chemicals (Ashbolt et al., 2013).

The present study was conducted to assess and evaluate BSR disease suppression in the presence of both BCAs applied as pre-treatments prior to *G. boninense* inoculation. Literature has it that a pathogen attack or the presence of an elicitor triggered various plant protective mechanisms specially developed to counteract the invasion of a pathogen causing an infection (Małolepsza & Różalska, 2005). Furthermore, several studies suggested that plant polymers, such as lignin and suberin, played a direct role in the breakdown of the pathogen cell wall (Treutter, 2006; Usall et al., 2000). Furthermore, Surekha et al. (2013) published those phenolic compounds act as antimicrobials, growth interceptors of pathogens, trigger plant defence genes, and structural barriers. Therefore, it is empirical to explore the effects of BCAs, such as *B. cereus* and *T. asperellum*, on their role in the heightening of oil palm defence mechanisms against *G. boninense* infection via enzymes, phenolic content, and metabolites.

MATERIALS AND METHODS

Plant Materials

The present study used three months old commercial oil palm seedlings (*dura* × *pisifera*). Before transplanting, a 3 : 2 : 1 soil mixture of topsoil, peat moss, and sand was made and sterilised in an autoclave for 30 minutes at 121°C and 100 kPa pressure at Laboratory of Biological Control , Department of Plant Protection, Faculty of Agriculture, Universiti Putra Malaysia (UPM).

Ganoderma boninense Artificial Inoculation

Artificial inoculation of *G. boninense* (UPM13) was carried out following the

dip, place, and drench (DPD) technique as described by Nusaibah et al. (2017). The seedlings were irrigated twice daily at 9 a.m. and 6 p.m. throughout the treatment. Commercial Nitrogen : Phosphorus : Potassium (N : P : K) (15 : 15 : 15) fertiliser (10 g per polybag) was applied at monthly intervals.

Inoculum of Microbes

Trichoderma asperellum isolate and *Bacillus cereus* bacterium was isolated from BSR-infested oil palm plantation soil. These microbes were identified using a universal internal transcribed spacer (ITS) primer set and 16S barcoding, respectively, and morphological identification in a previous study (Nusaibah et al., 2017; Syafiq et al., 2021). *Bacillus cereus* inoculum suspension was prepared using 48-hour grown culture on nutrient agar (NA). The concentration prepared was 10^8 colony-forming units (cfu) mL^{-1} (Zaiton et al., 2008). In addition, a 150 mL *B. cereus* suspension was administered to the seedlings 14 days before artificial inoculation with *G. boninense* inoculum by drenching the soil following a pre-designed treatment, as presented in Table 1.

Three days after the artificial inoculation of the seedlings with *G. boninense*, the application of *B. cereus* was made as a booster dose. Minor adjustments were made to Izzati and Abdullah's (2008) instructions while preparing the conidial suspension of *T. asperellum*.

Whatman® Grade 1 filter paper was used in place of muslin fabric. *Trichoderma asperellum* conidia were obtained from an inoculum cultured on potato dextrose agar (PDA) for seven days. After pipetting an aliquot of 10 mL sterile distilled water onto a PDA plate, the conidia were gently pushed with an L-shaped glass rod. The mixture was then passed via filter paper to eliminate the mycelial debris. The filtrate was diluted to a volume of 1 L using distilled water. The range of 10^7 conidia mL^{-1} was specified for conidia counts. Fourteen (14) days before *G. boninense* artificial inoculation, 250 mL of freshly prepared *T. asperellum* conidial suspension was applied to the seedlings via the drenching technique. Following five days of artificially inoculating the oil palm seedlings with *G. boninense*, a booster dose of *T. asperellum* was applied with a concentration similar to that of the initial treatment.

Table 1
Treatment design for greenhouse study

Treatment	Description
T1 (BT)	Plant + *Trichoderma asperellum* + *Bacillus cereus*
T2 (T)	Plant + *Trichoderma asperellum*
T3 (B)	Plant + *Bacillus cereus*
T4 (G)	Plant + *Ganoderma boninense*
T5 (BTG)	Plant + *Ganoderma boninense* + *Bacillus cereus* + *Trichoderma asperellum*
T6 (TG)	Plant + *Ganoderma boninense* + *Trichoderma asperellum*
T7 (BG)	Plant + *Ganoderma boninense* + *Bacillus cereus*
T8 (NC)	Plant (Untreated negative control)

Double-Sealed Plate Assay

Various studies have indicated that microbial volatile organic compounds (MVOCs) can stimulate plant growth and actively restrain fungal growth (Weisskopf, 2013). With a few minor adjustments, Gotor-Vila et al. (2017) technique was used to conduct the double-plate assay. The assay was to determine the antifungal effects of MVOCs emitted by *B. cereus* and *T. asperellum* on the growth of *G. boninense*. A 3-day-old *B. cereus* culture previously cultivated on NA was placed facing a PDA plate with a 5 mm *G. boninense* mycelium plug incubated into the plate's centre without a cover. The plates were parafilm-sealed and maintained at room temperature for 12 days. The conditions used in the test were: *B. cereus* culture as the base plate and *G. boninense* culture as the top plate. Seven replication was prepared for this assay. NA plates without *B. cereus* culture served as the control treatment. The diameter of *G. boninense* mycelium growth was recorded in millimetres after 12 days of incubation. A similar procedure was repeated using 7-day-old *T. asperellum* culture grown on PDA.

Experimental Design and Statistical Analysis

Table 1 displays the treatment design for the current trial. The greenhouse experiment was conducted using a randomised complete block design (RCBD) with eight treatments and twelve replications. All oil palm seedlings in the polythene bags were arranged on eight benches in a randomised manner. Every bench would be a block. Block factors, such as light, temperature, and moisture conditions that could affect the response variable were under contemplation. The area under the disease progress curve (AUDPC) was used to calculate disease reduction (DR). All the disease incidences and severity were arcsine transformed (Gomez & Gomez, 1984).

Disease Progress Assessment

The disease incidence (DI) is the proportion of seedlings with leaves that are chlorotic and necrotic, whether they have basidiocarps (Idris et al., 2006).

Equation 1:

$$\text{Disease incidence} = \frac{\text{Number of seedlings infected}}{\text{Total number of seedlings assessed}} \times 100$$

A decrease in the DI compared to the control measures how well a treatment suppresses a disease. In addition, a disease progression curve was created using the data to assess the treatments' effectiveness.

The following formula from Shaner and Finney (1977) was used to determine the AUDPC:

Equation 2:

$$AUDPC = (y_i + y_{i+1})/2(t_{i+1} + t_i)$$

whereby:

n = Number of assessment time
y = Disease incidence (DI)
t = Time (months) after inoculation

The efficacy of treatments in disease reduction (DR) was calculated using the following formula:

Equation 3:

$$\text{Disease reduction (DR)} = \frac{\text{AUDPC positive control} - \text{AUDPC treatment}}{\text{AUDPC positive control}} \times 100\%$$

The following Tarig et al. (1998) formula was used to determine the percentage of disease severity (DS) in the root tissues, and the severity scale was assessed by the severity index of Breton et al. (2006) (Table 2):

Equation 4:

$$\text{DS (\%)} = \frac{\Sigma\ (\text{Number of seedlings in the scale} \times \text{Severity scale})}{\text{Total number of seedlings assessed} \times \text{Highest scale}} \times 100$$

Table 2
The scale used for scoring disease (G. boninense) *severity index based on rotten root tissues of UPM13 seedlings*

Scale	Symptoms
0	Healthy, no internal rot
1	20% rotting of tissues
2	20% to 50% rotting of tissues
3	>50% rotting of tissues
4	>90% rotting of tissues

Source: Breton et al. (2006)

Data on disease incidence and disease severity were analysed by one-way Analysis of Variance (ANOVA). Mean values were compared by least significant difference (LSD) test ($P \leq 0.05$).

Establishment of Basal Stem Rot Disease and Biological Control Treatments

Scanning electron microscope (SEM) was used to examine the disease establishment via colonisation of the *G. boninense* pathogen and the BCAs on the roots of seedlings after one month of inoculation. SEM sample preparation was done following *in-house* procedures of the Microscopy Unit, Institute of Bioscience (IBS), UPM.

Enzyme Assay

Total Peroxidase (PO) Assay. Enzyme extract was created using, with some modifications, Samatha et al. (2012)'s methods. Approximately 1 g of the root was harvested during destructive sampling and subsequently immersed in liquid nitrogen. As soon as possible, the sample was homogenised in 2 mL of cold, 0.05 mol L^{-1} sodium phosphate buffer (pH 5) that had been adjusted with 5 mL of polyvinyl pyrrolidone (PVP) (Sigma-Aldrich, USA). The semi-solid mixture underwent a 20-minute, 18,922 × *g* centrifugation at 4°C. An aliquot of 200 µL of the supernatant was extracted. Three millilitres of a reaction mixture containing 0.1 mmol L^{-1} sodium acetate buffer (pH 6), 1 mmol L^{-1} H_2O_2 (3%, v/v), and 0.1 mmol L^{-1} *o*-methoxyphenol (guiacol) (Acros

Organics, USA) was prepared. The reaction mixture was mixed well with the previously removed supernatant and then left to sit at room temperature for 2 min. The mixture's absorbance was read at 470 nm with a spectrophotometer (Thermo Scientific Multiskan Go, Thermo Fisher Scientific, Finland). The reaction mixture was used to prepare blanks instead of the supernatant. Change in absorbance $min^{-1}g^{-1}$ protein was used to express PO activity (Kokkinakis & Brooks, 1979).

Data on enzyme concentration and activity were analysed by one-way ANOVA. Mean values were compared by Tukey's Studentized Range (HSD) Test at 5% level of significance.

Lignin Assay. One gram of frozen root from a damaging sample was dissolved in 5 mL of absolute methanol (Merck Schuchardt OHG, Hohenbrunn, Germany) for 48 hours (in four changes of methanol) (Doster & Bostock, 1988). After the root tissue samples were pulverised, 50 mL of them were put into an Eppendorf tube with 0.1 mL of thioglycolic acid and 0.9 millilitres of 2 N hydrochloric acid (HCl) (J.T. Baker®, USA) The samples were then heated for 4 hours in a water bath based on the method proposed by Bruce and West (1989) with some modification where the temperature of the water was reduced from 100°C to 95°C. Following cooling to room temperature, the heated sample test tubes underwent a 5-minute, 13902 × *g* centrifugation. Distilled water was used to clean the residue that had been collected. Finally, the samples were re-centrifuged to obtain the pellet. About 1 mL of 0.5 N sodium hydroxide (NaOH) (Systerm Chemicals, Malaysia) was added to the pellet tubes. The samples were incubated overnight at 28ºC and were later centrifuged. A 1 mL of concentrated HCl (37%) (Avantor Performance Materials, USA) was added to the resulting supernatant, centrifuged, and washed with distilled water. A solution of 1 N NaOH (Systerm Chemicals, Malaysia) in 1 mL was used to dissolve the pellet. After mixing 25 mL of the aliquot with 1 mL of 0.5 N NaOH (Systerm Chemicals, Malaysia), the results were read at 280 nm using Thermo Scientific Multiskan Go (ThermoFisher Scientific, Finland) (Dean & Kuc, 1987).

Total Phenolic Content (TPC) Analysis

The Folin-Ciocalteu colourimetric method was employed to determine the total phenolic content (TPC) (Singleton et al., 1999). The absorbance was measured at 725 nm using methanol as the blank and gallic acid as the reference standard. Gallic acid equivalents (GAE) were used to express the results.

Extraction of Metabolites for GC-MS (Gas Chromatography-Mass Spectrometry) Analysis. For metabolite profiling, the sample extraction method followed the procedure of Nusaibah et al. (2016) with some modifications. An amount of 1 g of oil palm leaf sample from the selected treatment was harvested, washed with sterile distilled water, ground in liquid nitrogen, and then transferred into a Falcon tube. A 5 mL methanol liquid chromatography grade (Merck, Germany) was added, and the

tube was vortexed to fully mix the sample. Subsequently, the mixture was stored for 48 hours at 4°C. The mixture was filtered through a 0.4 µm nylon syringe filter following an incubation period of roughly 40 hours. The compounds collected were evaporated at 38°C on a rotary evaporator until dry. An aliquot of 1 mL of methanol was added to the dried sample, syringe-filtered again, and transferred into a glass insert placed in an amber vial before subjecting it to GC-MS analysis.

Untargeted Metabolite Profiling of Treated Oil Palm Seedling Leaves. Based on the modified and improved approach of Fiehn (2002) and Nusaibah et al. (2016), GC-MS analysis was carried out at the Halal Product Research Institute, UPM. A DB5 capillary column (30 m long, 0.25 mm I.D. 155, and a 0.25 µm 5 % phenyl methylpolysiloxane column with an additional 10 m integrated guard column were used for chromatography). Agilent (USA) autosampler for GC (7890A) and MS (5975C) was equipped with a standard 10 µL injection needle. In a splitless mode, 2 µL of each sample was injected.

The column was heated to 180°C for 5 min, 180-260°C for 3 min, 260-280°C for 2 min, and lastly, 280°C for 5 min, with the injector temperature at 280°C and the detector temperature at 290°C. The carrier gas was helium, flowing at a rate of 0.7 mL min^{-1}. Following are the MS operational parameters: Ionisation potential of 70 eV, quadrupole temperature of 100°C, ion source temperature of 290°C, solvent delay of 7 min, the scan rate of 2000 amu sec^{-1}, the scan range of 30-600 amu, and EV voltage of 3000 V. Six biological replicates were run for each treatment and subjected to multivariate analysis. GC-MS results were run through the MetaboAnalyst 4.0 software (Canada, 2019) and based on the multivariate analysis method, specifically Partial Least Squares – Discriminant Analysis (PLS-DA). Metabolites detected from all treatments were discriminated in importance features analysis (Figures 5 and 6). Ten metabolites with the highest concentration were selected to help narrow down the result. The Variable Importance in Projection (VIP) scores estimate the importance of each variable in the projection used in a PLS model. A variable with a VIP Score close to or greater than one can be considered important in given model.

RESULTS

Double-Sealed Plate Test

The mycelial growth inhibition rate of pathogenic *G. boninense* in a double-plate test indicated the effectiveness of MVOCs produced by the BCA isolates. Figure 1 shows the mycelial growth of *G. boninense* when treated with *B. cereus* isolate, recorded after 12 days of incubation. This study showed that *B. cereus* could produce MVOCs that effectively inhibited mycelial growth with a mean of 51.3 mm compared to the control plates (85.0 mm). However, results for the *T. asperellum* assay failed to be recorded due to the overgrowth of *T. asperellum* mycelium on the surface of *G. boninense* culture plates.

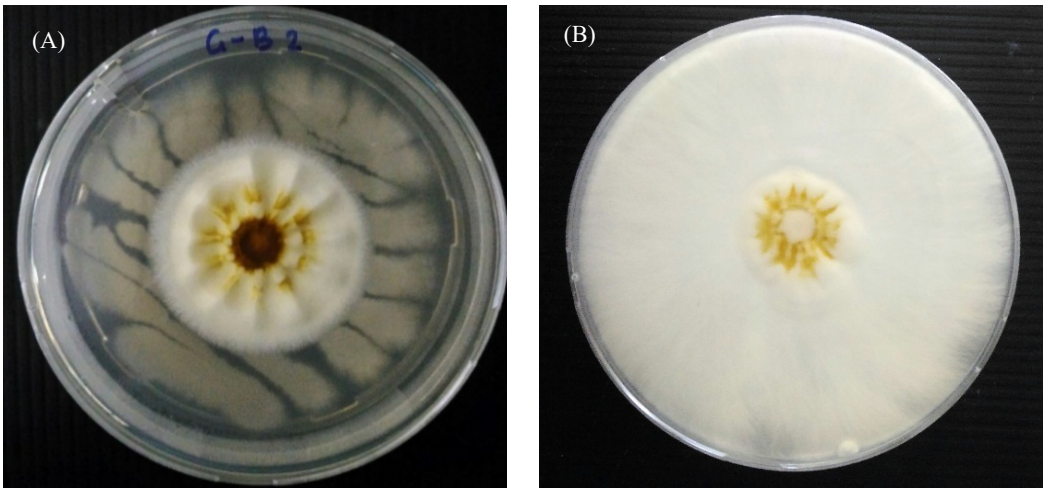

Figure 1. Growth inhibition of *Ganoderma boninense* (UPM13) by volatile compound emitted by *Bacillus cereus* (A) compared to the control plate (B)

Basal Stem Rot (BSR) Disease Assessment

The impact of treatments on disease suppression in oil palm seedlings was investigated during a 6-month greenhouse trial. Figure 2 presents visible proof of disease establishment in terms of root (A and B) and aerial parts (C and D). The percentage of DI was recorded and shown in Table 3. Data on DI recorded those

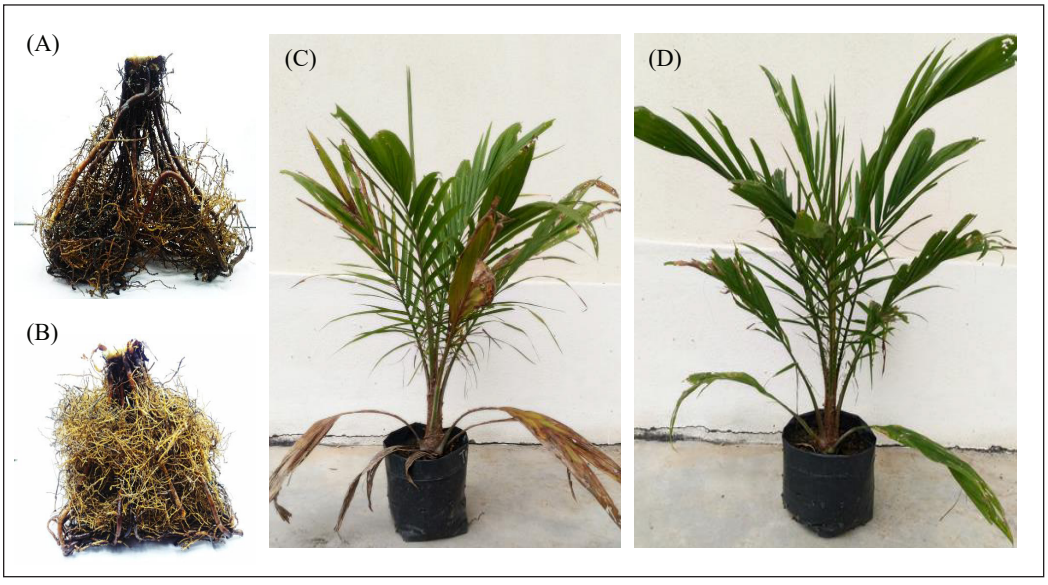

Figure 2. The visual appearance of basal stem rot establishment via artificial inoculation by dip, place, and drench (DPD) technique. (A) *G. boninense* inoculated roots from treatment G; (B) *G. boninense* uninoculated roots served as control; (C) showing external disease symptoms resulting from *G. boninense* inoculation; (D) showing no external disease symptoms observed on control palm

seedlings treated with a consortium or single treatment gave a lower percentage of DI after six months. At 3 months after inoculation (MAI), untreated Ganoderma-infected seedlings demonstrated the first DI at 25% infection, while the remaining treatments displayed DI at 4 to 5 MAI. At 6 MAI, the lowest DI was recorded in combination treatment (BTG) with 81.3%, followed by single treatments of B. cereus (87.5%) and T. asperellum (93.8%).

Based on methods developed by Breton et al. (2006), the DS on oil palm seedling root tissues was recorded after 6 MAI. Single treatment of T. asperellum (TG) recorded the lowest root DS at 50%, followed by consortium treatment (BTG) at 63%. Untreated Ganoderma-infected plants (G) gave the highest root DS at 84%.

Table 4 shows AUDPC and percentages of DR. Disease reduction was calculated using AUDPC values and the DR formula as described in Equation 3. Single treatment of T. asperellum gave the highest DR with 57.2%, followed by the consortium and single treatments of B. cereus, with both giving 50% DR.

Pathogen and BCA Colonization in Inoculated Oil Palm Roots

SEM image of root samples showed that BCAs and *G. boninense* had successfully colonised the root tissues, as depicted in Figures 3 and 4. Figure 3A demonstrates activities in the *Ganoderma*-infected seedling treated with a single application of *B. cereus* where *G. boninense* colonised the roots and *B. cereus* cells colonising *G. boninense* hypha.

In *Ganoderma*-inoculated seedlings treated with a single application of *T.*

Table 4
The effects of biological control agents *on the progression of basal stem rot disease in oil palm seedlings based on the severity of the root infection following a 6-month artificial infection with* G. boninense

Treatment	AUDPC[1]	DR[2]
Plant + *Ganoderma boninense*	263	-
Plant + *Trichoderma asperellum* + *Bacillus cereus*	131	50
Plant + *Trichoderma asperellum*	112	57.2
Plant + *Bacillus cereus*	131	50

Note. [1]AUDPC = Area under disease progress curve; [2]DR = Disease reduction

Table 3
Percentages of disease incidence in oil palm seedlings following inoculation with UPM13 (G. boninense)

Treatment	Disease incidence (%)*			
	3 MAI**	4 MAI	5 MAI	6 MAI
Ganoderma boninense (G)	25[a]	50[b]	93.8[d]	100[d]
Bacillus cereus + *Trichoderma asperellum* + *Ganoderma boninense* (BTG)	0	31.3[a]	56.3[b]	81.3[d]
Bacillus cereus + *Ganoderma boninense* (BG)	0	37.5[a]	68.8[c]	87.5[d]
Trichoderma asperellum + *Ganoderma boninense* (TG)	0	43.8[b]	81.3[d]	93.8[d]

* Means with the same letter in the same column are not significantly different by least significant difference (LSD) at $P \leq 0.05$, (n = 6)
** MAI = Months after inoculation with *G. boninense*

asperellum, the hyphae (of *T. asperellum*) were observed colonising *G. boninense* hyphae and the primary roots (Figure 3B). In Figure 4C, both BCAs were observed colonising the oil palm roots in a manner observed in the combination treatment. *Bacillus cereus* cells were also observed on *G. boninense* hyphae (Figure 4D).

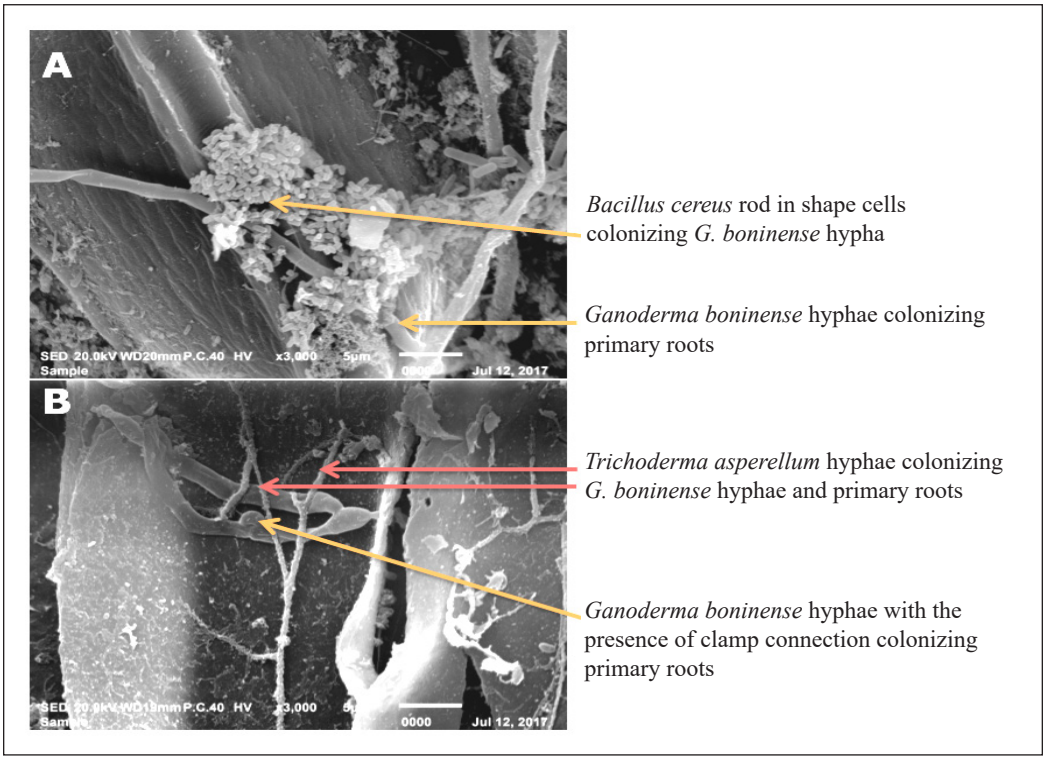

Figure 3. Oil palm seedling roots pre-inoculated with (A) *Bacillus cereus* (B) *Trichoderma asperellum* that were infected with *G. boninense*, and harvested after eight weeks of incubation

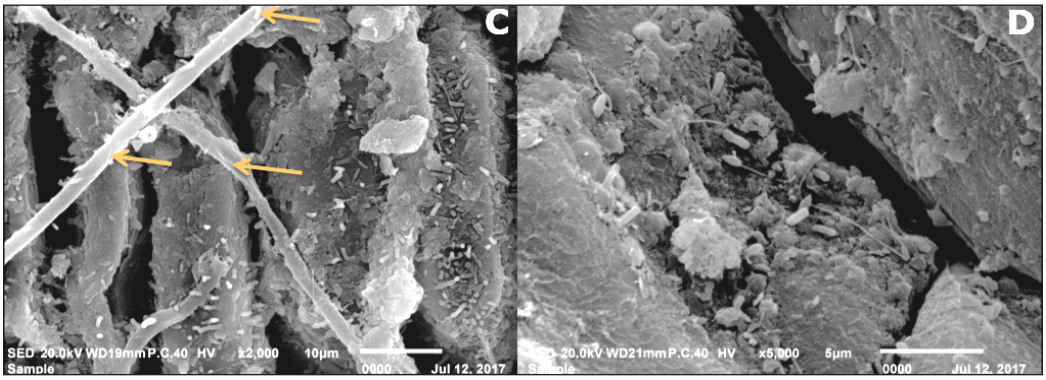

Figure 4. Oil palm seedling roots pre-inoculated with a mixture of *Bacillus cereus* and *Trichoderma asperellum* (C) infected with *G. boninense* and (D) non-infected with *G. boninense*. Roots were harvested after eight weeks of incubation

Enzyme Assay

Peroxidase Assay. Treatment with BG recorded the highest peroxidase (PO) activity with a value of 0.2601 unit^{-1}min^{-1}g, followed by treatment BTG with 0.2278 unit^{-1}min^{-1}g (Figure 5). Generally, all treatments treated with *B. cereus* (BT, B, BTG, and BG) yielded higher PO activities than untreated treatments (T, G, TG, and NC).

Lignin Assay. Figure 6 demonstrates that treatments T, BG, and NC recorded the highest lignin concentration with 10, 10.4, and 10.3 mg L^{-1}, respectively. Conversely, treatment G gave the lowest lignin concentration at 5.4 mg L^{-1} compared to other treatments. The lignin concentrations derived from a standard curve of lignin are presented in Figure 7.

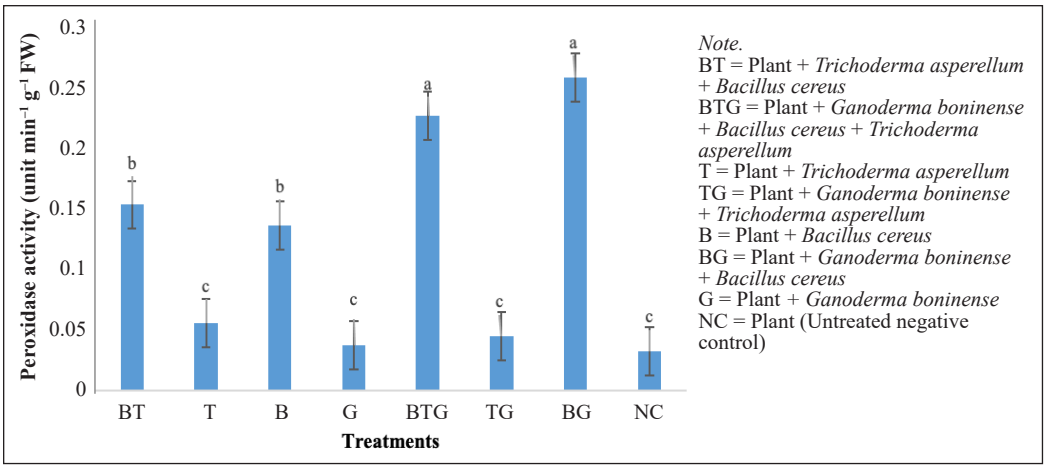

Figure 5. Induction of peroxidase activity in oil palm seedling roots treated with biological control agents. Values are means of five replications, and differences between means are separated by Tukey's studentised range (HSD) test at a 5% level of significance

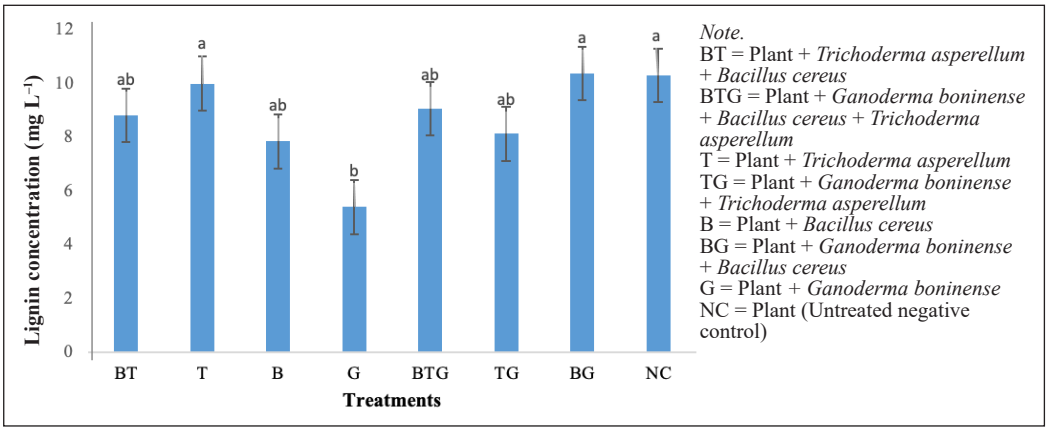

Figure 6. Oil palm lignin concentrations following effects of biological control agents. Values are means of three replications, and differences between means are separated by Tukey's studentised range (HSD) test at a 5% level of significance

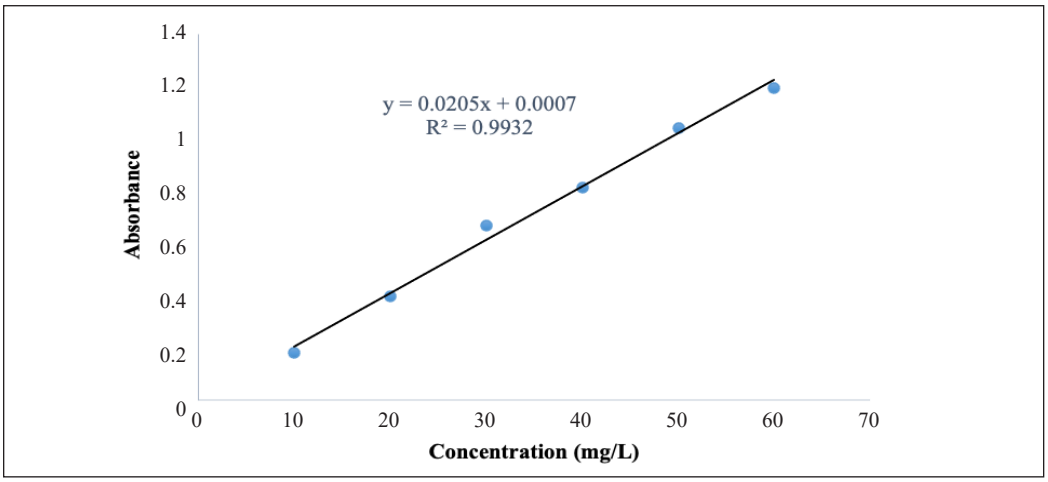

Figure 7. Standard curve of lignin with absorbance measured at 280 nm

Total Phenolic Content (TPC). The present study recorded high TPC extracted from oil palm roots in all treatments except for the consortium treatment, which was not infected with *G. boninense* (BT, as well as the untreated *Ganoderma*-infected treatment (G) (Figure 8). *Ganoderma*-infected seedlings treated with *B. cereus* (BG) gave the highest TPC (34.88 mg L^{-1}), followed by seedlings treated with *B. cereus* (B) (34.15 mg L^{-1}). Seedlings treated with consortium treatment (BT) gave the lowest TPC derived from the gallic acid standard curve shown in Figure 9.

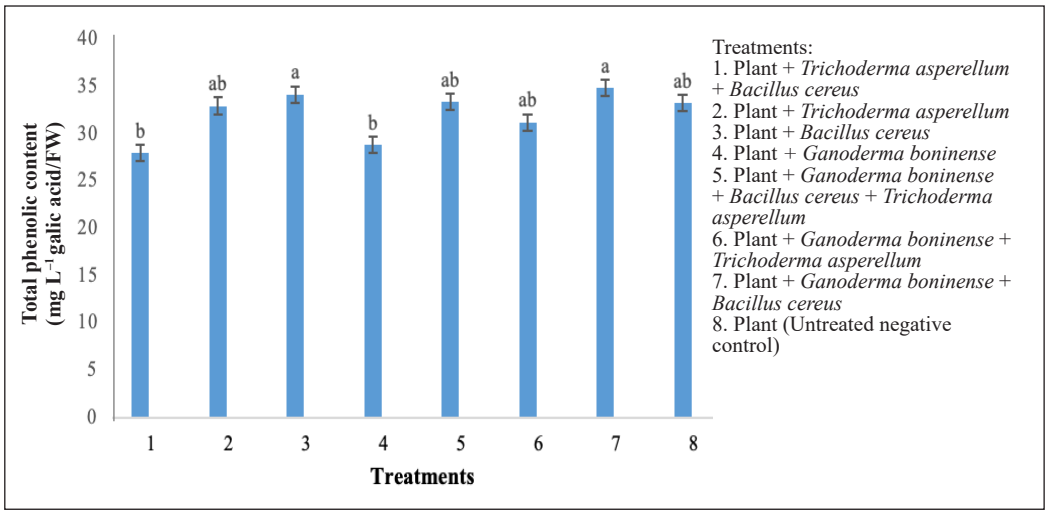

Figure 8. Total phenolic content of oil palm seedling roots following effects of treatments. Values are means of three replications, and differences between means are separated by Tukey's Studentized Range (HSD) Test at a 5% level of significance

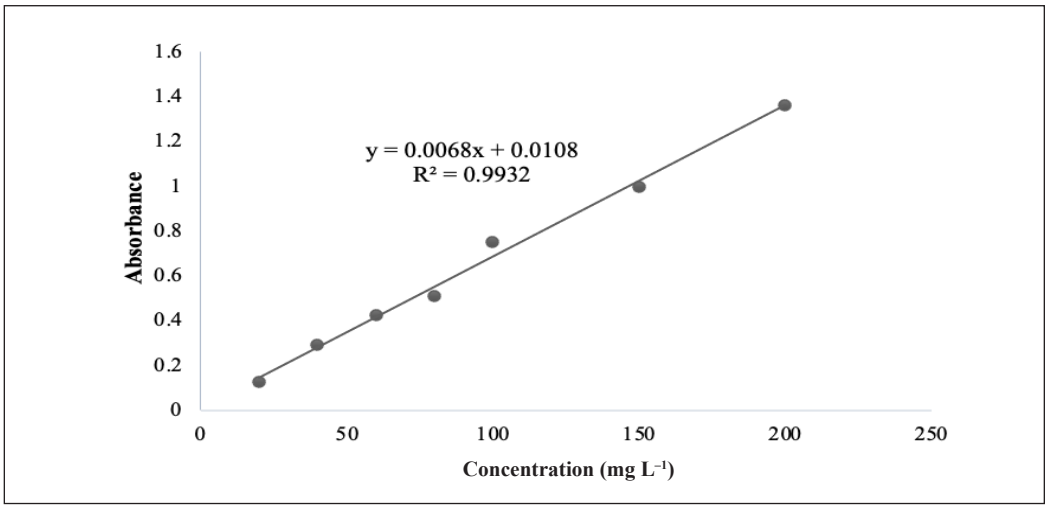

Figure 9. Standard curve of gallic acid with absorbance measured at 725 nm

Metabolite Profiling of Oil Palm Leave Extracts Treated with BCAs

For multivariate analysis, specifically partial least squares-discriminant analysis (PLS-DA), GC-MS findings were profiled and examined using MetaboAnalyst 4.0 software. Metabolites detected from all treatments were discriminated in the importance features analysis (Figure 10). Ten metabolites with the highest concentration were selected to narrow down the findings. Each variable's importance in the projection employed in a PLS model was estimated using the variable importance in projection (VIP) scores. In the presented model, a variable with a VIP score closer to one or higher can be regarded as essential (Gottfried, 2009). Based on VIP scores obtained, treatments BT and T produced three similar metabolites in relatively high concentrations, which were identified as phenol, 4-2-aminoethyl- (2.7-fold change), benzofuran, 2,3-dihydro- (2.4-fold change), and 9, 12, 15-octadecatrienoic acid (2.3-fold change). Treatments with BG and NC also had noticeable similarities in terms of metabolites profiled. They produced acetic acid, aminooxy-(2.7-fold-change), 2-furancarboxaldehyde, 5-hydroxymethyl-(2.3-fold change), and methyl 11, 14, 17-eicosatrienoate (1.9-fold change). The list of major metabolites detected in the leaves of treated seedlings and their potential bioactivity are presented in Table 5.

DISCUSSION

In recent years, studies on BCAs as an alternative method in plant protection have indicated positive results regardless of a single treatment or a combination of treatments (Hermosa et al., 2013; Nusaibah et al., 2017). The present study evaluated the ability to reduce BSR disease severity by *B. cereus* and *T. asperellum* in a greenhouse after positive outcomes were recorded *in vitro*.

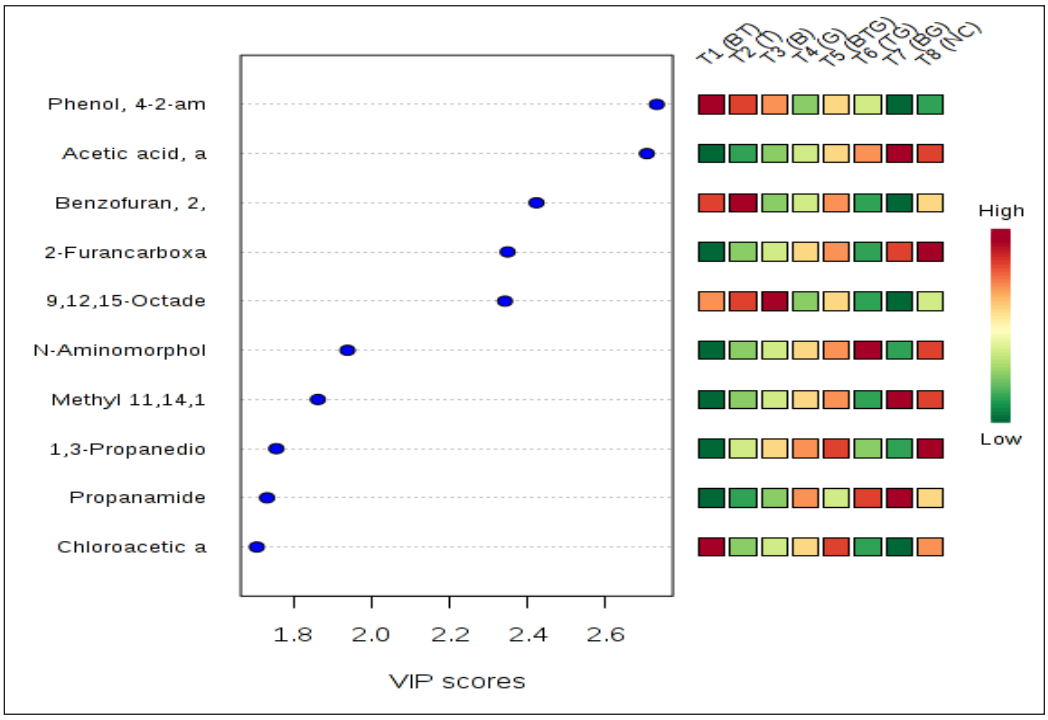

Figure 10. The importance features analysis of metabolites detected in the treatments. Coloured boxes on the right indicate relative concentrations of the corresponding metabolite in each group under study

The double-sealed plate method was used to determine the antifungal effects of MVOCs emitted by BCAs. Generally, MVOCs consist of various lower molecular weight lipophilic compounds that were naturally mixed. These compounds are by-products produced by microorganisms as part of their metabolism (Di Francesco et al., 2016; Mari et al., 2016). The study showed that *B. cereus* could produce MVOCs inhibiting *G. boninense* mycelial growth. The results were in line with Alexander et al. (2015), who observed that *Bacillus* spp. could suppress *G. boninense* growth *in vitro*.

In analysing disease suppression in the presence of both endophytes against BSR disease, the DPD technique (Nusaibah et al., 2017) was adopted. Since this technique is relatively new, SEM was used to determine disease establishment and efficacy of BCA treatment. The images observed through SEM effectively showed BSR disease establishment and successful BCA treatment on the roots of inoculated seedlings. Furthermore, the findings supported a study by Nusaibah et al. (2017), which concluded that the DPD technique could be considered an efficient technique in disease verification since *G. boninense* displayed vegetative growth with hyphae as the main mode of vegetative growth (Naher et al., 2014; Sundram et al., 2011).

BSR disease suppression was also assessed at a nursery trial. Both BCAs tested in the current study demonstrated efficacy in reducing BSR disease severity of oil

Table 5
Major metabolites detected in oil palm leaves and their potential bioactivities

Treatment	Metabolite	Synonyms	Activity / Reference
BT	Phenol, 4-2-aminoethyl-	Tyramin Tyramine Tyrosamine	Antimicrobial (Campos et al., 2014)
	Chloroacetic acid, 2,2-dimethylpropyl ester	Chloro-acetic acid neopentyl ester 2,2-dimethylpropyl 2-chloroacetate neopentyl 2-chloroacetate	
T	Benzofuran, 2,3-dihydro-	Coumaran Dihydrobenzofuran Dihydrocoumarone	Antifungal (Richardson et al., 2015), insecticidal activity (Huang et al., 2009)
B	9,12,15-Octadecatrienoic acid, Z, Z, Z-	α-linolenic acid Industrene 120	Antibacterial (Huang & Ebersole, 2010), antifungal (Walters et al., 2004)
TG	*N*-aminomorpholine	4-aminomorpholine 4-morpholinamine	
BG	Acetic acid, aminooxy-	Aminooxyacetate Aminooxyacetic acid Carboxymethoxyamine	Antifungal (Giorgio et al., 2015)
	Methyl 11,14,17-eicosatrienoate	Methyl 11,14,17-icosatrienoate Methyl icosa-11,14,17-trienoate	
	Propanamide	Propionamide Propylamide Propionic amide Propionimidic acid	Antimicrobial (Ölgen et al., 2008)
NC	2-furancarboxaldehyde, 5-hydroxymethyl-	2-furaldehyde, 5-(hydroxymethyl)- 5-oxymethylfurfurole 2-hydroxymethyl-5-furfural	Antifungal (Subramenium et al., 2018)
	1,3-propanediol, 2-ethyl-2-hydroxymethyl-	Ethriol Ethyltrimethylolmethane Etriol	

Treatments: BT = Plant + *Trichoderma asperellum* + *Bacillus cereus*; B = Plant + *Bacillus cereus*; BG = Plant + *Ganoderma boninense* + *Bacillus cereus*; T = Plant + *Trichoderma asperellum*; TG = Plant + *Ganoderma boninense* + *Trichoderma asperellum*; NC = Plant (Untreated negative control)

palm based on data recorded in DS and DR analysis. Single treatment of *T. asperellum*, with 50% DS and 57.2% DR, was more efficient in disease suppression compared to both single and combination treatments of *B. cereus*. Several studies have also indicated that *T. asperellum* could suppress several plant diseases (Bailey et al., 2008; Musa et al., 2018). According to Yang et al. (2011), *Trichoderma* spp. were shown to be effective soil inhabitants and root colonisers. However, the consortium treatment used in

this study still demonstrated better DR and lower DS to seedling roots compared to a single treatment of *B. cereus*.

Plant enzymes, such as PO and polyphenol oxidase (PPO), assist the formation of lignin and oxidative phenols that involve plant defence mechanisms against the pathogen (Avdiushko et al., 1993). The present study observed that seedlings treated with a single treatment of *B. cereus* recorded the highest PO enzyme activity. All treatments involving *B. cereus*, regardless of single application or combination, gave better PO enzyme activity than those without *B. cereus*. Parallel to the present study, Ramarathnam et al. (2011) observed that enzyme activity for strain *B. cereus* was higher than other treatments when inoculated with the pathogen. A study by Halfeld-Vieira et al. (2006) reported that leaf tissues exposed to *B. cereus* and inoculated with *Pseudomonas syringae* as a pathogen in tomatoes exhibited higher PO enzyme activities compared to other treatments. These studies confirmed that *B. cereus* efficiently induced PO enzyme activities.

Variables, such as the availability of sunlight and pathogen infection, have been reported to influence lignin content in plants (Xu et al., 2011). High levels of root lignin were a means of limiting fungal infection (Bennett et al., 2015). In their studies, lignin assays recorded that *Ganoderma*-infected seedlings treated with *B. cereus* (BG), seedlings treated with *T. asperellum* (T), and negative control (NC) yielded the highest lignin with no significant difference from each other. The data supported findings recorded on vegetative growth in the present study, where combination treatment and seedlings treated with *B. cereus* contributed higher root weight than the other treatments. *Ganoderma*-infected seedlings gave the lowest lignin accumulation. Adaskaveg et al. (1991) concluded that white rot fungi, such as *Ganoderma* spp., degraded wood components, especially lignin, making plants more susceptible to pathogens.

Epidemiological data by Hu and Kitts (2001) suggested that phenolic acid has strong inhibitory activity on oxidation induced by peroxyl radicals. According to Nikraftar et al. (2013), phenolic compounds in plants and the synthesis of those compounds in response to infection were linked to plant resistance. The present study also demonstrated that *Ganoderma*-infected seedlings treated with *B. cereus* yielded the highest TPC, followed by disease-free seedlings treated with *B. cereus*. These results matched those observed in an earlier study by Baydar et al. (2004), who confirmed that phenolics were the most important compound active against bacteria and explained the induction of TPC in seedlings treated with *B. cereus*. Endophytic *B. cereus* could have triggered the palms to produce TPC higher than the basal level as a defence tool against proteins synthesised by the bacterium. Seedlings treated with a combination of treatments contributed the lowest reading in TPC. It could be due to no virulent factors detected by the palm and endophytic *Trichoderma* spp. played a symbiotic role in plant-pathogen interaction.

Trichoderma asperellum had colonised the palm roots over *B. cereus*, as was seen in previous SEM observation.

Based on the GC-MS analysis of extracted oil palm leaves, phenol 4-2-aminoethyl- (syn: tyramine) was detected in treatment BT. Like any other biogenic amine, tyramines are mainly produced due to microbial enzymes or tissue bioactivity that causes certain amino acids to undergo an enzymatic decarboxylation process (Halász et al., 1994). Tyramine is the key enzyme that helps the production of hydroxycinnamic acid amides (HCAA) (Campos et al., 2014). HCAA strengthens a plant's cell walls, thus creating a barrier against microbial degradation (Hagel & Facchini, 2005). HCAA could also act directly as an antimicrobial agent. Newman et al. (2001) published that coumaroyltyramine (CT) and feruloyltyramine (FT) accumulated in pepper plants infected with the bacterial pathogen *Xanthomonas campestris* demonstrated antibacterial activity. FT extracted from *Allium* roots had been recorded to exhibit antifungal activity (Fattorusso et al., 1999). This study also detected acetic acid production in treatment with BG. Acetic acid (syn: aminooxyacetic acid, AOA) is known for its flavouring and preservative properties against microorganisms in various food products. It is also a natural compound throughout the biosphere (Alawlaqi & Alharbi, 2014). An *in vitro* study by Giorgio et al. (2015) observed that acetic acid could reduce mycelium growth arising from fungal plugs of *Sclerotinia sclerotiorum*.

The 2, 3-dihydrobenzofuran (DHB) skeleton is reportedly widespread in many natural products and biologically active molecules (Katritzky & Rees, 1984). Derivatives of benzofurans are sometimes discovered as metabolites of fungi, including endophytes of trees (Richardson et al., 2015). Several DHB products have been reported to have antioxidant, cytoprotective properties, and insecticidal activity (Z. Huang et al., 2009). In a study by Richardson et al. (2015), several benzofuran products were found to have antifungal properties and successfully reduced the growth of *Microbotryum violaceum*. Jang et al. (2006) also found that a dihydrobenzofuran derivative, awajanoran, exhibited antimicrobial activities against 5 strains.

Subramenium et al. (2018) studied 5-hydroxymethyl-2-furaldehyde (5HM2F) and found it to have antibiofilm and antivirulence activities against *Candida albicans*, pathogenic yeast. Based on the antifungal susceptibility testing results, the combination of antifungal and 5HM2F was more effective than a single antifungal treatment in reducing *C. albicans* biofilm. Chen et al. (2014) also discovered that 5HM2F and its derivatives extracted from the plant displayed antioxidant activity when tested in the laboratory. Furthermore, it was revealed that 5HM2F was naturally found in several plants (Lin et al., 2008), honey (Coco et al., 1996), and heat-treated food products (Almeida et al., 2009).

According to Burr and Burr (1930), 9, 12, 15-octadecatrienoic acid, Z, Z, Z- (syn: α-linolenic acid, ALA) is a polyunsaturated

fatty acid and is one of two human essential fatty acids. *In vitro* studies have shown that α-linolenic acid has been reported to have antibacterial activities against several oral pathogens such as *C. albicans*, *Streptococcus mutans*, and *Porphyromonas gingivalis* (C. B. Huang & Ebersole, 2010). In addition, Walters et al. (2004) reported that ALA demonstrated antifungal activities against mycelial growth of plant pathogenic fungi, namely, *Crinipellis pernicosa*, *Pyrenophora avanae*, *Pythium ultimum*, and *Rhizoctonia solani*. These findings suggested that ALA could play an important role in the search for alternative methods for controlling crucial plant pathogens.

CONCLUSION

The primary purpose of this study was to determine the contribution of BCA application on oil palm defence mechanism against *G. boninense* infection via greenhouse trial. Based on the results obtained, treatments positively impacted BSR disease suppression. PO enzyme activity, lignin content, TPC, and metabolites in BSR-diseased seedlings were affected in response to *B. cereus* and *T. asperellum* treatments. Treatments involving *B. cereus*, regardless of single application or combination, recorded enhanced PO activity. The present study showed that *B. cereus* induced the palms to produce more PO and TPC. Lignin assay showed that *Ganoderma*-infected seedlings treated with *B. cereus*, seedlings treated with *T. asperellum*, and negative control all produced the highest reading of lignin with no significant difference between them. The GC-MS analysis revealed that two metabolites with antifungal properties, phenol, and 4-2-aminoethyl, were the most abundant metabolite detected in the combination treatment, followed by acetic acid in the infected seedlings treated with *B. cereus*. Therefore, it could be concluded that treatments with a single or consortium of *T. asperellum* and *B. cereus* upregulated the oil palm defence mechanism against *G. boninense* infection. To further strengthen and support the outcome of this study, a field trial should be conducted using the currently designed treatments on palms still at the early stages of BSR infection.

ACKNOWLEDGEMENTS

Putra Grant-IPS via Research and Management Centre (RMC), Universiti Putra Malaysia (UPM) (Grant No: GP-IPS/2018/9667500).

REFERENCES

Adaskaveg, J. E., Blanchette, R. A., & Gilbertson, R. L. (1991). Decay of date palm wood by white-rot and brown-rot fungi. *Canadian Journal of Botany*, *69*(3), 615-629. https://doi.org/10.1139/b91-083

Alawlaqi, M. M., & Alharbi, A. A. (2014). Impact of acetic acid on controlling tomato fruit decay. *Life Science Journal*, *11*(3s), 114-119. https://doi.org/10.7537/marslsj1103s14.17

Alexander, A., Dayou, J., & Chong, K. P. (2015). Morphological changes of *Ganoderma boninense* mycelia after challenged by *Trichoderma* and *Bacillus*. In *AIP Conference Proceedings* (Vol. 1669, No. 1, p. 020075). AIP Publishing LLC. https://doi.org/10.1063/1.4919213

Almeida, J. R., Bertilsson, M., Gorwa-Grauslund, M. F., Gorsich, S., & Lidén, G. (2009). Metabolic effects of furaldehydes and impacts on biotechnological processes. *Applied Microbiology and Biotechnology*, *82*(4), 625-638. https://doi.org/10.1007/s00253-009-1875-1

Ashbolt, N. J., Amézquita, A., Backhaus, T., Borriello, P., Brandt, K. K., Collignon, P., Coors, A., Finley, R., Gaze, W. H., Heberer, T., Lawrence, J. R., Larsson, D. G. J., McEwen, S. A., Ryan, J. J., Schönfeld, J., Silley, P., Snape, J. R., Eede, C. V., & Topp, E. (2013). Human health risk assessment (HHRA) for environmental development and transfer of antibiotic resistance. *Environmental Health Perspectives*, *121*(9), 993-1001. https://doi.org/10.1289/ehp.1206316

Avdiushko, S. A., Ye, X. S., & Kuc, J. (1993). Detection of several enzymatic activities in leaf prints of cucumber plants. *Physiological and Molecular Plant Pathology*, *42*(6), 441-454. https://doi.org/10.1006/pmpp.1993.1033

Bailey, B. A., Bae, H., Strem, M. D., Crozier, J., Thomas, S. E., Samuels, G. J., Vinyard, B. T., & Holmes, K. A. (2008). Antibiosis, mycoparasitism, and colonization success for endophytic *Trichoderma* isolates with biological control potential in *Theobroma cacao*. *Biological Control*, *46*(1), 24-35. https://doi.org/10.1016/j.biocontrol.2008.01.003

Baydar, N. G., Özkan, G., & Sağdiç, O. (2004). Total phenolic contents and antibacterial activities of grape (*Vitis vinifera* L.) extracts. *Food Control*, *15*(5), 335-339. https://doi.org/10.1016/S0956-7135(03)00083-5

Bennett, A. E., Grussu, D., Kam, J., Caul, S., & Halpin, C. (2015). Plant lignin content altered by soil microbial community. *New Phytologist*, *206*(1), 166-174. https://doi.org/10.1111/nph.13171

Bivi, M. R., Noor Farhana, M. S., Khairulmazmi, A., & Idris, A. (2010). Control of *Ganoderma boninense*: A causal agent of basal stem rot disease in oil palm with endophyte bacteria *in vitro*. *International Journal of Agriculture and Biology*, *12*(6), 833-839.

Breton, F., Hasan, Y., Hariadi, S. S., Lubis, Z., & De Franqueville, H. (2006). Characterization of parameters for the development of an early screening test for basal stem rot tolerance in oil palm progenies. *Journal of Oil Palm Research*, (Special Issue – April), 24-36.

Bruce, R. J., & West, C. A. (1989). Elicitation of lignin biosynthesis and isoperoxidase activity by pectic fragments in suspension cultures of castor bean. *Plant Physiology*, *91*(3), 889-897. https://doi.org/10.1104/pp.91.3.889

Burr, G. O., & Burr, M. M. (1930). On the nature and role of the fatty acids essential in nutrition. *Journal of Biological Chemistry*, *86*(2), 587-621. https://doi.org/10.1016/S0021-9258(20)78929-5

Campos, L., Lisón, P., López-Gresa, M. P., Rodrigo, I., Zacarés, L., Conejero, V., & Bellés, J. M. (2014). Transgenic tomato plants overexpressing tyramine *N*-hydroxy cinnamoyl transferase exhibit elevated hydroxycinnamic acid amide levels and enhanced resistance to *Pseudomonas syringae*. *International Society for Molecular Plant-Microbe Interactions*, *27*(10), 1159-1169. https://doi.org/10.1094/MPMI-04-14-0104-R

Chen, P. X., Tang, Y., Zhang, B., Liu, R., Marcone, M. F., Li, X., & Tsao, R. (2014). 5-hydroxymethyl-2-furfural and derivatives formed during acid hydrolysis of conjugated and bound phenolics in plant foods and the effects on phenolic content and antioxidant capacity. *Journal of Agricultural and Food Chemistry*, *62*(20), 4754-4761. https://doi.org/10.1021/jf500518r

Coco, F. L., Valentini, C., Novelli, V., & Ceccon, L. (1996). High-performance liquid chromatographic determination of 2-furaldehyde and 5-hydroxymethyl-2-furaldehyde in honey. *Journal of Chromatography A*, *749*(1-2), 95-102. https://doi.org/10.1016/0021-9673(96)00392-5

Dean, R. A., & Kuć, J. (1987). Rapid lignification in response to wounding and infection as a mechanism for induced systemic protection in cucumber. *Physiological and Molecular Plant Pathology*, *31*(1), 69-81. https://doi.org/10.1016/0885-5765(87)90007-5

Di Francesco, A., Martini, C., & Mari, M. (2016). Biological control of postharvest diseases by microbial antagonists: How many mechanisms of action?. *European Journal of Plant Pathology*, *145*, 711-717. https://doi.org/10.1007/s10658-016-0867-0

Doster, M. A., & Bostock, R. M. (1988). Effects of low temperature on resistance of almond trees to *Phytophthora* pruning wound cankers in relation to lignin and suberin formation in wounded bark tissue. *Phytopathology*, *78*(4), 478-483. https://doi.org/10.1094/Phyto-78-478

Fattorusso, E., Lanzotti, V., & Taglialatela-Scafati, O. (1999). Antifungal *N*-feruloyl amides from roots of two *Allium species*. *Plant Biosystem*, *133*(2), 199-203. https://doi.org/10.1080/11263509909381549

Fiehn, O. (2002). Metabolomics – The link between genotypes and phenotypes. *Plant Molecular Biology*, *48*, 155-171. https://doi.org/10.1023/A:1013713905833

Giorgio, A., De Stradis, A., Lo Cantore, P., & Iacobellis, N. S. (2015). Biocide effects of volatile organic compounds produced by potential biocontrol rhizobacteria on *Sclerotinia sclerotiorum*. *Frontiers in Microbiology*, *6*, 1056. https://doi.org/10.3389/fmicb.2015.01056

Gomez, K. A., & Gomez, A. A. (1984). *Statistical procedures for agricultural research*. John Wiley & Sons.

Gotor-Vila, A., Teixidó, N., Di Francesco, A., Usall, J., Ugolini, L., Torres, R., & Mari, M. (2017). Antifungal effect of volatile organic compounds produced by *Bacillus amyloliquefaciens* CPA-8 against fruit pathogen decays of cherry. *Food Microbiology*, *64*, 219-225. https://doi.org/10.1016/j.fm.2017.01.006

Gottfried, J. L., De Lucia Jr, F. C., & Miziolek, A. W. (2009). Discrimination of explosive residues on organic and inorganic substrates using laser-induced breakdown spectroscopy. *Journal of Analytical Atomic Spectrometry*, *24*(3), 288-296. https://doi.org/10.1039/B818481J

Hagel, J. M., & Facchini, P. J. (2005). Elevated tyrosine decarboxylase and tyramine hydroxy cinnamoyl transferase levels increase wound-induced tyramine-derived hydroxycinnamic acid amide accumulation in transgenic tobacco leaves. *Planta*, *221*(6), 904-914. https://doi.org/10.1007/s00425-005-1484-x

Halász, A., Baráth, A., Simon-Sarkadi, L., & Holzapfel, W. (1994). Biogenic amines and their production by microorganisms in food. *Trends in Food Science and Technology*, *5*(2), 42-49. https://doi.org/10.1016/0924-2244(94)90070-1

Halfeld-Vieira, B. D. A., Vieira Júnior, J. R., Romeiro, R. D. S., Silva, H. S. A., & Baracat-Pereira, M. C. (2006). Induction of systemic resistance in tomato by the autochthonous phylloplane resident *Bacillus cereus*. *Pesquisa Agropecuaria Brasileira*, *41*(8), 1247-1252. https://doi.org/10.1590/S0100-204X2006000800006

Hermosa, R., Rubio, M. B., Cardoza, R. E., Nicolás, C., Monte, E., & Gutiérrez, S. (2013). The contribution of *Trichoderma* to balancing the costs of plant growth and defense. *International Microbiology*, *16*(2), 69-80. https://doi.org/10.2436/20.1501.01.181

Hu, C., & Kitts, D. D. (2001). Evaluation of antioxidant activity of epigallocatechin gallate in biphasic model systems *in vitro*. *Molecular and Cellular Biochemistry*, *218*, 147-155. https://doi.org/10.1023/A:1007220928446

Huang, C. B., & Ebersole, J. L. (2010). A novel bioactivity of omega-3 polyunsaturated fatty acids and their ester derivatives. *Molecular*

Oral Microbiology, *25*(1), 75-80. https://doi.org/10.1111/j.2041-1014.2009.00553.x

Huang, Z., Cui, Q., Xiong, L., Wang, Z., Wang, K., Zhao, Q., Bi, F., & Wang, Q. (2009). Synthesis and insecticidal activities and SAR studies of novel benzoheterocyclic diacylhydrazine derivatives. *Journal of Agricultural and Food Chemistry*, *57*(6), 2447-2456. https://doi.org/10.1021/jf8036193

Idris, A. S., Kushairi, D., Ariffin, D., & Basri, M. W. (2006). *Technique for inoculation of oil palm germinated seeds with* Ganoderma. http://palmoilis.mpob.gov.my/TOTV3/wp-content/uploads/2020/02/TT-314.pdf

Izzati, M. Z. N. A., & Abdullah, F. (2008). Disease suppression in *Ganoderma*-infected oil palm seedlings treated with *Trichoderma harzianum*. *Plant Protection Science*, *44*(3), 101-107. https://doi.org/10.17221/23/2008-PPS

Jang, J. H., Kanoh, K., Adachi, K., & Shizuri, Y. (2006). New dihydrobenzofuran derivative, awajanoran, from marine-derived *Acremonium* sp. AWA16-1. *The Journal of Antibiotics*, *59*, 428-431. https://doi.org/10.1038/ja.2006.60

Katritzky, A. R., & Rees, C. W. (Eds.). (1984). *Comprehensive heterocyclic chemistry*. Pergamon Press.

Kokkinakis, D. M., & Brooks, J. L. (1979). Hydrogen peroxide-mediated oxidation of indole-3-acetic acid by tomato peroxidase and molecular oxygen. *Plant Physiology*, *64*(2), 220-223. https://doi.org/10.1104/pp.64.2.220

Lin, A. S., Qian, K., Usami, Y., Lin, L., Itokawa, H., Hsu, C., Morris-Natschke, S. L., & Lee, K. H. (2008). 5-hydroxymethyl-2-furfural, a clinical trials agent for sickle cell anemia, and its mono/di-glucosides from classically processed steamed Rehmanniae Radix. *Journal of Natural Medicines*, *62*, 164-167. https://doi.org/10.1007/s11418-007-0206-z

Małolepsza, U., & Różalska, S. (2005). Nitric oxide and hydrogen peroxide in tomato resistance: Nitric oxide modulates hydrogen peroxide level in *o*-hydroxyethylorutin-induced resistance to *Botrytis cinerea* in tomato. *Plant Physiology and Biochemistry*, *43*(6), 623-635. https://doi.org/10.1016/j.plaphy.2005.04.002

Mari, M., Bautista-Baños, S., & Sivakumar, D. (2016). Decay control in the postharvest system: Role of microbial and plant volatile organic compounds. *Postharvest Biology and Technology*, *122*, 70-81. https://doi.org/10.1016/j.postharvbio.2016.04.014

Musa, H., Nusaibah, S. A., & Khairulmazmi, A. (2018). Assessment on *Trichoderma* spp. mixture as a potential biocontrol agent of *Ganoderma boninense* infected oil palm seedlings. *Journal of Oil Palm Research*, *30*(3), 403-415. https://doi.org/10.21894/jopr.2018.0035

Naher, L., Yusuf, U. K., Tan, S. G., Siddiquee, S., & Islam, M. R. (2014). *In vitro* and *in vivo* biocontrol performance of *Trichoderma harzianum* Rifai on *Ganoderma boninense* Pat. related to pathogenicity on oil palm (*Elaeis guineensis* Jacq.). *Journal of Pure and Applied Microbiology*, *8*(2), 973-978.

Newman, M. A., von Roepenack-Lahaye, E., Parr, A., Daniels, M. J., & Dow, J. M. (2001). Induction of hydroxycinnamoyl-tyramine conjugates in pepper by *Xanthomonas campestris*, a plant defense response activated by *hrp* gene-dependent and *hrp* gene-independent mechanisms. *International Society for Molecular Plant-Microbe Interactions*, *14*(6), 785-792. https://doi.org/10.1094/MPMI.2001.14.6.785

Nikraftar, F., Taheri, P., Rastegar, M. F., & Tarighi, S. (2013). Tomato partial resistance to *Rhizoctonia solani* involves antioxidative defence mechanisms. *Physiological and Molecular Plant Pathology*, *81*, 74-83. https://doi.org/10.1016/j.pmpp.2012.11.004

Nusaibah, S. A., Akmar, A. S. N., Idris, A. S., Sariah, M., & Pauzi, Z. M. (2016). Involvement of metabolites in early defence mechanism of oil palm (*Elaeis guineensis* Jacq.) against *Ganoderma* disease. *Plant Physiology and Biochemistry*, *109*, 156-165. https://doi.org/10.1016/j.plaphy.2016.09.014

Nusaibah, S. A., Saad, G., & Hun, T. G. (2017). Antagonistic efficacy of *Trichoderma harzianum* and *Bacillus cereus* against *Ganoderma* disease of oil palm via dip, place and drench (DPD) artificial inoculation technique. *International Journal of Agriculture and Biology*, *19*(2), 299-306. https://doi.org/10.17957/IJAB/15.0280

Ramarathnam, R., Fernando, W. D., & de Kievit, T. (2011). The role of antibiosis and induced systemic resistance, mediated by strains of *Pseudomonas chlororaphis*, *Bacillus cereus* and *B. amyloliquefaciens*, in controlling blackleg disease of canola. *BioControl*, *56*, 225-235. https://doi.org/10.1007/s10526-010-9324-8

Richardson, S. N., Nsiama, T. K., Walker, A. K., McMullin, D. R., & Miller, J. D. (2015). Antimicrobial dihydrobenzofurans and xanthenes from a foliar endophyte of *Pinus strobus*. *Phytochemistry*, *117*, 436-443. https://doi.org/10.1016/j.phytochem.2015.07.009

Samatha, T., Shyamsundarachary, R., Srinivas, P., & Swamy, N. R. (2012). Quantification of total phenolic and total flavonoid contents in extracts of *Oroxylum indicum* L. Kurz. *Asian Journal of Pharmaceutical and Clinical Research*, *5*(4), 177-179.

Sariah, M. C., Coo, C. W., Zakaria, H., & Norihan, M. S. (2005). Quantification and characterization of *Trichoderma* spp. from different ecosystems. *Mycopathologia*, *159*, 113-117. https://doi.org/10.1007/s11046-004-4432-6

Shaner, G., & Finney, R. E. (1977). The effect of nitrogen fertilization on the expression of slow-mildewing resistance in Knox wheat. *Phytopathology*, *67*(8), 1051-1056. https://doi.org/10.1094/Phyto-67-1051

Singleton, V. L., Orthofer, R., & Lamuela-Raventós, R. M. (1999). Analysis of total phenols and other oxidation substrates and antioxidants by means of folin-ciocalteu reagent. In L. Packer (Ed.), *Methods in enzymology* (Vol. 299, pp. 152-178). Academic press. https://doi.org/10.1016/S0076-6879(99)99017-1

Subramenium, G. A., Swetha, T. K., Iyer, P. M., Balamurugan, K., & Pandian, S. K. (2018). 5-hydroxymethyl-2-furaldehyde from marine bacterium *Bacillus subtilis* inhibits biofilm and virulence of *Candida albicans*. *Microbiological Research*, *207,* 19-32. https://doi.org/10.1016/j.micres.2017.11.002

Sundram, S., Sariah, M., Idris, A. S., & Radziah, O. (2011). Symbiotic interaction of endophytic bacteria with arbuscular mycorrhizal fungi and its antagonistic effect on *Ganoderma boninense*. *Journal Microbiology*, *49*(4), 551–557. https://doi.org/10.1007/s12275-011-0489-3

Surekha, C. H., Neelapu, N. R. R., Kamala, G., Prasad, B. S., & Ganesh, P. S. (2013). Efficacy of *Trichoderma viride* to induce disease resistance and antioxidant responses in legume *Vigna mungo* infested by *Fusarium oxysporum* and *Alternaria alternata*. *International Journal of Agricultural Science Research*, *3*(2), 285-294.

Syafiq, T. H. T. M., Nusaibah, S. A., & Rafii, M. Y. (2021). Effectiveness of bioinoculants *Bacillus cereus* and *Trichoderma asperellum* as oil palm seedlings growth promoters. *Pertanika Journal of Tropical Agricultural Science*, *44*(1), 157-170. https://doi.org/10.47836/pjtas.44.1.09

Tarig, S. A., Sariah, M., Sijam, K., & Marziah, M. (1998). Enhancements of growth and disease suppression by PGPF isolate, *Fusarium oxysporum* (Foc4), in banana seedlings. In Z. Wahab (Ed.), *Proceedings of the First National*

Banana Seminar (pp. 261-268). Malaysian Agricultural Information Portal.

Treutter, D. (2006). Significance of flavonoids in plant resistance: A review. *Environmental Chemistry Letters*, *4*, 147-157. https://doi.org/10.1007/s10311-006-0068-8

Usall, J., Teixidó, N., Fons, E. & Viñas, I. (2000). Biological control of blue mould on apple by a strain of *Candida sake* under several controlled atmosphere conditions. *International Journal of Food Microbiology*, *58*(1-2), 83-92. https://doi.org/10.1016/S0168-1605(00)00285-3

Walters, D., Raynor, L., Mitchell, A., Walker, R., & Walker, K. (2004). Antifungal activities of four fatty acids against plant pathogenic fungi. *Mycopathologia*, *157*(1),87-90. https://doi.org/10.1023/B:MYCO.0000012222.68156.2c

Weisskopf, L. (2013). The potential of bacterial volatiles for crop protection against phytopathogenic fungi. In A. Méndez-Vilas (Ed.), *Microbial pathogens and strategies for combating them: Science, technology and education* (pp. 1352-1363). Formatex.

Xu, L., Zhu, L., Tu, L., Liu, L., Yuan, D., Jin, L., & Zhang, X. (2011). Lignin metabolism has a central role in the resistance of cotton to the wilt fungus *Verticillium dahliae* as revealed by RNA-Seq-dependent transcriptional analysis and histochemistry. *Journal of Experimental Botany*, *62*(15), 5607-5621. https://doi.org/10.1093/jxb/err245

Yang, C. A., Cheng, C. H., Lo, C. T., Liu, S. Y., Lee, J. W., & Peng, K. C. (2011). A novel L-amino acid oxidase from *Trichoderma harzianum* ETS 323 associated with antagonism of *Rhizoctonia solani*. *Journal of Agricultural and Food Chemistry*, *59*(9), 4519-4526. https://doi.org/10.1021/jf104603w

Zaiton, S., Sariah, M., & Ahmad, Z. A. M. (2008). Effect of endophytic bacteria on growth and suppression of *Ganoderma* infection in oil palm. *International Journal of Agricultural and Biology*, *10*(2), 127-132.

Pertanika J. Trop. Agric. Sci. 46 (1): 153 - 176 (2023)

PERTANIKA JOURNALS

TROPICAL AGRICULTURAL SCIENCE

Journal homepage: http://www.pertanika.upm.edu.my/

Review Article

Replacement of Fishmeal in the Diet of African Catfish (*Clarias gariepinus*): A Systematic Review and Meta-Analysis

Abdulwakil Olawale Saba[1,9], Kafayat Adetoun Fakoya[1], Isa Olalekan Elegbede[2], Zakariyyah Olayiwola Amoo[3], Rasheed Olatunji Moruf[4], Musa Adamu Ibrahim[5], Taiwo Hassan Akere[6], Abdulrahman Muhammad Dadile[7], Morenike Adunni Adewolu[1], Akinloye Emmanuel Ojewole[8] and Mohammad Noor Azmai Amal[9,10]*

[1]*Department of Fisheries, Faculty of Science, Lagos State University, 102101 Ojo, Lagos, Nigeria*
[2]*Brandenburg University of Technology, 03042 Cottbus, Germany*
[3]*School of Agriculture, Lagos State University, 106101 Epe Campus, Lagos, Nigeria*
[4]*Department of Fisheries and Aquaculture, Faculty of Agriculture, Bayero University, 53011 Kano, Nigeria*
[5]*Department of Biological Sciences, University of Maiduguri, 600230 Maiduguri, Nigeria*
[6]*School of Geography, Earth and Environmental Science, University of Birmingham, Edgbaston Birmingham B15 2TT, United Kingdom*
[7]*Department of Aquaculture, Faculty of Agriculture, Universiti Putra Malaysia, 43400 Serdang, Selangor, Malaysia*
[8]*Department of Environmental Sciences, Southern Illinois University Edwardsville, IL 62026, USA*
[9]*Department of Biology, Faculty of Science, Universiti Putra Malaysia, UPM Serdang,43400, Selangor, Malaysia*
[10]*Aquatic Animal Health and Therapeutics Laboratory, Institute of Bioscience, Universiti Putra Malaysia, 43400 Serdang, Selangor, Malaysia*

ABSTRACT

Fishmeal is widely accepted as a protein source in fish feed formulation, making it a highly demanded ingredient, and this has probably contributed to its increased cost. Cheaper protein sources of plant and animal origin have been tested as potential replacements for fishmeal to reduce feed costs in fish production and guarantee a suitable nutrient supply for adequate growth. Therefore, this review assessed the effect of replacing fishmeal in the diet of African catfish, *Clarias gariepinus* based on empirical findings. Using a systematic literature review protocol, an extensive search of five databases resulted in the final inclusion of 32 articles for appraisal

ARTICLE INFO

Article history:
Received: 19 August 2022
Accepted: 13 September 2022
Published: 03 February 2023

DOI: https://doi.org/10.47836/pjtas.46.1.09

E-mail addresses:
sabaola@gmail.com (Abdulwakil Olawale Saba)
kafayat.fakoya@lasu.edu.ng (Kafayat Adetoun Fakoya)
isaelegbede@gmail.com (Isa Olalekan Elegbede)
azocowboyz@yahoo.com (Zakariyyah Olayiwola Amoo)
tunjimoruf@gmail.com (Rasheed Olatunji Moruf)
moosaad8@gmail.com (Musa Adamu Ibrahim)
taiwoakere@yahoo.com (Taiwo Hassan Akere)
ydadile02@gmail.com (Abdulrahman Muhammad Dadile)
madewolu@yahoo.com (Morenike Adunni Adewolu)
emmanuelakinloye@gmail.com (Akinloye Emmanuel Ojewole)
mnamal@upm.edu.my (Mohammad Noor Azmai Amal)
* Corresponding author

ISSN: 1511-3701
e-ISSN: 2231-8542

and meta-analysis. Fishmeal replacements were at levels ranging from 7–100%, while fish survival rate and feed conversion ratio recorded non-significant effects of fishmeal replacement ($p > 0.05$). However, final weight, weight gain, specific growth rate, and protein efficiency ratio revealed a significant effect of fishmeal replacement ($p < 0.05$) in the diet of African catfish. Our overall analyses suggest that feed ingredients such as microalgae and insects/worms are potentially perfect replacements for fishmeal.

Keywords: African catfish, alternative protein, aquaculture, fish growth, food security, nutrient utilization

INTRODUCTION

Over the years, aquaculture has increasingly contributed to the overall production of food fish, making it an essential practice that can help reduce hunger and improve food security in line with the United Nations' Sustainable Development Goals. A significant proportion of the costs involved in farmed fish production is related to feeds and feeding because of the high cost of protein-rich ingredients like fishmeal (Ansari et al., 2021; Tilami et al., 2020; Wan et al., 2019). Like fish species, feed ingredients differ in their nutritional characteristics and possible inclusion and replacement levels (Adeyemi et al., 2020). Therefore, the protein content, amino acid profile, and digestibility of the feed ingredients will influence their inclusion for replacement, making it crucial to ensure that the ingredients used for feed formulation possess the required nutrients for adequate growth and utilization by the fish species.

Being a source of protein, which is highly-priced, fishmeal is regarded as an essential ingredient in the diet of carnivorous and omnivorous aquatic organisms, mainly fishes (Alhazzaa et al., 2019; Olsen & Hasan, 2012). Consequently, efforts have been made to replace fishmeal partially or wholly with alternative protein sources in the diet of fish species. These efforts have sought to achieve similar or better output like fishmeal at a reduced cost (Adewolu et al., 2010; Ojewole et al., 2022; Raji et al., 2018; Taufek et al., 2016a).

Scientists must develop new strategies to provide the required amounts of high-quality protein to meet the growing demand (Boland et al., 2013). More so, a potentially viable feed component to replace fishmeal in aquafeeds must be at a reasonable cost, readily available, and simple to handle, transport, store, and use in feed production (Musyoka et al., 2019). Furthermore, high protein content, good amino acid profile, low-fat content, and excellent nutrient digestibility are some of the required characteristics (Luthada-Raswiswi et al., 2021).

Protein sources of plant and animal origin have been used in different fish species to replace fishmeal. In some cases, the growth, nutrient utilization, and other information such as enzyme activity and hematological parameters have been compared for fish (Huda et al., 2020; Kim et al., 2021; Lawal et al., 2017; Pongpet et al., 2016; Tippayadara et al., 2021; Wang et al., 2018; Zheng et al., 2012) and

shellfish (Moniruzzaman et al., 2020). Aside from fishmeal, several alternative feed ingredients, such as those of animal protein origin, insects, land animal by-products, fisheries by-products, worms, and plant-based protein sources, including algae such as *Chlorella* and spirulina, have been evaluated as feed ingredients in both fresh and marine water fish production (Ansari et al., 2021; Raji et al., 2018, 2019; Saleh, 2020).

Fishmeal has been totally or partially replaced in species' diets, such as tilapia *Oreochromis niloticus* (Abarra et al., 2017; Arunlertaree & Moolthongnoi, 2008; Djissou et al., 2019; Yousif et al., 2019), Atlantic salmon *Salmo salar* (Belghit et al., 2019), rose snapper *Lutjanus guttatus* (Hernández et al., 2014), snakehead *Channa argus* (Yu et al., 2015), and Russian sturgeon *Acipenser gueldenstaedtii* (Gong et al., 2016), among other species. Novriadi et al. (2017) performed a meta-analysis of fishmeal replacement with soybean meal. However, the African catfish *Clarias gariepinus* was not captured in the analysis. Luthada-Raswiswi et al. (2021) systematically reviewed and meta-analyzed the substitution of fishmeal by animal protein sources in aquaculture diets with valuable information about an array of fish species in whose diets fishmeal was replaced. Unfortunately, the study was not structured to assess individual fish species in-depth.

African catfish is an economically important fish species extensively cultured in various parts of the world. Especially in the tropics, due to its ability to accept a wide variety of feed, breed in captivity, grow fast, tolerate high stocking density, and resist common diseases (Abdel-Warith et al., 2019; Musa et al., 2021; Tahir et al., 2021). Fishes belonging to the genus *Clarias* are among the significant fish species produced worldwide, where approximately 2.3% of the world's catfish farming has contributed to total fish production (Food and Agriculture Organization of the United Nations [FAO], 2020). Efforts geared towards the further increase in its production through a reduction in the cost of feeding, its sustainability, and efficiency by using cheap but highly nutritious and sustainable ingredients are, therefore, outstanding contributions to food security around the globe. However, despite previous efforts, information regarding the performance of African catfish fed with diets where fishmeal was replaced partially or entirely remains scattered in the literature, making it challenging to identify the alternative feed ingredients with the best potential for growth and nutrient utilization of this species. Therefore, this study aims to systematically review existing studies regarding the replacement of fishmeal in the diet of African catfish. Besides, a meta-analysis to compare the recommended replacement levels of diets against the control was also conducted.

More specific information on these alternative protein sources may reduce feeding costs, increase growth and nutrient utilization parameters, and, therefore, add to the profits of fish farmers. Besides, there is a potential contribution of such information to

increased production of African catfish and fish food from the aquaculture sector due to efficient growth and nutrient utilization by the fish species. The successful replacement of fish meals in the diet of African catfish with cheaper yet nutritive alternatives can boost its production. This inclusion will improve aquaculture's contribution to food and nutrition security across the globe.

MATERIALS AND METHODS

Database Search and Screening

A search of databases, such as Scopus (https://www.scopus.com/), ScienceDirect (https://www.sciencedirect.com/), ProQuest (https://www.proquest.com/), and Wiley Online Library (https://onlinelibrary.wiley.com/), was conducted in addition to a search of the Google Scholar (https://scholar.google.com/) database. The following terms or phrases were used: "fishmeal replacement in "*Clarias gariepinus*", "fishmeal alternative in *Clarias gariepinus*", and "fishmeal substitution in *Clarias gariepinus*". The search was not limited to any time duration. From the databases, results produced for each search were exported as comma-separated values (CSV), research information systems (RIS), or text (txt) files to Rayyan QCRI (Qatar Computing Research Institute) software (Disner et al., 2021; Ouzzani et al., 2016). Rayyan is a free online tool for academics working on systematic review methodology and meta-analysis projects. Rayyan is one of several software products developed by QCRI, a creative and imaginative body of the Qatar Foundation for Education, Science, and Community Development, akin to the United States Department of Education in many aspects. Users may contribute citations and full-text articles as part of a single review, create several review projects, and even collaborate on publicly available projects using Rayyan (Johnson & Philips, 2018).

Duplicates were removed, after which articles were included or excluded based on title and abstract screening using predetermined criteria. Next, the first 500 publications from the Google Scholar search were screened for inclusion (Algera et al., 2020). Finally, the included articles were all downloaded for full-text screening. Studies included in the review were those published between the years 2010 and 2021 and reported at least three of the following: survival rate, growth parameters: final weight (FW), mean weight gain (MWG), and specific growth rate (SGR); nutrient utilization parameters: feed conversion ratio (FCR) and protein efficiency ratio (PER). Studies in which there were either no replicates, did not have a design directly related to the replacement of fishmeal, or did not provide clear information regarding the percentage replacement of fishmeal were excluded. For continuous data analysis, those with zero standard deviation (SD) values are not estimable and were excluded from the study. At the same time, data with the same percentage survival for the control and experimental groups are also non-estimable and, therefore, excluded.

Statistical Analysis

Microsoft Office Excel 2016 (Microsoft Inc., USA) was used to compute descriptive information about the included studies, while meta-analyses were conducted using Review Manager (RevMan) version 5.3 software for narrative synthesis. The primary outcome of this study was the performance of fish fed a fish meal-replaced diet in terms of growth and nutrient utilization. The odds ratio (OR) with 95% confidence intervals (CIs) for dichotomous data and standardized mean difference (SMD) with 95% CIs for continuous data were used to determine the relationship between fishmeal replacement and survival level. The forest plot was used to show pooled estimates. When the outcomes were not accessible, missing data were entirely random. In some cases, one study reported replacing fishmeal with more than one alternative ingredient, and these were treated individually, although with the same information for the control.

RESULTS

Database Search and Screening

A search of five databases yielded 2,562 individual records, with 2,021 articles remaining after duplicates were removed (Figure 1). After title and abstract screening, 112 articles were left for full-text screening. Seventy-four (74) publications were deleted from full-text screening for various reasons, including non-reportage of pertinent data, while six were excluded during data extraction. There were no more publications for data extraction after the full-text screening of grey literature sources from online searches.

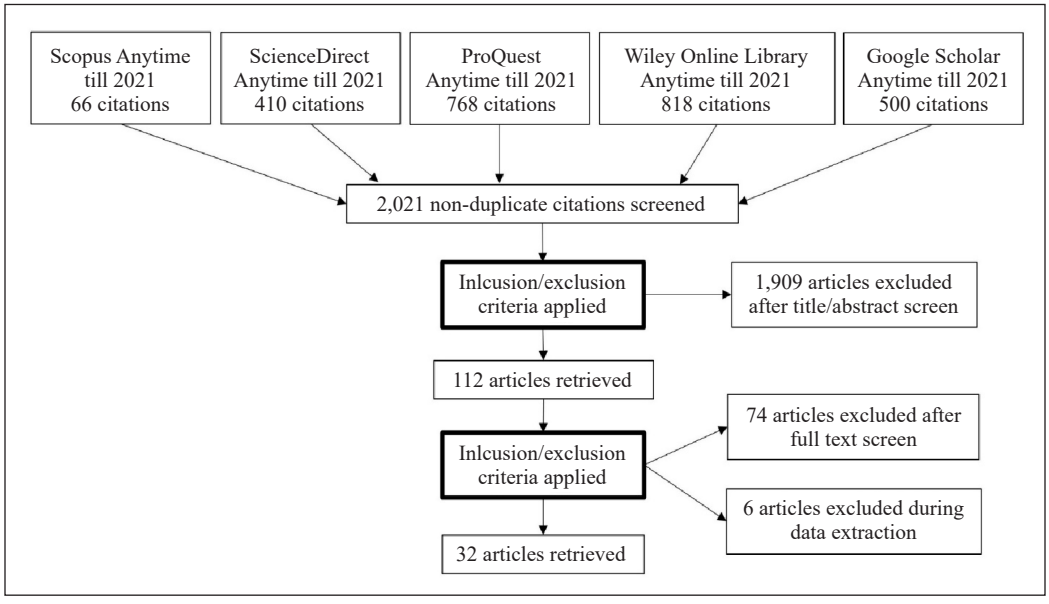

Figure 1. Flowchart of the database searched, screened, and included studies prepared using the PRISMA Flow Diagram Generator by Toronto Health Economics and Technology Assessment Collaboration (http://prisma.thetacollaborative.ca/)

Feed Ingredients and Recommended Replacement Levels

The included articles identified three main categories (animal products, insects/worms, and plant products) of protein sources used to replace fish meals in the diet of African catfish. The "animal products" being the first category include blood meal, poultry by-products, fish viscera, and shrimp heads. Various insects, including palm grub, palm weevil, black soldier fly, grasshopper, cricket meal, and worms, such as mopane and earthworm, were grouped under the second category, "insets/worms". Finally, the third category, or "plant products", consisted of spirulina, *Chlorella*, velvet bean, corn gluten, moringa leaf, marine seaweed, Bambara nut, and sweet lupin meal. The recommended replacement levels were 10–100% for insects/worms (with the highest recommended levels recorded for earthworm and maggot meal mix and cricket meal), while plant products had recommended replacement levels ranging from 10–75% (with the highest recommended levels recorded for spirulina and *Chlorella*). Generally, the feeding trial experiments ranged from 35 to 86 days, mostly feeding two times a day at 2.5–10% of fish body weight (Table 1).

Table 1
Summary of studies that assessed fishmeal replacement in the diet of African catfish using animal products, insects/worms, and algae/plants

	RRL (%)	D (days)	FF (times/ day)	FP (%BW)	NF	NR	Study
Animal products							
Cow blood meal	7.0	51	2	5	15	3	Ogunji et al. (2020)
Donkey blood meal	7.0	51	3	5	15	3	Ogunji et al. (2020)
Fish visceral meal	30.0	56	2	5	15	3	Jimoh et al. (2021)
Poultry offal meal	50.0	84	NS	5	10	3	Mamoon et al. (2018)
Blood and rumen blend	25.0	70	2	4	10	2	Lawal et al. (2017)
Blood meal and bovine rumen blend	50.0	86	2	5	12	2	Adewole et al. (2014)
Poultry offal meal	30.0	70	3	5	10	3	Falaye et al. (2011)
Snail offal meal	50.0	70	2	5	20	3	Okanlawon and Oladipupo (2010)
A mix of chicken feather and maggot	50.0	56	2	3	10	3	Adewolu et al. (2010)
Shrimp head meal	20.0	84	2	4	20	3	Nwanna et al. (2004)
Insect/worms							
Palm weevil meal	100.0	70	2	5	20	3	Agbanimu et al. (2020)
Black soldier fly meal	50.0	35	3	6	25	3	Huda et al. (2020)
Black soldier fly meal	50.0	42	2	AL	30	3	Adeoye et al. (2020)
Cricket meal	100.0	56	2	5-10	15	3	Taufek et al. (2018)

Table 1 *(continue)*

	RRL (%)	D (days)	FF (times/ day)	FP (%BW)	NF	NR	Study
Earthworm and maggot meal mix	100.0	42	3	5	50	3	Arnauld et al. (2016)
Earthworm meal	70.0	84	2	5	20	3	Monebi and Ugwumba (2016)
Cricket meal	75.0	49	2	AL	10	3	Taufek et al. (2016)
Variegated grasshopper meal	25.0	56	2	5	10	3	Alegbeleye et al. (2012)
Mopame worm meal	10.0	51	2	AL	100	3	Rapatsa and Moyo (2019)
Algae/plants							
Spirulina	68.5	56	2	4	10	3	Raji et al. (2019)
Chlorella	69.4	56	3	4	10	3	Raji et al. (2019)
Sweet lupin	50.0	63	3	5	10	3	Yalew et al. (2019)
Spirulina	75.0	84	2	2	15	3	Raji et al. (2018)
Chlorella	75.0	84	2	2	15	3	Raji et al. (2018)
Fenugreek seed meal	18.0	60	2	AL	30	3	Sheikhlar et al. (2018)
Corn gluten meal	50.0	70	2	NS	10	3	Adebayo and Obe (2017)
Moringa	15.0	56	2	5	10	2	Idowu et al. (2017)
Moringa leaf meal	10.0	56	2	5	10	3	Ezekiel et al. (2016)
Marine seaweed	10.0	70	2	3	15	3	Al-Asgah et al. (2016)
Bambara nut meal	75.0	56	NS	3	20	2	Orire et al. (2015)
Velvet bean	10.0	70	2	5	50	2	Aderolu et al. (2009)
Processed flamboyant meal	40.0	70	2	5	20	2	Adesina and Agbatan (2021)

Note. RRL (%) = Recommended replacement level in percentage; D = Duration of days; FF = Feeding frequency in times/day; FP = Feeding pattern in % body weight; NF = Number of fish per tank; NR = Number of replicates; AL = *Ad libitum*; NS = Not state

Survival, Growth, and Nutrient Utilization Parameters

Of the 32 included studies, 14, 28, 26, 31, 26, and 24 cases reported the survival rate, final weight, mean weight gain, specific growth rate, feed conversion ratio, and protein efficiency ratio, respectively, for both control and experimental groups of African catfish. The percentage survival of African catfish from the studies assessed recorded a mean of 89.40±5.30%. This value ranges from 77.78% to 100.0% for the control and 94.02±6.87%, ranging from 77.78% to 100.0% for the recommended replacement group. The final weights recorded a mean of 57.70 ± 93.59 g, ranging from 3.43 to 361.89 g for the control group, and 64.29 ± 97.97 g, ranging from 5.22 to 374.08 g for the recommended replacement group. Weight gain was at a mean of 60.85 ± 111.07 g, ranging from 1.31 to 413.82 g for the control group, and 82.43 ± 174.37 g, ranging from 1.55 to 819.05 g for the recommended replacement group. SGR recorded a mean of 2.06 ± 1.13 g, ranging from 0.06 to 5.48 g for the control group,

and 2.20 ± 1.17 g, ranging from 0.46 to 4.97 g for the recommended replacement group. FCR recorded a mean of 1.67 ± 0.80, ranging from 0.50 to 3.62 for the control group. At the same time, the mean FCR for the recommended replacement group was 1.54 ± 0.80 ranging from 0.50 to 4.18. Finally, a mean of 2.66 ± 4.74 was recorded for PER, ranging from 0.17 to 24.27 for the control group. Likewise, the recommended replacement group had a mean of 2.85 ± 4.70, ranging from 0.32 to 24.16.

Meta-Analysis

Analysis of the data gleaned from included studies was generally conducted for survival rate (1,448 samples), final weight (2,768 samples), weight gain (2,578 samples), SGR (3,548 samples), FCR (3,108 samples), and PER (3,108 samples). The outcome of the dichotomous analysis for survival rate revealed a non-significant effect of fishmeal replacement (OR = 1.28, 95% CI 0.86 to 1.89; $p > 0.05$; $I^2 = 0\%$) (Figure 2). Analyses of continuous data revealed that final weight (SMD = 5.43; 95% CI -2.72 to -1.45; $p < 0.001$; $I^2 = 99\%$) (Figure 3), weight gain (SMD = 5.59; 95% CI 4.08 to 7.10; $p < 0.001$; $I^2 = 99\%$) (Figure 4), SGR (SMD = 1.59; 95% CI 0.54 to 2.63; $p = 0.003$; $I^2 = 99\%$) (Figure 5), and PER (SMD = 2.54; 95% CI 1.68 to 3.40; $p < 0.001$; $I^2 = 99\%$) (Figure 6) revealed the significant effect of fishmeal replacement, while FCR (SMD = -0.24; 95% CI -0.21 to 0.81; $p = 0.61$; $I^2 = 99\%$) (Figure 7) establishing a non-significant overall effect of fish replacement in the diet of African catfish.

Analyses of continuous data for animal products revealed significant effects for the final weight (SMD = 4.86; 95% CI 1.73 to 7.99; $p = 0.002$; $I^2 = 99\%$) and weight gain (SMD = 3.07; 95% CI 1.07 to 5.07; $p = 0.003$; $I^2 = 99\%$), and non-significant effect for SGR (SMD = -0.14; 95% CI -1.64 to 1.36; $p = 0.86$; $I^2 = 99\%$) under the growth parameters. For the nutrient utilization parameters, a significant effect was recorded

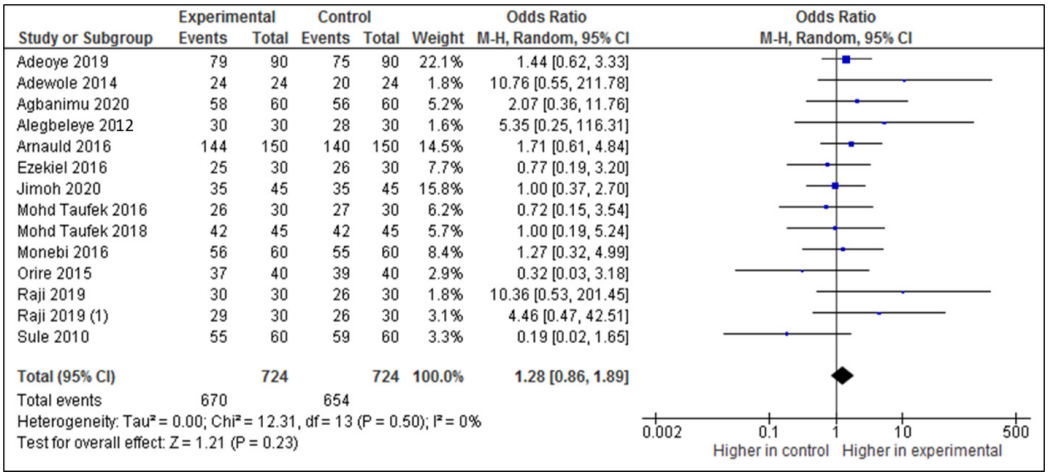

Figure 2. Forest plot of survival levels from different studies with recommended fishmeal replacement levels

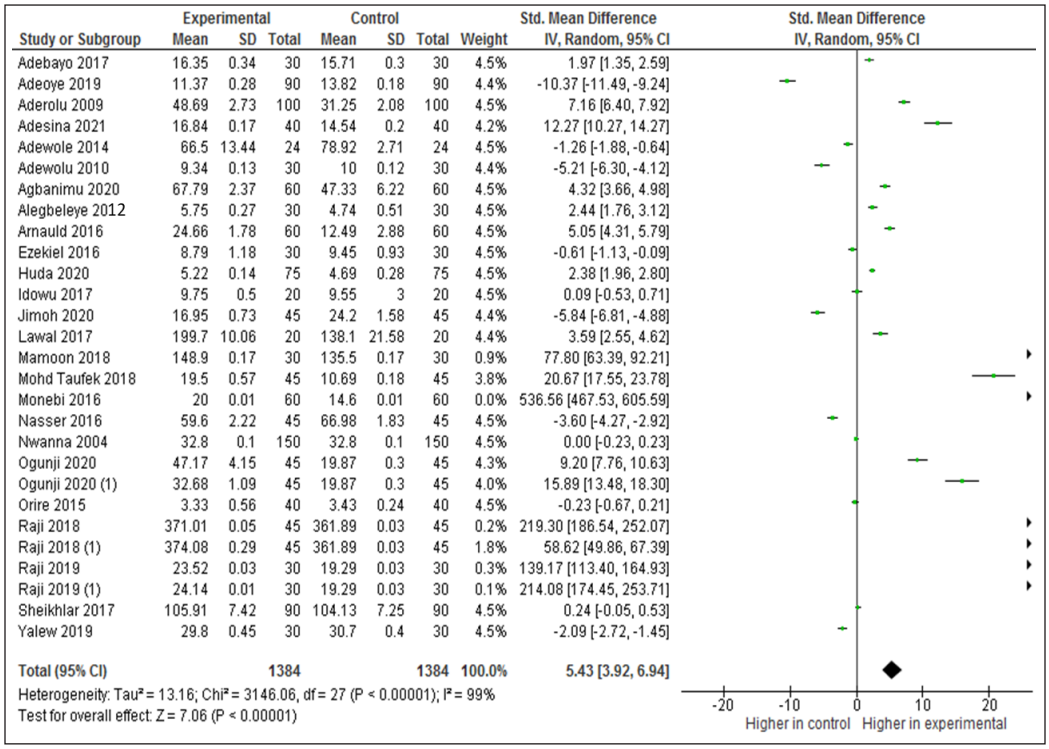

Figure 3. Forest plot of final weight from different studies with recommended fishmeal replacement levels

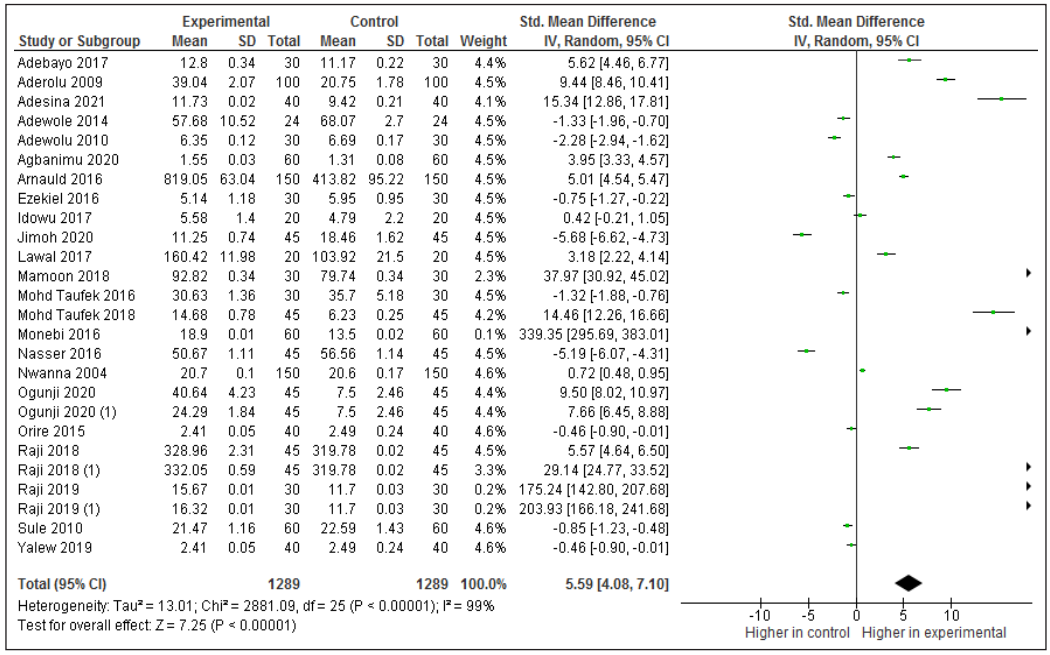

Figure 4. Forest plot showing the effect size for weight gain from different studies with recommended fishmeal replacement levels

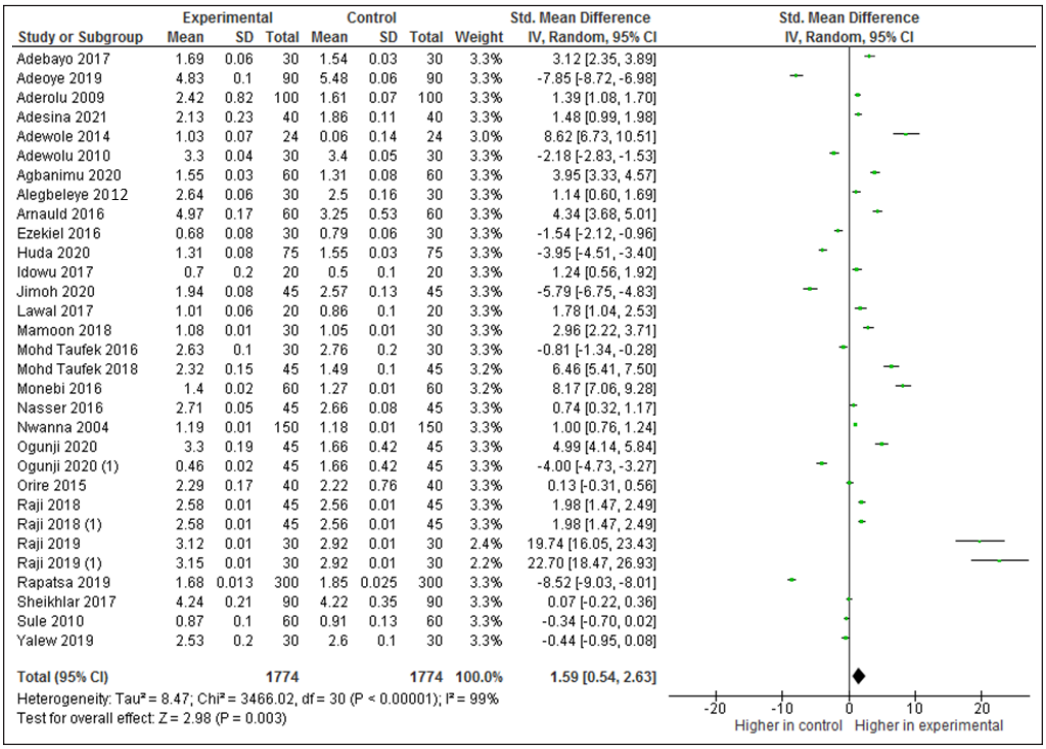

Figure 5. Forest plot of specific growth rates from different studies with recommended fishmeal replacement levels

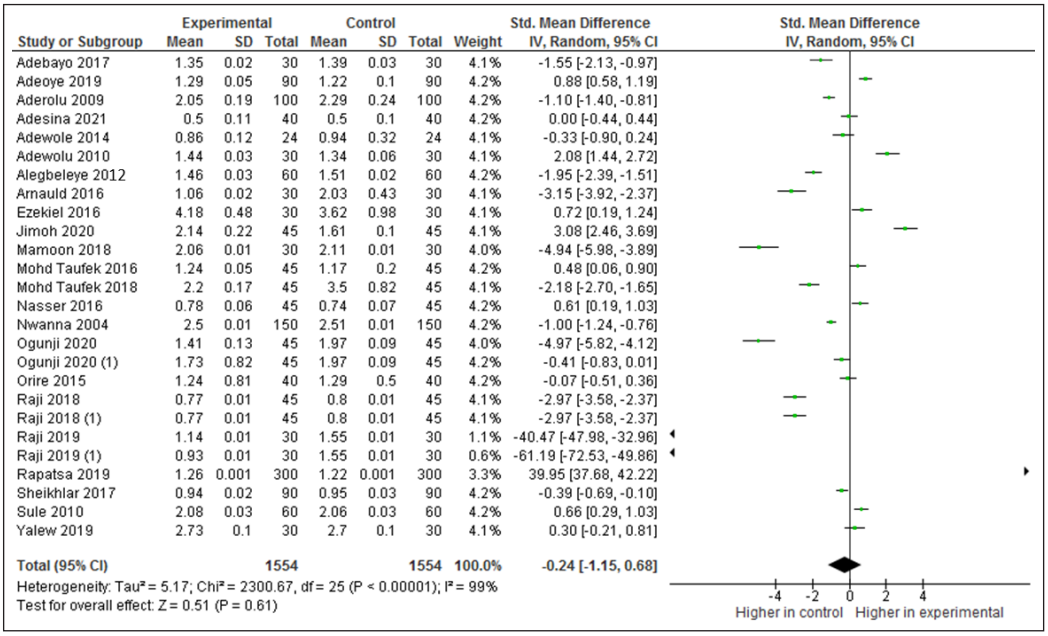

Figure 6. Forest plot of feed conversion ratio from different studies with recommended fishmeal replacement levels

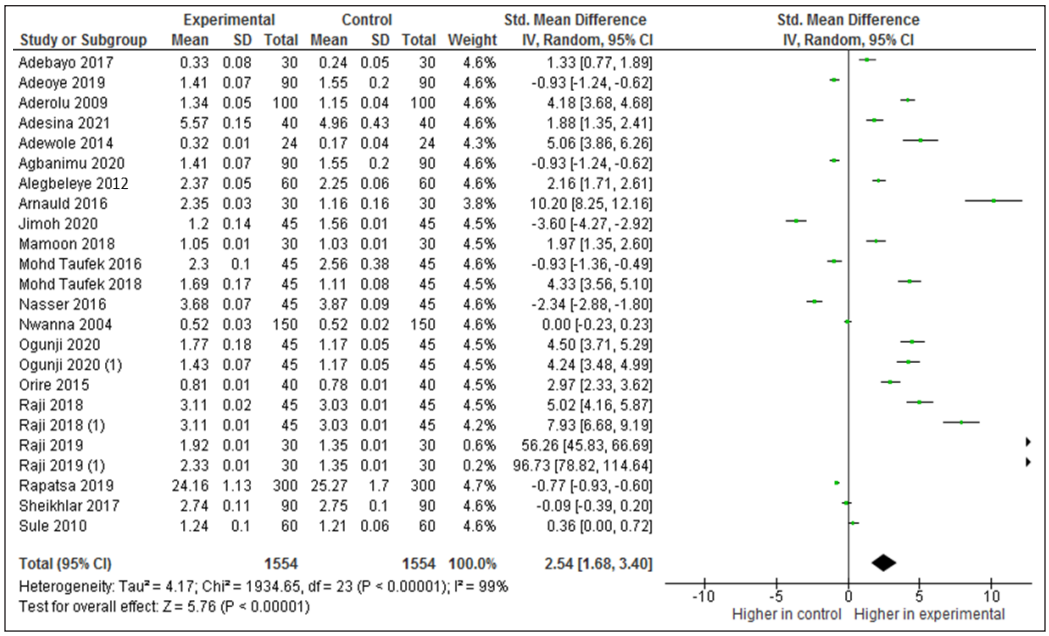

Figure 7. Forest plot of protein efficiency ratio from different studies with recommended fishmeal replacement level

for PER (SMD = 1.75; 95% CI 0.12 to 3.39; $p = 0.04$; $I^2 = 99\%$), while a non-significant effect was recorded for FCR (SMD = -0.69; 95% CI -2.00 to 0.63; $p = 0.31$; $I^2 = 98\%$) (Supplementary materials 1–2).

Analyses of continuous data for insects/worms revealed significant effects for the final weight (SMD = 5.74; 95% CI 1.60 to 9.88; $p = 0.007$; $I^2 = 99\%$) and weight gain (SMD = 9.23; 95% CI 4.45 to 14.00; $p < 0.001$; $I^2 = 99\%$), and non-significant effect for SGR (SMD = 0.32; 95% CI -9.03 to -8.01; $p = 0.86$; $I^2 = 100\%$) under the growth parameters. For the nutrient utilization parameters, a significant effect was recorded for PER (SMD = 1.50; 95% CI 0.32 to 2.67; $p = 0.01$; $I^2 = 99\%$), while a non-significant effect was recorded for FCR (SMD = -1.16; 95% CI -2.67 to 0.35; $p = 0.13$; $I^2 = 98\%$) (Supplementary materials 3–4).

Analyses of continuous data for algae/plants revealed significant effects for the final weight (SMD = 6.14; 95% CI 4.11 to 8.16; $p < 0.001$; $I^2 = 99\%$), weight gain (SMD = 7.42; 95% CI 4.69 to 10.15; $p < 0.001$; $I^2 = 99\%$), and specific growth rate (SMD = 2.16; 95% CI 1.30 to 3.03; $p < 0.001$; $I^2 = 97\%$). For the nutrient utilization parameters, a significant effect was recorded for FCR (SMD = -1.69; 95% CI -2.64 to 0.76; $p < 0.001$; $I^2 = 97\%$) and PER (SMD = 5.22; 95% CI 3.19 to 7.25; $p < 0.13$; $I^2 = 99\%$) (Supplementary materials 5-6).

DISCUSSION

To assess the potential of partially or wholly replacing fishmeal in the diet of an important aquaculture species, the African catfish, this review systematically selected and analyzed

previous research publications based on predetermined criteria. The focus on African catfish was to provide specific information regarding the performance of various alternative protein sources. Consequently, this review considered not only a higher number of studies but individuals of African catfish for the analyses of growth and nutrient utilization parameters compared to Luthada-Raswiswi et al. (2021). The latter reviewed the replacement of fish meal in various fish species.

The highest recommended fishmeal replacement level for animal products in the diet of African catfish did not exceed 50% for a blood meal and bovine rumen blend. The lowest was as low as 7% for bloodmeal, as opposed to insects/worms and plant products, which replaced as much as 75 to 100% of fishmeal at recommended levels. The limitation of using purely blood-based ingredients in the diet of African catfish is established due to the decline experienced with an increase in blood meal inclusion (Ogunji et al., 2020). Like its level of inclusion in the diet of African catfish, blood meal had been reportedly included at 6% to 10% in the diets of grouper *Epinephelus coioides* (Martins & Guzman, 1994), juvenile trout *Oncorhynchus mykiss* (Martins & Guzman, 1994), and gilthead sea bream *Sparus aurata* (Luzier et al., 1995).

Apart from Bambara nutmeal, spirulina, and *Chlorella* recorded the highest recommended replacement level in the algae/plant category and are the only algal taxa reported in the included studies. The performance and potential of algal species in the sustainable production of fish, especially African catfish, is revealed, making further research on the characteristics of this group of organisms quintessential. Microalgae have a high amount of protein with digestible amino acid profiles. Thus, they are equivalent to those found in other foods, such as antioxidants, sulfated polysaccharides, polyunsaturated fatty acids, β-carotene, and sterols (Raji et al., 2020; Reyes-Becerril et al., 2013). Sarker et al. (2020) reported the possibility of eliminating fish meal from the diet of Nile tilapia by replacing it with a microalgae blend. As a result, better protein quality, growth, and nutrient utilization parameters were reported. Besides, using microalgae could also help guarantee adherence to sustainability standards as it would reduce the dependence on wild fish, which are facing depletion due to overexploitation (Shah et al., 2018). Microalgae have also been noted to possess nutrient stability over a long period. For example, frozen microalgae-based aquafeed maintained stability for about nine months (Camacho-Rodríguez et al., 2018).

Ido et al. (2019) reported an improvement in growth performance and disease resistance of red sea bream *Pagrus major* when fishmeal was replaced with a yellow mealworm in its diet. However, according to Tilami et al. (2020), despite the potential for replacement of fish meal, some insects, such as house cricket *Acheta domesticus* and super worm *Zophobas morio*, in the diet of perch *Perca fluviatilis* negatively influenced its growth parameters.

The inclusion of insects may not give similar positive results in the diet of all fish species, indicating the need for more species-specific consideration in terms of insect inclusion. Insects are rich in amino acids, lipids, vitamins, and minerals (Pinotti et al., 2019). Also, their reproduction requires no arable land, energy, or water making their ecological footprint insignificant (Oonincx & de Boer, 2012). They have more natural reproduction with a faster development rate and convert low-quality organic materials into high-value proteins (Sánchez-Muros et al., 2014). Antifungal and antibacterial activities have also been reported for many insects, thereby improving the shelf-life of feeds containing them (Henry et al., 2015). However, the use of insects is not without limitations, such as low concentrations of sulfur-containing amino acids and varying nutritional value, depending on the species, stage of development, and substrate used to feed the insect.

Aqua feeds that result from the mixture of feed ingredients of different types may present a superior performance in the growth and nutrient utilization of African catfish and other fresh and marine water fish species. For example, the highest replacement level recorded in this review was achieved with a diet that stemmed from a mixture of two different animal products. This situation points to the possibility of achieving higher performance with blended animal products. More so, replacing fishmeal with insects/worms in the diet of African catfish appears to present the highest possible recommended replacement level. Again, one of the ingredients that recorded the highest possible recommended replacement level was blended earthworm and maggot meal, corroborating the possibility of recording better results when ingredients are blended or mixed to replace fishmeal as protein sources in fish species (Djissou et al., 2016).

Except for FCR, the experimental groups' growth and nutrient utilization parameters were higher at the recommended fish meal replacement levels. From this result, it could be deduced that fishmeal replacement at prescribed levels is undoubtedly more beneficial for African catfish growth and nutrient utilization. This situation is in line with the findings of Luthada-Raswiswi et al. (2021). They reported statistically significant differences in growth and nutrient utilization parameters based on a review of various fish species when the fish meal in their feeds was replaced. This review provides important information on the value of replacing fishmeal with other nutritive yet cheaper protein sources.

Meta-analysis corroborated the descriptive information and depicted the significant association between the recommended replacement levels versus growth and nutrient utilization parameters. Aside from survival level and FCR, all other parameters generally recorded a significant effect of fishmeal replacement. Again, it could be deduced that fishmeal replacement at prescribed levels is undoubtedly more beneficial for African catfish growth and nutrient utilization. As opposed to other categories, all the growth and nutrient

utilization parameters in the algae/plant category revealed a significant effect of fish meal replacement. Feed ingredients of plant origin, especially the microalgae followed by insects/worms, need to be researched in greater detail for African catfish and many other aquaculture species of commercial importance.

Generally, the level of heterogeneity in the included studies was high. The size, inclusion levels, and recommended protein levels were reported, which are the likely reasons our meta-analysis indicated heterogeneity in studies. Despite the heterogeneity observed, these animal protein sources have positively affected FCR, SGR, final weight, and survival of different fish species of varying size groups.

CONCLUSION

Based on their significant general effects on African catfish's growth and nutrient utilization parameters at higher recommended inclusion levels, feed ingredients of plant origin, especially the microalgae followed by insects/worms, are highly promising. Therefore, they need to be researched in greater detail for African catfish and many other aquaculture species of commercial importance. In addition, mixing ingredients at tested proportions to replace fishmeal may produce a better outcome. However, compared to single components usage for replacement, there seems to be a shortage of research in this regard. Therefore, systematic reviews and meta-analyses of studies regarding replacing fish meals with other protein sources should be approached more specifically on a species basis. This analysis will provide greater insights and guidance toward increasing fish production at reduced costs and contributing to global food security.

ACKNOWLEDGEMENTS

The authors acknowledge all anonymous reviewers for their suggestions towards improving the manuscript, and the Ministry of Higher Education, Malaysia for providing the Higher Institution Centre of Excellence (HiCoE) grant with vot. no.: 6369100.

REFERENCES

Abarra, S. T., Velasquez, S. F., Guzman, K. D. D., Felipe, J. L. F., Tayamen, M. M., & Ragaza, J. A. (2017). Replacement of fishmeal with processed meal from knife fish *Chitala ornata* in diets of juvenile Nile tilapia *Oreochromis niloticus*. *Aquaculture Reports*, *5*, 76-83. https://doi.org/10.1016/j.aqrep.2017.01.001

Abdel-Warith, A. A., Younis, E. M., Al-Asgah, N. A., & Mahboob, S. (2019). Effect of replacing fish meal by full fat soybean meal on growth performance, feed utilization and gastrointestinal enzymes in diets for African catfish *Clarias gariepinus*. *Brazilian Journal of Biology*, *80*(3), 535-543. https://doi.org/10.1590/1519-6984.214763

Adebayo, I. A., & Obe, B. W. (2017). Utilization of corn gluten meal in the diets of *Clarias gariepinus* juveniles. *International Journal of Fisheries and Aquatic Research*, *2*(4), 19-22. https://doi.org/10.3153/jfscom.2012008

Adeoye, A. A., Akegbejo-Samsons, Y., Fawole, F. J., & Davies, S. J. (2020). Preliminary assessment of black soldier fly (*Hermetia illucens*) larval meal in the diet of African catfish (*Clarias gariepinus*): Impact on growth, body index, and

hematological parameters. *Journal of the World Aquaculture Society*, *51*(4), 1024-1033. https://doi.org/10.1111/jwas.12691

Aderolu, A. Z., & Akpabio, V. M. (2009). Growth and economic performance of *Clarias gariepinus* juveniles fed diets containing velvet bean, *Mucuna pruriens*, seed meal. *African Journal of Aquatic Science*, *34*(2), 131-135. https://doi.org/10.2989/ajas.2009.34.2.3.890

Adesina, S. A., & Agbatan, O. D. (2021). Growth response and feed utilization in *Clarias gariepinus* fingerlings fed diets supplemented with processed flamboyant (*Delonix regia*) leaf meal. *Agro-Science*, *20*(1), 38-45. https://doi.org/10.4314/as.v20i1.7

Adewole, H. A., & Olaleye, V. F. (2014). Growth performance in *Clarias gariepinus* Burchell fingerlings fed blood meal–bovine rumen digesta blend diets. *Ife Journal of Science*, *16*(3), 495-503.

Adewolu, M. A., Ikenweiwe, N. B., & Mulero, S. M. (2010). Evaluation of an animal protein mixture as a replacement for fishmeal in practical diets for fingerlings of *Clarias gariepinus* (Burchell, 1822). *Israel Journal of Aquaculture-Bamidgeh*, *62*(4), 237-244.

Adeyemi, A. D., Kayode, A. P. P., Chabi, I. B., Odouaro, O. B. O., Nout, M. J., & Linnemann, A. R. (2020). Screening local feed ingredients of Benin, West Africa, for fish feed formulation. *Aquaculture Reports*, *17*, 100386. https://doi.org/10.1016/j.aqrep.2020.100386

Agbanimu, A. B., & Adeparusi, E. O. (2020). Growth performance and nutrient utilization of African catfish (*Clarias gariepinus*) juveniles fed varying inclusions of defatted African palm weevils (*Rhynchophorus phoenicis*) meal. *Aquaculture Studies*, *20*(2), 73-79. https://doi.org/10.4194/2618-6381-v20_2_01

Al-Asgah, N. A., Younis, E.-S. M., Abdel-Warith, A.-W. A., & Shamlol, F. S. (2016). Evaluation of red seaweed *Gracilaria arcuata* as dietary ingredient in African catfish, *Clarias gariepinus*. *Saudi Journal of Biological Sciences*, *23*(2), 205-210. https://doi.org/10.1016/j.sjbs.2015.11.006

Alegbeleye, W. O., Obasa, S. O., Olude, O. O., Otubu, K., & Jimoh, W. (2012). Preliminary evaluation of the nutritive value of the variegated grasshopper (*Zonocerus variegatus* L.) for African catfish *Clarias gariepinus* (Burchell. 1822) fingerlings. *Aquaculture Research*, *43*(3), 412-420. https://doi.org/10.1111/j.1365-2109.2011.02844.x

Algera, D. A., Rytwinski, T., Taylor, J. J., Bennett, J. R., Smokorowski, K. E., Harrison, P. M., Clarke. K. D., Enders, E. C., Power, M., Bevelhimer, M. S., & Cooke, S. J. (2020). What are the relative risks of mortality and injury for fish during downstream passage at hydroelectric dams in temperate regions? A systematic review. *Environmental Evidence*, *9*, 3. https://doi.org/10.1186/s13750-020-0184-0

Alhazzaa, R., Nichols, P. D., & Carter, C. G. (2019). Sustainable alternatives to dietary fish oil in tropical fish aquaculture. *Reviews in Aquaculture*, *11*(4), 1195-1218. https://doi.org/10.1111/raq.12287

Ansari, F. A., Guldhe, A., Gupta, S. K., Rawat, I., & Bux, F. (2021). Improving the feasibility of aquaculture feed by using microalgae. *Environmental Science and Pollution Research*, *28*(32), 43234-43257. https://doi.org/10.1007/s11356-021-14989-x

Arnauld. S. M. D, Adjahouinou, D. C., Koshio, S., & Fiogbe, E. D. (2016). Complete replacement of fish meal by other animal protein sources on growth performance of *Clarias gariepinus* fingerlings. *International Aquatic Research*, *8*(4), 333-341. https://doi.org/10.1007/s40071-016-0146-x

Arunlertaree, C., & Moolthongnoi, C. (2008). The use of fermented feather meal for

replacement fish meal in the diet of *Oreochromis niloticus*. *Environment and Natural Resources Journal*, *6*(1), 13-24.

Belghit, I., Liland, N. S., Gjesdal, P., Biancarosa, I., Menchetti, E., Li, Y., Waagbø, R., Krogdahl, Å., & Lock, E. J. (2019). Black soldier fly larvae meal can replace fish meal in diets of sea-water phase Atlantic salmon (*Salmo salar*). *Aquaculture*, *503*, 609-619. https://doi.org/10.1016/j.aquaculture.2018.12.032

Boland, M. J., Rae, A. N., Vereijken, J. M., Meuwissen, M. P., Fischer, A. R., van Boekel, M. A., Rutherfurd, S. M., Grippen, H., Moughan, P. J., & Hendriks, W. H. (2013). The future supply of animal-derived protein for human consumption. *Trends in Food Science and Technology*, *29*(1), 62-73. https://doi.org/10.1016/j.tifs.2012.07.002

Camacho-Rodríguez, J., Macías-Sánchez, M. D., Cerón-García, M. C., Alarcón, F. J., & Molina-Grima, E. (2018). Microalgae as a potential ingredient for partial fish meal replacement in aquafeeds: Nutrient stability under different storage conditions. *Journal of Applied Phycology*, *30*(2), 1049-1059. https://doi.org/10.1007/s10811-017-1281-5

Disner, G. R., Falcão, M. A. P., Andrade-Barros, A. I., Leite dos Santos, N. V., Soares, A. B. S., Marcolino-Souza, M., Gomes, K. S., & Lopes-Ferreira, M. (2021). The toxic effects of glyphosate, chlorpyrifos, abamectin, and 2, 4-D on animal models: A systematic review of Brazilian studies. *Integrated Environmental Assessment and Management*, *17*(3), 507-520. https://doi.org/10.1002/ieam.4353

Djissou, A. S. M., Adjahouinou, D. C., Koshio, S., & Fiogbe, E. D. (2016). Complete replacement of fish meal by other animal protein sources on growth performance of *Clarias gariepinus* fingerlings. *International Aquatic Research*, *8*(4), 333-341. https://doi.org/10.1007/s40071-016-0146-x

Djissou, A. S. M., Tossavi, C. E., Odjo, I. N., Koshio, S., & Fiogbe, E. D. (2019). Use of *Moringa oleifera* leaves and maggots as protein sources in complete replacement for fish meal in Nile tilapia (*Oreochromis niloticus*) diets. *Turkish Journal of Fisheries and Aquatic Sciences*, *20*(3), 177-183. https://doi.org/10.21077/ijf.2017.64.1.55317-05

Ezekiel, A. O., Fidelis, A. B., & Udeh G. N. (2016). Effect of partial replacement of fishmeal with *Moringa oleifera* leaf meal on the haematology, carcass composition and growth performance of *Clarias gariepinus* (Burchell 1822) fingerlings. *International Journal of Fisheries and Aquatic Studies*, *4*(4), 307-311.

Falaye, A. E., Omoike, A., Ajani, E. K., & Kolawole, O. T. (2011). Replacement of fishmeal using poultry offal meal in practical feeds for fry of the African catfish (*Clarias gariepinus*). *The Israeli Journal of Aquaculture-Bamidgeh*, *63*, 542. https://doi.org/10.46989/001c.20586

Food and Agriculture Organization of the United Nations. (2020). *The state of world fisheries and aquaculture: Sustainability in action*. FAO. https://doi.org/10.4060/ca9229en

Gong, Y. Y., Huang, Y. Q., Gao, L. J., Lu, J. X., & Huang, H. L. (2016). Substitution of krill meal for fish meal in feed for Russian Sturgeon, *Acipenser gueldenstaedtii*. *The Israeli Journal of Aquaculture-Bamidgeh*, *68*, 1319. https://doi.org/10.46989/001c.20797

Henry, M., Gasco, L., Piccolo, G., & Fountoulaki, E. (2015). Review on the use of insects in the diet of farmed fish: Past and future. *Animal Feed Science and Technology*, *203*, 1-22. https://doi.org/10.1016/j.anifeedsci.2015.03.001

Hernández, C., Osuna-Osuna, L., Benitez-Hernandez, A., Sanchez-Gutierrez, Y., González-Rodríguez, B., & Dominguez-Jimenez, P. (2014). Replacements of fish meal by poultry by-product meal, food-grade, in diets for juvenile spotted rose snapper (*Lutjanus guttatus*). *Latin American*

Journal Aquatic Research, *42*(1), 111-120. https://doi.org/10.3856/vol42-issue1-fulltext-8

Huda, M. A., Sunarno, M. T., & Nurhudah, M. (2020). Potential addition of black soldier fly carcass meal in sangkuriang catfish (*Clarias gariepinus*) feed formulation. *Aquaculture, Aquarium, Conservation and Legislation*, *13*(5), 2567-2576. https://doi.org/10.21534/ai.v21i1.174

Ido, A., Hashizume, A., Ohta, T., Takahashi, T., Miura, C., & Miura, T. (2019). Replacement of fish meal by defatted yellow mealworm (*Tenebrio molitor*) larvae in diet improves growth performance and disease resistance in red seabream (*Pargus major*). *Animals*, *9*(3), 100. https://doi.org/10.3390/ani9030100

Idowu, E., Adewumi, A., Oso, J., Edward, J., & Obaronbi, G. (2017). Effects of varying levels of *Moringa oleifera* on growth performance and nutrient utilization of *Clarias gariepinus* post-fingerlings. *American Academic Scientific Research Journal for Engineering, Technology, and Sciences*, *32*(1), 79-95.

Jimoh, W. A., Ayeloja, A. A., Rasak, I. A., Akintoye, E. A., Abubakar, A., & Olaifa, J. B. (2021). Responses by African catfish (*Clarias gariepinus*) fed diets containing fish visceral meal as fishmeal replacer. *Aquaculture Research*, *52*(2), 810-821. https://doi.org/10.1111/are.14936

Johnson, N., & Phillips, M. (2018). Rayyan for systematic reviews. *Journal of Electronic Resources Librarianship*, *30*(1), 46-48. https://doi.org/10.1080/1941126x.2018.1444339

Kim, J., Cho, S. H., Kim, T., & Hur, S. W. (2021). Substitution effect of fish meal with various sources of animal by-product meals in feed on growth, feed utilization, body composition, haematology and non-specific immune response of olive flounder (*Paralichthys olivaceus*, Temminck & Schlegel, 1846). *Aquaculture Research*, *52*(6), 2802-2817. https://doi.org/10.1111/are.15132

Lawal, B. M., Adewole, H. A., & Olaleye, V. F. (2017). Digestibility study and nutrient re-evaluation in *Clarias gariepinus* fed blood meal-rumen digesta blend diet. *Notulae Scientia Biologicae*, *9*(3), 344-349. https://doi.org/10.15835/nsb9310047

Luthada-Raswiswi, R., Mukaratirwa, S., & O'Brien, G. (2021). Animal protein sources as a substitute for fishmeal in aquaculture diets: A systematic review and meta-analysis. *Applied Sciences*, *11*(9), 3854. https://doi.org/10.3390/app11093854

Luzier, J. M., Summerfelt, R. C., & Ketola, H. G. (1995). Partial replacement of fish meal with spray-dried blood powder to reduce phosphorus concentrations in diets for juvenile rainbow trout, *Oncorhynchus mykiss* (Walbaum). *Aquaculture Research*, *26*(8), 577-587. https://doi.org/10.1111/j.1365-2109.1995.tb00948.x

Mamoon, M., Auta, J., & Babatunde, M. M. (2018). Growth performance of African mudfish *Clarias gariepinus* fingerling fed graded poultry offal meal as a replacement of fishmeal. *Bayero Journal of Pure and Applied Sciences*, *11*(1), 83-87. https://doi.org/10.4314/bajopas.v11i1.14s

Martins, S. N., & Guzmán, E. C. (1994). Effect of drying method of bovine blood on the performance of growing diets for tambaqui (*Colossoma macropomum*, Cuvier 1818) in experimental culture tanks. *Aquaculture*, *124*(1-4), 335-341. https://doi.org/10.1016/0044-8486(94)90406-5

Monebi, O. C., & Ugwumba, A. A. A. (2016). Culture and utilization of the earthworm *Alma millsoni* in the diet of *Clarias gariepinus* fingerlings. *Zoology and Ecology*, *26*(1), 35-46. https://doi.org/10.1080/21658005.2015.1111973

Moniruzzaman, M., Damusaru, J. H., Won, S., Cho, S. J., Chang, K. H., & Bai, S. C. (2020). Effects of partial replacement of dietary fish meal by bioprocessed plant protein concentrates on growth performance, hematology, nutrient

digestibility and digestive enzyme activities in juvenile Pacific white shrimp, *Litopenaeus vannamei*. *Journal of the Science of Food and Agriculture*, *100*(3), 1285-1293. https://doi.org/10.1002/jsfa.10141

Musa, S. O., Okomoda, V. T., Tiamiyu, L. O., Solomon, S. G., Adeyemo, B. T., Alamanjo, C. C., & Abol-Munafi, A. B. (2021). Dietary implications of toasted *Jatropha curcas* kernel on the growth, haematology, and organ histology of *Clarias gariepinus* fingerlings. *Tropical Animal Health and Production*, *53*, 232. https://doi.org/10.1007/s11250-021-02678-3

Musyoka, S. N., Liti, D. M., Ogello, E., & Waidbacher, H. (2019). Utilization of the earthworm, *Eisenia fetida* (Savigny, 1826) as an alternative protein source in fish feeds processing: A review. *Aquaculture Research*, *50*(9), 2301-2315. https://doi.org/10.1111/are.14091

Novriadi, R., Spangler, E., Rhodes, M., Hanson, T., & Davis, D. A. (2017). Effects of various levels of squid hydrolysate and squid meal supplementation with enzyme-treated soy on growth performance, body composition, serum biochemistry and histology of Florida pompano *Trachinotus carolinus*. *Aquaculture*, *481*, 85-93. https://doi.org/10.1016/j.aquaculture.2017.08.032

Nwanna, L. C., Balogun, A. M., Ajenifuja, Y. F. & Enujiugha, V. N. (2004). Replacement of fish meal with chemically preserved shrimp head in the diets of African catfish, *Clarias gariepinus*. *Journal of Food Agriculture and Environment*, *2*, 79-83.

Ogunji, J. O., Iheanacho, S. C., Abe, G. A., & Ikeh, O. R. (2020). Assessing effects of substituting dietary fish meal with boiled donkey and cow blood meal on growth performance and digestive enzyme activities of *Clarias gariepinus* juvenile. *Journal of the World Aquaculture Society*, *51*(4), 1066-1079. https://doi.org/10.1111/jwas.12716

Ojewole, A. E., Faturoti, E. O., & Ihundu, C. (2022). Nutrient utilization and growth performance of African catfish (*Clarias gariepinus*) fed varying levels of composite meal (CM) in replacement of fishmeal. *International Journal of Aquaculture and Fishery Sciences*, *8*(2), 54-58. https://doi.org/10.17352/2455-8400.000078

Okanlawon, S. S., & Oladipupo, S. A. (2010). Nutritional evaluation of snail offal meal as animal protein supplement in the diets of *Clarias gariepinus* (Burchell, 1822) fingerlings. *World Journal of Fish and Marine Sciences*, *2*(2), 103-108.

Olsen, R. L., & Hasan, M. R. (2012). A limited supply of fishmeal: Impact on future increases in global aquaculture production. *Trends in Food Science and Technology*, *27*(2), 120-128. https://doi.org/10.1016/j.tifs.2012.06.003

Oonincx, D. G., & De Boer, I. J. (2012). Environmental impact of the production of mealworms as a protein source for humans–a life cycle assessment. *PLOS One*, *7*(12), e51145. https://doi.org/10.1371/journal.pone.0051145

Orire, A. M., Sadiku, S., & Gana, S. N. (2015). Evaluation of growth performance and body composition of *Clarias gariepinus* fingerling fed graded level of Bambara nut meal (*Vigna substrarreana*). *Journal of Agriculture and Food Technology*, *5*(3), 7-13.

Ouzzani, M., Hammady, H., Fedorowicz, Z., & Elmagarmid, A. (2016). Rayyan — A web and mobile app for systematic reviews. *Systematic Reviews*, *5*, 210. https://doi.org/10.1186/s13643-016-0384-4

Pinotti, L., Giromini, C., Ottoboni, M., Tretola, M., & Marchis, D. (2019). Insects and former foodstuffs for upgrading food waste biomasses/streams to feed ingredients for farm animals. *Animal*, *13*(7), 1365-1375. https://doi.org/10.1017/s1751731118003622

Pongpet, J., Ponchunchoovong, S., & Payooha, K. (2016). Partial replacement of fishmeal by brewer's yeast (*Saccharomyces cerevisiae*) in the diets of Thai Panga (*Pangasianodon hypophthalmus* × *Pangasius bocourti*). *Aquaculture Nutrition*, *22*(3), 575-585. https://doi.org/10.1111/anu.12280

Raji, A. A., Alaba, P. A., Yusuf, H., Bakar, N. H. A., Taufek, N. M., Muin, H., Alias, Z., Milow, P., & Razak, S. A. (2018). Fishmeal replacement with *Spirulina platensis* and *Chlorella vulgaris* in African catfish (*Clarias gariepinus*) diet: Effect on antioxidant enzyme activities and haematological parameters. *Research in Veterinary Science*, *119*, 67-75. https://doi.org/10.1016/j.rvsc.2018.05.013

Raji, A. A., Jimoh, W. A., Bakar, N. H., Taufek, N. H., Muin, H., Alias, Z., Milow, P., & Razak, S. A. (2020). Dietary use of *Spirulina* (*Arthrospira*) and *Chlorella* instead of fish meal on growth and digestibility of nutrients, amino acids and fatty acids by African catfish. *Journal of Applied Phycology*, *32*, 1763-1770. https://doi.org/10.1007/s10811-020-02070-y

Raji, A. A., Junaid, O. Q., Milow, P., Taufek, N. M., Fada, A. M., Kolawole, A. A., Alias, Z., & Razak, S. A. (2019). Partial replacement of fishmeal with *Spirulina platensis* and *Chlorella vulgaris* and its effect on growth and body composition of African catfish *Clarias gariepinus* (Burchell 1822). *Indian Journal of Fisheries*, *66*(4), 100-111. https://doi.org/10.21077/ijf.2019.66.4.87193-13

Rapatsa, M. M., & Moyo, N. A. (2019). Enzyme activity and histological analysis of *Clarias gariepinus* fed on *Imbrasia belina* meal used for partial replacement of fishmeal. *Fish Physiology and Biochemistry*, *45*(4), 1309-1320. https://doi.org/10.1007/s10695-019-00652-3

Reyes-Becerril, M., Guardiola, F., Rojas, M., Ascencio-Valle, F., & Esteban, M. Á. (2013). Dietary administration of microalgae *Navicula* sp. affects immune status and gene expression of gilthead seabream (*Sparus aurata*). *Fish and Shellfish Immunology*, *35*(3), 883-889. https://doi.org/10.1016/j.fsi.2013.06.026

Saleh, H. H. (2020). Review on using of macro algae (seaweeds) in fish nutrition. *Journal of Zoological Research*, *2*(2), 6-11. https://doi.org/10.30564/jzr.v2i2.2054

Sánchez-Muros, M. J., Barroso, F. G., & Manzano-Agugliaro, F. (2014). Insect meal as renewable source of food for animal feeding: A review. *Journal of Cleaner Production*, *65*, 16-27. https://doi.org/10.1016/j.jclepro.2013.11.068

Sarker, P. K., Kapuscinski, A. R., McKuin, B., Fitzgerald, D. S., Nash, H. M., & Greenwood, C. (2020). Microalgae-blend tilapia feed eliminates fishmeal and fish oil, improves growth, and is cost viable. *Scientific Reports*, *10*, 19328. https://doi.org/10.1038/s41598-020-75289-x

Shah, M. R., Lutzu, G. A., Alam, A., Sarker, P., Chowdhury, K., Parsaeimehr, A., Liang, Y., & Daroch, M. (2018). Microalgae in aquafeeds for a sustainable aquaculture industry. *Journal of Applied Phycology*, *30*, 197-213. https://doi.org/10.1007/s10811-017-1234-z

Sheikhlar, A., Goh, Y. M., Ebrahimi, M., Romano, N., Webster, C. D., Alimon, A. R., Daud, H., & Javanmard, A. (2018). Replacement of dietary fishmeal for fenugreek seed meal on the growth, body composition, innate immunological responses and gene expression of hepatic insulin-like growth factors in African catfish (*Clarias gariepinus*). *Aquaculture Nutrition*, *24*(6), 1718-1728. https://doi.org/10.1111/anu.12806

Tahir, R., Ndimele, E. Saba, A., & Ibrahim, M. (2021). Growth response and nutrient utilization of *Clarias gariepinus* fingerlings exposed to Dichlorvos. *International Journal of Applied Biology*, *5*(1), 64-72.

Taufek, N. M., Aspani, F., Muin, H., Raji, A. A., Razak, S. A., & Alias, Z. (2016a). The effect

of dietary cricket meal (*Gryllus bimaculatus*) on growth performance, antioxidant enzyme activities, and haematological response of African catfish (*Clarias gariepinus*). *Fish Physiology and Biochemistry*, *42*(4), 1143-1155. https://doi.org/10.1007/s10695-016-0204-8

Taufek, N. M., Aspani, F., Muin, H., Raji, A. A., Razak, S. A., & Alias, Z. (2016b). The effect of dietary cricket meal (*Gryllus bimaculatus*) on growth performance, antioxidant enzyme activities, and haematological response of African catfish (*Clarias gariepinus*). *Fish Physiology and Biochemistry*, *42*(4), 1143-1155. https://doi.org/10.1007/s10695-016-0204-8

Taufek, N. M., Muin, H., Raji, A. A., Md Yusof, H., Alias, Z., & Razak, S. A. (2018). Potential of field crickets meal (*Gryllus bimaculatus*) in the diet of African catfish (*Clarias gariepinus*). *Journal of Applied Animal Research*, *46*(1), 541-546. https://doi.org/10.1080/09712119.2017.1357560

Tilami, S. K., Turek, J., Červený, D., Lepič, P., Kozák, P., Burkina, V., Sakalli, S., Tomčala, A., Samples, S., & Mráz, J. (2020). Insect meal as a partial replacement for fish meal in a formulated diet for perch *Perca fluviatilis*. *Turkish Journal of Fisheries and Aquatic Sciences*, *20*(12), 867-878. https://doi.org/10.4194/1303-2712-v20_12_03

Tippayadara, N., Dawood, M. A., Krutmuang, P., Hoseinifar, S. H., Doan, H. V., & Paolucci, M. (2021). Replacement of fish meal by black soldier fly (*Hermetia illucens*) larvae meal: Effects on growth, haematology, and skin mucus immunity of Nile tilapia, *Oreochromis niloticus*. *Animals*, *11*(1), 193. https://doi.org/10.3390/ani11010193

Wan, A. H.L., Davies, S. J., Soler-Vila, A., Fitzgerald, R., & Johnson, M. P. (2019). Macroalgae as a sustainable aquafeed ingredient. *Reviews in Aquaculture*, *11*(3), 458-492. https://doi.org/10.1111/raq.12241

Wang, M., Chen, N., Li, S., Lian, X., & Yan, C. (2018). Study on replacement of fish meal by two plant protein mixtures in diets for largemouth bass (*Micropterus salmoides*). *Journal of Shanghai Ocean University*, *27*(1), 37-47.

Yalew, A., Getahun, A., & Dejen, E. (2019). Effect of replacing fish meal by sweet lupin meal on growth performance of African catfish fingerlings, *Clarias gariepinus* (Burchell, 1822). *Ethiopian Journal of Science and Technology*, *12*(1), 1-17. https://doi.org/10.4314/ejst.v12i1.1

Yousif, R. A., Abdullah, O. J., Ahmed, A. M., Adam, M. I., Ahmed, F. A. M., & Idam, O. A. (2019). Effect of replacing fishmeal with water spinach (*Ipomoea aquatica*) on growth, feed conversion and carcass composition for Nile tilapia fry (*Oreochromis niloticus*). *Journal of Aquatic Sciences and Marine Biology*, *2*(4), 3-20. https://doi.org/10.21608/eajbsz.2019.61513

Yu, H., Zhang, Q., Cao, H., Tong, T., Huang, G., & Li, W. (2015). Replacement of fish meal by meat and bone meal in diets for juvenile snakehead *Ophiocephalus argus*. *Fisheries Science*, *81*(4), 723-729. https://doi.org/10.1007/s12562-015-0871-x

Zheng, Q., Wen, X., Han, C., Li, H., & Xie, X. (2012). Effect of replacing soybean meal with cottonseed meal on growth, hematology, antioxidant enzymes activity and expression for juvenile grass carp, *Ctenopharyngodon idellus*. *Fish Physiology and Biochemistry*, *38*(4), 1059-1069. https://doi.org/10.1007/s10695-011-9590-0

APPENDICES

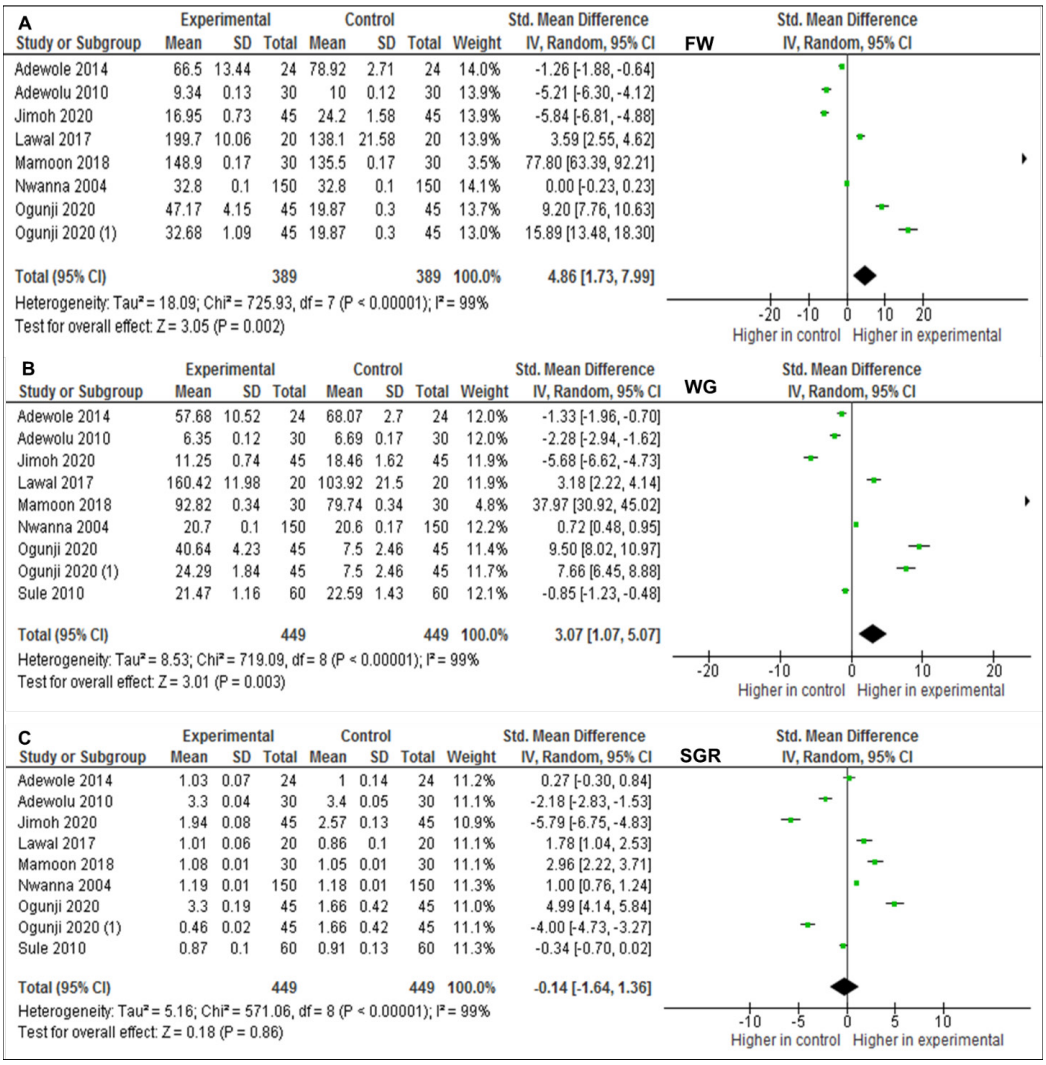

Supplementary material 1. Forest plot showing the effect sizes of growth parameters for fishmeal replacement with animal products in African catfish

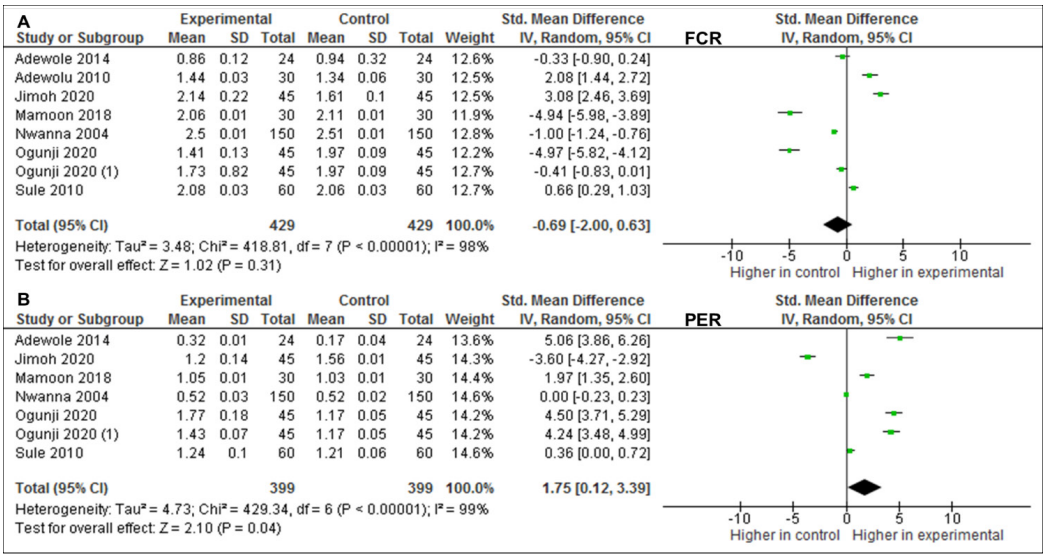

Supplementary material 2. Forest plot showing the effect sizes of nutrient utilization parameters after recommended fishmeal replacement with animal products in African catfish

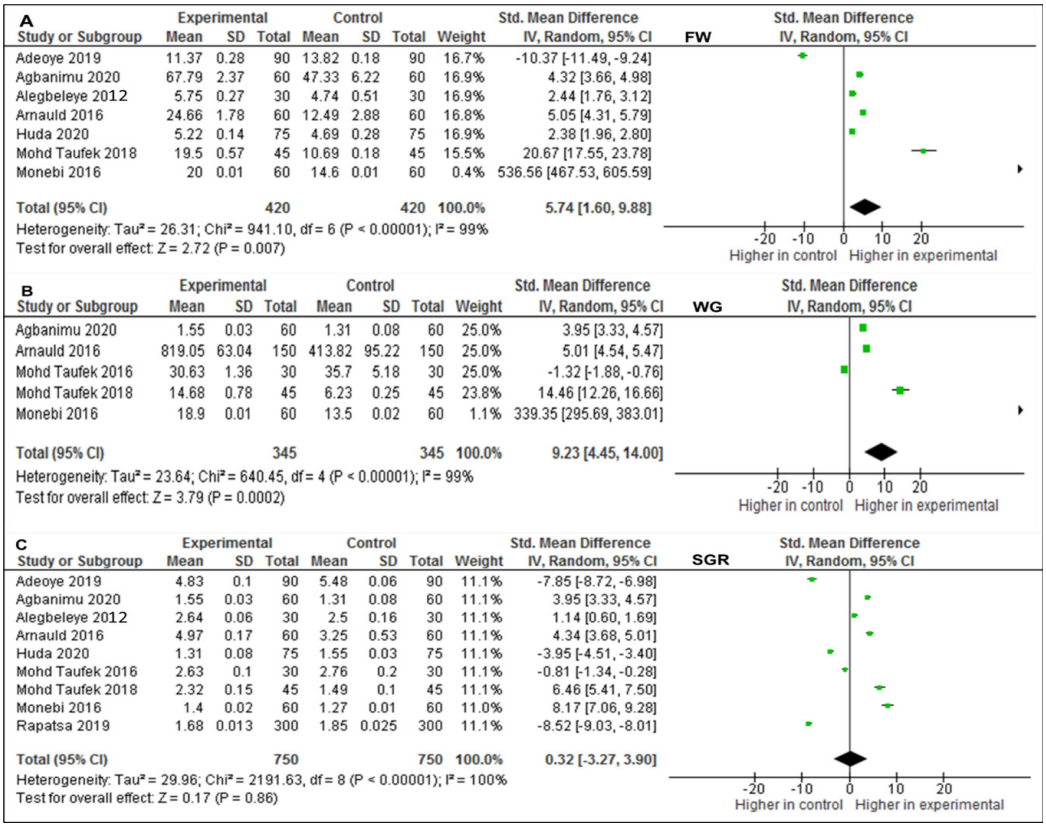

Supplementary material 3. Forest plot showing the effect sizes of growth parameters for fishmeal replacement with insects/worms in African catfish

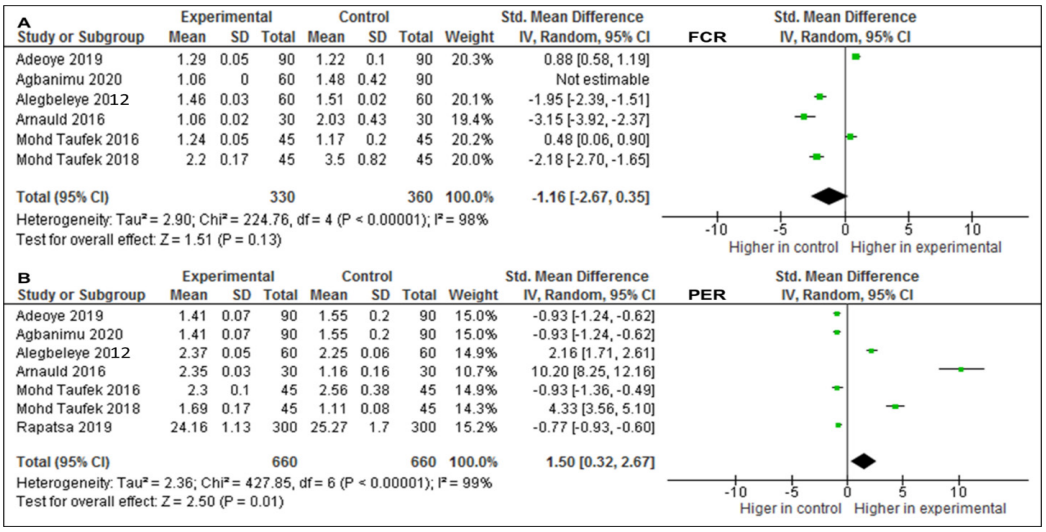

Supplementary material 4. Forest plot showing the effect sizes of nutrient utilization based on fishmeal replacement with insects/worms in African catfish

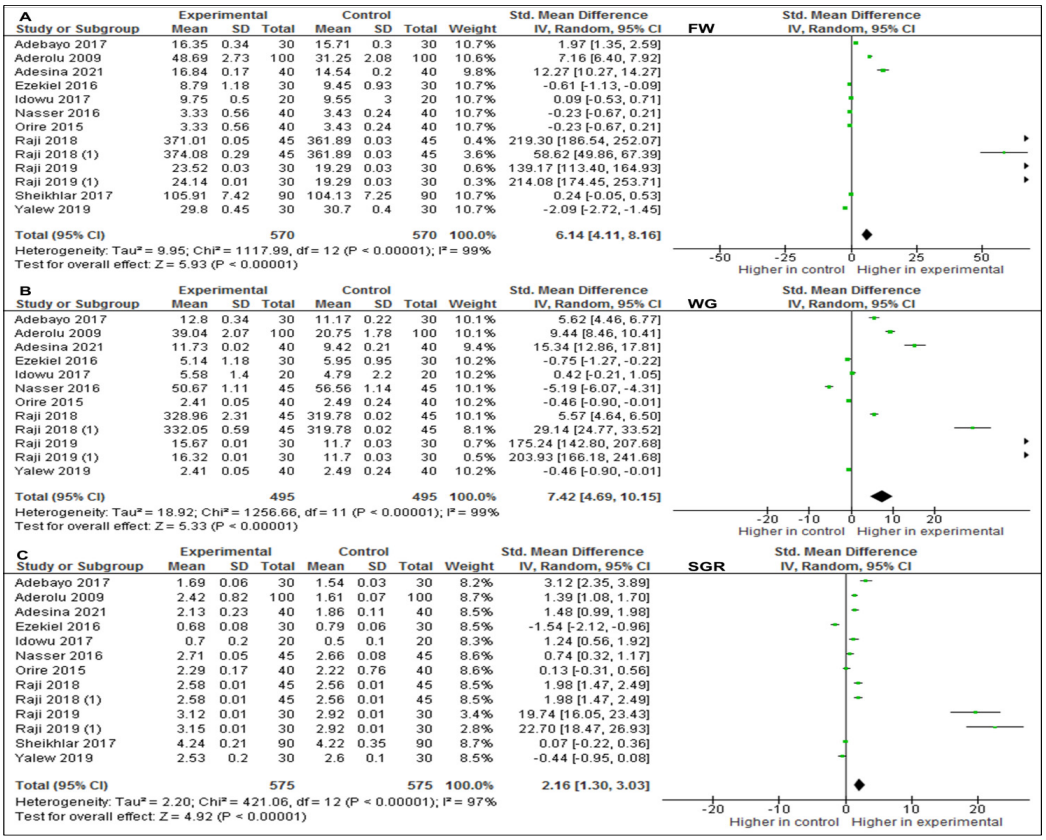

Supplementary material 5. Forest plot showing the effect sizes of growth parameters for fishmeal replacement with algae/plants in African catfish

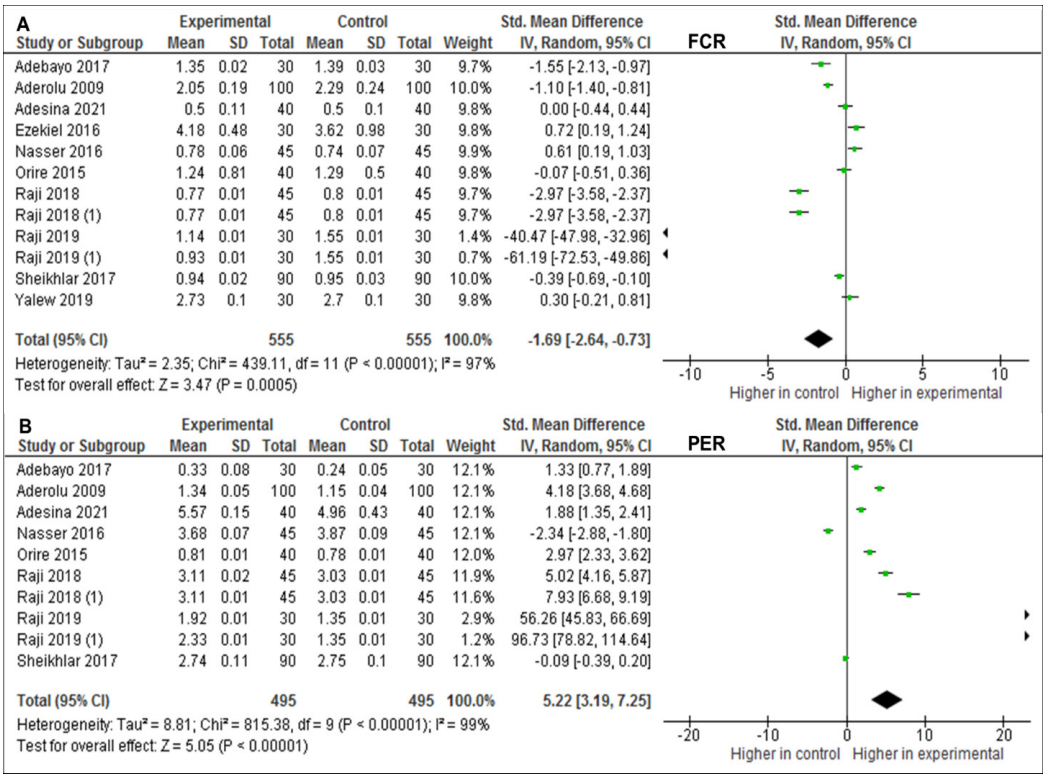

Supplementary material 6. Forest plot showing the effect sizes of nutrient utilization parameters for fishmeal replacement with algae/plants in African catfish

Pertanika J. Trop. Agri. Sci. 46 (1): 177 - 195 (2023)

PERTANIKA JOURNALS

TROPICAL AGRICULTURAL SCIENCE

Journal homepage: http://www.pertanika.upm.edu.my/

Review Article

Biological Control Strategies of Purple Witchweed, *Striga hermonthica*: A Review

Nadia Yasseen Osman[1,2], Muhammad Saiful Hamdani[3], Siti Nurbaya Oslan[4], Dzarifah Mohamed Zulperi[5] and Noor Baity Saidi[1,6]*

[1]Department of Cell and Molecular Biology, Faculty of Biotechnology and Biomolecular Sciences, Universiti Putra Malaysia, 43400 UPM Serdang, Selangor, Malaysia
[2]Environment, Natural Resources and Desertification Research Institute, The National Center for Research (NCR), 2404 Khartoum, Sudan
[3]Department of Crop Science, Faculty of Agriculture, Universiti Putra Malaysia, 43400 UPM Serdang, Selangor, Malaysia
[4]Department of Biochemistry, Faculty of Biotechnology and Biomolecular Sciences, Universiti Putra Malaysia, 43400 UPM Serdang, Selangor, Malaysia
[5]Department of Plant Protection Faculty of Agriculture, Universiti Putra Malaysia, 43400 UPM Serdang, Selangor, Malaysia
[6]Laboratory of Sustainable Agronomy and Crop Protection Universiti Putra Malaysia, 43400 UPM Serdang, Selangor, Malaysia

ABSTRACT

The genus of *Striga* spp., particularly *Striga hermonthica*, is an obligate root-hemiparasitic weed. *Striga* affects 25 African countries annually and is considered a major biotic threat to food security. This obnoxious weed species has been managed using various control strategies. However, the strategies have not been highly effective due to the complexity of the *Striga* life cycle and special interactions with its host. Biological control, considered a safer and 'greener' alternative, has drawn attention due to numerous reports on the potential of biological agents, including insects and microorganisms, to control *Striga*. Although researchers agree on the importance of the biocontrol approach as one of the alternative eco-friendly methods to manage *Striga* spp., the decreasing effectiveness of some biocontrol agents when introduced into new environments, in addition to requirements before and during

ARTICLE INFO

Article history:
Received: 27 July 2022
Accepted: 11 November 2022
Published: 03 February 2023

DOI: https://doi.org/10.47836/pjtas.46.1.10

E-mail addresses:
nadiaesam2013@gmail.com (Nadia Yasseen Osman)
s_ahmad@upm.edu.my (Muhammad Saiful Hamdani)
snurbayaoslan@upm.edu.my (Siti Nurbaya Oslan)
dzarifah@upm.edu.my (Dzarifah Mohamed Zulperi)
norbaity@upm.edu.my (Noor Baity Saidi)
*Corresponding author

ISSN: 1511-3701
e-ISSN: 2231-8542

the application, restricts the application of biological control on a large scale until today. This review focuses on the current knowledge of control strategies to manage *Striga*, emphasizing the biological control method. The challenges that limit the application of biological control to manage *Striga* on a broader scale are also highlighted.

Keywords: African agriculture, bio-protection, crop, microorganisms, parasitic weed

INTRODUCTION

Parasitic plants are a type of plant that attacks another plant to get all or part of nutrients and water (Samejima & Sugimoto, 2018). Moreover, parasitism among plants is one of the relationships that usually occurs among a considerable number of terrestrial plants. For example, more than 4,500 flowering plant species have parasitic behavior on other plants with wide distribution in different habitats. Consequently, various criteria have been used to classify the parasitic plants, including the site of attachment with a host, photosynthetic ability, and degree of dependency on the host plant (Erdogan, 2021; Joel et al., 2013).

Parasitic plants are morphologically distinct and range in size from diminutive herbaceous plants, generally known as weeds, to large trees. Among the parasitic plant families, the Orobanchaceae family has received great attention as it includes members of parasitic weeds that can cause severe damage to economic and cash crops leading to a critical agriculture problem of global food security (Joel et al., 2013; Okazawa et al., 2021). Witchweed (*Striga* spp.) and broomrape (*Orobanche* and *Phelipanche* spp.) are obligate root parasitic weeds that belong to the Orobanchaceae family (Clarke et al., 2019). The *Striga* genus comprises more than 35 species, including the two most widespread and economically important species, *Striga hermonthica* (Del.) Benth and *Striga asiatica* (L.) Kuntze. Both species parasitize sorghum, pearl millet, maize, and rice (Mutuku et al., 2021).

Striga hermonthica is considered the most serious biotic threat to cereal agriculture, particularly in developing countries (De Groote et al., 2008). The species affected the lives of more than 100 million people in Africa and caused economic damage, equivalent to approximately 1 billion USD per year (Labrada, 2008; Teka, 2014; Waruru, 2013). Furthermore, grain yield losses can reach 100% in susceptible cultivars under a high infestation level and drought conditions (Haussmann et al., 2000).

Biological control of *Striga* weed is a promising field with notable successes, as there are many reports on the potential of using various microorganisms to reduce damage caused by *Striga*. However, special consideration must be put in place to avoid unintended effects on the host plant due to the intimate relationship between *Striga* and the host plant. Therefore, rigorous testing and validation are necessary to evaluate their efficacy and reliability for *Striga* control (Hasan et al., 2021; Neondo et al.,

2017; Nzioki et al., 2016). Furthermore, a combination of compatible biocontrol agents with divergent modes of action is likely to yield better results than a single biocontrol agent (Neondo et al., 2017; Nzioki et al., 2016). In this review, the current state of knowledge on the biological control strategies to manage *Striga*, the mechanisms of control, and the obstacles that limit its application are described on a wider scale.

BIOLOGY AND LIFE CYCLE OF *STRIGA* SPP.

Striga spp. are annual root hemiparasitic plants that can produce an incredibly huge number of seeds per plant (up to 100,000 seeds plant-1) with high fecundity where it remains viable for more than 15 years, leading to a rapid increase in the seed bank (Samejima & Sugimoto, 2018; Teka, 2014). *Striga* spp. is characterized by a complex life cycle that initiates simultaneously with the life cycle of its host. The life cycle starts with germination, haustoria formation attachment, penetration, the establishment of vascular connections, the accretion of nutrients, flowering, and finally, the production of seeds (Cardoso et al., 2011; David et al., 2022). The distinct phases of the life cycles of both plants are harmonized through a signaling process before *Striga* sets new seeds (Figure 1). Before germination, *Striga* seeds must undergo a conditioning stage, which involves exposure to a sufficient temperature and high humidity conditions for two weeks to break seed dormancy and become responsive to germination stimulants (Cardoso et al., 2011). After the seeds germinate, germ tubes are produced and grown chemotropically toward the host root. Then radicals attach to the host root and form haustoria in response to the haustoria-inducing factor. An adhesive structure develops during the attachment phase to cement the parasite to the host surface. The haustorium then penetrates the root cortex of potential hosts and continues to connect with the xylem of the host plant. During the attachment phase, the parasite remains subterranean for several weeks and withdraws all the nutrients from the host plant before appearing above ground.

The Role of Strigolactones in the *Striga* Life Cycle

Soil deterioration correlates with *Striga* infestation via the increased production of secondary metabolites by the host plant in response to the poor soil condition that induces germination of the parasites (Jamil et al., 2014). The secondary metabolites, identified as strigolactones (SLs), which are abundantly present in mycotrophic plant roots, exudate in poor soil to help establish symbiotic interaction with mycorrhiza in the soil (Boari et al., 2016). SLs are also vital for the germination of *Striga* and other parasitic weeds. The first SLs to be characterized is strigol, isolated from cotton root, a trap host species (Aquino et al., 2021; Reigosa et al., 2006). Another established role for SLs is regulating root and shoot architecture based on phosphate availability. In a sufficient amount of phosphate, SLs inhibit lateral root formation, while in a

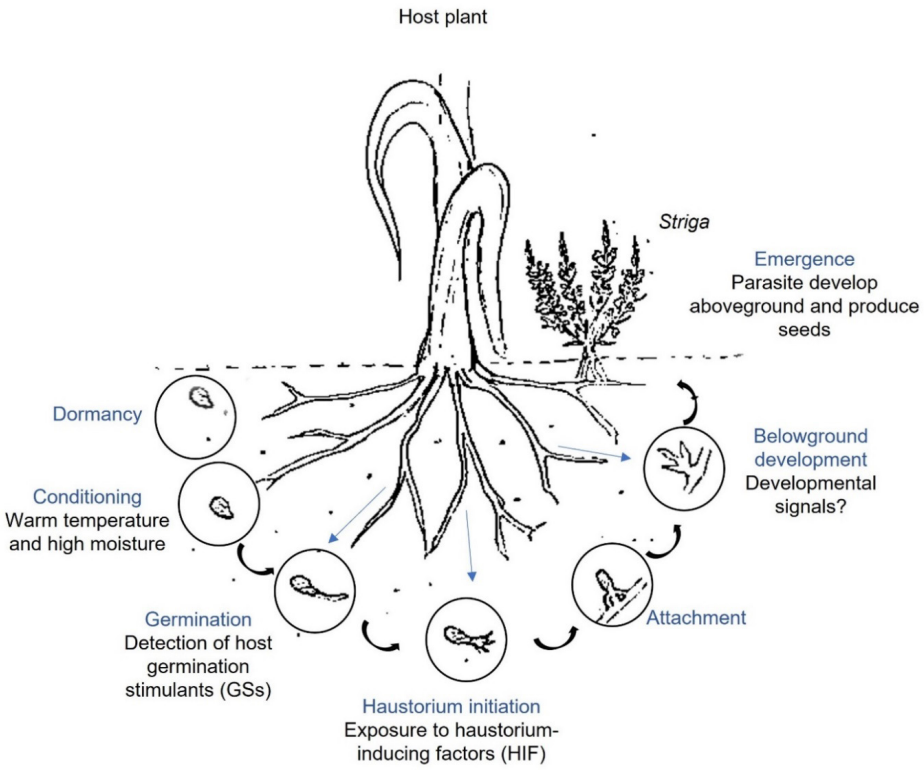

Figure 1. The life cycle of *Striga*

phosphate-limited environment, they can promote lateral root primordia formation (Xie et al., 2010). In addition to the effects on organ growth and development, SLs also affect plant metabolism through the biosynthesis of organic acids (Gamir et al., 2020). Previous research has confirmed that using nitrogen and phosphorus to improve soil fertility decreases SLs exudate and reduces *Striga* germination (Jamil et al., 2014; Mwangangi et al., 2021). Other than SLs, *Striga* seeds can also germinate in response to other compounds produced by plant roots, such as dihydrosorogoleone, kinetin, coumarin, jasmonate, ethylene, and fungal metabolites (Cardoso et al., 2011). However, the sensitivity of *Striga* seeds to these compounds is lower than their sensitivity to SLs. Furthermore, SLs can stimulate *Striga* seed germination even if secreted from the non-host roots, making SLs the most efficient compound for regulating *Striga* seed germination (Cardoso et al., 2011).

CURRENT PRACTICES IN MANAGING *STRIGA* AND THEIR LIMITATIONS

The management strategies of *Striga* rely on achieving the following targets: (1) limiting seed dispersal out of the endemic area via agriculture tools, irrigation water,

and pasture animals; (2) limiting new seed production by reducing the release of germination stimulants by the host, and (3) reducing seed bank accumulation in infested soil by stimulating the germination of *Striga* seed in the host's absence or blocking the germination of preconditioned seed (Jamil et al., 2021). Several control methods have been applied to attain at least one of the management targets, including chemical, cultural, and biological control, with varying degrees of success (Boari et al., 2016). However, many countries avoid the conventional (cultural) method, which involves hand pulling of emerging *Striga* stalk. It is ineffective since parasite damage already occurs at the subterranean phase (Figure 1). Likewise, crop rotation systems or using catch/trap crops and tolerant varieties are not considered efficient in eradicating this parasite, particularly if applied separately (Babiker, 2007; Hailu et al., 2018; Sibhatu et al., 2016).

Chemical control using herbicides, such as imazapyr and pyrithiobac, soil fumigation by methyl bromide, and ethylene as germination stimulants have been reported in numerous studies as effective methods to increase crop production and control *Striga* in the early season (Sibhatu et al., 2016). However, although the chemical approaches are widely adopted, their sustainability is compromised by the predicted emergence of herbicide-resistant weeds and unwanted off-target effects (Eizenberg et al., 2013). The latter can potentially disrupt biodiversity, reduce beneficial soil microbes, or compromise immunity against other pests and pathogens (Barzman et al., 2015; Druille et al., 2013). In addition, prolonged application of chemical herbicides was shown to have detrimental effects on humans by increasing the risk of cancer, congenital disabilities, and skin problems and by threatening the sustainability of natural resources (Bale et al., 2008; Kumar et al., 2021). Therefore, an eco-friendly approach to control *Striga* weed is critical and in high demand to avoid the negative impacts resulting from the accumulation of chemical residues and preserve environmental balance.

BIOLOGICAL CONTROL OF PARASITIC WEEDS

Biological agents to eliminate various noxious pests, including weeds, insects, and microbial pathogens, have been used for over a century. Regardless of the intentions, which may range from convenience to opportunism, the term 'biological control' has traditionally been used to describe actions to combat pests using other living agents (Cook & Baker, 1983; Stenberg et al., 2021). For example, the Weed Science Society of America (WSSA) defined the weed biological control method as 'the use of an agent, a complex of agents, or biological processes to bring about weed suppression' (Uludag et al., 2018). The ultimate advantage of biological control in terms of cost-effectiveness, safety, and benefits for the environment would be evident upon the establishment and reproduction of the released organisms (Teka, 2014).

Many reasons motivate the adoption of biological control in parasitic weeds. Among them are the restriction imposed on many common herbicides by the authorities, the evolution of herbicide-resistant parasitic weeds, increased understanding of weed control to target only unwanted species, conservation of environmentally sensitive or degradation-prone areas, contamination from chemical herbicides, and inclination to healthier and sustainable cropping systems (Myers & Cory, 2017; van Wilgen et al., 2013). Furthermore, the intimate relationship between the parasitic weed and its host hinders the application of chemical herbicides as they cannot all selectively distinguish between different species. On the other hand, the high specificity of some fungi, bacteria, and arthropods that feed exclusively on selected parasitic weeds leads to increased attention on exploiting these organisms as biocontrol agents, where other weed control options have failed (Teka, 2014; Uludag et al., 2018).

THE BIOLOGICAL APPROACHES FOR CONTROLLING *STRIGA*

Biological control of *Striga* is a system that relies on the interaction between three agents: the parasite (*Striga*), a living biocontrol agent targeting *Striga*, and a human stakeholder benefiting from the *Striga* control service provided by the biocontrol agent (Stenberg et al., 2021). In this case, the living biocontrol agents include bacteria, fungi, insects, and components extracted or synthesized from microorganisms *in situ*. According to the International Biocontrol Manufacturers Association (IBMA) (2018), bio-protection agents should originate from nature or be nature-identical when synthesized and have a low impact on human health and the environment.

Mechanisms of Action of Biological Control Against *Striga*

The biocontrol mechanisms of the living agents used for controlling *Striga* occur through direct or indirect antagonisms (Figure 2). The former involves natural enemies such as pathogens and insect predators that attack and consume *Striga* organs or produce secondary metabolites, which cause diseases that inhibit *Striga* seeds germination or interfere with host-*Striga* signaling (Ndambi et al., 2011). The latter occurs via disruption of the *Striga* life cycle or reduction of *Striga* attachment in the host root by enhancing nutrient acquisition, which consequently halts strigolactones biosynthesis in the host plant. Alternatively, indirect antagonism may occur via induced systemic resistance (ISR) in the host plants against *Striga* via changes in plant defense pathways, particularly salicylic acid, and jasmonic acid. It is worth mentioning that the precise knowledge of the control mechanism is behind the expansion of the term biocontrol to bio-protection to include the indirect effects of the living organisms on *Striga* (Masteling et al., 2019).

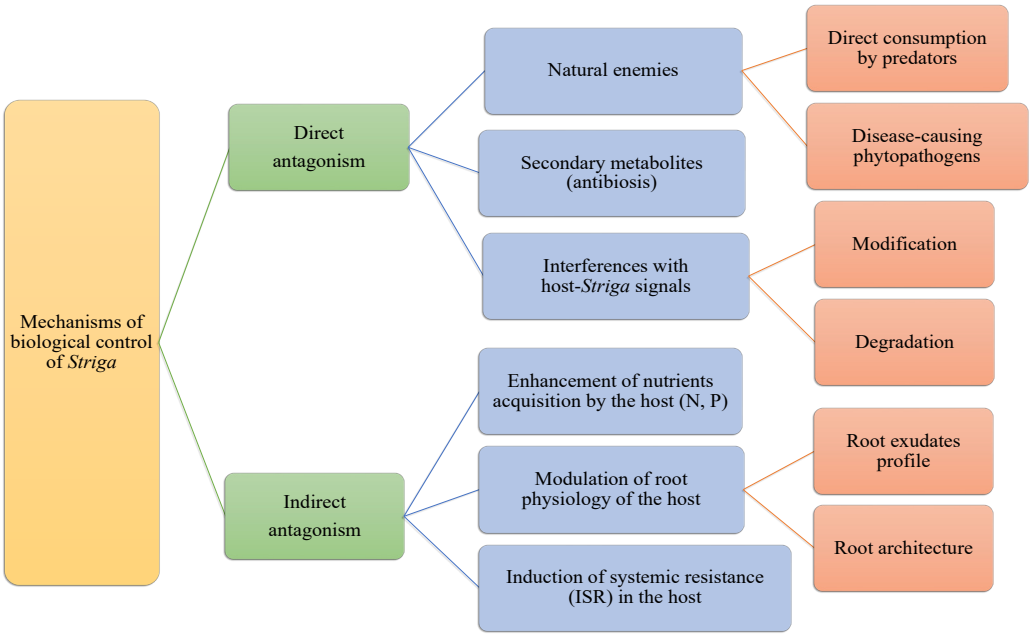

Figure 2. Mechanisms of biological control against *Striga*

Biocontrol of *Striga* Using Insects

Damaging *Striga* directly through natural enemies, such as herbivorous insects, is one of the most applied biocontrol techniques. Furthermore, many insects indigenous to India and Africa have been reported to attack *Striga* spp. The genus of greatest interest concerning biological control is *Smicronyx*, of which several species are highly specific to *Striga* (Parker & Riches, 1993). According to their effect on *Striga*, the insects are classified as defoliators, gall-formers, shoot borers, miners, inflorescence feeders, and fruit feeders (Bashir, 1987; Kroschel et al., 1999) (Table 1). For example, the release of *Smicronyx albovariegatus* and *Eulocastra argentisspara* in Ethiopia in 1974 signified the first attempt to adopt the classical biological control for *Striga*. The event was followed by a second release of *S. albovariegatus* four years later (Kroschel et al., 1999; Parker & Riches, 1993).

Table 1

Insects with the potential to control Striga *spp.*

Pathogen / Agent scientific name	Classification	Action / Response and mechanism	Reference(s)	Target of *Striga* spp.
Smicronyx albovariegatus	Insect	Induce gall formation on *Striga*	Kroschel et al. (1999)	*Striga hermonthica*

Table 1 *(Continue)*

Pathogen / Agent scientific name	Classification	Action /Response and mechanism	Reference(s)	Target of *Striga* spp.
Smicronyx umbrinus	Insect	Destroy seeds in the range of 80-95%	Smith and Webb (1996); Smith et al. (1993)	*Striga hermonthica*
Junonia spp.	Insect	Defoliator	Bashir (1987); Kroschel et al. (1999)	*Striga hermonthica*
Apanteles sp.	Insect	Shoot borer	Bashir (1987); Kroschel et al. (1999)	*Striga hermonthica*
Ophiomyia strigalis	Insect	Miner	Bashir (1987); Kroschel et al. (1999)	*Striga hermonthica*
Stenoptilodes thtaprobanes	Insect	Inflorescence feeder	Bashir (1987); Kroschel et al. (1999)	*Striga hermonthica*
Eulocastra spp.	Insect	Fruit feeder	Bashir (1987); Kroschel et al. (1999)	*Striga hermonthica*

Biocontrol of *Striga* Using Microorganisms

Apart from using insects, researchers interested in biological control to combat *Striga* have focused on exploiting microorganisms (Table 2) by directly applying or extracting and manipulating their biological compounds (Stenberg et al., 2021). Pathogenic fungi account for nearly 50% of the living organism candidates for biological control of *Striga*. Most candidates were reported to target *S. hermonthica*, except for *Fusarium oxysporum* f. sp. *strigae* (*Fos*), *Curvularia geniculate*, *Rhizoctonia solani*, and *Sclerotium rolfsii* that also target species other than *S. hermonthica*. For example, a direct application of *Fos* successfully blocked the xylem vessels of mature (emerged) plants by its hyphae or caused complete tissue digestion of younger plantlets belowground, leading to wilting and death on *Striga* (Ndambi et al., 2011). Alternatively, the application of amino acids L-leucine and L-tyrosine extracted from *Fusarium oxysporum* was found to be toxic to *Striga* and were able to inhibit its germination. However, at the same time, it is innocuous to the host.

Myriad signaling molecules, such as sterols, isothiocyanates, and organic acids, can induce germination and haustorium formation of parasitic root weed (RPW), including *Striga*, which are secreted by microbes in the plant rhizosphere. Arbuscular mycorrhiza fungi (AMF) enhance the growth performance of cereals to withstand

Striga damage by facilitating the uptake of water, phosphorus, and micronutrients from the soil through the wide net of extraradical fungal hyphae (Bonfante & Genre, 2010). Consequently, increased phosphorus uptake through symbiotic interaction by AMF could ultimately reduce SLs exudation by the host in the soil, thereby lowering *Striga* infection (Lendzemo et al., 2007; Lo´pez-Ra´ez et al., 2011).

In addition to fungi, bacteria also contribute to a large proportion of microbes in the plant rhizosphere. The root-associated bacteria mainly belong to the plant growth-promoting rhizobacteria (PGPR). They include various bacterial genera, such as *Bacillus* sp., *Azospirillum* sp., *Gluconacetobacter* sp., *Pseudomonas* sp., and *Rhizobium*. Augmentation of the rhizosphere microbiome by adding a new member might interfere with the signaling, thus suppressing seed germination, and disrupting the development of radical and/or haustoria (Masteling et al., 2019). Moreover, *Striga* seed germination and the number of attachments to the host root were reduced notably after treating sorghum root exudates with epiphytic bacteria from sorghum seeds. These occur following a change in the phenolic compound profile in the root exudates (Ali et al., 2013). These bacteria play an important role in plant growth by regulating the secretion of auxins, gibberellins, indole-3-acetic acid, and cytokinin, in addition to increasing soil mineral bioavailability by diazotrophic nitrogen fixation. Therefore, these bacteria contribute indirectly to managing *Striga* by strengthening the immune system in the host plant (Danhorn & Fuqua, 2007; Mounde et al., 2020; Taylor et al., 1996).

Though not pathogenic, other bacterial genera, such as *Bacillus*, can cause *Striga* seed decay by extracellular xylanases, pectinases, and amylases (Masteling et al., 2019). In another report, *Pseudomonas fluorescens* and *Pseudomonas putida* significantly inhibited *S. hermonthica* seed germination under screen house experiments (Babalola et al., 2007). In addition, Gafar et al. (2015) reported inhibition effects on *Striga* seed germination and haustorium initiation during conditioning with endophytic bacteria isolated from sugarcane suspected to belong to *Gluconacetobacter* spp. Conversely, ethylene from some *Pseudomonas* spp. and *Bradyrhizobium japonicum* can induce the germination of *Striga* seed in the absence of the host (suicidal germination), leading to a reduction of *Striga* seed bank (Table 2) (Ahonsi et al., 2003; Okazawa et al., 2021).

CHALLENGES AND LIMITATIONS IN THE BIOLOGICAL CONTROL OF PARASITIC WEED

In contrast to common weeds, controlling RPW, including *Striga*, is faced with several difficulties, as reviewed by Nzioki et al. (2016). Among them is the unique biology of parasitic weeds, which limits the number of metabolic pathways that current commercial herbicides can target. However, it can generate opportunities for discovering parasitic weed-specific herbicide targets (Fernández-Aparicio et al., 2017, 2020). In addition, the tiny size of RPW seeds,

Table 2

Microorganisms with the potential to control Striga *spp.*

Pathogen / Agent scientific name	Classification	Action / Response and mechanism	Reference (s)	Target of *Striga* spp.
Fusarium oxysporum	Phytopathogenic fungi	Disrupt amino acid homeostasis (Antibiosis)	Nzioki et al. (2016)	*Striga hermonthica*
Fusarium oxysporum f. sp. *strigae* (*Fos*)	Phytopathogenic fungi	Inhibit *Striga* emergence	Nzioki et al. (2016); Rebeka et al. (2013)	*Striga asiatica* and *Striga hermonthica*
Fusarium semitectum var. *majus*	Phytopathogenic fungi	Attack on *Striga* germ tube by the fungal spores and reduce *Striga* emergence by up to 82%	Abbasher et al. (1995)	*Striga hermonthica*
Fusarium solani	Phytopathogenic fungi	Culture filtrates inhibit *Striga* seed germination (mycotoxin)	Ahmed et al. (2001)	*Striga hermonthica*
Fusarium nygamai	Phytopathogenic fungi	Attack on *Striga* germ tube by the fungal spores and reduce *Striga* emergence by up to 97%	Abbasher et al. (1995)	*Striga hermonthica*
**Curvularia geniculate*	Phytopathogenic fungi	Cause disease in *Striga*	Meister and Eplee (1971)	*Striga* spp.
**Sclerotium rolfsii*	Phytopathogenic fungi	Cause disease in *Striga*	Meister and Eplee (1971)	*Striga* spp.
**Cercospora*	Phytopathogenic fungi	Cause disease in *Striga*	Zummo (1977)	*Striga hermonthica*
**Fusarium equiseti*	Phytopathogenic fungi	Cause disease in *Striga*	Zummo (1977)	*Striga hermonthica*

Table 2 *(Continue)*

Pathogen / Agent scientific name	Classification	Action / Response and mechanism	Reference (s)	Target of *Striga* spp.
Alternaria, *Aspergillus*, and *Verticillium*	Phytopathogenic fungi	Reduce *Striga* emergence and biomass	Joel et al. (2013)	*Striga hermonthica*
Glomus mosseae	Fungi	Increase total dry matter and yield of the host plant, reduce *Striga* emergence by up to 62%	Gworgwor and Weber (2003)	*Striga hermonthica*
Glomus clarum *Gigaspora margarita*	Fungi	Reduce *Striga* shoot number, increase the yield of the host plant, and reduce *Striga* germination by up to 97%	Lendzemo et al. (2007)	*Striga hermonthica*
Glomus and *Paraglomus* spp. alone or in combination with *Flavobacterium*, *Azotobacter*, or *Bacillus* sp.	Fungi and Bacteria	Reduce seed germination, interfere with seedling attachment and delay *Striga* emergence	Hassan, Abdelhalim, et al. (2011)	*Striga hermonthica*
Azospirillum brasilense	Bacteria	Inhibit seed germination and radicle elongation (antibiosis)	Miché et al. (2000)	*Striga hermonthica*
Azospirillum brasilense, *Pseudomonas putida*, and other isolates	Bacteria	Inhibit germination by 40–85%, haustorium initiation by 52–85%, and attachment by 78–81%	Hassan, Gani, et al. (2011)	*Striga hermonthica*
Pseudomonas	Bacteria	Reduce *Striga* seed germination via degradation of SLs (interference with host-*Striga* signals)	Ali et al. (2013)	*Striga hermonthica*
Pseudomonas syringae pathovar glycinea (*Psg*)	Bacteria	Promote seed germination (suicidal germination)	Berner et al. (1999)	*Striga hermonthica, Striga aspera*, *Striga gesnerioides*

Table 2 *(Continue)*

Pathogen / Agent scientific name	Classification	Action / Response and mechanism	Reference (s)	Target of *Striga* spp.
Pseudomonas syringae pv. *glycinea* with *Bradyrhizobium japonicum*	Bacteria	Promote seed death (suicidal germination) during non-host rotation	Ahonsi et al. (2003)	*Striga hermonthica*
Pseudomonas fluorescens *Pseudomonas putida*	Bacteria	Inhibit seed germination	Ahonsi et al. (2002); Babalola et al. (2007)	*Striga hermonthica*
Streptomyces and *Rhizobium* sp.	Bacteria	Produce compounds with antibiotic activity and extracellular enzymes, causing *Striga* seed decay	Neondo et al. (2017)	*Striga hermonthica*
Bacillus subtilis GBO3	Bacteria	Prevent *Striga* germination and promote the growth of the host plant	Mounde et al. (2015)	*Striga hermonthica*

*Recorded as the causal agent for diseases in *Striga* (natural control)

sometimes called dust seeds, can be easily spread over a wide range (Teka, 2014; Westwood et al., 2013). Moreover, intimate contact of the parasite with the host plant roots that lasts most of its life cycle makes controlling it more difficult because the control method must not harm the host plant. Further complicating the matter is the complex life cycle of *Striga* (Figure 1). Each phase requires a comprehensive study before any biological control agent can be applied in the field to adjust the optimum time of application.

Although biological control of weed can be effective, it is sometimes uneconomical because it requires in-depth studies on its efficacy, toxicological effects, and environmental effects before any biocontrol agent can be registered. Furthermore, even if the biocontrol agent is isolated locally, some still produce inconsistent results when applied at different locations due to a lack of adaptability to a new environment (Pereg & Mcmillan, 2015; Teka, 2014). For example, the inconsistency of *Fos* isolates to control genetically diverse *S. hermonthica* populations effectively lowers its reliability as an efficient mycoherbicide against *S. hermonthica* in various agroecological zones. Consequently, it hinders the widespread acceptability of *Fos* as a biocontrol agent against *S. hermonthica* (Velivelli et al., 2014; Massart et al., 2015). Furthermore, the viability of microbes may decrease during the traditional delivery system of packaged microbes for long-term storage to be distributed on a farm later because the microbes are still dormant when applied to the soil. Hence, a new and improved delivery technique is required to ensure maximum viability (Mohammadi, 2019; Nzioki et al., 2016).

While microbes effectively modify or degrade the host signals (Figure 2) and/or induce defense responses in the host plant *in vitro*, the in-planta efficacy and the impact on the mutualistic interactions between the host and the symbionts, such as AMF, are still under-explored. Hence, the underlying signal-transduction pathways and their conclusive role in *Striga* suppression are yet to be resolved. Furthermore, the knowledge gap is considered a challenge because the local environment interferes with the efficiency of microbes (Masteling et al., 2019). Finally, the usage of insects as classical biological control is costly and may be affected by political unrest in the African region. In addition, the inundative release of insects is not practical in third-world countries, mainly due to the infeasibility of mass rearing (Kroschel et al., 1999).

CONCLUSION

Various control methods have been applied to manage *Striga,* including chemical, cultural, and biological, with varying degrees of success. The limitations of the chemical and cultural methods and the list of benefits offered by the biological control method motivate the research on the latter and push its adoption. Insects and microorganisms are the two biocontrol agents used to control *Striga*, and they operate via both direct and indirect mechanisms. However, controlling parasitic weeds such as *Striga* poses more

challenges than common weeds. Among them is the unique and complex biology of the parasitic weed, the tiny size of the seeds, and the intimate contact of the parasite with the host plant roots that lasts most of its life cycle. Therefore, more research is needed, especially on the field adaptability of the biocontrol agents, delivery techniques, and *planta* efficacy.

ACKNOWLEDGMENTS

We thank Nurul Izzah Farhana Saidi for her valuable help with manuscript formatting. In addition, Nadia Yasseen Osman received a scholarship from OWSD (The Organization for Women in Science for the Developing World) and Sida (Swedish International Development Cooperation Agency). We also thank Southeast Asian Regional Center for Graduate Study, and Research in Agriculture (SEARCA) for the University Consortium Student Thesis Grant for Research Activities awarded to Nadia Yasseen Osman.

REFERENCES

Abbasher, A. A., Kroschel, J., & Sauerborn, J. (1995). Microorganisms of *Striga hermonthica* in northern Ghana with potential as biocontrol agents. *Biocontrol Science and Technology*, *5*(2), 157-162. https://doi.org/10.1080/09583159550039864

Ahmed, N., Sugimoto, Y., Babiker, A., Mohamed, O., Ma, Y., Inanaga, S., & Nakajima, H. (2001). Effects of *Fusarium solani* isolates and metabolites on *Striga* germination. *Weed Science*, *49*(3), 354-358. https://doi.org/10.1614/0043-1745(2001)049[0354:EOFSIA]2.0.CO;2

Ahonsi, M. O., Berner, D. K., Emechebe, A. M., Lagoke, S. T., & Sanginga, N. (2003). Potential of ethylene-producing *Pseudomonas* in combination with effective N_2-fixing *Bradyrhizobial* strains as supplements to legume rotation for *Striga hermonthica* control. *Biological Control*, *28*(1), 1-10. https://doi.org/10.1016/S1049-9644(03)00051-3

Ahonsi, M. O., Berner, D. K., Emechebem, A. M., & Lagoke, S. T. (2002). Selection of rhizobacterial strains for suppression of germination of *Striga hermonthica* (Del.) Benth. seeds. *Biological Control*, *24*(2), 143-152. https://doi.org/10.1016/S1049-9644(02)00019-1

Ali, H. A., Elamin, H. B., Dirar, H. A., & Sulieman, A. E. (2013). Biological control of *Striga hermonthica* Del. Benth: Screening for bacteria scavenging strigol. *American Journal of Biochemistry*, *3*(4), 89-92. https://doi.org/10.5923/j.ajb.20130304.01

Aquino, B., Bradley, J. M., & Lumba, S. (2021). On the outside looking in: Roles of endogenous and exogenous strigolactones. *The Plant Journal*, *105*(2), 322-334. https://doi.org/10.1111/tpj.15087

Babalola, O., Berner, D., & Amusa, N. (2007). Evaluation of some bacterial isolates as germination stimulants of *Striga hermonthica*. *African Journal of Agricultural Research*, *2*(1), 27-30.

Babiker, A. G. T. (2007). *Striga*: The spreading scourge in Africa. *Regulation of Plant Growth and Development*, *42*(1), 74-87. https://doi.org/10.18978/jscrp.42.1_74

Bale, J. S, van Lenteren, J. C., & Bigler, F. (2008). Biological control and sustainable food production. *Philosophical Transactions of the Royal Society B: Biological Science*, *363*(1492), 761-76. https://doi.org/10.1098/rstb.2007.2182

Barzman, M., Bàrberi, P., Birch, A. N. E., Boonekamp, P. M., Dachbrodt-Saaydeh, S., Graf, B., Hommel, B., Jensen, J. E., Kiss, J., Kudsk, P., Lamichhane, J. R., Messéan, A., Moonen, A. C., Ratnadass, A., Ricci, P., Sarah, J. L., &

Sattin, M. (2015). Eight principles of integrated pest management. *Agronomy for Sustainable Development*, *35*(4), 1199-1215. https://doi.org/10.1007/s13593-015-0327-9

Bashir, W.O. (1987). The potential for biocontrol of witchweeds. In L. J. Musselman (Ed.), *Parasitic weeds in agriculture* (Vol. 1, pp. 183-206). CRC Press.

Bekele, M. (2020). The importance of microorganisms in depleting *Striga* seed banks to enhance *Sorghum* productivity: A review. *International Journal of Advanced Research in Biological Sciences*, *7*(4), 107-115. https://doi.org/10.22192/ijarbs

Berner, D. K., Schaad, N. W., & Völksch, B. (1999). Use of ethylene-producing bacteria for stimulation of *Striga* spp. seed germination. *Biological Control*, *15*(3), 274–282. https://doi.org/10.1006/bcon.1999.0718

Boari, A., Ciasca, B., Pineda-Martos, R., Lattanzio, V. M., Yoneyama, K., & Vurro, M. (2016). Parasitic weed management by using strigolactone-degrading fungi. *Pest Management Science*, *72*(11), 2043–2047. https://doi.org/10.1002/ps.4226

Bonfante, P., & Genre, A. (2010). Mechanisms underlying beneficial plant–fungus interactions in mycorrhizal symbiosis. *Nature Communication*, *1*, 48. https://doi.org/10.1038/ncomms1046

Cardoso, C., Ruyter-Spira, C., & Bouwmeester, H. J. (2011). Strigolactones and root infestation by plant-parasitic *Striga*, *Orobanche* and *Phelipanche* spp. *Plant Science: An International Journal of Experimental Plant Biology*, *180*(3), 414–420. https://doi.org/10.1016/j.plantsci.2010.11.007

Clarke, C. R., Timko, M. P., Yoder, J. I., Axtell, M. J., & Westwood, J. H. (2019). Molecular dialog between parasitic plants and their hosts. *Annual Review of Phytopathology*, *57*, 279–299. https://doi.org/10.1146/annurev-phyto-082718-100043

Cook, R. J., & Baker, K. F. (1983). *The nature and practice of biological control of plant pathogens*. APS Press. https://doi.org/10.2307/2403361

Danhorn, T., & Fuqua, C. (2007). Biofilm formation by plant-associated bacteria. *Annual Review of Microbiology*, *61*, 401–422. https://doi.org/10.1146/annurev.micro.61.080706.093316

David, O. G., Ayangbenro, A. S., Odhiambo, J. J. O., & Babalola, O. O. (2022). *Striga hermonthica*: A highly destructive pathogen in maize production. *Environmental Challenges*, *8*, 100590. https://doi.org/10.1016/j.envc.2022.100590

De Groote, H., Wangareb, L., Kanampiua, F., Odendoc, M., Dialloa, A., Karayaa, H., & Friesend, D. (2008). The potential of a herbicide resistant maize technology for *Striga* control in Africa. *Agricultural Systems*, *97*(1-2), 83–94. https://doi.org/10.1016/j.agsy.2007.12.003

Druille, M., Omacini, M., Golluscio, R. A., & Cabello, M. N. (2013). Arbuscular mycorrhizal fungi are directly and indirectly affected by glyphosate application. *Applied Soil Ecology*, *72*, 143–149. https://doi.org/10.1016/j.apsoil.2013.06.011

Eizenberg, H., Hershenhorn, J., Ephrath, J. H., & Kanampiu, F. (2013). Chemical control. In D. M. Joel, J. Gressel, & L. J. Musselman (Eds.), *Parasitic Orobanchaceae: Parasitic mechanisms and control strategies* (pp. 415–432). Springer. https://doi.org/10.1007/978-3-642-38146-1_23

Erdogan, P. (2021). Parasitic plants in agriculture and management. In A. M. Gonzalez & H. A. Sato (Eds.), *Parasitic plants*. IntechOpen. https://doi.org/10.5772/intechopen.98760

Fernández-Aparicio, M., Bernard, A., Falchetto, L., Marget, P., Chauvel, B., Steinberg, C., Morris, C. E., Gibot-Leclerc, S., Boari, A., Vurro, M., Bohan, D. A., Sands, D. C., & Reboud, X. (2017). Investigation of amino acids as herbicides for control of *Orobanche minor* parasitism in red clover. *Frontiers in Plant Science*, *8*, 842. https://doi.org/10.3389/fpls.2017.00842

Fernández-Aparicio, M., Delavault, P., & Timko, M. P. (2020). Management of infection by parasitic weeds: A review. *Plants*, *9*(9), 1184. https://doi.org/10.3390/plants9091184

Gafar, N., Hassan, M., Rugheim, A., Osman, A., Mohamed, I., Abdelgani, M., & Babiker, A. G. T. (2015). Evaluation of endophytic bacterial isolates on germination and haustorium initiation of *Striga hermonthica* (Del.) Benth. *International Journal of Farming and Allied Sciences*, *4*(4), 302–308.

Gamir, J., Torres-Vera, R., Rial, C., Berrio, E., de Souza Campos, P. M., Varela, R. M., Macias, F. A., Pozo, M. J., Flors, V., & Lopez-Raez, J. A. (2020). Exogenous strigolactones impact metabolic profiles and phosphate starvation signalling in roots. *Plant, Cell and Environment*, *43*(7), 1655-1668. https://doi.org/10.1111/pce.13760

Gworgwor, N. A., & Weber, H. C. (2003). Arbuscular mycorrhizal fungi-parasite-host interaction for the control of *Striga hermonthica* (Del.) Benth. in sorghum [*Sorghum bicolor* (L.) Moench]. *Mycorrhiza*, *13*, 277-281. https://doi.org/10.1007/s00572-003-0238-5

Hailu, G., Niassy, S., Zeyaur, K.R., Ochatum, N., & Subramanian, S. (2018). Maize-legume intercropping and push-pull for management of fall armyworm, stemborers, and *Striga* in Uganda. *Agronomy Journal*, *110*(6), 2513-2522. https://doi.org/10.2134/agronj2018.02.0110

Hasan, M., Ahmad-Hamdani, M.S., Rosli, A.M., Hamdan, H. (2021). Bioherbicides: An eco-friendly tool for sustainable weed management. *Plants*, *10*(6), 1212. https://doi.org/10.3390/plants10061212

Hassan, M. M., Abdelhalim, T. S., Yagoub, S. O., Osman, A. G., Gani, M. E. A., & Babiker, A. G. E. (2011). Effects of arbuscular mycorrhiza fungi (AMF), plant growth promoting bacteria (PGPR) and interaction on *Striga hermonthica* management in sorghum. *International Journal of Agriculture: Research and Review*, *1*, 107–115.

Hassan, M. M., Azrag, M. A., Rugheim, A. M. E., Abusin, R. M. A., Elnasikh, M. H., Modawi, H., Ahmed, M. M., Abakeer, R. A., Osman, A. G., Abdelgani, M. E., & Babiker, A. G. E. (2019). Potential of *Trichoderma harzianum* as a biocontrol agent against *Striga hermonthica* in sorghum. *International Journal of Current Microbiology and Applied Sciences*, *8*(03), 195-206. https://doi.org/10.20546/ijcmas.2019.803.027

Hassan, M. M., Gani, M. E. A., & Babiker, A. G. T. (2011). Effects of bacterial strains and isolates on *in situ* germination, subsequent developmental stage of *Striga hermonthica* on to sorghum roots. *Advances in Environmental Biology*, *5*(10), 3263–3269.

Haussmann, B. I. G., Hess, D. E., Welz, H. G., & Geiger, H. (2000). Improved methodologies for breeding striga-resistant sorghums. *Field Crop Research*, *66*(3), 195-211. https://doi.org/10.1016/S0378-4290(00)00076-9

International Biocontrol Manufacturers Association. (2018). *IBMA white paper: New EU regulatory framework for bioprotection agents*. IBMA. https://ibma-global.org/latest-news-2/ibma-white-paper-ibma-vision-on-how-to-improve-regulation-in-the-european-union-a-new-eu-regulatory-framework-for-bioprotection-agents

Jamil, M., Charnikhova, T., Verstappen, F., Ali, Z., Wainwright, H., & Bouwmeester, H. J. (2014). Effect of phosphate-based seed priming on strigolactone production and *Striga hermonthica* infection in cereals. *Weed Research*, *54*(3), 307–313. https://doi.org/10.1111/wre.12067

Jamil, M., Kountche, B. A., & Al-Babili, S. (2021). Current progress in *Striga* management. *Plant Physiology*, *185*(4), 1339–1352. https://doi.org/10.1093/plphys/kiab040

Joel, D. M., Gressel, J., & Musselman, L. J. (Eds.) (2013). *Parasitic Orobanchaceae: Parasitic mechanisms and control strategies*. Springer. https://doi.org/10.1007/978-3-642-38146-1

Kroschel, J., Jost, A., & Sauerborn, J. (1999). Insects for *Striga* control – Possibilities and constraints. In J. Kroschel, H. Mercer-Quarshie, & J. Sauerborn (Eds.), *Advances in parasitic weed control at on-farm level: Joint action to control* Striga *in Africa* (Vol. 1, pp.117-132). Margraf Publishers.

Kumar, J., Ramlal, A., Mallick, D., & Mishra, V. (2021). An overview of some biopesticides and their importance in plant protection for commercial acceptance. *Plants*, *10*(6), 1185. https://doi.org/10.3390/plants10061185

Labrada, R. (2008). Farmer training on parasitic weed management. In R. Labrada (Ed.), *Progress on farmer training in parasitic weed management* (pp. 1-5). Food and Agriculture Organization of the United Nations.

Lendzemo, V. W., Kuyper, T. W., Matusova, R., Bouwmeester, H. J., & Ast, A. V. (2007). Colonization by arbuscular mycorrhizal fungi of sorghum leads to reduced germination and subsequent attachment and emergence of *Striga hermonthica*. *Plant Signaling and Behavior*, *2*(1), 58–62. https://doi.org/10.4161/psb.2.1.3884

Lo´pez-Ra´ez, J. A., Charnikhova, T., Ferna´ndez, I., Bouwmeester, H., & Pozo, M. J. (2011). Arbuscular mycorrhizal symbiosis decreases strigolactone production in tomato. *Journal of Plant Physiology*, *168*(3), 294–297. https://doi.org/10.1016/j.jplph.2010.08.011

Massart, S., Perazzolli, M., Höfte, M., Pertot, I., & Jijakli, M. H. (2015). Impact of the omic technologies for understanding the modes of action of biological control agents against plant pathogens. *Biocontrol*, *60*(6), 725–746. https://doi.org/10.1007/s10526-015-9686-z

Masteling, R., Lombard, L., de Boer, W., Raaijmakers, J. M., & Dini-Andreote, F. (2019). Harnessing the microbiome to control plant parasitic weeds. *Current Opinion in Microbiology*, *49*, 26–33. https://doi.org/10.1016/j.mib.2019.09.006

Meister, C. W., & Eplee, R. E. (1971). Five new fungal pathogens of witchweed (*Striga lutea*). *Plant Disease Reporter*, *55*, 861-863.

Miché, L., Bouillant, M. L., Rohr, R., Sallé, G., & Bally, R. (2000). Physiological and cytological studies on the inhibition of *Striga* seed germination by the plant growth-promoting bacterium *Azospirillum brasilense*. *European Journal of Plant Pathology*, *106*, 347–351. https://doi.org/10.1023/A:1008734609069

Mohammadi, G. (2019). Can soil microorganisms reduce broomrape (*Orobanche* spp.) infestation in cropping systems?. In V. Kumar, R. Prasad, M. Kumar, & D. Choudhary (Eds.), *Microbiome in plant health and disease* (pp. 385–402). Springer. https://doi.org/10.1007/978-981-13-8495-0_17

Mounde, L. G., Anteyi, W. O., & Rasche, F. (2020). Tripartite interaction between *Striga* spp., cereals, and plant root-associated microorganisms: A review. *CABI Reviews*, *15*(005), 1-17. https://doi.org/10.1079/PAVSNNR202015005

Mounde, L. G., Boh, M. Y., Cotter, M., & Rasche, F. (2015). Potential of rhizobacteria for promoting sorghum growth and suppressing *Striga hermonthica* development. *Journal of Plant Diseases and Protection*, *122*, 100–106. https://doi.org/10.1007/BF03356537

Mutuku, J. M., Cui, S., Yoshida, S., & Shirasu, K. (2021). Orobanchaceae parasite-host interactions. *The New Phytologist*, *230*(1), 46–59. https://doi.org/10.1111/nph.17083

Mwangangi, I. M., Büchi, L., Haefele, S. M., Bastiaans, L., Runo, S., & Rodenburg, J. (2021). Combining host plant defence with targeted nutrition: Key to durable control of hemiparasitic *Striga* in cereals in sub-Saharan Africa? *New*

Phytologist, *230*(6), 2164-2178. https://doi.org/10.1111/nph.17271

Myers, J. H., & Cory, J. S. (2017). Biological control agents: Invasive species or valuable solutions? In M. Vilà & P. E. Hulme (Eds.), *Impact of biological invasions on ecosystem services* (Vol. 12, pp. 191-202). Springer. https://doi.org/10.1007/978-3-319-45121-3_12

Ndambi, B., Cadisch, G., Elzein, A., & Heller, A. (2011). Colonization and control of *Striga hermonthica* by *Fusarium oxysporum f.* sp. *strigae*, a mycoherbicide component: An anatomical study. *Biological Control*, *58*(2), 149-159. https://doi.org/10.1016/j.biocontrol.2011.04.015

Neondo, J. O., Alakonya, A. E., & Kasili, R. W. (2017). Screening for potential *Striga hermonthica* fungal and bacterial biocontrol agents from suppressive soils in Western Kenya. *BioControl*, *62*, 705–717. https://doi.org/10.1007/s10526-017-9833-9

Nzioki, H. S., Oyosi, F., Morris, C. E., Kaya, E., Pilgeram, A. L., Baker, C. S., & Sands, D. C. (2016). *Striga* biocontrol on a toothpick: A readily deployable and inexpensive method for smallholder farmers. *Frontiers in Plant Science*, *7*, 1121. https://doi.org/10.3389/fpls.2016.01121

Okazawa, A., Samejima, H., Kitani, S., Sugimoto, Y., & Ohta, D. (2021). Germination stimulatory activity of bacterial butenolide hormones from *Streptomyces albus* J1074 on seeds of the root parasitic weed *Orobanche minor*. *Journal of Pesticide Science*, *46*(2), 242–247. https://doi.org/10.1584/jpestics.D21-014

Parker, C., & Riches, C. R. (1993). *Parasitic weed of the world: Biology and control*. CAB International.

Pereg, L., & McMillan, M. (2015). Scoping the potential uses of beneficial microorganisms for increasing productivity in cotton cropping systems. *Soil Biology and Biochemistry*, *80*, 349–358. https://doi.org/10.1016/j.soilbio.2014.10.020

Rebeka, G., Shimelis, H., Laing, M.D., Tongoona, P., & Mandefro, N. (2013). Evaluation of sorghum genotypes compatibility with *Fusarium oxysporum* under *Striga* infestation. *Crop Science*, *53*(2), 385–393. https://doi.org/10.2135/cropsci2012.02.0101

Reigosa, R. M. J., Pedrol, N., & Gonzalez, L. (2006). *Allelopathy: A physiological process with ecological implications*. Springer. https://doi.org/10.1007/1-4020-4280-9

Samejima, H., & Sugimoto, Y. (2018). Recent research progress in combatting root parasitic weeds. *Biotechnology and Biotechnological Equipment*, *32*(2), 221-240. https://doi.org/10.1080/13102818.2017.1420427

Sibhatu, B. (2016). Review on *Striga* weed management. *International Journal of Life Sciences Research*, *2*(2), 110-120.

Smith, M. C., & Webb, M. (1996). Estimation of the seedbank of *Striga* spp. (Scrophulariaceae) in Malian fields and the implications for a model of biocontrol of *Striga hermonthica*. *Weed Research*, *36*(1), 85-92. https://doi.org/10.1111/j.1365-3180.1996.tb01804.x

Smith, M. C., Holt, J. S., & Webb, M. (1993). Population model of the parasitic weed *Striga hermonthica* (Scrophulariaceae) to investigate the potential *Smicronyx umbrinus* (Coleoptera: Curculionidae) for biological control in Mali. *Crop Protection*, *12*(6), 470-476. https://doi.org/10.1016/0261-2194(93)90010-G

Stenberg, J. A., Sundh, I., Becher, P. G., Björkman, C., Dubey, M., Egan, P. A., Friberg, H., Gil, J. F., Jensen, D. F., Jonsson, M., Karlsson, M., Khalil, S., Ninkovic, V., Rehermann, G., Vetukuri, R. R., & Viketoft, M. (2021). When is it biological control? A framework of definitions, mechanisms, and classifications. *Journal of Pest*

Science, *94*(3), 665-676. https://doi.org/10.1007/s10340-021-01354-7

Taylor, A., Martin, J., & Seel, W. E. (1996). Physiology of the parasitic association between maize and witchweed (*Striga hermonthica*): Is ABA involved?. *Journal of Experimental Botany*, *47*(8), 1057-1065. https://doi.org/10.1093/jxb/47.8.1057

Teka, H. B. (2014). Advance research on *Striga* control: A review. *African Journal of Plant Science*, *8*(11), 492-506. https://doi.org/10.5897/AJPS2014.1186

Uludag, A., Uremis, I., & Arslan, M. (2018). Biological weed control. In K. J. Chauhan (Ed.), *Non-chemical weed control* (pp. 115-132). Academic Press. https://doi.org/10.1016/B978-0-12-809881-3.00007-3

van Wilgen, B. W., Moran, V. C., & Hoffmann, J. H. (2013). Some perspectives on the risks and benefits of biological control of invasive alien plants in the management of natural ecosystems. *Environmental Management*, *52*(3), 531–540. https://doi.org/10.1007/s00267-013-0099-4

Velivelli, S. L., De Vos, P., Kromann, P., Declerck, S., & Prestwich, B. D. (2014). Biological control agents: From field to market, problems, and challenges. *Trends in Biotechnology*, *32*(10), 493-496. https://doi.org/10.1016/j.tibtech.2014.07.002

Waruru, M. (2013). *East Africa: Deadly* Striga *weed spreading across Eastern Africa*. https://www.ghanamma.com/2013/02/08/east-africa-deadly-striga-weed-spreading-across-eastern-africa/

Westwood, J. (2013). The physiology of the established parasite–host association. In D. M. Joel, J. Gressel, & L. Musselman (Eds.), *Parasitic Orobanchaceae: Parasitic mechanisms and control strategies* (pp. 87–114). Springer. https://doi.org/10.1007/978-3-642-38146-1_6

Xie, X., Yoneyama, K., & Yoneyama, K. (2010). The strigolactone story. *Annual Review of Phytopathology*, *48*, 93–117. https://doi.org/10.1146/annurev-phyto-073009-114453

Zummo, N., (1977). Diseases of giant witchweed, *Striga hermonthica* in West Africa. *Plant Disease Reporter*, *61*(5), 428-430.

Pertanika J. Trop. Agric. Sci. 46 (1): 197 - 212 (2023)

PERTANIKA JOURNALS

TROPICAL AGRICULTURAL SCIENCE

Journal homepage: http://www.pertanika.upm.edu.my/

Diversity, Abundance, and Distribution of Macroalgae in Coastal Ecotourism Areas — A Case Study at Baluran National Park, Situbondo, Indonesia

Dinda Henes Aprilia[1], Muhammad Browijoyo Santanumurti[2,3], Mamdoh T. Jamal[3], Endang Dewi Masithah[4] and Suciyono[1,2]*

[1]Aquaculture Study Program, School of Health and Natural Science (SIKIA), Universitas Airlangga, 68422 Banyuwangi, East Java, Indonesia
[2]Department of Aquaculture, Faculty of Fisheries and Marine, Universitas Airlangga, 60115 Surabaya, East Java, Indonesia
[3]Department of Marine Biology, Faculty of Marine Sciences King Abdulaziz University, 21589 Jeddah, Mekkah, Kingdom of Saudi Arabia
[4]Department of Marine Science, Faculty of Fisheries and Marine, Universitas Airlangga, 60115 Surabaya, East Java, Indonesia

ABSTRACT

Indonesia is a mega biodiversity country with abundant macroalgae. The macroalgae are distributed along the coast and function to maintain the balance of the coastal marine ecosystem, including in Bama Beach, Baluran National Park, Situbondo, Indonesia. This study was to determine the abundance, distribution, and diversity of macroalgae in Bama Beach Baluran National Park, East Java, between April 2019 and June 2019. The research was conducted with a purposive sampling method at two stations, each consisting of five substations using transect blocks. Five species of macroalgae from the Phaeophyceae class (*Padina australis*, *Sargassum aquifolium*, *Polycladia myrica*, *Eucheuma edule*, and *Dictyota pinnatifida*), a Rhodophyta (*Jania pumila*), and Chlorophyta (*Halimeda macroloba*) were found in the study site. *Padina australis* was a species that had the highest abundance and dominated the observation station. Nonetheless, according to the Shannon-Weaver Index in the study area, overall macroalgae diversity was classified as a low category with a value of 0.35. The high availability of nutrients influences these conditions in ecosystems

ARTICLE INFO

Article history:
Received: 26 July 2022
Accepted: 17 October 2022
Published: 03 February 2023

DOI: https://doi.org/10.47836/pjtas.46.1.11

E-mail addresses:
Dindahenes71@gmail.com (Dinda Henes Aprilia)
m.browijoyo.s@fpk.unair.ac.id (Muhammad Browijoyo Santanumurti)
mjamal1@kau.edu.sa (Mamdoh T. Jamal)
endang_dm@fpk.unair.ac.id (Endang Dewi Masithah)
suciyono@fpk.unair.ac.id (Suciyono)
* Corresponding author

ISSN: 1511-3701
e-ISSN: 2231-8542

with the domination of *Padina australis*, followed by *Sargassum aquifolium* at Station I and II.

Keywords: Baluran National Park, diversity, macroalgae

INTRODUCTION

Indonesia is a maritime country with a coastline of 95,161 km and has a high potential for marine resources, such as macroalgae (Kusmana & Hikmat, 2015). Previous studies have shown that Indonesia produces the highest macroalgae in biomass culture in Southeast Asia, surpassing the Philippines (Hurtado et al., 2019; Rimmer et al., 2021). Another study also stated that 555 seaweed species are found in Indonesia, and 55 of them have high economic value, such as *Gracilaria* and *Euchema* (Meinita et al., 2021). As the primary producer in the coastal ecosystem, macroalgae are not a plant but an informal group of protists (Eliáš, 2021). Macroalgae are divided into three groups: brown algae (Phaeophyceae), green algae (Chlorophyta), and red algae (Rhodophyta) (Oryza et al., 2017). The presence of macroalgae is essential due to its function as a nursery, spawning, and feeding grounds for small fish and herbivorous animals (Burkepile et al., 2013; Rasher et al., 2013). It maintains the biodiversity of the coastal ecosystem (Wade et al., 2020).

Baluran National Park represents the forest ecosystem in Java Island (Indonesia), which consists of savanna, beach, coastal mangrove forests, and jungles (Nuzula et al., 2017). Bama Beach, with a length of 42 km, has a high diversity of macroalgae due to its clean and well-maintained sandy substrate (Arisandy et al., 2012). Therefore, Bama Beach is a suitable place to host a variety of aquatic organisms. At least eight macroalgae species were found in the recent study, with the dominance of *Padina australis* (Anugrah et al., 2019). This area also has a seagrass bed with a 48.9% abundance composition dominated by *Cymodocea serrulata* (Ulkhaq et al., 2016). Bama is often visited for tourism, research, and educational purposes. However, using this area as a tourist area threatens the preservation of existing ecosystems, including coastal areas. According to a previous study, there was an increase in visitors during the 2014–2015 period, which reached nearly sixty thousand visitors, an increase of 50% from the previous year due to its beautiful coastal area (Nuzula et al., 2017). A previous study stated that the development of the tourism sector degrades the quality of the ecosystem and organisms in Baluran National Park (Purnomo et al., 2020). Therefore, it will be a threat to the existing macroalgae ecosystem.

The purpose of this study was to observe the distribution of macroalgae to find out the phenomena and dynamics of ecosystems that occur as a basis for area management. The distribution of macroalgae in intertidal ecosystems depends on environmental conditions, such as location, shore level, salinity, temperature, and organic nutrients (Thongroy et al., 2007). This information is important to base an integrated understanding of conservation and restoration policies because if the water conditions change and are not following

their living conditions, macroalgae will be threatened. Furthermore, the movement of water and nutrients also distributed therein has an important role in determining seaweed productivity (Anderson et al., 2005). Baluran National Park has a dry climate type F with temperatures of 27.2 – 30.9 °C, average humidity of 77%, and wind speed of 7 knots (Nuzula et al., 2017). Furthermore, the rainy season occurs from November to April, while the dry season starts from April to October (Istomo & Ghifary, 2021).

MATERIAL AND METHODS

Research Location

The research was conducted in Bama Beach, Baluran National Park, East Java, Indonesia. The location is a semidiurnal tidal pattern described in a previous study (Putrisari et al., 2017). The location has a variety of habitats, such as mangroves, coral reefs, savanna, and beach. Moreover, these areas have a physical landscape structure for beach tourism, snorkeling, diving, and mangrove tours. Two stations were decided based on a purposive sampling method following the characteristic land uses, i.e., Station I (7°50'40.1" S and 114°27'41.5" E), which was an open tourist area. At the same time, Station II (7°50'40.7"S and 114°27'40.3"E) was an area protected with mangrove vegetation (Figure 1). The consideration for choosing this location is that both stations are in an open-access area for visitors. Other areas are inaccessible because there are many wild animals in the national park.

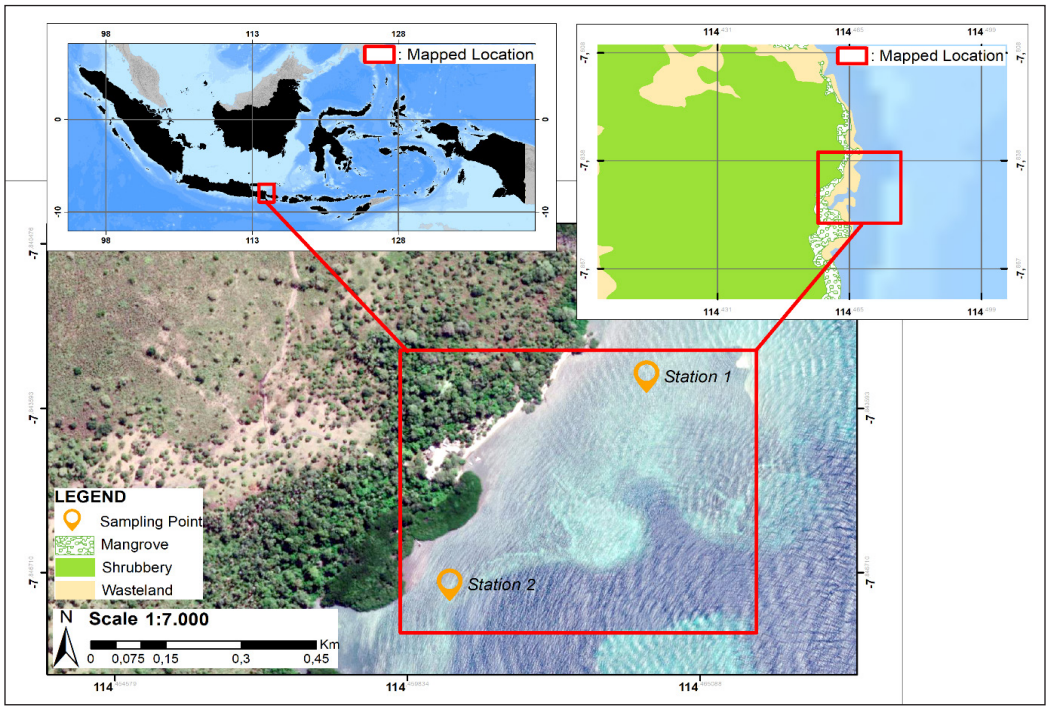

Figure 1. Map location of this study

Data Collection

The data collection was done in April, May, and June 2019. The sampling was conducted using the modified 2 m × 2 m transect block method installed from the coastline 50 m into the sea (Lelloltery et al., 2021). Furthermore, there were five sub-stations in each sample station with a distance between each sub-station of 10 m as replication. A camera (SeaLife Micro 3.0, Sony, Japan) observed the number of macroalgae samples when the tidal was low by diving at each sub-station. The representative macroalgae were taken at each transect block plot, preserved with 4% formaldehyde (Merck, German), and labeled to be analyzed in the laboratory (Khalil et al., 2021).

Analytical Method

The macroalgae identification was conducted by comparing external morphological characteristics in the previous study (Al-Yamani et al., 2015). The identified characteristics were body shape, color patterns, and thallus shape. Each characteristic was compared with the pictures in the references book, and the type of macroalgae was identified according to the compatibility between the sample and the references book. Also, chemical and physical parameters were measured from each station simultaneously with biota collection. It consists of in-situ parameters, i.e., temperature (AMTAST EC910, USA), sea surface current (Secchi Disk APAL-SCD, Indonesia), pH (AMTAST EC910, USA), salinity (refractometer; Atagao, Japan), and dissolved oxygen (DO) (AMTAST EC910, USA). In the meantime, the *ex-situ* parameters (nitrate and phosphate) were conducted using a volume sampler of 250 mL polyethylene bottle and kept in a cold box for analysis in the laboratory (Takarina et al., 2019). The nutrient analysis was conducted by spectrophotometer (Model AMV01 AMTAST, USA), as described in a previous study (Emilia, 2019). Soil and sediment samples from the two sampling stations were analyzed using the gravimetric triangle method to determine the criteria, the percentage of sediment composition, and the type of constituent textures (Anggraini et al., 2020).

Data Analysis

The distribution of macroalgae found at each research station was tabulated and presented descriptively. Furthermore, to determine the diversity of macroalgae (*H'*) by quantitative data (involving a number of individuals of each species or ni and the number of individuals of all types or N), the Shannon-Weaver formula was used (Shanon & Weaver, 1949). In addition, the evenness index value (*E*) was used to describe the individual components of each species contained in a community, and the dominance of macroalgae in waters was determined according to the Simpson Dominance Index (*C*) (Simpson, 1949). Finally, the Important Value Index (IVI) was added for assessing the importance of population structure (Curtis & Mcintosh, 1950).

$$H' = -\sum \left(\frac{ni}{N}\right) x \ ln \ (\frac{ni}{N})$$

Note.
H' = index of diversity
ni = number of individuals of each species
N = number of individuals of all types

$$E = \left(\frac{H'}{ln\ S}\right)$$

Note.
E = equitability index
H' = index of diversity
S = number of species

$$C = \sum \left(\frac{ni}{N}\right)^2$$

Note.
C = Index of dominance
ni = The number of individuals of each species
N = Number of individuals of all types

$$\mathbf{IVI = RD + RF + RDO}$$

Note.
IVI = Important Value Index
RD = Relative density
RF = Relative frequency
RDO = Relative dominance

The data was presented in graphs or images, then descriptively analyzed based on the relevant literature in discussing and concluding the results.

RESULTS AND DISCUSSION

Water Parameters

The results of the water parameters at both stations were generally suitable for the survival of macroalgae (Table 1). The data salinity, pH, and temperature from Station I showed 29.41 $g.L^{-1}$, 8.03, and 28.87 ^oC, while the data salinity, pH, and temperature from Station II showed 30.6 $g.L^{-1}$, 8.16, and 30.06 ^oC. Climate change impacts the temperature of seawater (Doney et al., 2012; Gaitán-espitia et al., 2014). The ideal temperature for macroalgae survival is 25–35 ^oC. Meanwhile, good salinity for macroalgae learning and success is 28–33 $g.L^{-1}$. Salinity that is too high or too low disrupts macroalgae growth (Kamer &

Table 1
Physical-chemical water quality measurement in the site study (90 samples size for each parameter at each station)

Parameters	Unit	Station I	Station II	Macroalgae's habitat standard
Temperature	^oC	28.87 ± 1.35	30.06 ± 1.17	24 – 32
Dissolved oxygen	$mg.L^{-1}$	7.33 ± 0.40	7.73 ± 0.47	8.4 – 9.2
Salinity	$g.L^{1}$	29.41 ± 1.80	30.6 ± 1.21	28 - 33
Sea surface current	$cm.s^{-1}$	50.36 ± 13.8	43.12 ± 14.79	20 – 40
pH		8.03 ± 0.11	8.16 ± 0.35	7 – 8.5
Nitrate (NO_3)	$mg.L^{-1}$	8.63 ± 1.19	13.33 ± 1.52	>0.04
Phosphate (PO_4)	$mg.L^{-1}$	0.26 ± 0.01	0.25 ± 0.02	>0.1
Substrate percentage		sand (45%), loam (20%), clay (35%)	sand (40%), loam (40%), clay (20%)	*Depend on macroalgae species
Substrate categories		Sandy clay	Sandy loam	

Fong, 2000). On the other hand, because pH is a carbon dioxide (CO_2) balance in the water, small fluctuations in value can affect macroalgae life (Gaitán-espitia et al., 2014). A common feature of these changes is a deterioration in water quality enriched with resources, particularly nitrogen nutrients, from land-based activities (Wahl et al., 2015).

In this study, the dissolved oxygen, nitrate, and phosphate values from Station I were 7.33 mg.L^{-1}, 8.63 mg.L^{-1}, and 0.26 mg.L^{-1}, respectively, with a substrate of sandy clay. Meanwhile, the dissolved oxygen, nitrate, and phosphate values from Station II were 7.33 mg.L^{-1}, 13.33 mg.L^{-1}, and 0.25 mg.L^{-1} with a substrate of sandy loam. Seaweed cannot survive in water with a low-brightness mud substrate. Therefore, clear waters ranging from 2 to 12 m with a sandy mud substrate are ideal. Furthermore, based on surface sea current measurements taken during observations, the speed range of the sea surface currents around the sampling range is approximately 30 m.s^{-1} (Figure 2). The speed of ocean currents significantly impacts macroalgae colony survival because they transport organic material that affects brightness. Furthermore, the high current velocity can uproot macroalgae from the substrate. Therefore, the ideal current for macroalgae growth ranges between 20 and 40 m.s^{-1} (Marianingsih et al., 2013).

Macroalgae Diversity

A total of seven macroalgae species were found during the study (Table 2). They consisted of the Phaeophyta class with five species (*Padina australis*, *Sargassum aquifolium*, *Polycladia myrica*, *Euleuma edule*, and *Dictyota pinnatifida*) and

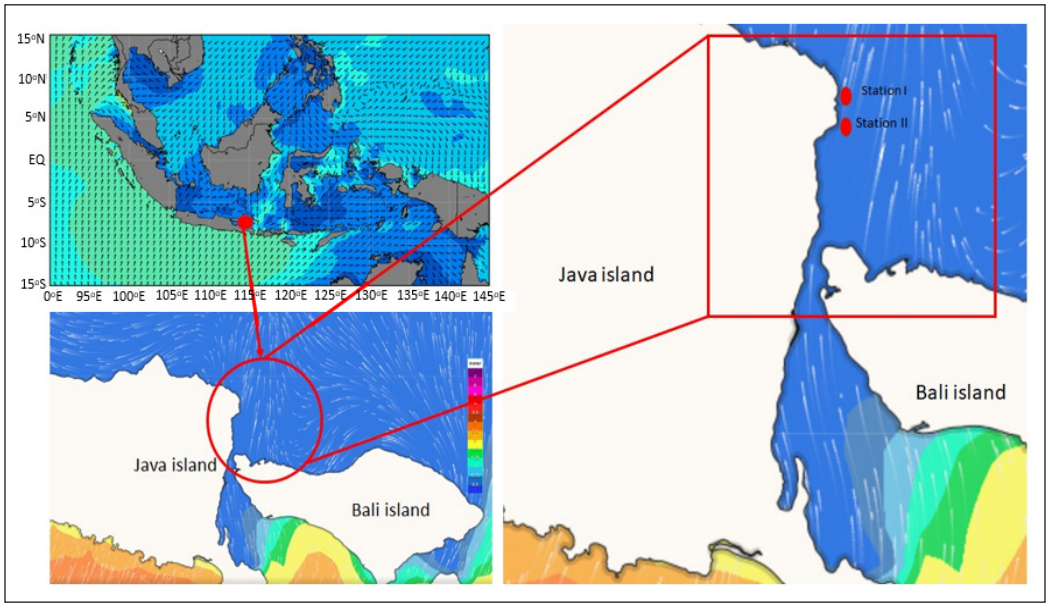

Figure 2. Characteristics of the sea at the study site (Badan Meteorologi, Klimatologi, dan Geofisika [BMKG], 2022)

Table 2
Macroalgae distribution at site study and habitat in the study location

Species	April 2019		May 2019		June 2019		Type of substrate
	St. I	St. II	St. I	St. II	St. I	St. II	
Padina australis	+	+	+	+	+	+	Sand and coral
Sargassum aquifolium	+	+	+	+	+	+	Sandy
Polycladia myrica	+	+	+	+	+	-	Sandy
Jania pumila	-	-	-	-	+	-	Coral and stone
Eucheuma edule	-	-	-	-	+	+	Coral and stone
Dictyota pinnatifida	+	-	-	-	-	-	Sandy
Halimeda macroloba	+	-	-	-	-	-	The mud around the seagrass

Note. + = Present; - = Absent

one species from the Rhodophyta and Chlorophyta classes (*Jania pumila* and *Halimeda macroloba)*. *Padina australis*, *Sargassum aquifolium*, and *Polycladia myrica* were found at each station for most of the observation. In contrast, *Jania pumila* and *Eucheuma edule* were only found at Station I in June. Furthermore, *Dictyota pinnatifida* and *Halimeda macroloba* also were only found in April.

The abundance data of macroalgae is presented in Table 3 and Figure 3. *Padina australis* and *Sargassum aquifolium* appeared consistently in each station. The previous study showed that *Padina* and *Sargassum* were found in Situbondo (Anugrah et al., 2019; Indahyani et al., 2019; Siswanto, 2005). Their presence indicated that water quality parameters in Bama Beach showed optimal values for the growth of *Padina australis* and *Sargassum aquifolium*, especially for nitrate and phosphate (Supardi & Nugroho et al., 2019; Wahyuningtyas et al., 2020). Nitrates and phosphorus also have a role in increasing the growth of macroalgae (Xu et al., 2020).

Interestingly, the presence of *Jania pumila*, *Euchema edule*, *Dictyita pinnatifida*, and *Halimeda macrobola* was not stable between April to June. The increase or decrease of macroalgae species in an area normally occurs. Previous research stated that this was caused by the natural process of species succession in the community (Jung & Choi, 2022). This phenomenon happens immediately with the appearance of ephemeral species after the detachment of old algae (Tytlyanov et al., 2014). For example, the presence of *Jania pumila* and *Eucheuma edule* only appeared in June might be due to currents that carried these types of seaweed from other areas and grew in Bama Beach. Meanwhile, ocean currents brought *Dictyota pinnifida* and *Halimeda macroloba* to Bama Beach in April. A previous study stated that in May and June (the new dry season), a southeast monsoon would appear in Indonesia and cause the macroalgae to bloom and more abundance (Setyawidati et al., 2018). However, when the southeast monsoon comes, the current will flow from Australia to Indonesia and

Table 3
Macroalgae abundance at site study and habitat in the study location

Species	April 2019		May 2019		June 2019		Total	
	St. I	St. II	St. I	St. II	St. I	St. II	St. I	St. II
Padina australis	2	5	2	1	2	1	6	7
Sargassum aquifolium	0	1	1	1	0	0	1	2
Polycladia myrica	1	1	0	1	0	0	1	2
Jania pumila	0	0	0	0	1	0	1	0
Eucheuma edule	0	0	0	0	1	1	1	1
Dictyota pinnatifida	2	2	0	0	0	0	2	2
Halimeda macroloba	1	0	0	0	0	0	1	0

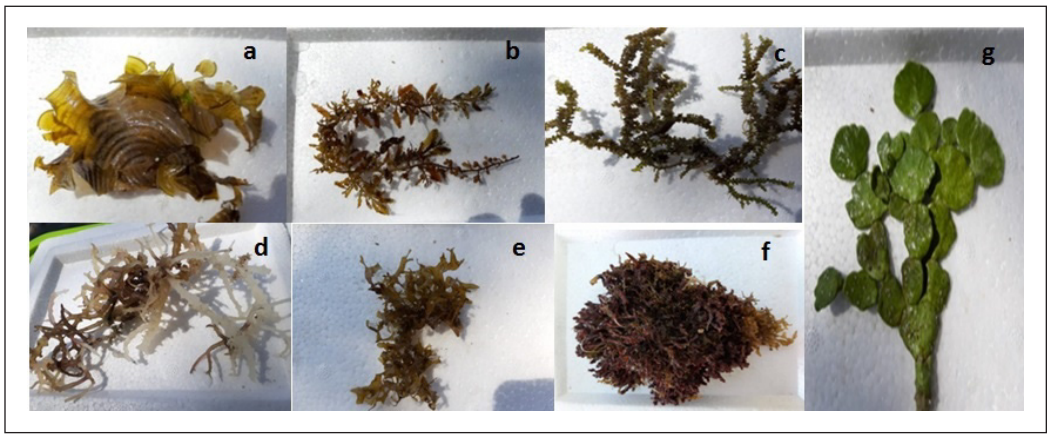

Figure 3. Macroalgae species discovered at the study site: a: *Padina australis*, b: *Sargassum aquifolium*, c: *Polycladia myrica*, d: *Eucheuma edule*, e: *Dictyota pinnatifida*, f: *Jania pumila*, g: *Halimeda macroloba*

change other water quality parameters (temperature, DO, pH) due to upwelling so that it can change the abundance of aquatic organisms (Hasyim et al., 2022).

DO parameters in this study were also low (7.33 ± 0.40 for Station I and 7.73 ± 0.47 for Station II). It causes the presence of *Jania pumila*, *Euchema edule*, *Dictyita pinnatifida*, and *Halimeda macrobola* to be unstable at the study site. DO is essential since macroalgae will invert it as oxygen for life (Subur et al., 2021). DO deficiency can cause mortality in macroalgae (Solidoro et al., 1997). This case differs from *Padina australis*, which is present every month in this study. Previous research stated that *Padina australis* could live with a DO value of only 3.51 ± 0.53 mg.L^{-1} at Lae-lae Island Makassar Marine Waters, South Sulawesi, Indonesia (Supardi & Nuhroho, 2019). Likewise, *Sargassum aquifolium* was also found in this study every month. Wahyuningtyas et al. (2020) stated that these macroalgae could live at DO 5.8 mg.L^{-1} in Sumenep, Madura, Indonesia. It indicated that the two macroalgae could be tolerant of low DO.

Species succession is also related to the different abilities of macroalgae to adapt to the environment. Environmental changes such as climate changes, land-use changes in coastal areas, and pollution affect the distribution, abundance, and physiological changes in aquatic organisms, including macroalgae (Firth & Hawkins, 2011). Macroalgae are sessile organisms; thus, they are susceptible to environmental changes and have a limited distribution (Coleman et al., 2011; Prathep et al., 2008). Janah et al. (2021) explain that there were at least three patterns in the distribution patterns, namely uniform, random, and clustered patterns. In addition, each species of macroalgae has a different distribution and habitat, which could affect the morphological characteristics, such as color, the shape of the thallus, and holdfast (Poloczanska et al., 2013).

This study revealed that *Sargassum aquifolium, Polycladia myrica*, and *Dicolota pinnatifida* have the form of stolon, distributed in sandy substrates. Meanwhile, *Jania pumila* are disk-shaped and found on rocky substrates. The form of holdfast stolon was generally an adaptation of macroalgae to a sandy substrate, while the shape of a disc is an adaptation of macroalgae that live on hard substrates (Wahl et al., 2015).

Based on the important value index, it was found that *Padina australis* had the highest value (Figure 4). It reflects that *Padina australis* has an important role in the ecosystem and species that will affect other components. In addition, this species also has the highest abundance compared to other species. Anugrah et al. (2019) also found that this species dominated during the observation in April. *Padina australis* is an organism that has fairly high adaptability, grows and attaches strongly to rocky substrates, and survives even in dry conditions (Kautsari & Ardiansyah, 2016). In contrast, *Halimeda macroloba* was the rarest species in April at Station I in seagrass areas with sand substrate, with the lowest abundance. *Halimeda macroloba* is often found on sandy substrates with a combination of coral fragments but not on dead coral substrates (Ain et al., 2014). The low *Halimeda macrolaba* found at the study site is influenced by the substrate available in the ecosystem and its relatively short life cycle (Nontji, 1993).

The diversity index calculation results of the two observation stations were 0.35 and included in the low category (Figure 5). These conditions describe an imbalance in the ecosystem, which was characterized by

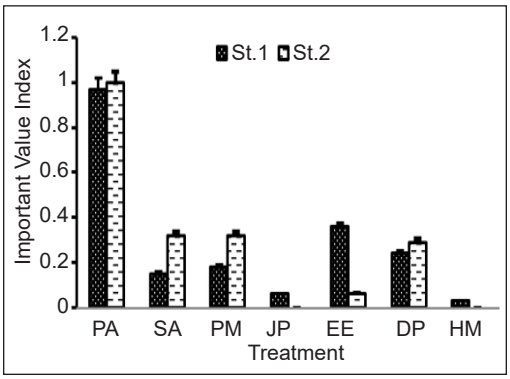

Figure 4. The important value index of macroalgae on the site study

Note. *Padina Australis* (PA), *Sargassum aquifoliu* (SA), *Polycladia myrica* (PM), *Jania pumila* (JP), *Eucheuma edul* (EE), *Dictyota pinnatifida* (DP), and *Halimeda macroloba* (HM)

the emergence of the dominance of certain species in the macroalgae community. Balanced ecosystems are characterized by stable community conditions and high species diversity (Jamilatun et al., 2020). The low value of the diversity of macroalgae might be caused by tourism activity in Bama Beach. The beach can attract up to 60,000 visitors yearly (Nuzula et al., 2017), with activities such as traveling, diving, and snorkeling (Mahendra et al., 2020). This activity can cause pollution, affect ecosystems, and damage marine biodiversity (Sidauruk et al., 2022). A previous study stated that this activity destroyed Bama Beach's diversity to a depth of 3 m (Fahmi et al., 2017).

Not only anthropogenic activity but the low value of the diversity of macroalgae species in the community is also due to environmental changes such as increased salinity, low availability of nitrates and orthophosphates, sunlight intensity, and the level of turbidity and sedimentation (Collado-Vides et al., 2007). Environmental changes, such as high-temperature fluctuations, influence the distribution of macroalgae, especially *Eucheuma* sp. and *Gracilaria* sp. (Martínez et al., 2012). A strong correlation between environmental variables and vegetation structure was observed in Baltic waters (Eriksson & Bergström, 2005). Interestingly, no *Gracilaria* was found in this study. *Gracilaria* is a species that is easily found almost all over the coast of Indonesia (Pamungkas & Djonu, 2022). It might be due to previous reasons regarding environmental changes and fluctuations that affected the existence of *Gracilaria* sp. It can disrupt its growth and metabolism (Hendri et al., 2018). Bama Beach's temperature changes easily due to another water parameter (Anugrah et al., 2019).

Furthermore, the evenness index for Station I in the medium category was 0.54, and the low category in Station II was 0.37 (Figure 5). One of the factors that influence the growth of macroalgae is the water flow and type of substrate, where both factors determine the form of the holdfast; it occurs due to the process of macroalgae adaptation to the environment (Eriksson & Bergström, 2005; Jamilatun et al., 2020; Litaay, 2014). Although the type of substrate determines the variation of macro types of algae that grow, the same type of substrate tends to have the same diversity (Herlinawati et al., 2017). In addition, the dominance index of the two stations was also included in the low category, which was 0.24 and 0.25, respectively (Figure 5). This condition was thought to be influenced by the basic characteristics of the waters in the study

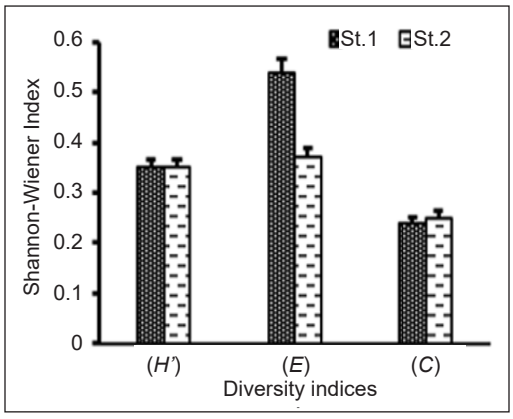

Figure 5. Diversity indices of macroalgae in the study site
Note. Diversity Index (*H'*), Evenness Index (*E*), and Dominance Index (*C*)

location and biotic component fluctuations. The dominance of seagrass in the exact location as the medium category was found during the transition season (Ulkhaq et al., 2016). In addition, International Association for Cryptologic Research (IACR) 1999 macroalgae will multiply at temperatures above 20 °C (1–2 weeks), while temperatures below 10 °C require longer (6–8 weeks).

Nonetheless, the overall state of the waters at the study site indicates that they are still within tolerance limits for macroalgae survival. Thus, the dynamics of the distribution and dominance of macroalgae on the Bama coast are likely influenced by environmental factors, such as nutrition and competition between species. Furthermore, environmental tolerance influences species distribution more strongly at high (sub-tropical) latitudes, whereas other factors, such as biotic interactions, play a more prominent role in the tropics (Keith et al., 2014).

CONCLUSION

Five species from the Phaeophyta group and one from the Chlorophyta and Rhodophyta groups were reported in Bama Beach, Baluran National Park, Situbondo, Indonesia. *Padina australis* from the class Phaeophyta was the highest distribution and abundance. However, each station's value of diversity, uniformity, and dominance was in a low category. The distribution and abundance of macroalgae showed the highest in areas with sufficient sunlight intensity and coral substrates and rocks.

ACKNOWLEDGMENTS

The authors want to express their gratitude to the Faculty of Fisheries and Maritime, Universitas Airlangga, as the funder of our research (1815/UN3/2019). The authors also express gratitude to the Laboratory at Banyuwangi Campus, Universitas Airlangga, Baluran National Park Manager, and Faculty of Marine Sciences, King Abdulaziz University, for the collaboration.

REFERENCES

Ain, N., Ruswahyuni, & Widyorini, N. (2014). Hubungan kerapatan rumput laut dengan substrat dasar berbeda di Perairan Pantai Bandengan, Jepara [The relationship between seaweed density and different basic substrates in Bandengan Coastal Waters, Jepara]. *Management of Aquatic Resources Journal*, *3*(1), 99–107. https://doi.org/10.14710/marj.v3i1.4426

Al-Yamani, F. Y., Skryabin, V., & Durvasula, S. R. V. (2015). Suspected ballast water introductions in the Arabian Gulf. *Aquatic Ecosystem Health and Management*, *18*(3), 282–289. https://doi.org/10.1080/14634988.2015.1027135

Anderson, R. J., McKune, C., Bolton, J. J., DeClerck, O., & Tronchin, E. (2005). Patterns in subtidal seaweed communities on coral-dominated reefs at Sodwana Bay on the KwaZulu-Natal coast, South Africa. *African Journal of Marine Science*, *27*(3), 529–537. https://doi.org/10.2989/18142320509504113

Anggraini, R. R., Yanuhar, U., & Risjani, Y. (2020). Characteristic of sediment at Lekok coastal waters, Pasuruan Regency, East Java. *Jurnal Ilmu dan Teknologi Kelautan Tropis*, *12*(1), 235-246. https://doi.org/10.29244/jitkt.v12i1.28705

Anugrah, D., Geovana, D., Ambarwati, A. D., Ismira, N. Z., Maulani, S., Khodikoh, S., Luthiyah, K., Meliyanti, K., Andini, Farhana, F., & Novitasari,

I. (2019). *Inventarisasi dan keaneragaman makroalga di Perairan Pesisir Pantai Bama Taman Nasional Baluran* [Inventory and diversity of macroalgae in the coastal waters of Bama Baluran National Park]. Academia Press. https://doi.org/10.13140/RG.2.2.32489.65126

Arisandy, K. R., Herawati, E. Y., & Suprayitno, E. (2012). Akumulasi logam berat timbal (Pb) dan gambaran histologi pada jaringan *Avicennia marina* (Forsk.) Vierh di Perairan Pantai Jawa Timur [Accumulation of heavy metal lead (Pb) and histology in *Avicennia marina* (Forsk.) Vierh tissue in East Java Coastal Waters]. *Jurnal Penelitian Perikanan*, *1*(1), 15–25.

Badan Meteorologi, Klimatologi, dan Geofisika. (2022). *Pusat meteorologi maritim* [Maritime Meteorological Center]. BMKG. https://peta-maritim.bmkg.go.id/ofs-static

Burkepile, D. E., Allgeier, J. E., Shantz, A. A., Pritchard, C. E., Lemoine, N. P., Bhatti, L. H., & Layman, C. A. (2013). Nutrient supply from fishes facilitates macroalgae and suppresses corals in a Caribbean coral reef ecosystem. *Scientific Reports*, *3*, 1493. https://doi.org/10.1038/srep01493

Coleman, M. A., Roughan, M., Macdonald, H. S., Connell, S. D., Gillanders, B. M., Kelaher, B. P., & Steinberg, P. D. (2011). Variation in the strength of continental boundary currents determines continent-wide connectivity in kelp. *Journal of Ecology*, *99*(4), 1026–1032. https://doi.org/10.1111/j.1365-2745.2011.01822.x

Collado-Vides, L., Caccia, V. G., Boyer, J. N., & Fourqurean, J. W. (2007). Tropical seagrass-associated macroalgae distributions and trends relative to water quality. *Estuarine, Coastal and Shelf Science*, *73*(3–4), 680–694. https://doi.org/10.1016/j.ecss.2007.03.009

Curtis, J. T., & Mcintosh, R. P. (1950). The interrelations of certain analytic and synthetic phytosociological characters. *Ecology*, *31*(3), 434-455. https://doi.org/10.2307/1931497

Doney, S. C., Ruckelshaus, M., Duffy, J. E., Barry, J. P., Chan, F., English, C. A., Galindo H. M., Grebmeier, J. M., Hollowed, A. B., Knowlton, N., Polloviba, J., Rabalais, N. N., Sydeman, W. J., & Talley, L. D. (2012). Climate change impacts on marine ecosystems. *Annual Review of Marine Science*, *4*, 11–37. https://doi.org/10.1146/annurev-marine-041911-111611

Eliáš, M. (2021). Protist diversity: Novel groups enrich the algal tree of life. *Current Biology*, *31*(11), R733-R735. https://doi.org/10.1016/j.cub.2021.04.025

Emilia, I. (2019). Analisa kandungan nitrat dan nitrit dalam air minum isi ulang menggunakan metode spektrofotometri UV-Vis [Analysis of nitrate and nitrite content in refillable drinking water using UV-Vis spectrophotometry method]. *Indobiosains*, *1*(1), 38-44. https://doi.org/10.31851/INDOBIOSAINS.V1I1.2441

Eriksson, B. K., & Bergström, L. (2005). Local distribution patterns of macroalgae in relation to environmental variables in the northern Baltic Proper. *Estuarine, Coastal and Shelf Science*, *62*(1–2), 109–117. https://doi.org/10.1016/j.ecss.2004.08.009

Fahmi, M. Y., Muttaqin, A. D., & Nurjanah, I. (2017, September 7). *Monitoring ekosistem laut dan pesisir di Taman Nasional Baluran, Situbondo* [Monitoring marine and coastal ecosystems in Baluran National Park, Situbondo] [Paper presentation]. Prosiding Seminar Nasional Kelautan dan Perikanan III 2017, Madura, Indonesia. http://ilmukelautan.trunojoyo.ac.id/wp-content/uploads/2018/02/6.pdf

Firth, L. B., & Hawkins, S. J. (2011). Introductory comments - Global change in marine ecosystems: Patterns, processes and interactions with regional and local scale impacts. *Journal of Experimental*

Marine Biology and Ecology, *400*(1–2), 1–6. https://doi.org/10.1016/j.jembe.2011.02.001

Gaitán-espitia, J. D., Hancock, J. R., Padilla-gamiño, J. L., Rivest, E. B., Blanchette, C. A., Reed, D. C., & Hofmann, G. E. (2014). Interactive effects of elevated temperature and pCO_2 on early-life-history stages of the giant kelp *Macrocystis pyrifera*. *Journal of Experimental Marine Biology and Ecology*, *457*, 51–58. https://doi.org/10.1016/j.jembe.2014.03.018

Hasyim, S., Hidayat, R., Farhum, S. A., & Zainuddin, M. (2022). The use of statistical models in identifying skipjack tuna habitat characteristics during the Southeast Monsoon in the Bone Gulf, Indonesia. *Biodiversitas Journal of Biological Diversity*, *23*(4), 2231-2237. https://doi.org/10.13057/biodiv/d230459

Hendri, M., Rozirwan, R., Apri, R., & Handayani, Y. (2018). *Gracilaria* sp. seaweed cultivation with net floating method in traditional shrimp pond in the Dungun River of Marga Sungsang Village of Banyuasin District, South Sumatera. *International Journal of Marine Science*, *8*. https://doi.org/10.5376/ijms.2018.08.0001

Herlinawati, N. D. P. D., Arthana, I. W., & Dewi, A. P. W. K. (2017). Keanekaragaman dan kerapatan rumput laut alami Perairan Pulau Serangan Denpasar Bali [Diversity and density of natural seaweed in Serangan Island Denpasar Bali]. *Journal of Marine and Aquatic Sciences*, *4*(1), 22-30. https://doi.org/10.24843/jmas.2018.v4.i01.22-30

Hurtado, A. Q., Neish, I. C., & Critchley, A. T. (2019). Phyconomy: The extensive cultivation of seaweeds, their sustainability and economic value, with particular reference to important lessons to be learned and transferred from the practice of eucheumatoid farming. *Phycologia*, *58*(5), 472-483. https://doi.org/10.1080/00318884.2019.1625632

Indahyani, D. E., Praharani, D., Barid, I., & Handayani, A. T. W. (2019). Aktivitas antioksidan dan total polisakarida ekstrak rumput laut merah, hijau dan coklat dari Pantai Jangkar Situbondo [Antioxidant activity and total polysaccharides of red, green and brown seaweed extract from Anchor Beach Situbondo]. *STOMATOGNATIC - Jurnal Kedokteran Gigi*, *16*(2), 64-69. https://doi.org/10.19184/stoma.v16i2.23094

Istomo, I., & Ghifary, S. (2021). Asosiasi bakau (*Rhizophora apiculata* Blume.) dengan jenis-jenis mangrove lainnya di Pantai Bama Taman Nasional Baluran Jawa Timur [Association of mangroves (*Rhizophora apiculata* Blume.) with other mangrove species in Bama Beach, Baluran National Park, East Java]. *Jurnal Silvikultur Tropika*, *12*(3), 135-143. https://doi.org/10.29244/j-siltrop.12.3.135-143

Jamilatun, A., Lestari, F., & Susiana, S. (2020). Patterns of macro algae types in the intertidal zone of Malang Rapat waters, Gunung Kijang District, Bintan Regency, Riau Islands, Indonesia. *Akuatikisle: Jurnal Akuakultur, Pesisir Dan Pulau-Pulau Kecil*, *4*(2), 65–71. https://doi.org/10.29239/j.akuatikisle.4.2.65-71

Janah, L. N., Rizkyta, A. N., Hidayah, A. N., Gavintri, M. B., Salsabila, N. S., Pratita, S. D., Nurahmah, Z., & Eprilurahman, R. (2021). The abundance and distribution patterns of echinoderms in the Intertidal Zone of Nglolang Beach, Gunungkidul, Yogyakarta. In *3rd KOBI Congress, International and National Conferences (KOBICINC 2020)* (Vol. 14, No. 1, pp. 31-36). Atlantis Press. https://doi.org/10.2991/absr.k.210621.007

Jung, S. W., & Choi, C. G. (2022). Seaweed community and succession on a trapezoidal-shaped artificial reef. *Ocean Science Journal*, *57*(1), 130-140. https://doi.org/10.1007/s12601-021-00053-9

Kamer, K., & Fong, P. (2000). A fluctuating salinity regime mitigates the negative effects of reduced salinity on the estuarine macroalga,

Enteromorpha intestinalis (L.) link. *Journal of Experimental Marine Biology and Ecology*, *254*(1), 53–69. https://doi.org/10.1016/S0022-0981(00)00262-8

Kautsari, N., & Ardiansyah, Y. (2016). Abundance, biomass and alginate yield of *Padina australis* in Sumbawa Aquatic. *Jurnal Perikanan Dan Kelautan*, *6*(1), 13–20.

Keith, S. A., Kerswell, A. P., & Connolly, S. R. (2014). Global diversity of marine macroalgae: Environmental conditions explain less variation in the tropics. *Global Ecology and Biogeography*, *23*(5), 517–529. https://doi.org/10.1111/geb.12132

Khalil, S., Mahnashi, M. H., Hussain, M., Zafar, N., Khan, F. S., Afzal, U., Shah, G. M., Niazi, U. M., Awais, M., & Irfan, M. (2021). Exploration and determination of algal role as bioindicator to evaluate water quality – Probing fresh water algae. *Saudi Journal of Biological Sciences*, *28*(10), 5728-5737. https://doi.org/10.1016/j.sjbs.2021.06.004

Kusmana, C., & Hikmat, A. (2015). The biodiversity of flora in Indonesia. *Journal of Natural Resources and Environmental Management*, *5*(2), 187–198. https://doi.org/10.19081/jpsl.5.2.187

Lelloltery, H., Rumanta, M., & Kunda, R. M. (2021). Strategy for marine ecotourism development based on natural resource management: Case study in Kotania Bay, Western Seram District, Maluku, Indonesia. *Nusantara Bioscience*, *13*(1), 91–99. https://doi.org/10.13057/nusbiosci/n130113

Litaay, C. (2014). Distribution and diversity of macro algae communities in the Ambon Bay. *Jurnal Ilmu Dan Tekonologi Kelautan Tropis*, *6*(1), 131–142. https://doi.org/10.29244/jitkt.v6i1.8636

Mahendra, A. A., Kusdianti, E. M., Wiradana, P. A., Susilo, R. J. K., Putranto, T. A. C., & Affandi, M. (2020). Checklist of coral reef fish species composition at Bama Coastal Waters, Situbondo, East Java, Indonesia: A preliminary study. *Economic Environmental and Conservation*, *26*(4), 1816-1819.

Marianingsih, P., Amelia, E., & Suroto, T. (2013). Inventarisasi dan identifikasi makroalga di Perairan Pulau Untung Jawa [Inventory and identification of macroalgae in the waters of Untung Jawa Island]. *Prosiding Semirata FMIPA Universitas Lampung*, *1*(1), 219–225.

Martínez, B., Arenas, F., Rubal, M., Burgués, S., Esteban, R., García-Plazaola, I., Figueroa F. L., Pereira, R., Saldaña L., Spusa-Pinto, I., & Viejo, R. M. (2012). Physical factors driving intertidal macroalgae distribution: Physiological stress of a dominant fucoid at its southern limit. *Physiological Ecology*, *170*, 341–353. https://doi.org/10.1007/s00442-012-2324-x

Meinita, M. D. N., Akromah, N., Andriyani, N., Setijanto, S., Harwanto, D., & Liu, T. (2021). Molecular identification of *Gracilaria* species (Gracilariales, Rhodophyta) obtained from the South Coast of Java Island, Indonesia. *Biodiversitas Journal of Biological Diversity*, *22*(7), 3046-3056. https://doi.org/10.13057/biodiv/d220759

Nontji, A. (1993). *Laut Nusantara* [Nusantara Sea]. Djambatan Jakarta.

Nuzula, N. I., Armono, H. D., & Rosyid, D. M. (2017). Management of Baluran National Park Resources for coastal ecotourism based on suitability and carrying capacity. *Applied Mechanics and Materials*, *862*, 161–167. https://doi.org/10.4028/www.scientific.net/amm.862.161

Oryza, D., Mahanal, S., & Sari, M. S. (2017). Identifikasi Rhodophyta sebagai bahan ajar di perguruan tinggi [Identification of Rhodophyta as teaching materials in higher education].

Jurnal Pendidikan: Teori, Penelitian, dan Pengembangan, *2*(3), 309–314. https://doi.org/10.17977/jptpp.v2i3.8582

Pamungkas, P. P., & Djonu, A. (2022). Microstructure with scanning electron microscope and sensory characteristics in nori red algae (*Gracilaria gigas*). *AGRITEPA: Jurnal Ilmu dan Teknologi Pertanian*, *9*(2), 275-286. https://doi.org/10.37676/agritepa.v9i2.2786

Poloczanska, E. S., Brown, C. J., Sydeman, W. J., Kiessling, W., Schoeman, D. S., Moore, P. J., Brander, K., Bruno, J. F., Buckley, L. B., Burrows, M. T., Duarte, C. M., Halpern, B. S., Holding, J., Kappel. C. V., O'Connor, M. I., Pandolfi, J. M., Parmesan, C., Schwing, F., Thompson, S. A., & Richardson, A. J. (2013). Global imprint of climate change on marine life. *Nature Climate Change*, *3*, 919–925. https://doi.org/10.1038/nclimate1958

Prathep, A., Mayakun, J., Tantiprapas, P., & Darakrai, A. (2008). Can macroalgae recover, 13 months after the 2004 Tsunami?: A case study at Talibong Island, Trang Province, Thailand. *Journal of Applied Phycology*, *20*(5), 907–914. https://doi.org/10.1007/s10811-007-9287-z

Purnomo, A., Idris, I., & Kurniawan, B. (2020). Understanding local community in managing sustainable tourism at Baluran National Park–Indonesia. *Geo Journal of Tourism and Geosites*, *29*(2), 508-520. https://doi.org/10.30892/gtg.29210-485

Putrisari, P., Suhartini, S., & Ratnawati, R. (2017). Keanekaragaman dan struktur vegetasi mangrove di Pantai Bama – Dermaga Lama Taman Nasional Baluran Jawa Timur [Diversity and vegetation structure of mangrove at Bama Beach – Dermaga Lama Baluran National Park East Java]. *Kingdom (The Journal of Biological Studies)*, *6*(3), 185-193.

Rasher, D. B., Hoey, A. S., & Hay, M. E. (2013). Consumer diversity interacts with prey defenses to drive ecosystem function. *Ecology*, *94*(6), 1347-1358. https://doi.org/10.1890/12-0389.1

Rimmer, M. A., Larson, S., Lapong, I., Purnomo, A. H., Pong-Masak, P. R., Swanepoel, L., & Paul, N. A. (2021). Seaweed aquaculture in Indonesia contributes to social and economic aspects of livelihoods and community wellbeing. *Sustainability*, *13*(19), 10946. https://doi.org/10.3390/su131910946

Setyawidati, N. A. R., Puspita, M., Kaimuddin, A. H., Widowati, I., Deslandes, E., Bourgougnon, N., & Stiger-Pouvreau, V. (2018). Seasonal biomass and alginate stock assessment of three abundant genera of brown macroalgae using multispectral high resolution satellite remote sensing: A case study at Ekas Bay (Lombok, Indonesia). *Marine Pollution Bulletin*, *131*(Part B), 40-48. https://doi.org/10.1016/j.marpolbul.2017.11.068

Shanon, C. E., & Weaver, W. (1949). *The mathematical theory of communication*. University of Illinois Press.

Sidauruk, T., Rahmadi, M. T., Sugiharto, S., Suciani, A., Sari, R. M., & Yuniastuti, E. (2022). Distribution analysis of coral reefs for development of marine tourism in Weh Island, Aceh, Indonesia. *Depik*, *11*(2), 237-245. https://doi.org/10.13170/depik.11.2.25919

Simpson, E. H. (1949). Measurement of diversity. *Nature*, *163*, 688. https://doi.org/10.1038/163688a0

Siswanto, D. A. (2005). *Studi populasi alga laut makrobentik di Pantai Pasir Putih Situbondo* [Study of macrobenthic marine algae populations at Situbondo White Sand Beach]. University of Muhammadiyah Malang Press.

Solidoro, C., Pecenik, G., Pastres, R., Franco, D., & Dejak, C. (1997). Modelling macroalgae (*Ulva rigida*) in the Venice Lagoon: Model structure identification and first parameters estimation. *Ecological Modelling*, *94*(2-3),

191-206. https://doi.org/10.1016/S0304-3800(96)00025-7

Subur, R., Irfan, M., & Akbar, N. (2021). The effect of NPK fertilizer with different dosage on the growth rate seaweed (*Caulerpa racemosa*). *Depik*, *10*(3), 207-210. https://doi.org/*10.13170/depik.10.3.20848*

Supardi, W., & Nugroho, A. P. (2019). Bioaccumulation of lead (Pb) in the macroalgae *Padina australis* Hauck in Makassar Marine Waters, South Sulawesi, Indonesia. In *IOP Conference Series: Earth and Environmental Science* (Vol. 380, No. 1, p. 012021). IOP Publishing. https://doi.org/10.1088/1755-1315/380/1/012021

Takarina, N. D., Nurliansyah, W., & Wardhana, W. (2019). Relationship between environmental parameters and the plankton community of the Batuhideung Fishing Grounds. *Biodiversitas Journal of Biological Diversity*, *20*(1), 171-180. https://doi.org/10.13057/biodiv/d200120

Thongroy, P., Liao, L. M., & Prathep, A. (2007). Diversity, abundance and distribution of macroalgae at Sirinart Marine National Park, Phuket Province, Thailand. *Botanica Marina*, *50*(2), 88–96. https://doi.org/10.1515/BOT.2007.010

Tytlyanov, E. A., Titlyanova, T. V., Huang, H., & Li, X. (2014). Seasonal changes in benthic algal communities of the upper subtidal zone in Sanya Bay (Hainan Island, China). *Journal of the Marine Biological Association of the United Kingdom*, *94*(1), 51-64. https://doi.org/10.1017/S0025315413001112

Ulkhaq M F., Sapto, A., Muhammad, Hanif, A., Hapsari, K., Daruti, Dinda, N., & Darmawan, setia, B. (2016). Dominance and diversity of seagrass and macrozoobenthos on transition season in Bama Beach, Baluran National Park, Situbondo. *Jurnal Ilmiah Perikanan dan Kelautan*, *8*(1), 36–45. https://doi.org/10.20473/jipk.v8i1.11191

Xu, N., Xu, K., Wang, W., Xu, Y., Ji, D., Chen, C., & Xie, C. (2020). Nutrient enrichment improves growth and food quality of two strains of the economic seaweed *Pyropia haitanensis*. *Frontiers in Marine Science*, *7*, 544582. https://doi.org/10.3389/fmars.2020.544582

Wade, R., Augyte, S., Harden, M., Nuzhdin, S., Yarish, C., & Alberto, F. (2020). Macroalgal germplasm banking for conservation, food security, and industry. *PLOS Biology*, *18*(2), e3000641. https://doi.org/10.1371/journal.pbio.3000641

Wahl, M., Molis, M., Hobday, A. J., Dudgeon, S., Neumann, R., Steinberg, P., Campbell, A. H., Marzinelli, E., & Connell, S. (2015). The responses of brown macroalgae to environmental change from local to global scales: Direct versus ecologically mediated effects. *Perspectives in Phycology*, *2*(1), 11–29. https://doi.org/10.1127/pip/2015/0019

Wahyuningtyas, A. F., Abdillah, A. A., Amin, M. N. G., & Alamsjah, M. A. (2020). The effectivity of plantation depth on seaweed *Sargassum* sp. growth using longline method. In *IOP Conference Series: Earth and Environmental Science* (Vol. 416, No. 1, p. 012021). IOP Publishing. https://doi.org/10.1088/1755-1315/416/1/012021

Pertanika J. Trop. Agric. Sci. 46 (1): 213 - 241 (2023)

PERTANIKA JOURNALS

TROPICAL AGRICULTURAL SCIENCE

Journal homepage: http://www.pertanika.upm.edu.my/

Review Article

Comprehensive Review of *Cratoxylum* Genus: Ethnomedical Uses, Phytochemistry, and Pharmacological Properties

Chui Yin Bok[1#], Eric Kat Jun Low[2#], Digsha Augundhooa[2], Hani' Ariffin[2], Yen Bin Mok[2], Kai Qing Lim[2], Shen Le Chew[2], Shamala Salvamani[3], Khye Er Loh[1], Chui Fung Loke[1], Baskaran Gunasekaran[2]* and Sheri-Ann Tan[1]*

[1]Department of Bioscience, Faculty of Applied Sciences, Tunku Abdul Rahman University of Management and Technology, Jalan Genting Kelang, 53300 Setapak, Kuala Lumpur, Malaysia
[2]Department of Biotechnology, Faculty of Applied Sciences, UCSI University, 56000 Cheras, Kuala Lumpur, Malaysia
[3]Division of Applied Biomedical Science and Biotechnology, School of Health Sciences, International Medical University, 57000 Bukit Jalil, Kuala Lumpur, Malaysia

ABSTRACT

In the past, the *Cratoxylum* genus has often been utilized as traditional medicines, culinary ingredients, health supplements, as well as manufacturing materials. This flowering plant belongs to the family Hypericaceae and is classified into six species: *Cratoxylum arborescens*, *Cratoxylum cochinchinense*, *Cratoxylum formosum*, *Cratoxylum glaucum*, *Cratoxylum maingayi*, and *Cratoxylum sumatranum*. The *Cratoxylum* genus is native to Asia as a traditional medicinal plant. It is currently being translated into conventional therapeutics as a preventive agent for diabetes mellitus and cardiovascular diseases. The phytochemical analysis and pharmacological investigations on the *Cratoxylum* species have unveiled the wide spectrum of phytoconstituents, including xanthones, triterpenoids, flavonoids, and phenolic compounds. These compounds are attributed to their significant pharmacological effects, such as antibacterial, antifungal, antioxidant, antimalarial, anti-gastric ulcer, anti-HIV-1 reverse transcriptase, antidiabetic, and anticancer activities. These research findings have strengthened the foundation

ARTICLE INFO

Article history:
Received: 28 August 2022
Accepted: 01 November 2022
Published: 03 February 2023

DOI: https://doi.org/10.47836/pjtas.46.1.12

E-mail addresses:
chuiyinbok@hotmail.com (Chui Yin Bok)
1001541907@ucsiuniversity.edu.my (Eric Kat Jun Low)
digshaaug04@gmail.com (Digsha Augundhooa)
1001850992@ucsiuniversity.edu.my (Hani' Ariffin)
1001851719@ucsiuniversity.edu.my (Yen Bin Mok)
1001851600@ucsiuniversity.edu.my (Kai Qing Lim)
1001852039@ucsiuniversity.edu.my (Shen Le Chew)
shamalasalvamani@imu.edu.my (Shamala Salvamani)
lohke@tarc.edu.my (Khye Er Loh)
lokecf@tarc.edu.my (Chui Fung Loke)
baskaran@ucsiuniversity.edu.my (Baskaran Gunasekaran)
tansw@tarc.edu.my (Sheri-Ann Tan)
* Corresponding author
# Equal contribution

ISSN: 1511-3701
e-ISSN: 2231-8542

of the *Cratoxylum* genus as a traditional medicinal plant to be further developed and applied as selective therapeutic drugs for various ailments. This paper discusses the *Cratoxylum* genus regarding its traditional uses, phytochemical compounds, and pharmacological properties.

Keywords: *Cratoxylum* genus, conventional therapeutics, ethnomedical uses, pharmacological properties, phytochemical compounds

INTRODUCTION

Cratoxylum is a genus of flowering plants categorized under the Hypericaceae family. The genus is known to be native to Southeast Asia, with six accepted species: *C. arborescens*, *C. cochinchinense*, *C. formosum*, *C. glaucum*, *C. maingayi*, and *C. sumatranum*. They are widely spread in the Southeast Asian region, including countries like Malaysia, Singapore, Indonesia, Vietnam, and Thailand. They are also found in Asian countries, such as India and China. *Cratoxylum* species have a long history in the traditional medicinal systems of these countries due to their health benefits aligned with proven pharmacological properties.

Over the years, several *Cratoxylum* species have been studied and were reported to possess various bioactivities such as antibacterial, antifungal, antioxidant, antimalarial, anti-gastric ulcer, anti-human immunodeficiency viruses (anti-HIV), antidiabetic, and anticancer effects. Furthermore, phytochemical analysis conducted on various *Cratoxylum* species elucidated a wide range of phytochemical compounds, which included flavonoids, xanthones, terpenoids, sterol, triterpenoids, benzophenone, quinone, and other phenolic compounds, which may contribute to its significant pharmacological properties. In this review, traditional medicinal uses, chemical constituents, and pharmacological characteristics of the *Cratoxylum* genus will be discussed systematically.

BACKGROUND

Cratoxylum is a genus of flowering plants that belongs to the family Hypericaceae. The genus is native to tropical Asia and distributed from India through South China to Malaysia. The name *Cratoxylum* is derived from the words '*kratos*' and '*xylon*' in Greek, which means strong wood, generally referring to its hard and durable timber (Soepadmo & Wong, 1995). To date, there are six recognized species in this genus: *C. arborescens* (Figure 1), *C. cochinchinense* (Figure 2), *C. formosum* (Figure 3), *C. glaucum* (Figure 4), *C. maingayi* (Figure 5), *C. sumatranum*; which are often integrated into traditional medicinal systems in the past (Neo et al., 2016).

Cratoxylum species are usually shrubs or small to medium-sized evergreen trees with five-petal flowers that are white, red, or pink (Neo et al., 2016). They are rare in primary forests and usually grow in the lowland areas such as gaps, forest fringes, and disturbed habitats. However, these species can also be found in well-drained soils and swampy areas (Neo et al., 2016; Soepadmo & Wong, 1995).

Figure 1. *Cratoxylum arborescens* (Ibrahim et al., 2015)

Figure 2. *Cratoxylum cochinchinense*. Photos were taken at Singapore Botanic Gardens (Photograph: Chui Yin Bok)

Figure 3. *Cratoxylum formosum*. Photos were taken at Singapore Botanic Gardens (Photograph: Chui Yin Bok)

Figure 4. *Cratoxylum glaucum*. Photos were taken at Bako National Park, Kuching, Sarawak (Photograph: Chui Yin Bok)

TRADITIONAL USES

In the past, various *Cratoxylum* species were used mainly for medicinal and manufacturing purposes. As a traditional medicine, the decoction of the bark and leaves of *C. cochinchinense* can relieve fever, while the decoction of roots can be served as a post-labor tonic for women. *Cratoxylum formosum* bark decoction and resin are used for colic and itch treatment, respectively. A pounded mixture of the bark and leaves of *C. formosum* with coconut oil is found to heal skin problems (Boo et al., 2003; Choi et al., 2012). In Thailand, leaves of *C. formosum* are used as herbal remedies as they are discovered to reduce the risk of cardiovascular diseases by preventing vascular dysfunction as well as conferring protection towards gastric

Figure 5. *Cratoxylum maingayi*. Photos taken at Singapore Botanic Gardens (Photograph: Chui Yin Bok)

mucosal to prevent the formation of gastric ulcers (Kukongviriyapan et al., 2007; Sripanidkulchai et al., 2010). The bark, roots, and leaves of *C. arborescens* are widely integrated into folk medicine to treat fever, coughs, diarrhea, itches, ulcers, and abdominal complaints (Sidahmed et al., 2013).

Apart from medicinal purposes, *Cratoxylum* species are also being consumed in daily diets. In Vietnam, *C. formosum* serves as a vegetable side dish or an ingredient in soup (Choi et al., 2012). In China, the leaves of *C. formosum* ssp. *pruniflorum* are substitutes for 'kuding tea' in Yunnan Province (Xiong et al., 2014). Furthermore, as mentioned earlier, the name *Cratoxylum* means 'strong wood' in Greek; hence the timbers are used in the manufacturing of various wood products, especially in construction and furniture production. This medium-weight hardwood is also used as charcoal and firewood as well as for carving purposes (Boo et al., 2003). A detailed summary of the ethnobotanical uses of the different species is shown in Table 1.

Table 1
Cratoxylum *species and its ethnomedical usages*

Plant	Parts	Traditional uses	References
Cratoxylum arborescens	Leaves	Treat gastric ulcer	Juanda et al. (2019)
Cratoxylum cochinchinense	Roots and stem	Function as diuretic	Juanda et al. (2019)
	Bark, root, and leaves	Treat diarrhea, itches, ulcer, abdominal complaints, fever, and coughs	Juanda et al. (2019)
	Roots	Post-labor tonic for women	Boo et al. (2003)
	Barks and leaves	Relieve fever	Boo et al. (2003)
Cratoxylum formosum	Leaves	To remedy food poisoning, internal bleeding, diarrhea, and liver cirrhosis	Juanda et al. (2019)
		Reduce the risk of cardiovascular diseases	Kukongviriyapan et al. (2007)
		Protective effects towards gastric mucosal	Sripanidkulchai et al. (2010)
	Barks and leaves	Treatment for skin problems and wound healing	Juanda et al. (2019)
	Flower	To cure coughs	Juanda et al. (2019)
	Barks	To treat colic	Boo et al. (2003)
Cratoxylum glaucum	Young stem	To decrease blood pressure Use as an ingredient in culinary	Juanda et al. (2019)
	Leaves, roots, and barks	To treat ulcers, diarrhea, itches, fever, cough, and abdominal complaints	Thaweboon et al. (2014)
Cratoxylum sumatranum	Decocted barks, leaves, and roots	To relieve cough, colds, and dysentery	Dapar (2020)
	Leaves	Relieve toothache To treat burns, scabies, and ulcers	Dapar et al. (2020)
	Leaves and stems	To relieve fever	Dapar et al. (2020)
	Barks	To treat abdominal pain	Dapar et al. (2020)

CHEMICAL CONSTITUENTS

Phytochemicals are chemical compounds synthesized naturally in plants. Based on their chemical structures and characteristics, these compounds can be categorized under six major classes: carbohydrates, lipids, terpenoids, phenolic acids, alkaloids, and other nitrogen-containing metabolites (Huang et al., 2016). These phytochemicals are also beneficial to human health. For example, they could function as antioxidant, antibacterial, antifungal, anti-inflammatory, anti-allergic, antispasmodic, chemopreventive, hepatoprotective, hypolipidemic, neuroprotective, hypotensive, immuno-modulator, and carminative agents. In addition, they were also reported to possess the ability to prevent the development of chronic diseases such as cancer, diabetes, heart disease, and osteoporosis (Thakur et al., 2020).

The major compounds elucidated from *Cratoxylum* species are phenolic compounds, such as xanthones, flavonoids, isoflavonoids, phenolic acids, vismiones, tocotrienols, and anthraquinones. These bioactive could be detected in various parts of the plant (leaves, stems, roots, and fruits). For example, xanthones (Figure 6) isolated from *C. cochinchinense* are cratoxylumxanthone B, cratoxylumxanthone C, and cratoxylumxanthone D, while 1,3,5,6-oxygenated xanthones are detected in *C. maingayi* (Figure 7) (Laphookhieo et al., 2009; Udomchotphruet et al., 2012). Furthermore, flavonoids, such as quercetin, quercitrin, isoquercitrin, and hyperin are reported in *C. formosum* (Choi et al., 2012).

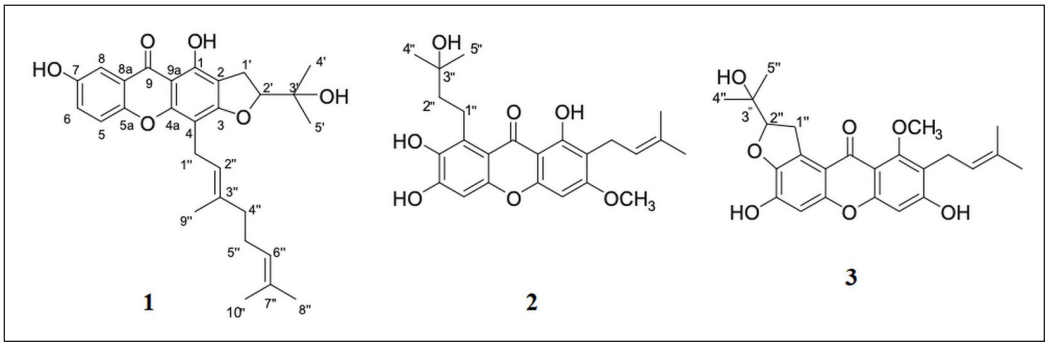

Figure 6. Xanthones isolated from *Cratoxylum cochinchinense*. (1) Cratoxylumxanthone B, (2) cratoxylumxanthone C, and (3) cratoxylumxanthone D (Udomchotphruet et al., 2012)

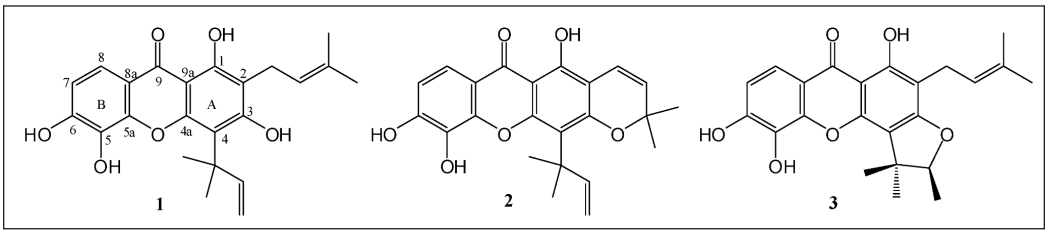

Figure 7. 1,3,5,6-oxygenated xanthones obtained from *Cratoxylum maingayi*. (1) Gerontoxanthone, (2) macluraxanthone, and (3) formoxanthone C (Laphookhieo et al., 2009)

Based on the rich phytochemical constituents present in the *Cratoxylum* genus, these compounds may have contributed to the known pharmacological activities of this genus, as illustrated in Table 2.

PHARMACOLOGICAL ACTIVITIES

Antibacterial

In the previous studies conducted on *Cratoxylum* species, it was found that

Table 2
Cratoxylum *species and its related pharmacological activities*

Plant	Parts	Pharmacological activity	Chemical constituents	References
Cratoxylum arborescens	Twigs and leaves	Anti-HIV-1 reverse transcriptase	Lup-20(29)-ene-3β,30-diol Betulinic acid Euxanthone 3β-hydroxylup-20(29)-en-30-oic acid 1,3,7-trihydroxy-6-methoxy-4,5-di(3-methylbut-2-en-yl)xanthone	Reutrakul et al. (2006)
	Stem bark	Antioxidant	Friedelin β-mangostin Vismiaquinone Fuscaxanthone C 5-demethoxycadensin 1,8-dihydoxy-3-methoxy-6-methylanthraquinonestigmasterol 3-geranyloxy-6-methyl-1,8-dihydroxyanthraquinone	Thaweboon et al. (2014)
		Anti-gastric ulcer	α-mangostin	Sidahmed et al. (2013)
		Antibacterial	α-mangostin	Sidahmed et al. (2013)
Cratoxylum cochinchinense	Stem	Antioxidant	Cratoxylumxanthone A Cratoxylumxanthone C Cochinxanthone D Cochinxanthone B Dulcisxanthone B Cudratricusxanthone E α-mangostin β-mangostin 2-geranyl-1,3,7-trihydroxy-4-(3-methylbut-2-enyl)xanthone tectochrystin	Sidahmed et al. (2013)
	Stem bark	Antibacterial	α-mangostin β-mangostin Cratoxylone Garcinone B Garcinone C Pruniflorone Q Pruniflorone R	Raksat et al. (2015)

Table 2 *(continue)*

Plant	Parts	Pharmacological activity	Chemical constituents	References
			Cochinchinone A Cochinchinone M 11-hydroxy-3-*O*-methyl-1-isomangostin 1,3,7-trihydroxy-2,4-diisoprenylaxanthone 3-*O*-methylmangostenone D 5,9-dihydroxy-8-methoxy-2,2-dimethyl-7-(3-methylbut-2-enyl)-2*H*,6*H*-pyrano[3,2-b]xanthen-6-one	
	Root	Antimalarial	5-*O*-methylcelebixanthone Celebixanthone β-mangostin Cochinchinone C	Maisuthisakul et al. (2007)
		Antibacterial	Cochinchinone A Celebixanthone methyl ether Cochinchinone L 7-geranyloxy-1,3-dihydroxyxanthone 3-geranyloxy-1,7-dihydroxyxanthone 1,3,7-trihydroxy-2,4-diisoprenylxanthone	Boonnak et al. (2009)
			Isocudraniaxanthone B Cudratricus-xanthone E Norathyriol	Mahabusarakam et al. (2008)
		Antioxidant	Cochinchinone A Cochinchinone B Cochinchinone C Cochinchinone D Cochinchinone E Cochinchinone F Caged-prenylated xanthone β-mangostin l,3,7-trihydroxy-2,4-bis(3-methyl-2-butenyl)xanthone Mangostin Macluraxanthone Garcinone B Celebixanthone Garcinone D	Mahabusarakam et al. (2008) Mahabusarakam et al. (2006)
		Cytotoxic	Cratochinone A Cratochinone B Pancixanthone-A Neriifolone A Macluraxanthone	Natrsanga et al. (2020)

Table 2 *(continue)*

Plant	Parts	Pharmacological activity	Chemical constituents	References
			10-*O*-methyxlmacluraxanthone Pruniflorone G Pruniflorone H 6-deoxyjacareubin 9-hydroxycalabaxanthone Cratoxylumxanthone A Formoxanthone B Cochinchinone J Cochinchinone A β-mangostin 3,8-dihydroxy-1,2-dimethoxyxanthone 1,5-dihydroxy-6-methoxyxanthone 1,3,7-trihydroxyxanthone	
	Root bark	Antidiabetic	α-mangostin ɣ-mangostin Pruniflorone S Cochinechinone A Cochinchinone Q Cochinxanthone A Cratoxylone Cratoxanthone E Cratoxanthone F Cratoxanthone A 1,3,7-trihydroxy-2,4-diisoprenylxanthone 7-geranyloxy-1,3-dihydroxyxanthone	Li, Lee, et al. (2018) Li, Song, et al. (2018)
	Twigs	Antioxidant	Dulcisxanthone B β-mangostin Cudratricusxanthone E Cochinchinone B	Chailap and Nuanyai (2019)
	Fruits and leaves	Antioxidant	α-tocopherol δ-tocotrienol γ-tocotrienol Cochinchinone G Fuscaxanthone E Vismiaquinone A 7-geranyloxy-1,3-dihydroxyxanthone	Chailap et al. (2017)
	Resin extract	Antifungal	α-mangostin Macluraxanthone	Boonnak et al. (2009)
		Antibacterial	α-mangostin β-mangostin Cochinchinone A Celebixanthone methyl ether	Boonnak et al. (2009)

Table 2 *(continue)*

Plant	Parts	Pharmacological activity	Chemical constituents	References
			Dulxis-xanthone Macluraxanthone Pruniflorone G 1,3,7-trihydroxy-2,4-diisoprenylxanthone Caged-prenylated xanthone	
	Fruits	Antimalarial	Fuscaxanthone E Vismione B Vismione F Vismione E	Maisuthisakul et al. (2007)
		Antibacterial	Cochinchinone L 7-geranyloxy-1,3-dihydroxyxanthone 3-geranyloxy-1,7-dihydroxyxanthon	Boonnak et al. (2009)
	Twigs	Antibacterial	β-mangostin Cochinchinone A	Mahabusarakam et al. (2008)
Cratoxylum formosum	Stem bark	Antibacterial	Gum extract	Boonsri et al. (2006)
	Leaves	Antioxidant Anti-inflammatory	Quercetin Isoquercitin Hyperin Quercitrin	Choi et al. (2012)
	Twigs	Antioxidant	Dulcisxanthone B β-mangostin Cudratricusxanthone E Cochinchinone B	Chailap and Nuanyai (2019)
Cratoxylum glaucum	Stem bark	Antioxidant	β-mangostin 5-demethoxycadensin Friedelin Fuscaxanthone C Vismiaquinone 3-geranyloxy-6-methyl-1,8-dihydroxyanthraquinone 1,8-dihydoxy-3-methoxy-6-methylanthraquinonestigmasterol	Thaweboon et al. (2014)
Cratoxylum maingayi	Stem bark	Antimalarial cytotoxic	Gerontoxanthone I Macluraxanthone Formoxanthone C	Maisuthisakul et al. (2007)
Cratoxylum sumatranum	Roots	Antibacterial	Cratosumatranone B Cratosumatranone D Pruniflorone N Pancixanthone B	Tantapakul et al. (2016)
		Antioxidant	Macluraxanthone	Tantapakul et al. (2016)

Table 2 *(continue)*

Plant	Parts	Pharmacological activity	Chemical constituents	References
	Twigs	Antibacterial	1,3,5,6-tetrahydroxyxanthone 1,3,6-trihydroxy-7-methoxyxanthone 1,5-dihydroxy-6,7-dimethoxyxanthone 1,5-dihydroxy-8-methoxyxanthone 1,7-dihydroxyxanthone 2,4,6-trimethoxybenzophenone 2,8-dihydroxy-1-methoxyxanthone 4-hydroxy-2,6-dimethoxybenzophenone Annulatomarin Cratosumatranone F Cratoxyarborenone F Trapezifolixanthone	Tantapakul et al. (2016)
		Antioxidant	1,3,5,6-tetrahydroxyxanthone	Tantapakul et al. (2016)

C. arborescens, *C. cochinchinense*, *C. formosum*, *C. maingayi*, and *C. sumatranum* possessed significant antibacterial activities towards *Bacillus cereus* (Tantapakul et al., 2016; Vu et al., 2015; Yahayu et al., 2013), *Bacillus subtilis* (Boonnak et al., 2009; Boonsri et al., 2006; Vu et al., 2015; Yahayu et al., 2013), *Escherichia coli* (Ngamsurach & Praipipat, 2021; Vu et al., 2015), *Enterococcus faecalis* (Boonnak et al., 2009), vancomycin-resistant *Enterococcus faecalis* (Boonnak et al., 2009), *Micrococcus luteus* (Tantapakul et al., 2016), *Pseudomonas aeruginosa* (Boonnak et al., 2009; Boonsri et al., 2006; Tantapakul et al., 2016; Vu et al., 2015), *Salmonella typhimurium* (Boonsri et al., 2006; Tantapakul et al., 2016; Yahayu et al., 2013), *Staphylococcus aureus* (Boonsri et al., 2006; Enggiwanto et al., 2019; Mahabusarakam et al., 2008; Ngamsurach & Praipipat, 2021; Tantapakul et al., 2016; Vu et al., 2015; Yahayu et al., 2013), methicillin-resistant *Staphylococcus aureus* (MRSA) (Boonnak et al., 2009; Mahabusarakam et al., 2008), *Staphylococcus epidermis* (Tantapakul et al., 2016), *Streptococcus mutans* (Suddhasthira et al., 2006), and *Streptococcus faecalis* (Boonsri et al., 2006).

The α-mangostin isolated from the stem bark of *C. arborescens* had shown potent reactivity against *B. cereus*, *B. subtilis*, *S. typhimurium*, and *S. aureus*, with the diameter of inhibition zones ranging from 16 to 20 mm, as compared to the standard drugs, tetracycline, and ampicillin (Yahayu et al., 2013). In the same study, β-mangostin was also isolated but demonstrated moderate antibacterial activity towards similar bacterial strains,

with the diameter of inhibition zones from 7 to 11 mm, which could be due to the loss of a hydroxyl group in its chemical structure compared to α-mangostin.

The antibacterial activities of *C. cochinchinense* were tested against Gram-positive and Gram-negative bacteria using the xanthones isolated from its green fruits and resin. The majority of the xanthones isolated possessed strong antibacterial effects against the tested Gram-positive bacteria (*B. subtilis*, *S. aureus*, *E. faecalis* TISTR 459, methicillin-resistant *S. aureus* (MRSA) ATCC 43300, vancomycin-resistant *E. faecalis* (VRE) ATCC 51299). However, among all the Gram-negative bacteria examined, xanthones, such as α-mangostin, β-mangostin, caged-prenylated xanthone, celebixanthone methyl ether, cochinchinone A, cochinchinone L, dulxisxanthone, macluraxanthone, pruniflorone G, 1,3,7-trihydroxy-2,4-diisoprenylxanthone, 3-geranyloxy-1,7-dihydroxyxanthone, and 7-geranyloxy-1,3-dihydroxyxanthone, did not show significant activities against *S. typhimurium* and *Shigella sonei* but were found to have strong antibacterial activities against *P. aeruginosa* (Boonnak et al., 2009). Interestingly, the compounds that showed inhibition towards *P. aeruginosa* were mostly 1,3,7-trihydroxy xanthones (cochinchinone A and 1,3,7-trihydroxy-2,4-diisoprenylxanthone) or 1,3,7-trioxygenated xanthones that have dihydroxyl groups and an oxygeranyl side chain either at C-3 or C-7 (7-geranyloxy-1,3-dihydroxyxanthone and 3-geranyloxy-1,7-dihydroxy- xanthone).

Besides, various xanthones (isocudraniaxanthone B, cudratricusxanthone E, norathyriol, β-mangsotin, and cochinchinone A) isolated from the fruits, roots, and twigs of *C. cochinchinense* exhibited strong antibacterial activities towards *S. aureus* and methicillin-resistant *S. aureus* (MRSA SK1) with minimum inhibitory concentration (MIC) values ranging from 16 to 128 μg mL^{-1}. In this study, isocudraniaxanthone B was found to possess the strongest antibacterial activities towards *S. aureus* and MRSA SK1 with a MIC value of 16 μg mL^{-1} compared with other xanthones (Mahabusarakam et al., 2008).

Antibacterial investigations using the crude hexane extracts from the roots of *C. formosum* were also conducted against *B. substilis*, *S. aureus*, *P. aeruginosa*, *S. faecalis*, and *S. typhimurium*. It was revealed that xanthone V_1, gerontoxanthone I, formoxanthone C, and macluraxanthone isolated from the crude roots extract of *C. formosum* were able to inhibit the growth of these bacteria (Boonsri et al., 2006). Besides, the gum extract from the stem bark of *C. formosum* was reported to exhibit antibacterial activities towards *S. mutans* based on the agar diffusion method. Inhibition zones were formed with a diameter ranging from 9.5 to 11.5 mm, and MIC values were between 48 mg mL^{-1} and 97 mg mL^{-1} (Suddhasthira et al., 2006). Another study by Ngamsurach and Praipipat (2021) used similar procedures to investigate the antibacterial potential of *C. formosum* leaves extract by synthesizing it into beads using sodium alginate. The study revealed that *C. formosum* beads (CFB) possessed antibacterial properties against *S. aureus* and

E. coli. CFB demonstrated a dose-dependent antibacterial potential indicating more effective results at a higher concentration range. As a result, the diameter of the inhibition zones on *S. aureus* was between 6.0 to 8.3 mm, while the diameter of the inhibition zones on *E. coli* was between 6.1 to 8.8 mm, with the increasing concentration of CFB from 100 to 400 mg mL^{-1}. Vu et al. (2015) also investigated the antibacterial activities of the leaf extracts of *C. formosum* by using the broth microdilution method. Three Gram-positive strains (*B. cereus* ATCC 21768, *B. subtilis* ATCC 6633, and *S. aureus* ATCC 6538) and two Gram-negative bacterial strains (*E. coli* American Type Culture Collection, ATCC 25922 and *P. aeruginosa* ATCC 9027) were used to test the antibacterial activities of the leaf extracts. The extracts were a potent antibacterial agent against all five strains, with the MIC concentration ranging from 125 to 2000 µg mL^{-1} (Vu et al., 2015).

Cratoxylum glaucum was also tested for its antibacterial activity toward *S. aureus*, as reported by Enggiwanto et al. (2019). The researchers emulsified the extracts into nanoemulsion, an effective drug delivery system for bacterial cells. The agar diffusion results showed inhibition zones with diameters ranging from 14.03 to 15.22 mm when the concentration of the extracts increased from 20 to 80%.

In another research conducted by Tantapakul et al. (2016), the roots and twigs of *C. sumatranum* ssp. *neriifolium* were found to consist of chemical constituents, such as benzophenones and xanthones. These chemical constituents were believed to have contributed to the antibacterial potentials of *C. sumatranum* towards *M. luteus*, *B. cereus*, *S. epidermis*, *S. aureus*, *S. typhimurium*, and *P. aeruginosa*.

Antifungal

The gum extract of *C. formosum* was tested against *Candida albicans* using disk diffusion and broth dilution assays. It was found that the gum extract demonstrated antifungal activity with MIC values between 0.50 and 1.25 mg mL^{-1} towards reference and clinical strains of *C. albicans* (Thaweboon et al., 2014). Another study by Boonnak et al. (2009) concluded that macluraxanthone and α-mangostin isolated from the resin of *C. cochinchinense* exhibited strong antifungal activity against the same fungus with MIC values of 2.4 and 4.7 µg mL^{-1}, respectively.

Antioxidant

Many antioxidant studies have been conducted over the years on *Cratoxylum* species. Phytochemicals confer human health benefits due to their antioxidative properties (Thakur et al., 2020). *Cratoxylum arborescens*, *C. cochinchinense*, *C. formosum*, *C. glaucum*, and *C. sumatranum* were found to be effective antioxidants as they have high contents of phytochemicals, such as anthraquinones, flavonoids, polyphenols, and triterpenoids.

Sim et al. (2010) reported that *C. arborescens* and *C. glaucum* possessed antioxidant properties as they effectively scavenged DPPH (2,2-diphenyl-1-

picrylhydrazyl) free radicals. These strong radical scavenging effects could be correlated to their high phenolic contents. In addition, the presence of xanthones and triterpenoids in the stems and leaves of *C. cochinchinense* also contributed to its antioxidant properties. Four xanthones isolated from the stem possessed potent activities in both DPPH radical scavenging and lipid peroxidation inhibition assays (Udomchotphruet et al., 2012). Furthermore, the leaves of *C. cochinchinense* also demonstrated antioxidant properties in ABTS [2,2'-azino-bis(3-ethylbenzothiazoline-6-sulfonic acid)] radical scavenging assay, recording the highest antioxidant activity in trolox equivalent antioxidant capacity (TEAC) values as well as total phenolic content (Tang, Whiteman, Peng, et al., 2004).

Our group evaluated the antioxidant activities of the methanolic leaf extracts of *C. cochinchinense* by using various antioxidant assays (Tan et al., 2021). The leaves were found to be antioxidant rich as they consisted of high phenolic and flavonoid contents, with the recorded values of 129.0 ± 2.55 mg GAE g^{-1} crude extract and 159.0 ± 2.15 mg QE g^{-1} crude extract, respectively. Expectedly, the leaves were reported to have strong dose-dependent radical scavenging activities towards both DPPH and ABTS free radicals. In addition, the extract also exerted its ability to reduce ferric ions with the ferric reducing antioxidant power (FRAP) value of 99.33 ± 13.28 mg Fe (II) g^{-1} crude extract, which could be due to the presence of reducing agents converting ferric ions to ferrous ions. However, the leaf extracts showed weak metal chelating activity at 31%, even though the extract concentration had been increased to 5 mg mL^{-1}.

Tea sample produced from *C. cochinchinense* was also tested using DPPH radical scavenging assay for its antioxidant activity, compared with the *Camellia* teas (green tea, pu-erh tea, and black tea) used. The tea sample possessed total phenolic content of 51.14 mg GAE g^{-1} dry weight, which was relatively lower than pu-erh tea (67.82 mg GAE g^{-1}) and green tea (80.07 mg GAE g^{-1}) but higher than black tea (39.77 mg GAE g^{-1}). In addition, the sample charted a half maximal effective concentration (EC_{50}) value of 294.73 μg mL^{-1}, which showed intermediate antioxidant activity as compared to trolox (17.67 μg mL^{-1}), green tea (44.23 μg mL^{-1}), pu-erh tea (108.10 μg mL^{-1}), and black tea (176.23 μg mL^{-1}) (Bi et al., 2016).

Antioxidant investigations were also conducted on *C. glaucum* recently. For example, Juanda et al. (2021) reported that the leaves, stems, and cortex extracts of *C. glaucum* contained phytochemicals, such as flavonoids, quinones, phenols, tannins, saponins, and steroids/triterpenoids. Three different solvents (n-hexane, ethyl acetate, and ethanol) were used to extract the plant, revealing total phenolic contents ranging from 6.62 to 48.77 g GAE 100 g^{-1} extract and total flavonoid contents ranging from 1.54 to 25.96 g QE 100 g^{-1} extract. Ethanol extracts possessed the highest total phenolic contents, ranging from 29.51 to 48.77 g GAE 100 g^{-1} extract. For total flavonoid contents, ethyl acetate stem extract had the highest content (25.96 g QE 100 g^{-1} extract),

while ethanol cortex extract reported the lowest content (1.54 g QE 100 g^{-1} extract). The plant contained phenolic and flavonoid compounds, so the extracts could scavenge DPPH free radicals and inhibit xanthine oxidase activities.

Xanthone is an abundant secondary plant metabolite in the twigs of *C. cochinchinense* and *C. formosum*. Chailap and Nuanyai (2019) successfully isolated and identified seven xanthones present in *C. cochinchinense* and *C. formosum*, which were β-mangostin, cudratricusxanthone E, cochinchinone A, cochinchinone B, 1,3,7-trihydroxy-2,4-di-(3-methylbut-2-eyl)-xanthone, dulcisxanthone B, and 2-geranyl-1,3,7-trihydroxy-4-(3,3-dimethylallyl)-xanthone. Meanwhile, xanthones with a hydroxyl group at C-6, such as dulcisxanthone B, β-mangostin, cudratricusxanthone E, and cochinchinone B, exhibited strong free radicals scavenging activities and low potential of oxidation peaks, in DPPH radical scavenging activity assay and cyclic voltammetry, respectively. Therefore, the hydroxyl moiety at the C-6 position could be concluded to play a crucial role in the antioxidant power of xanthone (Chailap & Nuanyai, 2019).

The *C. formosum* leaf extract contained chlorogenic acid (main phenolic acid), dicaffeoylquinic acid, and two ferulic acid derivatives. Antioxidant activities of the extract were assessed using DPPH and ABTS free radical scavenging assays. It was found that chlorogenic acid and another minor compound, dicaffeoylquinic acid, contributed to the antioxidant potential of the extract by demonstrating strong scavenging activities in both assays (Maisuthisakul et al., 2007).

In the past years, very few studies have been conducted on *C. sumatranum*. However, according to Tantapakul et al. (2016), *C. sumatranum* possessed antioxidant activities. The compounds elucidated from the ethanolic extract were evaluated using DPPH radical scavenging activity assay. Among all isolated compounds, it was found that only two compounds (macluraxanthone, 1,3,5,6-tetrahy-droxyxanthone) exhibited potent antioxidant activities, while the remaining compounds showed weak activities.

Antimalarial

Several studies had been conducted on *C. cochinchinense* to test its antimalarial effects against *Plasmodium falciparum*. Roots of *C. cochinchinense* were extracted, and prenylated xanthones were isolated. Among the isolated prenylated xanthones, 5-*O*-methylcelebixanthone, celebixanthone, β-mangostin, and cochinchinone C were found to be effective in inhibiting malarial activities, with half maximal inhibitory concentration (IC_{50}) values of 3.2 μg mL^{-1}, 4.9 μg mL^{-1}, 7.2 μg mL^{-1}, and 2.6 μg mL^{-1}, respectively, while the rest of the isolated compounds were shown inactive (Laphookhieo et al., 2006). Five phenolic compounds were also detected in the fruits of *C. cochinchinense*, and their antimalarial activities were determined. Among the five phenolic compounds identified, fuscaxanthone E, vismione B, vismione

F, and vismione E showed significant antimalarial effects. Vismione B showed the strongest activity at the IC_{50} value of 0.66 µg mL^{-1}, while vismione F and E recorded IC_{50} values of 2.02 µg mL^{-1} and 3.91 µg mL^{-1}, respectively. The structural variations of the vismione derivatives influenced antimalarial properties. As reported by Laphookhieo et al. (2009), a chromene ring was seen in the structure of vismione B at C-1 and C-2 positions, while in the chemical structure of vismione E and F, hydroxyl and isoprenyl groups were present at C-1 and C-2 instead of the chromene ring.

Three 1,3,5,6-oxygenated xanthones identified as formoxanthone C, gerontoxanthone I, and macluraxanthone were isolated from *C. maingayi* stem bark. All three xanthones exhibited strong antimalarial properties against *P. falciparum* with a low IC_{50} value of below 2 µg mL^{-1}. The strong antimalarial activity was observed among these 1,3,5,6-oxygenated xanthones because of two hydroxyl groups at C-5 and C-6 positions (Laphookhieo et al., 2009).

Anti-Gastric Ulcer

Cratoxylum arborescens exhibited anti-gastric ulcer properties due to its potential as an anti-*Helicobacter pylori* agent. This plant possessed high phytochemical contents consisting of xanthones, α-mangostin, and β-mangostin (Sharifi-Rad et al., 2018). Sidahmed et al. (2013) mentioned that α-mangostin isolated from the stem bark of *C. arborescens* demonstrated antibacterial properties towards *H. pylori*. The compound α-mangostin had shown a dose-dependent activity and was certainly able to protect the gastric mucosa from bacterial infection. Furthermore, it was revealed that α-mangostin interfered with the release of nitric oxides as well as the inhibition of cyclooxygenases (COX), thus validating the gastroprotective potential of *C. arborescens* to prevent the formation of gastric ulcers. In another study by Sidahmed et al. (2016), the stem bark of *C. arborescens* was found to contain β-mangostin, demonstrating gastroprotective activity by inducing the secretion of gastro-adherent mucus in the Sprague Dawley rats against the ethanol ulcer model system. Besides, this compound also exhibited antioxidant, anti-apoptotic, and anti-*H. pylori* effects strengthening its potential as an anti-gastric ulcer agent.

Anti-HIV-1 Reverse Transcriptase

Pentacyclic triterpenoids derivatives are one of the naturally occurring triterpenoids conferring anti-HIV potential. Lupanes, such as betulinic acid and lupene derivatives, are active in the inhibition activity of HIV-1 reverse transcriptase (Cassels & Asencio, 2010; Chinsembu, 2019). The leaves and twigs of *C. arborescens* were extracted and tested using the HIV-1 reverse transcriptase assay. Among the isolated compounds, betulinic acid and the lupene derivatives (lup-20(29)-ene-3β,30-diol and 3β-hydroxylup-20(29)-en-30-oic acid) were identified, along with other compounds, which were euxanthone and 1,3,7-trihydroxy-6-methoxy-4,5-di(3-methylbut-2-en-yl) xanthone. These compounds possessed IC_{50} values ranging from 8.7 µg mL^{-1}

to 84.9 μg mL^{-1}, indicating moderate to strong activities in the inhibition of HIV-1 reverse transcriptase. The result showed that 3β-hydroxylup-20(29)-en-30-oic acid exhibited the strongest inhibition activity towards HIV-1 reverse transcriptase with an IC_{50} value of 8.7 μg mL^{-1}. The isolated compounds were also tested using the syncytium assay that utilized $^{\Delta Tat/Rev}$MC99 virus and 1A2 cell line system. It was reported that lup-20(29)-ene-3β,30-diol, betulinic acid, euxanthone, 1,3,8-trihydroxy-2,4-dimethoxyxanthone, 3,4-dihydroxybenzoic acid, and 3β-hydroxylup-20(29)-en-30-oic acid possessed anti-HIV-1 activity based on the assay with the EC_{50} values ranging from below 3.9 to 32.2 μg mL^{-1} in which betulinic acid recorded the lowest EC_{50} value lesser than 3.9 μg mL^{-1} (Reutrakul et al., 2006).

In addition, a recent study was conducted on the stem bark of *C. formosum* ssp. *pruniflorum* for its anti-HIV-1 reverse transcriptase activity. Crude methanol extract and five fractions (CFA, CFB, CFC, CFD, and CFE) obtained from crude chloroform extract were tested. One of the chloroform fractions, CFE, exhibited effective anti-HIV-1 reverse transcriptase activity, similar to the positive control, Nevirapine, while the rest of the samples showed low inhibition (Srisombat et al., 2019).

Antidiabetic

The root bark of *C. cochinchinense* was reported to inhibit the activities of protein tyrosine phosphatase 1B (PTP1B) and α-glucosidase, which were the key target enzymes for the treatment of non-communicable chronic diseases such as obesity and diabetes mellitus. The isolated alkylated xanthones from *C. cochinchinense* demonstrated significant inhibitory activity with IC_{50} values ranging from 1.7 to 72.7 μM for α-glucosidase and 2.4 to 52.5 μM for PTP1B. Cratoxanthone A (IC_{50} = 4.8 μM), α-mangostin (IC_{50} = 5.7 μM), and ɣ-mangostin (IC_{50} = 1.7 μM) were the xanthones identified as the most active α-glucosidase inhibitors with IC_{50} values less than 10 μM. Li, Lee, et al. (2018) mentioned that subtle structural changes in the relevant compounds contributed to the α-glucosidase inhibitory potencies of xanthones. Xanthones with prenyl group on A-ring that bore free hydroxyl groups, such as cratoxanthone A, showed better inhibition towards α-glucosidase as compared to cochinchinone A. Furthermore, cratoxanthone A (IC_{50} = 2.4 μM), cochinchinone A (IC_{50} = 5.2 μM), and α-mangostin (IC_{50} = 5.5 μM) were the most active PTP1B inhibitors. Among the isolated alkylated xanthones, cratoxanthone A, and α-mangostin were the most potent inhibitors for α-glucosidase and PTP1B. In addition, two new xanthones, cratoxanthone E and F, were also identified from the *C. cochinchinense* root bark, demonstrating inhibition towards α-glucosidase and PTP1B (Li, Song, et al., 2018).

Besides, caged xanthones were also elucidated from the root bark of *C. cochinchinense*. As a result, six caged xanthones were isolated, and these compounds were studied for their

PTP1B inhibitory potentials. Among the isolated compounds, cochinchinoxanthone C, cochinchinoxanthone D, and cochinchinoxanthone recorded significant PTP1B inhibitory activities with IC_{50} values of 76.3, 46.2, and 6.6 µM, respectively. As such, cochinchinoxanthone was reported to be the most potent PTP1B inhibitor among the isolated caged xanthones (Li, Lee, et al., 2018).

Anticancer

The 1,3-dihydroxy-6,7-dimethoxy-2,8-diprenylxanthone and 2-geranylemodin were the xanthones compounds obtained from the *C. arborescens* stem bark with moderate cytotoxic effect towards NCI-H187 (lung cancer cell line) at IC_{50} values of 3.69 ± 1.27 and 3.08 ± 0.73 µg mL^{-1}, respectively (Pattanaprateeb et al., 2005). Besides, α-mangostin as the major bioactive compound in *C. arborescens*, was cytotoxic towards human cervix carcinoma cells (WRL-68) with IC_{50} value of 65 µg mL^{-1} but did not have any cytotoxic effect on normal kidney and liver cells as determined using *in vivo* mice model after 14 days of oral gavage with 100 mg kg^{-1}, 500 mg kg^{-1}, and 1000 mg kg^{-1} of compound (Ibrahim et al., 2015). Moreover, α-mangostin also showed a remarkable cytotoxic effect on the HeLa cancer cell line with an IC_{50} value of 24.53 ± 1.48 µM. However, no significant cytotoxic effects were shown towards normal human epithelial ovarian cells (SV40), where the IC_{50} value of 93.26 ± 3.92 µM was recorded after 24 hours of incubation. The proliferation and colony-forming capabilities of HeLa cells were significantly reduced and inhibited after treatment with α-mangostin isolated from *C. arborescens* in a dose and time-dependent manner. It was reported that the apoptosis in HeLa cells was induced by α-mangostin via the mitochondrial-dependent pathway. First, it disrupted the mitochondrial membrane potential with reactive oxygen species (ROS) due to high oxidative stress. It triggered the release of cytochrome C into the cytosol, which marked the early apoptosis process. Then, the free cytochrome C activated caspases (caspase-3, caspase-7, and caspase-9), which eventually led to apoptosis (El Habbash et al., 2017). In addition, Yahayu et al. (2013) showed that the α-mangostin and β-mangostin extracted from the *C. arborescens* stem bark exhibited high cytotoxicities against estrogen receptor-positive human breast adenocarcinoma cells (MCF-7) with IC_{50} values of 12.48 µg ml^{-1} and 28.42 µg ml^{-1}, respectively. The high cytotoxicity of α-mangostin towards MCF-7 cells was associated with the prenyl groups that affected the mitochondrial signal transduction pathway, which was responsible for the mitochondria permeability. In contrast, β-mangostin demonstrated a slightly lower cytotoxic effect on MCF-7 cells due to the loss of one hydroxyl group (Yahayu et al., 2013).

The cytotoxic effect of the less potent β-mangostin of *C. arborescens* isolated from stem bark was further studied by Syam et al. (2014) against the estrogen receptor-positive human breast adenocarcinoma

cells (MCF-7), estrogen receptor-negative human breast adenocarcinoma cells (MDA-MB 231), human liver hepatocellular cells (HepG2), human lung cancer cells (A-549), and human prostate cancer cells (PC3). This phytocompound exhibited a selective cytotoxic effect as the most significant cytotoxicity was observed for the two breast cancer cell lines, MCF-7 and MDA-MB-231. The MCF-7 and MDA-MB-231 cells showed prominent growth inhibition and cellular shrinkage after 24 hours post-treatment with β-mangostin. Meanwhile, animal experiments also validated that β-mangostin was non-hepatotoxic and nephrotoxic, with no significant changes in the body weight of mice models after treatment (Syam et al., 2014). Besides, β-mangostin also showed a significant antiproliferative effect on human promyelocytic leukemia cells (HL60) at a concentration of 58 µM post-treatment, with a 70% reduction in cellular viability. A similar apoptotic pathway was observed after induction with β-mangostin, which exhibited adverse effects on the mitochondrial membrane potential through the generation of an excessive amount of reactive oxygen species that led to the release of cytochrome C into the cytosol. Then, the free cytochrome C triggered the caspase-3 and caspase-9 activities, causing cell apoptosis. β-mangostin reduced the transcription of the mRNA of the apoptosis repressor genes Bcl-2 and HSP70 while upregulating the gene expression of caspase-9 as observed in quantitative real-time polymerase chain reaction (qPCR) reaction in a dose-dependent manner (Omer et al., 2017*).*

Hexane fraction of xanthones extracted from the roots of *C. cochinchinense* was significantly cytotoxic towards human lung cancer cells (NCI-H187) but demonstrated no antiproliferative effect on human mouth epidermoid carcinoma cells (KB) and breast cancer cells (BC-549). The geranyl moiety on the xanthones isolated from *C. cochinchinense* was considered responsible for its remarkable anticancer activity (Laphookhieo et al., 2006). Meanwhile, Mahabusarakam et al. (2008) reported that the dichloromethane fraction and methanolic fraction of xanthones from the roots of a similar plant consisting of 7-geranyloxy-1,3-dihydroxyxanthone and celebixanthone had strong cytotoxic effect towards MCF-7, HeLa, HT-29, and KB cancer cell lines, with IC_{50} values in the range of 0.32 to 0.45 mg mL^{-1}. The contradicting results for KB cancer cells may be due to the difference in the phytochemical contents in the various fractions tested by the researchers.

Laphookhieo et al. (2009) isolated formoxanthone C, gerontoxanthone I, and macluraxanthone from the bark of *C. cochinchinense*; vismione E and vismione F from the fruits of *C. cochinchinense* and these compounds were found to exhibit cytotoxic effects towards NCI-H187 cancer cells. Interestingly, formoxanthone C demonstrated the highest cytotoxic effect on NCI-H187 cancer cells with an IC_{50} value of 0.22 µg mL^{-1} compared to other isolated compounds and elliticine (IC_{50} = 0.45 µg mL^{-1}), a standard drug used in the sulforhodamine B (SRB) colorimetric cytotoxicity assay. In addition, pruniflorone

M, pruniflorone N, and 6-deoxyisojacareubin had been identified from the barks of *C. cochinchinense* with their significant antiproliferative effects on human breast cancer cells (MCF-7 and SKBR3), Ishikawa endometrial adenocarcinoma, ovarian carcinoma (BG-1), mesothelioma (IST-MES1), and human liver cancer cells (HepG2) based on MTT assays (Thu et al., 2017). Furthermore, fruits and leaves of *C. cochinchinense* also contained cochinchinone G, which showed a strong cytotoxic effect on the breast (BT474), lung (ChaGO-K-1), liver (HepG2), gastric (KATO-3), and colon (SW-620) cancer cell lines in MTT [3-(4,5-dimethylthiazol-2-yl)-2,5 diphenyl tetrazolium bromide] assays at IC_{50} values of 5.25 μg mL^{-1}, 5.44 μg mL^{-1}, 5.74 μg mL^{-1}, 5.32 μg mL^{-1}, and 4.64 μg mL^{-1}, respectively (Chailap et al., 2017).

On the other hand, Ren et al. (2011) identified α-mangostin as the most potent cytotoxic xanthone from the *C. cochinchinense* methanolic stem extract against the human colon cancer cell line (HT-29) with a median effective dose (ED_{50}) value of 4.1 μM. Meanwhile, the semi-synthetic derivatives of 6-*O*-benzoyl-α-mangostin and 3,6-di-*O*-acetyl-α-mangostin obtained from the chemical modification of α-mangostin were shown to be highly cytotoxic towards the HT-29 human colon cancer cells with ED_{50} values of 1.0 and 1.9 μM, respectively. This study discovered that the carboxyl group at C-18 and the prenyl groups at C-2 and C-4 were not responsible for the cytotoxicity of the xanthone compounds. The chemical modification of α-mangostin revealed that 3,6-diacetylation and 6-benzoylation could improve the cytotoxicity; at C-2 and C-3, the cyclization had retained the initial cytotoxicity, while at C-1, C-2, the cyclization, and 3,6-dimethylation would decrease the xanthone cytotoxicity. Besides, Ren et al. (2011) also found that 1,3,7-trihydroxy-2,4-diisoprenylxanthone isolated from the *C. cochinchinense* stem extracts possessed the highest inhibitory effect (IC_{50} value of 2.9 μM) on the nuclear factor-κB (NF-κB) p65. The transcriptional factor p65 plays a key role in the inflammatory responses on the NF-κB signaling pathway. Stimulation of the p65 transcriptional factor at aberrant levels would induce the canonical NF-κB signaling pathway above basal levels and indirectly trigger the development of tumors (Giridharan & Srinivasan, 2018).

In a study by Tang, Whiteman, Jenner, et al. (2004), a semipurified extract (YCT) containing at least 90% mangiferin was obtained from *C. cochinchinense*. This extract had induced a selective cytotoxic effect towards Jurkat T cells (T cell leukemia) by reducing 60% of cellular viability at 63.35 μg mL^{-1} after 48 hours of treatment but no significant effect on normal cell lines (Chang's liver cell (CL), Madin–Darby canine kidney (MDCK), human articular chondrocytes (HAC), rat pheochromocytoma cells (PC12), and human chondrosarcoma cells (HTB94)). It was postulated that YCT acted on the plasma membrane redox system (PMRS), such as cNOX (constitutive) and tNOX

(tumor-associated) plasma membrane oxidases that were active on T cell leukemia but inactive on normal lymphocytes. At first, YCT induced high oxidative stress by accumulating radical oxygen species (ROS) in the mitochondria. This action depolarized the mitochondrial membrane causing a rapid influx of calcium ions (Ca^{2+}) through the membrane's non-selective cation channel. Excessive Ca^{2+} led to a fall in mitochondria membrane potential, ultimately leading to cell death. Hepatotoxicity was observed in this experiment despite the positive effect of YCT on T cells. Human fetal liver cells (HFL) and human liver cancer cells were most susceptible to YCT, with reduced viability to 10% and 20%, respectively, after 48 hours of exposure at 63.35 μg mL^{-1} (Tang, Whiteman, Jenner, et al., 2004).

The anticancer properties of *C. cochinchinense* were mainly attributed to the xanthone compounds present in different parts of the plant. Studies have suggested that the selective cytotoxic effects of different xanthones on cancer cell lines largely depended on the molecular moiety present in the xanthones. For example, the hydroxyl moiety presents at C-5 of celebixanthone and the geranyl group at C-4 of cochinchinone A were responsible for the high cytotoxic effect towards human lung cancer cell (NCI-H187), but the opposite was observed for the methoxyl group at 5-*O*-methylcelebixanthone and prenyl group at 1,3,7-trihydroxy-2,4-di(3-methylbut-2-enyl) xanthone (Laphookhieo et al., 2006). This finding was supported by Chailap et al. (2017), who reported that cochinchinone G, which possessed two hydroxyl groups, expressed a high cytotoxic effect towards breast (BT474), lung (ChaGO-K-1), liver (HepG2), gastric (KATO-3), and colon (SW-620) cancer cell lines. Meanwhile, α,α,β-trimethylfuran ring on C-3/C-4 of formoxanthone C also contributed to the high cytotoxic effect towards NCI-H187. On the other hand, at C-4, the 1,1-dimethyl-2-propenyl moiety of gerontoxanthone I and macluraxanthone were reported to reduce the cytotoxic effect on NCI-H187 (Laphookhieo et al., 2009). Xanthone with an additional oxygenated heterocyclic ring fused with the xanthone nucleus at C-3/C-4 showed a high cytotoxic effect towards human breast cancer cells (MCF-7 and SKBR3), Ishikawa endometrial adenocarcinoma, ovarian carcinoma (BG-1), mesothelioma (IST-MES1), and human liver cancer cells (HepG2). However, an isoprenyl moiety in xanthone V_1 and macluraxanthone reduced the cytotoxic effect (Takamatsu et al., 2003). Chemical modifications, such as 3,6-diacetylation and 6-benzoylation, were reported to have improved the cytotoxicity towards cancer cell lines while cyclization at C-2 and C-3 on α-mangostin retained the initial cytotoxicity and cyclization at C-1 and C-2 and 3,6-dimethylation greatly reduced the cytotoxicity (Ren et al., 2011).

The crude methanol extracts (CME) of *C. formosum* ssp. *pruniflorum* (Teawdang) edible parts were found to be cytotoxic towards several cervical cancer cell lines, including HeLa (adenocarcinoma with HPV 18 positive), SiHa (squamous cell carcinoma grade II with HPV 16 positive),

and C-33A (carcinoma with non-HPV infection) cell lines, with IC_{50} of 208.32, 338.06, and 107.74 µg mL^{-1}, respectively. The crude methanol extract was reported to have phenolic contents, such as gallic acid, caffeine, caffeic acid, ferulic acid, quercetin, and resveratrol. Gallic acid was already proven to be cytotoxic to the hepatitis B virus as well as liver cancer cell lines (Promraksa et al., 2015; Waiyaput et al., 2012). Besides, the growth of HepG2 cancer cells was inhibited by 50% hydroethanolic extracts of *C. formosum* ssp. *pruniflorum* with the phytoconstituent of xanthones, terpenoids, tannin, saponin, alkaloids, and reducing sugars (IC_{50} value = 55.9 ± 10.6 µg mL^{-1}), as compared to non-cancerous vero cells (IC_{50} value more than 500 µg mL^{-1}) (Nonpunya et al., 2018). The cellular effect of *C. formosum* ssp. *pruniflorum* extracts towards HepG2 was apoptosis by activating caspase enzymes (Nonpunya et al., 2018).

In a study conducted by Senggunprai et al. (2016), the cytotoxic effect of the aqueous and ethanolic leaf extracts of *C. formosum* (Jack) Dyer towards human cholangiocarcinoma (KKU-M156) cells was shown in a concentration-dependent manner with the IC_{50} values ranging from 11.3 to 12.1 mg mL^{-1}. Apoptosis was observed in most cells, and necrosis was also seen in a small proportion of the cells after 24 hours of treatment. The percentage of apoptotic and necrotic cells increased dose-dependent for both aqueous and ethanolic extracts. In addition, the cells were arrested at the G2/M phase of the cell cycle, and the expression of cyclin A and Cdc25A, which were responsible for cell cycle regulation, were down-regulated. In another study by Putthawan et al. (2018), ethanolic leaf extracts of *C. formosum* exhibited a significant cytotoxic activity on human colorectal adenocarcinoma cell line (HT-29) and human liver cancer cell line (HepG2 cells) at 35.25 ± 5.95% and 17.13 ± 0.58%, at the concentration of 2000 µg mL^{-1}, respectively.

The ethanolic leaf extract of *C. formosum* (collected at Udon Thani province) showed significant cytotoxic effects on human breast cancer cells MCF-7 cells, as reported by Buranrat et al. (2017). The extract decreased the MCF-7 cell viability dose-dependently without altering the cellular morphology (IC_{50} values of 85.70 ± 4.52 mg mL^{-1} at 24 h and 53.74 ± 3.02 mg mL^{-1} at 48 h). Besides, this extract also lowered the colony-forming ability of the MCF-7 cell line with concentration (IC_{50} values of 36.37 ± 1.80 mg mL^{-1}) by reducing its cyclin D1 (cell cycle protein) expression. Furthermore, it potentiated the activity of anticancer drugs [5-fluorouracil (5-FU), cisplatin, doxorubicin, and gemcitabine] inducing MCF-7 cell death as compared to treatment groups with ethanolic leaf extract or anticancer drugs alone. Furthermore, the *C. formosum* ethanolic leaf extract significantly increased the intracellular ROS formation and caspase-3 activity, which led to mitochondrial membrane dysfunction, resulting in the apoptosis of cancer cells. It was found that 100 mg mL^{-1} of the leaf extract could reduce the mitochondrial function of MCF-7 cancer cells by 80% compared to

the untreated cell groups. In addition, this extract inhibited the MCF-7 cell migration by reducing the protein expression of matrix metalloproteinases MMP-2 and MMP-9, major proteins involved in the metastasis, migration, and invasion processes in tumor cells. It also interfered with the mevalonate pathway (cancer cell proliferation pathway) by significantly downregulating the gene expression of Rac1 and cdk6, which were responsible for breast cancer cell proliferation.

Ahn et al. (2019) synthesized *C. formosum* silver nanoparticles (AgNPs) with 0.25 mM silver nitrate and 0.02% of *C. formosum* ethanolic leaf extract. The result demonstrated high cytotoxicity against the human lung cancer cells (A549) compared to the *C. formosum* ethanolic leaf extracts alone. However, the cytotoxicity of *C. formosum* AgNPs towards the A549 cancer cell line was found to be greatly affected by the presence of fetal bovine serum (FBS). The viability of cancer cells treated by AgNPs was 49.9% in the presence of FBS, whereas, in the absence of FBS, it was 65.4%. Furthermore, the annexin V/ propidium iodide staining method used in the study suggested that the *C. formosum* AgNPs was a potential anticancer agent by inducing early apoptosis (21.36%) in A549 human lung cancer cells (Ahn et al., 2019).

Formoxanthone C was one of the bioactive compounds isolated and identified from the roots of *C. formosum* ssp. *pruniflorum* (Jack) Dyer. It exhibited a significant cytotoxic effect towards MCF-7, HeLa, HT-29, and KB cancer cell lines at IC_{50} values of 4.9, 3.7, 5.3, and 3.3 μg mL^{-1}, respectively. Meanwhile, it was determined that the catechol unit in the xanthone increased the cytotoxic effect (Boonsri et al., 2006).

Laphookhieo et al. (2009) characterized the three 1,3,5,6-oxygenated xanthones from the stem barks of *C. maingayi* as gerontoxanthone I, macluraxanthone, and formoxanthone C, as well as their cytotoxicities against NCI-H187, small cell lung carcinoma. It was found that all three 1,3,5,6-oxygenated xanthones exhibited a significant cytotoxic effect towards NCI-H187 at IC_{50} values of 6.63 μg mL^{-1} (gerontoxanthone I), 3.42 μg mL^{-1} (macluraxanthone), and 0.22 μg mL^{-1} (formoxanthone C). The highest cytotoxic effect of formoxanthone C was found to be associated with the α,α,β-trimethylfuran ring on C-3/C-4 as compared to the less potent gerontoxanthone I, which had only isoprenyl and hydroxyl groups at C-1 and C-2, respectively (Chailap et al., 2017).

New xanthones of cratoxyarborenones A-F and the four known compounds, vismione B, 2,4,6-trihydroxybenzophenone 4-*O*-geranyl ether, betulinic acid, and δ-tocotrienol as well as two novel anthraquinobenzophenones, cratoxyarborequinones A and B were found in the leaves, stem bark, and twigs of *C. sumatranum* using bioassay directed fractionation. Their cytotoxic effects were evaluated against the human oral epidermoid carcinoma (KB) cell line. The new xanthones of cratoxyarborenones A-F were all cytotoxic towards the KB

cell, with the highest being observed for cratoxyarborenones B at EC_{50} of 1.0 ± 0.1 µg mL^{-1} in comparison to vismione B (EC_{50} = 1.3 ± 0.1 µg mL^{-1}). In contrast, the two novel anthraquinobenzophenones, cratoxyarborequinones A and B, were inactive against the KB cell (Seo et al., 2002).

CONCLUSION

This review highlighted the vast bioactivities of the flowering plant, *Cratoxylum* genus, especially in the traditional medicinal system and as proven scientifically in many studies. Various parts of the plants are found to contain distinctive phytochemical compounds which may contribute to their observed pharmacological activities, such as antibacterial, antifungal, antioxidant, antimalarial, antiulcer, anti-HIV, antidiabetic, and anticancer effects. Nonetheless, there are still other novel bioactive molecules yet to be discovered from this plant species, thus, warrants further investigation. Furthermore, more in-depth research on the mechanistic actions of the plant extracts or their specific phytoconstituents towards the reported pharmacological actions should also be carried out to provide a better perspective on their bioactivities. In addition, *in vivo* model systems are highly recommended to be integrated into biological testing to validate results from *in vitro* studies. Pre-clinical and clinical trials are vital to further develop *Cratoxylum* species as a potent therapeutic agent for many ailments.

REFERENCES

Ahn, E.-Y., Jin, H., & Park, Y. (2019). Assessing the antioxidant, cytotoxic, apoptotic and wound healing properties of silver nanoparticles green-synthesized by plant extracts. *Materials Science and Engineering: C*, *101*, 204-216. https://doi.org/10.1016/j.msec.2019.03.095

Bi, W., He, C., Ma, Y., Shen, J., Zhang, L. H., Peng, Y., & Xiao, P. (2016). Investigation of free amino acid, total phenolics, antioxidant activity and purine alkaloids to assess the health properties of non-*Camellia* tea. *Acta Pharmaceutica Sinica B*, *6*(2), 170-181. https://doi.org/10.1016/j.apsb.2015.11.003

Boo, B. C., Omar-Hor, K., & Ou-Yang, C. L. (2003). *1001 Garden plants in Singapore* (2nd ed.). National Parks Board.

Boonnak, N., Karalai, C., Chantrapromma, S., Ponglimanont, C., Fun, H.-K., Kanjana-Opas, A., Chantrapromma, K., & Kato, S. (2009). Anti-*Pseudomonas aeruginosa* xanthones from the resin and green fruits of *Cratoxylum cochinchinense*. *Tetrahedron*, *65*(15), 3003-3013. https://doi.org/10.1016/j.tet.2009.01.083

Boonsri, S., Karalai, C., Ponglimanont, C., Kanjana-opas, A., & Chantrapromma, K. (2006). Antibacterial and cytotoxic xanthones from the roots of *Cratoxylum formosum*. *Phytochemistry*, *67*(7), 723-727. https://doi.org/10.1016/j.phytochem.2006.01.007

Buranrat, B., Mairuae, N., & Konsue, A. (2017). *Cratoxy formosum* leaf extract inhibits proliferation and migration of human breast cancer MCF-7 cells. *Biomedicine and Pharmacotherapy*, *90*, 77-84. https://doi.org/10.1016/j.biopha.2017.03.032

Cassels, B. K., & Asencio, M. (2010). Anti-HIV activity of natural triterpenoids and hemisynthetic derivatives 2004–2009. *Phytochemistry Reviews*, *10*(4), 545-564. https://doi.org/10.1007/s11101-010-9172-2

Chailap, B., & Nuanyai, T. (2019). Antioxidant activities and electrochemical behaviors of xanthones from *Cratoxylum cochinchinense* and *Cratoxylum formasum*. *Naresuan University Journal: Science and Technology*, *27*(3), 35-42. https://doi.org/10.14456/nujst.2019.24

Chailap, B., Nuanyai, T., Puthong, S., & Buakeaw, A. (2017). Chemical constituents of fruits and leaves of *Cratoxylum cochinchinense* and their cytotoxic activities. *Naresuan University Journal: Science and Technology*, *25*(3), 22-30.

Chinsembu, K. C. (2019). Chemical diversity and activity profiles of HIV-1 reverse transcriptase inhibitors from plants. *Revista Brasileira De Farmacognosia*, *29*(4), 504-528. https://doi.org/10.1016/j.bjp.2018.10.006

Choi, S.-J., Tai, B. H., Cuong, N. M., Kim, Y.-H., & Jang, H.-D. (2012). Antioxidative and anti-inflammatory effect of quercetin and its glycosides isolated from mampat (*Cratoxylum formosum*). *Food Science and Biotechnology*, *21*(2), 587-595. https://doi.org/10.1007/s10068-012-0075-4

Dapar, M. L. G. (2020). *Cratoxylum sumatranum* (Jack) Blume Hypericaceae. In F. M. Franco (Ed.), *Ethnobotany of mountain regions of Southeast Asia* (pp. 1-5). Springer. https://doi.org/10.1007/978-3-030-14116-5_114-1

Dapar, M. L. G., Alejandro, G. J. D., Meve, U., & Liede-Schumann, S. (2020). Quantitative ethnopharmacological documentation and molecular confirmation of medicinal plants used by the *Manobo* tribe of Agusan del Sur, Philippines. *Journal of Ethnobiology and Ethnomedicine*, *16*, 14. https://doi.org/10.1186/s13002-020-00363-7

El Habbash, A. I., Mohd Hashim, N., Ibrahim, M. Y., Yahayu, M., Omer, F. A. E., Abd Rahman, M., Nordin, N., & Lian, G. E. C. (2017). *In vitro* assessment of anti-proliferative effect induced by α-mangostin from *Cratoxylum arborescens* on HeLa cells. *PeerJ*, *5*, e3460. https://doi.org/10.7717/peerj.3460

Enggiwanto, S., Riyani, N., Pratama, Y., Roanisca, O., & Mahardika, R. G. (2019). Antibacterial effectiveness of formulations nanoemulsion *Cratoxylum glaucum* Korth. extract. In *IOP Conference Series: Earth and Environmental Science* (Vol. 353, No. 1, p. 012038). IOP Publishing. https://doi.org/10.1088/1755-1315/353/1/012038

Giridharan, S., & Srinivasan, M. (2018). Mechanisms of NF-κB p65 and strategies for therapeutic manipulation. *Journal of Inflammation Research*, *11*, 407-419. https://doi.org/10.2147/JIR.S140188

Huang, Y., Xiao, D., Burton-Freeman, B. M., & Edirisinghe, I. (2016). Chemical changes of bioactive phytochemicals during thermal processing. In *Reference module in food science*. Elsevier. https://doi.org/10.1016/b978-0-08-100596-5.03055-9

Ibrahim, M. Y., Hashim, N. M., Mohan, S., Abdulla, M. A., Abdelwahab, S. I., Arbab, I. A., Yahayu, M., Ali, L. Z., & Ishag, O. E. (2015). α-Mangostin from *Cratoxylum arborescens*: An *in vitro* and *in vivo* toxicological evaluation. *Arabian Journal of Chemistry*, *8*(1), 129-137. https://doi.org/10.1016/j.arabjc.2013.11.017

Juanda, D., Fidrianny, I., Ruslan, K., & Insanu, M. (2019). Overview of phytochemical compounds and pharmacology activities of *Cratoxylum* genus. *Rasayan Journal of Chemistry*, *12*(4), 2065-2073. https://doi.org/10.31788/rjc.2019.1245303

Juanda, D., Fidrianny, I., Wirasutisna, K. R., & Insanu, M. (2021). Evaluation of xanthine oxidase inhibitory and antioxidant activities of three organs of idat (*Cratoxylum glaucum* Korth.) and correlation with phytochemical content. *Pharmacognosy Journal*, *13*(4), 971-976. https://doi.org/10.5530/pj.2021.13.125

Kukongviriyapan, U., Luangaram, S., Leekhaosoong, K., Kukongviriyapan, V., & Preeprame, S. (2007). Antioxidant and vascular protective activities of *Cratoxylum formosum*, *Syzygium gratum* and *Limnophila aromatica*. *Biological and Pharmaceutical Bulletin*, *30*(4), 661-666. https://doi.org/10.1248/bpb.30.661

Laphookhieo, S., Maneerat, W., & Koysomboon, S. (2009). Antimalarial and cytotoxic phenolic compounds from *Cratoxylum maingayi* and *Cratoxylum cochinchinense*. *Molecules*, *14*(4), 1389-1395. https://doi.org/10.3390/molecules14041389

Laphookhieo, S., Syers, J. K., Kiattansakul, R., & Chantrapromma, K. (2006). Cytotoxic and antimalarial prenylated xanthones from *Cratoxylum cochinchinense*. *Chemical and Pharmaceutical Bulletin*, *54*(5), 745-747. https://doi.org/10.1248/cpb.54.745

Li, Z. P., Lee, H.-H., Uddin, Z., Song, Y. H., & Park, K. H. (2018). Caged xanthones displaying protein tyrosine phosphatase 1B (PTP1B) inhibition from *Cratoxylum cochinchinense*. *Bioorganic Chemistry*, *78*, 39-45. https://doi.org/10.1016/j.bioorg.2018.02.026

Li, Z. P., Song, Y. H., Uddin, Z., Wang, Y., & Park, K. H. (2018). Inhibition of protein tyrosine phosphatase 1B (PTP1B) and α-glucosidase by xanthones from *Cratoxylum cochinchinense*, and their kinetic characterization. *Bioorganic and Medicinal Chemistry*, *26*(3), 737-746. https://doi.org/10.1016/j.bmc.2017.12.043

Mahabusarakam, W., Nuangnaowarat, W., & Taylor, W. C. (2006). Xanthone derivatives from *Cratoxylum cochinchinense* roots. *Phytochemistry*, *67*(5), 470-474. https://doi.org/10.1016/j.phytochem.2005.10.008

Mahabusarakam, W., Rattanaburi, S., Phongpaichit, S., & Kanjana-Opas, A. (2008). Antibacterial and cytotoxic xanthones from *Cratoxylum cochinchinense*. *Phytochemistry Letters*, *1*(4), 211-214. https://doi.org/10.1016/j.phytol.2008.09.012

Maisuthisakul, P., Pongsawatmanit, R., & Gordon, M. H. (2007). Characterization of the phytochemicals and antioxidant properties of extracts from Teaw (*Cratoxylum formosum* Dyer). *Food Chemistry*, *100*(4), 1620-1629. https://doi.org/10.1016/j.foodchem.2005.12.044

Natrsanga, P., Jongaramruong, J., Rassamee, K., Siripong, P., & Tip-pyang, S. (2020). Two new xanthones from the roots of *Cratoxylum cochinchinense* and their cytotoxicity. *Journal of Natural Medicines*, *74*(2), 467-473. https://doi.org/10.1007/s11418-019-01376-7

Neo, L., Chong, K. Y., Tan, S. Y., Lim, R. C. J., Loh, J. W., Ng, W. Q., Seah, W. W., Yee, A. T. K., & Tan, H. T. W. (2016). Towards a field guide to the trees of the Nee Soon Swamp Forest (II): *Cratoxylum* (Hypericaceae). *Nature In Singapore*, *9*, 29-39.

Ngamsurach, P., & Praipipat, P. (2021). Modified alginate beads with ethanol extraction of *Cratoxylum formosum* and *Polygonum odoratum* for antibacterial activities. *ACS Omega*, *6*(47), 32215-32230. https://doi.org/10.1021/acsomega.1c05056

Nonpunya, A., Sethabouppha, B., Rufini, S., & Weerapreeyakul, N. (2018). *Cratoxylum formosum* ssp. *pruniflorum* activates the TRAIL death receptor complex and inhibits topoisomerase I. *South African Journal of Botany*, *114*, 150-162. https://doi.org/10.1016/j.sajb.2017.11.003

Omer, F. A. A., Mohd Hashim, N., Ibrahim, M. Y., Dehghan, F., Yahayu, M., Karimian, H., Salim, L. Z. A., & Mohan, S. (2017). Beta-mangostin from *Cratoxylum arborescens* activates the intrinsic apoptosis pathway through reactive oxygen species with downregulation of the HSP70 gene in the HL60 cells associated with a G_0/G_1 cell-cycle arrest. *Tumor Biology*, *39*(11). https://doi.org/10.1177/1010428317731451

Pattanaprateeb, P., Ruangrungsi, N., & Cordell, G. A. (2005). Cytotoxic constituents from *Cratoxylum arborescens*. *Planta Medica*, *71*(2), 181-183. https://doi.org/10.1055/s-2005-837788

Promraksa, B., Ponlatham, C., Chaiyarit, P., Ratree, T., Tueanjit, K., Narintorn, R., Roongpet, T., & Patcharee, B. (2015). Cytotoxicity of *Cratoxylum formosum* subsp. *pruniflorum* Gogel extracts in oral cancer cell lines. *Asian Pacific Journal of Cancer Prevention*, *16*(16), 7155-7159. https://doi.org/10.7314/apjcp.2015.16.16.7155

Putthawan, P., Poeaim, S., & Areekul, V. (2018). Cytotoxic activity and apoptotic induction of some edible Thai local plant extracts against colon and liver cancer cell lines. *Tropical Journal of Pharmaceutical Research*, *16*(12), 2927-2933. https://doi.org/10.4314/tjpr.v16i12.17

Raksat, A., Sripisut, T., & Maneerat, W. (2015). Bioactive xanthones from *Cratoxylum cochinchinense*. *Natural Product Communications*, *10*(11), 1969-1972. https://doi.org/10.1177/1934578x1501001141

Ren, Y., Matthew, S., Lantvit, D. D., Ninh, T. N., Chai, H., Fuchs, J. R., Soejarto, D. D., de Blanco, E. J. C., Swanson, S. M., & Kinghorn, A. D. (2011). Cytotoxic and NF-κB inhibitory constituents of the stems of *Cratoxylum cochinchinense* and their semisynthetic analogues. *Journal of Natural Products*, *74*(5), 1117-1125. https://doi.org/10.1021/np200051j

Reutrakul, V., Chanakul, W., Pohmakotr, M., Jaipetch, T., Yoosook, C., Kasisit, J., Napaswat, C., Santisuk, T., Prabpai, S., Kongsaeree, P., & Tuchinda, P. (2006). Anti-HIV-1 constituents from leaves and twigs of *Cratoxylum arborescens*. *Planta Medica*, *72*(15), 1433-1435. https://doi.org/10.1055/s-2006-951725

Senggunprai, L., Thammaniwit, W., Kukongviriyapan, V., Prawan, A., Kaewseejan, N., & Siriamornpun, S. (2016). *Cratoxylum formosum* extracts inhibit growth and metastasis of cholangiocarcinoma cells by modulating the NF-κB and STAT3 pathways. *Nutrition and Cancer*, *68*(2), 328-341. https://doi.org/10.1080/01635581.2016.1142580

Seo, E.-K., Kim, N.-C., Wani, M. C., Wall, M. E., Navarro, H. A., Burgess, J. P., Kawanishi, K., Kardono, L. B. S., Riswan, S., Rose, W. C., Fairchild, C. R., Farnsworth, N. R., & Kinghorn, A. D. (2002). Cytotoxic prenylated xanthones and the unusual compounds anthraquinobenzophenones from *Cratoxylum sumatranum*. *Journal of Natural Products*, *65*(3), 299-305. https://doi.org/10.1021/np010395f

Sharifi-Rad, M., Fokou, P. V. T., Sharopov, F., Martorell, M., Ademiluyi, A. O., Rajkovic, J., Salehi, B., Martins, N., Iriti, M., Sharifi-Rad, J. (2018). Antiulcer agents: From plant extracts to phytochemicals in healing promotion. *Molecules*, *23*(7), 1751. https://doi.org/10.3390/molecules23071751

Sidahmed, H. M. A., Abdelwahab, S. I., Mohan, S., Abdulla, M. A., Taha, M. M. E., & Hashim, N. M., Hadi, A. H. A., Vadivelu, J., Fai, M. L., Rahmani, M., & Yahayu, M. (2013). α-Mangostin from *Cratoxylum arborescens* (Vahl) Blume demonstrates anti-ulcerogenic property: A mechanistic study. *Evidence-Based Complementary and Alternative Medicine*, *2013*, 450840. https://doi.org/10.1155/2013/450840

Sidahmed, H. M. A., Mohd Hashim, N., Syam, M., Abdelwahab, S. I., Taha, M. M. E., Dehghan, F., Yahayu, M., Ee, G. C. L., Loke, M. F., & Vadivelu, J. (2016). Evidence of the gastroprotective and anti-*Helicobacter pylori* activities of β-mangostin isolated from *Cratoxylum arborescens* (Vahl) Blume. *Drug Design, Development and Therapy*, *10*, 297-313. https://doi.org/10.2147/dddt.s80625

Sim, W. C., Ee, G. C. L., Lim, C. J., & Sukari, M. A. (2010). *Cratoxylum glaucum* and *Cratoxylum arborescens* (Guttiferae) - Two potential source of antioxidant agents. *Asian Journal of Chemistry*, *23*(2), 569-572.

Soepadmo, E., & Wong, K. M. (1995). *Tree flora of Sabah and Sarawak*. Forest Research Institute Malaysia (FRIM).

Sripanidkulchai, K., Teepsawang, S., & Sripanidkulchai, B. (2010). Protective effect of *Cratoxylum formosum* extract against acid/alcohol-induced gastric mucosal damage in rats. *Journal of Medicinal Food*, *13*(5), 1097-1103. https://doi.org/10.1089/jmf.2009.1237

Srisombat, N., Bapia, S., Ratanabunyong, S., Choowongkomon, K., Vajrodaya, S., & Duangsrisai, S. (2019). Isolation of betulinic acid and antioxidant and anti-HIV-1 reverse transcriptase activity of *Cratoxylum formosum* subsp. *pruniflorum* (Kurz) Gogelein extract. *Agriculture and Natural Resources*, *53*(6), 674-680. https://doi.org/10.34044/j.anres.2019.53.6.16

Suddhasthira, T., Thaweboon, S., Dendoung, N., Thaweboon, B., & Dechkunakorn, S. (2006). Antimicrobial activity of *Cratoxylum formosum* on *Streptococcus mutans*. *Southeast Asian Journal of Tropical Medicine and Public Health*, *37*(6), 1156-1159.

Syam, S., Bustamam, A., Abdullah, R., Sukari, M. A., Mohd Hashim, N., Yahayu, M., Hassandarvish, P., Mohan, S., & Abdelwahab, S. (2014). Cytotoxicity and oral acute toxicity studies of β-mangostin isolated from *Cratoxylum arborescens*. *Pharmacognosy Journal*, *6*(1), 47-56. https://doi.org/10.5530/pj.2014.1.8

Takamatsu, S., Galal, A. M., Ross, S. A., Ferreira, D., ElSohly, M. A., Ibrahim, A.-R., & El-Feraly, F. S. (2003). Antioxidant effect of flavonoids on DCF production in HL-60 cells. *Phytotherapy Research*, *17*(8), 963-966. https://doi.org/10.1002/ptr.1289

Tan, S.-A., Yam, H. C., Cheong, S. L., Chow, Y. C., Bok, C. Y., Ho, J. M., Lee, P. Y., & Gunasekaran, B. (2021). Inhibition of *Porphyromonas gingivalis* peptidyl arginine deiminase, a virulence factor, by antioxidant-rich *Cratoxylum cochinchinense*: *In vitro* and *in silico* evaluation. *Saudi Journal of Biological Sciences*, *29*(4), 2573-2581. https://doi.org/10.1016/j.sjbs.2021.12.037

Tang, S. Y., Whiteman, M., Jenner, A., Peng, Z. F., & Halliwell, B. (2004). Mechanism of cell death induced by an antioxidant extract of *Cratoxylum cochinchinense* (YCT) in Jurkat T cells: The role of reactive oxygen species and calcium. *Free Radical Biology and Medicine*, *36*(12), 1588-1611. https://doi.org/10.1016/j.freeradbiomed.2004.03.018

Tang, S. Y., Whiteman, M., Peng, Z. F., Jenner, A., Yong, E. L., & Halliwell, B. (2004). Characterization of antioxidant and antiglycation properties and isolation of active ingredients from traditional Chinese medicines. *Free Radical Biology and Medicine*, *36*(12), 1575-1587. https://doi.org/10.1016/j.freeradbiomed.2004.03.017

Tantapakul, C., Maneerat, W., Sripisut, T., Ritthiwigrom, T., Andersen, R. J., Cheng, P., Cheenpracha, S., Raksat, A., & Laphookhieo, S. (2016). New benzophenones and xanthones from *Cratoxylum sumatranum* ssp. *neriifolium* and their antibacterial and antioxidant activities. *Journal of Agricultural and Food Chemistry*, *64*(46), 8755-8762. https://doi.org/10.1021/acs.jafc.6b03643

Thakur, M., Singh, K., & Khedkar, R. (2020). Phytochemicals. In *Functional and preservative properties of phytochemicals* (pp. 341-361). Academic Press. https://doi.org/10.1016/b978-0-12-818593-3.00011-7

Thaweboon, S., Thaweboon, B., Dechkunakorn, S., Nisalak, P., & Kaypetch, R. (2014). Anticandidal activity of *Cratoxylum formosum* gum and its cytotoxicity. *Advanced Materials Research*, *974*, 394-397. https://doi.org/10.4028/www.scientific.net/amr.974.394

Thu, Z. M., Aung, H. T., Sein, M. M., Maggiolini, M., Lappano, R., & Vidari, G. (2017). Highly cytotoxic xanthones from *Cratoxylum cochinchinense* collected in Myanmar. *Natural Product Communications*, *12*(11), 1759-1762. https://doi.org/10.1177/1934578x1701201127

Udomchotphruet, S., Phuwapraisirisan, P., Sichaem, J., & Tip-pyang, S. (2012). Xanthones from the stems of *Cratoxylum cochinchinense*. *Phytochemistry*, *73*, 148-151. https://doi.org/10.1016/j.phytochem.2010.04.028

Vu, T. T., Kim, H., Tran, V. K., Dang, Q. L., Nguyen, H. T., Kim, H., Kim, I. S., Choi, G. J., & Kim, J.-C. (2015). *In vitro* antibacterial activity of selected medicinal plants traditionally used in Vietnam against human pathogenic bacteria. *BMC Complementary and Alternative Medicine*, *16*, 32. https://doi.org/10.1186/s12906-016-1007-2

Waiyaput, W., Payungporn, S., Issara-Amphorn, J., & Panjaworayan, N. T.T. (2012). Inhibitory effects of crude extracts from some edible Thai plants against replication of hepatitis B virus and human liver cancer cells. *BMC Complementary and Alternative Medicine*, *12*, 246. https://doi.org/10.1186/1472-6882-12-246

Xiong, J., Liu, X.-H., Bui, V.-B., Hong, Z.-L., Wang, L.-J., Zhao, Y., Fan, H., Yang, G.-X., & Hu, J.-F. (2014). Phenolic constituents from the leaves of *Cratoxylum formosum* ssp. *pruniflorum*. *Fitoterapia*, *94*, 114-119. https://doi.org/10.1016/j.fitote.2014.02.002

Yahayu, A. M., Rahmani, M., Mohd Hashim, N., Ee G. C. L., Sukari, M. A., & Md Akim, A. (2013). Cytotoxic and antimicrobial xanthones from *Cratoxylum arborescens* (Guttiferae). *Malaysian Journal of Science*, *32*(1), 53-60. https://doi.org/10.22452/mjs.vol32no1.9

Pertanika J. Trop. Agric. Sci. 46 (1): 243 - 252 (2023)

PERTANIKA JOURNALS

TROPICAL AGRICULTURAL SCIENCE

Journal homepage: http://www.pertanika.upm.edu.my/

Breeding and Hybridization of Clownfish *Amphiprion ephippium* × *Amphiprion melanopus* in Captivity

Mohamad Saupi Ismail[1,2], Mei Ling Khoo[3]*, Baitul Ma'mor Dzulfikkar[2] and Annie Christianus[1]

[1]*Institute of Bioscience, Universiti Putra Malaysia, 43400 Serdang, Selangor, Malaysia*
[2]*Fisheries Research Institute (FRI) Batu Maung, 11960 Pulau Pinang, Malaysia*
[3]*Faculty of Science and Technology, Universiti Kebangsaan Malaysia, 43400 Bangi, Selangor, Malaysia*

ABSTRACT

Development of broodstock, spawning, and early rearing of the hybrid clownfish, *Amphiprion ephippium* (♂) × *Amphiprion melanopus* (♀), was studied under captive conditions. The fishes were successfully paired after being together for over a year. Spawning occurred between 0700 to 1000 hours every 3 weeks. More than 200 eggs were spawned each time, with an egg size of 1.5 ± 0.5mm. Fertilized eggs turned from bright orange to black to silvery before hatching after being incubated for 7–9 days. Out of 20 batches of eggs spawned, 5 batches were successfully hatched, with only 2 batches surviving to adulthood. The average survival rate for all the batches hatched was 21.16%. Newborn larvae measured about 3–4 mm long, with transparent fins that fused, forming a single fin fold. Larvae underwent metamorphosis on day 10 post hatched, where the fins started to separate, form, and develop body colorations. Two clear and thick bands were observed on the body (head and middle) as early as 14-day post hatched to 90-day post-hatched, where the banding reached its peak. The middle band then began fading as the juveniles grew. By 130-day post-hatched, the juveniles became adults with unique coloration featuring a headband and a black blotch, reaching the maximum size of 34 mm. The hybrid clownfish underwent metamorphosis earlier and reached marketable size much sooner compared to its parent species, making it a suitable candidate for ornamental fish culture. It is the first documentation on the production of hybrid clownfish *A. ephippium* and *A. melanopus* both in Malaysia and worldwide.

Keywords: Captive breeding, hybrid clownfish, juvenile rearing, Malaysia, marine ornamental

ARTICLE INFO

Article history:
Received: 08 September 2022
Accepted: 26 October 2022
Published: 03 February 2023

DOI: https://doi.org/10.47836/pjtas.46.1.13

E-mail addresses:
saupi@rocketmail.com (Mohamad Saupi Ismail)
meilingkhoo@ukm.edu.my (Mei Ling Khoo)
alfiks2001@gmail.com (Baitul Ma'mor Dzulfikkar)
annie@upm.edu.my (Annie Christianus)
* Corresponding author

ISSN: 1511-3701
e-ISSN: 2231-8542

INTRODUCTION

Aquaculture has been identified as a priority sector in the development of Malaysia's economy (Jumatli & Ismail, 2021). Its ornamental fish industry also played a significant role in the national economy, and this industry is now enjoying rapid growth (Othman et al., 2017). One of the most demanding marine fish in the aquarium trade is the clownfish or anemonefish (*Amphiprion* spp.). However, most of these species are wild-caught, increasing the chance or potential for the fish to be overharvested (Dhaneesh et al., 2012; Domínguez & Botella, 2014). One way to reduce the pressure on the ecosystem and meet the increasing demands for marine ornamentals is to improve the efficiency of the capture and the culture system for desirable marine species (Domínguez & Botella, 2014; Noh et al., 2013). Rearing fish in closed systems reduces pressure on wild populations and is likely to produce harder species that are far better in captivity and survive longer (Wittenrich, 2007). Today, as many as 18 clownfish from *Amphiprion* have been reared in captivity. However, their larvae rearing is still time-consuming and expensive (Arvedlund et al., 2000). Hence, knowledge of the life history of the species under study is crucial to the success of captive breeding (Olivotto et al., 2011).

Hybridization or crossbreeding has been a powerful tool to improve production and breeding qualities in fish (Chapman & ZoBell, 2010). Hybridization in ornamental fish was mostly performed on freshwater fish, although recently, there has been an attempt to crossbreed different species of clownfish (*Amphiprion percula* × *Amphiprion ocellaris*) and has been proven successful (Balamurugan & Kathiresan, 2018). Hence, there is a potential to develop hybrids with other clownfish species. Red saddleback anemonefish (*A. ephippium*) and fire clownfish (*A. melanopus*) are potential candidates. These two species can be found in Malaysian waters (Department of Fisheries Malaysia, 2009), while *A. ephippium* is considered a native species in Malaysia (Jenkins, Carpenter, et al., 2017). Both species were collected in the aquarium trade (Jenkins, Allen, et al., 2017; Jenkins, Carpenter, et al., 2017), causing the species to be overfished in localized areas and potentially endanger the local population (Domínguez & Botella, 2014).

Nowadays, clownfish breeding and conservation are very important to cater to the increasing demand in the ornamental trade. However, to our knowledge, the culture of hybrid clownfish has not yet been reported in Malaysia, despite Malaysia being one of the main exporters of marine ornamental fish (Rhyne et al., 2017). Furthermore, there is no report on the embryo development, larval-rearing methods, and production of any clownfish juveniles in Malaysia. Thus, this study will likely be the first documented nursery culture of hybrid clownfish of *A. ephippium* (♂) and *A. melanopus* (♀). This study was designed to determine the larval development and survival rate of hybrid clownfish of *A. ephippium* (♂) and *A. melanopus* (♀).

MATERIALS AND METHODS

Attaining Fish Samples and Holding Tank

Live juveniles of *A. ephippium* and *A. melanopus* bought from a local aquarium shop were used in this study. Experiments were conducted at an indoor and outdoor nursery of Fisheries Research Institute (FRI) Batu Maung in Pulau Pinang, Malaysia, from August 2017 to March 2020. The tanks were supplied with filtered seawater drawn from the treated reservoir tank. Continuous aeration was supplied, and 10–20% water exchange was done on alternate days. Water quality parameters such as dissolved oxygen (DO), pH, ammonia (NH_3), nitrate (NO_3^-), phosphate (PO_4^{3-}), and salinity were maintained and measured every 2 weeks (Table 1). For indoor tanks, the water temperature was kept at 28 °C and controlled by a 200 W submersible thermostat heater. A photoperiod of 10 h light and 14 h dark (lights on at 7 a.m. and lights off at 5 p.m.) were maintained throughout the study. For outdoor tanks, room temperature and natural photoperiod were provided. Both juveniles were reared and kept together in the same nursery tank (92 cm L × 46 cm W × 46 cm H) until pairs were formed.

Table 1
Water parameters maintained in the tanks

Parameter	Range
Dissolved oxygen (mg L^{-1})	5.78–6.12
pH	8.0
Ammonia (mg L^{-1})	0–0.5
Nitrate (mg L^{-1})	0
Phosphate (mg L^{-1})	0–0.5
Salinity (ppt)	31–35
Temperature (°C)	27–29

Experimental Design – Breeding Tank

Fish-forming pairs were transferred to a breeding glass tank (61 cm L × 46 cm W × 46 cm H). Substrates of dead coral chips and live rocks were provided at the bottom of the tank to mimic the reef environment. Flat rocks were used as a substrate on which the fish could attach their eggs to the surface. The pair was fed a combination of live adult *Artemia*, live mysids, and pellet marine food twice a day. Light emitting diode (LED) light was fixed on top of the tank to provide a light intensity of 3,000–4,000 lux for 10 h daily. After the pair deposited their eggs on the rock substrate, the rock with egg clutches will be removed into the rearing tanks one day before hatching.

Experimental Design – Rearing Tank

For the first 17 hatching events, the hatching tank used was an indoor squared glass tank (25 cm L × 25 cm W × 25 cm H) before changing to an outdoor cylindrical fiber tank (80 cm in diameter). The rock with the egg clutch was propped diagonally against the tank wall, with an air stone placed directly under the rock to aerate and agitate the eggs to aid in hatching. No other substrate was added inside the tank. All live newborns that hatched were then collected, counted, and transferred to a rearing tank (batches 1 to 17 in an indoor rectangular glass of 40 cm × 25 cm × 25 cm in size: batches 18–20 in an outdoor rectangular fiber tank of 2 m L × 0.5 m W × 0.5 m H in size). The sides of the indoor tank are covered with black panels to reduce light reflection. All tanks were aerated gently. Feeding began on the first

day of hatching, starting with green algae of *Nannochloropsis* sp. The juveniles were fed different types of diets, as in Table 2.

Table 2
Type of diets for hybrid clownfish according to days after hatching

Day	Food
1	Green algae (*Nannochloropsis* sp.)
2–10	Rotifer
11–30	Enriched rotifer + newly hatched *Artemia*
31–60	Enriched *Artemia* + small-sized pellet food
60 onwards	Marine pellet food

During the study, conditions in all tanks were kept the same. No substrate was used in the rearing tanks. The bottom of the tanks was cleaned, dead juveniles were removed, and 20-25% water exchange was carried out daily. A minimum of ten juveniles was randomly selected, and their total length and wet weight were measured. Measurements were made every 30 days for 6 months. Days of metamorphosis were noted. A gross estimate of the survival rate in all batches was made by counting the fish larvae in each batch at the time of hatching and the end of the experiment using the following formula:

$$\text{Survival rate (\%)} = (\text{Number of larvae surviving}/\text{Number of larvae hatched}) \times 100\%$$

RESULTS AND DISCUSSION

Spawning and Broodstock Development

After a year in captivity, the two fish began to form a pair bond. *A. melanopus* developed into a functional female, while *A. ephippium* became the functional male. Within a few months, the pair began to spawn. A day or two before spawning, the male *A. ephippium* cleaned the nest area. Spawning occurred approximately every two weeks and was observed to take place mostly between 0700 to 1000 hours. More than 200 eggs were spawned at a time, with an initial size of about 1.5 ± 0.5 mm in length, and were usually deposited on the flat rock (Figure 1). The male *A. ephippium* played an important role in the incubating stage, where it was observed to be aerating and guarding the eggs until they hatched. The eggs were initially bright orange before eventually turning transparent, where the eyes of the larvae can be seen developing within the egg case. The eggs normally hatched between days 7 to 9.

The pair spawned every month and produced an average of 2.2 egg clutches per month. A total of twenty batches of eggs from the same broodstock were obtained within 9 months (December 2018 to August 2019). However, only five batches of eggs managed to hatch successfully, and three

Figure 1. Amphiprion melanopus laying eggs on a flat rock

Table 3
Survival rates for batches that are successfully hatched

Batch	Date of laying eggs	Date of hatching	Incubation (days)	No. of hatchlings	No. of hatchlings survived	Survival rate (%)
3	18/01/19	27/01/19	9	1	0	0
9	10/04/19	19/04/19	9	1	0	0
18	12/07/19	19/07/19	7	52	44	84.62
19	22/07/19	29/07/19	7	61	3	4.92
20	16/08/19	22/08/19	7	7	0	0

had fewer hatchlings (less than 10). Only two batches survived and reached adult size (Table 3). The average survival rate for all the batches that hatched was 21.16%, with only batch 18 reaching 84.62%, while the rest (batches 3, 9, 20, and 19) were 0% and 4%, respectively.

Hybrid Larval Development

It is well established that the life cycle of most reef fishes can be divided into three distinct biological/ecological phases: larvae, juvenile, and adult (Olivotto et al., 2011). In this study, the larvae phase started after 7 days of incubation, which is the same case for most species of clownfish, such as *Amphiprion ocellaris* (7 days) (Balamurugan & Kathiresan, 2018), *Amphiprion melanopus* (7–8 days) (Uthayasiva et al., 2014), and *Amphiprion akallopisos* (7–9 days) (Dhaneesh et al., 2012). However, Rohini Krishna et al. (2018) reported that the hatching of *A. ephippium*'s eggs occurred as early as the sixth day of incubation.

The first batch of newborn hybrid clownfish was hatched in early January 2019. The larval was measured about 3–4 mm long. Its large dark eyes, open mouth, and internal organs can be seen through its transparent body. The fins were transparent and fused, forming a single fin fold. High initial mortality was commonly observed before the metamorphosis phase. Metamorphosis of the larvae started at day 10 post hatched when the fins started to separate and form as well as develop colors (Figure 2).

The newly hatched larvae were fed with algae as first feed and later with rotifers and finally *Artemia nauplii*. Rohini Krishna et al. (2018) reported that larvae of *A. ephippium* started feeding actively from the first day onwards. The given diets included rotifers, *Artemia*, and pellet feed. Algal-enriched

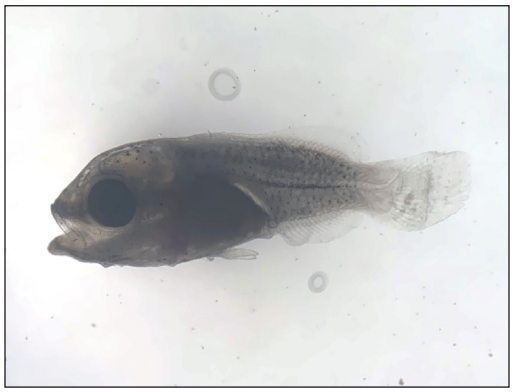

Figure 2. Microscopic observation (× 4.5) of ten-day-old larvae of hybrid *A. ephippium* and *A. melanopus*

rotifers and *Artemia* nutrition represent the underlying foundation for successful larval rearing. The difference in food quality may also play a role (Arvedlund et al., 2000). High survival rates were observed in larvae fed exclusively on enriched rotifers and *Artemia* (Olivotto et al., 2011), the same proven in this study for the hybrid clownfish larvae. After the metamorphosis stage, juvenile rearing was generally non-problematic if live feeds were enriched properly and good water quality was maintained.

The transformation of clownfish juveniles can be quite abrupt, with most clownfish species larvae starting to metamorphose 14 days after hatching (Wilkerson, 2001). However, the hybrid clownfish larvae started metamorphosis as soon as day 10 after hatching. The juveniles were observed to have developed well-defined fins (dorsal, pelvic, and caudal fins) their bodies turned dark. These results were also seen in reports by Rohini Krishna et al. (2018) on one of its parent species, *A. ephippium* (10 days after hatching). Its other parent species, *A. melanopus*, also reported undergoing a metamorphosis as early as day 8 after hatching (Arvedlund et al., 2000; Green & McCormick, 2001), which might contribute to the hybrid larvae starting to change faster than other species of clownfish, such as *Premnas biaculeatus* (11–12 days) (Madhu et al., 2006), *Amphiprion chrysogaster* (12–15 days) (Gopakumar et al., 2001), *Amphiprion sebae* (12–15 days) (Ignatius et al., 2001), *Amphiprion percula* (13-15 days) (Dhaneesh et al., 2009), and *Amphiprion akallopisos* (15–16 days) (Dhaneesh et al., 2012).

On day 15, post-hatched, the headband was visible with the fins, and body coloration turned red, resembling *Amphiprion frenatus*. At day 30 post-hatching, the headband was very clear, and the middle band could be seen from the dorsal part of the body, which was starting to take shape. The middle band has formed and reached half of the middle body at day 60 post-hatching. Two clear and thick bands were observed on the body (head and middle) at 90 days post-hatched, where the banding peaked. After that, the middle band began fading as the larvae grew, leaving only a white spot at the middle dorsal body by 120 days post-hatching. After that, the body color changed to dark red, resembling the color of an adult *A. melanopus*. The middle band completely disappeared by 130 days post-hatched, and a black blotch was seen at the sides when transitioning to adults with a maximum size of 34 mm. The adult hybrid clownfish has a clear headband resembling *A. melanopus* and a black blotch on the side and fin colors resembling *A. ephippium*, creating a new body pattern and coloration different from its parents (Figure 3).

The body transformation of the hybrid clownfish larvae closely followed the transformation of *A. ephippium* as reported by Rohini Krishna et al. (2018) in the early stages, whereby day 14 after hatching, larvae of hybrid clownfish and clownfish *A. ephippium* had the adult body coloration and clear headbands. Both also showed a clear middle band forming at day 30 post-hatched.

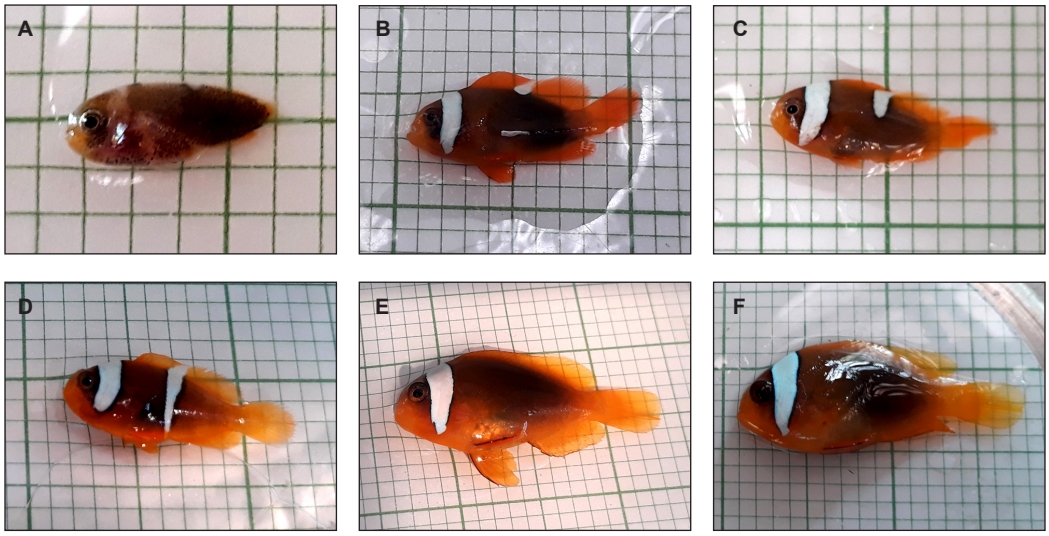

Figure 3. Larval development of hybrid *A. ephippium*♂ and *A. melanopus*♀. A: day 15 post-hatch; B: day 30 post-hatch; C: day 60 post-hatch; D: day 90 post-hatch; E: day 120 post-hatch; F: day 150 post-hatch. Each grid box represents 2mm in length

However, the peak banding for *A. ephippium* was reported at day 45 post hatched, much earlier than the peak banding of the hybrid clownfish 90 days post-hatch. Moreover, the middle band completely disappeared in *A. ephippium*, resembling the adult *A. frenatus* by 120 days after hatching. In contrast, remnants of the middle band were still present in the hybrid clownfish, and its body coloration turned darker, resembling *A. melanopus* 120 days post-hatch.

The headband in *A. ephippium* continued to fade as the larvae grew until it disappeared 310 days after hatched. Compared to its parent species, the hybrid clownfish larvae did not lose the headband as it grew and developed the black blotch on the side instead (a feature that distinguished the parent species *A. ephippium*) by day 130 post hatched. The transition from juvenile to adult body coloration in the hybrid clownfish was achieved within 130 days post hatched, much sooner than its parent species, *A. ephippium*, which takes 310 days to transform completely. The hybrid clownfish's final body pattern is unique; it consists of a white band near the head (resembling one of the parent species, *A. melanopus*) and a black blotch at the side (resembling the other parent species, *A. ephippium*).

The length of the hybrid larvae showed a substantial increase from day 20 post-hatch (8.60 ± 0.34 mm) to 130 days post-hatch (34.30 ± 1.63 mm) (Figure 4). Compared to its parent species, *A. ephippium*, the growth in the size of the larvae of the hybrid clownfish was much bigger and faster. *Amphiprion ephippium* is reported (Rohini Krishna et al., 2018) to reach its maximum length of 22.62 mm in 6 months, while the hybrid clownfish almost reached its maximum length of 34.30 mm in 130 days post hatched. In 6 months after hatching,

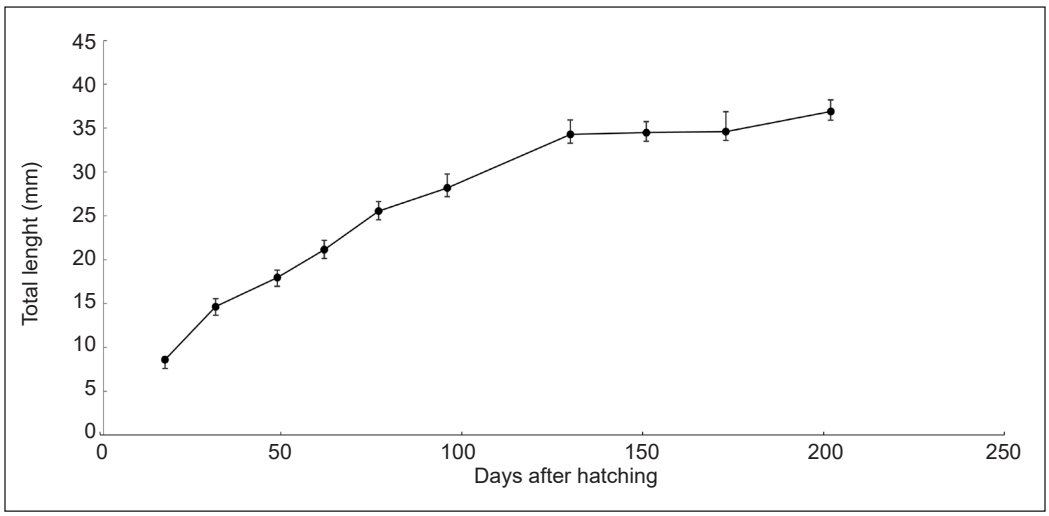

Figure 4. Total length (mm) of hybrid larvae (*Amphiprion ephippium*♂ × *Amphiprion melanopus*♀) post-hatching

the hybrid clownfish juveniles reached the maximum length of 36.90 ±1.32 mm, almost 14 mm larger than its parent species, *A. ephippium*. Therefore, the hybrid clownfish (*Amphiprion ephippium* ♂ × *Amphiprion melanopus* ♀) is a suitable candidate as a marine ornamental fish culture for the ornamental trade due to its unique body coloration and pattern that it inherited from both its parent species.

CONCLUSION

Compared to its parent species, *A. ephippium*, the hybrid clownfish (*Amphiprion ephippium* ♂ × *Amphiprion melanopus* ♀) larvae underwent metamorphosis earlier and reached the marketable size much faster. The body coloration is also unique, where the features from both parent species were inherited and expressed. The most remarkable finding in this study is that a clownfish can establish a sexual relationship with other clownfish species, and their offspring can indeed be successfully reared in captivity.

ACKNOWLEDGEMENTS

The authors wish to thank Mr. Abu Talib Ahmad, the former Senior Director of the Research Division of the Department of Fisheries, for making this project possible. Funding support was provided through the Akuarium Tunku Abdul Rahman (AkuaTAR) operational budgets for 2017 to 2020. The assistance of Ms. Siti Sarah Jamil is greatly acknowledged. The staff of AkuaTAR who have contributed their work is also appreciated.

REFERENCES

Arvedlund, M., McCormick, M. I., & Ainsworth, T. (2000). Effects of photoperiod on growth of larvae and juveniles of the anemonefish *Amphiprion melanopus*. *Naga: The ICLARM Quarterly*, *23*(2), 18-23.

Balamurugan, J., & Kathiresan, K. (2018). Interspecific hybridization and reproductive biology of marine clownfishes, the orange clownfish *Amphiprion percula* and clown anemonefish *A. ocellaris*. *North American Journal of Aquaculture*, *80*(3-4), 301-309. https://doi.org/10.1002/naaq.10033

Chapman, K. C., & ZoBell, D. (2010). *Applying principles of crossbreeding*. https://digitalcommons.usu.edu/cgi/viewcontent.cgi?article=1472&context=extension_curall

Department of Fisheries Malaysia. (2009). *Valid local name of Malaysian marine fishes*. Department of Fisheries Malaysia.

Dhaneesh, K. V., Ajith Kumar, T. T., & Shunmugaraj, T. (2009). Embryonic development of percula clownfish *Amphiprion percula* (Lacepede 1802). *Middle East Journal of Scientific Research, 4*(2), 84–89.

Dhaneesh, K. V., Nanthini Devi, K., Ajith Kumar, T. T., Balasubramanian, T., & Tissera, K. (2012). Breeding, embryonic development and salinity tolerance of Skunk clownfish *Amphiprion akallopisos*. *Journal of King Saud University – Science*, *24*(3), 201-209. https://doi.org/10.1016/j.jksus.2011.03.005

Domínguez, L. M., & Botella, A. S. (2014). An overview of marine ornamental fish breeding as potential support to the aquarium trade and to the conservation of natural fish population. *International Journal of Sustainable Development and Planning*, *9*(4), 608-632. https://doi.org/10.2495/SDP-V9-N4-608-632

Gopakumar, G., George, R. M., & Jasmine, S. (2001). Hatchery production of the clownfish *Amphiprion chrysogaster*. In N. G. Menon & P.P. Pillai (Eds.), *Perspective in mariculture* (pp. 305–310). The Marine Biological Association of India.

Green, B. S., & McCormick, M. I. (2001). Ontogeny of the digestive and feeding systems in the anemonefish *Amphiprion melanopus*. *Environmental Biology of Fishes*, *61*(1), 73–83. https://doi.org/10.1023/A:1011044919990

Ignatius, B., Rathore, G., Jagdis, I., Kandasami, D., & Victor, A. C. C. (2001). Spawning and larval rearing technique for tropical clownfish *Amphiprion sebae* under captive conditions. *Journal of Aquaculture in the Tropics*, *16*, 241–249.

Jenkins, A., Allen, G., Myers, R., Yeeting, B., & Carpenter, K. E. (2017). Amphiprion melanopus. The IUCN Red List of Threatened Species. https://doi.org/10.2305/IUCN.UK.2017-2.RLTS.T188491A1882866.en

Jenkins, A., Carpenter, K. E., Allen, G., Yeeting, B., & Myers, R. (2017). Amphiprion ephippium. The IUCN Red List of Threatened Species. https://doi.org/10.2305/IUCN.UK.2017-2.RLTS.T188463A1878690.en

Jumatli, A., & Ismail, M. S. (2021). Promotion of sustainable aquaculture in Malaysia. In F. A. Aya, L. D. de la Peña, N. D. Salayo, & E. A. Tendencia (Eds.), *Proceedings of the International Workshop on the Promotion of Sustainable Aquaculture, Aquatic Animal Health and Resource Enhancement in Southeast Asia* (pp. 31–40). Southeast Asian Fisheries Development Center (SEAFDEC). https://repository.seafdec.org.ph/bitstream/handle/10862/6253/JumatliA2021.pdf?sequence=1&isAllowed=y

Madhu, K., Madhu, R., Gopakumar, G., Sasidharan, C. S., & Venugopalan, K. M. (2006). Breeding larval rearing and seed production of maroon clown *Premnas biaculeatus* under captive conditions. *Marine Fisheries Information Service, Technical and Extension Series*, *190*, 1–5.

Noh, G. E., Rho, S., Chang, Y. J., Min, B. H., & Kim, J.-M. (2013). Gene encoding prolactin in cinnamon clownfish *Amphiprion melanopus* and its expression upon acclimation to low

salinities. *Aquatic Biosystems*, *9*, 1. https://doi.org/10.1186/2046-9063-9-1

Olivotto, I., Planas, M., Simoes, N., Holt, G. J., Avella, M. A., & Calado, R. (2011). Advances in breeding and rearing marine ornamentals. *Journal of the World Aquaculture Society*, *42*(2), 135-166. https://doi.org/10.1111/j.1749-7345.2011.00453.x

Othman, M. F, Mazuki, H., Yeo, M. E, Amal, M. N. A., Natrah, I., Ho, G. C., & Merican, Z. (2017). Transforming the aquaculture industry in Malaysia. *World Aquaculture*, *48*(2), 16-23.

Rhyne, A. L., Tlusty, M. F., Szczeback, J. T., & Holmberg, R. J. (2017). Expanding our understanding of the trade in marine aquarium animals. *PeerJ*, *5*, e2949. https://doi.org/10.7717/peerj.2949

Rohini Krishna, M. V., Anil, M. K., & Neethu Raj, P. (2018). Larval development and growth of red saddleback anemonefish, *Amphiprion ephippium* (Bloch, 1790) under captive conditions. *Indian Journal of Geo Marine Sciences*, *47*(12), 2421-2428.

Uthayasiva, M., Balamurugan, J., Kumar, T. T. A., Mohideen, A. B. H., & Arumugam, M. (2014). Seasonal disparity in fecundity and embryonic development of cinnamon anemone fish, *Amphiprion melanopus* (Bleeker, 1852) in captivity. *Journal of Marine Biology and Oceanography*, *3*(3), 1000130. https://doi.org/10.4172/2324-8661.1000130

Wilkerson, J. D. (2001). *Clownfishes: A guide to their captive care, breeding and natural history*. Microsom Ltd.

Wittenrich, M. L. (2007). *The complete illustrated breeder's guide to marine aquarium fishes*. T. F. H. Publications.

Pertanika J. Trop. Agri. Sci. 46 (1): 253 - 264 (2023)

PERTANIKA JOURNALS

TROPICAL AGRICULTURAL SCIENCE

Journal homepage: http://www.pertanika.upm.edu.my/

The Effect of Cadmium, Copper, and Lead on *Brassica juncea* in Hydroponic Growth Medium

Thang Quoc Nguyen[1], Tan Van Le[1]* and Tran Thanh Thi Le[2]

[1]*Chemical Engineering Faculty, Industrial University of Ho Chi Minh City, 12 Nguyen Van Bao, Go Vap, Ho Chi Minh City, 700000, Vietnam*
[2]*Chemical and Environmental Science Department, Dalat University, Lam Dong Province, 700000, Vietnam*

ABSTRACT

This study measured the accumulation of cadmium (Cd), lead (Pb), and copper (Cu) in *Brassica juncea* grown using the hydroponic method in a water environment contaminated with these heavy metals. The accumulated metal content in each part of the plant was monitored after one, three, and six weeks of exposure. The concentrations of Cd, Cu, and Pb in the biomass of *B. juncea* were determined using atomic absorption spectroscopy. The results showed that heavy metal pollution in water caused heavy metal accumulation in vegetable biomass. Pb tended to accumulate lower vegetable biomass than Cu and Cd. The metal accumulation level in Cu and Cd was in the order of roots > stems > leaves, while with Pb, the concentration accumulated in roots > leaves > stems. The translocation factors of Cu, Cd, and Pb from shoots to stems and shoots to leaves were less than 1.

Keywords: Accumulation, *Brassica juncea*, cadmium, copper, lead, translocation factor

INTRODUCTION

The contamination of heavy metals from the environment into food can result from industrial or agricultural activities, vehicle exhaust, or contamination during food processing and storage. Such contamination and its effects on human health are major challenges in many countries (Anwar et al., 2016). Vegetables have high amounts of vitamins, minerals, fibers, and antioxidants, making them valuable human food (Gupta et al., 2021). The quality of vegetables is highly dependent on the quality of the growing environment. Heavy metal contamination of

ARTICLE INFO

Article history:
Received: 16 September 2022
Accepted: 26 October 2022
Published: 14 February 2023

DOI: https://doi.org/10.47836/pjtas.46.1.14

E-mail addresses:
nguyenquocthang@iuh.edu.vn (Thang Quoc Nguyen)
levantan@iuh.edu.vn (Tan Van Le)
tranltt@dlu.edu.vn (Tran Thanh Thi Le)
*Corresponding author

ISSN: 1511-3701
e-ISSN: 2231-8542

vegetables may also occur due to irrigation in environments with heavy metal pollution.

Hydroponic vegetable cultivation is growing in interest worldwide due to the high quality of vegetables grown in this manner and the ability to control the vegetables' composition. The hydroponic technique involves soil-free gardening in which plants grow in nutrient-rich water without soil, gravel, rockwool, coconut fiber, or sawdust base (Sharma et al., 2018). The hydroponic technique is a relatively easy and clean method that reduces or eliminates pesticide use because crops do not incur soil-borne diseases or insect and pest infestations (AlShrouf, 2017; Wang et al., 2017). However, the quality of hydroponic vegetables depends largely on water quality. If the water is contaminated, pollutants can accumulate in agricultural products. Other factors include vegetable species, soil composition, growth stages, atmospheric and geographic conditions, and the types of metals present (Dulama et al., 2012; Radulescu et al., 2010, 2013).

Previous studies have documented that heavy metals are toxic and persistent and have the ability to bioaccumulate in aquatic atmospheres (Bai et al., 2018). Agriculture's increasing demand for water requires research on how to use other water sources and treated wastewater (TWW). TWW is rich in nutrients but may also contain various heavy metals (Mourato et al., 2015). Plants can uptake, transfer, and accumulate heavy metals in the growth stage because plants have a higher absorption capacity than mature plants (Souri et al., 2019). Additionally, roots have a higher concentration of heavy metals than other tissues of plants due to their direct contact with heavy metals in the environment (Mohtadi et al., 2012).

This study aimed to evaluate the effects of the accumulation of copper (Cu), cadmium (Cd), and lead (Pb) in the leaves, stems, and roots of *Brassica juncea* grown using the hydroponic technique.

MATERIALS AND METHODS

Vegetable and Conditional Experiments

In this study, young *B. juncea* were collected from a vegetable farm in the VI district of Ho Chi Minh City, Vietnam. The vegetables selected were 5.0 ± 0.5 cm in height and 4.0 ± 0.2 g in weight. First, 192 individual young *B. juncea* were kept under static hydroponic conditions in 48 tanks (30 cm × 20 cm × 16 cm = 9.6 L). Every tank contained four individual young *B. juncea*. The nutrient solution was purchased from Hydroponic Garden Company Limited (Vietnam), which composition was as follows: 2 mM calcium nitrate [$Ca(NO_3)_2$], 3 mM potassium nitrate (KNO_3), 0.50 mM magnesium nitrate ($MgSO_4$), 1 mM ammonium dihydrogen phosphate ($NH_4H_2PO_4$), 1 µM potassium chloride (KCl), 25 µM boric acid (H_3BO_3), 20 µM sodium ferric ethylenediaminetetraacetate [Fe(Na)-EDTA], 2 µM zinc sulfate ($ZnSO_4$), 2 µM manganese(II) sulfate ($MnSO_4$), and 0.1 µM ammonium heptamolybdate [$(NH_4)_6Mo_7O_{24}$]. After five days of acclimation, each tank was exposed to one

of four simulated heavy metal contamination levels. All experiments were triplicated (n = 3).

- Control sample: Only nutrient solution
- EXP 5 sample: Add 5 mg L^{-1} each of Cd, Pb, and Cu into the nutrient solution
- EXP 10 sample: Add 10 mg L^{-1} each of Cd, Pb, and Cu into the nutrient solution
- EXP 20 sample: Add 20 mg L^{-1} each of Cd, Pb, and Cu into the nutrient solution

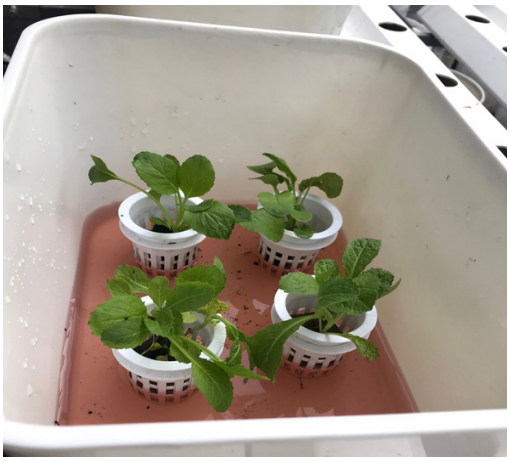

Figure 1. The tank of the experiment

The tanks were in a room with the temperature set at 30 ± 2°C by an air conditioner, and they received sunlight all day (Figure 1). Every six days, 100% of each tank's water was replaced to ensure consistency and that the nutrient solution's acidity remained at 5.5. Hydroponics experiments solution samples for total Cd, Pb, and Cu analysis were collected twice a week and analyzed by flame atomic absorption spectroscopy (ZA–3000, Hitachi, Japan) to check nominal concentrations of solutions. If the three metals measured and nominal concentrations were significantly different, the experiment solutions were adjusted to match the nominal concentration.

Sampling and Measurements

Sampling. On days 7, 21, and 42 of exposure, 20 plants from each treatment were randomly harvested and washed carefully in bidistilled water. All harvested plants were drained in room temperature for 2 hours and were weighed to determine the mass of plant. And then, all harvested plants were separated into roots, stems, and leaves. The roots were rinsed carefully for 15 min to remove the adsorbed metals on the surfaces of the root using a 10 mmol L^{-1} disodium ethylenediaminetetraacetate solution (Merck, Germany), followed by washing them again in bi-distilled water. The collected vegetable tissue samples were dried in an oven at 105°C for 24 h and then ground into a fine powder in a coffee grinder (HC-600, HeyCafé, Taiwan) before the Cd, Pb, and Cu concentrations were analyzed. Changes in the studied heavy metals content in the roots, stems, and leaves within six weeks from the time the vegetables were grown in contaminated water were monitored.

Cd, Pb, and Cu Analysis. To determine the concentrations of Cd, Pb, and Cu, a wet digestion method was used to digest 1 g of the powdered sample in a closed vessel using 4 ml of concentrated nitric acid (HNO_3, Merck, Germany) and 2 ml of concentrated hydrogen peroxide (H_2O_2,

Merck, Germany). The closed vessels were then heated to 85ºC for 30 min until preliminary mineralization was achieved. Next, the obtained solution was diluted to 25 mL using deionized water. Cd, Pb, and Cu concentrations were assayed using flame atomic absorption spectroscopy (ZA–3000, Hitachi, Japan). The method's detection limits were 3.6 μg kg^{-1} for Cd, 25 μg kg^{-1} for Pb, and 3.5 μg kg^{-1} for Cu. The method's quantification limits were 11.8 μg kg^{-1} for Cd, 83 μg kg^{-1} for Pb, and 11.8 μg kg^{-1} for Cu. The assay recovery was approximately 92.3% for Cd, 92.6% for Pb, and 97.1% for Cu. The relative standard deviation (RSD) was approximately 0.79% for Cd, 0.54% for Pb, and 3.55% for Cu.

Calculation and Statistical Analysis

The translocation factor (TF) indicates the ability to transfer metals in a plant from its roots to its stems and leaves. Following Deng et al. (2007), the TF of metal from a plant's roots to stems or leaves was calculated as follows: TF = leaves' or stems' metal concentration/roots' metal concentration.

The rootly, leafy, and stemly vegetable Cu, Cd, Pb concentrations were plotted against the Cu, Cd, Pb concentrations in nutrient solution, and a linear regression analysis was performed on the data to obtain the linear regression equation and R-squared.

All experiments were triplicated (n = 3), and the experimental data were presented in average ± standard deviation (SD). The analytical procedure was validated based on the Certified Reference Materials (white cabbage - trace elements, BCR®-679). The RSD of each analysis was found within ± 2.4% of the certified values. The one-way analysis of variance (ANOVA) was utilized to evaluate the significant differences between the lead content in particular vegetables and contaminated soil. Statistical significance was evaluated via the student's *t*-test with a *p*-value < 0.005.

RESULTS AND DISCUSSION

Effect of Cd, Pb, and Cu Concentration in the Nutrient Solution on the Growth Rate of *Brassica juncea*

The plant mass of the control and treatment plants is shown in Table 1. The toxicity of Cd, Pb, and Cu metals affected exposure plants' growth, and the absorption of these metals consequently depends on metabolic needs. The group of plants exposed to heavy metal showed clearly the changed metabolic

Table 1

Effect of Cd, Cu, and Pb on the growth of B. juncea *over time*

Treatments	Mass of plant (g)		
	Day 7th	Day 21st	Day 42nd
Control	10.94 ± 0.35	25.29 ± 0.69	41.45 ± 0.49
EXP 5 treatment	10.25 ± 0.39	24.35 ± 0.85	40.89 ± 0.82
EXP 10 treatment	9.95 ± 0.31	21.04 ± 0.74	34.99 ± 0.87
EXP 20 treatment	9.88 ± 0.36	18.73 ± 0.76	27.01 ± 0.69

Figure 2. Effect of Cu, Cd, and Pb to plant experiment

demands compared to the control group plants. As a result, the treatment plants reduced biomass yields compared to the control plants (Figure 2). For example, after 42nd days of treatment, the biomass yields of the EXP 5 sample, EXP 10 sample, and EXP 20 sample treatments were reduced by 88.3, 71.7, and 63.2% compared to control plants (Table 1).

The Accumulate Level of Cd, Cu, and Pb in the Biomass of *Brassica juncea*

The contents of Cu, Cd, and Pb accumulated in the biomass of *B. juncea* collected from each field after each week are presented in Figures 3, 4, and 5. Over time, the extent of accumulated studied metals in the roots, stems, and leaves of *B. juncea* increased.

Copper, this metal tends to accumulate in roots higher than in stems and leaves (Figure 3). In general, the copper content in the roots was, on average, 12.49 times higher than the copper in the stems and 16.59 times higher than the copper in the leaves. This result is consistent with the judgment of Feigl et al. (2013), under the stress of Cu, *B. juncea* and *Brassica napus* accumulated more Cu in roots than in shoots for 7 and 14 days in hydroponic solution when the amount of copper in the nutrient solution increased the amount of copper accumulated in the parts of *B. juncea*. On average, when doubling and quadrupling the amount of copper in the nutrient solution, the copper amount in the roots increased by 2.78 and

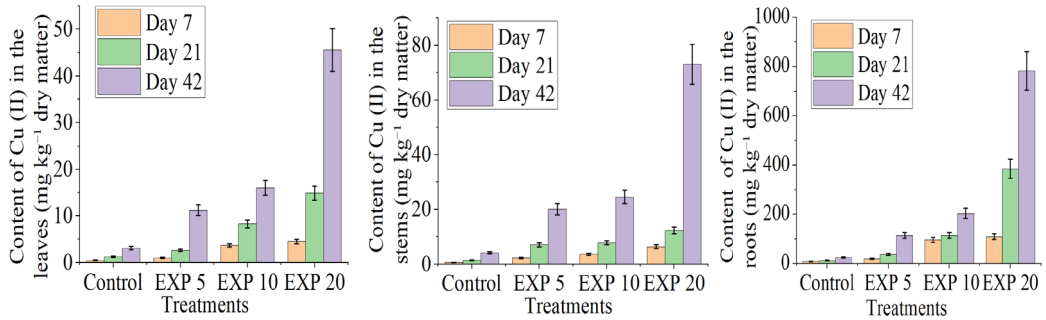

Figure 3. The accumulation of copper in the biomass of *B. juncea*

7.01 times, respectively. Meanwhile, the copper content in the stems increased by 1.22 and 2.92 times, respectively, and the content of this metal in the leaves increased by 2.77 and 4.71 times, respectively.

The accumulation of Cd in parts of *B. juncea* is lower than that of copper. When the Cd content in the nutrient solution was 5 mg/L, the amount of Cd accumulated in the roots was 18.15 times higher than its content in the stems and 15.24 times higher than in the leaves. At a content of 10 mg L^{-1} and 20 mg L^{-1} Cd in a nutrient solution, the amount of Cd in the roots was, on average, 6.59 times higher than the amount of Cd in the stems and 6.1 times higher than its content in the leaves (Figure 4). Jiang et al. (2001) reported that cadmium could accumulate in *Allium sativum* by hydroponically cultivated. In the group exposed to Cd at 0.01 M, Cd accumulation in plants was 1,826-fold higher than in the control group. Later, Barazani et al. (2004) reported that Cd was tolerant and hyperaccumulation in *Allium schoenoprasum*.

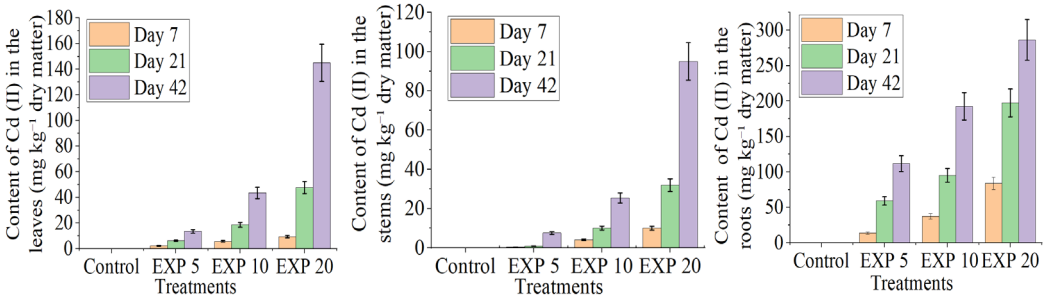

Figure 4. The accumulation of cadmium in the biomass of *B. juncea*

Unlike Cu and Cd, the amount of Pb accumulated in the roots of *B. juncea* is relatively large and much higher than the amount of lead in the stems and leaves. The heavy metals concentrations in the *B. juncea* tissue in this research were similar to the Zhou et al. (2016) reported that heavy metals concentrations in the edible tissue of different vegetable species were different. Because of the binds of Pb to cell walls and root surfaces, therefore, it reduced the transfer of Pb from roots to shoots or leaves (Cobb et al., 2000). Similarly, in this study, Pb accumulation was high in the roots compared to other tissue.

At the 5 mg L^{-1} content of the studied metal in the nutrient solution, the amount of lead accumulated in the roots of *B. juncea* was twice as high as cadmium and copper. At 10 mg/L concentration, the amount of lead accumulated in the roots was 1.44 and 1.80 times higher than that of copper and cadmium. These value at 20 mg L^{-1} metal contamination in the nutrient solution is 1.54 and 3.03, respectively (Figure 5).

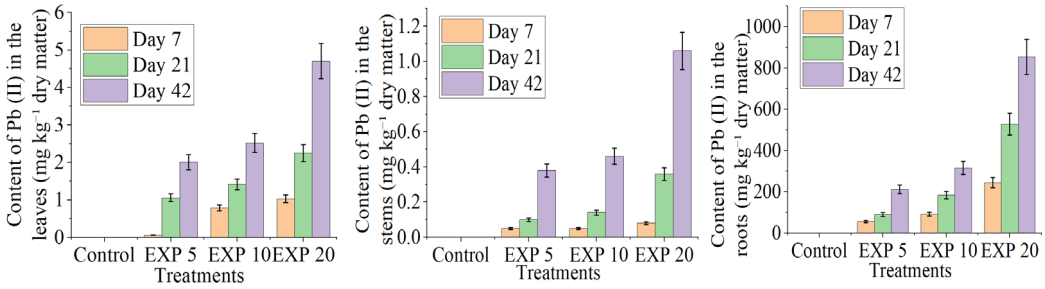

Figure 5. The accumulation of lead in the biomass of *B. juncea*

In general, the accumulated studied heavy metals in the roots were much higher than in the shoots and leaves because the roots were in direct contact with the nutrient solution. For copper, this vegetable's order of accumulation on biomass was roots > stems > leaves. Meanwhile, the order of accumulation for cadmium and lead was roots > leaves > stems. According to Soudek et al. (2009), the accumulation of heavy metals was predominantly in the root system, so its transport from roots to the bulbs was rather low. The heavy metal concentration in leaves resulted from the heavy metal absorption by roots, which then was transferred to leaves via stems. There were significantly different heavy metal levels in the different vegetable tissue, which linked to the characteristics of the plants and different heavy metals (Tom et al., 2014).

The accumulation of studied heavy metals in the biomass of *Brassica juncea* follows the order: Cd < Cu < Pb. This result proves that *B. juncea* has better Cd tolerance than Cu and Pb.

The Translocation Factors of *Brassica juncea* Grown in Polluted Condition by Cu, Cd, and Pb

The translocation of Cu in *B. juncea* clones is shown in Table 2. Under 5 mg L^{-1} Cu exposure, the stems and leaves TFs for Cu ranged from 0.114 to 0.186 and from 0.052 to 0.098, respectively. These results show that Cu tends to be accumulated in the roots rather than the stems and leaves. At 20 mg L^{-1} Cu exposure, the stems and leaves TFs of vegetable tissues were slightly increased. The order of TF values follows stems > leaves. In General, the TFs of vegetable tissues increased with time proceeds, whereas they decreased with increases in Cu concentration in the nutrient solution. The different TFs for Cu in *B. juncea* tissues showed different absorbing capacities and affinities for Cu. The decrease in TFs of vegetable tissues in *B. juncea* parts can be an informative sub-lethal response, indicating increased Cu availability and potential Cu stress in the *B. juncea*. Plants also can translocate and store micronutrients in their environment. Furthermore, toxic elements can have similar absorption, translocate, and storage mechanisms.

Table 2

The translocation factors (TFs) of B. juncea *with 5, 10, and 20 mg L^{-1} of Cu treatment in hydroponic culture for six weeks*

Days	The concentration of Cu (II) in nutrient solution (mg L^{-1})					
	5		10		20	
	Roots-stems TFs	Roots-leaves TFs	Roots-stems TFs	Roots-leaves TFs	Roots-stems TFs	Roots-leaves TFs
7th	0.114	0.052	0.037	0.038	0.058	0.041
21st	0.186	0.069	0.068	0.072	0.084	0.047
42nd	0.195	0.098	0.120	0.079	0.093	0.058

Compared to Cu exposure, the TF of Cd in *B. juncea* is larger than (Table 3). The stems and leaves TFs for Cd ranged from 0.025 to 0.332 and from 0.103 to 0.507, respectively. These results show that Cd tends to be accumulated in the roots rather than in other parts. The order of TF for Cd values in *B. juncea* was the following: leaves > stems. Perhaps Cd has similar properties to Ca, so *B. juncea* cannot recognize its toxicity. From there, Cd was absorbed and transported to the stems and leaves of *B. juncea*.

Table 3

The translocation factors of B. juncea *with 5, 10, and 20 mg L^{-1} of Cd treatment in hydroponic culture for six weeks*

Days	The concentration of Cd (II) in nutrient solution (mg L^{-1})					
	5		10		20	
	Roots-stems TFs	Roots-leaves TFs	Roots-stems TFs	Roots-leaves TFs	Roots-stems TFs	Roots-leaves TFs
7th	0.025	0.167	0.025	0.155	0.091	0.112
21st	0.071	0.103	0.106	0.196	0.129	0.242
42nd	0.090	0.121	0.166	0.226	0.332	0.507

The translocation of Pb in *B. juncea* clones is shown in Table 4. Similar to the case of Cu and Cd exposure, the stems TFs for Pb of *B. juncea* are higher than leaves TFs. However, the translocation factors of Pb in the stems and leaves of *B. juncea* are much lower than that of Cu and Cd. Therefore, it may indicate that *B. juncea* can recognize toxic of Pb so that they can limit absorption and transport to stems and leaves.

Similarly, several previous studies have documented that TFs were less than 1. Majid et al. (2014) studied *Typha angustifolia* and *Phragmites australis* species which TFs of Cu and Pb were 0.12 to 0.87 and 0.33 to 0.42, respectively. Takarina et al. (2017)

showed that TFs of Cu from roots to stems and from roots to leaves in *Rhizopora* sp. were 0.33 and 0.78. Rezapour et al. (2022), the TF values of Cu, Pb, and Cd were 0.72–0.85, 0.09–0.63, and 0.17–0.22, respectively. The values of TFs of Cu, Pb, and Cd ranged between 0.08 and 0.63 in the lettuce and spinach plants (Eissa & Negim, 2018).

Table 4

The translocation factors of B. juncea *with 5, 10, and 20 mg L^{-1} of Pb treatment in hydroponic culture for six weeks*

Days	The concentration of Pb (II) in nutrient solution (mg L^{-1})					
	5		10		20	
	Roots-stems TFs	Roots-leaves TFs	Roots-stems TFs	Roots-leaves TFs	Roots-stems TFs	Roots-leaves TFs
7th	0.0009	0.0011	0.0005	0.0085	0.0003	0.0042
21st	0.0011	0.0117	0.0008	0.0077	0.0007	0.0043
42nd	0.0018	0.0095	0.0015	0.0080	0.0012	0.0055

Relationship Between Rootly, Leafy, and Stemly Vegetable Cu, Cd, Pb Concentrations and Cu, Cd, Pb Concentrations in Nutrient Solution

A high correlation was observed between Cu, Cd, and Pb concentrations in tissues of *B. juncea* and Cu, Cd, and Pb concentrations in nutrient solution (Table 5). The significant positive correlation between Cu, Cd, or Pb concentrations in tissues of *B. juncea* and Cu, Cd, and Pb concentrations in nutrient solution may indicate that Cu, Cd, and Pb have similar uptake mechanisms. Roots absorbed trace elements through passive (which was nonmetabolic) and active (which was metabolic) mechanisms. The different uptake mechanisms depended on the kind of element. For example, Pb absorbed mechanisms passively, while Cu absorbed mechanisms actively (Kabata-Pendias, 2011). And then, Cu, Cd, and Pb were probably transported from roots to stems and leaves by similar transporters in the form of compounds or chelate metal complexes (Foy, 1983; Tyler et al., 1989).

Table 5

Correlation coefficients between Cu, Cd, and Pb concentrations in nutrient solution and Cu, Cd, and Pb concentrations in the tissue of B. juncea *(mg kg^{-1} dry matter)*

Treatments		Roots	Stems	Leaves
Cu	Linear regression	y = 46.444x - 174.5	y = 3.7197x - 4.11	y = 2.3846x - 3.52
	R-squared	R^2 = 0.9566	R^2 = 0.9352	R^2 = 0.9587

Table 5 *(Continue)*

Treatments		Roots	Stems	Leaves
Cd	Linear regression	y = 11.317x + 64.835	y = 8.9671x -37.25	y = 5.7574x - 21.47
	R-squared	R^2 = 0.9782	R^2 = 0.9871	R^2 = 0.9933
Pb	Linear regression	y = 44.412x - 57.125	y = 0.0474x + 0.08	y = 0.1849x + 0.92
	R-squared	R^2 = 0.9672	R^2 = 0.9499	R^2 = 0.9765

CONCLUSION

This study investigated the accumulation of heavy metals, including copper, cadmium, and lead, in the different parts of *B. juncea* planted by the hydroponic method. The research results show that the accumulation of these heavy metals in the different parts of *B. juncea* varied over time. However, generally, the results showed the highest concentration of all tested heavy metals in the root, and transport of metals to other plant parts (stems and leaves) was very low.

ACKNOWLEDGEMENTS

The authors are grateful to the Chemical Engineering Faculty, Industrial University of Ho Chi Minh City, for the support equipment for this study.

REFERENCES

AlShrouf, A. (2017). Hydroponics, aeroponic and aquaponic as compared with conventional farming. *American Scientific Research Journal for Engineering, Technology, and Sciences*, *27*(1), 247-255.

Anwar, S., Nawaz, M. F., Gul, S., Rizwan, M., Ali, S., & Kareem, A. (2016). Uptake and distribution of minerals and heavy metals in commonly grown leafy vegetable species irrigated with sewage water. *Environmental Monitoring and Assessment*, *188*(9), 541-550. https://doi.org/10.1007/s10661-016-5560-4.

Bai, L., Liu, X.-L., Hu, J., Li, J., Wang, Z.-L., Han, G., Li, S.-L., & Liu, C-Q. (2018). Heavy metal accumulation in common aquatic plants in rivers and lakes in the Taihu Basin. *International Journal of Environmental Research and Public Health*, *15*(12), 2857. https://doi.org/10.3390/ijerph15122857

Barazani, O., Dudai, N., Khadka, U. R., & Golan-Goldhirsh, A. (2004). Cadmium accumulation in *Allium schoenoprasum* L. grown in an aqueous medium. *Chemosphere*, *57*(9), 1213-1218. https://doi.org/10.1016/j.chemosphere.2004.08.037

Cobb, G. P., Sands, K., Waters, M., Wixson, B. G., & Dorward-King, E. (2000). Accumulation of heavy metals by vegetables grown in mine wastes. *Environmental Toxicology and Chemistry*, *19*(3), 600-607. https://doi.org/10.1002/etc.5620190311

Deng, D. M., Shu, W. S., & Zhang, J. (2007). Zinc and cadmium accumulation and tolerance in populations of *Sedum alfredii*. *Environmental Pollution*, *147*(2), 381-386. https://doi.org/10.1016/j.envpol.2006.05.024

Dulama, I. D., Popescu, I. V., Stihi, C., Radulescu, C., Cimpoca, G. V., Toma, L. G., Stirbescu, R., & Nitescu, O. (2012). Studies on accumulation

of heavy metals in *Acacia* leaf by EDXRF. *Romanian Report on Physics*, *64*(4), 1063–1071.

Eissa, M. A., & Negim, O. E. (2018). Heavy metals uptake and translocation by lettuce and spinach grown on a metal-contaminated soil. *Journal of Soil Science and Plant Nutrition*, *18*(4), 1097-1107. https://doi.org/10.4067/S0718-95162018005003101

Feigl, G., Kumar, D., Lehotai, N., Tugyi, N., Molnár, A., Ordög, A., Szepesi, A., Gémes, K., Laskay, G., Erdei, L., & Kolbert, Z. (2013). Physiological and morphological responses of the root system of Indian mustard (*Brassica juncea* L. Czern.) and rapeseed (*Brassica napus* L.) to copper stress. *Ecotoxicology and Environmental Safety*, *94*, 179–189. https://doi.org/10.1016/j.ecoenv.2013.04.029

Foy, C. D. (1984). Plant adaptation to mineral stress problem in soils. In D. Evered & G. M. Collins (Eds.), *Origins and development of adaptation* (Vol. 102, pp. 20-39). Ciba Foundation. https://doi.org/10.1002/9780470720837.ch3

Gupta, N., Yadav, K. K., Kumar, V., Cabral-Pinto, M. M. S., Alam, M., Kumar, S., & Prasad, S. (2021). Appraisal of contamination of heavy metals and health risk in agricultural soil of Jhansi City, India. *Environmental Toxicology and Pharmacology*, *88*, 103740. https://doi.org/10.1016/j.etap.2021.103740

Jiang, W., Liu, D., & Hou, W. (2001). Hyperaccumulation of cadmium by roots, bulbs and shoots of garlic (*Allium sativum* L.). *Bioresource Technology*, *76*(1), 9-13. https://doi.org/10.1016/S0960-8524(00)00086-9

Kabata-Pendias, A. (2011). *Trace elements in soils and plants* (4th ed.). CRC Press.

Majid, S. N., Khwakaram, A., Rasul, G. A. M., & Ahmed, Z. H. G. (2014). Bioaccumulation, enrichment and translocation factors of some heavy metals in *Typha angustifolia* and *Phragmites australis* species growing along Qalyasan Stream in Sulaimani City/IKR. *Journal of Zankoy Sulaimani-Part A*, *16*(4), 93-109.

Mohtadi, A., Ghaderian, S. M., & Schat, H. (2012). A comparison of lead accumulation and tolerance among heavy metal hyperaccumulating and non-hyperaccumulating metallophytes. *Plant and Soil*, *352*(1-2), 267–276. https://doi.org/10.1007/s11104-011-0994-5

Mourato, M. P., Moreira, I. N., Leitão, L., Pinto, F. R., Sales, J. R., & Martins, L. L. (2015). Effect of heavy metals in plants of the genus *Brassica*. *International Journal of Molecular Sciences*, *16*(8), 17975-17998. https://doi.org/10.3390/ijms160817975.

Radulescu, C., Stihi, C., Busuioc, G., Gheboianu, A. I., & Popescu, I. V. (2010). Studies concerning heavy metals bioaccumulation of wild edible mushrooms from industrial area by using spectrometric techniques. *Bulletin of Environmental Contamination and Toxicology*, *84*(5), 641–647. https://doi.org/10.1007/s00128-010-9976-1

Radulescu, C., Stihi, C., Popescu, I. V., Ionita, I., Dulama, I. D., Chilian, A., Bancuta, O. R., Chelarescu, E. D., & Let, D. (2013). Assessment of heavy metals level in some perennial medicinal plants by Flame Atomic Absorption Spectrometry. *Romanian Reports in Physics*, *65*(1), 246–260.

Rezapour, S., Moghaddam, S. S., Nouri, A., & Aqdam, K. K. (2022). Urbanization influences the distribution, enrichment, and ecological health risk of heavy metals in croplands. *Scientific Reports*, *12*(1), 3868-3884. https://doi.org/10.1038/s41598-022-07789-x

Sharma, N., Acharya, S., Kumar, K., & Chaurasia, O. P. (2018). Hydroponics as an advanced technique for vegetable production: An overview. *Journal of Soil and Water Conservation*, *17*(4), 364-371. https://doi.org/10.5958/2455-7145.2018.00056.5

Soudek, P., Kotyza, J., Lenikusova, I., Petrová, S., Benešová, D., & Vanek, T. (2009). Accumulation of heavy metals in hydroponically cultivated garlic (*Allium sativum* L.), onion (*Allium cepa* L.), leek (*Allium porrum* L.) and chive (*Allium schoenoprasum* L.). *Journal of Food, Agriculture and Environment*, *7*(3), 761-769.

Souri, M. K., Hatamian, M., & Tesfamariam, T. (2019). Plant growth stage influences heavy metal accumulation in leafy vegetables of garden cress and sweet basil. *Chemical and Biological Technologies in Agriculture*, *6*, 25. https://doi.org/10.1186/s40538-019-0170-3

Takarina, N. D., & Pin, T. G. (2017). Bioconcentration factor (BCF) and translocation factor (TF) of heavy metals in mangrove trees of Blanakan Fish Farm. *Makara Journal of Science*, *21*(2), 77-81. https://doi.org/10.7454/mss.v21i2.7308

Tom, M., Fletcher, T. D., & Mccarthy, D. T. (2014). Heavy metal contamination of vegetables irrigated by urban stormwater: A matter of time? *PLOS One*, *9*(11), e112441. https://doi.org/10.1371/journal.pone.0112441

Tyler, G., Balsberg Påhlsson, A. M., Bengtsson, G., Bååth, E., & Tranvik, L. (1989). Heavy metal ecology of terrestrial plants, microorganisms and invertebrates. *Water, Air, and Soil Pollution*, *47*, 189-215. https://doi.org/10.1007/BF00279327

Wang, L., Chen, X., Guo, W., Li, Y., Yan, H., & Xue, X. (2017). Yield and nutritional quality of water spinach (*Ipomoea aquatica*) as influenced by hydroponic nutrient solutions with different pH adjustments. *International Journal of Agriculture and Biology*, *19*(4), 635-642. https://doi.org/10.17957/IJAB/15.0311

Zhou, H., Yang, W.-T., Zhou, X., Liu, L., Gu, J.-F., Wang, W.-L., Zou, J.-L., Tian, T., Peng, P.-Q., & Liao, B.-H. (2016). Accumulation of heavy metals in vegetable species planted in contaminated soils and the health risk assessment. *International Journal of Environmental Research and Public Health*, *3*(3), 289-301. https://doi.org/10.3390/ijerph13030289

Pertanika J. Trop. Agric. Sci. 46 (1): 265 - 276 (2023)

PERTANIKA JOURNALS

TROPICAL AGRICULTURAL SCIENCE

Journal homepage: http://www.pertanika.upm.edu.my/

In vitro Bioactivity Evaluation of *Ziziphus mauritiana* Lam. (Bidara) Leaves Extract Against Vector Mosquitoes *Aedes* spp. and *Culex quinquefasciatus*

Ai Wei Lim[1], Azlinda Abu Bakar[1]*, Mohd Firdaus Lai[1] and Mohamad Nurul Azmi Mohamad Taib[2]

[1]School of Biological Sciences, Universiti Sains Malaysia, 11800 Minden, Pulau Pinang, Malaysia
[2]School of Chemical Sciences, Universiti Sains Malaysia, 11800 Minden, Pulau Pinang, Malaysia

ABSTRACT

Ziziphus mauritiana methanol crude extract was evaluated for its insecticidal properties against *Aedes aegypti*, *Ae. albopictus*, and *Culex quinquefasciatus* mosquito larvae. Bioassays against larvae mosquitoes were done following World Health Organization's guidelines. Late third and/or early fourth instar of mosquito larva were assayed for five different concentrations viz. 100, 150, 200, 250, and 300 mg ml^{-1} of *Z. mauritiana* crude extracts. From the results obtained, *Aedes aegypti* was the most susceptible to *Z. mauritiana* crude extracts. The percentage of mortality exhibited above 50% of 200, 250, and 300 mg ml^{-1} in 24, 48, and 72 hr exposure. Thus, it gives the lowest LC_{50} within 24 hr of exposure (121.98 mg L^{-1}), followed by *Ae. albopictus* (189.89 mg L^{-1}) and *Cx. quinquefasciatus* (246.22 mg L^{-1}). Observation of the morphology effect of the dead larvae shows *Ae. aegypti* was the most affected, followed by *Ae. albopictus* and *Cx. quinquefasciatus*. A ruptured midgut was observed in 100 and 200 mg ml^{-1} concentrations. In contrast, in higher concentrations of 300 mg ml^{-1}, the abdominal segments were indistinguishable, and the head and thorax regions were severely damaged. This study suggested that *Z. mauritiana* methanolic crude extracts were potent against *Ae. aegypti* larvae mosquitoes and have the potential to be used as an alternative larvicide in population control. However, further studies are required to establish the potential of *Z. mauritiana* larvicidal effects in the field setting.

Keywords: *Aedes* spp., bioactivity, crude extracts, *Culex quinquefasciatus*, *Ziziphus mauritiana*

ARTICLE INFO

Article history:
Received: 14 September 2022
Accepted: 27 October 2022
Published: 14 February 2023

DOI: https://doi.org/10.47836/pjtas.46.1.15

E-mail addresses:
aiweivip@gmail.com (Ai Wei Lim)
azlindaab@usm.my (Azlinda Abu Bakar)
firdausfir8881@gmail.com (Mohd Firdaus Lai)
mnazmi@usm.my (Mohamad Nurul Azmi Mohamad Taib)
* Corresponding author

ISSN: 1511-3701
e-ISSN: 2231-8542

INTRODUCTION

In many tropical and sub-tropical countries, mosquitoes such as *Aedes*, *Culex*, and *Anopheles* are vectors of many infectious pathogens, such as dengue, chikungunya, Zika, lymphatic filariasis, malaria, and yellow fever (World Health Organization [WHO], 2020). Malaysia is a tropical country that provides favourable and suitable breeding sites for mosquitoes to reproduce and survive throughout the year. In addition, Malaysia's favourable temperature and humidity play a huge role in aiding the increment of the mosquito population, thus encouraging viruses and disease transmission. The cumulative number of reported dengue cases in Malaysia as of September 2021 is 18,988, with 11 deaths, although there was a drastic drop compared to 74,443 reported dengue cases and 123 deaths in 2020 (WHO, 2021). On the other hand, according to European Centre for Disease Prevention and Control (ECDC) (2021), 1,102 reported chikungunya cases as of October 2021, with an increase of 134 new cases since 11 September 2021.

Until now, there has been no effective vaccine against these mosquito-borne diseases. Thus, chemical insecticides have been used as an effective tool to combat and control the disease outbreak due to their immediate effect on suppressing the vector population. However, continuous usage and repetitive exposure to these chemical insecticides have caused mosquitoes to develop resistance due to selective pressure and compromised the success of the control interventions. In addition, chemical insecticides have also caused irreversible environmental damage, hazards to non-target species, and food web disruption. Therefore, alternative approaches, such as botanical insecticides, have become more popular in mosquito control, either for larvicidal, adulticidal, or repellent (Bakar, 2020). Toxins and secondary metabolites, a complex of compounds which act as mosquitocidal agents, are hypothesised to be responsible for distinct biological activity found in different parts of plants (Aydin et al., 2017).

For instance, *Azolla pinnata* plants have shown their potential as larvicidal and adulticidal against *Aedes* mosquitoes. The extracts can alter the morphology and behaviour of *Ae. aegypti* larvae (Zulkrnin et al., 2018). Another study by Ravi et al. (2020) has shown that a significant increase in mortality was noted as test concentration increased, indicating the existence of bioactive chemicals responsible for adulticidal activity in *Aedes* mosquitoes. In addition, phytochemicals of plant extracts would have minimal effects on resistance development when exposed to mosquitoes (Şengül Demirak & Conpolat, 2022). Therefore, this study aimed to explore the bioactivity potential of the *Ziziphus mauritiana* plant against common mosquitoes vector in Malaysia. The plant is locally known as 'Bidara' and is commonly used in traditional Islamic medicine for its health-beneficial effect (Mohd Jailani et al., 2020). *Ziziphus mauritiana*, or Bidara, is commonly used in Malay traditional medicine (Mohd Jailani, 2020). *Ziziphus*

mauritiana dried fruits are anodyne, anticancer, pectoral, refrigerant, sedative, stomachache, styptic, and tonic as it is believed to have the ability to purify the blood and aid digestion. At the same time, the root treats dyspepsia and fever. Despite that, the fruits are crunchy and have a sweet and sour taste when eaten raw. Like many other commercialized medicinal plants, *Z. mauritiana* Bidara has also come to the attention of many small and medium company industries for similar purposes. Thus, products of *Z. mauritiana*-based have been used widely in all kinds of personal care products such as hair shampoo, body care, and facial care.

In Malaysia, however, there are limited to no studies conducted on their insecticidal properties. A thorough search of recent documented studies on *Z. mauritiana* has succeeded in finding a similar study conducted by researchers in Indonesia, which investigated the effectiveness of *Z. mauritiana* extracts against *Ae. aegypti* larva (Amaliyah et al., 2021; Askur et al., 2021). It has initiated the author(s) attention to give insight into *Z. mauritiana* larvicidal effects against common mosquitoes vector in Malaysia, such as *Ae. aegypti*, *Ae. albopictus*, and *Cx. quinquefasciatus*. While *Ae. aegypti* is commonly known as the primary dengue vector in Malaysia, *Ae. albopictus* is currently the most invasive mosquito in the world and serves as a potential vector of the dengue virus in rural and suburban areas (Benedict et al., 2007; Higa, 2011). In contrast to the *Aedes* spp. clean and clear water habitat, *Cx. quinquefasciatus* preferences of breeding in highly polluted water and being capable of surviving in high larval densities have allowed exploitation of the human-made polluted environment. As a result, it created a high risk of human transmission of zoonotic pathogen diseases (Harvey-Samuel et al., 2021). In the present study, the bioactivity of *Z. mauritiana* was evaluated *in vitro* against *Ae. aegypti*, *Ae. albopictus*, and *Cx. quiquefasciatus* for its larvicidal and morphological effects on dead larvae. The comparisons were discussed.

METHODOLOGY

Collection and Preparation of *Ziziphus mauritiana*

The leaves specimen of *Z. mauritiana* were collected at the Islamic Centre, Universiti Sains Malaysia (USM), Pulau Pinang, Malaysia (N 5° 24' 40.428''E 100° 20' 7.548''). The botanist staff of the School of Biological Sciences (SBS), USM, Pulau Pinang, identified the specimens. All collected leaves were brought to the SBS, USM laboratory for sample processing. The leaves were washed, cleaned thoroughly, and dried at room temperature (29.5–31.5°C) for three to four days. The cleaned and dried *Z. mauritiana* leaves were grounded using a household KitchenAid® blender (USA) and stored in zip-lock plastic bags until further use.

Maceration Extractions

In this study, crude extracts of the plant leaves were prepared with the maceration extractions method. The ratio applied was 1

g (grounded leaves) to 10 ml (solvents). The desired amounts of *Z. mauritiana* grounded leaves and methanol were measured and placed in tight containers for 72 hr. The mixture was stirred and shaken periodically to ensure complete extraction. At the end of the extraction process, the micelles were filtered with filter paper Whatman No.1. and concentrated with a rotary evaporator at a temperature of 50 to 60℃ and pressure of 1,000 mbar for eight hours. The extracted residue was carefully kept in the refrigerator at 4℃ in an amber glass vial for subsequent assay.

Mosquito Preparation

Mosquitoes used in this study were obtained from Vector Control Research Unit (VCRU), SBS, USM Pulau Pinang. The mosquito colony was cultured and reared in the laboratory with a temperature of 28.0 ± 2.0°C and relative humidity (RH %) of 80.5 ± 3.0 %. Throughout the maintenance period, mosquito larvae were provided with prepared portioned ratio powdered food (2 : 1 : 1 : 1): cat's biscuit, dried cow liver (grounded), powdered milk, yeast, and eight tablets of the vitamin B complex. The colony was continuously maintained during the study period.

Larval Bioassay

The bioassay larval was conducted according to the standard guidelines of the WHO (2005). Five concentrations of *Z. mauritiana* methanol extracts were prepared: 100, 150, 200, 250, and 300 mg ml^{-1}. Bioassay larvae were in five replicates of 20 instar larvae for each concentration. Larvae were aged between late instar three and early instar four. The number of dead larvae was recorded after 24 and 48 hr of exposure. The control solutions were prepared by mixing 1.0 ml methanol in 199.0 ml distilled water. During the observation, food was not supplied to the larvae.

Morphological Effects of Dead Larvae

All dead larvae mosquitoes were collected and transferred to a Petri dish to observe morphological effects. The observation was conducted under an Olympus® stereo microscope (Model: SZX16-CCD, Japan), and photos were captured.

Statistical Analysis

For any mortality in the control which is less than 20%, Abbott's formula was used (Abbot, 1925) as below:

$$Mortality\% = \frac{Test\ mortality\% - Control\ mortality\%}{100 - Control\ mortality\%} \times 100\%$$

The lethal concentrations 50% (LC_{50}) and 90% (LC_{90}) were calculated using probit analysis (Finney, 1971), respectively. All data obtained were analyzed with Statistical Product and Service Solutions (SPSS) software (version 27) with a confidence interval of 95%. Determination of the most effective concentration of the extract based on the analysis of variance (ANOVA) followed by least significant differences (LSD) tests.

RESULTS

Larvicidal Assays

Table 1 shows the mean mortality of mosquito larvae against *Z. mauritiana* leaves extracts at different concentrations and time exposure (hrs) during larvae assay. From the results obtained, mean mortality of different concentrations and time exposure among three mosquito species were increased with high concentrations and time exposure. Of these, *Ae. aegypti* larvae population was the most susceptible compared to *Ae. albopictus* and *Cx. quinquefasciatus*. It is notable that, at a concentration of 200 mg ml^{-1}, the mean mortality of *Ae. aegypti* population was the constant highest at 23.25 ± 0.48, 23.75 ± 0.25, and 24.25 ± 0.25 throughout the time exposure of 24, 48, and 72 hr, respectively, compared to *Ae. albopictus* and *Cx. quinquefasciatus*. The highest mean mortality was 25.00 ± 0.00 (100 % mortality), demonstrated by *Ae. aegypti* exposed to 300 mg ml^{-1} methanolic *Z. mauritiana* leaves extract for 48 and 72 hr. The *Ae. aegypti* larvae marked more than 50% mortality from exposure of 150 mg ml^{-1} and above for 24, 48, and 72 hr. The

Table 1
Mean mortality of Ziziphus mauritiana *extracts against mosquito larvae*

Mosquito species	Concentrations (mg ml^{-1})	Mean mortality ± S.E		
		24[a] hr	48 hr	72 hr
* [a]*Aedes aegypti*	100	5.00 ± 2.55	7.00 ± 2.94	9.50 ± 2.90
	150	17.3 ± 1.25	21.50 ± 0.87	22.50 ± 0.87
	200	23.25 ± 0.48	23.75 ± 0.25	24.25 ± 0.25
	250	23.25 ± 0.48	24.75 ± 0.25	25.00 ± 0.00
	300	24.75 ± 0.25	25.00 ± 0.00	25.00 ± 0.00
	Control	0	0	0
* *Aedes albopictus*	100	11.50 ± 1.85	13.25 ± 2.39	13.25 ± 2.39
	150	11.50 ± 1.55	13.50 ± 1.85	13.75 ± 1.89
	200	14.75 ± 3.09	18.00 ± 1.29	19.25 ± 1.44
	250	17.00 ± 3.67	19.50 ± 2.96	21.00 ± 2.12
	300	23.75 ± 0.63	25.00 ± 0.00	25.00 ± 0.00
	Control	0	0	0
* [a]*Culex quinquefasciatus*	100	1.00 ± 0.41	2.75 ± 0.25	3.75 ± 0.63
	150	2.75 ± 0.85	14.25 ± 1.89	15.75 ± 1.44
	200	13.25 ± 1.44	21.00 ± 0.00	22.50 ± 0.29
	250	16.25 ± 2.10	23.00 ± 0.41	23.50 ± 0.29
	300	13.50 ± 1.19	24.50 ± 0.29	24.75 ± 0.25
	Control	0	0	0

Note. Number of studies = 27; Number of effects = 216; Total $N = 5400$
*Significant difference in mean mortality of tested mosquito species, $p < 0.05$ ($p = 0.00$)
[a] Significant difference in mean mortality of 24 hr, $p < 0.05$ ($p = 0.015$)

mean mortality was 17.3 ± 1.25, 21.50 ± 0.87, and 22.50 ± 0.87, respectively. At the end of 72 hr observation, each concentration assayed of 100, 150, 200, 250, and 300 mg ml^{-1} *Z. mauritiana* methanolic extracts gives mean mortality of 9.50 ± 2.90, 22.50 ± 0.87, 24.25 ± 0.25, 25.00 ± 0.00, and 25.00 ± 0.00, respectively. In brief, *Ae. aegypti* larvae give the highest mean mortality throughout the time exposure period compared to *Ae. albopictus* and *Cx. quinquefasciatus*. Nevertheless, both mean mortality of *Ae. albopictus* and *Cx. quinquefasciatus* showed a gradual increment for each concentration with increasing exposure hours. However, extracts of *Z. mauritiana* were more effective against *Ae. albopictus* larvae compared to *Cx. quinquefasciatus*. Cx recorded no 100% mortality. *quinquefasciatus* at the highest concentrations in any time exposure of 24, 48, and 72 hr. Statistical analysis of one-way ANOVA analysis showed a significant difference ($p < 0.05$) in the mean mortality of all tested mosquito species and tested concentrations of *Z. mauritiana* leaves extract ($p = 0.00$). However, the paired samples test analysis revealed the significant difference ($p < 0.05$) in the mean mortality was only between *Ae. aegypti* and *Cx. quinquefasciatus* at 24 hr of methanolic *Z. mauritiana* leaves extract ($p = 0.015$).

Table 2 shows the lethal concentrations of LC_{50} and LC_{90} for each mosquito larvae assayed and time exposure (hr). Of these, mosquito larvae of *Ae. aegypti* was the most susceptible against *Z. mauritiana* leaves extracts. The LC_{50} and LC_{90} in three different time exposure, 24 hrs, 48 hrs, and 72 hr, were the lowest at 122.0, 111.7, 107.7, 200.1, 172.9, and 163.4 mg ml^{-1}, respectively compared to *Ae. albopictus* and *Cx. quinquefasciatus*. On the other hand, *Cx quinquefasciatus* gives the highest values of LC_{50} and LC_{90} of time exposure (hrs.). The lethal concentrations in 24 hrs, 48 hrs, and 72 hr were 246.2, 169.9,

Table 2
Lethal concentrations (LC_{50} and LC_{90}) of Ziziphus mauritiana *extracts against mosquito species*

Mosquito species	Exposure duration (hrs)	LC_{50} (mg ml^{-1})	95% CI (mg ml^{-1})		LC_{90} (mg ml^{-1})	95% CI (mg ml^{-1})		df
			LL	UL		LL	UL	
Aedes aegypti	24	122.0	117.1	126.6	200.1	192.0	209.6	3.5
	48	111.7	107.2	115.9	172.9	166.2	180.9	1.7
	72	107.7	103.3	111.8	163.4	157.1	171.0	1.9
Aedes albopictus	24	189.9	132.5	273.7	421.3	285.8	3044.3	42.2
	48	161.1	116.1	200.2	346.4	258.9	855.9	29.4
	72	150.1	111.4	180.9	306.7	240.5	570.9	25.5
Culex quinquefasciatus	24	246.2	221.0	285.3	496.4	393.5	768.8	8.5
	48	169.9	163.7	176.2	323.3	304.4	347.4	4.1
	72	144.5	137.7	150.9	296.6	278.4	319.8	2.2

Note. Number of studies = 27; Number of effects = 216; Total $N = 5400$. CI = Confidence intervals; df = Degree of freedom; LL = Lower limit; UL = Upper limit

144.5 mg ml^{-1} for LC_{50} and 496.4, 323.3, and 296.6 mg ml^{-1} for LC_{90}, respectively. In relative, lower values of LC_{50} and LC_{90} obtained from methanolic *Z. mauritiana* extracts indicate good effects against tested mosquito larvae.

Morphology Effect

The morphology effect of dead mosquito larvae was observed in different concentrations treatment of control, 0, 100, 200, and 300 mg ml^{-1}, as shown in Figure 1. Figure 1 (a)(i), (b)(i), and (c)(i) showed the

Figure 1. Morphology of mosquito larvae (a) *Aedes aegypti*, (b) *Aedes albopictus*, (c) *Culex quinquefasciatus* photographed at 0.69x by stereo microscope (Model: SZX16-CCD) after treated with different concentrations of *Ziziphus mauritiana* extracts in (i) 0 mg ml^{-1}, (ii) 100 mg ml^{-1}, (iii) 200 mg ml^{-1}, and (iv) 300 mg ml^{-1}

normal morphology features of the well-developed head, thorax, and abdominal region of *Ae. aegypti*, *Ae. albopictus*, and *Cx. quinquefasciatus* larvae with eight segments and anal segments, respectively. *Aedes aegypti* larvae treated with methanolic *Z. mauritiana* leaves extract concentrations of 100 and 200 mg ml^{-1} (Figure 1(a)(ii–iii)) showed ruptured midgut. In the 300 mg ml^{-1} treated concentration (Figure 1(a)(iii)), deformities of *Ae. aegypti* larvae's bodies were observed in which the abdominal segments were indistinguishable, and the head and thorax region were unidentified. On the other hand, observation of the dead larvae of *Ae. albopictus* in treated with methanolic *Z. mauritiana* leaves extract showed a normal morphological appearance with distinguishable head, thorax, and abdominal regions. However, darkening of the thorax, abdomen and anal gill was observed distinctly in larvae exposed to extract concentrations of 100, 200, and 300 mg ml^{-1} (Figure 1(b)(ii–iv)).

The observed morphology of dead *Cx. quinquefasciatus* exposed to 100, 200, and 300 mg ml^{-1} of methanolic *Z. mauritiana* leaves extract concentration after various exposure times were shown in Figure 1(c)(ii–iv). The *Cx. quinquefasciatus* larvae in control (Figure 1(c)(i)) showed normal morphological features with a well-developed head, thorax, eight segments abdominal region, and long siphon. While *Cx. quinquefasciatus* larvae treated with methanolic *Z. mauritiana* leaves extract of 200 mg ml^{-1} (Figure 1(c)(iii)) showed ruptured midgut, indistinguishable abdomen, and anal gill along with poorly developed thorax. On the other hand, larvae treated with 100 and 300 mg ml^{-1} (Figure 1(c)(i) and (iv)) showed well-developed morphology with distinguishable body regions as the larvae in control (Figure 1 (c)(i)). However, the darkening of the thorax and abdomen was notably observed. The results obtained in the morphological observation of dead mosquito larvae after being treated with different concentrations of *Z. mauritiana* leaves extract have confirmed the larvicidal assay findings in which *Ae. aegypti* was the most susceptible and thus exhibited severe deformities effect after being exposed to concentrations of 100, 200, and 300 mg ml^{-1} compared to *Ae. albopictus* and *Cx. quinquefasciatus*.

DISCUSSION

Theoretically, the higher the concentration, the more active compounds will directly contact the tested larvae. Askur et al. (2021) showed that ethanolic *Z. mauritiana* extracts cause greater mortalities against *Ae. aegypti* larvae with higher concentrations. These findings agreed with the present study conducted on methanolic extracts. Even though the solvent and concentrations used in each study were different, it has been shown that the *Z. mauritiana* extracts have larvicidal effects against *Ae. aegypti* if proper extractions technique and solvents are used. Another parameter observed in this study was the lethal concentration (LC) values. These values were analysed to evaluate the association between lethal concentrations and mortality. The lower

LC obtained indicated, the more effective the extracts used. Therefore, the larvicidal effects generally have good potential when the extract causes high mortality at a low LC value. Meyer et al. (1982) and Santos Pimenta et al. (2003) have classified the larvicidal effectiveness based on the ranges of LC values obtained: LC_{50} > 200 µg ml^{-1} (0.2 mg ml^{-1}) very weak (inactive), LC_{50} 20–200 µg ml^{-1} (0.02–0.2 mg ml^{-1}) as moderate, and LC_{50} < 200 µg ml^{-1} (0.2 mg ml^{-1}) as very good. The lowest LC_{50} values recorded of *Ae. aegypti* in this present study were 121.975, 111.726, and 107.734 mg ml^{-1}, while the LC_{90} were 200.100, 172.923, and 163.357 mg ml^{-1} for 24, 48, and 72 hr, respectively. These results obtained, however, are considered average in comparison with a study by Amaliyah et al. (2021), which reported a lower LC_{50} (46.97 mg ml^{-1}) and LC_{90} (86.48 mg ml^{-1}) values of *Z. mauritiana* leaves extract against *Ae. aegypti* for 24 hr.

The different larvicidal activities of different plant extracts are probably due to the extraction method and types of solvents used to extract the plants' leaves. According to Zhang et al. (2018), the solvent selection is crucial for plant extraction. The performance of solvent extraction can be enhanced by choosing solvents that have a polarity value near the polarity of the solute. In addition, the most crucial element in producing the best extract quality is the samples' phytochemicals themselves. A study by Velázquez-Martínez et al. (2022) has shown that the content and antioxidant activity of plant extracts remained stable across different extraction processes; however, different geographical regions of the plants obtained showed differences in the abundance of secondary metabolites in which related to the amount received of UV radiation, nutrient components, temperature, and water stress.

Morphological changes in all treated *Ae. aegypti*, *Ae. albopictus*, and *Cx. quinquefasciatus* larvae were demonstrated in which the most obvious deformities appear with poorly developed body regions. Most of the dead *Ae. aegypti* and *Cx. quinquefasciatus* larvae have ruptured midgut, and damaged tissues, possibly caused by the presence of chemical compounds in methanolic *Z. mauritiana* leaves extract that targets the larvae's osmoregulation system (Wang et al., 2019). For instance, the presence of tannins in methanolic *Z. mauritiana* leaves extract can cause disruption of membrane integrity and/or function of the midgut (Procópio et al., 2015). There were few notable observations on the body deformities of the *Ae. aegypti* and *Cx. quinquefasciatus* larvae, such as indistinguishable abdomen segments and poorly developed head and thorax, suggest that methanolic *Z. mauritiana* leaves extract has certain chemical properties that can cause structural distortion of larvae. Larvae of *Ae. albopictus* showed a typical appearance, but darker pigmentation was also observed, especially at the thorax, abdomen, and anal gills. The methanolic Z. mauritiana possibly causes the pigmentation leaves extract, which is dark green.

Montell and Zwiebel (2016) discussed that mosquito larvae usually do not discriminate against what they ingest. Thus, the high number percentage of mortality in larvae of *Ae. aegypti* compared to *Ae. albopictus* and *Cx. quinquefasciatus* were probably due to their feeding behaviour. According to Merritt et al. (1992), larvae of *Ae. aegypti* feed by swimming or diving to substrates in their habitats and thus are commonly known as "bottom feeders". Most methanolic *Z. mauritiana* leaves extract precipitation was found to be sediment or deposited on the bottom of the test cups, while the larval food powder was usually found. Thus, higher mortalities in *Ae. aegypti* larvae could be attributed to their feeding behaviours of "bottom feeders".

CONCLUSION

The results revealed that methanolic *Z. mauritiana* leaves extract at all tested concentrations cause mortality and morphology changes in *Ae. aegypti*, *Ae. albopictus*, and *Cx. quinquefasciatus* larvae associated with a higher concentration of the methanolic leaf extract and longer exposure time. It is concluded that these methanolic leaves extract of *Z. mauritiana* can induce morphological changes among larvae mosquito vectors. This study has also suggested that methanolic *Z. mauritiana* leaves extract can be a potent larvicide to reduce the mosquito population by controlling the larval stage. However, further studies on the active compounds, mechanisms, and mode of action of methanolic extracts of *Z. mauritiana* leaves against vector mosquitoes are required to understand the nature of its killing properties. Future initiatives of larvicidal bioassay using methanolic *Z. mauritiana* leaves extract against field strain mosquitoes are necessary. It is also crucial to further evaluate any toxicity and hazards established by *Z. mauritiana* extract towards the non-target organisms and environment. Different extraction methods associated with various solvents and *Z. mauritiana* plant parts can be considered against different mosquito species.

ACKNOWLEDGEMENTS

The authors want to thank the School of Biological Sciences and Chemical Sciences Universiti Sains Malaysia, Pulau Pinang, for providing the facilities.

REFERENCES

Abbott, W. S. (1925). A method of computing the effectiveness of an insecticide. *Journal of Economic Entomology*, *18*(2), 265-266. https://doi.org/10.1093/jee/18.2.265a

Amaliyah, N., Purnomo, A., Khayan, K., Wardoyo, S., & Anwar, T. (2021). *Z. mauritiana* leaves as larvasidal alternatives. *KEMAS: Jurnal Kesehatan Masyarakat*, *17*(1), 24-30. https://doi.org/10.15294/kemas.v17i1.24377

Askur, A., Adiningsih, R., & Ganning, A. (2021). Utilization of bidara eaf (*Ziziphus mauritiana* L.) extract as a natural larvacide. *Urban Health*, *3*(1), 103-107.

Aydin, T., Bayrak, N., Baran, E., & Cakir, A. (2017). Insecticidal effects of extracts of *Humulus lupulus* (hops) L. cones and its principal component, xanthohumol. *Bulletin*

Entomological Research, *107*(4), 543-549. https://doi.org/10.1017/S0007485317000256

Bakar, A. A. (2020). Bioactivity evaluation of *Melaleuca cajuputi* (Myrtales): Myrtaceae crude extracts against *Aedes* mosquito. *Pertanika Journal of Tropical Agricultural Science*, *43*(3), 303-313.

Benedict, M. Q., Levine, R. S., Hawley, W. A., & Lounibos, L. P. (2007). Spread of the tiger: Global risk of invasion by the mosquito *Aedes albopictus*. *Vector Borne and Zoonotic Diseases*, *7*(1), 76–85. https://doi.org/10.1089/vbz.2006.0562

European Centre for Disease Prevention and Control. (2021). *Chikungunya worldwide overview*. ECDC. https://www.ecdc.europa.eu/en/chikungunya-monthly

Finney, D. J. (1971). *Probit analysis* (3rd ed.). Cambridge University Press.

Harvey-Samuel, T., Ant, T. H., Sutton, J., Niebhur, C.-N., Asigau, S., Parker, P., Sinkins, S., & Alphey, L. (2021). *Culex quinquefasciatus*: Status as a threat to island avifauna and options for genetic control. *CABI Agriculture and Bioscience*, *2*, 9. https://doi.org/10.1186/s43170-021-00030-1

Higa, Y. (2011). Dengue vectors and their spatial distribution. *Tropical Medicine and Health*, *39*(4 Supplement), S17–S27. https://doi.org/10.2149/tmh.2011-S04

Merritt, R. W., Dadd, R. H., & Walker, E. D. (1992). Feeding behaviour, natural food, and nutritional relationships of larval mosquitoes. *Annual Review of Entomology*, *37*(1), 349-374. https://doi.org/10.1146/annurev.en.37.010192.002025

Meyer, B. N., Ferrigni, N. R., Putnam, J. E., Jacobsen, L. B., Nichols, D. E., & McLaughlin, J. L. (1982). Brine shrimp: A convenient general bioassay for active plant constituents. *Planta Medica*, *45*(5), 31–34. https://doi.org/10.1055/s-2007-971236

Mohd Jailani, F. N. A., Zaidan, U. H., Abdul Rahim, M. B. H., Abd Gani, S. S., & Effendi Halmi, M. I. (2020). Evaluation of constituents and physicochemical properties of Malaysian underutilized *Ziziphus mauritiana* (Bidara) for nutraceutical potential. *International Journal of Fruit Science*, *20*(3), 394-402. https://doi.org/10.1080/15538362.2019.1641458

Montell, C., & Zwiebel, L. J. (2016). Mosquito sensory systems. In A. S. Raikhel (Ed.), *Advances in insect physiology* (1st ed., pp. 293-328). Academic Press. https://doi.org/10.1016/bs.aiip.2016.04.007

Procópio, T. F., Fernandes, K. M., Pontual, E. V., Ximenes, R. M., de Oliveira, A. R., Souza, C., Melo, A. M., Navarro, D. M., Paiva, P. M., Martins, G. F., & Napoleão, T. H. (2015). *Schinus terebinthifolius* leaf extract causes midgut damage, interfering with survival and development of *Aedes aegypti* larvae. *PLOS One*, *10*(5), e0126612. https://doi.org/10.1371/journal.pone.0126612

Ravi, R., Rajendran, D., Oh, W. D., Mat Rasat, M. S., Hamzah, Z., Ishak, I. H., & Mohamad Amin, M. F. (2020). The potential use of *Azolla pinnata* as an alternative bio-insecticide. *Scientific Reports*, *10*(1), 19245. https://doi.org/10.1038/s41598-020-75054-0

Santos Pimenta, L. P., Pinto, G. B., Takahashi, J. A., e Silva, L. G., & Boaventura, M. A. (2003). Biological screening of annonaceous Brazilian medicinal plants using *Artemia salina* (brine shrimp test). *Phytomedicine: International Journal of Phytotherapy and Phytopharmacology*, *10*(2-3), 209–212. https://doi.org/10.1078/094471103321659960

Şengül Demirak, M. Ş., & Canpolat, E. (2022). Plant-based bioinsecticides for mosquito control: Impact on insecticide resistance and disease transmission. *Insects*, *13*(2), 162. https://doi.org/10.3390/insects13020162

Velázquez-Martínez, V., Valles-Rosales, D., Rodríguez-Uribe, L., Laguna-Camacho, J. R., López-Calderón, H. D., & Delgado, E. (2022). Effect of different extraction methods and geographical origins on the total phenolic yield, composition, and antimicrobial activity of sugarcane bagasse extracts. *Frontiers in Nutrition*, *9*, 834557. https://doi.org/10.3389/fnut.2022.834557

Wang, Z., Perumalsamy, H., Wang, X., & Ahn, Y.-J. (2019). Toxicity and possible mechanisms of action of honokiol from *Magnolia denudata* seeds against four mosquito species. *Scientific Reports*, *9*, 411. https://doi.org/10.1038/s41598-018-36558-y

World Health Organization. (2005). *Guidelines for laboratory and field testing of mosquito*. WHO. https://apps.who.int/iris/handle/10665/69101

World Health Organization. (2020). *Vector-borne diseases*. WHO. https://www.who.int/newsroom/fact-sheets/detail/vector-borne-diseases

World Health Organization. (2021). *Dengue situation*. WHO. https://www.who.int/docs/defaultsource/wprodocuments/emergency/surveillance/deue/dengue-20210923.pdf?sfvrsn=fc80101d_90

Zhang, Q. W., Lin, L. G., & Ye, W. C. (2018). Techniques for extraction and isolation of natural products: A comprehensive review. *Chinese Medicine*, *13*, 20. https://doi.org/10.1186/s13020-018-0177-x

Zulkrnin, N. S. H., Rozhan, N. N., Zulkfili, N. A., Nik Yusoff, N. R., Rasat, M., Abdullah, N. H., Ahmad, M. I., Ravi, R., Ishak, I. H., & Mohd Amin, M. F. (2018). Larvicidal effectiveness of *Azolla pinnata* against *Aedes aegypti* (Diptera: Culicidae) with its effects on larval morphology and visualization of behavioural response. *Journal of Parasitology Research*, *2018*, 50783339. https://doi.org/10.1155/2018/1383186

Pertanika J. Trop. Agric. Sci. 46 (1): 277 - 313 (2023)

PERTANIKA JOURNALS

TROPICAL AGRICULTURAL SCIENCE

Journal homepage: http://www.pertanika.upm.edu.my/

Characterisation of the Putative Antigenic Genes of the Outer Membrane Proteins of *Pasteurella multocida* B:2 Strain PMTB2.1 through *in silico* Analysis

Tahera Hashimi[1,4,5], Deborah Joyce[1], Sufia Mohd Nasir[1], Mas Jaffri Masarudin[1,3], Annas Salleh[2] and Sarah Othman[1,3]*

[1]*Department of Cell and Molecular Biology, Faculty of Biotechnology and Biomolecular Sciences, Universiti Putra Malaysia, 43400 Serdang, Selangor, Malaysia*
[2]*Department of Veterinary Laboratory Diagnostics, Faculty of Veterinary Medicine, Universiti Putra Malaysia, 43400 Serdang, Selangor, Malaysia*
[3]*UPM-MAKNA Cancer Research Laboratory, Institute of Bioscience, Universiti Putra Malaysia, 43400 Serdang, Selangor Darul Ehsan, Malaysia*
[4]*Department of Biology, Faculty of Education, Ghor Institute of Higher Education, Chaghcharan 3201, Ghor, Afghanistan*
[5]*Department of Biomedical Science, City University of Hong Kong, Kowloon, Hong Kong, China*

ABSTRACT

Outer membrane proteins (OMPs), usually found in Gram-negative bacteria, have long been shown to elicit immune responses in infected hosts. This tendency of OMPs to generate immune reactions makes them ideal candidates for vaccine development against pathogenic bacteria. *Pasteurella multocida* is a Gram-negative pathogen responsible for the economically significant veterinary disease, hemorrhagic septicemia (HS). HS is an endemic and highly fatal disease affecting buffaloes and cattle. In Malaysia, outbreaks of this disease cost about half a million USD each year. Thus, despite current treatment and prevention measures, HS is a prevalent issue that needs to be overcome. *Pasteurella multocida* subsp. *multocida* PMTB2.1, a Malaysian strain of the pathogen, has recently had its entire genome sequenced after being isolated from HS outbreaks in the region. Antigenic OMPs from this strain have since been identified and published for further characterisation. LptD, Wza, and TbpA are integral membrane proteins, while Pal is a peripheral membrane protein that has not been characterised in-depth. This study, therefore, aims to analyse these OMPs through *in silico* methods. First,

ARTICLE INFO

Article history:
Received: 20 August 2022
Accepted: 16 November 2022
Published: 14 February 2023

DOI: https://doi.org/10.47836/pjtas.46.1.16

E-mail addresses:
tahera.hashimi53@gmail.com (Tahera Hashimi)
deborahjoyce98@gmail.com (Deborah Joyce)
sufia.mohdnasir@gmail.com (Sufia Mohd Nasir)
masjaffri@upm.edu.my (Mas Jaffri Masarudin)
annas@upm.edu.my (Annas Salleh)
sarahothman@upm.edu.my (Sarah Othman)
* Corresponding author

ISSN: 1511-3701
e-ISSN: 2231-8542

protein homology modelling was performed using SWISS-MODEL, whereafter, the structures generated were validated using the SWISS-MODEL structure assessment page, PROCHECK, ERRAT, and PROSA programs. The Pal, Wza, and TbpA structures were good models, while the LptD structure was found to be a near-good model based on the validation performed. Analyses using BCPREDS, NetMHCpan4.1, and NetBoLAIIpan1.0 revealed that these four OMPs could potentially elicit humoral and cellular immune responses.

Keywords: Antigenic OMPs, hemorrhagic septicemia, homology modelling, outer membrane proteins, *Pasteurella multocida*

INTRODUCTION

Pasteurella multocida is a Gram-negative pathogen from the Pasteurerellaceae family responsible for an economically significant veterinary disease, hemorrhagic septicemia (HS). HS is a highly fatal and chronic disease affecting animals, such as buffaloes and cattle in tropical regions. *Pasteurella multocida* strains are categorised into five serogroups (A, B, D, E, and F) and 16 serotypes based on lipopolysaccharide antigens (Peng et al., 2018). In Malaysia, the strain *P. multocida* subsp. *multocida* PMTB2.1 has been isolated from HS outbreaks in the region and had its complete genome sequenced as of late (Jabeen et al., 2017).

Pasteurella multocida expresses a range of virulence factors, including capsule, fimbriae, lipopolysaccharides (LPS), adhesion proteins, toxins, iron control, iron acquisition proteins, sialic acid synthesis, hyaluronidases, and OMPs (Peng et al., 2016).

Many vaccines have been developed and routinely used to prevent this acute disease. For example, bacterin, oil-adjuvant, and alum-precipitated vaccines were used in Asia to control the disease (Muenthaisong et al., 2020).

However, due to a high record of cattle and buffalo mortality resulting in a loss of nearly USD3.9 million, none of the above control techniques or live attenuated vaccines developed so far were completely effective (Rafidah et al., 2010). The failure and low vaccination coverage against the disease originated from several reasons, such as the high viscosity of the oil adjuvant vaccine that causes difficulties in injection and the variety of cattle management methods (Benkirane & De Alwis, 2002; Zamri-Saad & Annas, 2016). In Malaysia, a parental strain was isolated from an outbreak, and the mutant strain derived was labelled as *P. multocida* B:2 GDH7. This mutant was weakened by deleting a housekeeping gene, *gdhA*, from *P. multocida* B:2 wild type (Sarah et al., 2006).

Subunit vaccine has been suggested to be a potential candidate vaccine that is stable and safe compared to the others. Furthermore, a study by Rita et al. (2018) reported that production of a recombinant subunit vaccine had successfully cloned the ABA392 gene isolated from *P. multocida* B:2 into a protein expression vector. Consequently, the vaccine triggered an immune response against HS disease, thus, confirming its potential as a vaccine candidate for further studies.

Outer membrane proteins (OMPs) of *P. multocida* are one of the virulence factors in host animals to allow the bacteria to adapt to host niches. *Pasteurella multocida* OMPs are classified into structural proteins, transport proteins, binding proteins, adhesion, protein-assembly machinery, and membrane-associated enzymes based on their functional characteristics (Peng et al., 2019).

Joshi et al. (2013) demonstrated the immunoprotective efficacy of *P. multocida* OMPs in mouse models by proving the survival of OMP-vaccinated animals when exposed to live pathogenic bacteria. Prasannavadhana et al. (2014) used a proteomics approach to identify OMPs unique to the Indian strain of *P. multocida* serotype B:2, while Azam et al. (2020) used *in silico* methods to identify and assess the antigenicity of antigenic OMPs of the Malaysian isolate of *P. multocida* B:2. Among the 105 OMPs identified by Azam et al. (2020), 53 of them were found to be possibly antigenic. Individual OMPs of *P. multocida* have also been reported to play a function in activating an immunological response in several studies (Hatfaludi et al., 2012).

Bioinformatics tools assist researchers in finding possible proteins or genes associated with a pathogen's antigenic or virulence components (Azam et al., 2020). Bioinformatics analysis of protein localisation in bacteria is also crucial in understanding their structure and function, especially in disease development by the pathogen. Efforts to identify antigenic genes of *P. multocida* OMPs have been seen through *in silico* analysis to select potential vaccine targets for other strains, such as avian influenza (Al-Hasani et al., 2007). However, bioinformatics analysis reveals that the composition of the subproteome of *P. multocida* outer membrane (OM) is far from comprehensive. Further experimental efforts are needed to identify the complete complement of OMPs and to scribe a role to each protein. Several tools are now available that are fast, accurate, and easy to use, particularly for users with no previous experience in bioinformatics research (Hensen et al., 2012).

In the previous study by Azam et al. (2020) and this current study, these methods were used to predict some crucial antigenic genes of OMPs and to further characterise the potential OMPs by identifying subcellular localisation, predicting OM lipoproteins, and predicting barrel integral OMPs.

The availability of genome sequencing provides a new approach to the study of pathogens. More than 100 genome sequences are available for *P. multocida* B:2; however, extensive and complete genome sequence analysis is restricted. Based on this current study and Jabeen et al. (2019), the genome of *P. multocida* subsp. *multocida* strain PMTB2.1 (accession no. CP007205.2) contains 2,315,138 bp DNA, 2,176 genes, and 2,065 SDS coding genes, with more than 40 coding regions for iron homeostasis and 140 virulence genes, such as the complete tad locus. Among them, a few genomes, such as the PM70 strain (serotype F) (May et al., 2001), PM36950 (serotype A) (Peng et al., 2016), and the genomes of *P. multocida* strains harbouring the *P. multocida* toxin (PMT) gene have been studied and analysed (W. Liu et al., 2012).

The previous study by Azam et al. (2020) identified 105 OMPs of *P. multocida*

B:2 PMTB2.1, a Malaysian strain that includes 53 integral membrane proteins (IMPs) and 52 peripheral membrane proteins (PMPs). The finding of Azam et al. (2020) was elaborated in this work, primarily on the potential antigenic OMPs, Pal, Wza, TbpA, and LptD of the strain. The details are summarised in Table 1. The purpose of this study was to characterise the 3D model structure predictions further and to identify the antigenic epitopes of each OMP for future applications.

MATERIALS AND METHODS

Protein Sequence Retrieval

Pasteurella multocida subsp. *multocida* PMTB2.1 is a pathogenic *P. multocida* B:2 isolated from an outbreak in Malaysia from buffaloes, and the genomic DNA of the bacteria has been sequenced in the NCBI database (accession no. CP007205.2) (Jabeen et al., 2017).

The protein sequences of the OMPs from *P. multocida* subsp. *multocida* PMTB2.1 Malaysian strains were retrieved from National Center for Biotechnology Information (NCBI) website (https://www.ncbi.nlm.nih.gov/). The retrieved protein sequences were used in additional computer analysis to find the antigenic gene sequences for vaccine development or treatment. The nucleotide sequences of antigenic OMP genes, *pal*, *tbpA*, *wza*, and *lptD*, were retrieved and analysed from the genomic DNA of *P. multocida* B:2 subsp. *multocida* PMTB2.1 strain. The protein sequences of the antigenic OMP genes were used as input in the protein-protein basic local alignment search tool (blastp) (https://blast.ncbi.nlm.nih.gov/Blast.cgi). The results of blastp were used to determine the exact location of the antigenic genes.

The complete genome of *P. multocida* subsp. *multocida* strain PMTB2.1 was retrieved and then downloaded from NCBI (https://www.ncbi.nlm.nih.gov/). The complete genomic DNA file of *P. multocida* subsp. *multocida* strain PMTB2.1 downloaded earlier, was opened using SnapGene viewer 5.2.3 software. Then, the sequence IDs obtained earlier were used to obtain the gene sequences of the putative antigenic genes using SnapGene viewer 5.2.3 software.

Table 1
Characterisation of the four antigenic OMPs of the P. multocida *B:2 PMTB2.1 Malaysian strain that were retrieved through* in silico *study*

Protein group	Accession Number	Function	Length (amino acids)	Molecular weight (kDa)	Protein type
Membrane assembly-associated proteins	AMM81068.1	Peptidoglycan associated lipoprotein	150	16.2	Perpheral membrane protein
	AMM81201.1	Thiamine ABC transporter substrate-binding protein	334	37.9	Integral membrane protein
	AMM81019.1	Sugar transporter	387	42.2	Integral membrane protein
	AMM82596.1	LPS assembly protein LptD	782	90.6	Integral membrane protein

Note. The table was adapted and modified from Azam et al. (2020) and the current study

The sequences of the four putative antigenic genes were retrieved from *in silico* study, and the primers were designed for each gene according to their sequences. First, the genes were amplified through polymerase chain reaction (PCR) using the extracted genomic DNA of *P. multocida* B:2. Then, the amplified genes were ligated into pJET1.2 plasmid vector using the *Escherichia coli* TOP10 as host cells.

The *in vitro* sequencing results of the cloned OMP genes (*pal*, *tbpA*, *wza*, and *lptD* into pJET1.2 plasmid vector) and the nucleotide sequences obtained from NCBI GenBank (https://www.ncbi.nlm.nih.gov) were uploaded to Expasy Translate Tool (https://web.expasy.org/translate/) to obtain the open reading frames (ORFs) and corresponding amino acid sequences. In addition, the frame with the longest and continuous amino acid sequence was retrieved for downstream analyses.

3D Homology Structure Modelling

In this study, the SWISS-MODEL server available at https://swissmodel.expasy.org/ was used for the 3D structure modelling of query proteins. The amino acid sequences retrieved from the Expasy Translate Tool were used as input. It was followed by a template search against the SWISS-MODEL template library (SMTL) derived from the Protein Data Bank (PDB) (Biasini et al., 2014) using two database search methods: BLAST (Camacho et al., 2009) and HHblits (Remmert et al., 2012). BLAST is useful for closely related templates, while HHblits is employed for distant homology searches. First, the template with a global model quality estimate (GMQE) score closest to 1, with a sequence identity of more than 30%, and a numerically lower structure resolution was chosen for building optimal models. 'Build models' was selected after that. Next, models with quality model energy analysis (QMEAN) Z-score above -4 and closer to 0 were selected. An updated GMQE score was also weighed, and models with a score closest to 1 were selected. The comparison plot was also evaluated for a visual representation of the models' Z-score before choosing a suitable homology model. Models of choice for Pal, LptD, Wza, and TbpA were saved in PDB format for further analysis. The steps applied in homology modelling using SWISS-MODEL are summarised in Figure 1.

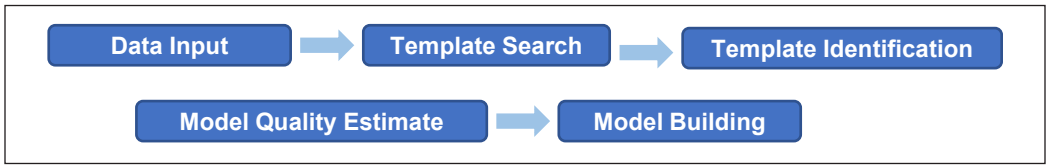

Figure 1. The general steps were taken to build 3D models of the outer membrance proteins in SWISS-MODEL. The target amino acid sequence inputs were provided in FASTA format. The input data served as a query sequence during the template search to identify evolutionary-related protein structures against the SWISS-MODEL template library. In template selection, the high reliability of a certain template is indicated by a high Global model quality estimate score that is expressed as a number between zero and one. Different models are built based on the templates selected. Following this, model building was continued with the generation of 3D models and model quality estimation using the Structure Assessment page of SWISS-MODEL

3D Homology Structure Validation

Evaluation of the 3D models were performed using several tools to determine their quality. Firstly, validation was performed using comparison plots and the local quality estimates available on the Structure Assessment page of the SWISS-MODEL server (https://swissmodel.expasy.org/). Following this, PROCHECK and ERRAT programs substantiated the model validation results. These programs are available in the SAVES 6.0 server, which is accessible at https://saves.mbi.ucla.edu/. The PROCHECK program makes a detailed scan of the stereochemistry of a protein structure, providing an assessment of the overall quality of the structure against highly refined structures of the same resolution (Laskowski et al., 1993). Meanwhile, the ERRAT program validates the model by the characteristic of atomic interactions and identifies the incorrect as well as the correct regions in a protein structure (Colovos & Yeates, 1993).

The ProSA server, which is available at https://prosa.services.came.sbg.ac.at/prosa.php, was then used to check the validity of the 3D structures. PDB files of the 3D structures were used as input data in all the servers mentioned above to verify the generated model. ProSA is a structure analysis program that displays scores and energy plots of local model quality for potential problems detected in protein structures. Global protein quality scores are displayed in the context of all known protein structures (Wiederstein & Sippl, 2007).

Protein Antigenicity Prediction and Comparison

Several parameters are important for predicting the immunogenicity of an antigen, such as flexibility, antigenicity, and solubility (Kim et al., 2013). The antigenicity of all OMPs was analysed by the ANTIGENpro server at http://scratch.proteomics.ics.uci.edu/. It is sequence-based, alignment-free, and pathogen-independent. A protein's antigenicity is predicted using protein antigenicity microarray data (Magnan et al., 2010). The input was provided in plain sequence format. Karplus Schulz's flexibility prediction method was used from the IEDB server (http://tools.iedb.org/bcell/) to determine the average flexibility of peptides within the OMPs. The flexible regions of the proteins are those shown above the threshold value of 1.0, following the method by Hasan et al. (2015). The SOLpro, which is available at http://scratch.proteomics.ics.uci.edu/, was used to predict the solubility of the OMPs and to report the solubility probabilities (above 0.5).

Epitope Prediction

B-cell epitopes were predicted using the B-cell epitope prediction server (BCPREDS), which is available at http://ailab-projects1.ist.psu.edu:8080/bcpred/predict.html. BCPREDS provides a selection of three prediction methods; the amino acid pairs (AAP) method (Chen et al., 2007), BCPred, and FBCPred (EL-Manzalawy et al., 2008b). The AAP method was chosen, and amino acid sequences were provided in plain text format, with epitope length set

to 12 and specificity set at default (75%) based on the method of Baliga et al. (2018). The program was also set to only report non-overlapping epitopes before submitting the query.

Prediction of major histocompatibility complex class I (MHC-I) T-cell epitopes and binding affinities were made using NetMHCpan 4.1 (Fisch et al., 2021), which is available at http://www.cbs.dtu.dk/services/NetMHCpan/. This server predicts the binding of peptides to MHC-I molecules of the known sequence using artificial neural networks (ANNs). The method is trained on quantitative binding affinity (BA) and mass-spectrometry eluted ligands (EL) peptides. The % rank threshold for strong binding peptides was set at 0.5, while the % rank threshold for weak binding peptides was set at 2. The peptide length selected was 9-mer, and the alleles chosen were BoLA-1:00901, BoLA-1:02301, BoLA-2:01201, BoLA-2:03001, BoLA-3:00101, and BoLA-3:00201. Input data was provided in FASTA format. Earlier findings reported that the vast majority (96.5%) of natural ligands are identified at a very high specificity (98.5%) using a percentile rank threshold of 2%. Input amino acid sequences are digested into 9-mer peptides. Research has shown that most presented MHC class I ligands are between 8-10 amino acids in length (Trolle et al., 2016). The BoLA alleles listed were also chosen as these were annotated in the IPD-MHC database (https://www.ebi.ac.uk/ipd/mhc/group/BoLA/).

Prediction of major histocompatibility complex class II (MHC-II) T-cell epitopes and binding affinities were made using the NetBoLAIIpan 1.0 server (http://www.cbs.dtu.dk/services/NetBoLAIIpan/) (Fisch et al., 2021). This server uses EL data derived from cell lines expressing a range of DRB3 alleles for model training. The % rank threshold for strong binding peptides was set at two, while the % rank threshold for weak binding peptides was set at 10. The peptide length selected was 13-mer, and all the alleles listed as BoLA-DRB3 alleles from mass spectrometry (MS) data were selected. Input amino acid sequences were digested into 13-mer peptides as research has shown that most presented MHC class II ligands are between 13–17 amino acids in length (Chang et al., 2006). Input data was provided in FASTA format, and additional configurations to display only the strongest binding core was selected alongside checking the 'Sort' output by prediction score option. The epitopes predicted by the BCPREDS, NetMHCpan 4.1, and NetBoLAIIpan 1.0 servers were manually combined to arrive at a consensus antigenic epitope sequence for each OMP.

RESULTS AND DISCUSSION

3D Homology Structure Modelling

Although X-ray crystallography or protein nuclear magnetic resonance spectroscopy (NMR) can be used to identify protein structures more precisely, these procedures are frequently time-consuming and expensive. In this sense, protein homology modelling using online servers and computer software can provide valuable models that help establish hypotheses about protein

function and drive additional experimental effort in the shortest time attainable while being cost-effective (Haddad et al., 2020). Such downstream applications include designing site-directed mutations through primer design and predictions of receptor-ligand binding for drug targeting (Sailapathi et al., 2020). Freely available sites for molecular docking are LightDock (Jiménez-García et al., 2018), MedusaDock 2.0 (Wang & Dokholyan, 2019), and LeDock (N. Liu & Xu, 2019).

Protein homology modelling generates 3D structures of proteins using a known experimental structure of a homologous protein as a template (Hasani & Barakat, 2016). 'Coverage' in templates quantifies the degree to which the template covers the target sequence. Although in most cases, achieving coverage of 100% is not possible, there is much to be inferred about a protein if the important domains are included within the template. As is observed with all the OMPs' models, none of the templates had 100% coverage. As such, other parameters were also taken into consideration. The number of amino acids perfectly matched between the target and template sequences is referred to as 'Identity.' Because the alignment of amino acids between the target and template sequences can be inferred, the higher the identity, the better the model. Because of the existence of a twilight zone, less than 30% of identities might be challenging to model. A homologous template backbone is no longer sufficient to regulate the exact assembly of protein side chains in this zone (Chung & Subbia, 1996). Thus, by default, the templates listed were filtered for those having an identity of 30% or above.

Models generated with the nearest GMQE score of 1 would indicate reliable templates (Biasini et al., 2014). This score estimates the model's quality given the target-template alignment and the template structure (Waterhouse et al., 2018). The models were also selected based on their QMEANDisCo global score, where a higher score is better as it shows the accuracy of local quality estimates (Waterhouse et al., 2018). High numeric values of 'resolution', such as 4 Å, mean poor resolution, while low numeric values, such as 1.5 Å, mean good resolution (Martz, 2014). For example, 2.05 Å is the PDB's median resolution for X-ray crystallographic results (Martz, 2014). Therefore, it is a crucial factor in modelling, as poor-resolution templates will give rise to poor-quality models. Details about the generated homology models are summarised in Table 2.

The Pal model in Figure 2A has a distinctly simpler structure compared to the LptD model in Figure 2B, owing to the shorter nucleotide sequence of *pal* and subsequently shorter amino acid sequence of Pal compared to that of LptD. The Pal model consists of four α-helices and four β-sheets linked by flexible loop regions, forming an α/β sandwich domain. This domain is characteristic of Pal proteins reported across the literature (Kumar et al., 2015; Mathelié-Guinlet et al., 2020). As for the LptD model, periplasmic and extracellular dimensions are obvious with the membrane annotations

Table 2
Details of P. multocida *PMTB2.1* outer membrance proteins*' homology models*

Outer membrane protein	Template SMTL ID	Coverage	Identity	GMQE	QMEAN DisCo Global	Resolution
Pal	4pwt.1	0.75	71.43	0.65	0.84	1.8 Å
TbpA	2qry.1	0.91	50.99	0.77	0.79	2.25 Å
Wza	2j58.1	0.86	56.46	0.75	0.78	2.25 Å
LptD	4q35.1	0.97	47.93	0.77	0.74	2.4 Å

Note. SMTL = SWISS-MODEL template library. A structural database produced from the Protein Data Bank comprises experimentally established protein structures. Global model quality estimate (GMQE) is a score between 0 and 1. A score closer to 1 is preferable. Qualitative model energy analysis distance constraint (QMEAN DisCo) global is a composite scoring function assessing the major geometrical aspects of protein structures

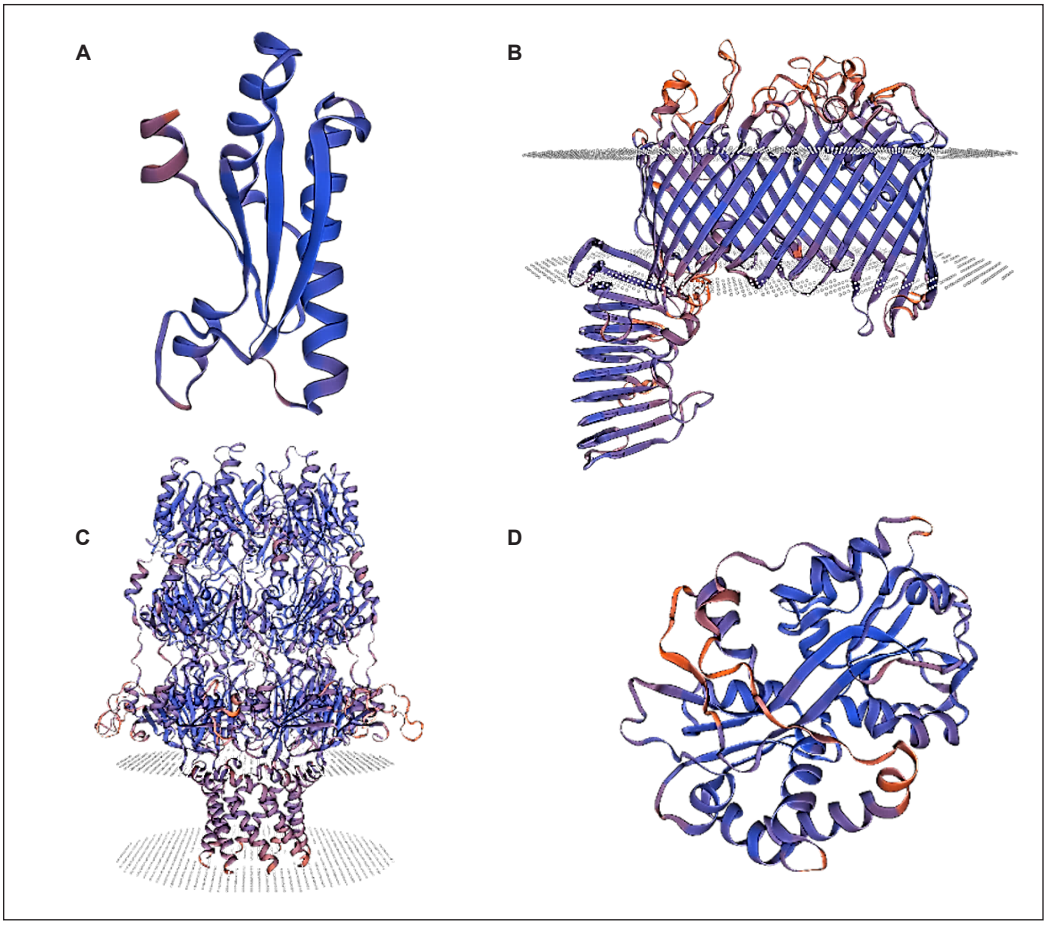

Figure 2. The 3D protein homology models of *Pasteurella multocida* PMTB2.1 outer membrance proteins. (A) 3D structure of Pal, (B) 3D structure of LptD, (C) 3D structure of Wza with membrane annotations transferred from the template, and (D) 3D structure of TbpA. The model colour scheme indicates regions of low confidence (red) and regions of high confidence (blue)

transferred from the template used. The modelled LptD structure was also observed to have a 26-stranded-β-barrel domain and a β-jellyroll domain consistent with LptD structures reported across literature (Qiao et al., 2014; Villa et al., 2013). SWISS-MODEL colour codes the modelled structures by indicating regions of low confidence in red and regions of high confidence in blue. It is visible in Figure 2B that the modelled LptD structure's loop regions on the extracellular dimension are mostly of low confidence and therefore coloured in red. It is because loop regions can be particularly difficult to model as sequences and structures might differ in these areas (Waterhouse et al., 2018). However, loop refinement or remodelling can be employed using other programs like the GalaxyLoop (Park et al., 2014), DaReUS-Loop (Karami et al., 2019), and MODELLER (Fiser & Šali, 2003).

Another region of homology models that can be hard to model is N-terminal tails (Waterhouse et al., 2018). Due to insufficient coverage between the template and target amino acid sequences (75% coverage, from residue 38 to 150), the N-terminal tail in the modelled Pal protein is found to be absent when compared to the template that was used to model the Pal protein (SMTL ID: 4pwt.1) and the structure of Pal protein reported by Mathelié-Guinlet et al. (2020). This N-terminal tail is, in fact, central to the role of the Pal protein. It functions to bind the Pal protein to the inner leaflet of the outer membrane (Cascales & Lloubès, 2004), while the C-terminal region of Pal interacts with the cell wall peptidoglycan (Lazzaroni & Portalier, 1992). Similarly, the LptD model's structure determines the protein's function. The β-barrel domain, along with the N-terminal β-jellyroll domain, forms a hydrophobic portal for the transport of lipopolysaccharide from the periplasm to the extracellular surface of the outer membrane (Botos et al., 2017). In brief, protein homology modelling can aid in characterising protein functions concerning their structures. It may direct predictions on how to regulate or modify proteins. However, limitations in this approach remain. These include the inability to predict sections of the sequence that do not align with the template sequence, as well as inaccuracies in modelling loop regions.

Wza is an inner membrane-lipoprotein (IM-lipoprotein) with the crystal structure of an octameric structure that is shaped like an amphora without its handles (Figure 2C) (Reid & Whitfield, 2005). Its transmembrane region is a novel α-helical barrel. The bulk of its structure is in the periplasm, which is also made up of three novel domains that create a large central cavity. It opens at a narrow 'neck' in the outer membrane towards the extracellular environment but is closed at its base at the periplasm (Dong et al., 2006). Wza's monomer structure comprises four domains. However, in ribbon format, Wza is an octameric structure made of four rings annotated as R1-R4 (Ford et al., 2009). Dong et al. (2006) mentioned the characteristics of each domain in Wza. Domain 1 comprises an anti-parallel β-sandwich with an α-helix at one edge representing a novel fold. Eight copies of Domain 1 would make up the Ring 1 structure at the bottom of Wza. Thus, Ring 1 has a centre filled with eight loops with a

concave surface at the base. The conserved polysaccharide biosynthesis/export (PES) motif is in Domain 1. Domain 2 shares a similar dimension to Domain 1 despite having a novel structure. An eightfold symmetric ring structure, Ring 2, is formed by eight copies of Domain 2. The domain comprises of central five-stranded mixed β-sheet with three α-helices. Domain 3 has a larger diameter than Domain 2 despite having the same structural duplication as Domain 2. N-terminus is located at the top of Ring 3. Hence, this indicates its location on Domain 3. Domain 4 is an amphipathic helix with a carboxy terminus of the monomers (Dong et al., 2006). An α-helical barrel was produced at the 'neck' of the structure due to the rotational symmetry of helices from eight monomers (Dong et al., 2006). Rings 1–3 are located inside the periplasmic (Kong et al., 2013), while Ring 4 has a C-terminus outside the cell (Dong et al., 2006). Ring 4 is a hydrophobic helical barrel, while Rings 1–3 consist of hydrophilic domains (Collins & Derrick, 2007; Ford et al., 2009).

According to a study by Soriano et al. (2008), the crystal structure of the thiamine-binding protein (TbpA) from *E. coli* in a complex with thiamine monophosphate (ThMP) was identified. Hence, it was referred to understand the crystal structure of TbpA from *P. multocida* in this study (Figure 2D). An adenosine triphosphate (ATP)-binding cassette (ABC) transporter in Gram-negative bacteria consists of periplasmic binding protein membrane permease and ATPase (Sippel et al., 2009). ABC transporters function by transporting ions and molecules into cells by utilising cellular energy (Jones & George, 2004), and in this case, it was used to take up the thiamine. Organisms used ABC transporters to take up thiamine. A study by Harper et al. (2006) mentioned that ABC transport protein is a predicted protein from the outer membrane of *P. multocida* A:3 strain P1059 that can stimulate cross-serotype protection (Rimler, 2001). TbpA structure consists of two domains with a flexible hinge region and a binding cleft between two domains (Soriano et al., 2008). Domain 1 consists of a three-layer αβα sandwich. The β layer has a five-stranded mix of β-sheet with a strand of the β-strand topology of ↑β2↑β1 ↑β3 ↓β9↑β4a. Meanwhile, for the α layer, five α-helices flanked the centre of the β-sheet with three helices below the β-sheet and two helices above it. Domain 2 also consists of a five-stranded mix of β-sheet with a strand of β-strand with a different topology compared to Domain 1, which is ↑β6↑β5 ↑β7↓β4b↑β8. Six and three α-helices flanked the above and below of the central β-sheet, respectively (Soriano et al., 2008). Jones and George (2004) stated that clarifying the mechanism and structure of ABC transporters is crucial to making pathways for rational protein design. Furthermore, it provides a guiding point for the proteins to be validated experimentally.

3D Homology Structure Validation

Determining the quality of a 3D protein homology model is a crucial step in understanding a model's utility and its potential downstream applications (Benkert et al., 2009).

Quality estimation was first done by analysing the local quality estimates of the generated 3D models. The local quality estimates in Figure 3 display sections of the models that are reliable and those that are not. The x-axis represents the residue number, while the y-axis represents predicted local similarity to the target. Red bars indicate residues of low confidence and low similarity between target and template residues, while blue bars are residues of high confidence that indicate high similarity between target and template residues, and therefore, high quality (Waterhouse et al., 2018) stretches below 0.6 hint towards regions of very low quality. Between the Pal (Figure 3A) and LptD models (Figure 3B), it can be observed that the LptD model has many more residues with stretches below the 0.6 threshold. It indicates that there are many erroneous regions in the LptD model. On closer inspection, it was noted that the stretches below 0.6 correspond to the loop regions of the LptD model, specifically from residues 260 to 737. This finding substantiates the observation made in the 3D protein homology model of LptD (Figure 2B), where the loop regions were also indicated in red. It was expected as loops are often the most vulnerable to model inaccuracies due to their increased variability in terms of sequence and structure when contrasted with the rest of the protein (Waterhouse et al., 2018). As for Wza and TbpA, the local quality estimates of the models are good, as most residues had scores close to 1. Wza (Figure 3C) and TbpA (Figure 3D) appear, with most residues between 0.8 and 0.9. Regions with low quality are indicated with residues that fall below 0.6. Wza shows a great number of residues in position 280-320 that falls below 0.6, while TbpA shows low-quality residues in regions 30-60, 180-210, and 210-250.

Further validation was performed with QMEAN, which relies on the database's context of all known experimental 3D structures by the scores representing energies (Haddad et al., 2020). These are shown in Figure 4. The comparison plots provide comparisons with a non-redundant set of PDB structures, a comparison to observe how well properties of known structures are represented in the model of interest. It consists of the x-axis representing the size of protein structures, the y-axis representing the normalised QMEAN4 scores of properties, and numerous dots, each representing one structure from the non-redundant set of PDB database structures. QMEAN4 refers to a version of the scoring system based solely on the statistical potentials of the four geometric aspects of the protein structure.

The red star represents the model of interest. The dark grey zone represents structures with a Z-score ranging from within one standard deviation of the mean in a normal distribution. Ideally, the star should be in the dark grey zone, indicating that the model behaves similarly to the experimentally determined PDB structure (Agrawal et al., 2013). Based on the comparison plots, the modelled structure of Pal (Figure 4A) ideally behaves as the star representing it is in the dark grey zone. It means that the modelled Pal structure has a QMEAN Z-score within one standard deviation of the mean in a

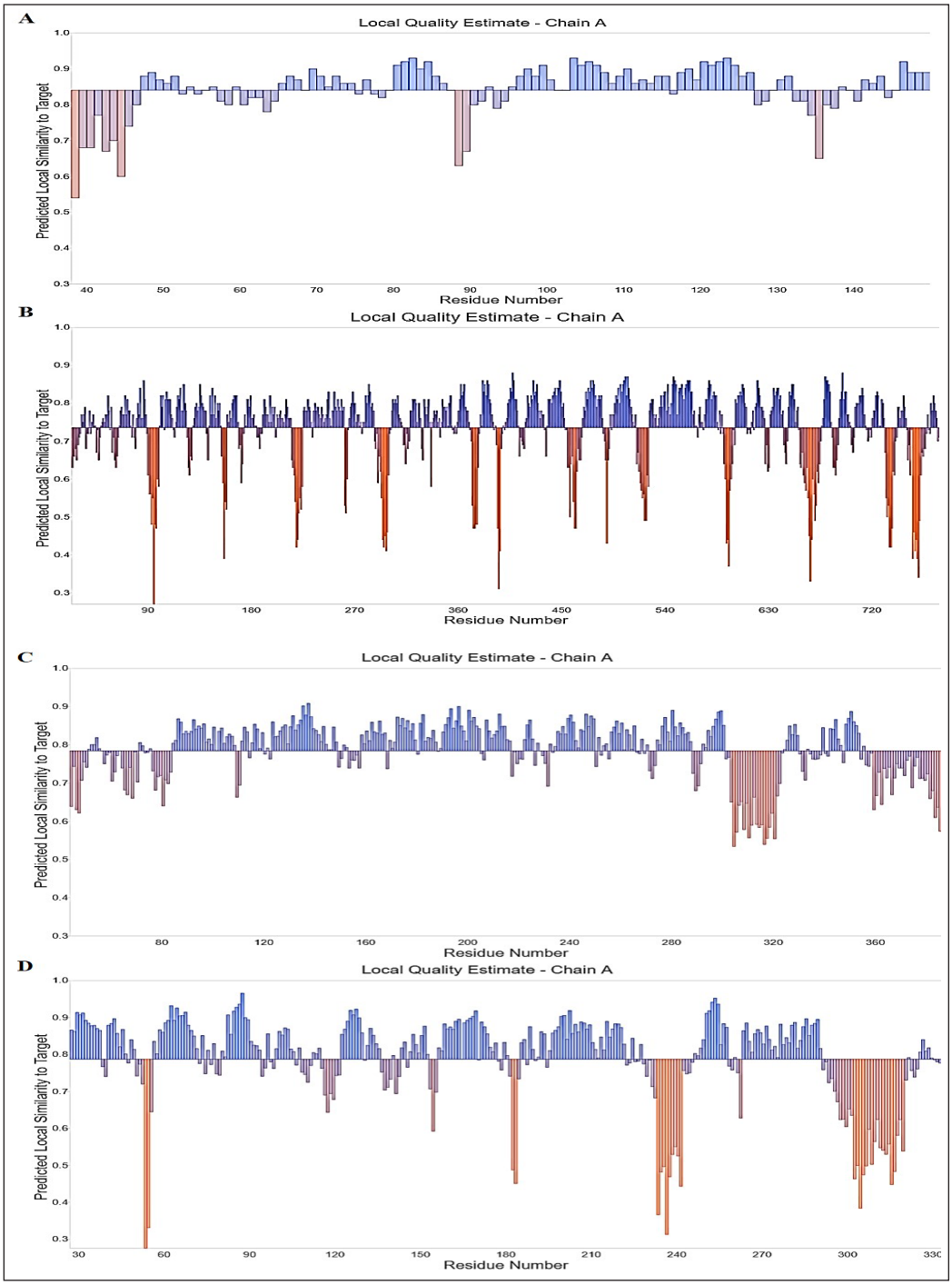

Figure 3. Local quality estimate of residues on modelled (A) Pal, (B) LptD, (C) Wza, and (D) TbpA structures. These were obtained from the Structure Assessment page of the SWISS-MODEL program. Low confidence residues are shown in red, while high confidence regions are displayed in blue. The threshold for the determination of very low-quality residues lies below 0.6 in predicted local similarity to target protein residues

normal distribution and, therefore, a higher "degree of nativeness" (Benkert et al., 2011) comparable to experimentally determined Pal structures of similar size in the PDB with a QMEAN Z-score of 0.15. In contrast, the LptD model (Figure 4B) is relatively not-ideal as the red star representing the model is located on the far right, with a QMEAN Z-score of -2.22, outside of the range of experimentally determined PDB structures. However, the LptD model is still acceptable as the QMEAN Z-score value is above -4.0 (Benkert et al., 2011). Meanwhile, Figure 4C shows that the Wza protein structure is reliable as it is within the range of other protein structures in PDB with a Z-score less than 1, -0.44. However, like LptD, the modelled TbpA protein structure lies outside the range of other structures in PDB (Figure 4D) with a Z-score of more than -2.63, indicating that the TbpA model is not ideal as well.

Validation was then continued with the PROCHECK program (Laskowski et al., 1993). PROCHECK validates the stereochemical quality and accuracy of the models and reports results as Ramachandran plots (Figure 5) that indicate residues in the favoured regions in red, allowed regions in yellow, generously allowed regions in light

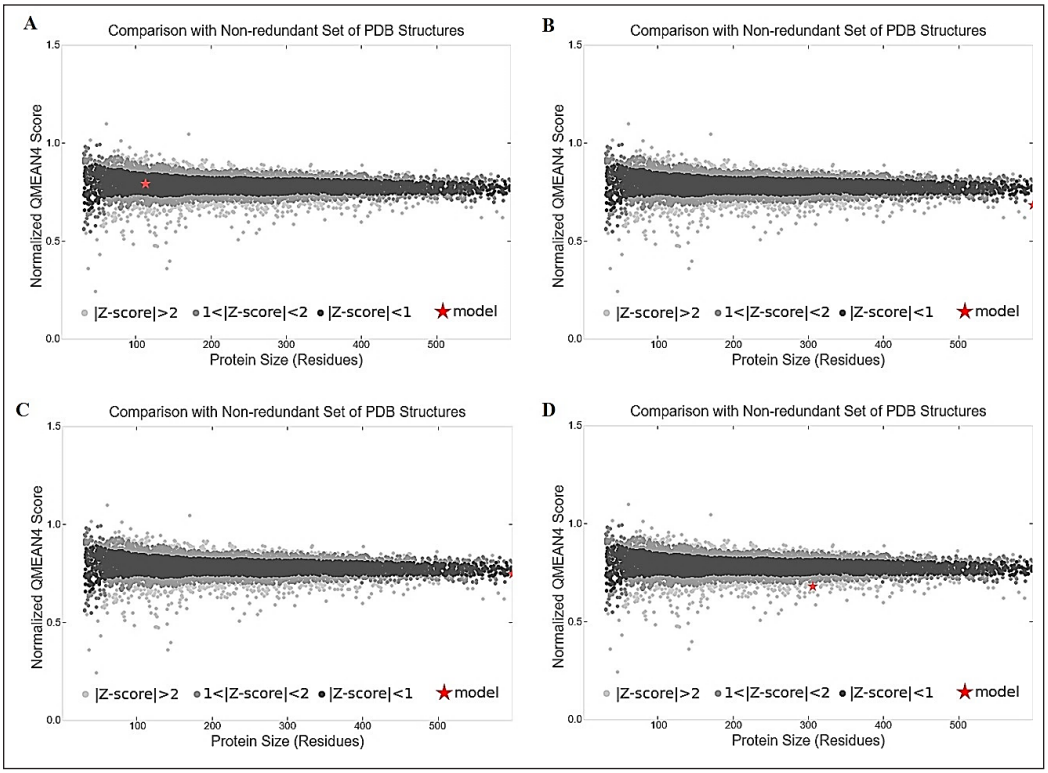

Figure 4. Comparison plot of the models represented by a red star (A) Pal, (B) LptD, (C) Wza, and (D) TbpA against a non-redundant set of Protein Data Bank structures (PDB). These were obtained from the Structure Assessment page of the SWISS-MODEL program. Each dot represents an individual protein crystal structure from the PDB database

yellow, and disallowed regions in white. In Figure 5, the red regions that determine the most favoured regions are marked as {A, B, L}. The additionally allowed regions are marked as {a, b, l, p} in yellow regions. Small black squares represent proline and non-glycine residues, while black triangles are glycine- residues (non-end). Disallowed residues are shown as red squares. In Ramachandran plot analyses, the percentage of residues in the most favoured regions must be more than 90% to ensure the reliability of the predicted structure. Meanwhile, G-factors measure how unusual the property is, with values below -0.5 and below -1.0 highly unusual.

The Ramachandran plot analyses indicate that the Pal model (Figure 5A) is a good model with more than 90% of its residues in the favoured region, while the LptD model (Figure 5B) is a near-good model with 88.7% residues in the favoured region (Prajapat et al., 2014). Both models are also observed to have an overall G-factor

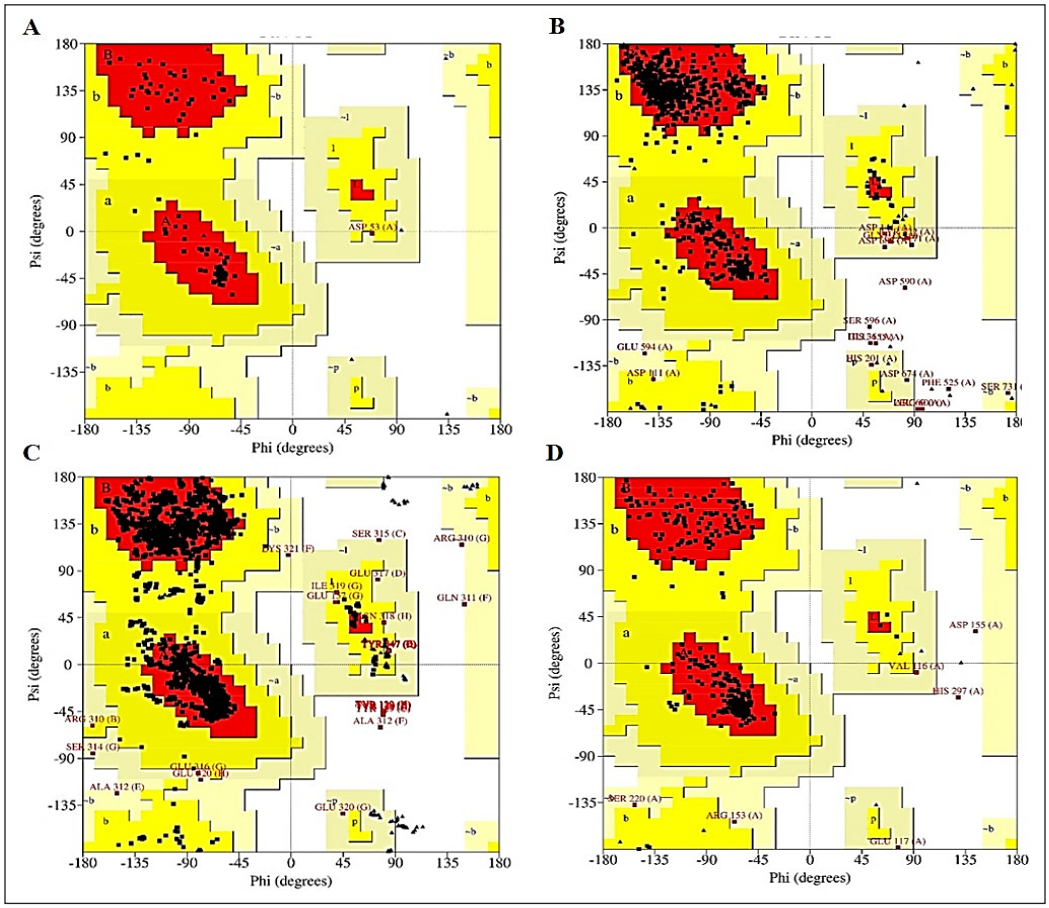

Figure 5. Main Ramachandran plot of the PROCHECK program for modelled (A) Pal, (B) LptD, (C) Wza, and (D) TbpA structures. Residues are indicated in favoured regions which are shown in red (represented by A, B, L), allowed regions in yellow (represented by a, b, l, p), generously allowed regions in light yellow (represented by ~a, ~b, ~l, ~p) and disallowed regions in white

of more than -0.5, indicating that they are reliable (Ramachandran et al., 1963). Similar to the LptD model, the Ramachandran plots for modelled Wza (Figure 5C) and TbpA (Figure 5D) did not record more than 90% of residues in the most favoured regions. Instead, the percentage of residues in the most favoured regions for Wza and TbpA is 89.5% and 89.9%, respectively. Thus, they are near-good quality models. Although both models did not exceed the 90% score in most favoured regions, they are still valid as the residues in disallowed regions are merely 0.5% and 0.7% (Prajapat et al., 2014). Hence, this represents only a slight steric hindrance between the model's side-chain C-beta methylene group and main-chain atoms. The overall G-factor for the Wza and TbpA structures are -0.08 and -0.17, respectively. Therefore, each modelled structure is acceptable as both scores are greater than the G-factor threshold value of -0.5. Data regarding the percentage residues in each region and overall G-factors have been summarised in (Table 3).

Quality estimation was done using the ERRAT server, where the overall quality factor for good high-resolution structures lies above 95%, while low resolutions have values of around 91% (Colovos & Yeates, 1993). Overall ERRAT quality factor values are expressed as the percentage of the proteins for which the calculated value falls below the 95% rejection limit. The quality factor values for Pal and LptD models were 100% and 91.3%, respectively (Figures 6A and 6B). It was established earlier that high-resolution structures generally produce values around 95% or higher (Colovos & Yeates,1993). Hence, the Pal model gets a maximum score as it was modelled after a high-resolution template (1.8 Å). On the other hand, the low ERRAT quality factor value for the LptD model is expected owing to its lower resolution template (2.4 Å). The Wza and TbpA were modelled after templates with a resolution of 2.25 Å. The overall quality factor of the Wza and TbpA models showed a score of 94.537 and 85.619, respectively, as shown in Figures 6C and 6D, respectively. It indicates that Wza has a good quality factor while TbpA might be considered near good as it is near 91%. Furthermore, the OMPs only had several regions that exceeded the error values of 95 and 99%. Thus, indicating that most residues are acceptable.

Lastly, ProSA was used to provide energy plots that can highlight potential errors in protein structures. The plots in

Table 3
Result summary of the Ramachandran plots from PROCHECK

Outer membrane protein	Residues in the favoured region (%)	Residues in the additionally allowed region (%)	Residues in the generously allowed region (%)	Residues in the disallowed region (%)	Overall G-factor
Pal	91.9	7.1	1.0	0.0	-0.02
LptD	88.7	8.7	1.5	1.0	-0.16
Wza	89.5	9.2	0.8	0.5	-0.08
TbpA	87.5	10.8	1.1	0.7	-0.17

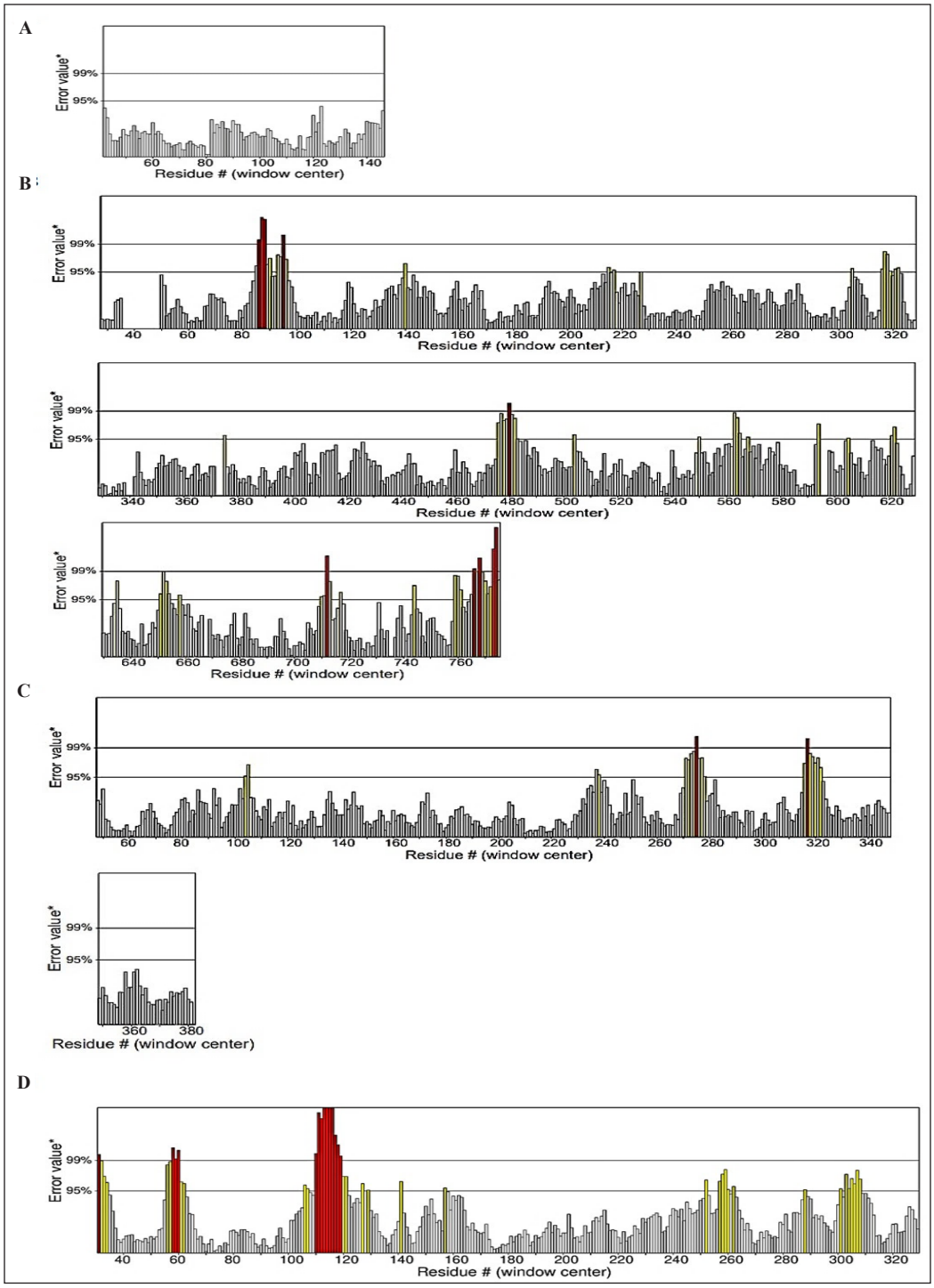

Figure 6. The ERRAT program evaluated the overall quality of the model. (A) Pal model, (B) LptD model, (C) Wza model, and (D) TbpA model. On the error axis, the two lines (95% and 99%) indicate the confidence with which it is possible to reject regions that exceed that error value

Figure 7 represent data obtained from the PDB regarding protein chains' scores discovered experimentally (Berman et al., 2002). All the plots were determined by X-ray crystallography (light blue) or NMR spectrophotometry (dark blue) about individual protein lengths (Agrawal et al., 2013). The inaccuracies of the models generated can be determined by the analysis of Z-scores being outside of the range of scores characteristic of native proteins. Analysing the position of the target protein (represented as black dots) in the Z-score plot could indicate whether the protein is in the typical range of scores as other proteins of similar length in PDB. The Z-score of the model presents the overall model quality.

The Z-score for the Pal model (−5.43) (Figure 7A) was within the range of scores typically found for the native proteins of similar size, while this was hardly the case for the LptD model (- 4.27) (Figure 7B). Figures 7C and 7D show the positioning according to individual Z- scores for Wza

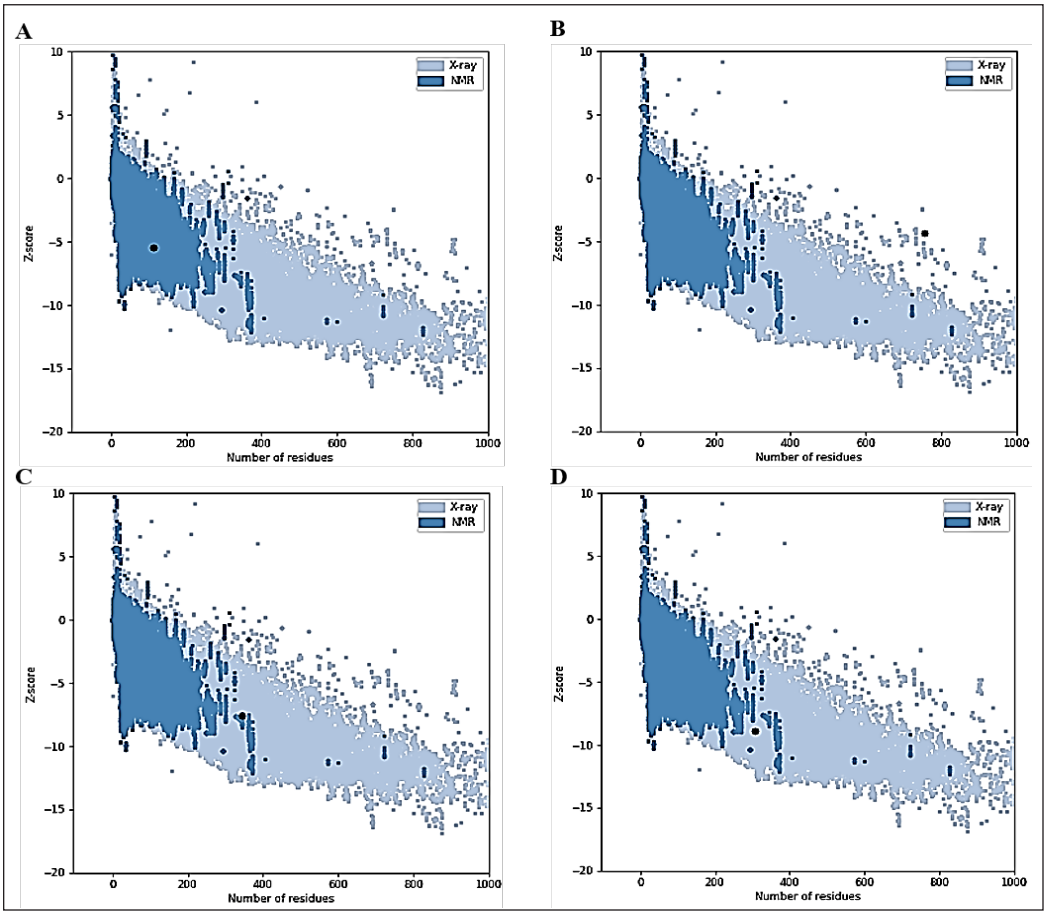

Figure 7. ProSA output of Z-scores for homology models using the ProSA-web server. (A) Pal model, (B) LptD model, (C) Wza model, and (D) TbpA model. The models are represented as black dots in the plot. These plots are used to identify whether the Z-score of protein is within the range with the typical range of scores for experimentally determined proteins of similar sizes

and TbpA with Z-score values of -7.57 and -8.85, respectively. The ProSA outputs indicate that the homology models for Pal, Wza, and TbpA are within the range of native protein conformations. It means that the 3D homology structures of Pal, Wza, and TbpA are highly reliable structures that are well within the range of scores typically found for proteins of similar size.

The plot of residue scores or energy plots provides local model quality by using knowledge-based energy to plot amino acid sequence position (Agrawal et al., 2013), where positive values correspond to problematic or erroneous parts of the input structure. This plot revealed that most of the calculated values were negative for Pal (Figure 8A), while a fair number of LptD residues had negative and positive scores (Figure 8B). It implies that there are many erroneous regions in the LptD model. The Wza model in the energy plot (Figure

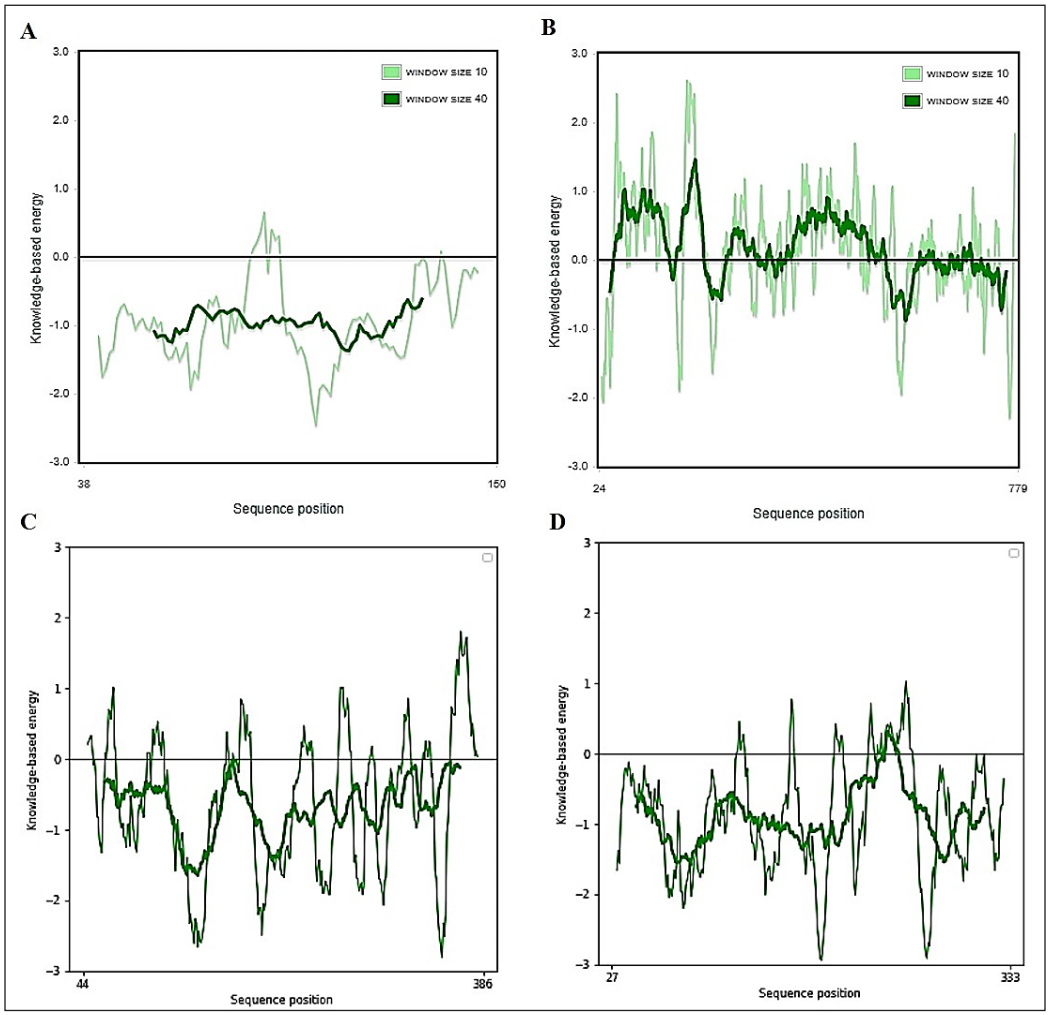

Figure 8. Plot of residue energies for (A) Pal model, (B) LptD model, (C) Wza model, and (D) TbpA model. Dark green and light green lines distinguish window sizes of 40 and 10 residues, respectively

8C) shows that all residues are positioned within the negative quadrant. It implies that the model has good energy stability. Meanwhile, the TbpA model (Figure 8D) shows that some residues are in the positive quadrant but still near zero, indicating that it has average energy stability (Bhattacharya et al., 2020).

Protein Antigenicity Prediction and Comparison

ANTIGENPro provides an accuracy of up to 82%, which surpasses other antigenicity predictors (Magnan et al., 2010). In addition, antigenic proteins in other pathogens were detected by this program (Chin et al., 2014; Magnan et al., 2010). ANTIGENpro server scores 0.816380 for Pal, 0.900650 for LptD, 0.779916 for Wza, and 0.804137 for TbpA. It shows that all proteins scored well above the minimum threshold of 0.7, indicating that they are all antigenic (Magnan et al., 2010) (Table 4). It substantiates the findings from Azam et al. (2020), whose study classified these four OMPs as antigenic following the results obtained from the Vaxijen v2.0 server (Doytchinova & Flower, 2007).

Solubility is crucial for maintaining the homeostasis of proteins. Identifying the solubility of a protein could give access to its conformation, concentration, and quaternary structure (Balch et al., 2008). Furthermore, maintaining a protein's function and preventing its aggregation requires solubility (Ciryam et al., 2013). Studies on structural and functional proteomics also require protein to be soluble (Chan et al., 2010). Therefore, identifying a protein's solubility is important for immunogenicity prediction. In Table 5, it was identified that Wza and LptD proteins are insoluble. Hence, they are not appropriate for the downstream analysis of the immunogenicity effect (Rahman et al., 2020). Meanwhile, Pal and TbpA are considered soluble. Hence, proving it to be suitable as a vaccine candidate for further analysis in the future. On the other hand, the area of a peptide that interacts with the antibody tends to be flexible, according to experimental findings (Hasan et al., 2015). The Karplus Schulz flexibility prediction program found the query protein's flexible regions in the IEDB server. As reported in Table 5, the OMP Pal recorded a flexibility score of 0.997, while the OMP TbpA scored 0.992. Between the two soluble OMPs,

Table 4
Antigenicity scores of outer membrane proteins derived from the ANTIGENpro server

Outer membrane proteins	Probable antigenicity	Prediction score
Pal	Antigen	0.816380
LptD	Antigen	0.900650
Wza	Antigen	0.779916
TbpA	Antigen	0.804137

Table 5
Flexibility and solubility of the OMPs, Pal, LptD, Wza, and TbpA

Outer membrane proteins	Flexibility (IEDB)	Solubility (SOLpro)
Pal	0.997	SOLUBLE with 0.762434
LptD	1.001	INSOLUBLE with 0.745939
Wza	0.996	INSOLUBLE with 0.700107
TbpA	0.992	SOLUBLE with 0.934680

Pal showed a higher flexibility score and is therefore considered relatively more immunogenic than the other OMPs reported in this study.

Epitope Prediction

T-cell or B-cell, epitope-based therapeutic and diagnostic rational design for pathogens, has long since been reported (Arévalo-Herrera et al., 2002; Sollner et al., 2008). Regarding T-cell epitopes, activation of both $CD4^+$ (MHC-II) and $CD8^+$ (MHC-I) T-cells are vital in many cases of infections (Jenkins et al., 2003). Therefore, in developing peptide-based vaccines, OMPs epitopes that elicit both the B-cell and T-cell (MHC-I and MHC-II) mediated immunities are the most advantageous (Bhattacharya et al., 2020).

B-cells are critical in the immune system's battle against invading pathogenic organisms because they secrete antibodies against antigens. A linear or continuous B-cell epitope is a sequence segment of a protein. Presently, the bulk of existing epitope prediction algorithms focuses on continuous epitopes due to the ease with which the amino acid sequence of a protein may be used as an input. These prediction approaches are based on the hydrophilicity, solvent accessibility, secondary structure, flexibility, and antigenicity of amino acids (Shen et al., 2015).

BCPred online server was used in predicting linear B-cell epitopes of the OMPs from their respective amino acid sequences. BCPred provides two algorithms for identifying an epitope's fixed lengths, which are BCPred and amino acid pair (AAP) (EL-Manzalawy et al., 2008a). The AAP technique is based on discovering that B-cell epitopes prefer some AAPs. The AAP technique outperformed conventional scales based on single amino acid propensity (Chen et al., 2007). The epitope length chosen for our study is 12 amino acids, which were motivated by previous work (Baliga et al., 2018). B-cell epitopes of lengths between 12 to 15 were shown to be potent inducers of the production of antibodies (EL-Manzalawy et al., 2008a). B-cell epitope prediction using the AAP method within the amino acid sequences of individual OMPs is summarised in (Supplementary material 1).

Identifying the shortest peptide in an antigen that triggers $CD4^+$ or $CD8^+$ T-cell mediated immunity is the objective in T-cell epitope prediction. In assays, immunogenicity was achieved using synthetic peptides derived from antigen that triggers T-cells (Ahmad et al., 2016). MHC aids in activating the adaptive immune response. MHC genes present peptide fragments from pathogens to T- cells to elicit an immune response. Therefore, the ability of the T-cell epitope region in antigenic proteins to bind to MHCs is essential in vaccine development (Patronov & Doytchinova, 2013). Epitope binding to MHC-I and MHC-II differs in length. For MHC-I binding prediction, input amino acid sequences were digested into 9-mer peptides, as research has shown that most presented MHC class I ligands are between 8 to 10 amino acids in length (Trolle et al., 2016). Meanwhile, the MHC-II binding epitope would be in the range of 13 to 17

amino acids in length (Chang et al., 2006). Considering the optimal epitope lengths for recognition and binding with B- cells and T-cells, antigenic sequences found to be recognised by B-cells and those with high binding affinities for MHC-I and MHC-II make for an effective epitope vaccine (Naz et al., 2015).

Based on data summarised in (Supplementary material 2), some peptide sequences of MHC-I and MHC-II can bind to more than one allele and have a part of a similar sequence to B-cell epitope prediction. Thus, a consensus antigenic sequence was obtained for each OMP by combining similar sequences found to be recognised by B-cells and those with high binding affinities for MHC-I and MHC-II. These sequences have been summarised in Table 6.

Table 6
B-cell, MHC-I, and MHC-II recognition sites within the amino acid sequences of Pal, LptD, Wza, and TbpA

OMP	Antigenic sequence	Amino acid position	Recognised by
Pal	LQQRYNTVY	41-49	B-cell
			MHC-I: BoLA-1:00901
			MHC-II: BoLA-DRB3_1001
LptD	ALFDSPLNF	393-401	B-cell
			MHC-I: BoLA-1:00901
			MHC-II: BoLA-DRB3_1001
			MHC-II: BoLA-DRB3_1201
Wza	LLVDGDIVH	631-657	B-cell
			MHC-I: BoLA-1:00901
TbpA	EPHFDALKATQM	287-322	B-cell
			MHC-II: BoLA-DRB3_2002
	KTKVQQPPK	770-796	B-cell
			MHC-I: BoLA-2:01201
	TQAVNVYTY	1,109-1,135	B-cell
			MHC-I: BoLA-1:00901
			MHC-I: BoLA-1:02301

CONCLUSION

The *in silico* generated 3D structures of Pal, Wza, and TbpA are considered good models, while the 3D structure of LptD is a near-good model. Good quality models are imperative as these are required for downstream applications, including protein function prediction, site-directed mutations, and ligand docking modelling in drug discovery. This study has also laid out the consensus epitope sequences within the OMPs that could elicit both humoral and cellular immune responses using bioinformatics approaches. Further *in silico* work can be directed towards molecular docking analysis between the identified epitopes and immunological elements to study the specific interactions involved.

Future investigations in validating B-cell and T-cell immunogenicity of the identified antigenic epitopes can be attempted through *in vitro* and *in vivo* means to prepare epitope or peptide-based vaccines against *P. multocida* infections.

ACKNOWLEDGMENTS

Universiti Putra Malaysia supported this research through the UPM Putra Research Grants, GP/2017/9560000 and GP/2017/9559200. The Higher Education Development Program (HEDP)-Afghanistan supported Tahera Hashimi.

REFERENCES

Agrawal, P., Thakur, Z., & Kulharia, M. (2013). Homology modelling and structural validation of tissue factor pathway inhibitor. *Bioinformation*, *9*(16), 808-812. https://doi.org/10.6026/97320630009808

Ahmad, T. A., Eweida, A. E., & El-Sayed, L. H. (2016). T-cell epitope mapping for the design of powerful vaccines. *Vaccine Reports*, *6*, 13-22. https://doi.org/10.1016/j.vacrep.2016.07.002

Al-Hasani, K., Boyce, J., McCarl, V. P., Bottomley, S., Wilkie, I., & Adler, B. (2007). Identification of novel immunogens in *Pasteurella multocida*. *Microbial Cell Factories*, *6*, 3. https://doi.org/10.1186/1475-2859-6-3

Arévalo-Herrera, M., Valencia, A. Z., Vergara, J., Bonelo, A., Fleischhauer, K., González, J. M., Restrepo, J. C., López, J. A., Valmori, D., Corradin, G., & Herrera, S. (2002). Identification of HLA-A2 restricted $CD8^+$ T-lymphocyte responses to *Plasmodium vivax* circumsporozoite protein in individuals naturally exposed to malaria. *Parasite Immunology*, *24*(3), 161-169. https://doi.org/10.1046/j.1365-3024.2002.00449.x

Azam, F. M., Zamri-Saad, M., Rahim, R. A., Chumnanpoend, P., E-kobon, T., & Othman, S. (2020). Antigenic outer membrane proteins prediction of *Pasteurella multocida* serotype B:2. *Asia-Pacific Journal of Molecular Biology and Biotechnology*, *28*(4), 102-116. https://doi.org/10.35118/apjmbb.2020.028.4.09

Balch, W. E., Morimoto, R. I., Dillin, A., & Kelly, J. W. (2008). Adapting proteostasis for disease intervention. *Science*, *319*(5865), 916–919. https://doi.org/10.1126/science.1141448

Baliga, P., Shekar, M., & Venugopal, M. N. (2018). Potential outer membrane protein candidates for vaccine development against the pathogen *Vibrio anguillarum*: A reverse vaccinology based identification. *Current Microbiology*, *75*(3), 368-377. https://doi.org/10.1007/s00284-017-1390-z

Benkert, P., Biasini, M., & Schwede, T. (2011). Toward the estimation of the absolute quality of individual protein structure models. *Bioinformatics*, *27*(3), 343-350. https://doi.org/10.1093/bioinformatics/btq662

Benkert, P., Künzli, M., & Schwede, T. (2009). QMEAN server for protein model quality estimation. *Nucleic Acids Research*, *37*(suppl_2), W510-W514. https://doi.org/10.1093/nar/gkp322

Benkirane, A., & De Alwis, M. C. L. (2002). Haemorrhagic septicaemia, its significance, prevention and control in Asia. *Veterinary Medicine Journal*, *47*(8), 234-240. https://doi.org/10.17221/5830-VETMED

Berman, H. M., Battistuz, T., Bhat, T. N., Bluhm, W. F., Bourne, P. E., Burkhardt, K., Feng, Z., Gilliland, G. L., Iype, L., Jain, S., Fagan, P., Marvin, J., Padilla, D., Ravichandran, V., Schneider, B., Thanki, N., Weissig, H., Westbrook, J. D., & Zardecki, C. (2002). The protein data bank. *Acta Crystallographica Section D: Biological Crystallography*, *58*(6), 899-907. https://doi.org/10.1107/S0907444902003451

Bhattacharya, M., Sharma, A. R., Sharma, G., Patra, P., Mondal, N., Patra, B. C., Lee, S.-S., & Chakraborty, C. (2020). Computer aided novel antigenic epitopes selection from the outer membrane protein sequences of *Aeromonas hydrophila* and its analyses. *Infection, Genetics and Evolution*, *82*, 104320. https://doi.org/10.1016/j.meegid.2020.104320

Biasini, M., Bienert, S., Waterhouse, A., Arnold, K., Studer, G., Schmidt, T., Kiefer, F., Cassarino, T. G., Bertoni, M., Bordoli, L., & Schwede, T. (2014). SWISS-MODEL: Modelling protein tertiary and quaternary structure using evolutionary information. *Nucleic Acids Research*, *42*(W1), W252-W258. https://doi.org/10.1093/nar/gku340

Botos, I., Noinaj, N., & Buchanan, S. K. (2017). Insertion of proteins and lipopolysaccharide into the bacterial outer membrane. *Philosophical Transactions of the Royal Society B: Biological Sciences*, *372*(1726), 20160224. https://doi.org/10.1098/rstb.2016.0224

Camacho, C., Coulouris, G., Avagyan, V., Ma, N., Papadopoulos, J., Bealer, K., & Madden, T. L. (2009). BLAST^{+}: Architecture and applications. *BMC Bioinformatics*, *10*, 421. https://doi.org/10.1186/1471-2105-10-421

Cascales, E., & Lloubès, R. (2004). Deletion analyses of the peptidoglycan-associated lipoprotein Pal reveals three independent binding sequences including a TolA box. *Molecular Microbiology*, *51*(3), 873-885. https://doi.org/10.1046/j.1365-2958.2003.03881.x

Chan, W. C., Liang, P. H., Shih, Y. P., Yang, U. C., Lin, W. C., & Hsu, C. N. (2010). Learning to predict expression efficacy of vectors in recombinant protein production. *BMC Bioinformatics*, *11*(Suppl 1), S21. https://doi.org/10.1186/1471-2105-11-S1-S21

Chang, S. T., Ghosh, D., Kirschner, D. E., & Linderman, J. J. (2006). Peptide length-based prediction of peptide–MHC class II binding. *Bioinformatics*, *22*(22), 2761-2767. https://doi.org/10.1093/bioinformatics/btl479

Chen, J., Liu, H., Yang, J., & Chou, K. C. (2007). Prediction of linear B-cell epitopes using amino acid pair antigenicity scale. *Amino Acids*, *33*(3), 423-428. https://doi.org/10.1007/s00726-006-0485-9

Chin, C. F., Teh, B. A., Anthony, A. A., Aziah, I., Ismail, A., Ong, E. B. B., & Lim, T. S. (2014). Overexpression, purification and validation of antigenic *Salmonella enterica* serovar Typhi proteins identified from LC-MS/MS. *Applied Biochemistry and Biotechnology*, *174*, 1897-1906. https://doi.org/10.1007/s12010-014-1173-y

Chung, S. Y., & Subbiah, S. (1996). A structural explanation for the twilight zone of protein sequence homology. *Structure*, *4*(10), 1123-1127. https://doi.org/10.1016/S0969-2126(96)00119-0

Ciryam, P., Tartaglia, G. G., Morimoto, R. I., Dobson, C. M., & Vendruscolo, M. (2013). Neurodegenerative diseases and widespread aggregation are associated with supersaturated proteins. *Cell Reports*, *5*(3), 781-790. https://doi.org/10.1016/j.celrep.2013.09.043 PMID: 24183671

Collins, R. F., & Derrick, J. P. (2007). Wza: A new structural paradigm for outer membrane secretory proteins?. *Trends in Microbiology*, *15*(3), 96-100. https://doi.org/10.1016/j.tim.2007.01.002

Colovos, C., & Yeates, T. (1993). ERRAT: An empirical atom-based method for validating protein structures. *Protein Science*, *2*(9), 1511-1519. https://doi.org/10.1002/pro.5560020916

Dong, C., Beis, K., Nesper, J., Brunkan-LaMontagne, A. L., Clarke, B. R., Whitfield, C., & Naismith, J. H. (2006). Wza the translocon for *E. coli* capsular polysaccharides defines a new class of membrane protein. *Nature*, *444*(7116), 226-229. https://doi.org/10.1038/nature05267

Doytchinova, I. A., & Flower, D. R. (2007). VaxiJen: A server for prediction of protective antigens, tumour antigens and subunit vaccines. *BMC Bioinformatics*, *8*, 4. https://doi.org/10.1186/1471-2105-8-4

EL-Manzalawy, Y., Dobbs, D., & Honavar, V. (2008a). Predicting linear B-cell epitopes using string kernels. *Journal of Molecular Recognition*, *21*(4), 243-255. https://doi.org/10.1002/jmr.893

EL-Manzalawy, Dobbs, D., & Honavar, V. (2008b). Predicting flexible length linear B-cell epitopes. *Computational Systems Bioinformatics*, *7*, 121-132. https://doi.org/10.1142/9781848162648_0011

Fisch, A., Reynisson, B., Benedictus, L., Nicastri, A., Vasoya, D., Morrison, I., Buus, S., Ferreira, B. R., de Miranda Santos, I. K. F., Ternette, N., Connelley, T., & Nielsen, M. (2021). Integral use of immunopeptidomics and immunoinformatics for the characterization of antigen presentation and rational identification of BoLA-DR–presented peptides and epitopes. *Journal of Immunology*, *206*(10), 2489-2497. https://doi.org/10.4049/jimmunol.2001409

Fiser, A., & Šali, A. (2003). Modeller: Generation and refinement of homology-based protein structure models. *Methods in Enzymology*, *374*, 461-491. https://doi.org/10.1016/S0076-6879(03)74020-8

Ford, R. C., Brunkan-LaMontagne, A. L., Collins, R. F., Clarke, B. R., Harris, R., Naismith, J. H., & Whitfield, C. (2009). Structure–function relationships of the outer membrane translocon Wza investigated by cryo-electron microscopy and mutagenesis. *Journal of Structural Biology*, *166*(2), 172-182. https://doi.org/10.1016/j.jsb.2009.02.005

Haddad, Y., Adam, V., & Heger, Z. (2020). Ten quick tips for homology modeling of high- resolution protein 3D structures. *PLOS Computational Biology*, *16*(4), e1007449. https://doi.org/10.1371/JOURNAL.PCBI.1007449

Harper, M., Boyce, J. D., & Adler, B. (2006). *Pasteurella multocida* pathogenesis: 125 years after pasteur. *FEMS Microbiology Letters*, *265*(1), 1–10. https://doi.org/10.1111/j.1574-6968.2006.00442.x

Hasan, M. A., Khan, M. A., Datta, A., Mazumder, M. H. H., & Hossain, M. U. (2015). A comprehensive immunoinformatics and target site study revealed the corner-stone toward Chikungunya virus treatment. *Molecular Immunology*, *65*(1), 189-204. https://doi.org/10.1016/j.molimm.2014.12.013

Hasani, H. J., & Barakat, K. H. (2016). Protein-protein docking: Are we there yet?. In *Methods and algorithms for molecular docking-based drug design and discovery* (pp. 173-195). IGI Global. https://doi.org/10.4018/978-1-5225-0115-2.ch007

Hatfaludi, T., Al-Hasani, K., Gong, L., Boyce, J. D., Ford, M., Wilkie, I. W., Quinsey, N., Dunstone, M. A. Hoke, D. E., & Adler, B. (2012). Screening of 71 *P. multocida* proteins for protective efficacy in a fowl cholera infection model and characterization of the protective antigen PlpE. *PLOS One*, *7*(7), e39973. https://doi.org/10.1371/journal.pone.0039973

Hensen, U., Meyer, T., Haas, J., Rex, R., Vriend, G., & Grubmüller, H. (2012). Exploring protein dynamics space: The dynasome as the missing link between protein structure and function. *PLOS One*, *7*(5), e33931. https://doi.org/10.1371/journal.pone.0033931

Jabeen, S., Yap, H. Y., Abdullah, F. F. J., Zakaria, Z., Isa, N. M., Tan, Y. C., Joo, Y. S., Satharasinghe, D. A., & Omar, A. R. (2019). Complete genome sequence analysis and characterization of selected iron regulation genes of *Pasteurella multocida* serotype A strain *PMTB2.1*. *Genes*, *10*(2), 81. https://doi.org/10.3390/genes10020081

Jabeen, S., Yong, Y. H., Abdullah, F. J. F., Zakaria, Z., Mat Isa, N., Tan, Y. C., Yee, W. Y., &

Omar, A. R. (2017). Complete genome sequence of *Pasteurella multocida* serotype A strain PMTB2.1 isolated from buffaloes that died of septicemia in Malaysia. *Genome Announcements*, *5*(44), e01190-17. https://doi.org/10.1128/genomeA.01190-17

Jenkins, M. K., Khoruts, A., Ingulli, E., Mueller, D. L., McSorley, S. J., Reinhardt, R. L., Itano, A., & Pape, K. A. (2003). *In vivo* activation of antigen-specific CD4 T cells. *Annual Reviews of Immunology*, *19*, 23–45. https://doi.org/10.1146/annurev.immunol.19.1.23

Jiménez-García, B., Roel-Touris, J., Romero-Durana, M., Vidal, M., Jiménez-González, D., & Fernández-Recio, J. (2018). LightDock: A new multi-scale approach to protein–protein docking. *Bioinformatics*, *34*(1), 49–55. https://doi.org/10.1093/bioinformatics/btx555

Jones, P. M., & George, A. M. (2004). The ABC transporter structure and mechanism: Perspectives on recent research. *Cellular and Molecular Life Sciences*, *61*(6), 682-699. https://doi.org/10.1007/s00018-003-3336-9

Joshi, S., Tewari, K., & Singh, R. (2013). Comparative immunogenicity and protective efficacy of different preparations of outer membrane proteins of *Pasteurella multocida* (B:2) in a mouse model. *Veterinarski Arhiv*, *83*(6), 665-676.

Karami, Y., Rey, J., Postic, G., Murail, S., Tufféry, P., & De Vries, S. J. (2019). DaReUS- Loop: A web server to model multiple loops in homology models. *Nucleic Acids Research*, *47*(W1), W423-W428. https://doi.org/10.1093/nar/gkz403

Kim, M., Song, L., Moon, J., Sun, Z. Y., Bershteyn, A., Hanson, M., Cain, D., Goka, S., Kelsoe, G., Wagner, G., Irvine, D., & Reinherz, E. L. (2013). Immunogenicity of membrane-bound HIV-1 gp41 membrane-proximal external region (MPER) segments is dominated by residue accessibility and modulated by stereochemistry. *Journal of Biological Chemistry*, *288*(44), 31888–31901. https://doi.org/10.1074/jbc.M113.494609

Kong, L., Harrington, L., Li, Q., Cheley, S., Davis, B. G., & Bayley, H. (2013). Single-molecule interrogation of a bacterial sugar transporter allows the discovery of an extracellular inhibitor. *Nature Chemistry*, *5*(8), 651–659. https://doi.org/10.1038/nchem.1695

Kumar, A., Mohanty, N. N., Chacko, N., Yogisharadhya, R., & Shivachandra, S. B. (2015). Structural features of a highly conserved Omp16 protein of *Pasteurella multocida* strains and comparison with related peptidoglycan-associated lipoproteins (PAL). *Indian Journal of Microbiology*, *55*(1), 50-56. https://doi.org/10.1007/s12088-014-0489-1

Laskowski, R. A., MacArthur, M. W., Moss, D. S., & Thornton, J. M. (1993). PROCHECK: A program to check the stereochemical quality of protein structures. *Journal of Applied Crystallography*, *26*(2), 283-291. https://doi.org/10.1107/S0021889892009944

Lazzaroni, J. C., & Portalier, R. (1992). The excC gene of *Escherichia coli* K-12 required for cell envelope integrity encodes the peptidoglycan-associated lipoprotein (PAL). *Molecular Microbiology*, *6*(6), 735-742. https://doi.org/10.1111/j.1365-2958.1992.tb01523.x

Liu, N., & Xu, Z. (2019). Using LeDock as a docking tool for computational drug design. In *IOP Conference Series: Earth and Environmental Science* (Vol. 218, No. 1, p. 012143). IOP Publishing. https://doi.org/10.1088/1755-1315/218/1/012143

Liu, W., Yang, M., Xu, Z., Zheng, H., Liang, W., Zhou, R., Wu, B., & Chen, H. (2012). Complete genome sequence of *Pasteurella multocida* HN06, a toxigenic strain of serogroup D. *Journal of Bacteriology*, *194*(12), 3292-3293. https://doi.org/10.1128/JB.00215-12

Magnan, C. N., Zeller, M., Kayala, M. A., Vigil, A., Randall, A., Felgner, P. L., & Baldi, P. (2010). High-throughput prediction of protein antigenicity using protein microarray data. *Bioinformatics*, *26*(23), 2936-2943. https://doi.org/10.1093/bioinformatics/btq551

Martz, F. (2014). *Développement d'une nouvelle méthode de docking basée sur les mécanismes enzymatiques et guidée par des groupes prosthétiques* [Development of a new mechanism-based molecular docking method guided by prosthetic groups] [Doctoral dissertation, Université Paris Sud-Paris XI]. HAL Portal Theses. https://tel.archives-ouvertes.fr/tel-01168482

Mathelié-Guinlet, M., Asmar, A. T., Collet, J. F., & Dufrêne, Y. F. (2020). Bacterial cell mechanics beyond peptidoglycan. *Trends in Microbiology*, *28*(9), 706-708. https://doi.org/10.1016/j.tim.2020.04.013

May, B. J., Zhang, Q., Li, L. L., Paustian, M. L., Whittam, T. S., & Kapur, V. (2001). Complete genomic sequence of *Pasteurella multocida*, Pm70. *Proceedings of the National Academy of Sciences*, *98*(6), 3460-3465. https://doi.org/10.1073/pnas.051634598

Muenthaisong, A., Nambooppha, B., Rittipornlertrak, A., Tankaew, P., Varinrak, T., Muangthai, K., Atthikanyaphak, K., Sawada, T., & Sthitmatee, N. (2020). An intranasal vaccination with a recombinant outer membrane protein H against haemorrhagic septicemia in swamp buffaloes. *Veterinary Medicine International*, *2020*, 3548973. https://doi.org/10.1155/2020/3548973

Naz, A., Awan, F. M., Obaid, A., Muhammad, S. A., Paracha, R. Z., Ahmad, J., & Ali, A. (2015). Identification of putative vaccine candidates against *Helicobacter pylori* exploiting exoproteome and secretome: A reverse vaccinology based approach. *Infection, Genetics and Evolution*, *32*, 280-291. https://doi.org/10.1016/j.meegid.2015.03.027

Park, H., Lee, G. R., Heo, L., & Seok, C. (2014). Protein loop modeling using a new hybrid energy function and its application to modeling in inaccurate structural environments. *PLOS One*, *9*(11), e113811. https://doi.org/10.1371/journal.pone.0113811

Patronov, A., & Doytchinova, I. (2013). T-cell epitope vaccine design by immunoinformatics. *Open Biology*, *3*(1), 120139. https://doi.org/10.1098/rsob.120139

Peng, Z., Liang, W., Liu, W., Wu, B., Tang, B., Tan, C., Zhou, R., & Chen, H. (2016). Genomic characterization of *Pasteurella multocida* HB01, a serotype A bovine isolate from China. *Gene*, *581*(1), 85-93. https://doi.org/10.1016/j.gene.2016.01.041

Peng, Z., Liang, W., Wang, F., Xu, Z., Xie, Z., Lian, Z., Hua, L., Zhou, Z., Chen, H., & Wu, B. (2018). Genetic and phylogenetic characteristics of *Pasteurella multocida* isolates from different host species. *Frontiers in Microbiology*, *9*, 1408. https://doi.org/10.3389/fmicb.2018.01408

Peng, Z., Wang, X., Zhou, R., Chen, H., Wilson, B. A., & Wu, B. (2019). *Pasteurella multocida*: Genotypes and genomics. *Microbiology and Molecular Biology Reviews*, *83*(4), e00014-19. https://doi.org/10.1128/MMBR.00014-19

Prajapat, R., Marwal, A., & Gaur, R. K. (2014). Recognition of errors in the refinement and validation of three-dimensional structures of AC1 proteins of *Begomovirus* strains by using ProSA-web. *Journal of Viruses*, *2014*, 752656. https://doi.org/10.1155/2014/752656

Prasannavadhana, A., Kumar, S., Thomas, P., Sarangi, L. N., Gupta, S. K., Priyadarshini, A., Nagaleekar, V. K., & Singh, V. P. (2014). Outer membrane proteome analysis of Indian strain of *Pasteurella multocida* serotype B:2 by MALDI-TOF/MS analysis. *The Scientific World Journal*, *2014*, 617034. https://doi.org/10.1155/2014/617034

Qiao, S., Luo, Q., Zhao, Y., Zhang, X. C., & Huang, Y. (2014). Structural basis for lipopolysaccharide insertion in the bacterial outer membrane. *Nature*, *511*(7507), 108-111. https://doi.org/10.1038/nature13484

Rafidah, O., Zamri-Saad, M., Nasip, E., Shahiruddin, S., & Saharee, A. A. (2010). Analysis of haemorrhagic septicaemia outbreaks in cattle and buffalo in Malaysia. *Online Journal of Veterinary Research*, *14*(2), 325-333.

Rahman, M. S., Biswas, C., Biswas, P. K., Kader, M. A., Alam, S. N., Sonne, C., & Kim, K. H. (2020). *In silico* analysis of the antigenic properties of iron-regulated proteins against *Neisseria meningitidis*. *Applied Sciences*, *10*(17), 6113. https://doi.org/10.3390/app10176113

Ramachandran, G. N., Ramakrishnan, C., & Sasisekharan, V. (1963). Stereochemistry of polypeptide chain configurations. *Journal of Molecular Biology*, *7*(1), 95–99. https://doi.org/10.1016/S0022-2836(63)80023-6

Reid, A. N., & Whitfield, C. (2005). Functional analysis of conserved gene products involved in assembly of *Escherichia coli* capsules and exopolysaccharides: Evidence for molecular recognition between Wza and Wzc for colanic acid biosynthesis. *Journal of Bacteriology*, *187*(15), 5470-5481. https://doi.org/10.1128/JB.187.15.5470-5481.2005

Remmert, M., Biegert, A., Hauser, A., & Söding, J. (2012). HHblits: Lightning-fast iterative protein sequence searching by HMM-HMM alignment. *Nature Methods*, *9*, 173-175. https://doi.org/10.1038/nmeth.1818

Rimler, R. B. (2001). Purification of a cross-protective antigen from *Pasteurella multocida* grown *in vitro* and *in vivo*. *Avian Diseases*, *45*(3), 572-580. https://doi.org/10.2307/1592897

Rita, D. V., Swee, K. C. W., Shamini, C., Kang, T. L., Nurshamimi, N. R., Hussin, A. R., Nurul, K., & Salmah, I. (2018). A recombinant subunit HSABA392 as a potential vaccine for haemorrhagic septicaemia disease in livestock. *Tropical Biomedicine*, *35*(4), 1075-1086.

Sailapathi, A., Murugan, G., Somarathinam, K., Gunalan, S., Jagadeesan, R., Yoosuf, N., Kanagaraj, S., & Kothandan, G. (2020). Proposing the promiscuous protein structures in JNK1 and JNK3 for virtual screening in pursuit of potential leads. *ACS Omega*, *5*(8), 3969–3978. https://doi.org/10.1021/acsomega.9b03458

Sarah, S. O., Zamri-Saad, M., Zunita, Z., & Raha, A. R. (2006). Molecular cloning and sequence analysis of *gdhA* gene of *Pasteurella multocida* B:2. *Journal of Animal and Veterinary Advances*, *5*(12), 1146- 1149.

Shen, W., Cao, Y., Cha, L., Zhang, X., Ying, X., Zhang, W., Ge, K., Li, W., & Zhong, L. (2015). Predicting linear B-cell epitopes using amino acid anchoring pair composition. *BioData Mining*, *8*, 14. https://doi.org/10.1186/s13040-015-0047-3

Sippel, K. H., Robbins, A. H., Reutzel, R., Boehlein, S. K., Namiki, K., Goodison, S., Agbandje, M. M., Rosser, C. J., & McKenna, R. (2009). Structural insights into the extracytoplasmic thiamine-binding lipoprotein p37 of *Mycoplasma hyorhinis*. *Journal of Bacteriology*, *191*(8), 2585-2592. https://doi.org/10.1128/JB.01680-08

Sollner, J., Grohmann, R., Rapberger, R., Perco, P., Lukas, A., & Mayer, B. (2008). Analysis and prediction of protective continuous B-cell epitopes on pathogen proteins. *Immunome Research*, *4*, 1. https://doi.org/10.1186/1745-7580-4-1

Soriano, E. V., Rajashankar, K. R., Hanes, J. W., Bale, S., Begley, T. P., & Ealick, S. E. (2008). Structural similarities between thiamin-binding protein and thiaminase-I suggest a common ancestor. *Biochemistry*, *47*(5), 1346-1357. https://doi.org/10.1021/bi7018282

Trolle, T., McMurtrey, C. P., Sidney, J., Bardet, W., Osborn, S. C., Kaever, T., Sette, A., Hildebrand, W. H., Nielsen, M., & Peters, B. (2016). The length distribution of class I–restricted T cell epitopes is determined by both peptide supply and MHC allele–specific binding preference. *The Journal of Immunology*, *196*(4), 1480-1487. https://doi.org/10.4049/jimmunol.1501721

Villa, R., Martorana, A. M., Okuda, S., Gourlay, L. J., Nardini, M., Sperandeo, P., Dehò, G., Bolognesi, M., Kahne, D., & Polissi, A. (2013). The *Escherichia coli* Lpt transenvelope protein complex for lipopolysaccharide export is assembled via conserved structurally homologous domains. *Journal of Bacteriology*, *195*(5), 1100-1108. https://doi.org/10.1128/JB.02057-12

Wang, J., & Dokholyan, N. V. (2019). MedusaDock 2.0: Efficient and accurate protein–ligand docking with constraints. *Journal of Chemical Information and Modeling*, *59*(6), 2509–2515. https://doi.org/10.1021/acs.jcim.8b00905

Waterhouse, A., Bertoni, M., Bienert, S., Studer, G., Tauriello, G., Gumienny, R., Heer, F. T., De Beer, T. A. P., Rempfer, C., Bordoli, L., Lepore. R., & Schwede, T. (2018). SWISS-MODEL: Homology modelling of protein structures and complexes. *Nucleic Acids Research*, *46*(W1), W296-W303. https://doi.org/10.1093/nar/gky427

Wiederstein, M., & Sippl, M. J. (2007). ProSA-web: Interactive web service for the recognition of errors in three-dimensional structures of proteins. *Nucleic Acids Research*, *35*(suppl_2), W407-W410. https://doi.org/10.1093/nar/gkm290

Zamri-Saad, M., & Annas, S. (2016). Vaccination against hemorrhagic septicemia of bovines: A review. *Pakistan Veterinary Journal*, *36*(1), 1-5.

APPENDICES

Supplementary Material 1

B-cell Epitope Predictions for Pal, LptD, Wza, and TbpA

Table I
B-cell epitope prediction within the amino acid sequence of Pal using the AAP prediction module in the BCPREDS server

Start position	Sequence
36	YSVQDLQQRYNT
75	TPATKVVVEGNT
108	HYLSAKGVQAGQ
21	GSSKKDESAGQM

Note. AAP = Amino acid pair prediction module in the BCPREDS server

Table II
B-cell epitope prediction within the amino acid sequence of LptD using the AAP prediction module in the BCPREDS server

Start position	Sequence
296	QGRAAEAEQVER
247	QAVHFDNKSPLM
360	NNAYLGFGYDSS
402	GTTRIYDKKGNE
375	QDYFGLFRDRRY
173	SDFDSAYGSSTD
231	YQNALFDSPLNF
159	LNLDYTRVSDQR
576	QTANQIFYDKSI
11	PQDNAWSIEAKE
418	SAGQIYYLQDSR
191	FRVAYYQPHYNI

Note. AAP = Amino acid pair prediction module in the BCPREDS server

Table III
B-cell epitope prediction within the amino acid sequence of Wza using the AAP prediction module in the BCPREDS server

Start position	Sequence
33	GVKVYAQGGPLD
238	RLLVDGDIVHVP
78	KIKAYQYRVGPG
95	TVWDHPELTTPA
339	GTEFYLKPYDVV
172	AYITGEVNRPGQ
369	PTLSGFDSITES
298	FVIRGQRSPSTT
259	IGEVAQPQMLKI

Note. AAP = Amino acid pair prediction module in the BCPREDS server

Table IV
B-cell epitope prediction within the amino acid sequence of TbpA using the AAP prediction module in the BCPREDS server

Start position	Sequence
178	HVYTENEVAQAW
295	EPHFDALKATQM
192	LAKHTVTVGKGW
134	IYDKTKVQQPPK
89	DNYNLEEAEKSG
24	TQAVNVYTYDSF
161	QDPRTSSVGRGL
76	EGKKTKADVVVG

Note. AAP = Amino acid pair prediction module in the BCPREDS server

Supplementary Material 2

MHC-I and MHC-II Binding Predictions for Pal, LptD, Wza, and TbpA

Table V
MHC-I and MHC-II binding peptide sequence prediction within the amino acid sequence of Pal through NetMHCpan 4.1 and NetBoLAIIpan 1.0, respectively

MHC	Start position	Peptide sequence
MHC-I: BoLA-1:00901	41	LQQRYNTVY
MHC-1: BoLA-1:02301	42	QQRYNTVYF
	1	MKKLTKVLL
	41	LQQRYNTVY
MHC-1: BoLA-2:01201	121	STVSYGEEK
MHC-1: BoLA-2:03001	102	RADAVKHYL
	125	YGEEKPAVL
	140	YSKNRRAVL
MHC-1: BoLA-3:00101	125	YGEEKPAVL
	90	GTPEYNIAL
	102	RADAVKHYL
MHC-1: BoLA-3:00201	90	GTPEYNIAL
MHC-II: BoLA-DRB3_1001	46	NTVYFGFDKYNIE
	137	EAAYSKNRRAVLA
MHC-II: BoLA-DRB3_1201	58	EGEYVQILDAHAA
MHC-II: BoLA-DRB3_1601	58	EGEYVQILDAHAA
MHC-II: BoLA-DRB3_2002	59	GEYVQILDAHAAF
	58	EGEYVQILDAHAA

Note. BoLA = Bovine leukocyte antigen

Table VI
MHC-I and MHC-II binding peptide sequence prediction within the amino acid sequence of LptD through NetMHCpan 4.1 and NetBoLAIIpan 1.0, respectively

MHC	Start position	Peptide sequence
MHC-I: BoLA-1:00901	326	SQQTFIEGY
	529	DQWAVVARH
	542	ALRKPVEQY
	234	ALFDSPLNF
	40	KVHGVPIFY
	105	WQLNGEFRY
MHC-1: BoLA-1:02301	612	GKLPYLQAF
	316	VKVDLQTVL
	234	ALFDSPLNF
	609	LQRGKLPYL
	39	FKVHGVPIF

Table VI *(continue)*

MHC	Start position	Peptide sequence
	326	SQQTFIEGY
	207	KQFQIFNEV
	542	ALRKPVEQY
	517	KQLGLTVAW
MHC-I: BoLA-2:01201	463	YQYDTRLNK
MHC-I: BoLA-2:03001	614	LPYLQAFSL
	44	VPIFYTPYL
	347	RPYKDQSNI
	545	KPVEQYLGL
MHC-I: BoLA-3:00101	87	IAPNLDATM
	48	YTPYLQLPI
	264	FHAEPSINL
	585	KSIGINIEL
	289	VHFDNKSPL
MHC-I: BoLA-3:00201	87	IAPNLDATM
	585	KSIGINIEL
	48	YTPYLQLPI
MHC-II: BoLA-DRB3_0101	339	EPHVQYLYRPYKD
	307	RKINRVLPQVKVD
MHC-II: BoLA-DRB3_1001	207	KQFQIFNEVDIGP
	225	QVDFNYYQNALFD
	217	IGPYRALPQVDFN
	45	PIFYTPYLQLPIG
	193	VAYYQPHYNIAIS
	28	QEEYAEMWHARFK
	36	HARFKVHGVPIFY
	309	INRVLPQVKVDLQ
	239	PLNFKLFSQAVHF
	528	TDQWAVVARHYQD
	448	ASNWKINDQWRWQ
	108	NGEFRYLSPIGEG
MHC-II: BoLA-DRB3_1101	108	NGEFRYLSPIGEG
	119	EGKIAGEYLKQDR
	241	NFKLFSQAVHFDN
	321	QTVLASQQTFIEG
MHC-II: BoLA-DRB3_1201	225	QVDFNYYQNALFD
	343	QYLYRPYKDQSNI
	419	AGQIYYLQDSRID
	207	KQFQIFNEVDIGP

Table VI *(continue)*

MHC	Start position	Peptide sequence
	375	QDYFGLFRDRRYS
	160	NLDYTRVSDQRYF
	45	PIFYTPYLQLPIG
	217	IGPYRALPQVDFN
MHC-II: BoLA-DRB3_1601	419	AGQIYYLQDSRID
	160	NLDYTRVSDQRYF
	261	AWRFHAEPSINLP
	168	DQRYFSDFDSAYG
	82	PFYWNIAPNLDAT
	578	ANQIFYDKSIGIN
	197	QPHYNIAISAKQF
MHC-II: BoLA-DRB3_2002	108	NGEFRYLSPIGEG
	217	IGPYRALPQVDFN

Note. BoLA = Bovine leukocyte antigen

Table VII
MHC-I and MHC-II binding peptide sequence prediction within the amino acid sequence of Wza through NetMHCpan 4.1 and NetBoLAIIpan 1.0, respectively

MHC-class: BoLA	Position	Peptide sequence
MHC-I: BoLA-1:00901	60	KQLAPSIPF
	112	AAESGSQVH
	165	ATYQSKKAY
	202	GLSEHADWH
	239	LLVDGDIVH
MHC-I: BoLA-1:02301	2	YKLSRLLIL
	45	AQKAVDAYL
	60	KQLAPSIPF
	76	DQKIKAYQY
	165	ATYQSKKAY
	183	QQYLTNVPL
	263	AQPQMLKIM
	343	YLKPYDVVY
MHC-I: BoLA-2:01201	20	YLKPYDVVY
	70	RANPPLDQK
	138	LTVSQIRNK
	141	SQIRNKLTK
	162	VSVATYQSK
	163	SVATYQSKK
	223	ISVEALIQR
	313	TSSEENIEK

Table VII *(continue)*

MHC-class: BoLA	Position	Peptide sequence
MHC-I: BoLA-2:03001	29	SPVSGVKVY
	50	DAYLITPSL
	111	SAAESGSQV
	127	YPYVGSIHV
	206	HADWHNVTL
	363	VISQIVPTL
MHC-I: BoLA-3:00101	28	KSPVSGVKV
	54	ITPSLVKQL
	71	ANPPLDQKI
	86	VGPGDVLNI
	130	VGSIHVSGL
	178	VNRPGQQYL
	206	HADWHNVTL
	231	RGDLSQNRL
	263	RGDLSQNRL
	273	YGMTLTEAI
MHC-I: BoLA-3:00201	28	KSPVSGVKV
	54	ITPSLVKQL
	71	ANPPLDQKI
	86	VGPGDVLNI
	130	VGSIHVSGL
	263	AQPQMLKIM
	273	YGMTLTEAI
MHC-II:BoLA-DRB3_0101	59	VKQLAPSIPFARA
	60	KQLAPSIPFARAN
	61	QLAPSIPFARANP
	134	HVSGLTVSQIRNK
	135	VSGLTVSQIRNKL
	136	SGLTVSQIRNKLT
	137	GLTVSQIRNKLTK
	159	QIEVSVATYQSKK
	374	FDSITESMLRIRN
	375	DSITESMLRIRNW
MHC-II:BoLA-DRB3_1001	90	DVLNITVWDHPEL
	91	VLNITVWDHPELT
	92	LNITVWDHPELTT
	93	NITVWDHPELTTP
	151	LANYISEPQIEVS
	152	ANYISEPQIEVSV
	340	TEFYLKPYDVVYV

Table VII *(continue)*

MHC-class: BoLA	Position	Peptide sequence
	341	EFYLKPYDVVYVT
	342	FYLKPYDVVYVTT
MHC-II: BoLA-DRB3_1101	322	IADIYQLDVTDAT
MHC-II: BoLA-DRB3_1201	152	LANYISEPQIEVS
	153	ANYISEPQIEVSV
MHC-II:BoLA-DRB3_1501	20	CSVMLPSTKSPVS
	21	SVMLPSTKSPVSG
	345	KPYDVVYVTTAPV
	346	PYDVVYVTTAPVA
	347	YDVVYVTTAPVAR
MHC-II: BoLA-DRB3_1601	151	LANYISEPQIEVS
	152	ANYISEPQIEVSV
	153	NYISEPQIEVSVA
MHC-II: BoLA-DRB3_2002	294	ATGIFVIRGQRSP

Note. BoLA = Bovine leukocyte antigen

Table VIII
MHC-I and MHC-II binding peptide sequence prediction within the amino acid sequence of TbpA through NetMHCpan 4.1 and NetBoLAIIpan 1.0, respectively

MHC	Start position	Peptide sequence
MHC-I: BoLA-1:00901	22	AQTQAVNVY
	24	TQAVNVYTY
	44	KVKKAFETH
	97	EKSGLFVQH
	187	QAWQKLAKH
	213	GEADVVLSY
	219	LSYNTSPLY
	229	MVFEQKDQY
	251	ETAARVAQH
	271	LIHPEAQGH
	289	VINTNIEPH
MHC-I: BoLA-1:02301	22	AQTQAVNVY
	24	TQAVNVYTY
	45	VKKAFETHF
	80	TKADVVVGL
	118	WKNQTFLPY
	160	YQDPRTSSV
	213	GEADVVLSY
MHC-I: BoLA-2:01201	98	KSGLFVQHK
	137	KTKVQQPPK

Table VIII *(continue)*

MHC	Start position	Peptide sequence
	140	VQQPPKSLK
	145	KSLKELVER
	219	LSYNTSPLY
	315	KVNAEQVKK
MHC-I: BoLA-3:00101	5	KTSFFFTAL
	41	AGPKVKKAF
	99	SGLFVQHKV
	142	QPPKSLKEL
	223	TSPLYHMVF
	272	IHPEAQGHL
MHC-I:BoLA-2:03001	106	KVDLTPLSL
	110	TPLSLPVEW
	139	KVQQPPKSL
	142	QPPKSLKEL
	160	YQDPRTSSV
	223	TSPLYHMVF
MHC-I:BoLA-3:00201	5	KTSFFFTAL
	41	AGPKVKKAF
	223	TSPLYHMVF
MHC-II: BoLA-DRB3_0101	190	QKLAKHTVTVGKG
	291	NTNIEPHFDALKA
	292	TNIEPHFDALKAT
	293	NIEPHFDALKATQ
	298	FDALKATQMNTKV
	299	DALKATQMNTKVL
MHC-II: BoLA-DRB3_1001	97	EKSGLFVQHKVDL
	98	KSGLFVQHKVDLT
	99	SGLFVQHKVDLTP
	120	NQTFLPYDFGQFA
	203	WSDTYGAFLKGEA
	204	SDTYGAFLKGEAD
	205	DTYGAFLKGEADV
	322	KKWIAVWQTILTQ
MHC-II: BoLA-DRB3_1101	105	HKVDLTPLSLPVE
	106	KVDLTPLSLPVEW
	107	VDLTPLSLPVEWK
	108	DLTPLSLPVEWKN
	263	CADHFLAFLIHPE
	264	ADHFLAFLIHPEA
	265	DHFLAFLIHPEAQ

Table VIII *(continue)*

MHC	Start position	Peptide sequence
MHC-II: BoLA-DRB3_1201	57	QVNFTAFGDSGTM
	58	VNFTAFGDSGTMF
	99	SGLFVQHKVDLTP
	100	GLFVQHKVDLTPL
MHC-II: BoLA-DRB3_1501	90	NYNLEEAEKSGLF
	91	YNLEEAEKSGLFV
	247	VLQIETAARVAQH
	248	LQIETAARVAQHD
MHC-II: BoLA-DRB3_1601	130	QFAFIYDKTKVQQ
	131	FAFIYDKTKVQQP
	208	GAFLKGEADVVLS
MHC-II: BoLA-DRB3_2002	7	SFFFTALSTLSLS
	294	IEPHFDALKATQM
	295	EPHFDALKATQMN
	296	PHFDALKATQMNT

Note. BoLA = Bovine leukocyte antigen

Pertanika J. Trop. Agric. Sci. 46 (1): 315 - 328 (2023)

PERTANIKA JOURNALS

TROPICAL AGRICULTURAL SCIENCE

Journal homepage: http://www.pertanika.upm.edu.my/

The Effectiveness of Rice Husk Ash as Additive in Palm Oil-Based Compost in Enhancing the Nitrogen Uptake by *Brassica oleracea* var. *alboglabra* L. (Chinese Kale) Plant

Nor Hanuni Ramli[1]*, Nur Eliza Badrul Hisham[1] and NorFhairna Baharulrazi[2]

[1]*Faculty of Chemical and Process Engineering Technology, Universiti Malaysia Pahang, Lebuhraya Tun Razak, 26300 Gambang, Kuantan, Pahang, Malaysia*

[2]*Faculty of Chemical and Energy Engineering, Universiti Teknologi Malaysia, 81310 Johor Bahru, Johor, Malaysia*

ABSTRACT

Rice husk ash (RHA), palm oil mill effluent (POME) sludge, and decanter cake can be utilized as compost to reduce environmental pollution. This research attempted to investigate the effect of RHA addition to palm oil-based compost in boosting the nitrogen (N) uptake and the growth of *Brassica oleracea* var. *alboglabra* L. (Chinese kale plant). Two categories of compost treatment were prepared in this study: Treatment 1 (control) and Treatment 2 [consisting of 10% (wt/wt) of RHA]. Both treatments were composted for 60 days until it was matured. The temperature and pH of the composts were recorded daily throughout the study. The treatments were analyzed for moisture, water-holding capacity, and nutrient content. The Chinese kale plant was grown in growing media and applied with Treatment 1 and Treatment 2 composts. The progress of plant growth was tracked every week. Based on the analysis, Treatment 2 exhibited a higher temperature and pH profile than Treatment 1. Meanwhile, the contents of N, P, and K were higher in Treatment 1 compost. However, Treatment 2 compost had higher silicon (Si) content, moisture content, and water-holding capacity. Based on the field test study carried out on the Chinese kale plant, the N uptake, and the growth of the plant, were found to be significantly higher when applied with Treatment 2 compost compared to Treatment 1 by 19% to 31% and 13% to 53%, respectively. It was proven that the addition of 10% RHA managed to provide an adequate amount of Si, moisture content, and water-holding capacity in Treatment 2

ARTICLE INFO

Article history:
Received: 22 July 2022
Accepted: 26 October 2022
Published: 14 February 2023

DOI: https://doi.org/10.47836/pjtas.46.1.17

E-mail addresses:
drhanuni@ump.edu.my (Nor Hanuni Ramli)
elizahisham21@gmail.com (Nur Eliza Badrul Hisham)
norfhairna@utm.my (NorFhairna Baharulrazi)
* Corresponding author

ISSN: 1511-3701
e-ISSN: 2231-8542

compost that can enhance the N uptake and improve the growth of the Chinese kale plant in this study.

Keywords: Chinese kale, decanter cake, POME sludge, rice husk ash

INTRODUCTION

The increasing demand for rice in several countries, such as Malaysia, India, and China, has triggered the expansion of rice processing industries (Babaso & Sharanagouda, 2017). As rice production keeps increasing, the industry will produce the main product and waste materials. One of the valuable waste materials produced is rice husk ash (RHA). RHA is the ashes produced in abundance when the rice husk undergoes the burning process as a disposal method. According to Theeba et al. (2012), RHA contains high silica (Si) content, which makes it valuable in the agricultural industry, as it can be utilized to enhance the moisture content of the soil. Phonphuak and Chindaprasirt (2015) claimed that the presence of Si could help maintain the soil's moisture content since this element is highly porous and has a large surface area. Therefore, RHA can be applied in the composting process with other compost materials, such as palm oil mill wastes, to enhance the quality of the compost produced.

The wastes from the palm oil industry, which are palm oil mill effluent (POME) sludge and decanter cake, have been utilized in the composting process to reduce the disposal of these wastes to the environment. POME and decanter cake have contributed to the highest waste management cost in palm oil mill operations, as they contribute to a massive volume of waste. However, the utilization of the treated POME sludge can be potentially explored as it could provide sufficient essential macronutrients, such as nitrogen (N), potassium (K), phosphorus (P), and many other nutrients, to the soil and plant. Compared to other palm oil mill wastes, POME sludge is a great choice to be utilized as a biofertilizer due to its significantly high nutrient contents essential for crop growth (Sapie et al., 2019). Meanwhile, another palm oil mill waste, decanter cake, also contains high nutrient composition, making it suitable to be utilized as a bio-fertilizer. Decanter cake can be added to compost production to enhance the moisture content of the compost materials (Adam et al., 2016). RHA, together with POME sludge and decanter cake, can be utilized in the compost-making process and applied to soil to facilitate the uptake of nitrogen by the plants, especially for leafy vegetables.

For leafy vegetables, such as kale, lettuce, and cabbage, N is the macronutrient needed most for the growth of the leaves. N is normally taken by plants in ammonium form (NH_4^+) and nitrate form (NO_3^-). N is required by the plant sufficiently as this element affects various plant function levels, including plants' metabolism, growth, and development (Yousaf et al., 2021).

In Malaysia, an abundance of waste generated from the rice processing and palm oil mill industries could be potentially

utilized. The disposal of these wastes, such as RHA, POME sludge, and decanter cake, can be reduced by turning them into valuable compost materials. Prior research by Hisham and Ramli (2019) discovered that the combination of POME sludge and decanter cake at a ratio of 1:1 with different percentages of RHA has proven to enhance the physicochemical properties of the compost produced. The compost produced can be applied to soil to improve the nutrient uptake by the plant and hence, promote the production of good-quality plants. Although research has been conducted to study the compost made from palm oil mill wastes, the utilization of these wastes and other organic materials, such as RHA, is worth discovering. Apart from that, current research also disregards the effect of RHA in combination with palm oil-based compost in enhancing the N uptake by the plant. Prior research by Hisham and Ramli (2019), Khairuddin et al. (2016), and Theeba et al. (2012) only covered the physicochemical properties of the compost produced from rice processing and palm oil mill wastes and not the application of these wastes on the plant.

Hence, there is a need to diversify the existing data available for the growth study related to the N uptake by the plant by applying the compost on leafy vegetables, such as *Brassica oleracea* var. *alboglabra* L. (Chinese kale) plant, which requires a high amount of N for the growth of its leaves. Therefore, the effect of RHA and palm oil-based compost can be easily observed on this vegetable. Other than that, there is a need to conduct a field test study to refine the existing data obtained by previous researchers such as Di Mola et al. (2020), Xiang et al. (2019), and Y. Wang et al. (2022), who also studied about the nitrogen uptake by leafy vegetables like Chinese kale plant. Therefore, this study attempted to investigate the effect of RHA addition to palm oil-based compost in enhancing the nitrogen uptake by the Chinese kale plant.

MATERIALS AND METHODS

Preparation of Compost

Compost preparation was prepared by adapting the same procedure used by Hisham and Ramli (2020) and Ramli et al. (2019). The rice husk ash (RHA) was acquired from a nursery in Kuantan, Pahang, while palm oil mill effluent (POME) sludge was obtained from the aerobic pond at Lembaga Kemajuan Perusahaan Pertanian (LKPP) Lepar, Pekan, Pahang. Meanwhile, the raw material for DC was collected from the oil clarification section of LKPP Lepar. This research developed two compost treatments, Treatment 1 and Treatment 2. Treatment 1 (control) consisted of 50% POME sludge and 50% decanter cake with a total weight of 5 kg. For Treatment 2 (RHA_{10}), the compost was made up of 10% RHA, 45% POME sludge, and 45% decanter cake with the same total weight as Treatment 1, as referred to the previous study by Hisham and Ramli (2020) since current work is a continuation from the previous work done in Hisham and Ramli (2019). The details of the weight composition of raw materials used in this study are tabulated in Table 1.

Table 1
Weight composition of sample preparation

Treatments	Composition of RHA added (%)	Weight of RHA (kg)	Weight of POME sludge (kg)	Weight of decanter cake (kg)	Total weight (kg)
Control	0	0	2.50	2.50	5.00
RHA_{10}	10	0.50	2.25	2.25	5.00

Note. RHA: rice husk ash; POME: palm oil mill effluent

Two containers, as illustrated in Figure 1, with a size of 16 cm (H) × 30 cm (L) × 18 cm (W), were used for composting process. The samples were allowed to be decomposed in the containers for 60 days, whereby the maturity stage was expected to achieve within this period. Throughout this period, the compost's temperature and pH were recorded daily using the AMT-300 4-in-1 Soil Survey Instrument (Microtemp Electrics, Taiwan). The matured composts were then analyzed based on physicochemical properties (moisture content, water holding capacity, N, P, K, and Si contents). The experiment was set up based on a completely randomized design (CRD), and three replicates of samples were prepared for each analysis.

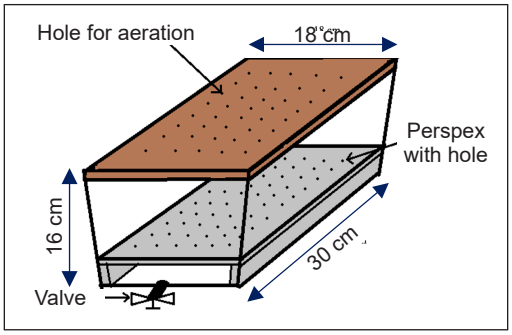

Figure 1. Illustration of composting bin

Characterization of Matured Compost

The matured composts were analyzed for moisture, water-holding capacity, and nutrient contents. For moisture content analysis, the fresh weight of the sample was measured and recorded. Then, the sample was dried for 5 hr in an oven, in which the temperature was set at 105 ± 2°C. After 5 hr, the dry weight of the sample was measured, and the standard test ASTM D4442-16 (2016) was referred to determine the percentage of moisture content.

For water holding capacity analysis, approximately 10 g of sample was mixed with 50 ml of distilled water. The sample was allowed to stand for 30 min and moved onto filter paper in a funnel. When the weight remained unchanged, the wet sample weight in the filter was measured. For every 30 min, the drop-off water was recorded until the sample began to dry. Then, the sample was oven-dried at 105 ± 2°C for 48 hr and reweighed again. Standard test ASTM D2980-02 (2002) was used to calculate the water holding capacity.

Meanwhile, for chemical analysis, the sample was dried in an oven for 24 hr at 105 ± 2°C. Then, the dried sample was pulverized using a grinder (IKA A11, Germany) to change it into powder. The micro-Kjeldahl method was performed to determine the N content. A standard method of the test using ASTM E1621-13

was utilized to determine the content of K, P, and Si by using wavelength dispersive X-ray fluorescence (WDXRF) spectrometer instrument (model Axios^{mAX}, PANalytical, Netherlands).

Field Tests and Sampling

To validate the effectiveness of Treatment 1 and Treatment 2 samples in enhancing the N uptake and plant growth, a field test study was conducted on *Brassica oleracea* var. *alboglabra* L. (Chinese kale). The experiment was based on a completely randomized design (CRD). The Chinese kale seed was germinated on a seedling tray filled with peat moss for 21 days. After 21 days, the seedlings were transferred into polybags (22.8 cm x 22.8 cm) containing cocopeat (800 g) as the growing medium. The seedlings were allowed to grow for six weeks (42 days). For analysis, the seedlings were prepared in three replications each week until they were ready to be harvested. Treatment 1 and Treatment 2 composts were applied to the plant in the first and second weeks after planting (Purbajanti et al., 2019). For analysis, the Chinese kale plant grown in the polybags was harvested weekly. The plant's fresh weight was recorded. Only the aboveground part was weighed as referred to the method described in Wijitkosum and Jiwnok (2019).

Determination of N Uptake and Crop Yield

The N uptake was investigated on the leaf part of the plant. First, the leaf part of Chinese kale was separated from the stem and roots to estimate dry matter accumulation. Next, the leaf sample was dried in an oven at 70°C until a constant weight was achieved and weighed for the dry weight (DW). The sample was then pulverized to 20 mesh and analyzed for N content using the micro-Kjeldahl method referred to as N. K. Sharma et al. (2012). The formula mentioned in N. K. Sharma et al. (2012) work was used to determine the total uptake of nitrogen.

$$Uptake\ of\ N\left(\frac{g}{pot}\right) = \frac{N\ \%\ \text{in leaf} \times dry\ weight\left(\frac{g}{pot}\right)}{100}$$

Equation 1

Statistical Analysis

All data obtained in this study were subjected to analysis of variance (ANOVA) by using MINITAB®18 Statistical Software (version 18.1). To determine the significant difference among means, a least significant difference (LSD) was performed at a significant level of $p \leq 0.05$, as referred to by Majbar et al. (2018) and Oviedo-ocaña et al. (2021).

RESULTS AND DISCUSSION

Temperature Profile of Compost

Temperature is an important parameter that needs to be closely monitored to determine the completion of the composting process. Therefore, the temperature profile for Treatment 1 (control) and Treatment 2 (RHA_{10}) composts were presented in Figure 2.

Based on Figure 2, the mesophilic stage was observed from day 1 to day 17. During

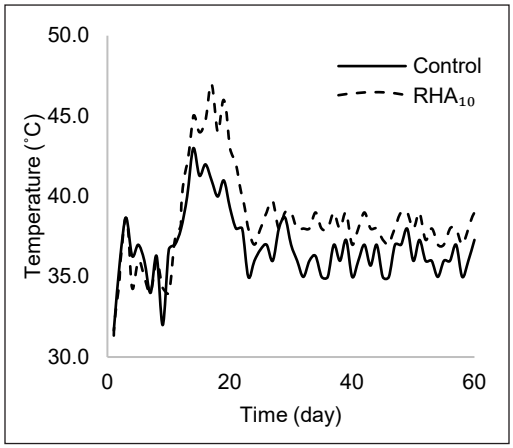

Figure 2. Temperature profile throughout the 60 days composting period

this period, the composts' temperature increased and remained within the mesophilic temperature below 45°C (Biyada et al., 2021). The highest temperature was recorded by Treatment 2 on day 17, with the temperature being around 47°C, compared to Treatment 1. The high temperature obtained by Treatment 2 might occur due to the presence of RHA in the formulated compost, which can enhance the compost's moisture content. A proper moisture content level can improve the oxygen uptake rate by aerobic microorganisms and increase microbial activity (Rastogi et al., 2020). As a result, the compost temperature would rise due to the increase in oxygen consumption and microbial activity that will generate more heat.

After the mesophilic stage, the compost temperature for Treatments 1 and 2 gradually decreased and fluctuated from day 18 until day 60. It is because the microbial activity started to slow down, though they stayed within the range of 34 to 40°C. Based on Figure 2, the temperatures fell within the range of the mesophilic stage throughout the composting period and did not enter the thermophilic stage. The thermophilic stage was not reached, probably due to the minimal microbial activity inside the composts (Hayawin et al., 2016). Moreover, although the temperature range still lies under the mesophilic stage, the stage can be identified as the curing stage based on the trend of the graph. In this stage, the compost temperature will gradually decrease until it reaches the ambient temperature, which indicates the completion of the composting process (Román et al., 2015). The matured compost can be identified based on the physical appearance of the compost, such as the black color of the material, which is almost similar to soil texture, and reduced particle size (Román et al., 2015).

pH Profile of Compost

Other than temperature, the pH of both treatments was also monitored, and the profile is illustrated in Figure 3.

Based on Figure 3, low pH values in pH 4.6 to pH 5.6 were recorded for the first ten days. Then, the pH values rose from pH 5 to pH 7. The increase in pH is due to the metabolic degradation of organic acids inside the compost (Hock et al., 2009). Other than that, it also occurred due to the transformation of N into ammonium (NH_4^+) or ammonia (NH_3) via the ammonification process (Irvan et al., 2019).

At the beginning of the composting process, Treatment 1 had a lower pH than Treatment 2 due to the original pH of the decanter cake, which was quite acidic.

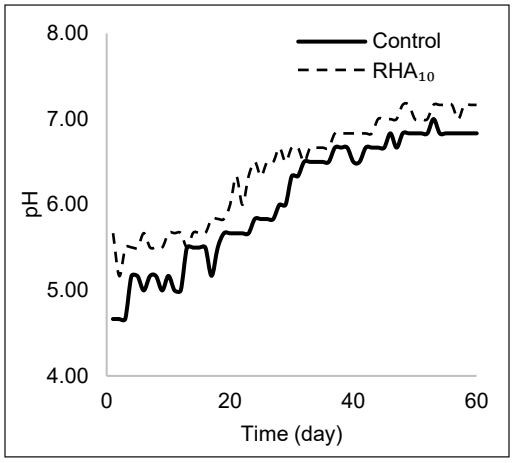

Figure 3. pH profile throughout the 60 days composting period

Meanwhile, a higher pH was obtained by Treatment 2, which might be due to the high composition of alkaline RHA. The presence of RHA in compost can ameliorate the acidity of compost; this finding has been proven by Yin et al. (2022). Eventually, the pH of both treatments reached close to a neutral level from day 45 onwards. In the composting process, the neutral pH indicates that the organic acids that exist in the compost are neutralized, which is caused by the humic substances' buffering effect, as claimed by Hock et al. (2009). According to D. Sharma et al. (2017), the final pH value between pH 6 and 8 is acceptable in composting.

Physicochemical Properties of Compost

For physical properties, the result presented in Table 2 clearly shows that Treatment 2 compost had a higher moisture content and water-holding capacity compared to Treatment 1. Meanwhile, for chemical properties, Treatment 1 contained the highest N and P contents, while Treatment 2 had the highest K and Si contents. Based on the ANOVA, the difference between the treatments was significant at $p \leq 0.05$ for all parameters.

As presented in Table 2, Treatment 2 compost had the highest moisture content and water-holding capacity, which might be due to high Si content, as referred to in the same table. According to Siddika et al. (2021), the Si content in RHA could reach as high as 90%. Si is widely used for various

Table 2
Physicochemical properties of finished composts

Parameters	Treatments (Mean ± SD)	
	Treatment 1 (Control)	Treatment 2 (RHA_{10})
Physical properties		
Moisture content (%)	47.37 ± 0.38^{b}	53.21 ± 0.32^{a}
Water holding capacity (%)	55.39 ± 0.85^{b}	59.52 ± 0.82^{a}
Chemical properties		
N (%)	3.31 ± 0.02^{a}	2.97 ± 0.08^{b}
P (%)	0.87 ± 0.03^{a}	0.67 ± 0.02^{b}
K (%)	3.46 ± 0.04^{b}	3.74 ± 0.07^{a}
Si (%)	18.32 ± 0.87^{b}	28.12 ± 0.66^{a}

Note. Means that columns with the same letters are not significantly different at $p \leq 0.05$; RHA: rice husk ash

purposes for its porosity and large surface area (Lumbanraja et al., 2019). These structures allow Si to retain more water and increase the water-holding capacity of this element. As a result, the moisture content will increase as these parameters are closely related. Previous work done by Schaller et al. (2020) has proved that the soil's water-holding capacity was improved with the presence of Si since this element has an amorphous structure with a high surface area that can hold more water.

Apart from that, based on the chemical analysis result, Treatment 1 compost contained the highest N and P contents. It is because Treatment 1 had the largest weight composition of palm oil mill wastes, as shown in Table 1. Palm oil mill wastes, such as POME sludge and decanter cake, contain a substantial amount of important nutrients for plants, as claimed by Nizar et al. (2018). Therefore, these wastes contribute to the high percentage of N and P content in Treatment 1 as this treatment only contained the palm oil mill wastes without adding RHA.

Meanwhile, for K and Si contents, these elements were observed to be higher in Treatment 2 than in Treatment 1. However, the result of K content was slightly contradicted by the predicted result, whereby it was expected that Treatment 1 would have a higher K content than Treatment 2. It is because palm oil mill wastes also contain an appreciable amount of K in their composition. Treatment 2 had a lower weight composition of palm oil mill wastes, as referred to in Table 1, and supposedly, it contained a lower K content than Treatment 1. The reduction of K content in Treatment 1 might occur due to the leaching process that occurred during the composting process. K is highly soluble in water, and the availability of K inside the sample is greatly affected by leaching (Krishnan et al., 2021). Other than that, K is also a mobile ion and can be lost when K inputs surpass the soil retention capacity (Alfaro et al., 2017).

For Si content, it was found that Treatment 2 had a higher Si content compared to Treatment 2 since Treatment 2 compost contained 10% RHA composition in its components. As mentioned, RHA contained a high amount of Si in its components, which could enhance the Si content inside the compost. Moreover, work done by Hisham and Ramli (2019) also proved this finding, in which the authors discovered that adding RHA in compost production enhanced the Si content inside the finished compost.

Nitrogen Uptake and the Growth of Chinese Kale Plant

Both compost treatments were applied to the Chinese kale plant *Brassica oleracea* var. *alboglabra* L.) to validate the effectiveness of the treatments on N uptake and plant growth. The effect of N uptake on the growth of the Chinese kale plant in terms of weight is presented in Figure 4. Based on the figure, higher N uptake and weight of Chinese kale were observed on the plant that was applied with Treatment 2 (RHA_{10}) compost compared to Treatment 1 (Control).

As shown in Figure 4, the results obtained for N uptake by both treatments were significantly different since the *p*-value obtained is less than 0.05 ($p \leq 0.05$). However, high N uptake was observed on Chinese kale that was applied with Treatment 2, which could be related to the properties of high moisture content and water-holding capacity of Treatment 2 compost, as shown in Table 2. These properties of Treatment 2 compost could enhance the water availability inside the growing medium and boost the N uptake by Chinese kale grown in the medium. Water availability is crucial for plants since it carries essential nutrients from the soil to the upper parts of plants. Other than that, the presence of RHA in Treatment 2 compost enhanced the Si content in the form of amorphous silica (SiO_2), which could improve water absorption inside the growing medium.

As buttressed by Rios et al. (2017), the presence of Si in soil could regulate water uptake by the plant roots as this element was claimed to be able to promote the hydraulic conductance of the roots. Other than that, the presence of Si in Treatment 2 compost could also boost the aquaporin genes. According to Maurel et al. (2015), in most living things, aquaporin is the membrane channel that is responsible for the transport of small neutral molecules and water across the biological membrane. According to Gao et al. (2018), aquaporin genes regulate the water flow, which could regulate the movement of N

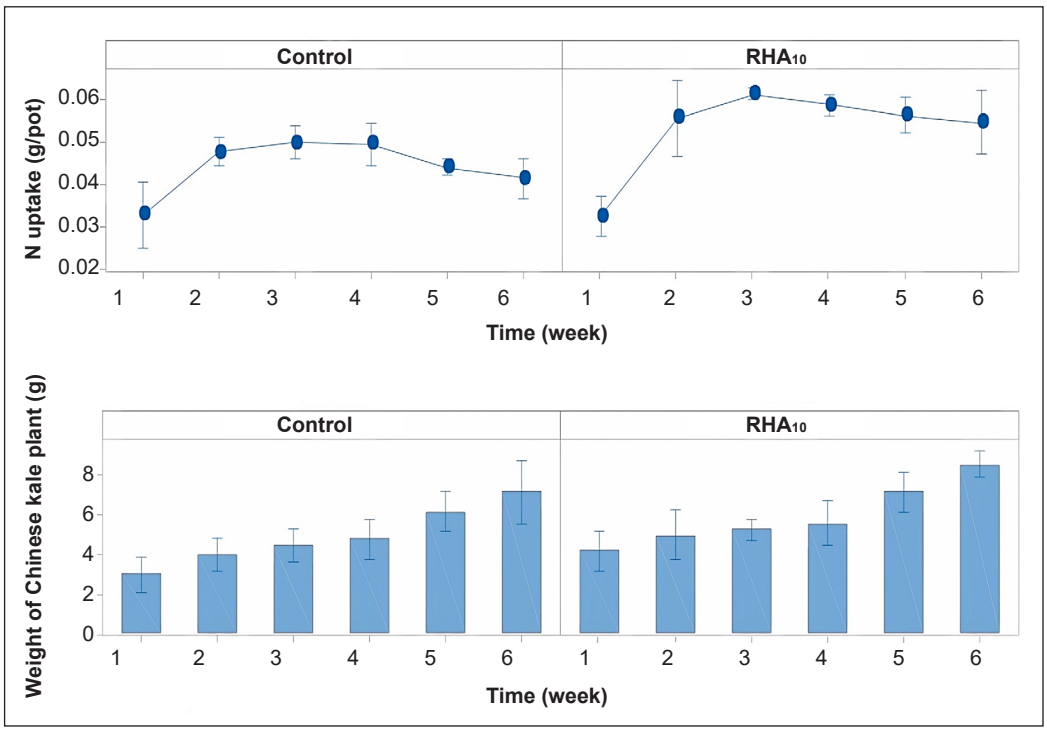

Figure 4. The N uptake and Chinese kale growth in terms of weight of plant (g) for six weeks
Note. Individual standard deviations are used to calculate the intervals

in plants. Other than that, it also plays a prominent role in N absorption and the soil's mobilization and detoxification (M. Wang et al., 2016). Hence, the sufficient amount of Si in the growing medium applied with Treatment 2 compost was proven to enhance the N uptake by Chinese kale via the role of water as the carrier of the important nutrient.

Moreover, in this study, the trend of N uptake obtained for both treatments was comparable with the work done by Onwonga et al. (2017), who also investigated the N uptake by the kale plant. The trend of N uptake by kale was claimed to have rapidly occurred at the early stage of growth since kale requires a high amount of N for the growth of its leaves. The trend will decline after reaching the maximum N uptake, indicating the growth's maturity phase. They also stated that when the growth of kale reached the maturity phase, the plant only required the N element in moderate amounts. In contrast, the uptake of other nutrients will increase. As proved in previous research conducted by Teuber et al. (2020), the increase of N uptake by kale will positively affect the biomass yield of the plant. The same correlation could be observed in Figure 2, whereby the weight of Chinese kale recorded in the growing medium applied with Treatment 2 compost was higher compared to Treatment 1 due to the high uptake of N by the plant.

Based on the result obtained for the average weight of Chinese kale, the statistical analysis indicates that the results recorded for both treatments were significantly different at $p \leq 0.05$. This finding suggests that both compost treatments significantly affected the growth of Chinese kale. By referring to Teuber et al. (2020), the availability of N strongly affects kale growth since this plant belongs to the forage Brassica species. The plant categorized in this species would require a substantial amount of N for the development and growth of its leaves. High N uptake by the leafy vegetable will enhance the photosynthetic activities and improve the conductance of stomatal and chlorophyll content (Dinh et al., 2017). As buttressed by Erwin and Gesick (2017), when the photosynthetic rate is increased, the plant's mass increases concurrently. The findings have proved that, for leafy vegetables, high N uptake is prominent in enhancing plant biomass.

Hence, the results of this work have confirmed that RHA can be utilized in composting to enhance the moisture content, water holding capacity, and Si content in the growing medium. However, in compost production, RHA is suggested to be used with other suitable compost material to enhance the nutrient contents inside the compost. The high-water content attributed to the presence of RHA is crucial in transporting important nutrients, such as N, to the leaves of leafy vegetables. High N uptake, but not excessive, will ensure plant growth is at the right trend.

CONCLUSION

This work proved that adding RHA in palm oil-based compost (Treatment 2) enhanced the temperature and pH profile during the composting process. Other than that, the presence of RHA also improves

the physical properties of the compost produced. The compost needs to have a well-balanced condition of physical and chemical properties to produce high-quality compost. Treatment 2 compost has successfully improved the N uptake and the growth of the Chinese kale plant in this study due to high moisture content and water-holding capacity with a proper amount of nutrients inside the compost. It was noted in the study that the N uptake and the growth of plants applied with Treatment 2 compost were found to be significantly higher by 13% to 53% compared to Treatment 1. Overall, it is evident that applying RHA in compost production can improve the availability of nutrient-enriched water in the growing media, leading to more nutrients, especially N, being taken up by the plant for its growth.

ACKNOWLEDGEMENTS

The authors are grateful for the financial support from the Ministry of Education Malaysia and Universiti Malaysia Pahang through the Fundamental Research Grant Scheme (RDU190136) with reference code FRGS/1/2018/TK10/UMP/02/7 and Collaborative Research Grant (RDU 192322).

REFERENCES

Adam, S., Ahmad, S. S. N. S., Hamzah, N. M., & Darus, N. A. (2016). Composting of empty fruit bunch treated with palm oil mill effluent and decanter cake. In *Regional Conference on Science, Technology and Social Sciences (RCSTSS 2014)* (pp. 437–445). Springer, Singapore. https://doi.org/10.1007/978-981-10-0534-3_43

Alfaro, M. A., Rosolem, C. A., Goulding, K. W. T., & Wang, H. (2017, January 25-27). *Potassium losses and transfers in agricultural and livestock systems* [Paper presentation]. Proceedings for the Frontiers of Potassium Science Conference, Rome, Italy. https://www.apni.net/wp-content/uploads/2020/05/IPNI-FOPS-2017-Proceedings.pdf

ASTM D2980-02. (2002). *Standard test method for volume weights, water-holding capacity, and air capacity of water-saturated peat materials.* ASTM International. https://doi.org/10.1520/D2980-02

ASTM D4442-16. (2016). *Standard test methods for direct moisture content measurement of wood and wood-based materials*. ASTM International. https://doi.org/10.1520/D4442-16

Babaso, P. N., & Sharanagouda, H. (2017). Rice husk and its applications: Review. *International Journal of Current Microbiology and Applied Sciences*, *6*(10), 1144–1156. https://doi.org/10.20546/ijcmas.2017.610.138

Biyada, S., Merzouki, M., Dėmčėnko, T., Vasiliauskienė, D., Ivanec-Goranina, R., Urbonavičius, J., Marčiulaitienė, E., Vasarevičius, S., & Benlemlih, M. (2021). Microbial community dynamics in the mesophilic and thermophilic phases of textile waste composting identified through next-generation sequencing. *Scientific Reports*, *11*, 23624. https://doi.org/10.1038/s41598-021-03191-1

Di Mola, I., Cozzolino, E., Ottaiano, L., Nocerino, S., Rouphael, Y., Colla, G., El-Nakhel, C., & Mori, M. (2020). Nitrogen use and uptake efficiency and crop performance of baby spinach (*Spinacia oleracea* L.) and lamb's lettuce (*Valerianella locusta* L.) grown under variable sub-optimal N regimes combined with plant-based biostimulant application. *Agronomy*, *10*(2), 278. https://doi.org/10.3390/agronomy10020278

Dinh, T. H., Watanabe, K., Takaragawa, H., Nakabaru, M., & Kawamitsu, Y. (2017). Photosynthetic response and nitrogen use efficiency of sugarcane under drought stress conditions with different nitrogen application levels. *Plant Production Science*, *20*(4), 412–422. https://doi.org/10.1080/1343943X.2017.1371570

Erwin, J., & Gesick, E. (2017). Photosynthetic responses of swiss chard, kale, and spinach cultivars to irradiance and carbon dioxide concentration. *HortScience*, *52*(5), 706–712. https://doi.org/10.21273/HORTSCI11799-17

Gao, L., Lu, Z., Ding, L., Guo, J., Wang, M., Ling, N., Guo, S., & Shen, Q. (2018). Role of aquaporins in determining carbon and nitrogen status in higher plants. *International Journal of Molecular Sciences*, *19*(1), 35. https://doi.org/10.3390/ijms19010035

Hayawin, Z. N., Astimar, A. A., Ropandi, M., Faizah, J. N., & Hamid, F. A. (2016). Rapid composting of oil palm biomass by using aerobic thermophilic composter. *Palm Oil Engineering Bulletin*, *119*, 19–26.

Hisham, N. E. B., & Ramli, N. H. (2020). Incorporation of rice husk ash with palm oil mill wastes in enhancing physicochemical properties of the compost. *Pertanika Journal of Tropical Agricultural Science*, *44*(1), 221–236. https://doi.org/10.47836/pjtas.44.1.13

Hisham, N. E. B., & Ramli, N. H. (2019). Effect of rice husk ash on the physicochemical properties of compost. *Indonesian Journal of Chemistry*, *19*(4), 967–974. https://doi.org/10.22146/ijc.39704

Hock, L. S., Baharuddin, A. S., Ahmad, M. N., Hassan, M. A., Shah, U. K. M., Rahman, N. A. A., Abd-Aziz, S., & Shirai, Y. (2009). Physicochemical changes in windrow co-composting process of oil palm mesocarp fiber and palm oil mill effluent anaerobic sludge. *Australian Journal of Basic and Applied Sciences*, *3*(3), 2809–2816.

Irvan, Rahman, M., Anwar, D., Trisakti, B., & Daimon, H. (2019). Production of compost from non-shredded empty fruit bunches mixed with activated liquid organic fertilizer in tower composter. *Malaysian Journal of Analytical Science*, *23*(1), 138–146. https://doi.org/10.17576/mjas-2019-2301-17

Khairuddin, M. N., Zakaria, A. J., Isa, I. M., Jol, H., Nazri Wan Abdul Rahman, W. M., & Salleh, M. K. S. (2016). The potential of treated palm oil mill effluent (POME) sludge as an organic fertilizer. *Agrivita*, *38*(2), 142–154. https://doi.org/10.17503/agrivita.v38i2.753

Krishnan, K., Ngerong, A. A., Ahim, K., Ahmed, O. H., Ali, M., Omar, L., & Musah, A. A. (2021). Mitigating potassium leaching from muriate of potash in a tropical peat soil using clinoptilolite zeolite, forest litter compost, and chicken litter biochar. *Agronomy*, *11*(10), 1900. https://doi.org/10.3390/agronomy11101900

Lumbanraja, S., Nainggolan, H., & Sitohang, C. (2019). Improving porosity of glycerol-plated silica from rice husk silica. *Journal of Chemical Natural Resources*, *1*(2), 88–97. https://doi.org/10.32734/jcnar.v1i2.1257

Majbar, Z., Lahlou, K., Ben Abbou, M., Ammar, E., Triki, A., Abid, W., Nawdali, M., Bouka, H., Taleb, M., El Haji, M., & Rais, Z. (2018). Co-composting of olive mill waste and wine-processing waste: An application of compost as soil amendment. *Journal of Chemistry*, *2018*, 7918583. https://doi.org/10.1155/2018/7918583

Maurel, C., Boursiac, Y., Luu, D. T., Santoni, V., Shahzad, Z., & Verdoucq, L. (2015). Aquaporins in plants. *Physiological Reviews*, *95*(4), 1321–1358. https://doi.org/10.1152/physrev.00008.2015

Nizar, M. K., Isharudin, M. I., Jamil, A. Z., & Hazandy, A. H. (2018). Influence of treated palm oil mill effluent sludge on maize (*Zea mays*) growth performance and gas exchange.

Sains Malaysiana, *47*(5), 961–969. https://doi.org/10.17576/jsm-2018-4705-11

Onwonga, R. N., Chepkoech, C., Wahome, R. G., Jensen, H. H., & Freyer, B. (2017, September 20-22). *Synchronizing legume residue nutrient release with kale (*Brassica oleracea *var.* acephala*) uptake in a nitisol of Kabete, Kenya* [Paper presentation]. International Research on Food Security, Natural Resource Management and Rural Development 2017, Bonn, North Rhine-Westphalia, Germany. https://backend.orbit.dtu.dk/ws/portalfiles/portal/134276995/Paper_til_Tropentag_sept_2017_1075.pdf

Oviedo-ocaña, E. R., Hernández-gómez, A. M., Ríos, M., Portela, A., Sánchez-torres, V., Domínguez, I., & Komilis, D. (2021). A comparison of two-stage and traditional co-composting of green waste and food waste amended with phosphate rock and sawdust. *Sustainability*, *13*(3), 1109. https://doi.org/10.3390/su13031109

Phonphuak, N., & Chindaprasirt, P. (2015). Types of waste, properties, and durability of pore-forming waste-based fired masonry bricks. In F. Pacheco-Torgal, P. B. Lourenco, J. A. Labrincha, S. Kumar, & P. Chindaprasirt (Eds.), *Eco-efficient masonry bricks and blocks* (pp. 103–127). Woodhead Publishing. https://doi.org/10.1016/B978-1-78242-305-8.00006-1

Purbajanti, E. D., Slamet, W., Fuskhah, E., & Rosyida. (2019). Effects of organic and inorganic fertilizers on growth, activity of nitrate reductase and chlorophyll contents of peanuts (*Arachis hypogaea* L.). In *IOP Conference Series: Earth and Environmental Science* (Vol. 250, No. 1, p. 012048). IOP Publishing. https://doi.org/10.1088/1755-1315/250/1/012048

Ramli, N. H., Hisham, N. E. B., Said, F. M., Hisham, N. E. B., & Olalere, O. A. (2019). The role of wood vinegar in enhancing the microbial activity and physicochemical properties of palm oil-based compost. *Pertanika Journal of Tropical Agricultural Science*, *42*(4), 1391–1403.

Rastogi, M., Nandal, M., & Khosla, B. (2020). Microbes as vital additives for solid waste composting. *Heliyon*, *6*(2), e03343. https://doi.org/10.1016/j.heliyon.2020.e03343

Rios, J. J., Martínez-Ballesta, M. C., Ruiz, J. M., Blasco, B., & Carvajal, M. (2017). Silicon-mediated improvement in plant salinity tolerance: The role of aquaporins. *Frontiers in Plant Science*, *8*, 948. https://doi.org/10.3389/fpls.2017.00948

Román, P., Martínez, M. M., & Pantoja, A. (2015). *Farmer's compost handbook: Experiences in Latin America*. Food and Agriculture Organization of the United Nations.

Sapie, S., Jumali, S. S., Mustaffha, S., & Pebrian, D. E. (2019). Analysis of POME discharge quality from different mill in Perak, Malaysia: A case study. In *IOP Conference Series: Earth and Environmental Science* (Vol. 327, No. 1, p. 012022). IOP Publishing. https://doi.org/10.1088/1755-1315/327/1/012022

Schaller, J., Cramer, A., Carminati, A., & Zarebanadkouki, M. (2020). Biogenic amorphous silica as main driver for plant available water in soils. *Scientific Reports*, *10*, 2424. https://doi.org/10.1038/s41598-020-59437-x

Sharma, D., Varma, V. S., Yadav, K. D., & Kalamdhad, A. S. (2017). Evolution of chemical and biological characterization during agitated pile composting of flower waste. *International Journal of Recycling of Organic Waste in Agriculture*, *6*, 89–98. https://doi.org/10.1007/s40093-017-0155-9

Sharma, N. K., Singh, R. J., & Kumar, K. (2012). Dry matter accumulation and nutrient uptake by wheat (*Triticum aestivum* L.) under poplar (*Populus deltoides*) based agroforestry system. *International Scholarly Research Notices*, *2012*, 359673. https://doi.org/10.5402/2012/359673

Siddika, A., Mamun, M. A. Al, Alyousef, R., & Mohammadhosseini, H. (2021). State-of-the-

art-review on rice husk ash: A supplementary cementitious material in concrete. *Journal of King Saud University - Engineering Sciences*, *33*(5), 294–307. https://doi.org/10.1016/j.jksues.2020.10.006

Teuber, O., Samarappuli, D., & Berti, M. (2020). Nitrogen and sulfur fertilization in kale and swede for grazing. *Agronomy*, *10*(5), 619. https://doi.org/10.3390/agronomy10050619

Theeba, M., Bachmann, R. T., Illani, Z. I., Zulkefli, M., Husni, M. H. A., & Samsuri, A. W. (2012). Characterization of local mill rice husk charcoal and its effect on compost properties. *Malaysian Journal of Soil Science*, *16*(1), 89–102.

Wang, M., Ding, L., Gao, L., Li, Y., Shen, Q., & Guo, S. (2016). The interactions of aquaporins and mineral nutrients in higher plants. *International Journal of Molecular Sciences*, *17*(8), 1229. https://doi.org/10.3390/ijms17081229

Wang, Y., Zhang, X., Liu, H., Sun, G., Song, S., & Chen, R. (2022). High NH_4^+/NO_3^- ratio inhibits the growth and nitrogen uptake of Chinese kale at the late growth stage by ammonia toxicity. *Horticulturae*, *8*(1), 8. https://doi.org/10.3390/horticulturae8010008

Wijitkosum, S., & Jiwnok, P. (2019). Effect of biochar on chinese kale and carbon storage in an agricultural area on a high rise building. *AIMS Agriculture and Food*, *4*(1), 177–193. https://doi.org/10.3934/agrfood.2019.1.177

Xiang, Y., Zou, H., Zhang, F., Qiang, S., Wu, Y., Yan, S., Wang, H., Wu, L., Fan, J., & Wang, X. (2019). Effect of irrigation level and irrigation frequency on the growth of mini Chinese cabbage and residual soil nitrate nitrogen. *Sustainability*, *11*(1), 111. https://doi.org/10.3390/su11010111

Yin, M., Li, X., Liu, Q., & Tang, F. (2022). Rice husk ash addition to acid red soil improves the soil property and cotton seedling growth. *Scientific Reports*, *12*, 1704. https://doi.org/10.1038/s41598-022-05199-7

Yousaf, M., Bashir, S., Raza, H., Shah, A. N., Iqbal, J., Arif, M., Bukhari, M. A., Muhammad, S., Hashim, S., Alkahtani, J., Alwahibi, M. S., & Hu, C. (2021). Role of nitrogen and magnesium for growth, yield and nutritional quality of radish. *Saudi Journal of Biological Sciences*, *28*(5), 3021–3030. https://doi.org/10.1016/j.sjbs.2021.02.043

Pertanika J. Trop. Agric. Sci. 46 (1): 329 - 345 (2023)

PERTANIKA JOURNALS

TROPICAL AGRICULTURAL SCIENCE

Journal homepage: http://www.pertanika.upm.edu.my/

Phylogeny Study of 20 Selected Species of Zingiberaceae from *Ex situ* Collections in Peninsular Malaysia

Seemab Akram[1], Shamsul Khamis[2], Shahrizim Zulkifly[1], Rishzuan Talib[3] and Nurul Izza Ab Ghani[1,4]*

[1]Department of Biology, Faculty of Science, Universiti Putra Malaysia, 43400 Serdang, Selangor, Malaysia
[2]Faculty of Science and Technology, Universiti Kebangsaan Malaysia, 43600 Bangi, Selangor, Malaysia
[3]Biodiversity Unit, Institute of Bioscience, Universiti Putra Malaysia, 43400 Serdang, Selangor, Malaysia
[4]Laboratory of Sustainable Animal Production and Biodiversity, Institute of Tropical Agriculture and Food Security, Universiti Putra Malaysia, 43400 Serdang, Selangor, Malaysia

ABSTRACT

Zingiberaceae is widely distributed in Malaysia, with 750 species and 31 genera. This family comprises a different number of subfamilies and genera according to different taxonomic classification methods — classical taxonomy: one subfamily and four tribes *vs* molecular taxonomy: four subfamilies and six tribes. However, the taxonomic classification of Zingiberaceae is still debated, especially the classical taxonomy. It is due to some Zingiberaceae species showing cryptic morphologies that make it difficult to classify them through classical taxonomy, which refers to the unique morphological characteristics of a tribe/species. Therefore, accurate taxonomic classification is required by using a molecular approach. In this study, 20 selected species of Zingiberaceae collected from the Agricultural Conservatory Park, Institute of Bioscience (IBS), Universiti Putra Malaysia (UPM) were taxonomically classified using a molecular method with the help of three random amplified polymorphic DNA (RAPD) and three inter simple sequence repeat (ISSR) markers until the tribe level. The combined RAPD and ISSR unweighted pair group method with arithmetic mean (UPGMA) phylogenetic tree was comparable to Zingiberaceae's current molecular and classical taxonomy. The 20 selected species were grouped into three tribes (Alpinieae, Zingiberaceae, and Globbeae). This finding has contributed additional biological information to better manage the 20 Zingiberaceae species in the Agricultural Conservatory Park, IBS,

ARTICLE INFO

Article history:
Received: 30 August 2022
Accepted: 29 November 2022
Published: 22 February 2023

DOI: https://doi.org/10.47836/pjtas.46.1.18

E-mail addresses:
seemabakram@ymail.com (Seemab Akram)
shamsulk@ukm.edu.my (Shamsul Khamis)
shahrizim@upm.edu.my (Shahrizim Zulkifly)
rishzuan@upm.edu.my (Rishzuan Talib)
nurul_izza@upm.edu.my (Nurul Izza Ab Ghani)
* Corresponding author

ISSN: 1511-3701
e-ISSN: 2231-8542

UPM. Further studies are needed to explore the genetic diversities and properties of Zingiberaceae species.

Keywords: ISSR, phylogenetic tree, RAPD, taxonomy, Zingiberaceae

INTRODUCTION

Zingiberaceae is the largest family in the order Zingiberales and is widely distributed all over the world, mainly in the tropical and subtropical countries: America, Indonesia, Indochina, Malaysia, and Thailand (Burtt & Smith, 1972; Holttum, 1950; Kress et al., 2002; Larsen, 2007; Nagappan et al., 2019; Newman et al., 2004; Ridley, 1899; Schumann, 1904; Zahara, 2020). Zingiberaceae contains 55 genera with approximately 1,300 species (Royal Botanic Garden Edinburgh [RBGE], n.d.). In Malaysia, 750 species belonging to 31 genera can be found (Govaerts et al., 2022). At the same time, around 200 species belonging to 19 genera have been reported in Peninsular Malaysia (Nagappan et al., 2019).

The characteristics of the ovary, such as the number of locules and placentation, development of staminodia, and modifications of the fertile anther, as well as the rhizome and shoot-leaf orientation, have been used for classical taxonomy classification (Larsen et al., 1998). Accordingly, four tribes have been identified: Alpinieae, Hedychieae, Globbeae, and Zingiberaceae (Burtt & Smith, 1972; Holttum, 1950; Larsen et al., 1998; Schumann, 1904). On the other hand, Kress et al. (2002) classified Zingiberaceae by combining classical (used floral and vegetative characteristics) and molecular (used internal transcribed spacer [ITS] and *matK* markers) taxonomy classifications into four subfamilies and six tribes. The four subfamilies and six tribes are (i) subfamily Siphonochiloideae (tribe Siphonochileae), (ii) subfamily Tamijioideae (tribe Tamijieae), (iii) subfamily Alpinioideae (tribe Alpinieae and tribe Reidelieae), and (iv) subfamily Zingiberoideae (tribe Zingiberaceae and tribe Globbeae). However, discrepancies among the number of genera and species have remained for the family Zingiberaceae. Apart from ITS and *matK* markers, RAPD and ISSR have been used to assess the genetic diversity and genetic relationships/ molecular taxonomy of Zingiberaceae species (Bidyaleima et al., 2019; Siriluck et al., 2014; Theanphong et al., 2016, 2018). RAPD is a dominant marker that allows random sampling of a marker over whole genomic DNA (Morell et al., 1995; Welsh & McClelland, 1990). ISSR relies on repeat motifs of DNA sequences and is also a dominant marker (Mohanta et al., 2015).

The 20 selected Zingiberaceae species used in this study were a part of the Agricultural Conservatory Park, Institute of Bioscience (IBS), Universiti Putra Malaysia (UPM) *ex situ* collection. The Agricultural Conservatory Park, IBS, UPM is an *ex situ* conservation centre for Malaysia's many important, endangered, and unique plant species. The park has about 100 species of Zingiberaceae, and almost half of the Zingiberaceae species can be found.

The 20 selected Zingiberaceae species included in this study are known for their traditional and medicinal value (Baruaha et al., 2019; Behera, 2006; Chan et al., 2011; Chattopadhyay et al., 2004; Habsah et al., 2005; Hussain et al., 1992; Larsen et al., 1999; Malek et al., 2011; Srivastava et al., 2006). There are threatened and endangered species: *Alpinia rafflesiana*, *Scaphochlamys kunstleri*, and *Zingiber puberulum* (International Union for Conservation of Nature [IUCN], n.d.). However, only a few species have been scientifically studied in relation to their biological value and characteristics (Awang et al., 2011; Md-Mustafa et al., 2014; Wijekoon et al., 2011). Meanwhile, the taxonomic information for the 20 selected species in this study also needs to be updated. It has been classified taxonomically (Larsen et al., 1998). Nevertheless, some have confusing cryptic morphological characteristics, such as *Etlingera* and *Hornstedtia*. It has caused difficulty classifying them according to their morphological characteristics, especially for those not experts in taxonomy. Hence, this study aims to construct an accurate phylogeny tree of the 20 selected Zingiberaceae species using the molecular taxonomy method, which does not require the identification of tribes based on their morphological characteristics.

MATERIALS AND METHODS

Sampling Collection

Twenty species from three tribes and ten genera of Zingiberaceae (Table 1; 2–9 leaves for each plant — n = 1–3 per species) collected from the Agricultural Conservatory Park, IBS, UPM, Serdang, Selangor (3º00'01"N, 101º43'27"E). The samples were collected based on their morphological characteristics with the assistance of Dr Shamsul Khamis (a botanist) and Mr Rishzuan Talib (the park coordinator). Several references were used to identify them (Burtt & Smith, 1976; Larsen et al., 1998, 1999; Lim, 2000; Nurainas & Arbain, 2017). All leaves were washed with tap water and rinsed with distilled water to get rid of any debris. Then leaves were left overnight to dry at room temperature (26–30°C). Each sample was photographed using a Redmi Note 7 (China) with a megapixel dual camera of 1,080 × 2,340 pixels. All samples were stored in a -20°C freezer with labelled plastic bags before DNA extraction.

Table 1
List of 20 collected Zingiberaceae species from the Agricultural Conservatory Park, IBS, UPM

Plant	Individuals	Label	Voucher number
Alpinia mutica Roxb.	1	AM/1	ACP110/2005
Alpinia conchigera Griff.	1	AC/1	ACP51/2003
Alpinia rafflesiana Wall. ex. Baker	1	AR/1	ACP43/2003
Boesenbergia plicata (Ridl.) Holttum	1	BP/1	ACP226/2017
Boesenbergia rotunda (L.) Mansf.	1	BR/1	ACP38/2002
Curcuma longa L.	1	CL/1	ACP27/2002

Table 1 *(continue)*

Plant	Individuals	Label	Voucher number
Elettariopsis smithiae Y. K. Kam	1	ES/1	ACP112/2010
Elettariopsis smithiae var. *rogusa* (Y. K. Kam) C. K. Lam	1	ES v. R/1	ACP119/2010
Elettariopsis curtisii Baker	1	EC/1	ACP164/2013
Etlingera elatior (Jack) R. M. Sm.	1, 2, 3	EE/1, EE/2, EE/3	ACP42/2002
Etlingera terengganuensis C. K. Lim	1, 2, 3	ET/1, ET/2, ET/3	ACP125/2015
Globba nawawii Ibrahim & K. Larsen	1	GN/1	ACP107/2014
Hornstedtia leonurus (J. Keonig) Retz	1, 2, 3	HL/1, HL/2, HL/3	ACP201/2016
Kaempferia galanga L.	1	KG/1	ACP39/2002
Kaempferia pulchra Ridl.	1	KP/1	ACP118/2007
Scaphochlamys biloba (Ridl.) Holttum	1	SB/1	ACP181/2017
Scaphochlamys mat-kilau C. K. Lim	1	SM/1	ACP190/2017
Scaphochlamys kunstleri (Baker) Holttum	1	SK/1	ACP219/2017
Zingiber spectabile Griff.	1, 2, 3	ZS/1, ZS/2, ZS/3	ACP178/2015
Zingiber puberulum Ridl.	1, 2, 3	ZP/1, ZP/2, ZP/3	ACP184/2015

Data Collection and Analysis

Genomic DNAs were extracted from fresh or frozen leave samples (0.1 g) using the Qiagen DNeasy plant mini kit (Germany) following the manufacturer's protocol with some modifications. Modifications were made at the beginning of the DNA extraction protocol. The modifications included adding up 400 µl Buffer AP1 and 4 µl RNase into the tube containing the well-grinned sample before vortex vigorously and incubating the mixture at 65°C overnight to allow complete lysis of the cells. Samples were ground to a fine powder with the help of liquid nitrogen using sterilised pestles and mortars to begin the genomic DNA extractions. Successfully extracted genomic DNA was verified by using 0.8% agarose gel electrophoresis. Gel electrophoresis was run at 80 V, 250 current for 80 min. Clear and sharp visualisation of bands showed a successful DNA extraction. The bands were observed under UV light and photographed using ENDURO™ GDS Gel Documentation System (USA). High polymorphic RAPD (n = 11) and ISSR (n = 6) markers that were used by Singh et al. (2012) to assess genetic diversity among and within the agro-climatic zones of several Zingiberaceae species were used for PCR amplification. RAPD and ISSR markers were selected due to their extensive use for assessing genetic variations at different DNA levels and their cost-effectiveness and sensitivity. Moreover, they provide concise genetic information for taxonomy classification, conservation, breeding, and genetic improvement strategies (Ismail et al., 2016).

Furthermore, both markers have been used to identify the species of Zingiberaceae, including *Alpinia* spp. (Siriluck et al., 2014), *Boesenbergia* spp. (Vanijajiva et al., 2005), *Curcuma* spp. (Basak et al., 2017; Das et al., 2011; Kitamura et al., 2007; Prashanth

et al., 2015; Sahoo et al., 2017; Senan et al., 2013; Siriluck et al., 2014; Theanphong et al., 2016; Zou et al., 2011), and *Kaempferia* spp. (Devi et al., 2015; Pojanagaroon et al., 2004; Theanphong et al., 2018; Vanijajiva et al., 2005). PCR amplification for RAPD was performed as follows: initial denature at 94°C for 5 min, followed by 34 cycles of denaturing at 92°C for 1 min, annealing at 50–30°C for 1 min and extension at 72°C for 1½ min with a final extension at 72°C for 7 min. Whilst for ISSR, PCR amplifications were performed as follows: initial denature at 94°C for 1 min, followed by 34 cycles of denaturing at 94°C for 5 min, annealing at 70–40°C for 1½ min and extension at 72°C for 2 min with a final extension at 72°C for 7 min. PCR amplifications contained ≥ 50 ng template DNA, 50 ρmol primer, 25 mM magnesium chloride ($MgCl_2$), 1.5 mM Promega GoTaq® DNA Polymerase (USA), 7.5 mM buffer, 10 mM dNTPs mixed and topped up with ddH_2O to a final volume of 15 µL. PCR amplifications were performed using a BIO-RAD T100™ Thermal cycler (USA).

Amplified PCR regions were genotyped manually as "0" and "1," which showed the absence and presence of the bands for both RAPD and ISSR molecular markers. Only sharp bands were considered for the analysis, and then they were computerized/rechecked using PyElph 3.1 software as binary data (Table 2). The binary data were later used for computing similarity matrixes which were later used for building a dendrogram. A dendrogram was constructed using the SAHN module with a UPGMA in NTSYS-PC 2.10e software (Rohlf, 1998) to check the genetic relationship among 20 selected Zingiberaceae species. UPGMA is selected due to its common and valuable use for clustering trees using distance matrices (Nei & Kumar, 2000). UPGMA usually constructs a node at each stage and then makes a new node on a tree. This process continues from bottom to top and develops a new node at each step (Durbin et al., 1998; Rizzo & Eric, 2007). UPGMA combines a pair of operational taxonomic units (OTU) with high similarity into a new OTU, and OTU is composed of DNA or protein sequences (Nei & Kumar, 2000; Yujian & Xu, 2010). Furthermore, UPGMA constructs a tree which assumes a constant rate of evolution (Nei, 1987; Nei & Kumar, 2000).

Table 2
Binary data of combined data using three RAPD markers (OPD16, OPD08, and OPD20) and three ISSR (SPS04, SPS07, and SPS08) markers for 20 selected Zingiberaceae from Agricultural Conservatory Park, IBS, UPM

Primers	OPD16	OPD08	OPD20	SPS04	SPS07	SPS08
Expected band size (bp)	450-2,200	650-2,000	400-2,050	250-1,350	250-1,500	200-1,950
Species	Binary data using observed band size (bp)					
Alpinia mutica	1	1	1	1	1	1
Alpinia conchigera	1	1	1	1	1	1
Alpinia rafflesiana	1	1	1	1	1	1

Table 2 *(continue)*

Primers	OPD16	OPD08	OPD20	SPS04	SPS07	SPS08
Expected band size (bp)	450-2,200	650-2,000	400-2,050	250-1,350	250-1,500	200-1,950
Species	Binary data using observed band size (bp)					
Boesenbergia plicata	1	1	1	1	1	1
Boesenbergia rotunda	1	1	1	1	0	1
Curcuma longa	1	1	0	1	0	1
Elettariopsis smithiae	1	1	0	1	1	1
Elettariopsis smithiae var. *rugosa*	1	1	1	0	1	1
Elettariopsis curtisii	1	1	0	0	1	1
Etlingera elatior	1	1	1	1	1	1
Etlingera terengganuensis	1	1	0	1	1	1
Globba nawawii	1	1	0	1	0	0
Hornstedtia leonurus	1	1	1	1	1	1
Kaempferia galanga	1	1	1	1	1	0
Kaempferia pulchra	1	1	1	1	1	1
Scaphochlamys biloba	1	1	1	0	1	1
Scaphochlamys mat-kilau	1	1	1	1	1	1
Scaphochlamys kunstleri	1	1	1	1	1	1
Zingiber spectabile	1	1	1	1	1	1
Zingiber puberulum	1	1	1	1	1	1

There are three UPGMA phylogenetic trees (RAPD only, ISSR only, and combined RAPD and ISSR). However, RAPD-only and ISSR-only trees do not provide clear taxonomic classification until the tribe level. Some of the Alpinieae species were grouped into the Zingiberaceae tribe. Hence, RAPD-only and ISSR-only trees were rejected. However, the combined RAPD and ISSR tree provided clear taxonomic classification until the tribe level.

RESULTS

Among the three UPGMA phylogenetic trees, the combined tree of RAPD (OPD16, OPD08, and OPD20 markers) and ISSR (SPS04, SPS07, and SPS08 markers) (Figure 1) was the best and comparable to current molecular and classical taxonomy of Zingiberaceae (Kress et al., 2002, 2005, 2007; Larsen et al., 1998; Pederson, 2004; Rangsiruji et al., 2000; Xia et al., 2004). When compared to the taxonomy studies of Zingiberaceae reported by Kress et al. (2005), Larsen et al. (1998), Rangsiruji et al. (2000), Pederson (2004), and Xia et al. (2004), the 20 studied species were grouped according to their tribes (Alpinieae, Zingiberaceae, and Globbeae) similarly in the studies mentioned above. In this study, three clades were formed. Clade i comprised the Alpinieae tribe, the clade comprised the Zingiberaceae tribe and clade iii comprised the Globbeae tribe.

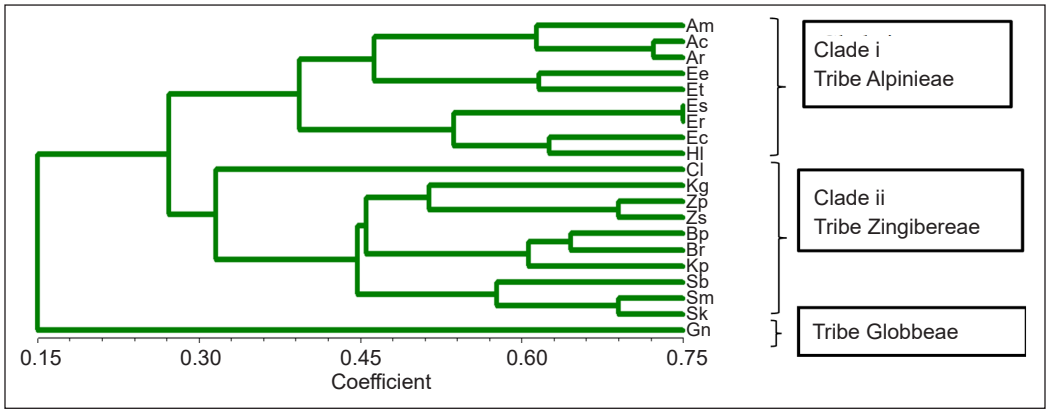

Figure 1. A UPGMA phylogenetic tree using combined data of three RAPD (OPD16, OPD08, and OPD20) and three ISSR (SPS04, SPS07, and SPS08) markers

Note. *Alpinia mutica* (Am), *Alpinia conchigera* (Ac), *Alpinia rafflesiana* (Ar), *Etlingera elatior* (Ee), *Etlingera terengganuensis* (Et), *Elettariopsis smithiae* (Es), *Elettariopsis smithiae* var. *rogusa* (Er), *Elettariopsis curtisii* (Ec), *Hornstedtia leonurus* (Hl), *Curcuma longa* (Cl), *Kaempferia galanga* (Kg), *Zingiber puberulum* (Zp), *Zingiber spectabile* (Zs), *Boesenbergia plicata* (Bp), *Boesenbergia rotunda* (Br), *Kaempferia pulchra* (Kp), *Scaphochlamys biloba* (Sb), *Scaphochlamys mat-kilau* (Sm), *Scaphochlamys kunstleri* (Sk), and *Globba nawawii* (Gn)

Clade i comprised all nine species from four genera (*Alpinia*, *Elettariopsis*, *Etlingera*, and *Hornstedtia*) of the tribe Alpinieae. All *Alpinia* species were grouped in one cluster. *Alpinia conchigera* (Ac) and *Alpinia rafflesiana* (Ar) were grouped in one cluster and shared the same root with *Alpinia mutica* (Am). The two *Etlingera* species, *Etlingera elatior* (Ee), and *Etlingera terengganuensis* (Et) were grouped in one cluster and connected to the genus *Alpinia*. Meanwhile, three *Elettariopsis* species and one *Hornstedtia* species were grouped in one cluster and connected to the genera *Alpinia* and *Etlingera*. *Elettariopsis smithiae* (Es) and *Elettariopsis smithiae* var. *rogusa* (Er) were grouped in one cluster and connected to *Elettariopsis curtisii* (Ec), which was grouped with *Hornstedtia leonurus* (Hl).

Clade ii comprised all ten species from five genera (*Boesenbergia*, *Curcuma*, *Kaempferia*, *Scaphochlamys*, and *Zingiber*) of the tribe Zingiberaceae. All *Scaphochlamys* species were grouped in one cluster. *Scaphochlamys mat-kilau* (Sm) and *Scaphochlamys kunstleri* (Sk) were grouped in one cluster and shared the same root with *Scaphochlamys biloba* (Sb). The two *Boesenbergia* species, *Boesenbergia plicata* (Bp) and *Boesenbergia rotunda* (Br) were grouped in one cluster and connected to *Kaempferia pulchra* (Kp). The two *Zingiber* species, *Zingiber puberulum* (Zp) and *Zingiber spectabile* (Zs) were grouped in one cluster and connected to *Kaempferia galanga* (Kg). The *Kaempferia* species, *Kaempferia pulchra* (Kp) and *Kaempferia galanga* (Kg) mixed with *Boesenbergia* and *Zingiber* species. Meanwhile, *Curcuma longa* (Cl) branched alone and connected to the four genera (*Boesenbergia*, *Kaempferia*, *Scaphochlamys*, and *Zingiber*) of the tribe

Zingiberaceae. Clade iii is comprised of one species of Globbeae tribe, which is *Globba nawawii*.

DISCUSSION

The RAPD and ISSR markers were used for studying the molecular taxonomy of 20 selected Zingiberaceae species from the Agricultural Conservatory Park, IBS, UPM. These 20 selected Zingiberaceae species are important to the endangered and unique *ex situ* collections of Zingiberaceae species from Peninsular Malaysia. A UPGMA phylogenetic tree built from three RAPD and three ISSR markers showed that the 20 selected Zingiberaceae species can be successfully grouped until the tribe level. Three clades were formed: (1) Clade i of tribe Alpinieae, (2) Clade ii of tribe Zingiberaceae, and (3) Clade iii of tribe Globbeae.

The combined RAPD and ISSR UPGMA phylogenetic tree were comparable to Zingiberaceae's recent molecular and classical taxonomy (Kress et al., 2002, 2005, 2007; Pederson, 2004; Rangsiruji et al., 2000; Xia et al., 2004). This UPGMA phylogenetic tree agrees with Kress et al. (2002, 2005, 2007) and Pederson (2004), whereby both have grouped the tribe Alpinieae and tribe Zingiberaceae as two major clades. Within the tribe Alpinieae, the genus *Alpinia* was separated from other genera (*Elettariopsis*, *Etlingera*, and *Hornstedtia*). Meanwhile, within the tribe Zingiberaceae, the genus *Scaphochlamys* was separated from other genera (*Boesenbergia*, *Kaempferia*, and *Zingiber*), and the genus *Curcuma* branched out from other genera (*Scaphochlamys*, *Boesenbergia*, *Kaempferia*, and *Zingiber*). It agrees with other studies (Kress et al., 2002, 2005, 2007; Pederson, 2004; Xia et al., 2004). The present study grouped *Elettariopsis* and *Hornstedtia* in one cluster but separated it from *Etlingera*. Hence, they do not support *Etlingera* and *Hornstedtia* as two complex genera with confusing taxonomic classifications and cryptic morphologies (Kress et al., 2002; Pederson, 2004). *Etlingera* and *Hornstedtia* are sister groups because both have sterile bracts and a fertile bract that subtends a single flower (Kress et al., 2002), except for *Hornstedtia leonurus* (Pederson, 2004). *Hornstedtia leonurus* is unique in the genus, having more than one flower per bract and a tubular bracteole that is occasionally open to the base in Lambir plants. Flower of this species is not easily recognised in dark forests, while during the day, they can be easily identified due to dense brown hairs on leaf margins, truncate, subcordate leaf bases, and 1-2 cm prominent petiole (Sakai & Nagamasu, 2003). Genus *Kaempferia* was confounded with genera *Boesenbergia* and *Zingiber*. It is different from Kress et al. (2002). In addition, this study showed tribe Globbeae connected with the tribe Alpinieae and the tribe Zingiberaceae. However, this contradicts Kress et al. (2002, 2005) — the tribe Globbeae is not distinguished from the tribe Zingiberaceae.

The selected RAPD and ISSR markers used in this study have shown high success amplification in 55 accessions of *Curcuma longa* and five cultivars from different

agroclimatic zones of Zingiberaceae (Singh et al., 2012). One of the species studied by Singh et al. (2012), *Curcuma longa*, is used in this study. RAPD and ISSR markers are simple, dominant, highly reproducible, polymorphic, and easily handle molecular markers (RAPD: Zietkiewicz et al., 1994; Bornet & Branchard, 2001, 2004; ISSR: Welsh & McClelland, 1990; Williams et al., 1990). RAPD and ISSR have been used for genetic diversity and genetic relationship/taxonomy studies within Zingiberaceae species (RAPD: Das et al., 2011; Jatoi et al., 2008; Saha et al., 2016; Techaprasan et al., 2008; ISSR: Das et al., 2015; Siriluck et al., 2014; Taheri et al., 2012). Applications to molecular markers to identify and characterise species according to their genetic information differ according to their efficiency, including the level of polymorphism, locus specificity, genomic abundance, technical requirements, and reproducibility (Spooner et al., 2005). In the present study, RAPD is more reproducible than ISSR because all 11 RAPD markers amplified and produced clear and sharp bands.

Taxonomy classification of the family Zingiberaceae is still under debate because new species are being discovered in the 21st century and are taxonomically classified by referring to their morphological characteristics. Hence, there is a need to revise the taxonomy classification of the family Zingiberaceae to correctly place all newly identified species under their correct tribes and subfamilies. For instance, two new species of Zingiberaceae: *Amomum bungoensis* and *Sundamomum corrugatum*, have been reported in Malaysia (Mohamad et al., 2020; Syazana et al., 2018). Another new Zingiberaceae species: *Etlingera terengganuensis* is an endemic species to Terengganu and was discovered in the year 2000 (Khaw, 2001; Lim, 2000) and 11 new species of Zingiberaceae from the genus *Scaphochlamys*: *Scaphochlamys durga*, *Scaphochlamys hasta*, *Scaphochlamys nigra*, *Scaphochlamys uniflora*, *Scaphochlamys multifolia*, *Scaphochlamys lucens*, *Scaphochlamys lanjakensis*, *Scaphochlamys penyama*, *Scaphochlamys graveolens*, *Scaphochlamys scintillans*, and *Scaphochlamys peuedoreticosa* have been investigated in Borneo (Im Hin et al., 2017). Five new species of Zingiberaceae including *Boesenbergia bella*, *Boesenbergia phenklaii*, *Boesenbergia putianai*, *Kaempferia phuphanensis*, and *Globba sirirugsae* have been discovered in Thailand (Mood et al., 2019). Two new Zingiberaceae species have been reported in Indonesia: *Zingiber alba* (Nurainas & Arbain, 2017) and *Etlingera megalocheilos* (Trimanto & Haspari, 2018).

All 20 selected species of Zingiberaceae have valuable uses for medicinal and economic ornamental purposes. Rhizome of *Alpinia conchigera* and *Alpinia mutica* is used to treat gastrointestinal disorders, and *Alpinia conchigera* is used in traditional Thai dishes (Awang et al., 2011; Malek et al., 2011). The fruit and rhizome of *Alpinia rafflesiana* have been used for their anti-microbial and anti-inflammatory properties (Ahmad et al., 2006; Jusoh et al., 2013). Rhizome of *Boesenbergia rotunda* is used

to treat dyspepsia, gastrointestinal disorders, mouth ulcers, dermatitis, diarrhoea, and dry cough (Md-Mustafa et al., 2014; Tewtrakul et al., 2003) and dried leaves are used in treating food poisoning and controlling allergies (Eng-Chong et al., 2012). Leaves of *Boesenbergia plicata* are used in treating human immunodeficiency viruses (HIV), protease inhibitory activity, and as an anti-inflammatory (Tewtrakul et al., 2003; Tuchinda et al., 2002). Rhizome of *Curcuma longa* is used in wound healing, common cold, stomachache, treatment of piles, antidiabetic, anti-chlorotic, anti-rheumatic, hypocholesterolemic, anti-fibrotic, antiviral, antihepatotoxic, antivenomous, anti-microbial, and for its anti-inflammatory and anti-cancerous properties (Akinyemi et al., 2015; Behera, 2006; Chattopadhyay et al., 2004; Hussain et al., 1992; Srivastava et al., 2006). Leaves of *Curcuma longa* are used in Peninsular Malaysia as a flavouring agent in spicy and savoury dishes (Larsen et al., 1999). Leaves, rhizomes, flower buds, and fruit of *E. elatior* are used to cure earaches and heal wounds and are used for their anticancer, antibacterial, antioxidant, antiproliferative, and cytotoxic activity. The flower bud is used in dishes, such as nasi kerabu, nasi ulam, and asam laksa in Peninsular Malaysia (Chan, Han, et al., 2007; Chan, Lim, et al., 2007; Jackie et al., 2011; Khaw, 2001; Lachumy et al., 2010; Larsen et al., 1999; Wijekoon et al., 2011). Furthermore, *E. elatior* is grown for ornamental and commercial purposes (Chan et al., 2007b; Khaw et al., 2001; Larsen et al., 1999). *Etlingera curtisii* whole plant is used for carminative, antioxidant and antibacterial properties, and leaves are eaten as vegetables, added in chilly spices to enhance the flavour, as decoration and bath, and to stimulate gastric secretions (Chairgulprasert et al., 2008). *Keampferia galanga* leaves and rhizomes are used in cosmetic powder, flavouring agents, and traditional medicine to treat swelling, toothache, headache, stomach-ache, and rheumatism (Ibrahim, 1999; Larsen et al., 1999; Mitra et al., 2007). In addition, leaves, rhizome, and stem of *Zingiber spectabile* are eaten as salad and used as a flavouring agent in food, as an antiproliferative, antioxidant, and anticancer purpose (Lim, 2020; Rahman, Rasedee, Abdul, et al., 2014; Rahman, Rasedee, Yeap, et al., 2014).

CONCLUSION

This study provided additional biological information to the 20 selected Zingiberaceae species to help better conserve the species in the Agricultural Conservatory Park, IBS, UPM. The combined RAPD and ISSR UPGMA phylogenetic tree classed them according to their three tribes (Alpinieae, Zingiberaceae, and Globbeae). However, the 20 selected Zingiberaceae species cannot be classed until their genera. Hence, additional markers are required. In addition, further studies are needed to explore the genetic diversities and properties of Zingiberaceae species.

ACKNOWLEDGEMENTS

We sincerely thank the Genome-Wide Association Laboratory (GWA Lab.)

members for their support in completing this project. Also, we are thankful to the anonymous reviewers for their comments and improvements in the writing of this paper. This study is a part of a PhD project entitled "Molecular study of selected Zingiberaceae species from *ex situ* collections of Peninsular Malaysia". It is partially funded by the Universiti Putra Malaysia through International Graduate Student Scholarship (IGSS).

REFERENCES

Ahmad, S., Israf, D. A., Lajis, N. H., Shaari, K., Mohamed, H., Wahab, A. A., & Somchit, M. N. (2006). Cardamonin, inhibits pro-inflammatory mediators in activated RAW 264.7 cells and whole blood. *European Journal of Pharmacology*, *538*(1-3), 188-194. https://doi.org/10.1016/j.ejphar.2006.03.070

Akinyemi, A. J., Adedara, I. A., Thome, G. R., Morsch, V. M., Rovani, M. T., Mujica, L. K. S., Duarte, T., Duarte, M., Oboh, G., & Schetinger, M. R. C. (2015). Dietary supplementation of ginger and turmeric improves reproductive function in hypertensive male rats. *Toxicology Reports*, *2*, 1357-1366. https://doi.org/10.1016/j.toxrep.2015.10.001

Awang, K., Ibrahim, H., Rosmy, S. D., Mohtar, M., Mat, A. R., & Azah, M. A. N. (2011). Chemical constituents and antimicrobial activity of the leaf and rhizome oils of *Alpinia pahangensis* Ridl., an endemic wild ginger from Peninsular Malaysia. *Chemistry and Biodiversity*, *8*(4), 668-673. https://doi.org/10.1002/cbdv.201000225

Baruaha, J., Sudin, K. P., Twahira, B., Neelav, S., Manabi, P., & Mohan, L. (2019). Molecular diversity assessed amongst high dry rhizome recovery Ginger germplasm (*Zingiber officinale* Roscoe) from NE-India using RAPD and ISSR markers. *Industrial Crops and Products*, *129*, 463-471. https://doi.org/10.1016/j.indcrop.2018.12.037

Basak, S., Kesari, V., Ramesh, A. M., Rangan, L., Parida, A., & Mitra, S. (2017). Assessment of genetic variation among nineteen turmeric cultivars of Northeast India: Nuclear DNA content and molecular marker approach. *Acta Physiologiae Plantarum*, *39*, 45. https://doi.org/10.1007/s11738-016-2341-1

Behera, K. K. (2006). Ethnomedicinal plants used by the tribals of Similipal Bioreserve, Orissa, India: A pilot study. *Ethnobotanical Leaflets*, *2006*(1), 17.

Bidyaleima, L., Kishor, R., & Sharma, G. J. (2019). Chromosome numbers, RAPD and ISSR profiles of six *Zingiber* species found in Manipur, India. *Biodiversitas*, *20*(5), 1389-1397. https://doi.org/10.13057/biodiv/d200531

Bornet, B., & Branchard, M. (2001). Nonanchored inter simple sequence repeat (ISSR) markers: Reproducible and specific tools for genome fingerprinting. *Plant Molecular Biology Reporters*, *19*, 209-215. https://doi.org/10.1007/BF02772892

Bornet, B., & Branchard, M. (2004). Use of ISSR fingerprints to detect microsatellites and genetic diversity in several related *Brassica* taxa and *Arabidopsis thaliana*. *Hereditas*, *140*(3), 245-248. https://doi.org/10.1111/j.1601-5223.2004.01737.x

Burtt, B. L., & Smith, R. M. (1972). Key species in the taxonomic history of Zingiberaceae. *Notes from the Royal Botanic Garden Edinburgh*, *31*, 177-227.

Burtt, B. L., & Smith, R. M. (1976). Notes on the collection of Zingiberaceae. *Flora Malesiana Bulletin*, *29*(1), 2599-2601.

Chairgulprasert, V., Somporn, P., Supanun, J., & Matira, S. (2008). Chemical constituents of

the essential oil, antioxidant and antibacterial activities from *Elettariopsis curtisii* Baker. *Songklanakarin Journal of Science and Technology*, *30*(5), 591-596.

Chan, E. W. C., Han, Y.Y. L., & Lim, T.Y. (2007). Total phenolic content and antioxidant activity of leaves and rhizomes of some ginger species in Peninsular Malaysia. *The Gardens' Bulletin Singapore*, *59*(1-2), 47-56.

Chan, E. W. C., Lim, Y. Y., & Omar, M. (2007). Antioxidant and antibacterial activity of leaves of *Etlingera* species (Zingiberaceae) in Peninsular Malaysia. *Food Chemistry*, *104(*4), 1586-1593. https://doi.org/10.1016/j.foodchem.2007.03.023

Chan, E. W. C., Lim, Y. Y., & Wong, S. K. (2011). Antioxidant properties of ginger leaves: An overview. *Free Radicals and Antioxidants*, *1*(1), 6-16. https://doi.org/10.5530/ax.2011.1.3

Chattopadhyay, I., Biswas, K., Bandyopadhyay, U., & Banerjee, R. K. (2004). Turmeric and curcumin: Biological actions and medicinal applications. *Current Science*, *87*(1), 44-53.

Das, A., Kesari, V., Satyanarayana, V. M., Parida, A., & Rangan, L. (2011). Genetic relationship of *Curcuma* species from Northeast India using PCR-based markers. *Molecular Biotechnology*, *49*(1), 65-76. https://doi.org/10.1007/s12033-011-9379-5

Das, A., Kesari, V., Satyanarayana, V. M., Parida, A., Mitra, S., & Rangan, L. (2015). Genetic diversity in ecotypes of the scarce wild medicinal crop *Zingiber moran* revealed by ISSR and AFLP marker analysis and chromosome number assessment. *Plant Biosystems-An International Journal Dealing with all Aspects of Plant Biology*, *149*(1), 111-120. https://doi.org/10.1080/11263504.2013.795197

Devi, K. D., Singh, S. B., Singh, N. S., Chingakham, B. S., Punyarani, K., & Devi, H. S. (2015). Evaluation of genetic relationships and chemical assay of *Kaempferia galanga* L. cultivars found in Manipur, North-East India. *International Journal of Recent Scientific Research*, *6*(6), 4366-4373.

Durbin, R., Eddy, S., Krogh, A., & Mitchison, G. (1998). *Biological sequence analysis: Probabilistic models of proteins and nucleic acids*. Cambridge University Press. https://doi.org/10.1017/CBO9780511790492

Eng-Chong, T., Lee, Y. K., Chee, C. F., Heh, C. H., Wong, S. M., Christina, T. L. P., Foo, G. T., Norzulaani, K., Noorsaadah, A. R.,Saiful, A. K., Shatrah,O., & Rozana, O. (2012). *Boesenbergia rotunda*: From ethnomedicine to drug discovery. *Evidence-Based Complementary and Alternative Medicine*, *2012*, 473637. https://doi.org/10.1155/2012/473637

Govaerts, R., Newman, M., & Lock, J. M. (2022). *World checklist of Zingiberaceae*. https://checklistbuilder.science.kew.org/reportbuilder.do

Habsah, M., Ali, A. M., Lajis, N. H., Sukari, M. A., Yap, Y. H., Kikuzaki, H., & Nakatani, N. (2005). Antitumour-promoting and cytotoxic constituents of *Etlingera elatior*. *Malaysian Journal of Medical Sciences*, *12*(1), 6-12.

Holttum, R. E. (1950). The Zingiberaceae of the Malay Peninsula. *The Gardens' Bulletin, Singapore*, *13*, 1-249.

Hussain, A., Virmani, O. P., Popli, S. P., Mishra, L. N., Gupta, M. M., Srivastava, G. N., & Singh, A. K. (1992). *Dictionary of Indian medicinal plants*. Central Institute of Medical and Aromatic Plants (CIMAP).

Ibrahim, H. (1999). *Kaempferia*. In L. S. de Padua, N. Bunyapraphatsara, & R. H. M. J. Lemmens (Eds.), *Plant resources of South-East Asia* (Vol. 12, pp. 331-335). Backhuys Publishers.

Im Hin, O. O. I., Kalu, M., & Yeng, W. S. (2017). A review of *Scaphochlamys* (Zingiberaceae) from Borneo, with description of eleven new

species. *Phytotaxa*, *317*(4), 231-279. https://doi.org/10.11646/phytotaxa.317.4.1

International Union for Conservation of Nature. (n.d.). *The IUCN Red List of Threatened Species*™. IUCN. https://www.iucnredlist.org/

Ismail, N. A., Rafii, M. Y., Mahmud, T. M. M., Hanafi, M. M., & Miah, G. (2016). Molecular markers: A potential resource for ginger genetic diversity studies. *Molecular Biology Reports*, *43*(12), 1347-1358. https://doi.org/10.1007/s11033-016-4070-3

Jackie, T., Haleagrahara, N., & Chakravarthi, S. (2011). Antioxidant effects of *Etlingera elatior* flower extract against lead acetate-induced perturbations in free radical scavenging enzymes and lipid peroxidation in rats. *BMC Research Notes*, *4*, 67. https://doi.org/10.1186/1756-0500-4-67

Jatoi, S. A., Kikuchi, A., Mimura, M., Yi, S., & Watanabe, K. N. (2008). Relationships of *Zingiber* species, and genetic variability assessment in ginger (*Zingiber officinale*) accessions from *ex situ* gene bank, on–farm and rural markets. *Breeding Science*, *58*(3), 261-270. https://doi.org/10.1270/jsbbs.58.261

Jusoh, S., Hasnah, M. S., & Farediah, A. (2013). Essential oils of *Alpinia rafflesiana* and their antimicrobial activities. *Natural Product Communications*, *8*(9), 1317-1320. https://doi.org/10.1177/1934578X1300800933

Khaw, S. H. (2001). The genus *Etlingera* (Zingiberaceae) in Peninsular Malaysia including a new species. *The Gardens' Bulletin, Singapore*, *53*(1-2), 191-239.

Kitamura, C., Nagoe, T., Prana, M. S., Agusta, A., Ohashi, K., & Shibuya, H. (2007). Comparison of *Curcuma* sp. in Yakushima with *C. aeruginosa* and *C. zedoaria* in Java by *trn*K gene sequence, RAPD pattern and essential oil component. *Journal of Natural Medicines*, *61*, 239-243. https://doi.org/10.1007/s11418-006-0131-6

Kress, W. J., Liu, A., Newman, M., & Li, Q. (2005). The molecular phylogeny of *Alpinia* (Zingiberaceae): A complex and phylogenetic genus of gingers. *American Journal of Botany*, *92*(1), 167-178. https://doi.org/10.3732/ajb.92.1.167

Kress, W. J., Newman, M. F., Poulsen, A. D., & Specht, C. (2007). An analysis of generic circumscriptions in tribe Alpinieae (Alpinioideae: Zingiberaceae). *Gardens' Bulletin Singapore*, 59(1-2), 113-128.

Kress, W. J., Prince, L. M., & Williams, K. J. (2002). The phylogeny and a new classification of the gingers (Zingiberaceae): Evidence from molecular data. *American Journal of Botany*, *89*(10), 1682-1696. https://doi.org/10.3732/ajb.89.10.1682

Lachumy, S. J. T., Sasidharan, S., Sumathy, V., & Zuraini, Z. (2010). Pharmacological activity, phytochemical analysis, and toxicity of methanol extract of *Etlingera elatior* (torch ginger) flowers. *Asian Pacific Journal of Tropical Medicine*, *3*(10), 769-774. https://doi.org/10.1016/S1995-7645(10)60185-X

Larsen, K. (2007). The exploration of gingers in SE Asia – Some milestones and perspectives symposium. *The Gardens' Bulletin Singapore*, *59*(2), 1-12.

Larsen, K., Ibrahim, H., Khaw, S. H., & Saw, L. G. (1999). *Gingers of Peninsular Malaysia and Singapore*. Natural History Publications (Borneo).

Larsen, K., Lock, J. M., Maas, H., & Maas, P. J. M. (1998). Zingiberaceae. In K. Kubitzki (Ed.), *Flowering plants monocotyledons* (pp. 474-495). Springer. https://doi.org/10.1007/978-3-662-03531-3_49

Lim, C. K. (2000). Taxonomic notes on *Etlingera* Giseke (Zingiberaceae) in Peninsular Malaysia: The "*Nicolaia*" taxa. *Folia Malaysiana*, *1*(1), 1-12.

Malek, S. N. A., Phang, C. W., Ibrahim, H., Abdul Wahab, N., & Sim, K. S. (2011). Phytochemical and cytotoxic investigations of *Alpinia mutica* rhizomes. *Molecules*, *16*(1), 583-589. https://doi.org/10.3390/molecules16010583

Md-Mustafa, N. D., Khalid, N., Gao, H., Peng, Z., Alimin, M. F., Bujang, N., & Othman, R. Y. (2014). Transcriptome profiling shows gene regulation patterns in a flavonoid pathway in response to exogenous phenylalanine in *Boesenbergia rotunda* cell culture. *BMC Genomics*, *15*, 984. https://doi.org/10.1186/1471-2164-15-984

Mitra, R., Orbell, J., & Muralitharan, M. S. (2007). Agriculture - Medicinal plants of Malaysia. *Asia-Pacific Biotech News*, *11*(2), 105-110. https://doi.org/10.1142/S0219030307000110

Mohamad, S., Kalu, M., & Poulsen, A. D. (2020). A new species and a new combination of *Sundamomum* (Zingiberaceae) from Sarawak, Borneo. *Kew Bulletin*, *75*, 58. https://doi.org/10.1007/s12225-020-09919-y

Mohanta, S., Swain, P. K., Sial, P., & Rout, G. R. (2015). Morphological and molecular screening of turmeric (*Curcuma longa* L.) cultivars for resistance against parasitic nematode, *Meloidogyne incognita*. *Journal of Plant Pathology and Microbiology*, *6*, 270. https://doi.org/10.4172/2157-7471.1000270

Mood, J. D., Veldkamp, J. F., Mandakova, T., Prince, L. M., & de Boer, H. J. (2019). Three new species of *Boesenbergia* (Zingiberaceae) from Thailand and Lao P. D. R. *The Gardens' Bulletin Singapore*, *71*(2), 473-495.

Morell, M. K., Peakall, R., Appels, R., Preston, L. R., & Lloyd, H. L. (1995). DNA profiling techniques for plant variety identification. *Australian Journal of Experimental Agriculture*, *35*(6), 807-819. https://doi.org/10.1071/EA9950807

Nagappan, T., Tatin, Y., & Skornickova, J. L. (2019). Investigation on bioactive potential of selected wild ginger, genus *Etlingera* from Tasik Kenyir, Terengganu. In M. Abdullah, A. Mohammad, M. Nor Zalipah, & M. Safiih Lola (Eds.), *Greater Kenyir landscapes* (pp. 75-82). Springer. https://doi.org/10.1007/978-3-319-92264-5_7

Nei, M. (1987). *Molecular evolutionary genetics*. Columbia University Press.

Nei, M., & Kumar, S. (2000). *Molecular evolution and phylogenetics*. Oxford University Press.

Newman, M., Lhuillier, A., & Poulsen, A. D. (2004). Checklist of the Zingiberaceae of Malesia. *Blumea Supplement*, *16*, 1-166.

Nurainas, N., & Arbain, D. (2017). A new species and a new record of Zingiberaceae from Sumatra, Indonesia. *Taiwania*, *62*(3), 294-298. https://doi.org/10.6165/tai.2017.62.294

Pederson, L. M. (2004). Phylogenetic analysis of the subfamily Alpinioideae (Zingiberaceae), particularly *Etlingera* Giseke, based on nuclear and plastid DNA. *Plant Systematics and Evolution*, *245*(3), 239-258. https://doi.org/10.1007/s00606-004-0126-2

Pojanagaroon, S., Praphet, R., Kaewrak, C., & Yotdi, A. (2004). Characterization of Krachai-Dam (*Kaempferia parviflora*) cultivars using RAPD markers, morphological traits and chemical components of essential oil from rhizomes. In *Proceedings of the 42nd Kasetsart University Annual Conference* (pp. 56-65). Kasetsart University Press.

Prashanth, N., Yugander, A., & Bhavani, N. L. (2015). DNA isolation and PCR amplification of turmeric varieties from Telangana State. *International Journal of Current Microbiology and Applied Sciences*, *4*(5), 485-490.

Rahman, H. S., Rasedee, A., Abdul, A. B., Zeenathul, N. A., Othman, H. H., Yeap, S. K., & Hafiza, W. A. G. W. N. (2014). Zerumbone-loaded nanostructured lipid carrier induces G2/M cell cycle arrest and apoptosis via mitochondrial

pathway in a human lymphoblastic leukemia cell line. *International Journal of Nanomedicine*, *9*(1), 527-538. https://doi.org/10.2147/IJN.S54346

Rahman, H. S., Rasedee, A., Yeap, S. K., Othman, H. H., Chartrand, M. S., Namvar, F., Abdul, AB., & How, C. W. (2014). Biomedical properties of a natural dietary plant metabolite, zerumbone, in cancer therapy and chemoprevention trials. *BioMed Research International*, *2014*, 920742. https://doi.org/10.1155/2014/920742

Rangsiruji, A., Newman, M. F., & Cronk, Q. C. B. (2000). A study of the infrageneric classification of *Alpinia* (Zingiberaceae) based on the *ITS* region of nuclear rDNA and the *trnL-F* spacer of chloroplast DNA. In K. L. Wilson & D. A. Morrison (Eds.), *Monocots-systematics and evolution* (pp. 695-709). Commonwealth Scientific and Industrial Research Organisation.

Ridley, H. N. (1899). The Scitamineae of the Malay Peninsula. *Journal of the Straits Branch of the Royal Asiatic Society*, (32), 85-184.

Rizzo, J., & Eric, C. R. (2007). *Review of phylogenetic tree construction*. http://bioinformatics.louisville.edu/lab/localresources/papers/TR-ULBL-2007-01.pdf

Rohlf, F. J. (1998). *NTSYSpc: Numerical taxonomy and multivariate analysis system – Getting started guide* (version 2.0). Applied Biostatistics Inc.

Royal Botanic Garden Edinburgh. (n.d.). *Zingiberaceae*. https://www.rbge.org.uk/science-and-conservation/tropical-diversity/taxonomy-and-phylogenetics/zingiberaceae/

Saha, K., Sinha, R. K., Basak, S., & Sinha, S. (2016). ISSR fingerprinting to ascertain the genetic relationship of *Curcuma* sp. of Tripura. *American Journal of Plant Sciences*, *7*(2), 259-266. https://doi.org/10.4236/ajps.2016.72025

Sahoo, A., Jena, S., Kar, B., Sahoo, S., Ray, A., Singh, S., & Nayak, S. (2017). EST-SSR marker revealed effective over biochemical and morphological scepticism towards identification of specific turmeric (*Curcuma longa* L.) cultivars. *3 Biotech*, *7*, 84. https://doi.org/10.1007/s13205-017-0701-1

Sakai, S., & Nagamasu, H. (2003). Systematic studies of Bornean Zingiberaceae IV. Alpinioideae of Lambir Hills, Sarawak. *Edinburgh Journal of Botany*, *60*(2), 181-216. https://doi.org/10.1017/S0960428603000143

Schumann, K. (1904). Zingiberaceae. *In* A. Engler (Ed.), *Das pflanzenreich* [The plant kingdom] (Vol. IV, pp. 1-458). Wilhelm Engelmann.

Senan, S., Kizhakayil, D., Sheeja, T. E., Sasikumar, B., Bhat, A. I., & Parthasarathy, V. A. (2013). Novel polymorphic microsatellite markers from turmeric, *Curcuma longa* L. (Zingiberaceae). *Acta Botanica Croatica*, *72*(2), 407-412. https://doi.org/10.2478/botcro-2013-0002

Singh, S., Manoj, K. P., & Sanghamitra, N. (2012). Evaluation of genetic diversity in turmeric (*Curcuma longa* L.) using RAPD and ISSR markers. *Industrial Crops and Products*, *37*(1), 284-291. https://doi.org/10.1016/j.indcrop.2011.12.022

Siriluck, I., Ratchanok, T., Worakij, H., & Thitamin, K. (2014). Identification of 24 species of Zingiberaceae in Thailand using ISSR technique. *Thai Journal of Agricultural Science*, *47*(1), 1-6.

Spooner, D., Treuren, V. R., & de Vicente, M. C. (2005). *Molecular markers for germplasm and genebank management*. International Plant Genetic Resources Institute.

Srivastava, S., Srivastava, M., Rawat, A. K. S., & Mehrotra, S. (2006). Pharmacognostic evaluation of *Curcuma amada* Roxb. *Proceedings of National Academy of Sciences*, *India Section B*, *76*(2), 153-160.

Syazana, S., Meekiong, K., Afifah, N., & Syauqina, M. Y. (2018). *Amomum bungoensis*: A new species of *Amomum* (Zingiberaceae) from Sarawak, Malaysia. *Journal of Botany*, *2018*, 1978607. https://doi.org/10.1155/2018/1978607

Taheri, S., Abdullah, T. L., Abdullah, N. A., & Ahmad, Z. (2012). Genetic relationships among five varieties of *Curcuma alismatifolia* (Zingiberaceae) based on ISSR markers. *Genetics and Molecular Research*, *11*(3), 3069-3076. https://doi.org/10.4238/2012.August.31.4

Techaprasan, J., Klinbunga, S., & Jenjittikul, T. (2008). Genetic relationships and species authentication of *Boesenbergia* (Zingiberaceae) in Thailand based on AFLP and SSCP analyses. *Biochemical Systematics and Ecology*, *36*(5-6), 408-416. https://doi.org/10.1016/j.bse.2007.10.006

Tewtrakul, S., Subhadhirasakul, S., Puripattanavong, J., & Panphadung, T. (2003). HIV-1 protease inhibitory substances from the rhizome of *Boesenbergia pandurata* Holtt. *Songklanakarin Journal of Science and Technology*, *25*(4), 503-508.

Theanphong, O., Jenjittikul, T., Mingvanish, W., & Rungsihirunrat, K. (2018). Phylogenetic relationships of *Kaempferia* plants based on inter-simple sequence repeat fingerprints. *Songklanakarin Journal of Science and Technology*, *40*(3), 617-622. https://doi.org/10.14456/sjst-psu.2018.81

Theanphong, O., Thanakijcharoenpath, W., Palanuvej, C., Ruangrungsi, N., & Rungsihirunrat, K. (2016). RAPD marker for determination of phylogenetic relationships of 15 *Curcuma* species from Thailand. *Bulletin of Health Science and Technology*, *14*(1), 45-56.

Trimanto, T., & Hapsari, L. (2018). A new record of *Etlingera megalocheilos* (Griff.) A. D. Poulsen (Zingiberaceae) in Sulawesi, Indonesia. *Biodiversitas Journal of Biological Diversity*, *19*(4), 1227-1235. https://doi.org/10.13057/biodiv/d190407

Tuchinda, P., Reutrakul, V., Claeson, P., Pongprayoon, U., Sematong, T., Santisuk, T., & Taylor, W. C. (2002). Anti-inflammatory cyclohexenyl chalcone derivatives in *Boesenbergia pandurata*. *Phytochemistry*, *59*(2), 169-173. https://doi.org/10.1016/S0031-9422(01)00451-4

Vanijajiva, O., Sirirugsa, P., & Suvachittanont, W. (2005). Confirmation of relationships among *Boesenbergia* (Zingiberaceae) and related genera by RAPD. *Biochemical Systematics and Ecology*, *33*(2), 159-170. https://doi.org/10.1016/j.bse.2004.06.012

Welsh, J., & McClelland, M. (1990). Fingerprinting genomes using PCR with arbitrary primers. *Nucleic Acids Research*, *18*(24), 7213-7218. https://doi.org/10.1093/nar/18.24.7213

Wijekoon, M. M. J. O., Bhat, R., & Karim, A. A. (2011). Effect of extraction solvents on the phenolic compounds and antioxidant activities of bunga kantan (*Etlingera elatior* Jack.) inflorescence. *Journal of Food Composition and Analysis*, *24*(4-5), 615-619. https://doi.org/10.1016/j.jfca.2010.09.018

Williams, J. G., Kubelik, A. R., Livak, K. J., Rafalski, J. A., & Tingey, S. V. (1990). DNA polymorphisms amplified by arbitrary primers are useful as genetic markers. *Nucleic Acids Research*, *18*(22), 6531-6535. https://doi.org/10.1093/nar/18.22.6531

Xia, Y. M., Kress, W. J., & Prince, L. M. (2004). Phylogenetic analyses of *Amomum* (Alpinioideae: Zingiberaceae) using ITS and *matK* DNA sequence data. *Systematic Botany*, *29*(2), 334-344. https://doi.org/10.1600/036364404774195520

Yujian, L., & Liye, X. (2010). Unweighted multiple group method with arithmetic mean. In *2010 IEEE Fifth International Conference on Bio-Inspired Computing: Theories and Applications (BIC-TA)* (pp. 830-834). IEEE. https://doi.org/10.1109/BICTA.2010.5645232

Zahara, M. (2020). Identification of morphological and stomatal characteristics of Zingiberaceae as medicinal plants in Banda Aceh, Indonesia. In *IOP Conference Series: Earth and Environmental Science* (Vol. 425, No. 1, p. 012046). IOP Publishing. https://doi.org/10.1088/1755-1315/425/1/012046

Zietkiewicz, E., Rafalski, A., & Labuda, D. (1994). Genome fingerprinting by simple sequence repeat (SSR)-anchored polymerase chain reaction amplification. *Genomics*, *20*(2), 176-183. https://doi.org/10.1006/geno.1994.1151

Zou, X., Dai, Z., Ding, C., Zhang, L., Zhou, Y., & Yang, R. (2011). Relationships among six medicinal species of *Curcuma* assessed by RAPD markers. *Journal of Medicinal Plants Research*, *5*(8), 1349-1354.

Pertanika J. Trop. Agric. Sci. 46 (1): 347 - 357 (2023)

PERTANIKA JOURNALS

TROPICAL AGRICULTURAL SCIENCE

Journal homepage: http://www.pertanika.upm.edu.my/

Effectiveness of *Samia cynthia ricini* Boisduval (Lepidoptera: Saturniidae) Cocoon Extract as UV Protectant of *Bacillus thuringiensis kurstaki* in Controlling Beet Armyworm *Spodoptera exigua* (Hübner) (Lepidoptera: Noctuidae) under Sunlight

Rahmatullah Rahmatullah[1], Sukirno[2]*, Nindita Sabila Ningtyas[1], Aryo Seto Pandu Wiranto[1], Nadya Sofia Siti Sa'adah[1], Hipny Alwandri[1], Tiara Purti Arssalsabila[1], Asma' Asma'[1] and Hanindyo Adi[2]

[1]Faculty of Biology, Universitas Gadjah Mada, Jalan Teknika Selatan Sekip Utara Depok Sleman, 55281 Yogyakarta, Indonesia
[2]Entomology Laboratory, Faculty of Biology, Universitas Gadjah Mada, Jalan Teknika Selatan Sekip Utara Depok Sleman, 55281 Yogyakarta, Indonesia

ABSTRACT

Bacillus thuringiensis (Bt) is a biological agent for insect pest management. Its toxins effectively control *Spodoptera exigua* Hübner (Lepidoptera: Noctuidae) larvae, but it is sensitive to ultraviolet (UV) radiation from the sunlight. This study aimed to investigate the effect of sericin extract from *Samia ricini* Boisduval (Lepidoptera: Saturniidae) cocoons as a UV protectant for Bt after exposure under direct sunlight for 1, 2, 3, and 4 weeks. After being exposed to sunlight, the Bt formulae were tested against 20 larvae of 24 hr old, the first larval instar in the laboratory. The larval mortality was observed 72 hr after the treatment. The results indicated that the mortality of *S. exigua* in Bt + sericin extract treatment was significantly different compared with Bt alone. For the first week, the mortality of *S. exigua* in exposed Bt + sericin exposed Bt alone, unexposed (Bt + sericin, and unexposed Bt alone were 80, 61, 85, and 97%, respectively. Scanning electron microscopy analysis revealed that Bt + sericin, after being exposed to sunlight, still showed the presence of spore and crystal protein comparable to the unexposed Bt.

ARTICLE INFO

Article history:
Received: 26 August 2022
Accepted: 30 November 2022
Published: 22 February 2023

DOI: https://doi.org/10.47836/pjtas.46.1.19

E-mail addresses:
rahmatullah95@mail.ugm.ac.id (Rahmatullah Rahmatullah)
sukirnobiougm@ugm.ac.id (Sukirno Sukirno)
sabilaningtyas25@mail.ugm.ac.id (Nindita Sabila Ningtyas)
aryo.seto.p@mail.ugm.ac.id (Aryo Seto Pandu Wiranto)
nadya.sofia88@mail.ugm.ac.id (Nadya Sofia Siti Sa'adah)
hipny.a@mail.ugm.ac.id (Hipny Alwandri)
tiarapurti@mail.ugm.ac.id (Tiara Purti Arssalsabila)
asma.BI@mail.ugm.ac.id (Asma' Asma')
hanindyo.adi@mail.ugm.ac.id (Hanindyo Adi)
* Corresponding author

ISSN: 1511-3701
e-ISSN: 2231-8542

Based on the results, sericin provides good protection against sunlight and prevents the Bt spores from light-induced damage.

Keywords: Bt, *Samia*, *Spodoptera exigua*, UV protectant

INTRODUCTION

The beet armyworm, *Spodoptera exigua* (Hübner) (Lepidoptera: Noctuidae), is a polyphagous insect pest that can damage many plants, such as wheat, cotton, pea, cauliflower, tomato, onion, and soybean (Adamczyk et al., 2008; Saeed et al., 2010; Taylor & Riley, 2008; Zheng et al., 2000; Zhou et al., 2011). The larvae can feed on leaves and attack flowers, buds, and fruits, causing slow growth and a decrease quantity and quality of the crops (Khattab, 2013). Thus, controlling the insect pest population is critical, thereby promoting the use of chemical and biological insecticides (Meissle et al., 2011). Chemical pesticide reliance results in increased insecticide resistance, a greater risk to human health because of the lack of appropriate safety standards, and environmental pollution (Day et al., 2017). *Bacillus thuringiensis* (Bt) is an alternative solution for reducing insect pests. With a narrow species spectrum, these bioinsecticides are safe, eco-friendly, residual-free, and safe for most other organisms (Maagd et al., 2001; Schnepf et al., 1998).

Bt is a Gram-positive bacterium that can produce toxic proteins (para-spore crystals) when reaching the sporulation stage (Bravo et al., 2005). These insecticidal crystal proteins are predominantly encoded by *Cry* and *Cyt* genes, known as δ-endotoxins (Aronson, 2002). When insect larvae ingest such toxins during feeding, spore, and toxins (δ-endotoxins) are produced in the midgut. These molecules (Cry and Cyt) bind to receptors on the intestinal epithelium, causing irreversible damage to the epithelial cells by generating pores or lysing the target membrane of the midgut (Gill, 1995). Cry proteins show a highly specific spectrum and effectiveness in insect taxa, such as Diptera, Lepidoptera, Coleoptera, and Hymenoptera (Maagd et al., 2001). In addition, Cry1C is a major specificity determinant for *S. exigua* (Maagd et al., 2000). However, biological pesticides are easily degradable and unstable when applied in the field. For example, sunlight's ultraviolet (UV) radiation might deactivate the Bt toxin (Sansinenea et al., 2015). Therefore, treatment measures are necessary to address this difficulty.

Recently, scientists tried to improve the stability of bio-pesticides by covering Bt spores and toxins using biomaterials as UV protectants. For example, *Bacillus thuringiensis kurstaki* (Btk) was formulated with a biomaterial derived from olive oil (Maghsoudi & Jalali, 2017), tea leaves (Ningrum & Sumarmi, 2020), aloe vera (Tarigan et al., 2020), spinach leaves (Sumarmi et al., 2020), and sericin extract from eri and atlas silkworm (Sukirno et al., 2022). Silk sericin is a biological polymer consisting of glycoprotein, essential for protecting the cocoon and pupa from UV radiation during pupal stages (Kaur et al., 2013). It also has antioxidant activity

that can protect against UV radiation and overcome oxidation (Kumar & Mandal, 2019).

Recently, sericin from eri and atlas cocoon has been proven effective as a UV protectant of Btk (Sukirno et al., 2022) against tobacco armyworm. This study evaluated the effectiveness of formulation of Btk and sericin extract of eri silkworm cocoon when sunlight against beet armyworm. In addition, the potency and viability of Btk spore crystals with the addition of sericin extract were evaluated in the laboratory. The results of this work will support the integrated management of insect pests in Indonesia.

MATERIALS AND METHODS

Beet Armyworm Insect Rearing

Beet armyworm larvae were collected from onion farms in Magelang, Central Java, Indonesia. The larvae were maintained in the lab using an artificial diet (Shorey & Hale, 1965) with some modifications (Sukirno et al., 2018) until pupation. Thirty pupae were each transferred in a glass jar (7 cm × 23 cm) with an opaque paper supporting adult emergence, mating, and egg laying. Adults were provided with a cotton ball dipped in a 10% honey solution for feeding. Eggs were monitored and collected daily, then kept in plastic cups (6.5 cm × 4 cm) containing an artificial diet and then covered with tissue until hatched into first instar larvae. Insects were kept in lab conditions of 28 ± 5°C and relative humidity of 50 – 70%. A 24 hr old first larval instar of F_2 was used in this study.

Bio-pesticide and Sericin Extract Preparations

Dipel WP®, a commercial product by Abbot Co. (Indonesia), was used as a source of *B. thuringiensis kurstaki*, whereas eri silkworm cocoon was collected from Jantra Mas Sejahtera (JAMTRA, Indonesia) wild silk production house. Five grams of dried cocoon was cut into small pieces and added into 100 mL of autoclaved distilled water (dH_2O) containing 1 g of Turkey Red Oil (TRO, Indonesia) powder. Then, the mixture was boiled for 60 min using a stirring machine and filtered to obtain a stock of 5% sericin solution. Before the experiment, the stock solution was diluted using autoclaved dH_2O to make a 1% sericin solution.

Larval Toxicity Bioassay

The 1% sericin extract was added to make a Bt suspension at 10 times the lethal concentration of 95% (LC_{95}) (2×10^8 CFU/ml) (Sukirno et al., 2022). Autoclaved dH_2O as a negative control was used to compare the effectiveness of UV protectants. One milliliter of each Bt suspension was transferred homogenously to the surface of the disposable Petri dish (55 mm × 15 mm). After that, the Petri dishes were exposed to direct sunlight for 1, 2, 3, and 4 weeks. After respective exposure, the dried Bt was then homogenously mixed with 10 ml of autoclaved dH_2O to make the final concentration at LC_{95}. Afterward, 1 ml of each formula was poured onto an artificial diet surface in a plastic cup (6.5 cm × 4 cm). The Bt-contaminated diet was

allowed at room temperature for 2 hr before adding the 24 hr old first larval instar of *S. exigua*. The experiment used five replicates on each formula and exposure period, with 20 larvae per replicate, for a total of 2,000 treated larvae. The mortality was recorded at 72 hr after treatment and scored as dead when there was no movement when touched with a fine brush. In this study, the first larval instar of beet armyworm was used as an indicator for the effectivity of UV protectant of Bt as it is susceptible.

Sublethal Effects of Bt Formulation on Beet Armyworm Larvae

Sublethal effects can be physiological, behavioral, survival rate, and body weight after treatment with sublethal amounts of toxic compounds (Desneux et al., 2007; Rajathi et al., 2010; Tao & Wu, 2006). The sublethal effects of Bt on the larval body weight beet armyworm in the present were observed on the sixth day after the treatment.

Scanning Electron Microscopic Observation of Bt Formulation

Scanning electron microscopy (SEM) (JSM-6510LA, JEOL Ltd., Japan) was used to evaluate the presence and the structure of spores and crystals. One milliliter of Btk suspension was centrifuged at 16,000 × *g* for 15 min at 4°C and air dried on a castable vacuum system. Samples were then placed on a brass stub, sputter coated with gold at 3.3 Pa and 20 mA for 120 s, and photographed in a JEC-3000 FC (JEOL Ltd., Japan) at 15 kV.

Statistical Analysis

Before statistical analysis, the data on mortality percentage was corrected using the Abbott formula (Abbott, 1925; Finney, 1977). Then, the mortality percentage and larval weight were analyzed using a one-way analysis of variance (ANOVA). The exposure period and formula were used as independent factors, with mortality and larval weight as dependent factors for analysis. Before the ANOVA, the mortality percentage was arcsine-transformed. After the ANOVA, the means were subjected to post hoc multiple pairwise comparisons across each formula and exposure period ($P < 0.05$; least significant difference [LSD]). Statistical Product and Service Solutions (SPSS) Statistic (ver. 23.0) was used for all statistical analyses.

RESULTS

Mortality of the First Instar Larvae of *S. exigua*

The percentage of larval mortality was significantly different for each formula during the first week of exposure ($F_{4,20} = 12.75$; $P = 0.000$) and the fourth week of exposure ($F_{4,20} = 9.14$; $P = 0.001$). Meanwhile, no statistically significant differences were identified after the second week of exposure ($F_{4,20} = 2.75$; $P = 0.077$), the third week of exposure ($F_{4,20} = 0.36$; $P = 0.782$), and without sunlight exposure ($F_{4,20} = 2.11$; $P = 0.139$).

In the first week, the pathogenicity of the Bt + sericin had higher toxicity against beet armyworm larvae (80%) than the Bt without sericin (61%). By contrast, Bt +

sericin and Bt without sericin in unexposed sunlight had relatively higher pathogenicity to *S. exigua* larvae, with mortality of 85 and 97%, respectively. It showed that the formula of Bt mixed with sericin was more pathogenic to *S. exigua* than Bt alone when exposed under sunlight, with values ranging from 56 to 93%, except on the second week of exposure. The pathogenicity value of the combination of Bt + sericin without exposure to *S. exigua* ranged from 85 to 98%, whereas that of Bt alone without exposure ranged from 81 to 99%. The death rate showed a synergistic effect of sericin when added to Bt and tested against beet armyworm (Table 1).

Delayed Mortality and Sublethal Effects on the First Instar Larvae of *S. exigua*

Figure 1 shows that the percentage of surviving larvae during the exposure period until the sixth day was not significantly different in all treatments. The percentages were 3.97, 3.97, 1.48, and 0.72% ($F_{3,12}$ = 1.36; P = 0.300) for exposed Bt + sericin, exposed Bt without sericin, unexposed Bt + sericin, and unexposed Bt without sericin, respectively. The average larval weight in Bt + sericin is greater than that of exposed Bt without sericin, unexposed Bt + sericin, and unexposed Bt without sericin treatments (Figure 2). The larval weight on those treatments was 1.67; 0.93; 0.29, and 1.00 mg ($F_{3,12}$ = 0.37; P = 0.774), respectively. Meanwhile, the larval weight during the 2-week exposure period was significantly different and higher than other exposure periods, whereas 1, 2, 3, and 4 weeks was 0.38, 3.27, 0.20, and 0.03 mg ($F_{3,12}$ = 7.05; P = 0.005), respectively. On the other hand, based on the larvae survivorship, it showed that there was no significant difference

Table 1
Mortality percentage of the first instar larvae of Spodoptera exigua *(mean ± SE) after being treated with* Bacillus thuringiensis kurstaki *formulation at different exposure periods*

Period (Week)	Mortality exposed (%)		Mortality non-exposed (%)		Statistic
	Bt + sericin	Bt without sericin	Bt + sericin	Bt without sericin	
0	93.63 ± 2.31aA	82.60 ± 6.51aA	96.35 ± 0.92aA	93.04 ± 3.39aAB	$F_{4,20}$ = 2.11; P = 0.139
1	80.00 ± 4.18abA	61.14 ± 7.08aB	85.00 ± 3.53bA	97.14 ± 2.85cB	$F_{4,20}$ = 12.75; P = 0.000
2	56.00 ± 13.72aB	86.33 ± 5.71aA	93.78 ± 5.06aA	81.76 ± 5.02aA	$F_{4,20}$ = 2.75; P = 0.077
3	91.04 ± 5.57aA	87.00 ± 4.89aA	89.00 ± 8.57aA	96.04 ± 0.98aAB	$F_{4,20}$ = 0.36; P = 0.782
4	93.09 ± 2.52abA	86.00 ± 1.87aA	98.00 ± 1.22bA	99.04 ± 0.95bB	$F_{4,20}$ = 9.14; P = 0.001
Statistic	$F_{4,20}$ = 3.34; P = 0.030	$F_{4,20}$ = 2.99; P = 0.044	$F_{4,20}$ = 1.73; P = 0.183	$F_{4,20}$ = 3.37; P = 0.029	

Note. Means with the same row followed by the same lowercase letters are not significantly different at P < 0.05. The numbers with the same column followed by the same uppercase letters are not significantly different at P < 0.05

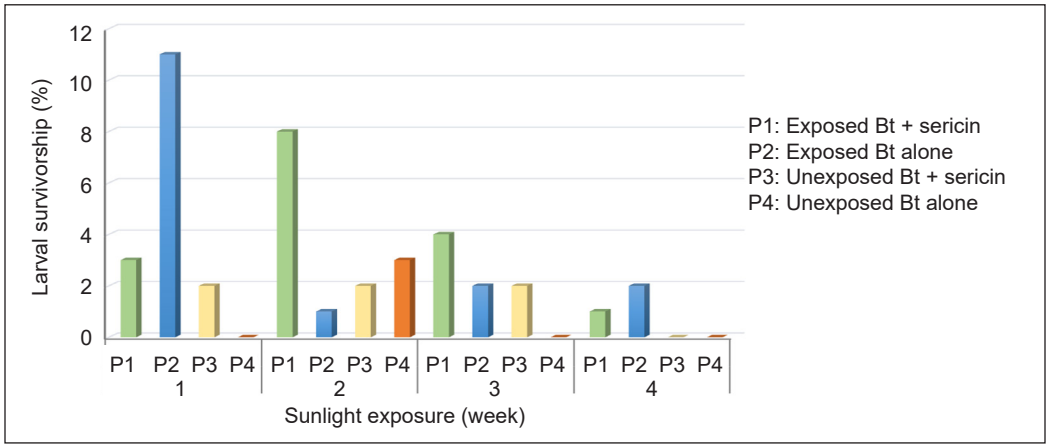

Figure 1. Effects of different Bt formulations on the average number of *Spodoptera exigua* survival on the sixth day after treatment

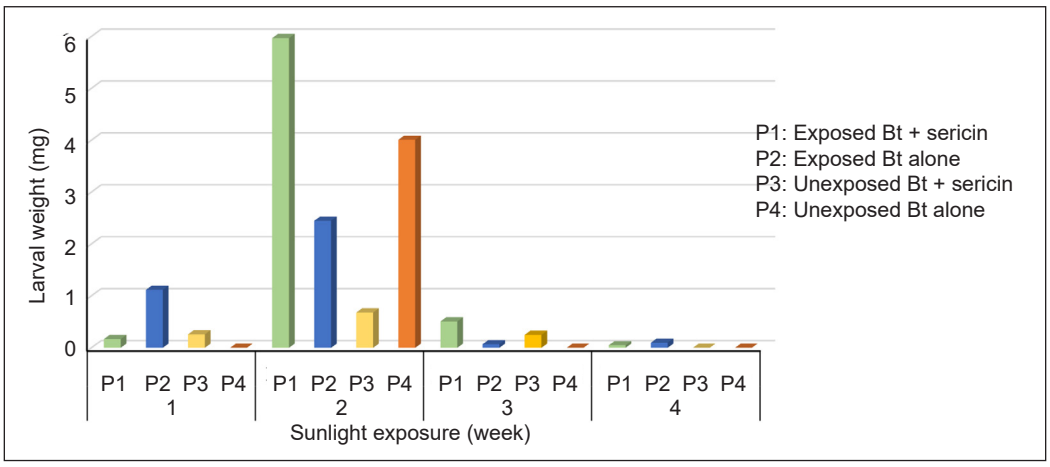

Figure 2. Sublethal effects of different Bt formulations on the larval weight of *Spodoptera exigua* on the sixth day after treatment

in 1-, 2-, 3-, and 4-week treatment. The survivorship on those treatments was 3.97, 3.45, 1.98, and 0.74% ($F_{3,12}$ = 0.94; P = 0.448), respectively.

Scanning Electron Microscopy

Scanning electron microscopy (SEM) ((JSM-6510LA, JEOL Ltd., Japan) has successfully detected the spore and crystal of Bt in the treatment, especially on the formula with and without exposure to direct sunlight. This research found many spores within various crystal shapes, including bipyramidal, cuboidal, and spherical crystals (Figures 3 and 4).

DISCUSSION

The protein sericin content in silkworm cocoons is lower than fibroin, around 20–30% (Eom et al., 2020). Sericin is rich in

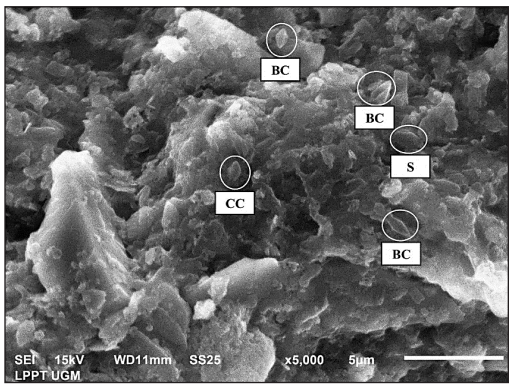

Figure 3. Scanning electron microscopy of the mixture of Bt spores, crystals, and sericin extract (1%) without exposure
Note. S = Spore; CC = Cuboid crystals; BC = Bipyramidal crystal

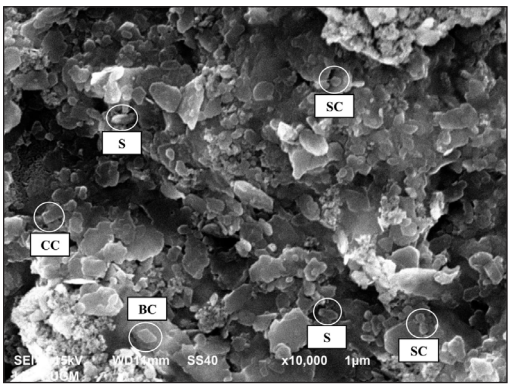

Figure 4. Scanning electron microscopy of the mixture of Bt spores, crystals, and sericin extract (1%) after three weeks of exposure
Note. S = Spore; CC = Cuboid crystals; BC = Bipyramidal crystal; SC = Spherical crystal

amino acids, particularly serine and aspartic acid, and each cocoon layer has different sericin contents (Aramwit et al., 2010). Several studies have shown that sericin has a high concentration of antioxidant molecules, which play an important role in preventing UV-induced oxidative damage (Kaur et al., 2013). A previous study has demonstrated that sericin from eri silkworm can absorb UVA and UVB radiation and has a high toxicity effect on *Spodoptera litura* larvae when mixed with Btk for bioassay (Sukirno et al., 2022). UV radiation is an electromagnetic spectrum that is categorized into three regions: 320–400 nm as ultraviolet A (UVA), 280–320 nm as ultraviolet B (UVB), and 200–280 nm as ultraviolet C (UVC). UVA accounts for 90–98% of total UV radiation reaching the earth, whereas UVB accounts for 1–10%. Moreover, UVC radiation is absorbed by the ozone layer (Hou et al., 2015; Kaur et al., 2013).

We evaluated a small concentration (1%) of sericin extract as UV protectant Bt under direct sunlight exposure in the present study. The results showed that sericin significantly affected the persistence of Bt to prolonged time exposure, as revealed by the mortality percentage of *S. exigua* larvae, which was greater in Bt with sericin than in Bt alone (Table 1). This extensive research also tested the efficacy and survivability of Bt spore crystals. SEM analysis revealed that after prolonged exposure to the formula with the addition of sericin extract (1%), spores and crystals were still observed despite being exposed to sunlight for three weeks. Many spores within various crystal shapes were found (Figures 3 and 4), which included bipyramidal, cuboidal, and spherical crystals. These results are consistent with the research results of Lozano et al. (2018), who discovered the crystal shape of Btk S-1905. Larvicidal toxicity was commonly due to spores and crystal proteins. The Cry 1 protein, which is efficient against Lepidoptera, is associated with bipyramidal crystals, whereas the Cry 2 protein, which

is effective against Diptera and Lepidoptera, is associated with cuboidal crystals (Silva et al., 2004). Other factors, including the structure and function of the intestine, toxin diversity, structure and solubilization of protein, and toxin interactions, were also investigated (Gill, 1995). The presence of spores and germination can affect Bt insecticidal activity (Liu et al., 1998). The spores can be protected by various localized biological structures, such as spore coats on Bt, allowing crystal formation to continue during sporulation. Spores of *Bacillus* species are seven to 50 times more resistant to UV radiation at 254 nm, the wavelength that kills most cells, than vegetative cell killing (Setlow et al., 1998). Furthermore, according to Hart et al. (2006), spores have an outer layer known as an exosporium, which surrounds the dense spore and serves as a protective barrier. This layer is present in some spore species, such as *Bacillus anthracis* and *Bacillus thuringiensis*, but absent in others.

Larval body weight as an indicator of sublethal effects was significantly related to the proportion of surviving larvae, which led to major changes in the biology of the treated larvae and their offspring. The results showed that the Bt formulation with sericin extract after the fourth week of exposure decreased the proportion of survivors. In addition, the larval weight emergence rate was significantly reduced on the sixth day after treatment for all formulas. The percentage of larval survival in P1 and P2 formulas had the same value but not with their body weight. Our hypotheses indicate that differences in survival ability can be observed among larvae, with a high adaptation to diet contamination. Another factor may be due to the different counts of spore present in each formula. According to Apaydin et al. (2008), almost all strains of Bt suppress the growth and development of the larvae, which might cause pupal stage failure.

CONCLUSION

The study showed that sericin (1%) from cocoons of *S. cynthia ricini* protected Bt from exposure to direct sunlight and that the formula was efficient against *S. exigua* larvae. In addition, the mortality percentage, sublethal effect, and existence of spores and crystals indicated the efficacy of the treatment. However, all bioassay processes are still conducted on a laboratory scale; thus, further studies may be required to evaluate their protective effectiveness directly in field conditions, particularly on onion crops.

ACKNOWLEDGMENTS

The authors want to express gratitude and appreciation for the PDUPT research grant (4346/UN1/DITLIT/DIT-LIT/PT.01.06/2022). This research was also partly funded by LPDP (Lembaga Pengelola Dana Pendidikan) Finance Ministry of the Republic of Indonesia. Thank you also to the farmers in Magelang for allowing us to collect *Spodoptera exigua*, the research team, who assisted with the rearing process, and the reviewers who provided feedback to help improve this study.

REFERENCES

Abbott, W. S. (1925). A method of computing the effectiveness of an insecticide. *Journal of Economic Entomology*, *18*(2), 268–267. https://doi.org/10.1093/JEE%2F18.2.265A

Adamczyk, J. J., Greenberg, S., Armstrong, J. S., Mullins, W. J., Braxton, L. B., Lassiter, R. B., & Siebert, M. W. (2008). Evaluations of Bollgard®, Bollgard II®, and WideStrike® technologies against beet and fall armyworm larvae (Lepidoptera: Noctuidae). *Florida Entomologist*, *91*(4), 531–536. https://doi.org/10.1653/0015-4040-91.4.531

Apaydin, O., Cinar, C., Turanli, F., Harsa, S., & Gunes, H. (2008). Identification and bioactivity of native strains of *Bacillus thuringiensis* from grain-related habitats in Turkey. *Biological Control*, *45*(1), 21–28. https://doi.org/10.1016/j.biocontrol.2008.01.011

Aramwit, P., Kanokpanont, S., Nakpheng, T., & Srichana, T. (2010). The effect of sericin from various extraction methods on cell viability and collagen production. *International Journal of Molecular Sciences*, *11*(5), 2200–2211. https://doi.org/10.3390/ijms11052200

Aronson, A. (2002). Sporulation and δ-endotoxin synthesis by *Bacillus thuringiensis*. *Cellular and Molecular Life Sciences*, *59*(3), 417–425. https://doi.org/10.1007/s00018-002-8434-6

Bravo, A., Soberon, M., & Gill, S. S. (2005). *Bacillus thuringiensis*: Mechanisms and use. In L. I. Gilbert & S. S. Gill (Eds.), *Comprehensive molecular insect science* (Vol. 6, pp. 175-205). Academic Press. https://doi.org/10.1016/B0-44-451924-6/00081-8

Day, R., Abrahams, P., Bateman, M., Beale, T., Clottey, V., Cock, M., Colmenarez, Y., Corniani, N., Early, R., Godwin, J., Gomez, J., Moreno, P. G., Murphy, S. T., Oppong-Mensah, B., Phiri, N., Pratt, C., Silvestri, S., & Witt, A. (2017). Fall armyworm: Impacts and implications for Africa. *Outlooks on Pest Management*, *28*(5), 196–201. https://doi.org/10.1564/v28_oct_02

Desneux, N., Decourtye, A., & Delpuech, J. (2007). The sublethal effects of pesticides on beneficial arthropods. *Annual Review of Entomology*, *52*, 81–106. https://doi.org/10.1146/annurev.ento.52.110405.091440

Eom, S. J., Lee, N. H., Kang, M. C., Kim, Y. H., Lim, T.-G., & Song, K.-M. (2020). Silk peptide production from whole silkworm cocoon using ultrasound and enzymatic treatment and its suppression of solar ultraviolet-induced skin inflammation. *Ultrasonics Sonochemistry*, *61*, 104803. https://doi.org/10.1016/j.ultsonch.2019.104803

Finney, D. J. (1977). Estimation of the response curve in radiology and assays. *Annals of the Institute of Statistical Mathematics*, *29*, 467–477. https://doi.org/10.1007/BF02532806

Gill, S. S. (1995). Mechanism of action of *Bacillus thuringiensis* toxins. *Memorias do Instituto Oswaldo Cruz*, *90*(1), 69–74. https://doi.org/10.1590/S0074-02761995000100016

Hart, S. J., Terray, A., Leski, T. A., Arnold, J., & Stroud, R. (2006). Discovery of a significant optical chromatographic difference between spores of *Bacillus anthracis* and its close relative, *Bacillus thuringiensis*. *Analytical Chemistry*, *78*(9), 3221–3225. https://doi.org/10.1021/ac052221z

Hou, W., Gao, W., Wang, D., Liu, Q., Zheng, S., & Wang, Y. (2015). The protecting effect of deoxyschisandrin and schisandrin B on HaCaT cells against UVB-induced damage. *PLOS One*, *10*(5), e0127177. https://doi.org/10.1371/journal.pone.0127177

Kaur, J., Rajkhowa, R., Tsuzuki, T., Millington, K., Zhang, J., & Wang, X. (2013). Photoprotection by silk cocoons. *Biomacromolecules*, *14*(10), 3660–3667. https://doi.org/10.1021/bm401023h

Khattab, M. (2013). Isolation of *nucleopolyhedrovirus* (NPV) from the beet armyworm *Spodoptera exigua* (Hübner) (*Spex*NPV). *International Journal of Environmental Science and Engineering*, *4*, 75–83.

Kumar, J. P., & Mandal, B. B. (2019). The inhibitory effect of silk sericin against ultraviolet-induced melanogenesis and its potential use in cosmeceutics as an anti-hyperpigmentation compound. *Photochemical and Photobiological Sciences*, *18*(10), 2497–2508. https://doi.org/10.1039/c9pp00059c

Liu, Y. B., Tabashnik, B. E., Moar, W. J., & Smith, R. A. (1998). Synergism between *Bacillus thuringiensis* spores and toxins against resistant and susceptible diamondback moths (*Plutella xylostella*). *Applied and Environmental Microbiology*, *64*(4), 1385–1389. https://doi.org/10.1128/aem.64.4.1385-1389.1998

Lozano, E. R., Neves, P. M. O. J., Alves, L. F. A., Potrich, M., Vilas-Boas, G. F. L. T., & Monnerat, R. G. (2018). Action of natural phytosanitary products on *Bacillus thuringiensis* subsp. *kurstaki* S-1905. *Bulletin of Entomological Research*, *108*(2), 223–231. https://doi.org/10.1017/S0007485317000670

Maagd, R. A., Bravo, A., & Crickmore, N. (2001). How *Bacillus thuringiensis* has evolved specific toxins to colonize the insect world. *Trends in Genetics*, *17*(4), 193–199. https://doi.org/10.1016/S0168-9525(01)02237-5

Maagd, R. A., Weemen-Hendriks, M., Stiekema, W., & Bosch, D. (2000). *Bacillus thuringiensis* delta-endotoxin Cry1C domain III can function as a specificity determinant for *Spodoptera exigua* in different, but not all, Cry1-Cry1C hybrids. *Applied and Environmental Microbiology*, *66*(4), 1559–1563. https://doi.org/10.1128/AEM.66.4.1559-1563.2000

Maghsoudi, S., & Jalali, E. (2017). Noble UV protective agent for *Bacillus thuringiensis* based on a combination of graphene oxide and olive oil. *Scientific Reports*, *7*(1), 7–12. https://doi.org/10.1038/s41598-017-11080-9

Meissle, M., Romeis, J., & Bigler, F. (2011). *Bt* maize and integrated pest management - A European perspective. *Pest Management Science*, *67*(9), 1049–1058. https://doi.org/10.1002/ps.2221

Ningrum, A. D., & Sumarmi, S. (2020). The extract of tea leaves (*Camellia sinensis* (L.) Kuntze) as protectant of *Bacillus thuringiensis* var. *kurstaki* against ultraviolet light for control of armyworm (*Spodoptera litura* Fab.) larvae. In *AIP Conference Proceedings* (Vol. 2260, No. 1, p. 030022). AIP Publishing. https://doi.org/10.1063/5.0015744

Rajathi, A., Pandiarajan, J., & Krishnan, M. (2010). Effect of RH-2485 on development, metamorphosis, and synthesis of major proteins in female silkworm *Bombyx mori*. *Versita*, *65*(5), 903-913. https://doi.org/10.2478/s11756-010-0104-9

Saeed, S., Sayyed, A. H., & Ahmad, I. (2010). Effect of host plants on life-history traits of *Spodoptera exigua* (Lepidoptera: Noctuidae). *Journal of Pest Science*, *83*(2), 165–172. https://doi.org/10.1007/s10340-009-0283-8

Sansinenea, E., Salazar, F., Ramirez, M., & Ortiz, A. (2015). An ultra-violet tolerant wild-type strain of melanin-producing *Bacillus thuringiensis*. *Jundishapur Journal of Microbiology*, *8*(7), e20910. https://doi.org/10.5812/jjm.20910v2

Schnepf, E., Crickmore, N., Van Rie, J., Lereclus, D., Baum, J., Feitelson, J., Zeigler, D. R., & Dean, D. H. (1998). *Bacillus thuringiensis* and its pesticidal crystal proteins. *Microbiology and Molecular Biology Reviews*, *62*(3), 775–806. https://doi.org/10.1128/mmbr.62.3.775-806.1998

Setlow, B., Tautvydas, K. J., & Setlow, P. (1998). Small, acid-soluble spore proteins of the α/β type do not protect the DNA in *Bacillus subtilis* spores against base alkylation. *Applied and*

Environmental Microbiology, *64*(5), 1958–1962. https://doi.org/10.1128/aem.64.5.1958-1962.1998

Shorey, H. H., & Hale, R. L. (1965). Mass-Rearing of the larvae of nine noctuid species on a simple artificial medium. *Journal of Economic Entomology*, *58*(3), 522–524. https://doi.org/10.1093/jee/58.3.522

Silva, S. M. B., Silva-Werneck, J. O., Falcao, R., Gomes, A. C., Fragoso, R. R., Quezado, M. T., Neto, O. B. O., Aguiar, J. B., De Sa, M. F. G., Bravo, A., & Monnerat, R. G. (2004). Characterization of novel Brazilian *Bacillus thuringiensis* strains active against *Spodoptera frugiperda* and other insect pests. *Journal of Applied Entomology*, *128*(2), 102–107. https://doi.org/10.1046/j.1439-0418.2003.00812.x

Sukirno, S., Lukmawati, D., Hanum, S. S. L., Ameliya, V. F., Sumarmi, S., Purwanto, H., Suparmin, S., Sudaryadi, I., Soesilohadi, R. C. H., & Aldawood, A. S. (2022). The effectiveness of *Samia ricini* Drury (Lepidoptera: Saturniidae) and *Attacus atlas* L. (Lepidoptera: Saturniidae) cocoon extracts as ultraviolet protectants of *Bacillus thuringiensis* for controlling *Spodoptera litura* Fab. (Lepidoptera: Noctuidae). *International Journal of Tropical Insect Science*, *42*(1), 255–260. https://doi.org/10.1007/s42690-021-00540-5

Sukirno, S., Tufail, M., Rasool, K. G., El Salamouny, S., Sutanto, K. D., & Aldawood, A. S. (2018). The efficacy and persistence of *Spodoptera littoralis* nucleopolyhedrovirus (*Spli*MNPV) applied in UV protectants against the beet armyworm, *Spodoptera exigua* (Hübner) (Lepidoptera: Noctuidae) under Saudi field conditions. *Pakistan Journal of Zoology*, *50*(5), 1895–1902. https://doi.org/10.17582/JOURNAL.PJZ/2018.50.5.1895.1902

Sumarmi, S., Arlinda, M., & Sukirno, S. (2020). The effectiveness of red spinach (*Amaranthus tricolor* L.) and green spinach (*Amaranthus hybridus* L.) extracts for *Bacillus thuringiensis* var. *kurstaki* protectant against UV-B radiation for the control of armyworm (*Spodoptera litura* Fab.). *Journal of Tropical Biodiversity and Biotechnology*, *5*(2), 143–148. https://doi.org/10.22146/jtbb.53004

Tao, S., & Wu, F. (2006). Sublethal effect of chlorpyrifos on dynamics of experimental *Tetranychus cinnabarinus* population. *Journal of Applied Ecology*, *17*(7), 1351-1353.

Tarigan, A., Sumarmi, S., & Sukirno, S. (2020). Effectiveness of aloe (*Aloe vera* L.) as a protectant of *Bacillus thuringiensis* var *kurstaki* against ultraviolet light and biological control agenst of *Spodoptera litura* Fab. In *AIP Conference Proceedings: Biological Science ICBS* (Vol. 2260, No. 1, p. 030003). AIP Publishing. https://doi.org/10.1063/5.0015743

Taylor, J. E., & Riley, D. G. (2008). Artificial infestations of beet armyworm, *Spodoptera exigua* (Lepidoptera: Noctuidae), used to estimate an economic injury level in tomato. *Crop Protection*, *27*(2), 268–274. https://doi.org/10.1016/j.cropro.2007.05.014

Zheng, S., Henken, B., Wietsma, W., Sofiari, E., Jacobsen, E., Krens, F. A., & Kik, C. (2000). Development of bio-assays and screening for resistance to beet armyworm (*Spodoptera exigua* Hübner) in *Allium cepa* L. and its wild relatives. *Euphytica*, *114*, 77–85. https://doi.org/10.1023/A:1004089424419

Zhou, C., Liu, Y., Yu, W., Deng, Z., Gao, M., Liu, F., & Mu, W. (2011). Resistance of *Spodoptera exigua* to ten insecticides in Shandong, China. *Phytoparasitica*, *39*(4), 315–324. https://doi.org/10.1007/s12600-011-0157-5

Pertanika J. Trop. Agric. Sci. 46 (1): 359 - 372 (2023)

PERTANIKA JOURNALS

TROPICAL AGRICULTURAL SCIENCE

Journal homepage: http://www.pertanika.upm.edu.my/

Paralytic Shellfish Profiles Produced by the Toxic Dinoflagellate *Pyrodinium bahamense* from Sepanggar Bay, Malaysia

Asilah Al-Has[1], Normawaty Mohammad-Noor[1]*, Sitti Raehanah Muhamad Shaleh[2], Mohd Nor Azman Ayub[3], Deny Susanti[1] and Ghaffur Rahim Mustakim[2]

[1]Kuliyyah of Science, International Islamic University Malaysia, 25200 Kuantan, Pahang, Malaysia
[2]Borneo Marine Research Institute, Universiti Malaysia Sabah, 88400 Kota Kinabalu, Sabah, Malaysia
[3]Fisheries Research Institute, 11960 Batu Maung, Penang, Malaysia

ABSTRACT

Pyrodinium bahamense var *compressum* is a harmful dinoflagellate that produces saxitoxin, which causes paralytic shellfish poisoning (PSP) that is deadly to humans. A non-axenic culture of *P. bahamense* was established using f/2 media from samples collected from Sepanggar Bay, Kota Kinabalu, Sabah. Toxin analyses of cultures harvested on days 60, 120, 180, and 360 were performed using high-performance liquid chromatography with a fluorescence detector and compared with samples collected at the same location during the bloom in 2021. The highest cell toxin content was found in the bloom sample (86.2 fmole/cell), and no toxin was detected in the culture 60 days old. In addition, cell toxin content for the *P. bahamense* culture was low (9.4-16.5 fmole/cell). Based on the toxin profile, *P. bahamense* comprises 84-98% of gonyautoxin 4. In summary, the current findings add to the existing knowledge of the toxin profiling of *P. bahamense*, a toxic, harmful algal bloom species, thus, leading to better toxin management.

Keywords: Gonyautoxin, HPLC, PSP, *Pyrodinium bahamense*, saxitoxin

ARTICLE INFO

Article history:
Received: 02 August 2022
Accepted: 13 October 2022
Published: 22 February 2023

DOI: https://doi.org/10.47836/pjtas.46.1.20

E-mail addresses:
asilah.alhas@live.iium.edu.my (Asilah Al-Has)
normawaty@iium.edu.my (Normawaty Mohammad-Noor)
sittirae@ums.edu.my (Sitti Raehanah M. Shaleh)
mohayo01@yahoo.com (Mohd Nor Azman Ayub)
deny@iium.edu.my (Deny Susanti)
grmustakim@gmail.com (Ghaffur Rahim Mustakim)
* Corresponding author

INTRODUCTION

Pyrodinium bahamense var. *compressum* is a thecate dinoflagellate and one of the most harmful algal bloom (HAB) organisms. The *P. bahamense* bloom is mainly distributed in the tropical Indo-Pacific and the pacific Atlantic coasts of Central America, including Florida (Usup et al., 2012). Paralytic shellfish poisoning (PSP) consists of more than 57 saxitoxin

ISSN: 1511-3701
e-ISSN: 2231-8542

analogues (Oyaneder-Terrazas et al., 2017). The highest PSP concentration is usually recorded during or after an algal bloom. PSP is an illness caused by consuming shellfish contaminated with toxic dinoflagellates, a vector of PSP in humans due to the presence of saxitoxin (STX) in their tissue (Wiese et al., 2010). The STX PSP outbreak is usually associated with the algal bloom of toxic dinoflagellates, such as *P. bahamense*, *Gymnodinium catenatum*, and *Alexandrium* spp., often responsible for the paralytic shellfish poisoning toxin (PST) that can impact human health. Saxitoxin was isolated and named after the Alaskan butter clam (*Saxidomus gigantes*) in 1957 (Schantz et al., 1957).

Pyrodinium bahamense bloom has been a constant occurrence in Sepanggar Bay, Sabah, Malaysia, for decades. This species is the main cause of harmful algal blooms (HABs) in Sabah coastal waters besides *Margalefidinium polykrikoides*. Therefore, this area is regularly monitored for PSP by the Department of Fisheries, Sabah (DOFS). A warning will be released to the public once the *P. bahamense* population exceeds 7,000 cells/L and the shellfish toxicity level exceeds 80 µg poison 100/g of meat (Jipanin et al., 2019). In 2013, 64 patients were hospitalised, and four deaths were recorded (Jipanin et al., 2019; Suleiman et al., 2017) due to the consumption of contaminated shellfish, such as mussels (*Atrina fragilis*), green mussels (*Perna viridis*), and oyster (*Crassostrea belcheri*) collected from Kota Kinabalu (Suleiman et al., 2017). In addition, PSP cases have become increasingly common along the west coast of Sabah, including Tuaran, Kuala Penyu, and Membakut (Suleiman et al., 2017). Generally, shellfish toxins, especially in green mussels (Montojo et al., 2006; Suleiman et al., 2017), remain in their tissue as decarbomyl and other STX derivatives for up to two years before being released as waste (Mustakim et al., 2016).

Besides *P. bahamense*, other marine dinoflagellates, such as *Alexandrium minutum*, *Alexandrium tamiyavanichii*, and *G. catenatum*, are also associated with PSP in Malaysia (Mohammad-Noor et al., 2018; Usup et al., 2006). Despite that, *P. bahamense* has caused more fatalities than other species (Usup et al., 2006, 2012). The *P. bahamense* is challenging to culture in the laboratory and is not widely distributed, hence the lack of studies on the physiology of this species. In the laboratory, *P. bahamense* can grow in the enriched seawater media (ES-DK) (Usup et al., 1994) and f/2 medium (Gedaria et al., 2007; Mustakim et al., 2019), yielding less than 10,000 cells/mL; much lower than other saxitoxin producers, such as *Alexandrium* spp. (Usup et al., 2012). Since 1976, there has been no record of *P. bahamense* blooming in other Malaysian coastal waters (Yñiguez et al., 2021). Moreover, field data obtained during *P. bahamense* bloom suggests that this species thrives in waters with high salinity and temperature (Adam et al., 2011; Banguera-Hinestroza et al., 2016; Lorons et al., 2022; Mohammad-Noor et al., 2014; Morquecho, 2019; Phlips et al., 2006). Meanwhile, the specific growth rate of *P. bahamense*

increased when cultured at higher salinities under laboratory conditions (Gedaria et al., 2007; Muhammad Shaleh et al., 2010). *Pyrodinium bahamense* also coexists with *Margalefidinium polykrikoides* and *G. catenatum*; hence salinity, temperature, and pH may not be limiting factors of the bloom (Adam et al., 2011).

Generally, PSP is caused by exposure to STX (an alkaloid) and other analogues, such as gonyautoxins (GTXs), neosaxitoxin (NeoSTX), dicarbamoyl-saxitoxin (dcSTXs), decarbamoyl-neosaxitoxin (decneoSTX), and decarbamoyl-gonyautoxins (dcSTXs) through the consumption of contaminated shellfish (Farabegoli et al., 2018). Therefore, it is essential to discover the toxin produced by various algae to protect consumers from lethal food poisoning (Farabegoli et al., 2018; Hummert et al., 1997). Natural and cultured *P. bahamense* samples from the Indo-Pacific coasts contain dc-STX, STX, neo-STX, B1, and B2 (Usup et al., 2012). Meanwhile, the toxin content of *P. bahamense* batch culture from Kota Kinabalu and the Philippines is higher during the exponential phase based on the high-performance liquid chromatography (HPLC) analysis (Gedaria et al., 2007; Usup et al., 1994; Yahumin et al., 2022).

The cellular toxin content of *P. bahamense* might increase with a lower growth rate and remains unaffected by different growth conditions (Usup et al., 2012). Microalgae release toxins in the water body and toxicity levels of shellfish are affected by the abundance and duration of exposure to the toxic microalgae (Tang et al., 2021). In this study, a post-column oxidation HPLC-FLD method was performed according to Oshima (1995) to analyse the toxin level and profile of *P. bahamense* at different culture ages (60, 120, 180, and 360 days) after the death phase to see how long the toxin can be sustained and bloom according to the AOAC Official Method 2011.02 (AOAC International, 2011). The findings will act as additional information regarding the toxin content of *P. bahamense*.

MATERIALS AND METHODS

Cultures and Field Sample Collection

Pyrodinium bahamense culture (CC-UHABS-040(M)) was obtained from the Borneo Marine Research Institute (BMRI), isolated during blooms in Sepanggar Bay in 2012, and established into unialgal non-axenic cultures in f/2 media (Guillard & Ryther, 1962). The media was prepared using autoclaved filtered seawater, with a salinity of 30 and pH of 8 ± 0.1. The culture was maintained at 25–26^{o}C with a 12:12 light-dark cycle illuminated by LED lights with an intensity of 100 µmol quanta/$m^{2/}$s. For the experiment, *P. bahamense* was cultured for 360 days at a similar condition. In addition, *P. bahamense* was collected from the field during the bloom in December 2021 at Sepanggar Bay using a plankton net (20 µm) and transported to the lab for further analysis.

Sample Preparation for Toxin Analysis (Figure 1)

For toxin extraction, about 1 to 2 L of *P. bahamense* at different culture ages (60,

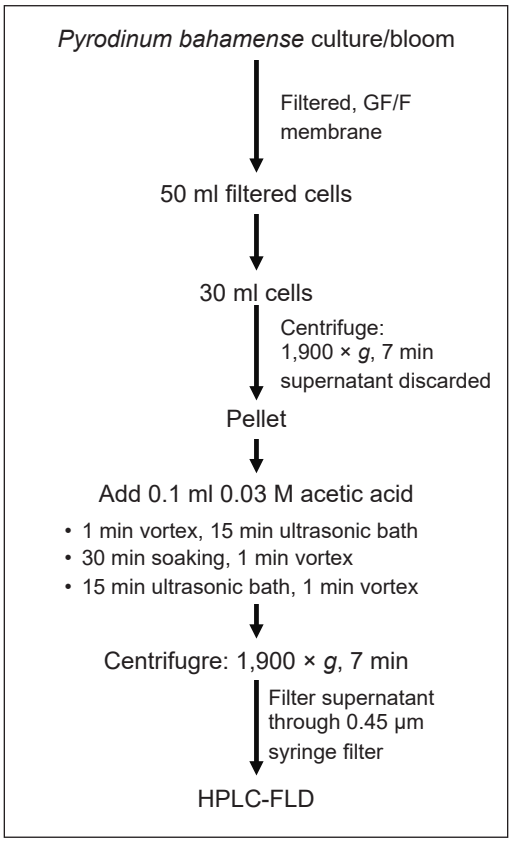

Figure 1. Sample preparation for toxin analysis

120, 180, and 360 days) and bloom samples were harvested and filtered using 45 mm glass-fibre GF/F filter paper (Whatman) to obtain a volume of 50 ml. A volume of 30 ml filtered cells was used for toxin extraction. Pellets were obtained by centrifuging the filtered cells at 1,900 × *g* for 7 min and discarding the supernatant. Afterwards, the pellets were mixed with 1 ml 0.03 M acetic acid (Merck, Germany) using a vortex for 1 min and homogenised in the ultrasonic water bath (Branson 2510, USA) for 15 min. Next, the samples were soaked in the mixture for 30 min and homogenised again for 15 min, followed by centrifugation at 1,900 × *g* for 7 min. Next, the supernatant was filtered using the 0.45 µm syringe filters (Whatman). The protocol was repeated on bloom samples collected from the field. Finally, cell densities were calculated using the Sedgewick Rafter chamber for the cultured and field samples at 400× magnification under the light microscope (Zeiss Axiostar, Germany), and the cell sizes (n = 20) were recorded.

Toxin Analysis by HPLC

For PSP toxin calibration, gonyautoxin-4/1 (GTX4/GTX1), gonyautoxin-3/2 (GTX3/GTX2), gonyautoxin-5 (GTX 5), dcSTX, and STX standards were purchased from the National Research Council (NRC), Halifax, Canada. The PSP toxins were analysed via HPLC (Shimadzu, Japan) with the post-column device and fluorescence detector utilising the isocratic post-column derivation with a slight modification from Oshima (1995). First, the samples were separated using a Luna C18(2) column (150 mm × 4.6 mm inner diameter, 120 Å, 5 µm) (Phenomenex) with a security guard cartridge (C18, 4.0 mm × 3.0 mm inner diameter) (Phenomenex, USA) at a flow rate of 0.8 ml/min. The column temperature was kept at 27ºC, while the post-column temperature was set at 65ºC for all runs. Toxin verification was performed in non-oxidising post-column conditions by substituting distilled water for the oxidising reagent. The reaction coil was kept in an ice bath during the analysis.

The chromatographic conditions are as follows: 1) STX = the mobile phase was 2

mM heptanesulfonate (Fisher Scientific, USA) in 30 mM ammonium phosphate buffer (Fisher Scientific, USA) and 5% (v/v) of acetonitrile (v/v, pH 7.1; 2) (J. T. Baker®, USA), and for the GTXs mobile phase was 2 mM heptanesulphonate (Fisher Scientific, USA) in 10 mM ammonium phosphate buffer (Fisher Scientific, USA) and 1% of acetonitrile (v/v, pH 7.1) (J. T. Baker®, USA). The acidifier was 0.5 M acetic acid (J. T. Baker®, USA), and the post-column oxidising reagent was 7 mM periodic acid (J. T. Baker®, USA) in 10 mM sodium phosphate buffer (Fisher Scientific, USA) at pH 9.0. The sample injection volume was 10 to 20 µl at a flow rate of 0.4 ml/min for each post column. Detection wavelengths were set at 330 nm for excitation and 390 nm for emissions. Toxin identification and quantification were carried out via comparisons with standard toxin materials. The concentrations of each toxin or epimeric pair (GTX1/4, GTX2/3, GTX5, STX, and dcSTX) were calculated with linear calibration curves achieved using PSP-certified references standards. The results were expressed in relative amounts of each toxin on a molar basis (mole %) and cellular toxin content as fmole/cell.

Statistical Analysis

After the data normality was tested, a one-way analysis of variance (ANOVA) was conducted, with a significance level of $p \leq 0.05$, followed by a Tukey post hoc test using Statistical Package for Social Science (SPSS) ver. 21.

RESULTS

The PST profile in the *Pyrodinium bahamense* culture isolated from Sepanggar Bay in 2012 and the seawater sample collected during a bloom of *P. bahamense* in 2021 from the same area was characterised by HPLC-FLD. The data obtained show that the culture and field bloom of *P. bahamense* produces dcSTX, STX, GTX1, GTX2, GTX3, GTX4, and GTX 5 (Figure 2). No toxin was detected on day 60, and GTX4 was the major toxin, constituting about 84-98 mole% among whole PSP toxins in other samples (Figure 3). The SXT toxin was absent in 120 days culture but comprised 4.3 mole% in the field bloom sample. However, no dcSTX toxin was detected in the field bloom sample, but high dcSTX was detected in the 360 days culture (5.4%). The proportion of GTX 1 in 180 and 360 days of culture was 5.4 and 5.9 mole%, respectively. The contribution of other toxins, such as GTX 2, GTX 3, and GTX 5 was less than 5 mole% in all samples.

The study findings also show that the cell size of cultured *P. bahamense* was not significantly different ($p < 0.05$) from the field bloom sample (Table 1). The highest cell toxin content was found in *P. bahamense* of the field bloom sample at 86.2 fmol/cell, and no cell toxin content was found in a culture of 60 days. The high number of *P. bahamense* cells (18,000 cells/mL) from the field bloom contains a high toxicity potential per cell at 63.92 fmol STXequiv./cell. There were no significant differences in the total

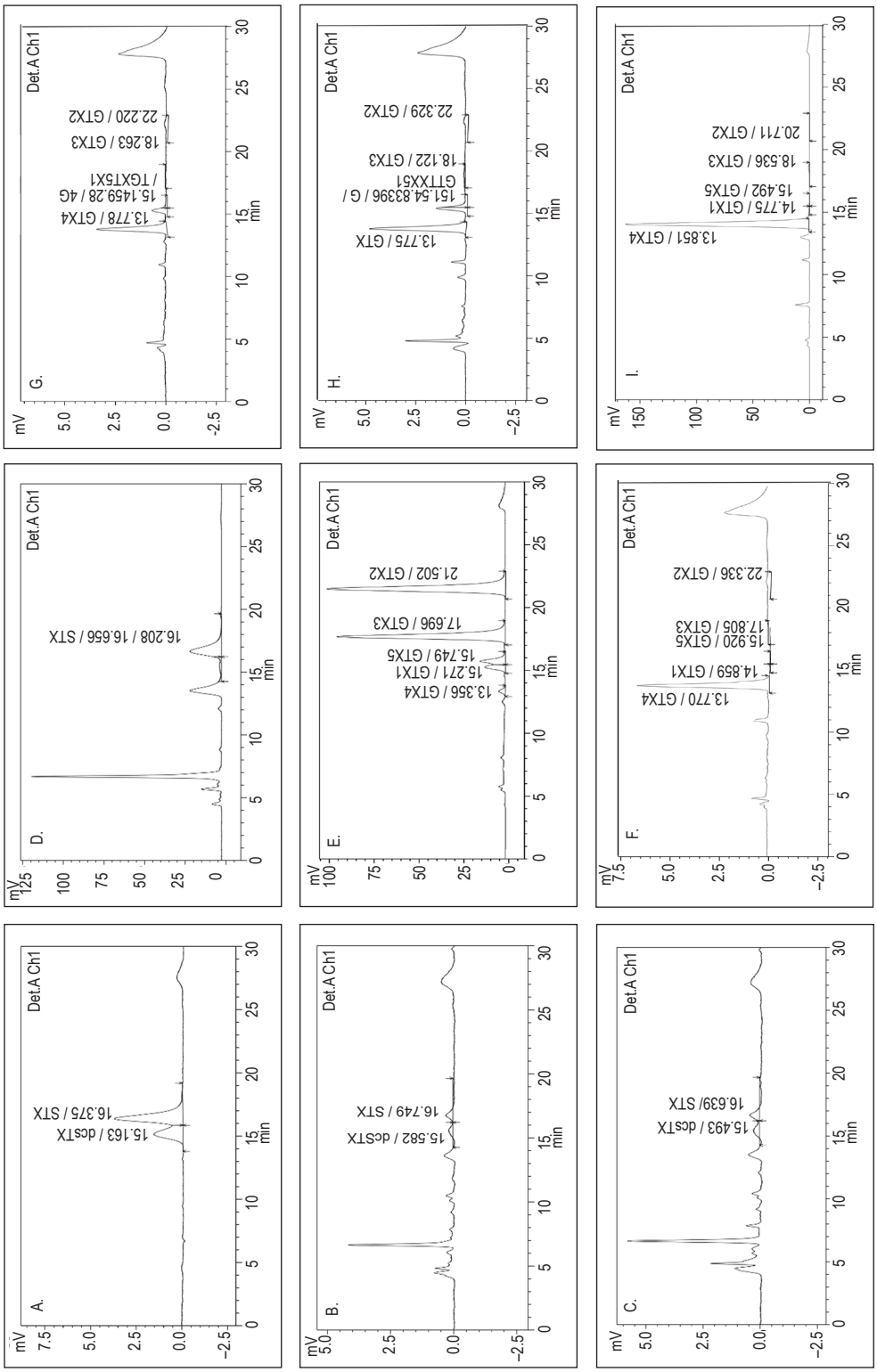

Figure 2. HPLC chromatogram profile of the culture and field bloom of *Pyrodinium bahamense*. A) STX standard; B-C) STX at 180 and 360 days, respectively; D) STX at field bloom sample; E) GTX standard; F-H) GTX at 120, 180, and 360 days, respectively; I) GTX at field bloom sample

toxicity potential per cell of *P. bahamense* samples at different culture ages (120, 180, and 360 days) ranging from 6.7-12.0 fmole STXequiv./cell.

DISCUSSION

This study detected six toxin compounds from *P. bahamense* sampled at Sepanggar Bay: GTX1, GTX2, GTX3, GTX4, GTX5,

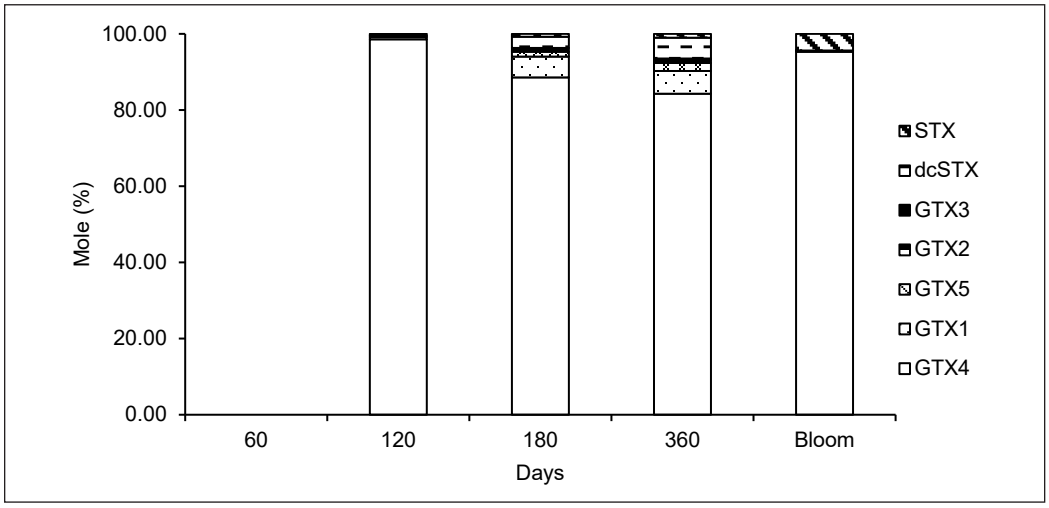

Figure 3. Toxin profile (mole%) of *Pyrodinium bahamense* from the Sepanggar Bay cultivated in f/2 media at different culture ages and field bloom sample

Table 1
Cell size (µm), cell count (cells/mL), toxin profile, and toxin content (f mole/cell) of the Pyrodinium bahamense *in different culture ages and field bloom*

	Culture age (days)				Bloom
	60	120	180	360	
Size (µm)					
Width	14.17 ± 1.42	14.34 ± 1.67	14.25 ± 2.33	14.35 ± 1.99	14.17 ± 2.43
Length	13.65 ± 1.80	14.36 ± 1.57	13.43 ± 1.65	14.29 ± 1.70	14.10 ± 2.03
Cell count (cells/mL)	1,866	2,910	4,050	4,116	18,000
Toxin (fmol/cell)					
GTX1	n.d.	0.10 (0.09)	0.52 (0.51)	0.78 (0.78)	0.16 (0.15)
GTX2	n.d.	0.08 (0.03)	0.10 (0.03)	0.12 (0.04)	0.03 (0.009)
GTX3	n.d.	n.d.	n.d.	0.04 (0.03)	0.05(0.03)
GTX4	n.d.	16.24 (11.85)	8.37 (6.11)	11.15 (8.14)	82.22 (60.02)
GTX 5	n.d.	0.06 (0.003)	0.12 (0.007)	0.28 (0.02)	0.06 (0.004)
dcSTX	n.d.	n.d.	0.28 (0.14)	0.72 (0.37)	n.d.
STX	n.d.	n.d.	0.07 (0.06)	0.13 (0.13)	3.71 (3.71)
Total toxin/cell	0	16.47	9.45	13.23	86.22
STXequiv./cell	0	11.97	6.86	9.51	63.92

Note. n.d. = Not detected. Figure in brackets is the STX equivalent value for the derivative

dcSTX, and STX via HPLC-FLD analysis (Figure 2). Based on a previous study, these compounds also were detected in *P. bahamense* from nature, cultures, and vectors (shellfish, fish) exposed to *P. bahamense* (Table 2). The GTX4 was the major toxin compound found in different culture ages and field bloom samples collected. However, GTX3 was found as the primary toxin using the same culture but at an exponential phase (Yahumin et al., 2022). It indicates that growth phases will determine the type of toxin produced besides other factors, such as temperature, medium, and chain length (Band-schmidt et al., 2006). In the *P. bahamense* batch culture, GTX 5 increased from 25 to 55% as the temperature increased from 22 to 34°C, but NeoSTX decreased from 70 to 40%. In addition, the high light intensity can cause an inversion of the NEO/B1 ratio (Usup et al., 1994), while STX and dcSTX decrease by approximately 20 mole% when *P. bahamense* is cultured in a high salinity environment (Gedaria et al., 2007). However, there was also the biotransformation of the of PSTs where less toxic PSTs into analogues of greater toxicity has been reported, such as C-toxin conversion into GTXs or GTX to STX (Wiese et al., 2010). The most toxic analogues are STX, NeoSTX, and gonyautoxin (GTX 1-4), followed by the decarbamoyl group consisting of the decarbamoyl derivatives of STX, GTX 1-4, and Neo (Oshima, 1995).

During the bloom of PSP producers, shellfish concentrate the toxins in their tissue from the water they filter when feeding (Montojo et al., 2006; Wiese et al., 2010). For instance, *Alexandrium catenella* at a low density (10 cells/ml) can accumulate up to 80 ug toxin 100/g in mussel tissue (Nishitani & Chew, 1984). During the *P. bahamense* bloom in 2013, the shellfish toxin level was 360–2920 µg STXequiv. 100/g meat with a population of 34, 200 cells/L (Suleiman et al., 2017). Furthermore, GTX 4 was found in green mussels two years after the *P. bahamense* bloom in Sabah (Mustakim et al., 2016). It is probably due to toxins that can be maintained in the cells even after cell death and the main toxin compound in GTX4, as observed in this study. Some bivalve species can maintain toxicities in their tissues for a long time after exposure to algal bloom (Mustakim et al., 2016; Oyaneder-Terrazas et al., 2022). For instance, STX, NeoSTX, GTX 5, and GTX 6 were found in bivalves after exposure to *P. bahamense* bloom. The exact analogues were present in *P. bahamense* in nature and cultures, but the toxin levels differ depending on the bivalve species (Montojo et al., 2006). The varying toxin profiles among shellfish may be attributed to the selective retention or elimination of toxins or enzymatic conversions by the molluscs (Oyaneder-Terrazas et al., 2022). Determining toxin profile or PST analogues in shellfish, fish, and organisms accumulating the toxin is crucial due to the association with human health (Vilariño et al., 2018). Meanwhile, the green mussel showed high toxicity during the *P. bahamense* bloom, and the bivalve toxicity receded instantly when the bloom subsided (Montojo et al., 2006). The human intestinal

Table 2
Toxin profile and toxicity of Pyrodinium bahamense *in bloom, culture, shellfish, and fish exposed to* P. bahamense

	Paralytic shellfish toxin (PST)																			
	Carbamate						N-sulfocarbamoyl						Decarbamoyl							
Reference/ Medium	STX	Neo STX	GTX1	GTX2	GTX3	GTX4	GTX5 (B1)	GTX6 (B2)	C1	C2	C3	C4	dsSTX	dcneo STX	dc GTX1	dc GTX2	dc STX3	dc STX4	Toxin level	Region
Bloom																				
Montojo et al. (2006)	X	X					X	X											1624 fmole/cell	Philippines
Landsberg et al. (2006)	X						X						X						3.28 pg STXeq/cell	USA
Culture																				
Usup et al. (1994)	X	X					X	X					X						200 - 400 fmol/cell	Malaysia
Montojo et al. (2006)	X	X					X	X											165-402 fmole/cell	Philippines
Landsberg et al. (2006)	X						X												2.02 - 12.74 pg STXeq/cell	USA
Usup et al. (2006)	X	X					X	X					X						59 fmole STXeq/cell	Malaysia
Gedaria et al. (2007)	X						X						X						50 to 250 fmole/cell	Philippines
Yahumin et al. (2022)	X	X	X		X	X	X						x						None	Malaysia
Shellfish																				
Montojo et al. (2006)	X	X					X	X											500-2916 mg STXeq 100/g	Philippines
Mustakim et al. (2016)						X													30 µgeq 100/g	Malaysia
Fish																				
Landsberg et al. (2006)	X						X						X						6.25 - 9,039 µg STXeq 100/g	USA

epithelium can absorb almost all PST analogues after consuming the contaminated shellfish (Rodrigues et al., 2021). Multiple factors must be considered in analysing the toxin content and toxic profile of shellfish; thus, Hayashi et al. (2006) recommend using a cell bioassay for routine monitoring.

This study shows that *P. bahamense* can survive in low cell numbers for up to 360 days. After the cell entered the death phase, the morphology remained the same, and the cell size did not experience significant changes. This observation indicates the cell's ability to utilise the nutrients from degraded cells and store them for later use (Phlips et al., 2006). Meanwhile, the *P. bahamense* from the Philippines had a low growth rate (0.2 div/d) that declined on day 35 and entered the death phase on day 43 (Gedaria et al., 2007). There were significant differences in toxin levels between field-collected and cultured *P. bahamense*, which aligned with previous reports. Toxin production rate is related to production of arginine (Arg) within the cells due to cell division (Anderson et al., 1990). PSP toxin content of a cell also relates to nitrogen within the cells (Usup et al., 2006). In this study, the toxin content of culture *P. bahamense* was constant. However, Usup et al. (2006) reported that the total toxicity potential per cell was higher in the field bloom sample with a toxin of 63.92 fmole STXequiv./cell compared to 59 fmole STXequiv./cell of *P. bahamense* culture. The high *P. bahamense* cell numbers reflect the high STX levels (Lopez et al., 2021). Moreover, Usop et al. (1994) found that the toxin level of isolated *P. bahamense* from Sabah increased at the beginning of the exponential phase and achieved maximum toxin content during the mid-exponential phase (400 fmole/cell), followed by a rapid decrease and plateau at 200 fmole/cell. Contrary to *G. catenatum*, no significant changes in toxin content with culture age were observed (Band-schmidt et al., 2006). In contrast, Montojo et al. (2006) reported no significant difference in toxin content from five strains of *P. bahamense* harvested at the late exponential phase in the Philippines. *Pyrodinium bahamense* toxin content is not significantly influenced by different growth conditions but could affect the toxin profile in terms of the ratio of different PSTs (Usop et al., 2012). Furthermore, minimal differences were identified in PSTs detected in *P. bahamense* and shellfish (Montojo et al., 2006). Since there are discrepancies in the existing literature, it is essential to monitor *P. bahamense* bloom regularly to understand better the ecology and toxin mechanism of these STX producers. Furthermore, the findings can be utilised in developing a HAB programme to preserve human health and food safety.

CONCLUSION

This preliminary study showed that *P. bahamense* could sustain its growth for up to 360 days and produce toxins in low concentrations. Toxins GTX 4 is the main analogue found in *P. bahamense*, and a constant toxin cell content was found during the death phase. Furthermore, fresh

samples may contain more analogues than cultured cells, as observed in the bloom sample collected from the field. The study results align with previous findings that toxins are retained in the cell for a long time, although at low concentrations. Consequently, the vectors, such as the shellfish, will continuously accumulate toxins through filter-feeding after a bloom (death phase). Therefore, it is crucial to identify the environmental factors that trigger toxin production in harmful algae, such as *P. bahamense*, to ensure human and food safety and security.

ACKNOWLEDGEMENTS

This work was financially supported by a Fundamental Research Grant (19-038-0646/FRGS/1/2018/WAB09/UIAM/O2/4) provided by the Ministry of Higher Education, Malaysia and under the License Ref. No. JKM/MBS.1000-2/2 JLD.12 (37) from the Sabah Biodiversity Centre (SeBC). We want to thank the Department of Fisheries Sabah, the Department of Meteorology Department, Kota Kinabalu, Sabah, the Borneo Marine Research Institute and the Fisheries Research Institute, Batu Maung, for supporting this study.

REFERENCES

Adam, A., Mohammad-Noor, N., Anton, A., Saleh, E., Saad, S., & Shaleh, S. R. M. (2011). Temporal and spatial distribution of harmful algal bloom (HAB) species in coastal waters of Kota Kinabalu, Sabah, Malaysia. *Harmful Algae*, *10*(5), 495–502. https://doi.org/10.1016/j.hal.2011.03.006

Anderson, D. M., Kulis, D. M., Sullivan, J. J., Hall, S., & Lee, C. (1990). Dynamics and physiology of saxitoxin production by the dinoflagellates *Alexandrium* spp. *Marine Biology*, *104*, 511-524. https://doi.org/10.1007/BF01314358

AOAC International. (2011). *Paralytic shellfish toxins in mussels, clams, scallops and oysters by liquid chromatography post-column oxidation*. AOAC International.

Band-schmidt, C. J., Bustillos-Guzman, J., Morquecho, L., Grate-Lizarraga, I., Alonso-Rodríguez, R., Reyes-Salinas, A., Erler, K., & Luckas, B. (2006). Variations of PSP toxin profiles during different growth phases in *Gymnodinium catenatum* (Dinophyceae) strains isolated from three location in the Gulf of California, Mexico. *Journal of Phycology*, *42*(4), 757–768. https://doi.org/10.1111/j.1529-8817.2006.00234.x

Banguera-Hinestroza, E., Eikrem, W., Mansour, H., Solberg, I., Cúrdia, J., Holtermann, K., Edvardsen, B., & Kaartvedt, S. (2016). Seasonality and toxin production of *Pyrodinium bahamense* in a Red Sea lagoon. *Harmful Algae*, *55*, 163–171. https://doi.org/10.1016/j.hal.2016.03.002

Farabegoli, F., Blanco, L., Rodríguez, L. P., Juan, M. V., & Ana, G. C. (2018). Phycotoxins in marine shellfish: Origin, occurrence and effects on humans. *Marine Drugs*, *16*(6), 188. https://doi.org/10.3390/md16060188

Gedaria, A. I., Luckas, B., Reinhardt, K., & Azanza, R. V. (2007). Growth response and toxin concentration of cultured *Pyrodinium bahamense* var. *compressum* to varying salinity and temperature conditions. *Toxicon*, *50*(4), 518–529. https://doi.org/10.1016/j.toxicon.2007.04.021

Guillard, R. R., & Ryther, J. H. (1962). Studies of marine planktonic diatoms: I. *Cyclotella nana* Hustedt, and *Detonula confervacea* (cleve) Gran. *Canadian Journal of Microbiology*, *8*(2), 229-239. https://doi.org/10.1139/m62-029

Hayashi, R., Saito, H., Okumura, M., & Kondo, F. (2006). Cell bioassay for paralytic shellfish poisoning (PSP): Comparison with postcolumn derivatization liquid chromatographic analysis and application to the monitoring of PSP in shellfish. *Journal of Agricultural and Food Chemistry*, *54*(2), 269–273. https://doi.org/10.1021/jf050649t

Hummert, C., Ritscher, M., Reinharde, K., & Luckas, B. (1997). Analysis of the characteristic PSP profiles of *Pyrodinium bahamense* and several strains of *Alexandrium* by HPLC based on ion-pair chromatographic separation, post-column oxidation, and fluorescence detection. *Chromatographia*, *45*, 312–316. https://doi.org/10.1007/BF02505576

Jipanin, S. J., Shaleh, S. M., Lim, P. T., Leaw, C. P., & Mustapha, S. (2019). The monitoring of harmful algae blooms in Sabah, Malaysia. In *IOP conference series: Journal of Physics* (Vol. 1358, No. 1, p. 012014). IOP Publishing. https://doi.org/10.1088/1742-6596/1358/1/012014

Landsberg, J. H., Hall, S., Johannessen, J. N., White, K. D., Conrad, S. M., Abbott, J. P., Flewelling, L. J., Richardson, R. W., Dickey, R. W., Jester, E. L. E., Etheridge, S. M., Deeds, J. R., Dolah, F. M. V., Leighfield, T. A., Zou, Y., Beaudry, C. G., Benner, R. A., Rogers, P. L., Scott, P. S., … Steidinger, K. A. (2006). Saxitoxin puffer fish poisoning in the United States, with the first report of *Pyrodinium bahamense* as the putative toxin source. *Environmental Health Perspectives*, *114*(10), 1502–1507. https://doi.org/10.1289/ehp.8998

Lopez, C. B., Tilney, C. L., Muhlbach, E., Bouchard, J. N., Villac, M. C., Henschen, K. L., Markley, L. R., Abbe, S. K., Shankar, S., Shea, C. P., Flewelling, L., Garrett, M., Badylak, S., Phlips, E. J., Hall, L. M., Lasi, M. A., Parks, A. A., Paperno, R., Adams, D. H., … Hubbard, K. A. (2021). High-resolution spatiotemporal dynamics of harmful algae in the Indian River Lagoon (Florida) — A case study of *Aureoumbra lagunensis*, *Pyrodinium bahamense*, and *Pseudo-nitzschia*. *Frontiers in Marine Science*, *8*, 769877. https://doi.org/10.3389/fmars.2021.769877

Lorons, D., Jafar-Sidik, M., Ali, N., Mohamad-Azaini, F., Rodrigues, K. F., & Chin, G. J. W. L. (2022). The variation of environmental profiles during harmful algal bloom in Sepanggar Bay, Sabah, Malaysia. *Journal of Oceanography*, *78*(2), 121–132. https://doi.org/10.1007/s10872-022-00634-9

Mohammad-Noor, N., Weliyadi, E., Aung, T., Adam, A., & Hanan, D. S. M. (2014). Effects of meteorological conditions on the occurrence of *Cochlodinium polykrikoides* and *Pyrodinium bahamense* var. *compressum* in coastal waters of Kota Kinabalu, Sabah, Malaysia. *Sains Malaysiana*, *43*(1), 21–29.

Mohammad-Noor, N., Adam, A., Lim, P. T., Leaw, C. P., Lau, W. L., Liow, G. R., Muhamad-Bunnori, N., Hamdan, N. A., Md-Nor, A., Kemat, N., & Muniandi, D. (2018). First report of paralytic shellfish poisoning (PSP) caused by *Alexandrium tamiyavanichii* in Kuantan Port, Pahang, East Coast of Malaysia. *Phycological Research*, *66*(1), 37-44. https://doi.org/10.1111/pre.12205

Montojo, U. M., Sakamoto, S., Cayme, M. F., Gatdula, N. C., Furio, E. F., Relox, J. R., Sato, S., Fukuyo, Y., & Kodama, M. (2006). Remarkable difference in accumulation of paralytic shellfish poisoning toxins among bivalve species exposed to *Pyrodinium bahamense* var. *compressum* bloom in Masinloc Bay, Philippines. *Toxicon*, *48*(1), 85–92. https://doi.org/10.1016/j.toxicon.2006.04.014

Morquecho, L. (2019). *Pyrodinium bahamense* one the most significant harmful dinoflagellate in Mexico. *Frontiers in Marine Science*, *6*, 1. http://doi.org/10.3389/fmars.2019.00001

Muhammad Shaleh, S. R., Doinsing, J., Peter, C. Anton, A., & Saleh, E. (2010). Effects on

salinity on interspecific growth interactions between 2 harmful algal species *Pyrodinium* var. *compressum* and *Cochlodinium polykrikoides* in laboratory cultures. In *Proceedings of the 13th International Conference on Harmful Algae* (95-97). Environmental Publication Department. https://www.researchgate.net/publication/233985327_Effects_of_salinity_on_interspecific_growth_interactions_between_2_harmful_algal_species_Pyrodinium_bahamanse_var_Compressum_and_Cochlodinium_polykrikoides_in_laboratory_cultures

Mustakim, G. R., Anton, A., Samsur, M., & Ayub, M. N. A. (2016). Determination of PSP concentration in shellfish from Kuala Penyu, Sabah using HPLC method. *Transactions on Science and Technology*, *3*(2–2), 433–438.

Mustakim, G. R., Muhammad Shaleh, S. R., & Ayub, M. N. A. (2019). Effect of different concentration of soil extracts on the growth of *Pyrodinium bahamense* var. *compressum*. *International Journal of Fisheries and Aquatic Studies*, *7*(5), 353–355.

Nishitani, L., & Chew, K. K. (1984). Recent developments in paralytic shellfish poisoning research. *Aquaculture*, *39*(1-4), 317–329. https://doi.org/10.1016/0044-8486(84)90274-6

Oshima, Y. (1995). Postcolumn derivation liquid chromatographic method for paralytic shellfish toxins. *Journal of AOAC International*, *78*(2), 528-532. https://doi.org/10.1093/jaoac/78.2.528

Oyaneder-Terrazas, J., Contreras, H. R., & García, C. (2017). Prevalence, variability and bioconcentration of saxitoxin-group in different marine species present in the food chain. *Toxins*, *9*(6), 190. https://doi.org/10.3390/toxins9060190

Oyaneder-Terrazas, J., Figueroa, D., Araneda, O. F., & García, C. (2022). Saxitoxin group toxins accumulation induces antioxidant responses in tissues of *Mytilus chilensis*, *Ameghinomya antiqua*, and *Concholepas concholepas* during a bloom of *Alexandrium pacificum*. *Antioxidants*, *11*(2), 392. https://doi.org/10.3390/antiox11020392

Phlips, E. J., Badylak, S., Bledsoe, E., & Cichra, M. (2006). Factors affecting the distribution of *Pyrodinium bahamense* var. *bahamense* in coastal waters of Florida. *Marine Ecology Progress Series*, *322*, 99–115. https://doi.org/10.3354/meps322099

Rodrigues, E. T., Nascimento, S. F., Pires, C. L., Godinho, L. P., Churro, C., Moreno, M. J., & Pardal, M. A. (2021). Determination of intestinal absorption of the paralytic shellfish toxin GTX-5 using the Caco-2 human cell model. *Environmental Science Pollution Research*, *28*, 67256-67266. https://doi.org/10.1007/s11356-021-15342-y

Schantz, E. J., Mold, J. D., Warren Stanger, D., John, S., Riel, F. J., Bowden, J. P., Lynch, J. M., Wayler, R. S., Riegel, B., & Sommer, H. (1957). Paralytic shellfish poison. VI. A procedure for the isolation and purification of the poison from toxic clam and mussel tissues. *Journal of the American Chemical Society*, *79*(19), 5230–5235. https://doi.org/10.1021/JA01576A044

Suleiman, M., Jelip, J., Rundi, C., & Chua, T. H. (2017). Case report: Paralytic shellfish poisoning in Sabah, Malaysia. *The American Journal of Tropical Medicine and Hygiene*, *97*(6), 1731–1736. https://doi.org/10.4269/ajtmh.17-0589

Tang, Y., Zhang, H., Wang, Y., Fan, C., & Shen, X. (2021). Combined effects of temperature and toxic algal abundance on paralytic shellfish toxic accumulation, tissue distribution and elimination dynamics in mussels *Mytilus coruscus*. *Toxins*, *13*(6), 425. https://doi.org/10.3390/toxins13060425

Usup, G., Ahmad, A., Matsuoka, K., Teen, P., & Pin, C. (2012). Biology, ecology and bloom dynamics

of the toxic marine dinoflagellate *Pyrodinium bahamense*. *Harmful Algae*, *14*, 301–312. https://doi.org/10.1016/j.hal.2011.10.026

Usup, G., Cheah, M. Y., Ng, B. K., Leaw, C. P., & Ahmad, A. (2006). Toxin profile and relative toxicity of three paralytic shellfish poisoning toxin-producing dinoflagellates from Malaysia. *Malaysian Applied Biology*, *35*, 41–45.

Usup, G., Kulis, D. M., & Anderson, D. M. (1994). Growth and toxin production of the toxic dinoflagellate *Pyrodinium bahamense* var. *compressum* in laboratory cultures. *Natural Toxins*, *2*(5), 254–262. https://doi.org/10.1002/nt.2620020503

Vilariño, N., Louzao, M. C., Abal, P., Cagide, E., Carrera, C., Vieytes, M. R., & Botana, L. M. (2018). Human poisoning from marine toxins: Unknowns for optimal consumer protection. *Toxins*, *10*(8), 324. https://doi.org/10.3390/toxins10080324

Wiese, M., D'Agostino, P. M., Mihali, T. K., Moffitt, M. C., & Neilan, B. A. (2010). Neurotoxic alkaloids: Saxitoxin and its analogs. *Marine Drugs*, *8*(7), 2185–2211. https://doi.org/10.3390/md8072185

Yahumin, S., Rodrigues, K. F., & Chin, G. J. W. L. (2022). Characterization of the saxitoxin biosynthetic starting gene, *sxt4*, in the toxic dinoflagellate, *Pyrodinium bahamense* var. *compressum*. *Journal of Sustainability Science and Management*, *7*(7), 152-165. http://doi.org/10.46754/jssm.2022.07.011

Yñiguez, A. T., Lim, P. T., Leaw, C. P., Jipanin, S. J., Iwataki, M., Benico, G., & Azanza, R. V. (2021). Over 30 years of HABs in the Philippines and Malaysia: What have we learned?. *Harmful Algae*, *102*, 101776. https://doi.org/10.1016/j.hal.2020.101776

REFEREES FOR THE PERTANIKA
JOURNAL OF TROPICAL AGRICULTURAL SCIENCE

Vol. 46 (1) Feb. 2023

The Editorial Board of the Pertanika Journal of Tropical Agricultural Science wishes to thank the following:

Ahmed Osumanu Haruna
(UNISSA, Brunei)

Alimuddin Ali
(UNM, Indonesia)

Amir Hamzah Ahmad Ghazali
(USM, Malaysia)

Anjas Asmara@Ab. Hadi Samsudin
(UPM, Malaysia)

Aslizah Mohd-Aris
(UiTM, Malaysia)

Asnuzilawati Asari
(UMT, Malaysia)

Azzreena Mohd Azzeme
(UPM, Malaysia)

Banpot Napompeth
(KU, Thailand)

Chew Li Lee
(UCSI, Malaysia)

Chonchanok Muangnapoh
(Chula, Thailand)

Chong Khim Phin
(UMS, Malaysia)

Chuah Cheng Hock
(UM, Malaysia)

Chye Fook Yee
(UMS, Malaysia)

Danner Sagala
(Unihaz, Indonesia)

Emily Wynn
(USDA, USA)

Fahrul Zaman Huyop
(UTM, Malaysia)

Farah Alia Nordin
(USM, Malaysia)

Farhan Hafeez
(CUI, Pakistan)

Fatimah Kayat
(UMK, Malaysia)

Gan Chee Yuen
(USM, Malaysia)

Graham Matthews
(IC, United Kingdom)

Hayati Mohd Yusof
(UMT, Malaysia)

Husnul Azan Tajarudin
(USM, Malaysia)

Intan Shameha Abdul Razak
(UPM, Malaysia)

Jameel R. Al-Obaidi
(UPSI, Malaysia)

Jamilah Mohd Salim@Halim
(UMT, Malaysia)

Keeren Sundara Rajoo
(UPM, Malaysia)

Lela Susilawati
(UIN, Indonesia)

Luciano Pinotti
(UniMi, Italy)

Mahadimenakbar Mohamed Dawood
(UMS, Malaysia)

Malik Abdul Malik
(Uniska, Indonesia)

Md. Kamal Uddin
(UPM, Malaysia)

Miftahul Khair Kadim
(UNG, Indonesia)

Mohammad Anwar Mohamed Iqbal
(USM, Malaysia)

Mohd Azlan Jayasilan bin Abdul Gulam Azad
(UNIMAS, Malaysia)

Mohd Nazre Saleh
(UPM, Malaysia)

Monsuru Salisu
(UPSI, Malaysia)

Nadzifah Yaakub
(UniSZA, Malaysia)

Nazahatul Anis Amaludin
(UMK, Malaysia)

Neena Singla
(PAU, India)

Nor Hayati Ibrahim
(UMT, Malaysia)

Nozlena Abdul Samad
(USM, Malaysia)

Nurul Shamsinah Mohd Suhaimi
(UM, Malaysia)

Patrick Skoth Michael
(Unitech, Papua New Guinea)

Piotr Salachna
(ZUT, Poland)

Rabiatul Adawiah Zainal Abidin
(MARDI, Malaysia)

Sakina Zerizer
(UMC, Algeria)

Samsur Mohamad
(UNIMAS, Malaysia)

Saw Leng Guan
(Malaysia)

Shahrul Anuar Mohd Sah
(USM, Malaysia)

Shamshuddin Jusop
(UPM, Malaysia)

Sharina Omar
(UPM, Malaysia)

Siti Noor Hajjar Md Latip
(UiTM, Malaysia)

Somchai Butnan
(SNRU, Thailand)

Supat Isarangkool Na Ayutthaya
(KKU, Thailand)

Suzan Benedick
(UMS, Malaysia)

Tuan Noorkorina Tuan Kub
(USM, Malaysia)

Ubedullah Kaka
(UPM, Malaysia)

Uma Rani Sinniah
(UPM, Malaysia)

Wahizatul Afzan Azmi
(UMT, Malaysia)

Wasiu Adeyemi Jimoh
(Unilorin, Nigeria)

Wasiu Adeyemi Jimoh
(Unilorin, Nigeria)

Yap Chee Kong
(UPM, Malaysia)

Yeo Freddy Kuok San
(UNIMAS, Malaysia)

Zaiton Sapak
(UiTM, Malaysia)

Chula – Chulalongkorn University
CUI – COMSATS University Islamabad, Abbottabad Campus
IC – Imperial College London
KKU – Khon Kaen University
KU – Kasetsart University
MARDI – Malaysian Agricultural Research and Development Institute
PAU – Punjab Agricultural University
SNRU – Sakon Nakhon Rajabhat University
UCSI – UCSI University
UIN – Universitas Islam Negeri Sunan Kalijaga
UiTM – Universiti Teknologi MARA
UM – Universiti Malaya
UMC – Université Frères Mentouri Constantine I
UMK – Universiti Malaysia Kelantan
UMS – Universiti Malaysia Sabah
UMT – Universiti Malaysia Terengganu
UNG – Universitas Negeri Gorontalo
Unihaz – Universitas Prof. Dr. Hazairin SH
Unilorin – University of Ilorin
UNIMA – Universiti Malaysia Sarawak
UniMi – Università degli Studi di Milano
Uniska – Universitas Islam Kalimantan
UNISSA – Universiti Islam Sultan Sharif Ali
UniSZA – Universiti Sultan Zainal Abidin
Unitech – Papua New Guinea University of Technology
UNM – Universitas Negeri Makassar
UPM – Universiti Putra Malaysia
UPSI – Universiti Pendidikan Sultan Idris
USDA – United States Department of Agriculture
USM – Universiti Sains Malaysia
UTM – Universiti Teknologi Malaysia
ZUT – Zachodniopomorski Uniwersytet Technologiczny w Szczecinie

---

While every effort has been made to include a complete list of referees for the period stated above, however if any name(s) have been omitted unintentionally or spelt incorrectly, please notify the Chief Executive Editor, *Pertanika* Journals at executive_editor.pertanika@upm.edu.my

Any inclusion or exclusion of name(s) on this page does not commit the *Pertanika* Editorial Office, nor the UPM Press or the university to provide any liability for whatsoever reason.

Pertanika Journal of Tropical Agricultural Science
Vol. 46 (1) Feb. 2023

Content

Pertanika Editorial Office, Journal Division,
Putra Science Park,
1st Floor, IDEA Tower II,
UPM-MTDC Center,
Universiti Putra Malaysia,
43400 UPM Serdang,
Selangor Darul Ehsan
Malaysia

http://www.pertanika.upm.edu.my
Email: executive_editor.pertanika@upm.edu.my
Tel. No.: +603- 9769 1622

PENERBIT UPM PRESS
UNIVERSITI PUTRA MALAYSIA

http://www.penerbit.upm.edu.my
Email: penerbit@upm.edu.my
Tel. No.: +603- 9769 8851

ISSN 1511-3701
02
9 771511 370234